Methods in Molecular Biology 1354

Springer Protocols

Vinayaka R. Prasad
Ganjam V. Kalpana *Editors*

HIV Protocols

Third Edition

Humana Press

METHODS IN MOLECULAR BIOLOGY

Series Editor
John M. Walker
School of Life and Medical Sciences
University of Hertfordshire
Hatfield, Hertfordshire, AL10 9AB, UK

For further volumes:
http://www.springer.com/series/7651

HIV Protocols

Third Edition

Edited by

Vinayaka R. Prasad

Department of Microbiology & Immunology, Albert Einstein College of Medicine, Bronx, NY, USA

Ganjam V. Kalpana

Department of Genetics, Albert Einstein College of Medicine, Bronx, NY, USA

Humana Press

Editors
Vinayaka R. Prasad
Department of Microbiology & Immunology
Albert Einstein College of Medicine
Bronx, NY, USA

Ganjam V. Kalpana
Department of Genetics
Albert Einstein College of Medicine
Bronx, NY, USA

ISSN 1064-3745 ISSN 1940-6029 (electronic)
Methods in Molecular Biology
ISBN 978-1-4939-3045-6 ISBN 978-1-4939-3046-3 (eBook)
DOI 10.1007/978-1-4939-3046-3

Library of Congress Control Number: 2015960182

Springer New York Heidelberg Dordrecht London

Cover illustration: A human macrophage infected with HIV-1 carrying GFP embedded in Gag
Courtesy: Dr. Paul Bieniasz, Aaron Diamond AIDS Research Center and Rockefeller University

Printed on acid-free paper

Humana Press is a brand of Springer
Springer Science+Business Media LLC New York is part of Springer Science+Business Media (www.springer.com)

Preface

It has been about 5 years since the publication of the *HIV Protocols* 2nd edition. Thus, when we were approached by John Walker asking us to compile a new edition, we were pleased to know that previous edition had been quite popular both in print and in terms of online downloads. During the intervening years, there has been a considerable advance in the methods employed in HIV research—especially those pertaining to virology. Therefore, we readily agreed, and now here is *HIV Protocols* 3rd edition!

The protocols included in this book were chosen to complement those in the previous edition. Therefore, these two editions are companion volumes and there are no overlaps. The HIV protocols are written for use by researchers at all levels including technicians, graduate students, and postdoctoral fellows working in HIV/AIDS laboratories both in academia and pharmaceutical industry. The protocols include chapters that investigate various aspects of HIV-1 replication and hence are helpful for investigating the mechanisms of HIV-1 replication or pathogenesis. The book contains 25 chapters grouped into six parts: (1) HIV early events; (2) HIV-1 RNA structure and RNA-protein interactions; (3) HIV-1 post-integration events; (4) HIV-1 pathogenesis in animal models; (5) Tools to study HIV-1 latency; and (6) NeuroAIDS. Chapters within each part are related to each other in the overall goals, but they are distinct from each other and cover a specific protocol or sets of protocols. For each of the chapters, we have sought out experts who have developed the technique, improved it significantly or simplified it, and applied it to HIV research.

As is typical to all MiMB series of books, these chapters are complete with a Notes section. These notes come from the experts and contain many tips, tricks, and little details that are rarely mentioned in standard protocols. All our authors made a special effort to think up those, seemingly small, but highly significant tips that are crucial for the protocols to work.

We would like to thank Springer for the opportunity to edit this book, the series editor Dr. John Walker for his continuous support and guidance, and Patrick Marton and David Casey for their unwavering support. We extend our sincere gratitude to all contributors for submitting their valuable contributions to this collection and for their prompt communication with us. We wish to specially express our gratitude to the members of our two research groups (Arthur Ruiz, Annalena La Porte, Christine Timmons, Vasudev Rao, and David Ajasin) who have helped with reading the chapters for scientific content and with creating the subject index. Arthur Ruiz deserves a very special mention for his careful corrections and for piloting the chapters from the user point of view. His contribution was above and beyond the call of duty.

Bronx, NY, USA

Vinayaka R. Prasad, Ph.D.
Ganjam V. Kalpana, Ph.D.

Contents

Preface . . . . . *v*
Contributors . . . . . *xi*

PART I HIV-1 REPLICATION—EARLY EVENTS

1 Quantifying CD4/CCR5 Usage Efficiency of HIV-1 Env Using the Affinofile System 3
Nicholas E. Webb and Benhur Lee

2 Measuring T Cell-to-T Cell HIV-1 Transfer, Viral Fusion, and Infection Using Flow Cytometry 21
Natasha D. Durham and Benjamin K. Chen

3 HIV-1 Capsid Stabilization Assay 39
Thomas Fricke and Felipe Diaz-Griffero

4 Detection and Tracking of Dual-Labeled HIV Particles Using Wide-Field Live Cell Imaging to Follow Viral Core Integrity 49
João I. Mamede and Thomas J. Hope

5 HIV-1 Reverse Transcriptase-Based Assay to Determine Cellular dNTP Concentrations 61
Joseph A. Hollenbaugh and Baek Kim

6 Rapid Determination of HIV-1 Mutant Frequencies and Mutation Spectra Using an mCherry/EGFP Dual-Reporter Viral Vector 71
Jonathan M.O. Rawson, Christine L. Clouser, and Louis M. Mansky

PART II HIV-1 RNA STRUCTURE AND RNA-PROTEIN INTERACTIONS

7 Novel Biochemical Tools for Probing HIV RNA Structure 91
Jason W. Rausch, Joanna Sztuba-Solinska, Sabrina Lusvarghi, and Stuart F.J. Le Grice

8 Analysis of HIV-1 Gag-RNA Interactions in Cells and Virions by CLIP-seq 119
Sebla B. Kutluay and Paul D. Bieniasz

9 Isolation of Cognate Cellular and Viral Ribonucleoprotein Complexes of HIV-1 RNA Applicable to Proteomic Discovery and Molecular Investigations 133
Deepali Singh, Ioana Boeras, Gatikrushna Singh, and Kathleen Boris-Lawrie

PART III HIV-1 REPLICATION—POST-INTEGRATION EVENTS

10 Methods for the Analyses of Inhibitor-Induced Aberrant Multimerization of HIV-1 Integrase 149
Jacques J. Kessl, Amit Sharma, and Mamuka Kvaratskhelia

11 Quantification of HIV-1 Gag Localization Within Virus Producer Cells 165
Annalena La Porte and Ganjam V. Kalpana

12 Methods to Study Determinants for Membrane Targeting of HIV-1 Gag In Vitro 175
Gabrielle C. Todd and Akira Ono

PART IV STUDYING HIV-1 REPLICATION AND PATHOGENESIS IN ANIMAL MODELS

13 Visualizing the Behavior of HIV-Infected T Cells In Vivo Using Multiphoton Intravital Microscopy 189
Radwa Sharaf, Thorsten R. Mempel, and Thomas T. Murooka

14 Modeling HIV-1 Mucosal Transmission and Prevention in Humanized Mice 203
Milena Veselinovic, Paige Charlins, and Ramesh Akkina

15 High-Throughput Humanized Mouse Models for Evaluation of HIV-1 Therapeutics and Pathogenesis. 221
Tynisha Thomas, Kieran Seay, Jian Hua Zheng, Cong Zhang, Christina Ochsenbauer, John C. Kappes, and Harris Goldstein

PART V TOOLS TO STUDY HIV-1 LATENCY AND PATHOGENESIS

16 Measuring the Frequency of Latent HIV-1 in Resting $CD4^+$ T Cells Using a Limiting Dilution Coculture Assay 239
Gregory M. Laird, Daniel I.S. Rosenbloom, Jun Lai, Robert F. Siliciano, and Janet D. Siliciano

17 LGIT In Vitro Latency Model in Primary and T Cell Lines to Test HIV-1 Reactivation Compounds 255
Ulrike Jung, Mayumi Takahashi, John J. Rossi, and John C. Burnett

18 Improved Methods to Detect Low Levels of HIV Using Antibody-Based Technologies 265
Eliseo A. Eugenin and Joan W. Berman

19 Analysis of ABCA1 and Cholesterol Efflux in HIV-Infected Cells 281
Nigora Mukhamedova, Beda Brichacek, Christina Darwish, Anastas Popratiloff, Dmitri Sviridov, and Michael Bukrinsky

20 The Proteomic Characterization of Plasma or Serum from HIV-Infected Patients. 293
Nicole A. Haverland, Lance M. Villeneuve, Pawel Ciborowski, and Howard S. Fox

21 Proteomic Characterization of Exosomes from HIV-1-Infected Cells 311
Ming Li and Bharat Ramratnam

PART VI NEUROAIDS

22 Detecting HIV-1 Tat in Cell Culture Supernatants by ELISA or Western Blot. 329
Fabienne Rayne, Solène Debaisieux, Annie Tu, Christophe Chopard, Petra Tryoen-Toth, and Bruno Beaumelle

23 Protocol for Detection of HIV-Tat Protein in Cerebrospinal Fluid by a Sandwich Enzyme-Linked Immunosorbent Assay 343
Tory P. Johnson and Avindra Nath

24 Measuring the Uptake and Transactivation Function of HIV-1 Tat Protein in a Trans-Cellular Cocultivation Setup 353
Arthur P. Ruiz and Vinayaka R. Prasad

25 Evaluating the Role of Viral Proteins in HIV-Mediated Neurotoxicity Using Primary Human Neuronal Cultures 367
Vasudev R. Rao, Eliseo A. Eugenin, and Vinayaka R. Prasad

Erratum *E1*

Index *377*

Contributors

Ramesh Akkina • *Department of Microbiology, Immunology and Pathology, Colorado State University, Fort Collins, CO, USA*

Bruno Beaumelle • *CPBS, UMR 5236 CNRS, University of Montpellier, Montpellier Cedex 05, France*

Joan W. Berman • *Departments of Pathology, The Albert Einstein College of Medicine, Bronx, NY, USA; Department of Microbiology and Immunology, The Albert Einstein College of Medicine, Bronx, NY, USA*

Paul D. Bieniasz • *Laboratory of Retrovirology, Aaron Diamond AIDS Research Center, The Rockefeller University, New York, NY, USA; Howard Hughes Medical Institute, Aaron Diamond AIDS Research Center, The Rockefeller University, New York, NY, USA*

Ioana Boeras • *Department of Veterinary Biosciences, The Ohio State University, Columbus, OH, USA; Center for Retrovirus Research, The Ohio State University, Columbus, OH, USA; Center for RNA Biology, The Ohio State University, Columbus, OH, USA*

Kathleen Boris-Lawrie • *Department of Veterinary Biosciences, The Ohio State University, Columbus, OH, USA; Center for Retrovirus Research, The Ohio State University, Columbus, OH, USA; Center for RNA Biology, The Ohio State University, Columbus, OH, USA*

Beda Brichacek • *Department of Microbiology, Immunology and Tropical Medicine, George Washington University School of Medicine and Health Sciences, Washington, DC, USA*

Michael Bukrinsky • *Department of Microbiology, Immunology and Tropical Medicine, George Washington University School of Medicine and Health Sciences, Washington, DC, USA*

John C. Burnett • *Department of Molecular and Cellular Biology, Beckman Research Institute of City of Hope, Duarte, CA, USA; Irell & Manella Graduate School of Biological Sciences, Beckman Research Institute of City of Hope, Duarte, CA, USA*

Paige Charlins • *Department of Microbiology, Immunology and Pathology, Colorado State University, Fort Collins, CO, USA*

Benjamin K. Chen • *Division of Infectious Diseases, Department of Medicine and Immunology Institute, Icahn School of Medicine at Mt. Sinai, New York, NY, USA*

Christophe Chopard • *CPBS, UMR 5236 CNRS, University of Montpellier, Montpellier Cedex 05, France*

Pawel Ciborowski • *Department of Pharmacology and Experimental Neuroscience, University of Nebraska Medical Center, Omaha, NE, USA*

Christine L. Clouser • *Institute for Molecular Virology, University of Minnesota, Minneapolis, MN, USA; Department of Diagnostic and Biological Sciences, School of Dentistry, University of Minnesota, Minneapolis, MN, USA*

Christina Darwish • *Department of Microbiology, Immunology and Tropical Medicine, George Washington University School of Medicine and Health Sciences, Washington, DC, USA*

Solène Debaisieux • *CPBS, UMR 5236 CNRS, University of Montpellier, Montpellier Cedex 05, France*
Felipe Diaz-Griffero • *Department of Microbiology and Immunology, Albert Einstein College of Medicine Bronx, Bronx, NY, USA*
Natasha D. Durham • *Division of Infectious Diseases, Department of Medicine and Immunology Institute, Icahn School of Medicine at Mt. Sinai, New York, NY, USA*
Eliseo A. Eugenin • *Public Health Research Institute (PHRI), Rutgers University, Newark, NJ, USA; Departments of Microbiology and Molecular Genetics, Rutgers University, Newark, NJ, USA*
Howard S. Fox • *Department of Pharmacology and Experimental Neuroscience, University of Nebraska Medical Center, Omaha, NE, USA*
Thomas Fricke • *Department of Microbiology and Immunology, Albert Einstein College of Medicine Bronx, Bronx, NY, USA*
Harris Goldstein • *Departments of Microbiology & Immunology, Albert Einstein College of Medicine, Bronx, NY, USA; Departments of Pediatrics, Albert Einstein College of Medicine, Bronx, NY, USA*
Stuart F.J. Le Grice • *Reverse Transcriptase Biochemistry Section, HIV Drug Resistance Program, Frederick National Laboratory for Cancer Research, Frederick, MD, USA*
Nicole A. Haverland • *Department of Pharmacology and Experimental Neuroscience, University of Nebraska Medical Center, Omaha, NE, USA*
Joseph A. Hollenbaugh • *Center for Drug Discovery, Emory Center for AIDS Research, Laboratory of Biochemical Pharmacology, Department of Pediatrics, Emory University School of Medicine, Atlanta, GA, USA*
Thomas J. Hope • *Department of Cell and Molecular Biology, Feinberg School of Medicine, Northwestern University, Chicago, IL, USA*
Tory P. Johnson • *Section of Infections of the Nervous System, National Institute of Neurological Diseases and Stroke, National Institutes of Health, Bethesda, MD, USA*
Ulrike Jung • *Department of Molecular and Cellular Biology, Beckman Research Institute of City of Hope, Duarte, CA, USA*
Ganjam V. Kalpana • *Department of Genetics, Albert Einstein College of Medicine, Bronx, NY, USA*
John C. Kappes • *Department of Medicine, University of Alabama at Birmingham, Birmingham, AL, USA; Birmingham Veterans Affairs Medical Center, Research Service, Birmingham, AL, USA*
Jacques J. Kessl • *Center for Retrovirus Research and Comprehensive Cancer Center, College of Pharmacy, Ohio State University, Columbus, OH, USA*
Baek Kim • *Center for Drug Discovery, Emory Center for AIDS Research, Laboratory of Biochemical Pharmacology, Department of Pediatrics, Emory University School of Medicine, Atlanta, GA, USA; College of Pharmacy, Kyung-Hee University, Seoul, South Korea*
Sebla B. Kutluay • *Laboratory of Retrovirology, Aaron Diamond AIDS Research Center, The Rockefeller University, New York, NY, USA; Department of Molecular Microbiology, Washington University School of Medicine, St. Louis, MO, USA*
Mamuka Kvaratskhelia • *Center for Retrovirus Research and Comprehensive Cancer Center, College of Pharmacy, Ohio State University, Columbus, OH, USA*
Jun Lai • *Department of Medicine, Johns Hopkins University School of Medicine, Baltimore, MD, USA*

Gregory M. Laird • *Department of Medicine, Johns Hopkins University School of Medicine, Baltimore, MD, USA*
Benhur Lee • *Department of Microbiology, Icahn School of Medicine at Mount Sinai, New York, NY, USA*
Ming Li • *Laboratory of Retrovirology, Division of Infectious Diseases, Department of Medicine, The Warren Alpert Medical School of Brown University, Providence, RI, USA*
Sabrina Lusvarghi • *Laboratory of Bioorganic Chemistry, National Institute of Diabetes, and Digestive and Kidney Diseases, National Institutes of Health, Bethesda, MD, USA*
João I. Mamede • *Department of Cell and Molecular Biology, Feinberg School of Medicine, Northwestern University, Chicago, IL, USA*
Louis M. Mansky • *Institute for Molecular Virology, University of Minnesota, Minneapolis, MN, USA; Department of Diagnostic and Biological Sciences, School of Dentistry, University of Minnesota, Minneapolis, MN, USA; Molecular, Cellular, Developmental Biology & Genetics Graduate Program, University of Minnesota, Minneapolis, MN, USA; Department of Microbiology, University of Minnesota, Minneapolis, MN, USA*
Thorsten R. Mempel • *Center for Immunology and Inflammatory Diseases, Division of Rheumatology, Allergy and Immunology, Massachusetts General Hospital, Harvard Medical School, Boston, MA, USA*
Nigora Mukhamedova • *Baker IDI Heart and Diabetes Institute, Melbourne, VIC, Australia*
Thomas T. Murooka • *Departments of Immunology and Medical Microbiology, University of Manitoba, Winnipeg, MB, Canada*
Avindra Nath • *Section of Infections of the Nervous System, National Institute of Neurological Diseases and Stroke, National Institutes of Health, Bethesda, MD, USA*
Christina Ochsenbauer • *Department of Medicine, University of Alabama at Birmingham, Birmingham, Al, USA*
Akira Ono • *Department of Microbiology and Immunology, University of Michigan Medical School, Ann Arbor, MI, USA*
Anastas Popratiloff • *Office of VP for Research, George Washington University Center for Microscopy and Image Analysis, Washington, DC, USA*
Annalena La Porte • *Department of Genetics, Albert Einstein College of Medicine, Bronx, NY, USA*
Vinayaka R. Prasad • *Department of Microbiology and Immunology, Albert Einstein College of Medicine, Bronx, NY, USA*
Bharat Ramratnam • *Laboratory of Retrovirology, Division of Infectious Diseases, Department of Medicine, The Warren Alpert Medical School of Brown University, Providence, RI, USA*
Vasudev R. Rao • *Department of Microbiology and Immunology, Albert Einstein College of Medicine, Bronx, NY, USA*
Jason W. Rausch • *Reverse Transcriptase Biochemistry Section, HIV Drug Resistance Program, Frederick National Laboratory for Cancer Research, Frederick, MD, USA*
Jonathan M.O. Rawson • *Institute for Molecular Virology, University of Minnesota, Minneapolis, MN, USA; Molecular, Cellular, Developmental Biology & Genetics Graduate Program, University of Minnesota, Minneapolis, MN, USA*
Fabienne Rayne • *CPBS, UMR 5236 CNRS, University of Montpellier, Montpellier Cedex 05, France*
Daniel I.S. Rosenbloom • *Department of Biomedical Informatics, Columbia University Medical Center, New York, NY, USA*

John J. Rossi • *Department of Molecular and Cellular Biology, Beckman Research Institute of City of Hope, Duarte, CA, USA; Irell & Manella Graduate School of Biological Sciences, Beckman Research Institute of City of Hope, Duarte, CA, USA*
Arthur P. Ruiz • *Department of Microbiology and Immunology, Albert Einstein College of Medicine, Bronx, NY, USA*
Kieran Seay • *Department of Microbiology and Immunology, Albert Einstein College of Medicine, Bronx, NY, USA*
Radwa Sharaf • *Center for Immunology and Inflammatory Diseases, Division of Rheumatology, Allergy and Immunology,, Massachusetts General Hospital, Harvard Medical School, Boston, MA, USA*
Amit Sharma • *Center for Retrovirus Research and Comprehensive Cancer Center, College of Pharmacy, Ohio State University, Columbus, OH, USA; Human Biology Division, Fred Hutchinson Cancer Research Center, Seattle, WA, USA*
Janet D. Siliciano • *Department of Medicine, Johns Hopkins University School of Medicine, Baltimore, MD, USA*
Robert F. Siliciano • *Department of Medicine, Johns Hopkins University School of Medicine, Baltimore, MD, USA; Howard Hughes Medical Institute, Baltimore, MD, USA*
Deepali Singh • *Department of Veterinary Biosciences, The Ohio State University, Columbus, OH, USA; Center for Retrovirus Research, The Ohio State University, Columbus, OH, USA; Center for RNA Biology, The Ohio State University, Columbus, OH, USA*
Gatikrushna Singh • *Department of Veterinary Biosciences, The Ohio State University, Columbus, OH, USA; Center for Retrovirus Research, The Ohio State University, Columbus, OH, USA; Center for RNA Biology, The Ohio State University, Columbus, OH, USA*
Dmitri Sviridov • *Baker IDI Heart and Diabetes Institute, Melbourne, VIC, Australia*
Joanna Sztuba-Solinska • *Reverse Transcriptase Biochemistry Section, HIV Drug Resistance Program, Frederick National Laboratory for Cancer Research, Frederick, MD, USA*
Mayumi Takahashi • *Department of Molecular and Cellular Biology, Beckman Research Institute of City of Hope, Duarte, CA, USA*
Tynisha Thomas • *Department of Microbiology and Immunology, Albert Einstein College of Medicine, Bronx, NY, USA*
Gabrielle C. Todd • *Department of Microbiology and Immunology, University of Michigan Medical School, Ann Arbor, MI, USA*
Petra Tryoen-Toth • *Institut des Neurosciences Cellulaires et Intégratives, CNRS UPR3212, University of Strasbourg, Strasbourg, France*
Annie Tu • *Institut des Neurosciences Cellulaires et Intégratives, CNRS UPR3212, University of Strasbourg, Strasbourg, France*
Milena Veselinovic • *Department of Microbiology, Immunology and Pathology, Colorado State University, Fort Collins, CO, USA*
Lance M. Villeneuve • *Department of Pharmacology and Experimental Neuroscience, University of Nebraska Medical Center, Omaha, NE, USA*
Nicholas E. Webb • *Department of Microbiology, Immunology, and Molecular Genetics, University of California, Los Angeles, CA, USA*
Cong Zhang • *Department of Microbiology and Immunology, Albert Einstein College of Medicine, Bronx, NY, USA*
Jian Hua Zheng • *Department of Microbiology and Immunology, Albert Einstein College of Medicine, Bronx, NY, USA*

Part I

HIV-1 Replication—Early Events

Chapter 1

Quantifying CD4/CCR5 Usage Efficiency of HIV-1 Env Using the Affinofile System

Nicholas E. Webb and Benhur Lee

Abstract

Entry of HIV-1 into target cells involves the interaction of the HIV envelope (Env) with both a primary receptor (CD4) and a coreceptor (CXCR4 or CCR5). The relative efficiency with which a particular Env uses these receptors is a major component of cellular tropism in the context of entry and is related to a variety of pathological Env phenotypes (Chikere et al. Virology 435:81–91, 2013). The protocols outlined in this chapter describe the use of the Affinofile system, a 293-based dual-inducible cell line that expresses up to 25 distinct combinations of CD4 and CCR5, as well as the associated Viral Entry Receptor Sensitivity Assay (VERSA) metrics used to summarize the CD4/CCR5-dependent infectivity results. This system allows for high-resolution profiling of CD4 and CCR5 usage efficiency in the context of unique viral phenotypes.

Key words Affinofile, Virus entry, CD4, CCR5, Receptor usage efficiency, Env, Entry efficiency, HIV

1 Introduction

HIV-1 entry is driven by the envelope glycoproteins gp120 and gp41 (Env). Fusion between the viral and cellular membrane is driven by a multistage, concerted mechanism that first requires binding of gp120 to cell-surface CD4. This engagement triggers conformational changes in gp120 that expose a coreceptor binding region, which subsequently binds to one of two chemokine coreceptors: CCR5 (R5) or CXCR4 (X4). Coreceptor interactions trigger the release of a fusion peptide in gp41, which induces membrane fusion, ultimately leading to infection.

While HIV Envs can be classified as either R5, X4, or dual R5/X4 tropic based on the coreceptor recognized [1], coreceptor tropism alone does not predict target-cell tropism or pathology. For example, although macrophages express higher levels of CCR5 than CD4+ T cells, many R5-tropic viruses can infect CD4+ T cells but not macrophages. The majority of transmitted HIV-1 Env's are exclusively R5-tropic [2–4], which persist throughout the course

Vinayaka R. Prasad and Ganjam V. Kalpana (eds.), *HIV Protocols*, Methods in Molecular Biology, vol. 1354,
DOI 10.1007/978-1-4939-3046-3_1,

of infection to the onset of clinical AIDS, where nearly half of all subtype B infections evolve X4-tropism [5–7]. However, X4-tropism is not a requirement of advanced disease as R5 Env's are also associated with disease progression, T-cell depletion, and clinical AIDS [8, 9]. Indeed, the relative efficiency of CCR5 usage among certain Env's has been linked to transmission [10, 11], macrophage tropism [12–14], and neurovirulence [12, 15–17], underscoring the importance of CD4 and CCR5 usage efficiency in pathological contexts.

Prior studies of CD4 and CCR5 usage efficiency commonly evaluate infection on multiple cell lines expressing distinct and homogenous CD4/CCR5 surface densities [18–20], which, although informative, offers a limited resolution of CD4 and CCR5 expression combinations. Additionally, differences in postentry infection susceptibility and viral gene expression can confound interpretations of entry efficiency. We describe the Affinofile system [21], a 293-derived CD4/CCR5 dual-inducible cell line, and the associated Viral Entry Receptor Sensitivity Assay (VERSA) metrics used to assess CD4 and CCR5 usage efficiency in an interdependent context on a single clonal cell line.

Affinofile cells express CD4 through the tet-on system where, in the presence of tetracycline, inhibition of CD4 expression by the tet transactivator is released providing concentration-dependent expression of CD4. CCR5 is expressed through the ecdysone system where ponasterone A promotes dimerization of constitutively expressed VgEcr and RXR nuclear receptor proteins, which drives CCR5 expression in a concentration-dependent manner. A schematic of this inducible system is shown in Fig. 1, and more detail regarding the mechanisms of induction can be found in the literature [21, 22]. Affinofile cells can be induced to generate up to 25 distinct combinations of CD4 and CCR5 (as measured by CD4/CCR5 antibody epitopes per cell), recapitulating a wide, biologically relevant range of receptor/coreceptor surface densities [13]. CD4 expression generally ranges between 2000 and 150,000 CD4 antibody biding sites per cell (ABS/cell) and CCR5 expression ranges between 1500 and 25,000 ABS/cell. These induction matrices are then infected to profile viral infectivity across the entire range of combined CD4 and CCR5 expression levels. This profile is distilled by the VERSA algorithm into three metrics that describe the overall infectivity of an Env (mean induction, M), the stoichiometric contribution of CD4 and CCR5 to infectivity (angle, θ), and the responsiveness of an Env to the most efficient combination of CD4 and CCR5 expression (amplitude, Δ). These three parameters have been used to identify specific mechanisms of entry inhibitor resistance [23–28], target-cell tropism [12–14, 29], and transmission [10, 11] in terms of an Env's response to changing levels of CD4 and CCR5 expression on Affinofile cells.

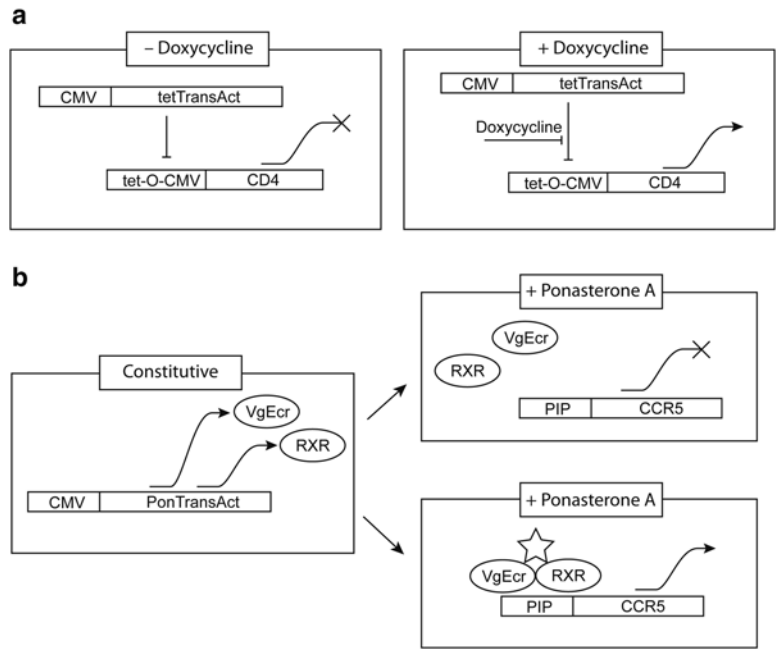

Fig. 1 Schematic of the Affinofile system. (**a**) The Tet-On system drives CD4 expression where tetracycline prevents the tet transactivator from repressing CD4 expression in a dose-dependent fashion. (**b**) CCR5 expression is driven by the ecdysone-inducible system. Ponasterone A (*star*) induces dimerization of the constitutively expressed insect nuclear hormone receptor subunits (VgEcR and RXR, represented as PonTransAct) forming VgRXR, which binds the ponasterone inducible promoter, driving expression of CCR5 in a manner dependent on ponasterone A concentration.

A more in-depth description of these metrics and how they have been applied to specific Env phenotypes is reviewed in [22].

The protocols provided in this chapter are intended as a guide for using the Affinofile system and interpreting the results in any context and, thus, are not specific for analyzing a particular Env phenotype. The experiments described can be easily adjusted to fit specific research needs so long as the fundamental requirements and core concepts discussed are satisfied. The first procedure quantifies CD4 and CCR5 expression in terms of induction with doxycycline and ponasterone A, respectively, to calibrate this system and determine the range of induction to be used in further experiments (Subheading 3.1). We then describe the preparation and infection of an Affinofile matrix composed of 25 distinct CD4/CCR5 expression levels (Subheading 3.2). This chapter then closes with an in-depth discussion of the fundamental meaning and derivation of each VERSA metric to provide users with a strong foundation from which to interpret relative differences in CD4 and CCR5 usage efficiency in a wide range of contexts (Subheading 3.3).

2 Materials

2.1 Cell Culture

1. Affinofile media: Dulbecco's Modified Eagle Medium (DMEM) supplemented with 10 % dialyzed fetal bovine serum (*see* **Note 1**) with 50 μg/mL Blasticidin S HCl.
2. Affinofiles are normally cultured in 10 cm culture dishes and split every 2–3 days at 1/5× for no more than 35 passages.

2.2 Induction, Staining, and Quantification

1. One 24-well plate.
2. Doxycycline hyclate (10 μM in sterile water). Store in 50–100 μL aliquots at −20 °C.
3. Ponasterone A resuspended and stored according to manufacturer's instructions.
4. PE quantification beads. These are used to quantify expression of CCR5 by correlating the geometric mean fluorescence of a variety of bead populations with distinct fluorophore-per-bead quantities to the fluorescence of stained Affinofiles. We routinely use QuantiBrite PE beads.
5. APC quantification beads. These are used to quantify expression of CD4 by correlating the geometric mean fluorescence of a variety of bead populations with distinct fluorophore-per-bead quantities to the fluorescence of stained Affinofiles. We routinely use Quantum™ APC MESF beads.
6. APC mouse antihuman CD4 (Clone RPA-T4) and appropriate isotype (APC isotype for CD4 antibody).
7. PE mouse antihuman CCR5 (Clone 2D7) and appropriate isotype (PE isotype for CCR5 antibody).
8. FACS buffer: 2 % FBS in DPBS.
9. FACS buffer supplemented with 5 mM EDTA.
10. CD4 staining solution: 1/2× APC mouse antihuman CD4 in FACS buffer.
11. CCR5 staining solution: 1/2× PE mouse antihuman CCR5 in FACS buffer.
12. CD4 isotype staining solution: 1/2× APC mouse IgG1κ isotype in FACS buffer.
13. CCR5 isotype staining solution: 1/2× PE mouse IgG2aκ isotype.
14. Paraformaldehyde (2 %).
15. Flow cytometer with APC (635 nm excitation/660–668 emission) and PE (488 nm excitation/575–566 nm emission) channels.

2.3 Infection

1. Two 24-well plates.
2. Doxycycline hyclate (10 μM in sterile water). Store in 50–100 μL aliquots at −20 °C.
3. Ponasterone A (powder) resuspended and stored according to manufacturer's instructions.
4. Pseudotyped HIV reporter virus (5×10^5 IU minimum per matrix to achieve an MOI of 0.2). Affinofiles express low, basal levels of CXCR4 and can be infected by both R5- and X4-tropic envelopes. Only R5-tropic envelopes will respond to different levels of CCR5 induction. The particular envelope chosen should be relevant to one's specific research purposes.
5. Relevant pseudotype reporter detection reagents.

3 Methods

3.1 Quantitative Determination of CD4 and CCR5 Induction

The induction range of each thawed batch of Affinofiles must be determined before use. This protocol uses a minimized sample set whereby CD4 and CCR5 are measured simultaneously across a range of combined doxycycline and ponasterone A serial dilutions. Figure 2 shows the sample set and plate map for this protocol, where each induction dilution is indicated by samples *1–8* and *U1* and *U2* (uninduced), and isotype controls are indicated by samples *A–D* and cytometer voltage adjustment samples *E–H*. This sample set is intended to provide excess controls for cytometer voltage adjustments. CD4 and CCR5 are measured simultaneously using APC-labeled CD4 antibody (clone RPA-T4) and PE-labeled CCR5 antibody (clone 2D7) such that no fluorescence

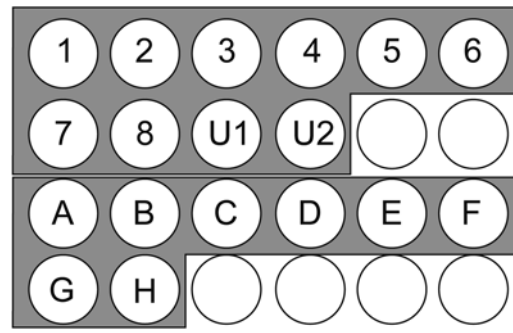

Fig. 2 Plate map for quantitative determination of CD4/CCR5 expression. Samples 1–8 are concomitant serial dilutions of doxycycline and ponasterone A with samples U1 and U2 remaining uninduced. Samples A–B and C–D are duplicate CD4/CCR5 isotype staining controls, respectively, while samples E–F are induced for maximum CD4/CCR5 expression for cytometer voltage adjustment. Samples G and H are uninduced Affinofiles used for live cell gating and FSC/SSC voltage calibration.

compensation is necessary. This protocol can be adjusted for single color analysis of both CD4 and CCR5 by doubling the sample set and staining each replicate with CD4 or CCR5 antibodies. Refer to Subheading 3.1.3 for a more thorough description of the CD4/CCR5 antibodies used.

3.1.1 Induction and Staining

1. Seed one 24-well plate with Affinofiles at a minimum density of 1×10^5 cells/well (*see* Fig. 2) using Affinofile media (*see* **Note 2**).
2. Incubate at 37 °C (5 % CO_2) until the cells have adhered and wells have reached 70–80 % confluency.
3. Prepare 100 μL maximum induction solution with 78 ng/mL doxycycline and 52 μM ponasterone A (*see* **Note 3**).
4. Prepare seven 0.5× serial dilutions of the maximum induction solution by serial diluting 30 μL maximum induction solution through seven additional tubes containing 30 μL Affinofile media.
5. Add 20 μL of the appropriate induction dilution to wells *1–8* (Fig. 2).
6. Add 20 μL of the maximum induction solution to wells *E–F* (Fig. 2).
7. Add 20 μL Affinofile media to wells *U* and *A–D* (Fig. 2).
8. Swish plate left-right and up-down gently to mix.
9. Incubate at 37 °C (5 % CO_2) for 16–20 h.
10. Prepare labeled FACS tubes with 2 mL FACS buffer each, one tube for each well in Fig. 2.
11. Aspirate media from each well and replace with FACS buffer supplemented with 5 mM EDTA.
12. Incubate for 2–5 min at room temperature and visually confirm cell detachment.
13. Transfer cells to appropriate FACS tubes using a minimum 700 μL of FACS buffer from the destination FACS tube to wash the well surface.
14. Pellet cells at $300 \times g$ for 5 min at 4 °C.
15. Decant supernatant and break up pellet by vortexing gently.
16. Add 2 mL FACS buffer without EDTA and pellet cells at $300 \times g$ for 5 min at 4 °C.
17. Decant supernatant and break up pellet by vortexing gently.
18. Add 2 μL CD4 staining solution to tubes *1–8*, *U1* and *U2*, and *E* and *F*. Vortex immediately after addition.
19. Add 2 μL CCR5 staining solution to tubes *1–8*, *U1* and *U2*, and *E* and *F*. Vortex immediately after addition.

20. Add 2 μL CD4 isotype staining solution to tubes *A* and *B* and 2 μL CCR5 isotype staining solution to tubes *C* and *D*. Vortex immediately after addition.
21. Incubate at 4 °C in the dark for 60 min.
22. Add 2 mL FACS buffer to each tube.
23. Pellet cells at 300 × *g* for 5 min at 4 °C.
24. Decant supernatant and break up pellet by vortexing gently.
25. Resuspend cells in 200 μL paraformaldehyde (2 %) and vortex gently to mix.
26. Store at 4 °C in the dark until samples can be analyzed using flow cytometry.

3.1.2 Flow Cytometry Analysis

Quantitative PE and APC beads are analyzed concurrently with the Affinofile samples described in Subheading 3.1.1. These should be prepared according to the manufacturer's specification.

Samples *G*, *H* are intended for FSC/SSC voltage adjustment and live cell gating while samples *A*, *B* and *C*, *D* are CD4 and CCR5 isotype controls, respectively. One replicate of these sets is intended for fluorescence voltage adjustment (it is also recommended that PE and APC voltage should consider the fluorescence of PE and APC quantitative bead populations) while the other will be recorded as an isotype background for subtraction. Samples *E* and *F* are replicates of sample *1* (max CD4/CCR5 induction) for fluorescence channel voltage adjustment. Figure 3a shows a sample FSC/SSC plot with a live cell gate. Once the cytometer voltage is adjusted appropriately, a minimum of 5×10^4 live cell events should be recorded from samples *1–8*, *U1* and *U2* (induced and uninduced samples), one of *A* or *B* (CD4 isotype control), and one of *C* or *D* (CCR5 isotype control). Once these samples are recorded, the quantitative PE and APC bead samples should be recorded after adjusting FSC/SSC voltage appropriately. Fluorescence channel voltage should not be adjusted to ensure that the bead fluorescence is representative of the fluorescence observed on Affinofile cells.

Quantitative calibration of APC and PE fluorescence is determined by comparing the geometric mean fluorescence of each bead population with the manufacturer-indicated APC/PE molecules per bead. Figure 3b, d shows calibration curves for both the Quantum™ APC MESF (Fig. 3b) and QuantiBrite PE beads (Fig. 3d), respectively. Follow the manufacturer's instructions for converting the geometric mean fluorescence of each bead population to fluorophore molecules. This calibration is then applied to the isotype-subtracted geometric mean fluorescence of each Affinofile induction sample (*1–8*, *U1* and *U2*) to calculate fluorophore molecules per cell, which is directly equal to antibody binding sites per cell (Fig. 3c, e).

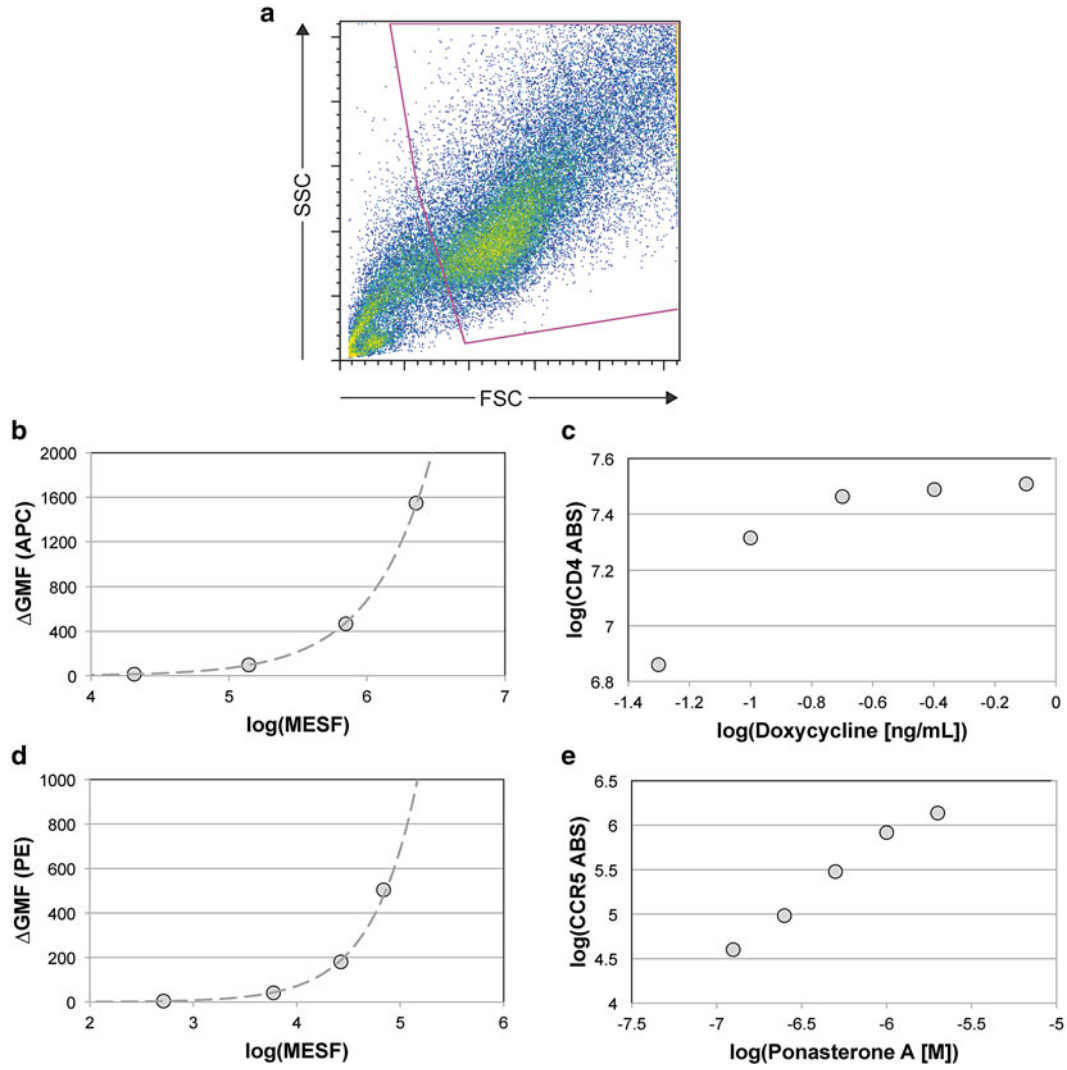

Fig. 3 Quantifying CD4 and CCR5 antibody binding sites per cell. Geometric mean fluorescences for PE (CCR5) and APC (CD4) are calculated from live cells (**a**). Quantitative APC and PE beads are used to correlate geometric mean fluorescence to fluorophore molecules per bead (**b**, **d**). These calibration curves are then used to calculate antibody binding sites per cell for each induced Affinofile sample (**c**, **e**).

Induction ranges for all future experiments involving this particular batch of Affinofiles may be determined from these induction-response curves. The quantity of antibody binding sites, once determined for an individual thaw of Affinofiles, does not change significantly until late passages (>25–30).

3.1.3 Antibody Usage

We refer the reader to our recent review [22] and references therein for the CD4 and CCR5 monoclonal antibodies (MAbs) used. Many anti-CD4 MAbs that bind to the D1–D2 domain of CD4 with low (single digit) nanomolar Kd and compete well for gp120

binding (e.g., clone RPA-T4 and Q4120) can be used for quantifying CD4 ABS/cell on Affinofiles. However, CCR5 is conformationally heterogeneous and some epitopes recognized by commercially available anti-CCR5 MAbs might not coincide with those necessary for productive gp120-CCR5 interactions [30]. The 2D7 anti-CCR5 Mab is most often used for quantifying CCR5 for HIV entry studies and has been used in almost all Affinofile studies to date. Although some CCR5 MAbs such as PA14 may recognize an even larger spectrum of relevant CCR5 conformations [30]. For historical consistency and comparison purposes, we recommend that 2D7 be used for quantifying CCR5 ABS/cell on Affinofiles.

3.2 Induction Matrix and Infection

This protocol describes infection of a 5×5 induction matrix containing 25 distinct combinations of CD4 and CCR5 expression in a 24-well format (Fig. 4). Doxycycline and ponasterone A concentrations for this matrix should be determined from the quantitative induction responses described in Subheading 3.1. Preparation

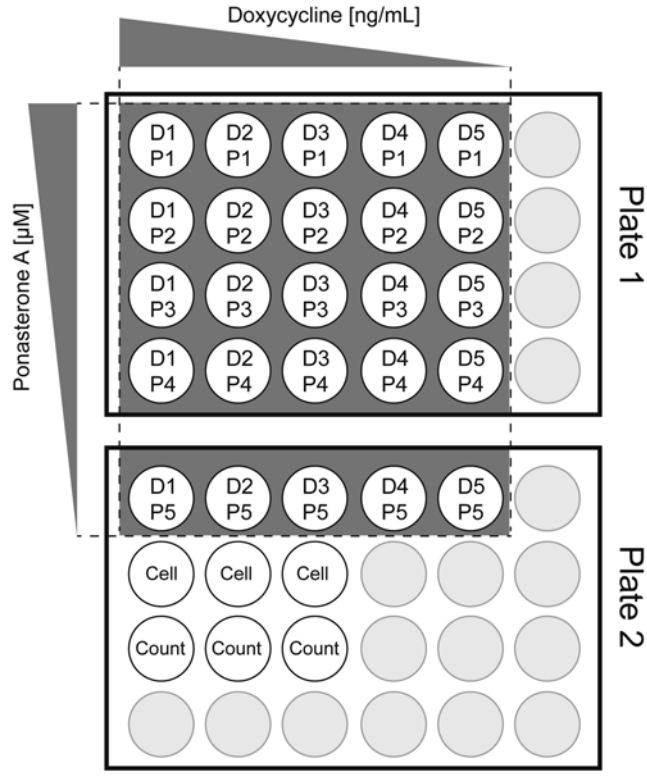

Fig. 4 Infection matrix plate map. This matrix consists of five doxycycline (D1–D5, high to low) and five ponasterone A (P1–P5, high to low) inductions. Uninfected cell samples are included for reporter background measurement [27], and additional cell counting wells (Count) are included for proper MOI determination.

of induction solutions is greatly simplified when serial dilution can be used, although this is not required. The induction matrix is infected with reporter-pseudotyped HIV virus. We recommend infecting at an MOI of 0.2 (*see* **Note 4**) as determined on Ghost R5 cells which express saturating levels of CD4 and CCR5 [31].

1. Seed two 24-well plates with 8×10^4 cells/well in Affinofile media (*see* **Note 5**).
2. Incubate at 37 °C (5 % CO_2) until the cells have adhered and reached 50–60 % confluence.
3. Prepare five doxycycline induction solutions at 52× the final desired concentration, with the fifth solution containing no doxycycline. Each solution should have a minimum, final volume of 60 μL.
4. Prepare five ponasterone A induction solutions at 52× the final desired concentration, with the fifth solution containing no ponasterone A. Each solution should have a minimum, final volume of 60 μL.
5. Add 10 μL of each doxycycline dilution to appropriate wells (*see* Fig. 4) and swish plate left-right and up-down gently to mix.
6. Add 10 μL of each ponasterone A dilution to appropriate wells (*see* Fig. 4) and swish plate left-right and up-down gently to mix.
7. Incubate 16–20 h at 37 °C (5 % CO_2).
8. Trypsinize and count the three *Count* wells (*see* **Note 6**).
9. Remove media from *Cell* wells (Fig. 4) and replace with the same media used to dilute viral stock.
10. Remove media from all induction wells and add viral inoculant at an MOI of 0.2 to each well (*see* **Note 7**).
11. Centrifuge plates at $700 \times g$ for 2 h at 37 °C.
12. Remove inoculant/media from all wells and replace with fresh Affinofile media.
13. Incubate at 37 °C (5 % CO_2) to allow reporter expression (typically 48–72 h).
14. Measure the reporter signal from each of the induction wells and subtract reporter signal from the background signal obtained from the three *Cell* wells.

3.2.1 VERSA Metric Processing

Using the ABS calibration curve determined in Subheading 3.1, determine the CD4 and CCR5 ABS quantities for each doxycycline and ponasterone A concentration used in the induction matrix (Subheading 3.2). The VERSA algorithm accepts single header (Fig. 5a) and double header (Fig. 5b) formats. The single

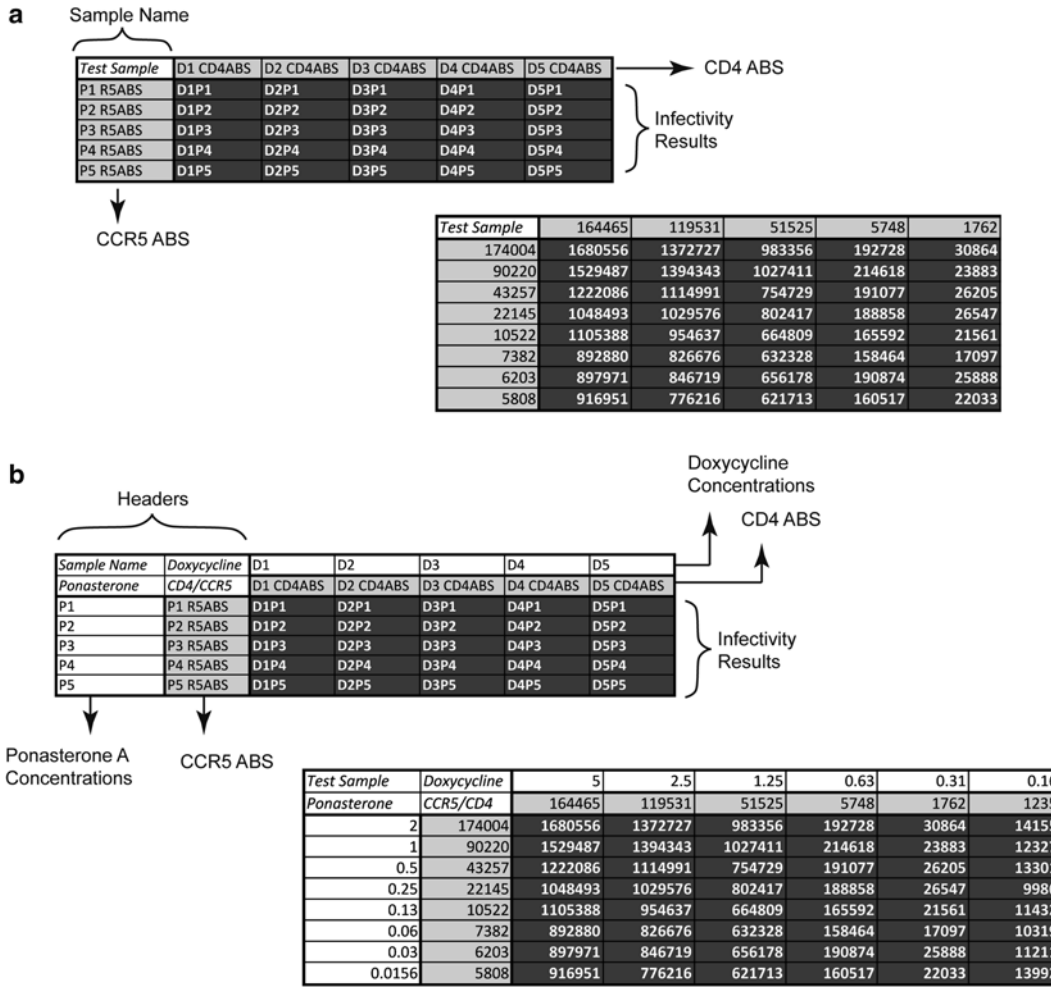

Fig. 5 VERSA format. VERSA includes a single header format (**a**) that associates antibody binding sites to infectivity reporter values and a double header format (**b**) that includes doxycycline and ponasterone A concentrations. Example formats are shown below format descriptions using background-subtracted reporter signals.

header format correlates CD4/CCR5 ABS to infectivity directly while the double header format includes additional fields for doxycycline and ponasterone A concentrations associated with each CD4/CCR5 ABS value. Example single and double header formats are shown to the lower left of each format description (Fig. 5a, b, respectively). The infectivity itself may be reported as either background-subtracted reporter signal values or normalized infection (*see* **Note 8**).

The following formatting criteria must be met for VERSA analysis:

1. The data must be converted to CSV format.
2. The first (or only) matrix data set must start at the first row of the CSV file.

These are the Angle, Magnitude and Mean Induction values for each datasets

Strain	Vector Angle	Vector Magnitude	Mean Induction
Matrix 1	13.21	0.76	0.28
Matrix 2	12.59	0.75	0.32
Matrix 3	13.95	0.79	0.35
Matrix 4	13.26	0.77	0.32

These are the fitting polynomials for each datasets.

The polynomials are of the form: $F(X,Y)=a_0 + a_1X + a_2Y + a_3XY + a_4X^2 + a_5Y^2$.

Strain	a_0	a_1	a_2	a_3	a_4	a_5
Matrix 1	0.02	0.06	-0.09	0.43	0.47	0.05
Matrix 2	0.03	0.21	-0.05	0.39	0.33	0.02
Matrix 3	0.00	0.54	-0.12	0.47	-0.01	0.08
Matrix 4	0.02	0.27	-0.09	0.43	0.26	0.05

Fig. 6 VERSA output. VERSA metrics (vector angle, vector amplitude, and mean induction) are reported for each matrix in this 4-matrix data set, along with the polynomial fitting parameters (a0–a5) used to construct the surface (*boxed rectangle*). It is not necessary for the user to know the values of these fitting parameters in order to understand the biological meaning of the VERSA metrics.

3. Multiple matrices may be included in the same file so long as they are separated by a single empty row and have the same number of headers (*see* **Note 9**).

Open the VERSA website – http://versa.biomath.ucla.edu/ – in any browser and click on *DATA ANALYSIS* (upper left hand menu). Select the number of headers and indicate the total number of data sets (matrices) included in the file. Select *Choose File* and locate the appropriate csv file, and then click on *Process File* to begin calculation.

Figure 6 shows a sample of the VERSA output that includes the VERSA metric summary (mean induction M, angle θ, and vector amplitude Δ) and $F(x,y)$ polynomial fitting parameters (a0–a5). While the metrics summarize each matrix in terms of overall infectivity and CD4/CCR5 usage efficiency, the fitting parameters can be used to reconstruct the surface fit $F(x,y)$.

3.3 Analysis of VERSA Metrics

VERSA metrics are derived by fitting an Env's infectivity profile to a second-order polynomial surface function $F(x,y)$ (Fig. 7a). The mean infectivity across the entire surface (M) describes the overall infectivity of the Env throughout all levels of CD4 and CCR5 expression (Fig. 7b). The gradient of $F(x,y)$ (S) is defined by a vector anchored at the lowest CD4/CCR5 expression level that points in the direction of the steepest path along the surface (Fig. 7c). This sensitivity vector (S) is composed of an amplitude of responsiveness

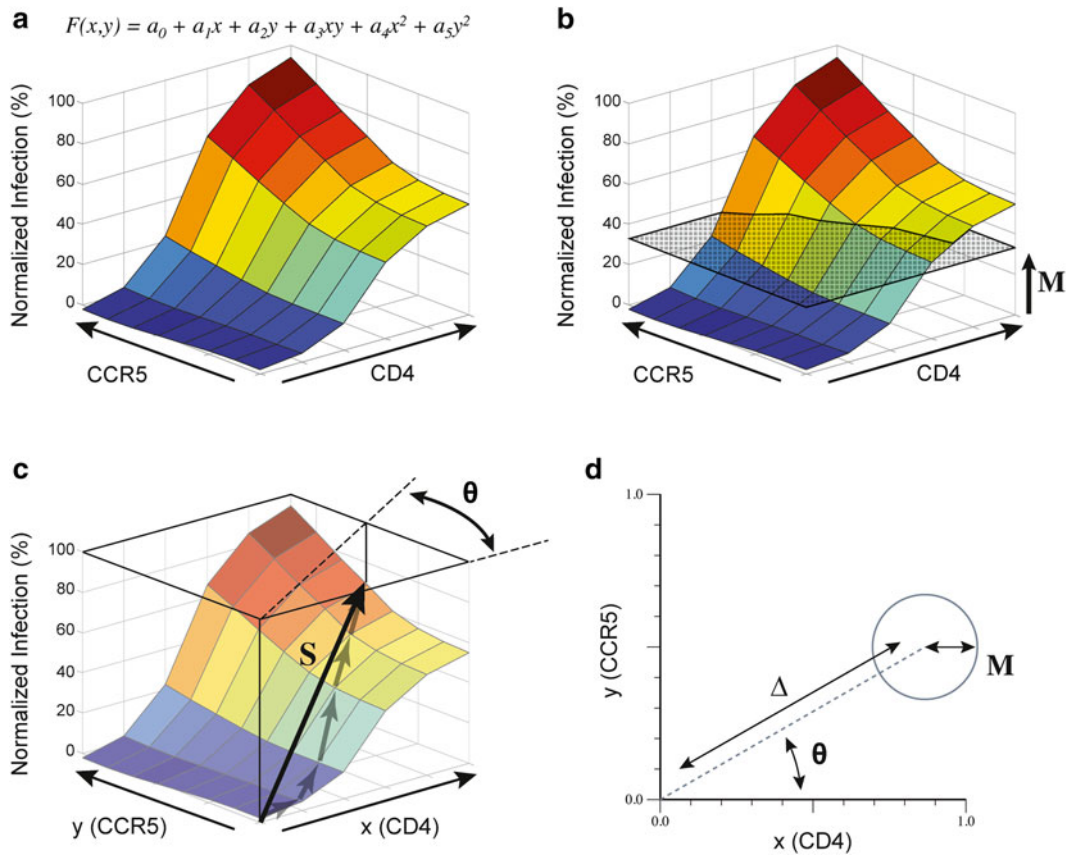

Fig. 7 VERSA metrics. The VERSA metrics θ, Δ, and M are calculated by fitting the surface function $f(x,y)$ (**a**) to infectivity data across all combined CD4/CCR5 expression levels. Mean infectivity (M) is the mean infectivity observed across the entire surface (**b**). A sensitivity vector ($\vec{S}$) is fit to the gradient of $f(x,y)$ (**c**). The vector is composed of an angle (θ) indicating the direction of greatest infectivity response (in the x,y plane) and the amplitude (Δ) of responsiveness. A polar plot (**d**) summarizes these three metrics where θ is defined as the angle of a line anchored at the origin, Δ is the length of that line, and M is the size of the circle set at the end of the line.

(Δ) to a specific stoichiometric combination of CD4 and CCR5 expression defined as an angle (θ, e.g., the direction of S in the x,y plane). By convention, low angles ($\theta<45°$) indicate that the path of greatest responsiveness is weighted toward CD4, while high angles ($\theta>45°$) indicate a CCR5-weighted responsiveness.

As the mean level of infection observed across the entire surface, M is generally indicative of overall infection efficiency. This is most evident when comparing infection profiles in the absence and presence of entry inhibitors [25, 28].

However, M is inherently bound by the maximum and minimum levels of infection observed. For example, the infectivity profile of YU2 reveals a distinct ability to mediate high levels of infection at low CD4 surface densities compared to JRCSF [12],

which necessarily increases the mean infectivity (by increasing the minimum). The dynamic range and steepness of an infectivity surface has a lesser impact on M, for example, a short and dramatic increase in infectivity that plateaus at low levels of CD4 and CCR5 will naturally increase the mean by weighting more CD4/CCR5 expression levels at high infection. Collectively, these unique effects describe specific mechanistic components of generalized entry efficiency.

The sensitivity vector (S) identifies the path of the greatest increase in infection from the lowest CD4/CCR5 combination, taking into account the curvature of the entire surface (Fig. 7c). S is more easily visualized as the average of a stepwise path of greatest increase in infectivity starting at the lowest CD4/CCR5 level (shadow arrows in Fig. 7c). The sensitivity vector has two components: an amplitude (Δ) that describes the vertical slope and a direction defined by coordinates in the x,y (or CD4/CCR5) plane, which is summarized as an angle (θ). The angle is a balance of the CD4 and CCR5 expression associated with the gradient path and, as such, is interpreted as the most efficient stoichiometric combination of CD4 and CCR5 used by an Env. By convention, θ is defined off of the CD4 axis; thus, Env's that exhibit a stronger responsiveness to changes in CD4 expression will yield a lower angle ($\theta < 45°$), while Env's exhibiting a stronger responsiveness to CCR5 expression will give higher angles ($\theta > 45$). For example, a relative increase in θ that is not associated with significant changes in Δ or M indicates that the Env is more responsive to CCR5 (by comparison).

The amplitude (Δ) quantifies the strength of responsiveness to this most efficient, θ-defined combination of CD4/CCR5. In the simplest context, such as the comparison of two Env's that exhibit no dramatic differences in θ, a higher Δ suggests a greater efficiency of infection in response to the ideal CD4/CCR5 combination and will necessarily be associated with an increase in M.

The metrics themselves can be represented in a polar format (Fig. 7d) that clearly illustrates the functional clustering of Env's. Each infectivity profile is represented as a single point surrounded by a circle with radius M, angled off the x axis (CD4) by θ at a distance Δ. It is important to note that these three metrics (M, Δ, and θ) are derived from a mathematically smoothed surface and describe only the properties of the surface itself. The more intricate details of an Env's response to CD4 and CCR5 expression may not result in significant metric differences due to the fact that the metrics are intended to accommodate the entire surface [32]. Alternative representations of these data can offer additional insight without the need for mathematical fitting, such as 2D profiles or 2D infectivity response plots (published in Fig. 5g, d, e, respectively [32]).

4 Notes

1. Some lots and brands of FBS have residual tetracyclines that may induce CD4 expression. We routinely use dialyzed FBS, Thermo Scientific.
2. The growth rate of Affinofile cells can decrease approximately 50–75 % under induction. A high-density seed or longer preinduction culture is necessary to ensure a minimum of 5×10^4 live cell events during flow cytometry analysis. Some labs routinely seed their Affinofile cells onto polylysine-coated plates to mitigate cell loss. This is appropriate for infectivity experiments (*see* **Note 5**) but is not recommended when the cells are to be used for FACS determination of CD4 and CCR5 expression levels.
3. In this protocol, doxycycline and ponasterone A concentrations are prepared at 26× of the final concentration. Alternatively, the culture media can be entirely replaced with Affinofile media containing the proper doxycycline/ponasterone A concentrations; however, as Affinofiles are weakly adherent, some cell loss may occur.
4. An MOI of 0.2 as determined on Ghost R5 cells (which are highly susceptible to HIV infection due to high expression of both CD4 and CCR5) is the upper limit of the linear range of infection. This MOI is used to, first, ensure that the majority of infected Affinofiles were infected by a single infectious unit and, second, to maximize the dynamic range of infection across the CD4/CCR5 expression matrix.
5. As mentioned in **Note 2**, the growth rate of Affinofiles decreases during induction; it is also slower after infection. The cell seed used for an infection matrix should be informed by both this decreased growth rate and the postinfection culture time required for adequate reporter signal. The cell seed provided is optimized for luciferase reporter pseudotype virus requiring a 48 h postinfection culture period. Longer culture periods will require lower cell seeds to prevent overgrowth. The ultimate goal is to achieve a healthy and adherent cell density on the day of infection that is low enough to prevent overgrowth until infection is measured. Seeding Affinofile cells onto polylysine-coated plates can result in less well-to-well variability, especially when highly passaged Affinofile cells begin to lose their already weak baseline adherence.
6. For the most accurate count, we recommend counting two separate 10 μL volumes from each trypsinized well sample.
7. Viral inoculant should be diluted in the same solution the virus was stored/cultured.

8. Both background-subtracted reporter signal and normalized infection are valid for VERSA processing. When normalizing, the subtracted signals should be normalized to the signal observed at saturating or near-saturating CD4 and CCR5 induction levels. When properly normalized, there is little difference in θ; however, the scale of mean induction (M) and amplitude (Δ) is necessarily dependent on whether the data is normalized or not. A more thorough discussion of normalization can be found in [22]. Normalization is our current standard.
9. Multiple matrices may have different CD4 and CCR5 ABS quantities as each matrix is processed independently.

References

1. Berger EA, Doms RW, Fenyö EM, Korber BT, Littman DR, Moore JP, Sattentau QJ, Schuitemaker H, Sodroski J, Weiss RA (1998) A new classification for HIV-1. Nature 391:240. doi:10.1038/34571
2. Long EM, Rainwater SMJ, Lavreys L, Mandaliya K, Overbaugh J (2002) HIV type 1 variants transmitted to women in Kenya require the CCR5 coreceptor for entry, regardless of the genetic complexity of the infecting virus. AIDS Res Hum Retroviruses 18:567–576. doi:10.1089/088922202753747914
3. Salvatori F, Scarlatti G (2001) HIV type 1 chemokine receptor usage in mother-to-child transmission. AIDS Res Hum Retroviruses 17:925–935. doi:10.1089/088922201750290041
4. van't Wout AB, Kootstra NA, Mulder-Kampinga GA, Albrecht-van Lent N, Scherpbier HJ, Veenstra J, Boer K, Coutinho RA, Miedema F, Schuitemaker H (1994) Macrophage-tropic variants initiate human immunodeficiency virus type 1 infection after sexual, parenteral, and vertical transmission. J Clin Invest 94:2060–2067. doi:10.1172/JCI117560
5. Melby T, Despirito M, Demasi R, Heilek-Snyder G, Greenberg ML, Graham N (2006) HIV-1 coreceptor use in triple-class treatment-experienced patients: baseline prevalence, correlates, and relationship to enfuvirtide response. J Infect Dis 194:238–246. doi:10.1086/504693
6. Moyle GJ, Wildfire A, Mandalia S, Mayer H, Goodrich J, Whitcomb J, Gazzard BG (2005) Epidemiology and predictive factors for chemokine receptor use in HIV-1 infection. J Infect Dis 191:866–872. doi:10.1086/428096
7. Wilkin TJ, Su Z, Kuritzkes DR, Hughes M, Flexner C, Gross R, Coakley E, Greaves W, Godfrey C, Skolnik PR, Timpone J, Rodriguez B, Gulick RM (2007) HIV type 1 chemokine coreceptor use among antiretroviral-experienced patients screened for a clinical trial of a CCR5 inhibitor: AIDS Clinical Trial Group A5211. Clin Infect Dis 44:591–595. doi:10.1086/511035
8. Brown BK, Darden JM, Tovanabutra S, Oblander T, Frost J, Sanders-Buell E, de Souza MS, Birx DL, McCutchan FE, Polonis VR (2005) Biologic and genetic characterization of a panel of 60 human immunodeficiency virus type 1 isolates, representing clades A, B, C, D, CRF01_AE, and CRF02_AG, for the development and assessment of candidate vaccines. J Virol 79:6089–6101. doi:10.1128/JVI.79.10.6089-6101.2005
9. Huang W, Eshleman SH, Toma J, Fransen S, Stawiski E, Paxinos EE, Whitcomb JM, Young AM, Donnell D, Mmiro F, Musoke P, Guay LA, Jackson JB, Parkin NT, Petropoulos CJ (2007) Coreceptor tropism in human immunodeficiency virus type 1 subtype D: high prevalence of CXCR4 tropism and heterogeneous composition of viral populations. J Virol 81:7885–7893. doi:10.1128/JVI.00218-07
10. Ping L-H, Joseph SB, Anderson JA, Abrahams M-R, Salazar-Gonzalez JF, Kincer LP, Treurnicht FK, Arney L, Ojeda S, Zhang M, Keys J, Potter EL, Chu H, Moore P, Salazar MG, Iyer S, Jabara C, Kirchherr J, Mapanje C, Ngandu N, Seoighe C, Hoffman I, Gao F, Tang Y, Labranche C, Lee B, Saville A, Vermeulen M, Fiscus S, Morris L, Karim SA, Haynes BF, Shaw GM, Korber BT, Hahn BH, Cohen MS, Montefiori D, Williamson C, Swanstrom R, CAPRISA Acute Infection

Study and the Center for HIV-AIDS Vaccine Immunology Consortium (2013) Comparison of viral Env proteins from acute and chronic infections with subtype C human immunodeficiency virus type 1 identifies differences in glycosylation and CCR5 utilization and suggests a new strategy for immunogen design. J Virol 87:7218–7233. doi:10.1128/JVI.03577-12

11. Parker ZF, Iyer SS, Wilen CB, Parrish NF, Chikere KC, Lee F-H, Didigu CA, Berro R, Klasse PJ, Lee B, Moore JP, Shaw GM, Hahn BH, Doms RW (2013) Transmitted/founder and chronic HIV-1 envelope proteins are distinguished by differential utilization of CCR5. J Virol 87:2401–2411. doi:10.1128/JVI.02964-12
12. Salimi H, Roche M, Webb N, Gray LR, Chikere K, Sterjovski J, Ellett A, Wesselingh SL, Ramsland PA, Lee B, Churchill MJ, Gorry PR (2013) Macrophage-tropic HIV-1 variants from brain demonstrate alterations in the way gp120 engages both CD4 and CCR5. J Leukoc Biol 93:113–126. doi:10.1189/jlb.0612308
13. Joseph SB, Arrildt KT, Swanstrom AE, Schnell G, Lee B, Hoxie JA, Swanstrom R (2014) Quantification of entry phenotypes of macrophage-tropic HIV-1 across a wide range of CD4 densities. J Virol 88:1858–1869. doi:10.1128/JVI.02477-13
14. Sterjovski J, Roche M, Churchill MJ, Ellett A, Farrugia W, Gray LR, Cowley D, Poumbourios P, Lee B, Wesselingh SL, Cunningham AL, Ramsland PA, Gorry PR (2010) An altered and more efficient mechanism of CCR5 engagement contributes to macrophage tropism of CCR5-using HIV-1 envelopes. Virology 404:269–278. doi:10.1016/j.virol.2010.05.006
15. Gorry PR, Bristol G, Zack JA, Ritola K, Swanstrom R, Birch CJ, Bell JE, Bannert N, Crawford K, Wang H, Schols D, De Clercq E, Kunstman K, Wolinsky SM, Gabuzda D (2001) Macrophage tropism of human immunodeficiency virus type 1 isolates from brain and lymphoid tissues predicts neurotropism independent of coreceptor specificity. J Virol 75:10073–10089. doi:10.1128/JVI.75.21.10073-10089.2001
16. Gorry PR, Taylor J, Holm GH, Mehle A, Morgan T, Cayabyab M, Farzan M, Wang H, Bell JE, Kunstman K, Moore JP, Wolinsky SM, Gabuzda D (2002) Increased CCR5 affinity and reduced CCR5/CD4 dependence of a neurovirulent primary human immunodeficiency virus type 1 isolate. J Virol 76:6277–6292
17. Martín J, LaBranche CC, González-Scarano F (2001) Differential CD4/CCR5 utilization, gp120 conformation, and neutralization sensitivity between envelopes from a microglia-adapted human immunodeficiency virus type 1 and its parental isolate. J Virol 75:3568–3580. doi:10.1128/JVI.75.8.3568-3580.2001
18. Kozak SL, Platt EJ, Madani N, Ferro FE, Peden K, Kabat D (1997) CD4, CXCR-4, and CCR-5 dependencies for infections by primary patient and laboratory-adapted isolates of human immunodeficiency virus type 1. J Virol 71:873–882
19. Platt EJ, Madani N, Kozak SL, Kabat D (1997) Infectious properties of human immunodeficiency virus type 1 mutants with distinct affinities for the CD4 receptor. J Virol 71:883–890
20. Platt EJ, Wehrly K, Kuhmann SE, Chesebro B, Kabat D (1998) Effects of CCR5 and CD4 cell surface concentrations on infections by macrophagetropic isolates of human immunodeficiency virus type 1. J Virol 72:2855–2864
21. Johnston SH, Lobritz MA, Nguyen S, Lassen K, Delair S, Posta F, Bryson YJ, Arts EJ, Chou T, Lee B (2009) A quantitative affinity-profiling system that reveals distinct CD4/CCR5 usage patterns among human immunodeficiency virus type 1 and simian immunodeficiency virus strains. J Virol 83:11016–11026. doi:10.1128/JVI.01242-09
22. Chikere K, Chou T, Gorry PR, Lee B (2013) Affinofile profiling: how efficiency of CD4/CCR5 usage impacts the biological and pathogenic phenotype of HIV. Virology 435:81–91. doi:10.1016/j.virol.2012.09.043
23. Pugach P, Ray N, Klasse PJ, Ketas TJ, Michael E, Doms RW, Lee B, Moore JP (2009) Inefficient entry of vicriviroc-resistant HIV-1 via the inhibitor-CCR5 complex at low cell surface CCR5 densities. Virology 387:296–302. doi:10.1016/j.virol.2009.02.044
24. Pfaff JM, Wilen CB, Harrison JE, Demarest JF, Lee B, Doms RW, Tilton JC (2010) HIV-1 resistance to CCR5 antagonists associated with highly efficient use of CCR5 and altered tropism on primary CD4+ T cells. J Virol 84:6505–6514. doi:10.1128/JVI.00374-10
25. Roche M, Jakobsen MR, Sterjovski J, Ellett A, Posta F, Lee B, Jubb B, Westby M, Lewin SR, Ramsland PA, Churchill MJ, Gorry PR (2011) HIV-1 escape from the CCR5 antagonist maraviroc associated with an altered and less-efficient mechanism of gp120-CCR5 engagement that attenuates macrophage tropism. J Virol 85:4330–4342. doi:10.1128/JVI.00106-11
26. Roche M, Jakobsen MR, Ellett A, Salimiseyedabad H, Jubb B, Westby M, Lee B, Lewin SR, Churchill MJ, Gorry PR (2011) HIV-1 predisposed to acquiring

resistance to maraviroc (MVC) and other CCR5 antagonists in vitro has an inherent, low-level ability to utilize MVC-bound CCR5 for entry. Retrovirology 8:89. doi:10.1186/1742-4690-8-89

27. Flynn JK, Paukovics G, Moore MS, Ellett A, Gray LR, Duncan R, Salimi H, Jubb B, Westby M, Purcell DFJ, Lewin SR, Lee B, Churchill MJ, Gorry PR, Roche M (2013) The magnitude of HIV-1 resistance to the CCR5 antagonist maraviroc may impart a differential alteration in HIV-1 tropism for macrophages and T-cell subsets. Virology 442:51–58. doi:10.1016/j.virol.2013.03.026
28. Roche M, Salimi H, Duncan R, Wilkinson BL, Chikere K, Moore MS, Webb NE, Zappi H, Sterjovski J, Flynn JK, Ellett A, Gray LR, Lee B, Jubb B, Westby M, Ramsland PA, Lewin SR, Payne RJ, Churchill MJ, Gorry PR (2013) A common mechanism of clinical HIV-1 resistance to the CCR5 antagonist maraviroc despite divergent resistance levels and lack of common gp120 resistance mutations. Retrovirology 10:43. doi:10.1186/1742-4690-10-43
29. Loftin LM, Kienzle MF, Yi Y, Lee B, Lee F-H, Gray L, Gorry PR, Collman RG (2010) Constrained use of CCR5 on CD4+ lymphocytes by R5X4 HIV-1: efficiency of Env-CCR5 interactions and low CCR5 expression determine a range of restricted CCR5-mediated entry. Virology 402:135–148. doi:10.1016/j.virol.2010.03.009
30. Berro R, Klasse PJ, Lascano D, Flegler A, Nagashima KA, Sanders RW, Sakmar TP, Hope TJ, Moore JP (2011) Multiple CCR5 conformations on the cell surface are used differentially by human immunodeficiency viruses resistant or sensitive to CCR5 inhibitors. J Virol 85:8227–8240. doi:10.1128/JVI.00767-11
31. Lee B, Sharron M, Montaner LJ, Weissman D, Doms RW (1999) Quantification of CD4, CCR5, and CXCR4 levels on lymphocyte subsets, dendritic cells, and differentially conditioned monocyte-derived macrophages. Proc Natl Acad Sci U S A 96:5215–5220
32. Chikere K, Webb NE, Chou T, Borm K, Sterjovski J, Gorry PR, Lee B (2014) Distinct HIV-1 entry phenotypes are associated with transmission, subtype specificity, and resistance to broadly neutralizing antibodies. Retrovirology 11:48. doi:10.1186/1742-4690-11-48

Chapter 2

Measuring T Cell-to-T Cell HIV-1 Transfer, Viral Fusion, and Infection Using Flow Cytometry

Natasha D. Durham and Benjamin K. Chen

Abstract

Direct T cell-to-T cell HIV-1 infection is a distinct mode of HIV-1 infection that requires physical contact between an HIV-1-infected "donor" cell and an uninfected, CD4-expressing "target" cell. In vitro studies indicate that HIV-1 cell-to-cell infection is much more efficient than infection by cell-free viral particles; however, the exact mechanisms of the enhanced efficiency of this infection pathway are still unclear. Several assays have been developed to study the mechanism of direct cell-to-cell HIV-1 transmission and to assess sensitivity to neutralizing antibodies and pharmacologic inhibitors. These assays are based on the coculture of donor and target cells. Here, we describe methods that utilize flow cytometry, which can discriminate donor and target cells and can assess different stages of entry and infection following cell-to-cell contact. HIV Gag-iGFP, a clone that makes fluorescent virus particles, can be used to measure cell-to-cell transfer of virus particles. HIV NL-GI, a clone that expresses GFP as an early gene, facilitates the measure of productive infection after cell-to-cell contact. Lastly, a variation of the β-lactamase (BlaM)-Vpr fusion assay can be used to measure the viral membrane fusion process after coculture of donor and target cells in a manner that is independent of cell-cell fusion. These assays can be performed in the presence of neutralizing antibodies/inhibitors to determine the 50 % inhibitory concentration (IC_{50}) required to block infection specifically in the target cells.

Key words HIV entry, Cell-to-cell transfer, Cell-to-cell infection, Virological synapse, Neutralization assay, Fluorescent reporter virus, Gag-iGFP, β-lactamase (BlaM) fusion assay

1 Introduction

Direct cell-to-cell HIV-1 infection is a major mode of HIV-1 transmission between T cells in vitro and is likely to make a significant contribution to in vivo HIV-1 spread and pathogenesis in lymph nodes, gut-associated lymphatic tissue (GALT), and other tissues containing high numbers of HIV-1 susceptible cells. In $CD4^+$ T cells, two major modes of HIV-1 infection have been documented—infection by cell-free virus and infection facilitated by cell-cell contact. Traditional "cell-free" infection involves the release of viral particles from a productively infected cell, followed by particle diffusion, viral attachment, and entry into an uninfected cell.

Vinayaka R. Prasad and Ganjam V. Kalpana (eds.), *HIV Protocols*, Methods in Molecular Biology, vol. 1354,
DOI 10.1007/978-1-4939-3046-3_2,

The T cell-to-T cell virological synapse is distinct from the synapse formed between dendritic cells (DCs) and T cells [1, 2]. HIV-1 infection of the donor DC is not required for DC-to-T cell infection. Rather, virus particles are concentrated at the DC-T cell junction and transferred in *trans* to the target cell after exposure of donor DCs to virus particles [3]. T cell-to-T cell infection is mediated by a stable adhesion called a virological synapse (VS) [4], formed between a de novo HIV-1-infected donor T cell and an uninfected target T cell (also see reviews [5–7]). T cell-to-T cell infection was first observed for HTLV-1, a retrovirus that produces poorly infectious cell free virions [8]. For HIV-1, T cell-to-T cell infection has also been recognized as a much more efficient mode of HIV-1 infection compared to cell-free HIV-1 [9, 10]. HIV-1 Env and CD4 are required on the infected and uninfected T cells, respectively [4], and integrins may facilitate or reinforce the cell-cell adhesions [11–13]. Once contact is established, cell-surface Env, Gag, and CD4 polarize to the site of cell contact through actin cytoskeleton rearrangement, forming an adhesive structure that is defined as a "virological synapse," as it resembles the immunological synapse formed during T cell activation, but with unique characteristics (reviewed in [14] and [15]).

After virological synapse formation, viral particles have been described as following different pathways to viral entry. Some studies suggest that particles bud from the infected donor cell into the synaptic cleft and fuse at the plasma membrane of the uninfected target cell, similar to cell-free infection, but without extensive particle diffusion [4, 16, 17]. Alternatively, particles may be transferred directly into the target cell within intracellular compartments in a co-receptor-independent manner [18], before fusion of the viral and intracellular membranes which requires the presence of either CXCR4 or CCR5 co-receptor [19–21] (Fig. 1). Subsequent to viral fusion, the viral life cycle (uncoating, integration, and viral gene expression) is thought to be similar to cell-free infection.

Some antiviral drugs and antibodies have been described as having lower inhibitory potency when blocking cell-to-cell infection as compared to cell-free infection [22–24]. Cell-to-cell transmission may promote viral persistence when suboptimal therapy or immune responses are present. Recently, these have been tested extensively in various in vitro cell-to-cell entry/infectivity assays [9, 17, 23–30].

A challenge in measuring cell-to-cell infection is clearly distinguishing the infectious signal in the target cells from the input signal of the infected donor cells. A common feature of the assays described here is the use of inert fluorescent cell-labeling dyes to accurately distinguish between donor and target cells. On the day of the synapse-forming assay, donor cells are Ficoll purified, and target cells are differentially labeled with cell proliferation dye, cocultured for a given duration, trypsinized, fixed, and analyzed by

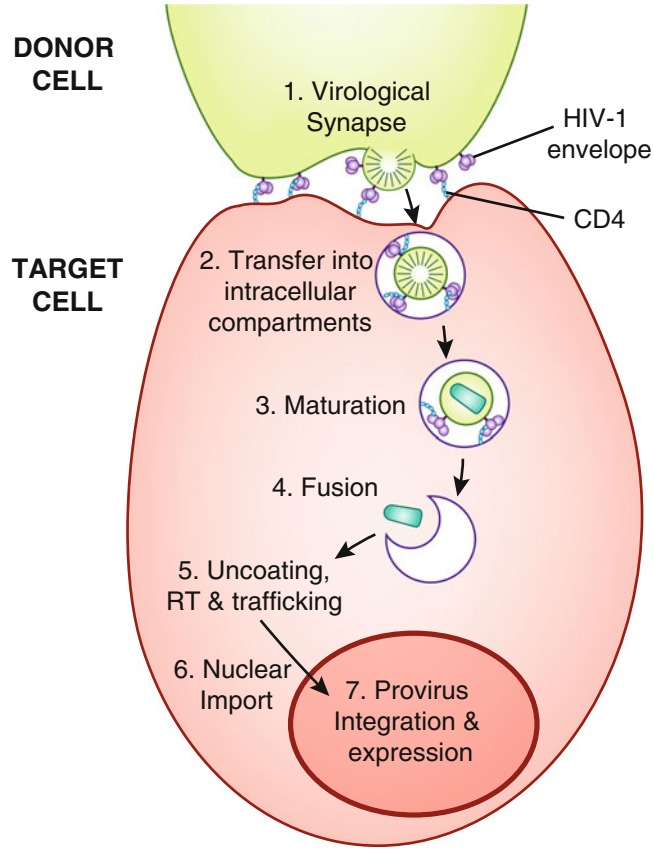

Fig. 1 Schematic representation of direct T cell-to-T cell HIV-1 entry, illustrating a multistep entry model. An HIV-1-infected donor T cell (*top*) expressing cell-surface envelope binds to CD4 on the surface of an uninfected target T cell (*bottom*), forming a virological synapse. Gag and other molecules also co-localize to the site of adhesion. Virions bud and may be transferred directly into intracellular compartments where viral maturation and co-receptor binding occur, followed by fusion of the viral and intracellular membranes, uncoating, reverse transcription (RT), trafficking to the nucleus, nuclear import, provirus integration, and HIV-1 proviral gene expression. Alternatively, virions may bud into the synaptic cleft and undergo maturation, CD4 and co-receptor binding, and fusion of the viral and cell plasma membranes, similar to cell-free infection (not shown).

flow cytometry. Methods that employ flow cytometry enable rapid measurements of thousands of cells per second on a highly quantitative single-cell basis. The three assays in the following sections use flow cytometry and functional fluorescent indicators to detect distinct stages of cell-to-cell infection through T cell virological synapses:

1. *Cell-to-cell transfer assay* utilizes fluorescent virus particles to measure the CD4-dependent steps that lead up to transfer of virus particles to the target cell during cell-to-cell infection (Fig. 2a).

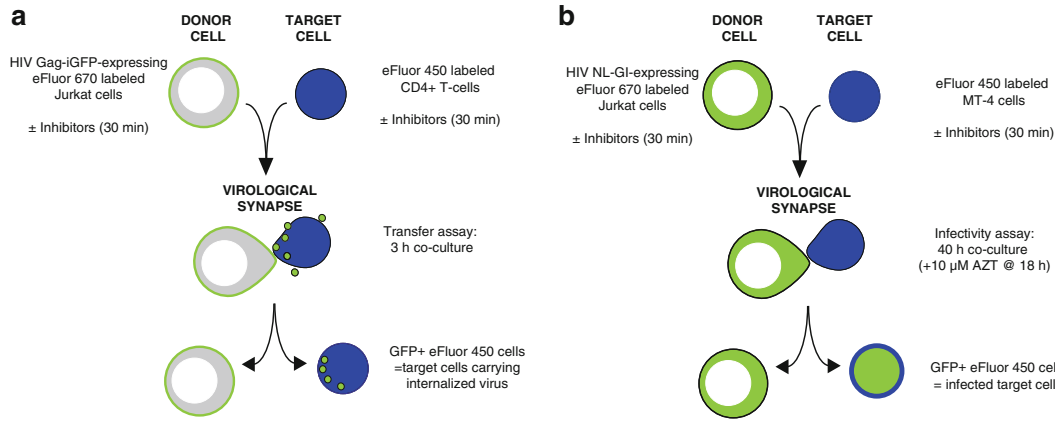

Fig. 2 Overview of cell-to-cell viral transfer and cell-to-cell infection assays. (**a**) In the cell-to-cell transfer assay, donor Jurkat cells are nucleofected with HIV Gag-iGFP proviral DNA 24 h prior to the assay. Donor Jurkat cells and primary $CD4^+$ target cells are labeled with Cell Proliferation dyes eFluor 670 and eFluor 450, respectively, and may be preincubated separately for 30 min with inhibitors or antibodies before mixing at a 1:1 ratio. After 3 h coculture, GFP expression levels in target cells are detected by flow cytometry, indicating HIV-1 transfer. (**b**) In the cell-to-cell infectivity assay, donor Jurkat cells are nucleofected with HIV NL-GI proviral DNA 24 h prior to the assay. Donor Jurkat cells and MT-4 target cells are labeled with Cell Proliferation dyes eFluor 670 and eFluor 450, respectively, and may be preincubated separately for 30 min with inhibitors or antibodies before mixing at a 1:1 ratio. After 18 h coculture, cell culture media is replaced with media containing 10 μM AZT. 40 h after initial coculture, GFP expression levels in donor and target cells are detected by flow cytometry, indicating HIV-1 infection.

2. *Cell-to-cell infection assay* utilizes a virus that expresses fluorescent protein as an early gene and thus measures all the steps that lead to productive viral infection, up to and including new viral gene expression (Fig. 2b).
3. *Cell-to-cell viral membrane fusion assay* measures the efficiency of viral membrane fusion with target cells by adapting a well-described BlaM-Vpr enzymatic assay for detecting viral fusion to a cell-to-cell transmission format.

These assays can be performed with or without antibodies/inhibitors, using the 96-well plate format described here. The assays described here employ the $CD4^+$ T cell line, Jurkat clone E6-1, as donor cells. While other T cell lines or even primary cells may be employed, we use Jurkat cells as they are a well-studied and infectable $CD4^+$ T cell line that we have optimized for transfection by nucleofection methods. By transfecting the cells one can ensure that virus has been made de novo in donor cells, as is the case during acute infection, and is not derived from residual cell-free virus that is bound to the cell surface. The cell-to-cell transfer assay uses primary resting $CD4^+$ T cells as target cells. The cell-to-cell infectivity and viral membrane fusion assays use MT-4 cells as target cells because of their robust infectivity. With some modification, these protocols can also be utilized with activated primary $CD4^+$ T cells.

2 Materials

2.1 Plasmids

1. The plasmid encoding the fluorescent reporter virus HIV Gag-iGFP (Fig. 3a) is expressed in donor cells for the cell-to-cell transfer assay (Subheading 3.4). This construct expresses green fluorescent protein (GFP) as a fusion with the viral Gag protein, inserted between MA and CA, allowing the GFP to be packaged into particles at high copy number. Viral particles contain stoichiometric quantities of fluorescent protein in addition to Gag [20, 31]. Acquisition of fluorescence in the target cell is indicative of a CD4- and Env-dependent process that transfers virus to the target cell and does not require viral fusion, integration, or viral gene expression.
2. A second reporter virus HIV NL-GI (Fig. 3b) is expressed in donor cells for the cell-to-cell infectivity assay (Subheading 3.5). This reporter construct expresses GFP in place of the viral *nef* gene, providing an indicator of early viral gene expression, which requires viral integration [32]. GFP is not tagged to a viral protein, so these viral particles are nonfluorescent. To restore Nef expression in this clone, an internal ribosome entry site (IRES) is inserted upstream of the Nef open reading frame.

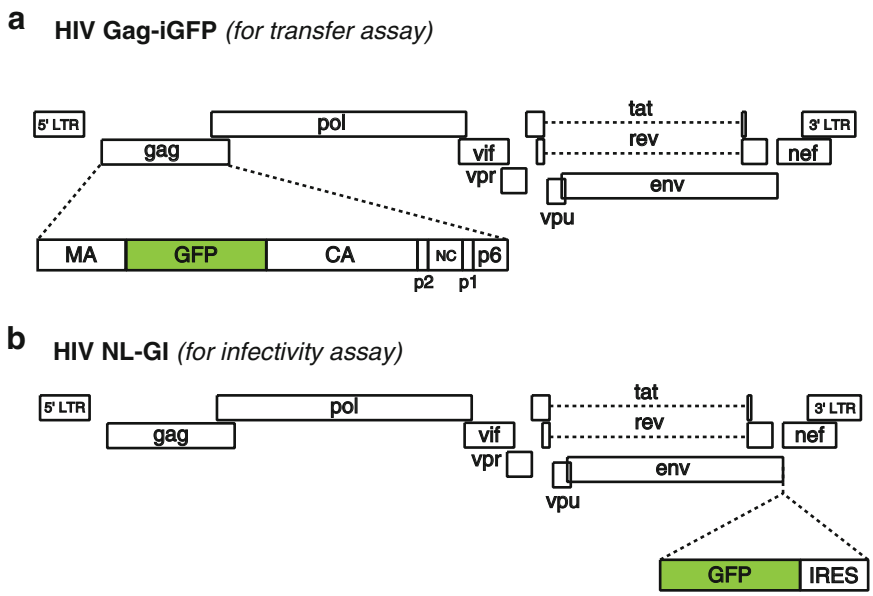

Fig. 3 Fluorescent HIV-1 reporter virus clones. (**a**) HIV Gag-iGFP proviral DNA contains the fluorescent protein GFP in the gag gene between matrix (MA) and capsid (CA), flanked by viral protease cleavage sites, as described in [20]. Viral particles contain GFP in addition to MA, CA, and the other viral structural proteins. (**b**) HIV NL-GI proviral DNA contains GFP and an internal ribosomal entry site (IRES) directly upstream of the nonstructural gene nef [32]. GFP is expressed in infected cells in place of nef, during early viral gene expression. Nef expression is driven from the IRES.

3. Full-length HIV-1 molecular clone pNL4-3 [33] for cell-to-cell viral membrane fusion assay (Subheading 3.6).
4. pMM310 encodes the BlaM-Vpr fusion protein [34, 35] that packages the β-lactamase Vpr fusion protein into virus particles when cotransfected with an HIV proviral plasmid, e.g., pNL4-3. The cell-to-cell viral membrane fusion assay described in Subheading 3.6 is a variation of the FRET-based virion fusion assay described by Cavrois et al. [34, 36]. A green to blue shift in the BlaM fluorescent substrate CCF2-AM indicates fusion of cell-associated virus with target cells.

2.2 Cell Culture and Nucleofection Reagents

1. Nucleofection media: RPMI-1640 medium supplemented with 10 % heat inactivated fetal bovine serum (FBS).
2. RPMI complete: RPMI-1640 medium supplemented with 10 % FBS, 100 U/mL penicillin, 100 μg/mL streptomycin, and 200 μM L-glutamine.
3. Phosphate-buffered saline (PBS).
4. Trypsin-EDTA (0.05 % trypsin, 1 mM ethylenediaminetetraacetic acid).
5. 2 % paraformaldehyde (PFA) solution in PBS.
6. Recombinant Human IL-2 (IL-2).
7. Cell Proliferation dye eFluor 450, 10 mM stock in DMSO.
8. Cell Proliferation dye eFluor 670, 5 mM stock in DMSO.
9. Amaxa Cell Line Nucleofector Kit V containing Supplement V; stored at 4 °C, warmed to room temperature before use.
10. Ficoll-Paque PLUS.
11. Jurkat Clone E6-1 cells.
12. MT-4 cells (for cell-to-cell infectivity assay).
13. 0.4 % trypan blue solution.
14. Unactivated (resting) primary human $CD4^+$ T cells (for cell-to-cell transfer assay).
15. 6-well flat-bottom tissue culture plates.
16. 96-well round-bottom tissue culture plates.
17. Zidovudine (AZT).

2.3 Additional Reagents for Cell-to-Cell Viral Membrane Fusion Assay

1. CO_2-independent media.
2. CCF2-AM substrate and β-lactamase loading solutions.
3. Probenecid stock solution: 250 mM probenecid in 250 mM NaOH.
4. Solution B: 100 mg/mL of Pluronic-F127 and 0.1 % acetic acid.

5. Loading solution (1 mL): 1 μL of 1 mM CCF2-AM stock + 9 μL Solution B + 1 mL CO2-independent media.
6. Development media (1 mL): 10 μL probenecid stock solution + 100 μL FBS + 1 mL CO_2-independent media.

2.4 Additional Reagents for Intracellular p24 Staining of Donor Cells for Viral Membrane Fusion Assay (Optional)

1. 1 % PFA solution in PBS.
2. FIX & PERM Cell Permeabilization Kit (Invitrogen).
3. Wash Buffer: 1 % FBS in PBS; at 4 °C.
4. Anti-p24-PE or anti-p24-FITC monoclonal antibody.
5. 96-well V-bottom tissue culture plates.

2.5 Specialized Equipment

1. Nucleofector Device (single cuvette-based model) (Amaxa, Lonza).
2. BD LSR II Flow Cytometer (BD Biosciences).

3 Methods

Subheadings 3.1–3.3 describe the shared protocol for the preparation of donor Jurkat cells and target cells used in the subsequent assays (Subheadings 3.4–3.6). The plasmid DNA used for nucleofection in Subheading 3.1 will depend on the assay being performed (see above and *see* **Note 1**). The cell-to-cell assays in Subheadings 3.4–3.6 are performed in a 96-well round-bottom tissue culture plate and can be adapted to include neutralizing antibody/inhibitor titrations, as described in Subheading 3.4.

3.1 Nucleofection of Jurkat Donor Cells

Virus-producing Jurkat donor cells are generated by nucleofection of proviral DNA the day before the cell coculture. This method yields high transfection efficiencies and ensures that virus examined in the assay was produced in the donor cell. Nucleofection should be performed using Amaxa Cell Line Nucleofector Solution V containing Supplement V. Allow the solution to warm to room temperature before use. Cell survival after nucleofection will vary depending on the amount of DNA transfected. In general, approximately 50 % cell death is expected. Perform additional nucleofection reactions as needed, to prepare sufficient numbers of live cells for subsequent assays:

1. For each reaction, place 8 mL of nucleofection media per well in a 6-well tissue culture plate (*see* **Note 2**). Incubate at 37 °C for 10 min to warm media.
2. Count Jurkat cells. For each nucleofection reaction, spin 7×106 cells at $400 \times g$ for 5 min to pellet cells. Carefully remove as much supernatant as possible and discard (*see* **Note 3**).

3. Resuspend cell pellet in 140 μL of room temperature Amaxa Cell Line Nucleofector Solution V containing Supplement V (*see* **Note 4**).
4. Immediately add DNA to cell suspension and pipette several times to mix (*see* **Notes 1** and **5**).
5. Immediately transfer suspension to Amaxa cuvette and cover with cap (*see* **Note 6**).
6. Select the program "S-18" on the Nucleofector Device, insert cuvette, and press the start button to transfect cells.
7. After successful transfection (i.e., "OK" message on the Nucleofector Device), remove cuvette. Immediately remove the cells gently with a single-use pipette provided with the Nucleofector Kit. Slowly add the cell suspension dropwise to the pre-warmed nucleofection media.
8. Use the single-use pipette to carefully rinse the cuvette with pre-warmed media to remove residual cells. Add cells to the 6-well plate.
9. Incubate overnight at 37 °C (*see* **Note 7**).

3.2 Density Gradient Purification of Nucleofected Jurkat Donor Cells Using Ficoll

The day after nucleofection, donor cells are spun through a Ficoll density gradient to remove dead cells:

1. For each 8 mL nucleofection reaction, place 4 mL of Ficoll in a sterile 15 mL centrifuge tube. Carefully layer nucleofected cells onto Ficoll using a 10 mL pipette.
2. Use 1 mL of RPMI complete to rinse the well and remove residual cells. Add cells to the 15 mL tube.
3. Spin at 400 × g for 20 min. Set centrifuge brake to "low" or off to prevent disruption of layers when centrifuge brakes at the end of the spin.
4. Carefully remove tubes from centrifuge. A layer of live cells should be visible at the interface of Ficoll and media.
5. Remove and discard a few mL of media from the top of the tube. Carefully remove the layer of live cells from the Ficoll-media interface using a pipette, and transfer to a clean 15 mL centrifuge tube. Avoid removing excess Ficoll.
6. Fill the tube containing live cells with RPMI complete, cap, and invert several times to mix. Spin at 400 × g for 5 min to wash cells (*see* **Note 8**). Discard supernatant.
7. Resuspend cell pellet in 1 or 2 mL of RPMI complete. Remove a sample of cell suspension and determine cell count (*see* **Notes 9** and **10**).

3.3 Cell Labeling

Cell labeling should be optimized for the cells and dye combination that one chooses to use. We often use Jurkat donor cells labeled with 4 μM Cell Proliferation dye eFluor 670 and MT-4 or

$CD4^+$ target cells labeled with 6 μM Cell Proliferation dye eFluor 450, except in the viral membrane fusion assay where donor cells are unlabeled and target cells are labeled with eFluor 670. Labeling cells with eFluor 670 and eFluor 450 allows detection of distinct donor and target populations by flow cytometry using APC and Pacific Blue filter sets, respectively, with minimal spectral compensation required. Depending upon the flow cytometer you use, you may also choose to use other inert fluorescent dyes from other manufacturers that are compatible with formaldehyde-based fixatives. As a flow cytometry control in the assays, it is useful to also label uninfected Jurkat cells:

1. Spin Ficoll-purified Jurkat donor cells and the desired amount of target cells at 400 × g for 5 min to pellet (*see* **Note 11**). Use a 15 or 50 mL sterile centrifuge tube for target cells, as appropriate. Discard supernatant and resuspend cell pellet in PBS.
2. Fill tube with PBS and spin at 400 × g for 5 min to pellet cells. Discard supernatant.
3. Prepare a working solution of 6 μM Cell Proliferation dye eFluor 450 in PBS for labeling target cells. Use 1 mL for a maximum of 10×106 cells.
4. Prepare a working solution of 4 μM Cell Proliferation dye eFluor 670 in PBS for labeling donor cells. Use 1 mL for a maximum of 10×106 cells.
5. Resuspend target cells in the appropriate volume of 6 μM Cell Proliferation dye eFluor 450. Resuspend donor cells in the appropriate volume of 4 μM Cell Proliferation dye eFluor 670.
6. Incubate cells at 37 °C for 10 min in the dark.
7. Add 4–5 volumes of RPMI complete to stop the labeling reaction. Spin at 400 × g for 5 min.
8. Remove supernatant and resuspend cells in 4–5 volumes of RPMI complete. Spin at 400 × *g* for 5 min to wash cells (wash #1).
9. Remove supernatant and resuspend cell pellet in 1 or 2 mL of RPMI complete. Remove a sample of cell suspension and determine live cell count using trypan blue (*see* **Note 12**).
10. Add to 4–5 volumes of RPMI complete and spin at 400 × g for 5 min to pellet cells (wash #2).
11. Resuspend each cell type at 2.5×10^6 cells/mL in RPMI complete.

3.4 Cell-to-Cell Transfer and Neutralization Assay

Steps 1–3 describe the preparation of eight dilutions of antibody/inhibitors for neutralization of cell-to-cell transfer from infected Jurkat donor cells to uninfected resting $CD4^+$ human T cells. A positive control antibody such as Leu3a (an anti-CD4, HIV-blocking antibody) should be included to ensure the assay is

performed correctly. Leu3a should neutralize both cell-to-cell transfer and cell-to-cell infection at 0.5 μg/mL. A negative control of RPMI complete (no antibody) should also be included in the assay:

1. Prepare 150 μL of each antibody/inhibitor at twice the highest desired concentration in RPMI complete. For example, prepare 150 μL of Leu3a at 1 μg/mL in RPMI complete. Mix and add to well A1 of a 96-well round-bottom tissue culture plate. Repeat for additional inhibitors, using wells B1 to H1, as needed (*see* **Note 13**).
2. Add 120 μL of RPMI complete to columns 2–8 for each row being used.
3. Make fivefold titrations by adding 30 μL of antibody/inhibitor from column 1 to column 2. Mix and repeat using a multichannel pipette, making serial fivefold dilutions until column 8. Discard 30 μL from column 8.
4. Mix donor cells gently to resuspend cells. Add 50 μL of donor cells (i.e., 0.125×10^6 cells) to each well of a clean 96-well round-bottom tissue culture plate (plate 1). Reserve remaining cells.
5. Repeat **step 4** for target cells, using a clean 96-well round-bottom tissue culture plate (plate 2) (*see* **Note 14**).
6. Add 50 μL of antibody/inhibitor to the corresponding wells in plate 1 containing donor cells. Pipette several times to mix (*see* **Note 15**).
7. Repeat **step 6** for plate 2.
8. Incubate plate 1 and plate 2 for 30 min at 37 °C.
9. During incubation, fix samples of donor and target cells to determine infectivity levels at the time of coculture. Add 50 or 100 μL of donor or target cells to separate wells in a clean 96-well round-bottom tissue culture plate (plate 3). Samples can be prepared in duplicate. Proceed to **steps 12–17**.
10. After 30 min, pipette donor cells (plate 1) to resuspend cells, and transfer the entire suspension to corresponding wells containing target cells (plate 2).
11. Incubate for 3 h at 37 °C.
12. Spin plate at 500 × g for 5 min to pellet cells. Discard supernatant by quickly flicking the plate contents once into a waste container or by carefully using a multichannel pipette without disrupting the cell pellet.
13. Add 50 μL 0.05 % trypsin-EDTA to each well and mix to resuspend cells. Incubate for 4 min at 37 °C (*see* **Note 16**).

14. Add 150 µL of RPMI complete to each well to stop reaction.
15. Spin plate at 500 × g for 5 min. Discard supernatant.
16. Add 200 µL of PBS to each well and mix to resuspend cells. Spin plate at 500 × g for 5 min to wash cells. Discard supernatant.
17. Add 200 µL of 2 % PFA to each well to fix cells. Mix to resuspend cells.
18. Seal plate and store at 4 °C in the dark until samples are analyzed by flow cytometry for up to 48 h. Figure 4 shows example data and a suggested gating strategy for data analysis.

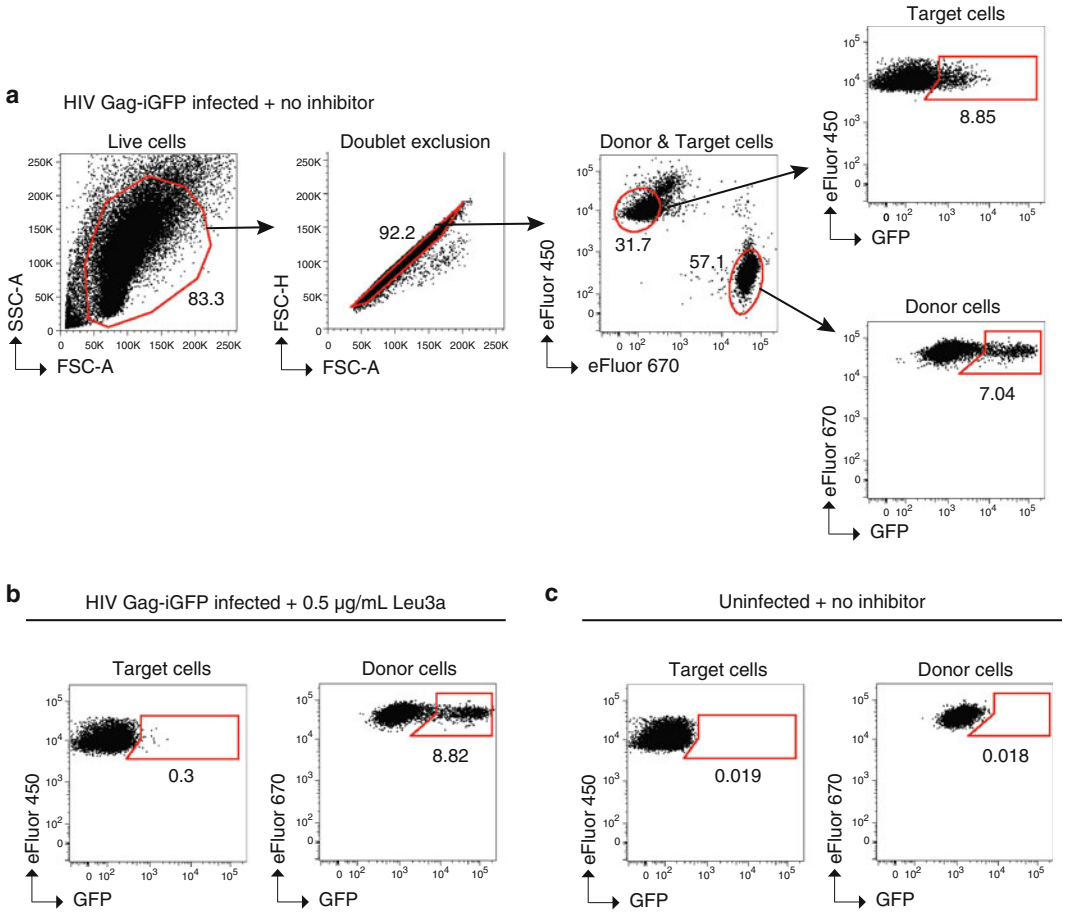

Fig. 4 Detection of cell-to-cell transfer and inhibition by flow cytometry. Example flow cytometry plots of a typical cell-to-cell transfer assay using HIV Gag-iGFP. Gating strategy to determine live cells, doublet exclusion, eFluor 670 (APC)-positive Jurkat donor cells vs. eFluor 450 (Pacific Blue)-positive primary $CD4^+$ target cells, GFP-positive (i.e., HIV+) $CD4^+$ target cells, and GFP-positive (i.e., HIV+) Jurkat donor cells. $CD4^+$ target cells are cocultured for 3 h with (**a**) Jurkat donor cells expressing HIV Gag-iGFP in the absence of neutralizing antibody, (**b**) donor cells expressing HIV Gag-iGFP in the presence of the antibody Leu3a at 0.5 µg/mL, and (**c**) uninfected donor cells.

19. If using neutralizing antibodies/inhibitors, calculate % inhibition:

    100 – [(% infected target cells with inhibitor/% infected target cells without inhibitor) × 100].

3.5 Cell-to-Cell Infectivity and Neutralization Assay

1. Label Jurkat donor cells with eFluor 670 and MT-4 target cells with eFluor 450 as described in Subheading 3.3.
2. Prepare antibodies/inhibitors, infected Jurkat donor cells, and uninfected MT-4 target cells as described in Subheading 3.4, **steps 1–10**.
3. Incubate for 18 h at 37 °C.
4. 18 h after coculture, spin plate at 500 × g for 5 min to pellet cells. Discard supernatant.
5. Resuspend cell pellet in 200 μL per well of RPMI complete containing 10 μM AZT. Mix well. Incubate for an additional 22 h at 37 °C (i.e., for a total of 40 h after coculture).
6. Spin plate at 500 × g for 5 min to pellet cells. Discard supernatant.
7. Treat cells with trypsin-EDTA and fix with 2 % PFA as described in Subheading 3.4, **steps 13–19**. Figure 5 shows example data and a suggested gating strategy for data analysis.

3.6 Cell-to-Cell Viral Membrane Fusion Assay

1. Label MT-4 target cells with 4 μM Cell Proliferation dye eFluor 670 as described in Subheading 3.3.
2. Prepare antibodies/inhibitors, infected Jurkat donor cells, and uninfected MT-4 target cells as described in Subheading 3.4, **steps 1–10** (*see* **Note 17**).
3. Incubate for 5 h at 37 °C.
4. Prepare appropriate amount of loading solution and development media.
5. 5 h after coculture, spin plate at 800 × *g* for 5 min to pellet cells. Discard supernatant.
6. Resuspend cells in 200 μL per well of CO_2-independent media to wash cells. Spin plate at 800 × g for 5 min to pellet cells. Discard supernatant.
7. Resuspend cells in 100 μL per well of loading solution, and incubate for 1–1.5 h in the dark at room temperature.
8. Spin plate at 800 × g for 5 min to pellet cells. Discard supernatant.
9. Resuspend cells in 200 μL per well of Development media to wash cells.
10. Spin plate at 800 × g for 5 min to pellet cells. Discard supernatant.

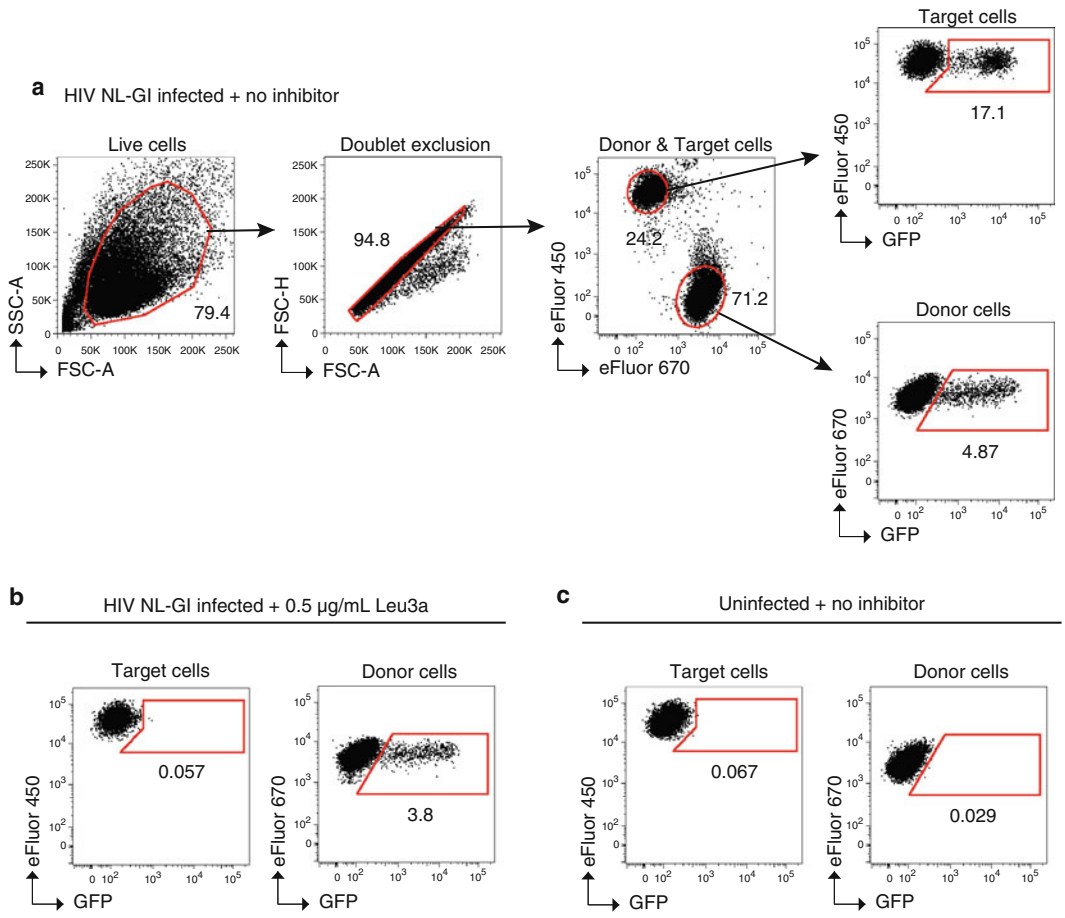

Fig. 5 Detection of cell-to-cell infection and inhibition by flow cytometry. Example flow cytometry plots of a typical cell-to-cell infectivity assay using NL-GI. Gating strategy to determine live cells, doublet exclusion, eFluor 670 (APC)-positive Jurkat donor cells vs. eFluor 450 (Pacific Blue)-positive MT-4 target cells, GFP-positive (i.e., HIV+) MT-4 target cells, and GFP-positive (i.e., HIV+) Jurkat donor cells. MT-4 target cells are cocultured for 40 h with (**a**) Jurkat donor cells expressing HIV NL-GI in the absence of neutralizing antibody, (**b**) donor cells expressing HIV NL-GI in the presence of the antibody Leu3a at 0.5 µg/mL, and (**c**) uninfected donor cells.

11. Resuspend cell pellet in 200 µL per well of Development media and incubate at room temperature in the dark for 16–18 h.
12. Spin plate at 800 × g for 5 min to pellet cells. Discard supernatant.
13. Treat cells with trypsin-EDTA, stop trypsinization, and wash cells with PBS as described in Subheading 3.4, **steps 13–16**.
14. Add 200 µL of 1 % PFA to each well to fix cells. Mix to resuspend pellet.
15. Seal plate and store at 4 °C in the dark until samples are analyzed by flow cytometry for up to 48 h. Figure 6 shows example data and a suggested gating strategy for data analysis.

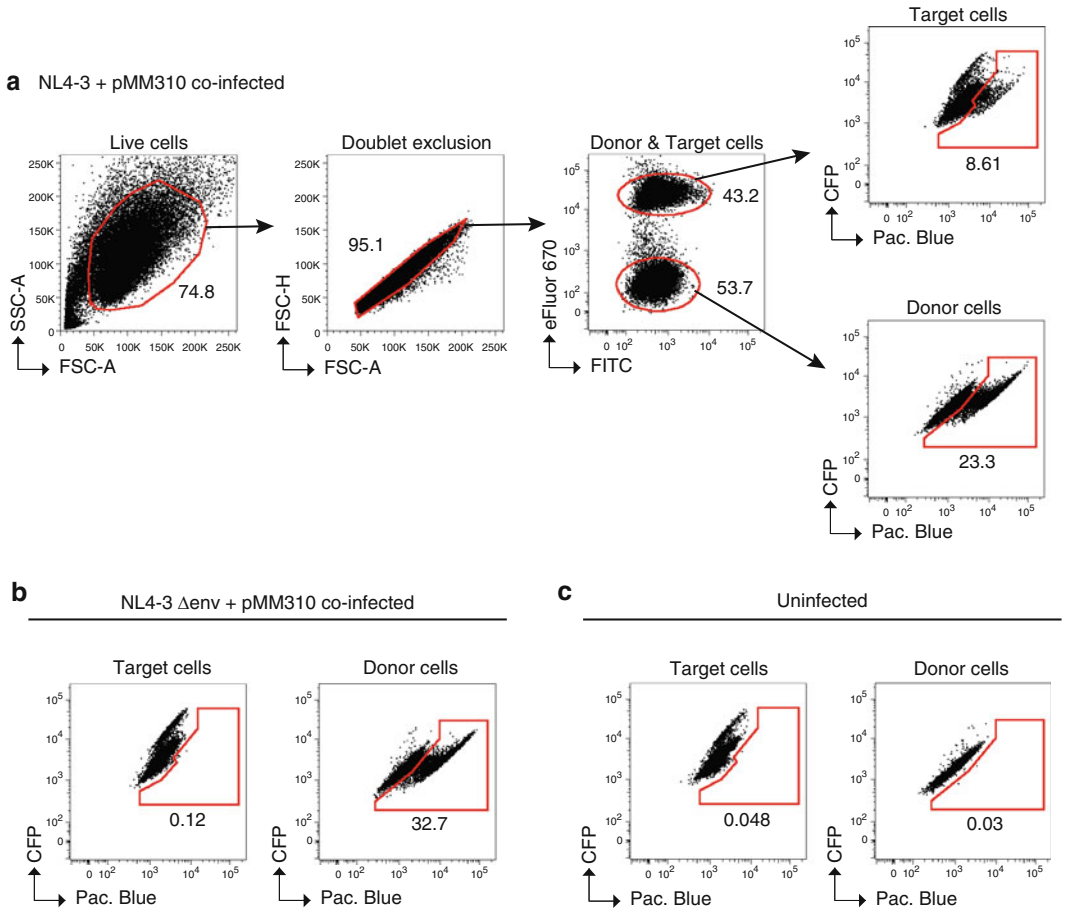

Fig. 6 Detection of cell-to-cell viral membrane fusion by flow cytometry. Example flow cytometry plots of a typical cell-to-cell viral membrane fusion assay using donor Jurkat cells co-expressing NL4-3 and pMM310 and MT-4 target cells. Gating strategy to determine live cells, doublet exclusion, eFluor 670 (APC)-positive MT-4 target cells and eFluor 670 (APC)-negative Jurkat donor cells, and Pacific Blue-positive (i.e., cleaved CCF2-AM) MT-4 target cells and Pacific Blue-positive (i.e., cleaved CCF2-AM) Jurkat donor cells. MT-4 target cells are cocultured for 5 h with (**a**) Jurkat donor cells co-expressing NL4-3 and the plasmid pMM310, which encodes BlaM-Vpr, (**b**) donor cells co-expressing NL4-3 Δenv and pMM310, and (**c**) uninfected donor cells.

4 Notes

1. When preparing donor cells for the cell-to-cell transfer assay (Subheading 3.4), use HIV Gag-iGFP proviral DNA. If donor cells will be used in the cell-to-cell infectivity assay (Subheading 3.5), use HIV NL-GI proviral DNA. Other versions of these proviral constructs that contain another fluorescent protein, e.g., mCherry, instead of GFP, can also be used. If donor cells will be used in the cell-to-cell viral membrane fusion assay (Subheading 3.6), use a 3:1 ratio of pNL4-3 proviral DNA to pMM310 DNA. Other pNL4-3 genetic variants

can also be tested, for example, pNL4-3 Δenv, by co-transfection with pMM310 (*see* Fig. 6b).

2. Up to two (i.e., duplicate) reactions can be placed in the same well containing 8 mL of media.
3. If cells are $\geq 1 \times 106$/mL at the time of counting, wash cells once with PBS before **step 3**.
4. **Steps 3–8** should be performed separately for each nucleofection reaction, to avoid keeping cells in Nucleofector Solution for longer than necessary.
5. Use endotoxin-free purified HIV-1 proviral DNA, prepared at a concentration of approximately 1 μg/μL. The amount of DNA used will vary depending on the desired transfection efficiency. Typically 5 μg of fluorescent reporter proviral DNA will result in approximately 10–20 % positive cells when detected by flow cytometry the day after nucleofection.
6. Avoid air bubbles when adding the cell suspension to the cuvette to prevent an "error" message during nucleofection. This is easiest if the exact volume of the suspension (approximately 160 μL) is transferred to the cuvette with a 1 mL pipette. Gently tap the bottom of the cuvette to dispense air bubbles and ensure the suspension covers the bottom of the cuvette.
7. For nucleofection of proviral DNA encoding a fluorescent reporter virus, fluorescent virus-expressing cells should be readily visible with a fluorescent microscope the day after transfection.
8. If excess Ficoll was removed in **step 5** and is visible after washing in **step** 6, remove and discard the top layer of RPMI complete, resuspend remaining volume up to 15 mL, invert tube several times to mix, and repeat spin.
9. The cell count here is used to determine the volume required for cell labeling.
10. An aliquot of cells can be fixed in a 96-well round-bottom tissue culture plate (*see* Subheading 3.4, **steps 12–17**) and analyzed by flow cytometry to determine the percentage of HIV-1-positive donor cells. If several HIV-1 genetic variants are being compared, it may be desirable to normalize samples to equal transfection efficiency if the efficiency of nucleofection varies between samples. Measure the transfection efficiency by flow cytometry and add uninfected cells to the nucleofected donor cells to achieve uniform transfection efficiency before proceeding to Subheading 3.3.
11. Label approximately 1.5× or 2× more target cells than needed, as cells are frequently lost during labeling wash **steps**.

12. Cells can be incubated at 37 °C in sterile centrifuge tubes for up to 2 h before proceeding to **step 10**.
13. You may also use wells B2-B11 through G2-G11 and fill outside wells with PBS during coculture to avoid sample evaporation from outer wells of the plate.
14. If no antibody/inhibitor is being tested, target cells can be added directly to donor cells. Add 100 µL of RPMI complete, pipette several times to mix, and proceed to **step** 11.
15. Mixing the antibody/inhibitor with an equal volume of cells dilutes it in half, to the desired final concentration, e.g., from 1 to 0.5 µg/mL for Leu3a.
16. Treating samples with 0.05 % trypsin-EDTA reduces the number of cell doublets before flow cytometry. In the cell-to-cell transfer assay, it also removes cell-surface bound fluorescent virus, ensuring that any fluorescent signal is from internalized virus only [9].
17. Optional: to determine the transfection efficiency of donor Jurkat cells, stain for intracellular p24 using anti-p24-PE or anti-p24-FITC monoclonal antibodies.

Acknowledgments

We thank members of the B. K. Chen Lab for helpful comments and the Flow Cytometry Shared Resource Facility, Icahn School of Medicine at Mount Sinai, for assistance. This work was supported by NIH/NIDA DA028866 and NIH/NIAID A1074420.

References

1. McDonald D, Wu L, Bohks SM, KewalRamani VN, Unutmaz D, Hope TJ (2003) Recruitment of HIV and its receptors to dendritic cell-T cell junctions. Science 300:1295–1297. doi:10.1126/science.1084238
2. Cameron PU, Freudenthal PS, Barker JM, Gezelter S, Inaba K, Steinman RM (1992) Dendritic cells exposed to human immunodeficiency virus type-1 transmit a vigorous cytopathic infection to CD4+ T cells. Science 257:383–387
3. Arrighi JF, Pion M, Garcia E, Escola JM, van Kooyk Y, Geijtenbeek TB, Piguet V (2004) DC-SIGN-mediated infectious synapse formation enhances X4 HIV-1 transmission from dendritic cells to T cells. J Exp Med 200:1279–1288. doi:10.1084/jem.20041356
4. Jolly C, Kashefi K, Hollinshead M, Sattentau QJ (2004) HIV-1 cell to cell transfer across an Env-induced, actin-dependent synapse. J Exp Med 199:283–293. doi:10.1084/jem.20030648
5. Piguet V, Sattentau Q (2004) Dangerous liaisons at the virological synapse. J Clin Invest 114:605–610. doi:10.1172/jci22812
6. Dale BM, Alvarez RA, Chen BK (2013) Mechanisms of enhanced HIV spread through T-cell virological synapses. Immunol Rev 251:113–124. doi:10.1111/imr.12022
7. Puigdomenech I, Massanella M, Cabrera C, Clotet B, Blanco J (2009) On the steps of cell-to-cell HIV transmission between CD4 T cells. Retrovirology 6:89. doi:10.1186/1742-4690-6-89
8. Igakura T, Stinchcombe JC, Goon PK, Taylor GP, Weber JN, Griffiths GM, Tanaka Y, Osame M, Bangham CR (2003) Spread of HTLV-I between lymphocytes by virus-induced polarization

of the cytoskeleton. Science 299:1713–1716. doi:10.1126/science.1080115

9. Chen P, Hubner W, Spinelli MA, Chen BK (2007) Predominant mode of human immunodeficiency virus transfer between T cells is mediated by sustained Env-dependent neutralization-resistant virological synapses. J Virol 81:12582–12595. doi:10.1128/jvi.00381-07
10. Sourisseau M, Sol-Foulon N, Porrot F, Blanchet F, Schwartz O (2007) Inefficient human immunodeficiency virus replication in mobile lymphocytes. J Virol 81:1000–1012. doi:10.1128/jvi.01629-06
11. Arthos J, Cicala C, Martinelli E, Macleod K, Van Ryk D, Wei D, Xiao Z, Veenstra TD, Conrad TP, Lempicki RA, McLaughlin S, Pascuccio M, Gopaul R, McNally J, Cruz CC, Censoplano N, Chung E, Reitano KN, Kottilil S, Goode DJ, Fauci AS (2008) HIV-1 envelope protein binds to and signals through integrin alpha4beta7, the gut mucosal homing receptor for peripheral T cells. Nat Immunol 9:301–309. doi:10.1038/ni1566
12. Rudnicka D, Feldmann J, Porrot F, Wietgrefe S, Guadagnini S, Prevost MC, Estaquier J, Haase AT, Sol-Foulon N, Schwartz O (2009) Simultaneous cell-to-cell transmission of human immunodeficiency virus to multiple targets through polysynapses. J Virol 83:6234–6246. doi:10.1128/jvi.00282-09
13. Jolly C, Mitar I, Sattentau QJ (2007) Adhesion molecule interactions facilitate human immunodeficiency virus type 1-induced virological synapse formation between T cells. J Virol 81:13916–13921. doi:10.1128/jvi.01585-07
14. Haller C, Fackler OT (2008) HIV-1 at the immunological and T-lymphocytic virological synapse. Biol Chem 389:1253–1260. doi:10.1515/bc.2008.143
15. Vasiliver-Shamis G, Dustin ML, Hioe CE (2010) HIV-1 virological synapse is not simply a copycat of the immunological synapse. Viruses 2(5):1239–1260. doi:10.3390/v2051239
16. Sattentau Q (2010) Cell-to-cell spread of retroviruses. Viruses 2:1306–1321
17. Martin N, Welsch S, Jolly C, Briggs JA, Vaux D, Sattentau QJ (2010) Virological synapse-mediated spread of human immunodeficiency virus type 1 between T cells is sensitive to entry inhibition. J Virol 84:3516–3527. doi:10.1128/jvi.02651-09
18. Gupta P, Balachandran R, Ho M, Enrico A, Rinaldo C (1989) Cell-to-cell transmission of human immunodeficiency virus type 1 in the presence of azidothymidine and neutralizing antibody. J Virol 63:2361–2365
19. Dale BM, McNerney GP, Thompson DL, Hubner W, de Los RK, Chuang FY, Huser T, Chen BK (2011) Cell-to-cell transfer of HIV-1 via virological synapses leads to endosomal virion maturation that activates viral membrane fusion. Cell Host Microbe 10:551–562. doi:10.1016/j.chom.2011.10.015
20. Hubner W, McNerney GP, Chen P, Dale BM, Gordon RE, Chuang FY, Li XD, Asmuth DM, Huser T, Chen BK (2009) Quantitative 3D video microscopy of HIV transfer across T cell virological synapses. Science 323:1743–1747. doi:10.1126/science.1167525
21. Sloan RD, Kuhl BD, Mesplede T, Munch J, Donahue DA, Wainberg MA (2013) Productive entry of HIV-1 during cell-to-cell transmission via dynamin-dependent endocytosis. J Virol 87:8110–8123. doi:10.1128/jvi.00815-13
22. Sigal A, Kim JT, Balazs AB, Dekel E, Mayo A, Milo R, Baltimore D (2011) Cell-to-cell spread of HIV permits ongoing replication despite antiretroviral therapy. Nature 477:95–98. doi:10.1038/nature10347
23. Abela IA, Berlinger L, Schanz M, Reynell L, Gunthard HF, Rusert P, Trkola A (2012) Cell-cell transmission enables HIV-1 to evade inhibition by potent CD4bs directed antibodies. PLoS Pathog 8:e1002634. doi:10.1371/journal.ppat.1002634
24. Durham ND, Yewdall AW, Chen P, Lee R, Zony C, Robinson JE, Chen BK (2012) Neutralization resistance of virological synapse-mediated HIV-1 Infection is regulated by the gp41 cytoplasmic tail. J Virol 86:7484–7495. doi:10.1128/jvi.00230-12
25. Swartz TH, Esposito AM, Durham ND, Hartmann B, Chen BK (2014) P2X-selective purinergic antagonists are strong inhibitors of HIV-1 fusion during both cell-to-cell and cell-free infection. J Virol 88:11504. doi:10.1128/jvi.01158-14
26. Massanella M, Puigdomenech I, Cabrera C, Fernandez-Figueras MT, Aucher A, Gaibelet G, Hudrisier D, Garcia E, Bofill M, Clotet B, Blanco J (2009) Antigp41 antibodies fail to block early events of virological synapses but inhibit HIV spread between T cells. AIDS 23:183–188. doi:10.1097/QAD.0b013e32831ef1a3
27. Sanchez-Palomino S, Massanella M, Carrillo J, Garcia A, Garcia F, Gonzalez N, Merino A, Alcami J, Bofill M, Yuste E, Gatell JM, Clotet B, Blanco J (2011) A cell-to-cell HIV transfer assay identifies humoral responses with broad neutralization activity. Vaccine 29:5250–5259. doi:10.1016/j.vaccine.2011.05.016
28. Malbec M, Porrot F, Rua R, Horwitz J, Klein F, Halper-Stromberg A, Scheid JF,

Eden C, Mouquet H, Nussenzweig MC, Schwartz O (2013) Broadly neutralizing antibodies that inhibit HIV-1 cell to cell transmission. J Exp Med 210:2813–2821. doi:10.1084/jem.20131244

29. Agosto LM, Zhong P, Munro J, Mothes W (2014) Highly active antiretroviral therapies are effective against HIV-1 cell-to-cell transmission. PLoS Pathog 10:e1003982. doi:10.1371/journal.ppat.1003982
30. Titanji BK, Aasa-Chapman M, Pillay D, Jolly C (2013) Protease inhibitors effectively block cell-to-cell spread of HIV-1 between T cells. Retrovirology 10:161. doi:10.1186/1742-4690-10-161
31. Hubner W, Chen P, Del Portillo A, Liu Y, Gordon RE, Chen BK (2007) Sequence of human immunodeficiency virus type 1 (HIV-1) Gag localization and oligomerization monitored with live confocal imaging of a replication-competent, fluorescently tagged HIV-1. J Virol 81:12596–12607. doi:10.1128/jvi.01088-07
32. Cohen GB, Gandhi RT, Davis DM, Mandelboim O, Chen BK, Strominger JL, Baltimore D (1999) The selective downregulation of class I major histocompatibility complex proteins by HIV-1 protects HIV-infected cells from NK cells. Immunity 10:661–671
33. Adachi A, Gendelman HE, Koenig S, Folks T, Willey R, Rabson A, Martin MA (1986) Production of acquired immunodeficiency syndrome-associated retrovirus in human and nonhuman cells transfected with an infectious molecular clone. J Virol 59:284–291
34. Cavrois M, De Noronha C, Greene WC (2002) A sensitive and specific enzyme-based assay detecting HIV-1 virion fusion in primary T lymphocytes. Nat Biotechnol 20:1151–1154. doi:10.1038/nbt745
35. Tobiume M, Lineberger JE, Lundquist CA, Miller MD, Aiken C (2003) Nef does not affect the efficiency of human immunodeficiency virus type 1 fusion with target cells. J Virol 77:10645–10650
36. Cavrois M, Neidleman J, Bigos M, Greene WC (2004) Fluorescence resonance energy transfer-based HIV-1 virion fusion assay. Methods Mol Biol 263:333–344. doi:10.1385/1-59259-773-4:333

Chapter 3

HIV-1 Capsid Stabilization Assay

Thomas Fricke and Felipe Diaz-Griffero

Abstract

The stability of the HIV-1 core in the cytoplasm is crucial for productive HIV-1 infection. Mutations that stabilize or destabilize the core showed defects in HIV-1 reverse transcription and infection. We developed a novel and simple assay to measure stability of in vitro-assembled HIV-1 CA-NC complexes. This assay allowed us to demonstrate that cytosolic extracts strongly stabilize the HIV-1 core (Fricke et al., J Virol 87:10587–10597, 2013). By using our novel assay, one can measure the ability of different drugs to modulate the stability of in vitro-assembled HIV-1 CA-NC complexes, such as PF74, CAP-1, IXN-053, cyclosporine A, Bi2, and the peptide CAI. We also found that purified CPSF6 (1-321) protein stabilizes in vitro-assembled HIV-1 CA-NC complexes (Fricke et al., J Virol 87:10587–10597, 2013). Here we describe in detail the use of this capsid stability assay. We believe that our assay can be a powerful tool to assess HIV-1 capsid stability in vitro.

Key words HIV-1, Capsid, Stability, Core, Uncoating

1 Introduction

In its simplest definition, uncoating is the shedding of monomeric capsid proteins from the retroviral core or ribonucleoprotein complex. Because only ~40 % of the total capsid in the virion comprises the retroviral core [1–3], a simple model is that the monomeric capsid is in dynamic equilibrium with the assembled capsid (viral core). This implies that the core might exist in a meta-stable state only when the soluble capsid is in high concentration, keeping the equilibrium shifted toward the core formation by mass action. The fact that complexes containing capsid have been detected in the cytoplasm of cells early during infection implies that cellular factors might be involved in stabilization of the core [4, 5].

The capsid protein is required for the successful completion of several early steps of HIV-1 replication: (1) successful infection requires that capsid uncoating occurs during or after reverse transcription [6–9]; (2) elegant experiments have shown that the capsid sequence is the genetic determinant for the ability of

Vinayaka R. Prasad and Ganjam V. Kalpana (eds.), *HIV Protocols*, Methods in Molecular Biology, vol. 1354,
DOI 10.1007/978-1-4939-3046-3_3,

lentiviruses to infect nondividing cells [10–13]; and (3) the stability provided by the capsid protein assembled into the viral core is important for the occurrence of reverse transcription and productive infection [14–16].

Over the years, sensitive assays to biochemically measure core stability have been developed, such as the "fate of the capsid" assay that measures core stability during infection of cells over time [6, 7, 17]. Even though this assay is widely used [7, 8, 14, 17–23], it is intensive and laborious and a more rapid assay to measure core stability is desirable.

Here we present a rapid and simple assay to measure capsid stability in vitro using in vitro-assembled HIV-1 CA-NC complexes as a surrogate for the HIV-1 core [24]. This assay will assist the evaluation of drugs or proteins that change the stability of capsid. Furthermore, this assay could be used to identify novel cellular factors that bind to the HIV-1 core.

2 Materials

Prepare all solutions using ultrapure water and analytical grade reagents. Prepare and store all reagents at room temperature (unless indicated otherwise). Diligently follow all waste disposal regulations when disposing waste materials.

2.1 Capsid Assembly

1. 1 M Tris–HCl, pH 8.0.
2. 5 M NaCl.
3. 10 mg/ml oligo $(TG)_{25}$ (store at –20 °C).
4. HIV-1 CA-NC protein purified as described previously [25].

2.2 Stability Assay

1. *Destabilization buffer (DB) 5×*: 50 mM Tris–HCl (pH 8.0), 300 mM NaCl, 2 mM $MgCl_2$, 10 % (v/v) glycerol, 0.5 % (v/v) (NP-40). Make fresh every time.
2. *Stabilization buffer (SB)*: 10 mM Tris–HCl (pH 8.0), 10 mM KCl, 2 mM $MgCl_2$, 0.5 mM DTT. Store at 4 °C for up to 1 week.
3. PBS 1×.
4. Human 293 T cells.
5. Refrigerated tabletop centrifuge.
6. CAI peptide (amino acid sequence, ITFEDLLDYYGP) and the CAIctrl peptide (amino acid sequence, IYDPTLYGLEFD) (95 % purity) [26]. Prepare stock solutions at 10 mM in dimethyl sulfoxide (DMSO). Store at –20 °C.
7. PF74 (PF-3450074), stock solution 100 mM in DMSO (store at –20 °C) [27].

8. CPIPB (4-{2-[3-(3-chlorophenyl)-1H-pyrazol-4-yl]-1-[3-(1H-imidazol-1-yl)propyl]-1H-benzimidazol-5-yl}benzoic acid dihydrochloride) stock solution of 20 mM in DMSO [28–30]. Store at −20 °C.
9. CPSF6 (1-321) purified as described previously [31].

2.3 Differential Ultracentrifugation

1. 70 % (w/v) sucrose (ACS reagent > 99%purity) in 1× PBS.
2. Ultracentrifuge.
3. SW55 Rotor.
4. SW55 centrifuge tubes.

2.4 PAGE and Western Blot

1. 1× SDS sample buffer: 60 m M Tris–HCl (pH 6.8), 2 % (w/v) SDS, 5 % (v/v) β-mercaptoethanol, 0.02 % (w/v) bromophenol blue, 9 % (v/v) glycerol.
2. 5× SDS sample buffer: 0.3 M Tris–HCl (pH 6.8), 10 % (w/v) SDS, 25 % (v/v) β-mercaptoethanol, 0.1 % (w/v) bromophenol blue, 45 % (v/v) glycerol. Store aliquots at −20 °C.
3. 10 % (w/v) polyacrylamide NuPAGE gel.

3 Methods

To measure HIV-1 core stability, we developed an assay that measures the stability of HIV-1 CA-NC complexes in vitro (Fig. 1). The assay consists of determining the stability of in vitro-assembled HIV-1 CA-NC complexes in the presence of different agents such as proteins or small-molecule inhibitors to subsequently measure the remaining amount of assembled HIV-1 CA-NC complexes using a sucrose cushion. *To measure whether an agent stabilizes the capsid*, in vitro-assembled HIV-1 CA-NC complexes are incubated with the agent in question in destabilization buffer (Fig. 1). The total amount of stabilized capsid complexes is measured using a sucrose cushion, and the amount of stabilized complexes is compared to complexes obtained in the absence of the agent in question. *To measure whether an agent destabilizes the capsid*, in vitro-assembled HIV-1 CA-NC complexes are incubated with the agent in stabilization buffer (Fig. 1). The amount of destabilized capsid complexes is measured by subtracting the amount of complexes obtained in the presence of the agent from the amount of complexes obtained in the absence of the agent.

3.1 Capsid Assembly

1. Add 2.5 µl 1 M Tris–HCl (pH 8.0), 5 µl 5 M NaCl, and 10 µl oligo$(TG)_{25}$ to 25 µl of 10–20 mg/ml purified CA-NC protein (*see* **Note 1**).
2. Add 7.5 µl water to the suspension. The mixture is incubated for 5 min at room temperature. Successful assembly is noted by

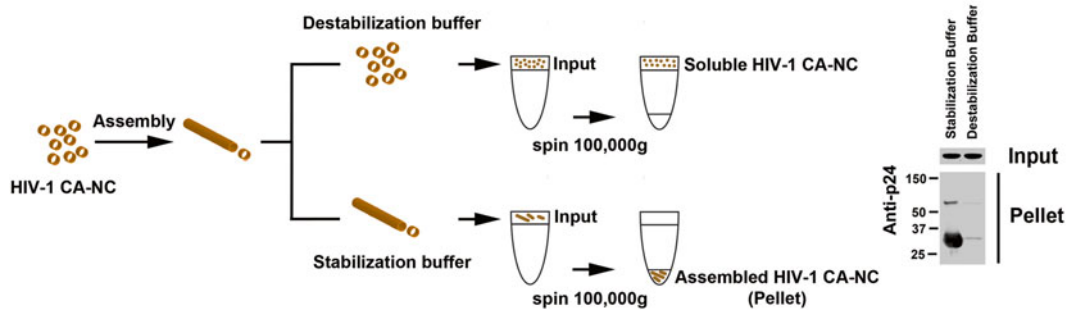

Fig. 1 Diagram of the stabilization assay. In vitro-assembled HIV-1 CA-NC complexes, shown here as tubular structures, are formed by monomeric recombinant HIV-1 CA-NC fusion proteins under highly ionic conditions and recapitulate the surface of the HIV-1 core. When HIV-1 CA-NC complexes are incubated in destabilization buffer, they disassemble spontaneously. Disassembled capsids are layered on top of a 70 % sucrose cushion; however, the disassembled capsid does not cross the cushion after spinning at 100,000 × *g* for 1 h. In contrast, incubation of HIV-1 CA-NC in stabilization buffer preserves the assembled structures, which pellet when layered onto a 70 % sucrose cushion with spinning at 100,000 × *g* for 1 h. Input, a fraction of the sample layered onto the sucrose cushion before the centrifugation step. Pellet, a fraction of the capsid pelleted after the sample has been centrifuged at 100,000 × *g* for 1 h. Input and pellet samples were analyzed by Western blotting using anti-p24 antibodies.

the appearance of white complexes in solution. The size of the complexes can be determined by dynamic light scattering (*see* **Note 2**).

3.2 Stabilization Assay

1. Prepare up to six Eppendorf test tubes with 400 µl stabilization buffer. Add additional 100 µl stabilization buffer in the first test tube. To the other test tubes, add 100 µl of 5× destabilization buffer. Final volume is 500 µl.
2. Add the indicated agents to test tubes 3–6 (Fig. 2a). Incubate 3 µl of in vitro-assembled HIV-1 CA-NC complexes in the presence of PF74, CAI peptide, CAIctrl peptide, or purified CPSF6 (1-321) (Fig. 2a). As a second example, the ability of CPIPB to change the stability of in vitro-assembled HIV-1 CA-NC complexes is determined. For this purpose, incubate 3 µl of in vitro-assembled HIV-1 CA-NC complexes in the presence of different concentrations of CPIPB (Fig. 3) (*see* **Note 3**).
3. Incubate 3 µl of in vitro-assembled HIV-1 CA-NC complexes with the different agents at room temperature for 1 h (*see* **Notes 4** and **5**).
4. Store an aliquot of this mixture at −20 °C for further analysis, henceforth referred to as "input." For this purpose, add 5× SDS sample buffer. Proceed with ultracentrifugation below.

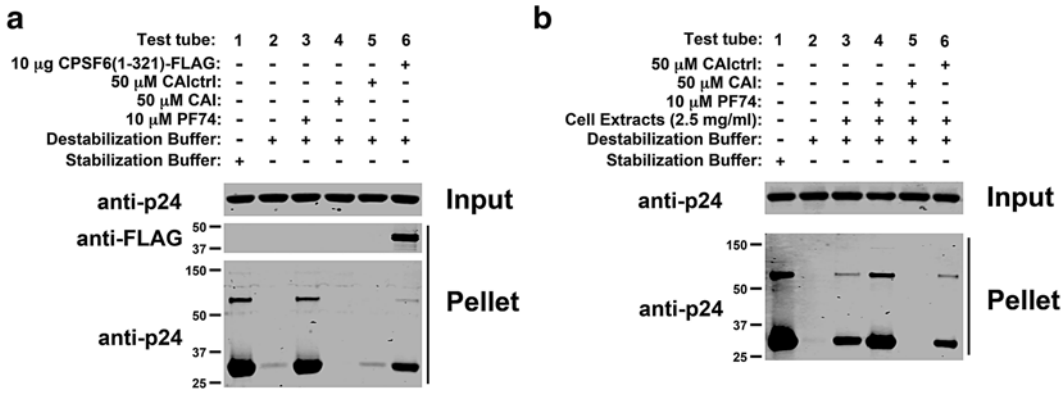

Fig. 2 PF74 and CPSF6 (1-321) increase the stability of in vitro-assembled HIV-1 CA-NC complexes, whereas the CAI peptide decreases the stability. In contrast, the CAI peptide with a randomized sequence (CAIctrl) did not show an effect on the stability of HIV-1 CA-NC complexes. The stability of HIV-1 CA-NC complexes in destabilization buffer (stabilization assay) (**a**) or destabilization buffer in cell extracts (destabilization assay) (**b**) supplemented with 10 μM PF74, 50 μM CAI, or CAIctrl peptide was measured. The assay without cellular extract was performed additionally using 10 μg of the protein CPSF6 (amino acids 1-321).

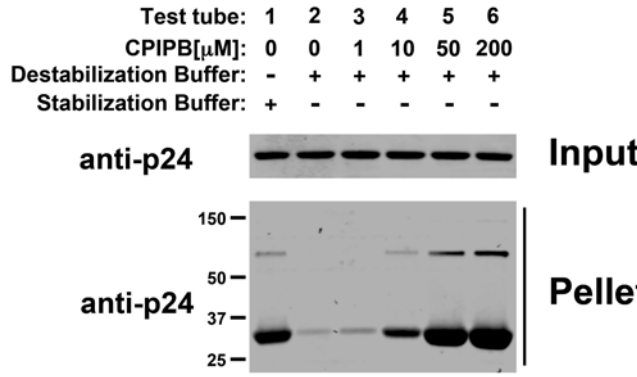

Fig. 3 The capsid drug CPIPB (4-{2-[3-(3-chlorophenyl)-1H-pyrazol-4-yl]-1-[3-(1H-imidazol-1-yl)propyl]-1H-benzimidazol-5-yl}benzoic acid dihydrochloride) stabilizes in vitro-assembled HIV-1 CA-NC complexes. The stability of HIV-1 CA-NC complexes in destabilization buffer using increasing concentrations of the drug CPIPB was measured. CPIPB has been shown previously to strongly increase HIV-1 capsid crystallization and competes with the novel restriction factor M×B for binding to the HIV-1 capsid [29, 30].

3.3 Destabilization Assay

1. Culture 293 T cells in DMEM containing 10 % FBS and antibiotics (penicillin and streptomycin) in an incubator calibrated at 37 °C and 5 % CO_2. Cells are detached from nearly confluent dishes with trypsin-EDTA. Five million cells are seeded in 10 ml medium in 100 mm plastic culture dishes and cultured for 1 day prior to the assay. The next day, cultures will have grown to approximately 100 % confluence.

Discard the media by decanting and add 400 µl of stabilization buffer (*see* **Note 6**).

2. Scrape the cells on the 100 mm plate using a cell scraper and transfer cells into 1.5 ml tube.
3. Incubate sample for 15 min on ice.
4. Centrifuge with maximum speed using a 4 °C refrigerated tabletop centrifuge.
5. Carefully take the tubes from the centrifuge and transfer the supernatant (cell extract) into a fresh tube.
6. Prepare up to six test tubes and fill the first two with 400 µl stabilization buffer. Add 400 µl of cell extracts resuspended in stabilization buffer into test tubes 3–6. Add additional 100 µl of stabilization buffer in the first test tube. To the test tubes 2–6, add 100 µl of 5× destabilization buffer.
7. Add the agents/drugs you would like to assay to test tubes 4–6. In this example, the well-known HIV-1 capsid drug PF74 and the peptides CAI and CAIctrl are tested (Fig. 2b) (*see* **Note 3**).
8. Add 3 µl of in vitro-assembled HIV-1 CA-NC complexes to all test tubes, and incubate the mixture at room temperature for 1 h (*see* **Notes 4** and **5**).
9. An aliquot of this mixture, henceforth referred to as "input," was stored at –20 °C for further analysis. For this purpose, add 5× SDS sample buffer.

3.4 Ultra-centrifugation

1. Prepare six centrifuge tubes containing 3 ml 70 % sucrose at 4 °C (*see* **Note 7**). Check the sucrose levels and if necessary adjust using a 200 µl pipette (keep the tubes in the cold room until needed).
2. Load the sample from Subheading 3.2, **step 4** above carefully on top of the sucrose cushion (*see* **Note 8**).
3. Centrifuge at 100,000×*g* (30,000 rpm using a SW55 rotor) for 1 h at 4 °C.
4. Aspirate the supernatant carefully and resuspend pellet in 1× SDS loading buffer (*see* **Note 9**).

3.5 PAGE and Western Blot

1. Load input and pellet with a molecular size marker on a 10 % acrylamide NuPAGE gel.
2. Analyze gel by standard western blot using anti-p24 antibodies against HIV-1 capsid and anti-FLAG antibodies to detect CPSF6 (1-321).

4 Notes

1. The protein should assemble within 5 min; the solution turns into a white suspension. These complexes could be used for at least 5 days.
2. The capsid should be assembled at least one night before the experiment and stored at 4 °C.
3. If the drug is soluble in an organic solvent, then add the same amount of solvent to the control in test tubes 1 and 2.
4. Use the 10 μl pipette about halfway into the solution and slowly add the capsid.
5. Do not shake the tube during the incubation time.
6. Remove remaining media using vacuum aspirator.
7. Use a serological 5 ml pipette and load 3.0 ml of the 70 % sucrose solution into the SW55 tube. Consider that the 5 ml serological pipette retains at least 0.5 ml of the sucrose.
8. Mix the sample carefully before applying to the sucrose cushion by pipetting once up and down.
9. First remove the supernatant carefully, change the tip and remove the sucrose layer, and allow time for the sucrose to move down from the tube walls.

Acknowledgments

Projects AI087390, AI10282401, R56AI108432, and AI104476 to F.D.-G supported this work. We are grateful to the NIH HIV-1/AIDS repository for providing reagents such as antibodies and small-molecule inhibitors that were crucial for this work.

References

1. Briggs JA, Simon MN, Gross I, Krausslich HG, Fuller SD, Vogt VM, Johnson MC (2004) The stoichiometry of Gag protein in HIV-1. Nat Struct Mol Biol 11:672–675
2. Briggs JA, Wilk T, Welker R, Krausslich HG, Fuller SD (2003) Structural organization of authentic, mature HIV-1 virions and cores. EMBO J 22:1707–1715
3. Lanman J, Lam TT, Emmett MR, Marshall AG, Sakalian M, Prevelige PE Jr (2004) Key interactions in HIV-1 maturation identified by hydrogen-deuterium exchange. Nat Struct Mol Biol 11:676–677
4. McDonald D, Vodicka MA, Lucero G, Svitkina TM, Borisy GG, Emerman M, Hope TJ (2002) Visualization of the intracellular behavior of HIV in living cells. J Cell Biol 159:441–452
5. Fassati A, Goff SP (2001) Characterization of intracellular reverse transcription complexes of human immunodeficiency virus type 1. J Virol 75:3626–3635
6. Stremlau M, Perron M, Lee M, Li Y, Song B, Javanbakht H, Diaz-Griffero F, Anderson DJ, Sundquist WI, Sodroski J (2006) Specific recognition and accelerated uncoating of retroviral

capsids by the TRIM5alpha restriction factor. Proc Natl Acad Sci U S A 103:5514–5519

7. Diaz-Griffero F, Kar A, Lee M, Stremlau M, Poeschla E, Sodroski J (2007) Comparative requirements for the restriction of retrovirus infection by TRIM5alpha and TRIMCyp. Virology 369:400–410, Epub 2007 Oct 24
8. Roa A, Hayashi F, Yang Y, Lienlaf M, Zhou J, Shi J, Watanabe S, Kigawa T, Yokoyama S, Aiken C, Diaz-Griffero F (2012) RING domain mutations uncouple TRIM5alpha restriction of HIV-1 from inhibition of reverse transcription and acceleration of uncoating. J Virol 86:1717–1727
9. Arfi V, Lienard J, Nguyen XN, Berger G, Rigal D, Darlix JL, Cimarelli A (2009) Characterization of the behavior of functional viral genomes during the early steps of human immunodeficiency virus type 1 infection. J Virol 83:7524–7535
10. Yamashita M, Emerman M (2004) Capsid is a dominant determinant of retrovirus infectivity in nondividing cells. J Virol 78:5670–5678
11. Yamashita M, Perez O, Hope TJ, Emerman M (2007) Evidence for direct involvement of the capsid protein in HIV infection of nondividing cells. PLoS Pathog 3:1502–1510
12. Yamashita M, Emerman M (2006) Retroviral infection of non-dividing cells: old and new perspectives. Virology 344:88–93
13. Diaz-Griffero F (2012) The role of TNPO3 in HIV-1 replication. Mol Biol Int 2012:868597
14. Yang Y, Fricke T, Diaz-Griffero F (2013) Inhibition of reverse transcriptase activity increases stability of the HIV-1 core. J Virol 87:683–687
15. Forshey BM, von Schwedler U, Sundquist WI, Aiken C (2002) Formation of a human immunodeficiency virus type 1 core of optimal stability is crucial for viral replication. J Virol 76:5667–5677
16. Ohagen A, Gabuzda D (2000) Role of Vif in stability of the human immunodeficiency virus type 1 core. J Virol 74:11055–11066
17. Diaz-Griffero F, Kar A, Perron M, Xiang SH, Javanbakht H, Li X, Sodroski J (2007) Modulation of retroviral restriction and proteasome inhibitor-resistant turnover by changes in the TRIM5alpha B-box 2 domain. J Virol 81:10362–10378
18. Shi J, Zhou J, Shah VB, Aiken C, Whitby K (2011) Small-molecule inhibition of human immunodeficiency virus type 1 infection by virus capsid destabilization. J Virol 85:542–549
19. De Iaco A, Santoni F, Vannier A, Guipponi M, Antonarakis S, Luban J (2013) TNPO3 protects HIV-1 replication from CPSF6-mediated capsid stabilization in the host cell cytoplasm. Retrovirology 10:20
20. Perron MJ, Stremlau M, Lee M, Javanbakht H, Song B, Sodroski J (2007) The human TRIM5alpha restriction factor mediates accelerated uncoating of the N-tropic murine leukemia virus capsid. J Virol 81:2138–2148
21. Diaz-Griffero F, Perron M, McGee-Estrada K, Hanna R, Maillard PV, Trono D, Sodroski J (2008) A human TRIM5alpha B30.2/SPRY domain mutant gains the ability to restrict and prematurely uncoat B-tropic murine leukemia virus. Virology 378:233–242
22. Ohkura S, Goldstone DC, Yap MW, Holden-Dye K, Taylor IA, Stoye JP (2011) Novel escape mutants suggest an extensive TRIM5alpha binding site spanning the entire outer surface of the murine leukemia virus capsid protein. PLoS Pathog 7, e1002011
23. Berube J, Bouchard A, Berthoux L (2007) Both TRIM5alpha and TRIMCyp have only weak antiviral activity in canine D17 cells. Retrovirology 4:68
24. Fricke T, Brandariz-Nunez A, Wang X, Smith AB 3rd, Diaz-Griffero F (2013) Human cytosolic extracts stabilize the HIV-1 core. J Virol 87:10587–10597
25. Ganser BK, Li S, Klishko VY, Finch JT, Sundquist WI (1999) Assembly and analysis of conical models for the HIV-1 core. Science 283:80–83
26. Sticht J, Humbert M, Findlow S, Bodem J, Muller B, Dietrich U, Werner J, Krausslich HG (2005) A peptide inhibitor of HIV-1 assembly *in vitro*. Nat Struct Mol Biol 12: 671–677
27. Blair WS, Pickford C, Irving SL, Brown DG, Anderson M, Bazin R, Cao J, Ciaramella G, Isaacson J, Jackson L, Hunt R, Kjerrstrom A, Nieman JA, Patick AK, Perros M, Scott AD, Whitby K, Wu H, Butler SL (2010) HIV capsid is a tractable target for small molecule therapeutic intervention. PLoS Pathog 6, e1001220
28. Goudreau N, Lemke CT, Faucher AM, Grand-Maitre C, Goulet S, Lacoste JE, Rancourt J, Malenfant E, Mercier JF, Titolo S, Mason SW (2013) Novel inhibitor binding site discovery on HIV-1 capsid N-terminal domain by NMR and X-ray crystallography. ACS Chem Biol 8:1074–1082
29. Lemke CT, Titolo S, Goudreau N, Faucher AM, Mason SW, Bonneau P (2013) A novel inhibitor-binding site on the HIV-1 capsid N-terminal domain leads to improved

crystallization via compound-mediated dimerization. Acta Crystallogr D Biol Crystallogr 69:1115–1123

30. Fricke T, White TE, Schulte B, de Souza Aranha Vieira DA, Dharan A, Campbell EM, Brandariz-Nunez A, Diaz-Griffero F (2014) MxB binds to the HIV-1 core and prevents the uncoating process of HIV-1. Retrovirology 11:68
31. Fricke T, Valle-Casuso JC, White TE, Brandariz-Nunez A, Bosche WJ, Reszka N, Gorelick R, Diaz-Griffero F (2013) The ability of TNPO3-depleted cells to inhibit HIV-1 infection requires CPSF6. Retrovirology 10:46

Chapter 4

Detection and Tracking of Dual-Labeled HIV Particles Using Wide-Field Live Cell Imaging to Follow Viral Core Integrity

João I. Mamede and Thomas J. Hope

Abstract

Live cell imaging is a valuable technique that allows the characterization of the dynamic processes of the HIV-1 life cycle. Here, we present a method of production and imaging of dual-labeled HIV viral particles that allows the visualization of two events. Varying release of the intravirion fluid phase marker reveals virion fusion and the loss of the integrity of HIV viral cores with the use of live wide-field fluorescent microscopy.

Key words Live cell imaging, HIV uncoating, HIV fusion, Wide-field microscopy, HIV early steps of infection, HIV viral core

1 Introduction

The two steps that define retroviral infections are the reverse transcription of the positive sense viral RNA genome into double-stranded DNA and the integration of this reverse-transcribed DNA into the host genome. Our understanding of these earliest aspects of the HIV replication cycle remain incomplete even though there have been significant recent advances in our knowledge of the viral and cellular determinants in the pathway of infection. Interestingly, determinants in the viral capsid can have a large influence on events that happen in the nucleus including the pathway of nuclear import and integration site selection. During virion maturation, the capsid (CA) protein assembles into a conical shell that contains the viral genome known as the "viral core." This structure is able to assemble through the interaction of CA monomers that form hexameric and pentameric rings, which arrange themselves into a conical structure that shields and contains several viral proteins such as RT, NC, IN, PR, Vpr, the viral RNA, as well as several host cell proteins such as cyclophilin A.

Vinayaka R. Prasad and Ganjam V. Kalpana (eds.), *HIV Protocols*, Methods in Molecular Biology, vol. 1354,
DOI 10.1007/978-1-4939-3046-3_4,

During the progression of reverse transcription, the conical capsid is lost. The timing of the disassembly of the conical core structure, a process known as uncoating, remains controversial and appears to be dynamic. For example, multiple lines of evidence have revealed a relationship between reverse transcription and the disassembly of the viral core. However, details of the changes in the conical capsid structure are poorly defined relating to the spatial, temporal, and mechanistic specifics of HIV-1 uncoating. Single particle imaging of HIV has revealed important details about the viral life cycle informing our understanding of trafficking and the step-progressive uncoating from in situ imaging of fixed cells [1–6]. However, an in vivo fluorescent assay needs to be developed to provide insights into the dynamics and kinetics of the uncoating process. Here, we present a detailed method for live cell imaging of HIV-1, allowing changes in the integrity of the conical capsid to be detected in real time. These changes in the conical capsid are considered to be the earliest steps in the process of uncoating.

It has been previously reported that Vpr remains attached to HIV-1 reverse transcribing complexes (RTC) after the uncoating process has taken place as revealed by the loss of readily detectable CA [3, 4, 7]. Based on these observations, HIV-1 particles can be tracked by fusing fluorescent proteins to Vpr, such as GFP, mCherry, or tdTomato [3]. Recently, a new system has been developed that labels HIV particles using a fluid phase marker. This is accomplished by the insertion of a fluorescent protein (GFP or mCherry) between the matrix (MA) and CA cleavage sites of Gag. This insertion allows the selected fluorophore to be released from Gag by proteolytic cleavage and trapped inside the virion upon budding [8]. The fluid phase fluorescent protein is located both within the assembled core and in the virion space between the core and the viral membrane. Based on the calculation of a volume estimate for a virion, only a minority of the fluid phase marker (eGFP or mCherry) will be located in the intact conical core. We have previously reported that the fluid phase marker can be retained within intact cores as shown by membrane-stripping ultracentrifugations and with a TRIM5 capture assay in the presence of MG132 [9]. With the knowledge of these data, it is possible to perform live cell time-lapse imaging using dual-labeled HIV-1 particles. Therefore, by using this system during infection, we anticipate two changes in the levels of intravirion fluid phase markers that co-localize with signal from tagged Vpr. The first loss of fluid phase marker will take place upon fusion, as has been previously reported [10]. However, the subsequent complete loss of the fluid phase marker reveals changes in the integrity of the conical capsid structure, allowing the fluorescent protein to escape the reverse transcribing complex, a change consistent with the initiation of uncoating. This system can be utilized to provide important new

insights into the process of uncoating and the behavior of the HIV viral particles and the genome moving toward its ultimate goal of integrating into the target cell genome. Here, we present a method to produce and image the infection of HIV-iGFP + CherryVpr or HIV-iCherry + GFPVpr viruses.

2 Materials

2.1 Cell Culture Materials

1. HEK-293 T cells (ATCC). Keep in culture with DMEM supplemented with 10 % FBS and 2 mM L-glutamine.
2. CHO-pgsA-745 cells. Keep in culture with DMEM supplemented with 10 % FBS, 2 mM L-glutamine, and MEM-NEAA (*see* **Note 1**).
3. Dulbecco's Modified Eagle's Medium (DMEM).
4. Fetal bovine serum (FBS).
5. FluoroBrite DMEM Media (Life Technologies).
6. L-Glutamine.
7. MEM Non-Essential Amino Acids Solution (MEM-NEAA).
8. Polybrene (hexadimethrine bromide).
9. 10 cm diameter culture dishes.
10. 0.45 μm filters.
11. 20 ml syringes.
12. Cryovials.

2.2 Virus Production

1. PEI 1 mg/ml in water.
2. HIV-Gag-iGFPΔEnv (AIDS Reagent Repository) or HIV-Gag-iCherryΔEnv plasmids. These molecular clones of HIV (pNL4-3 derived) had GFP or mCherry inserted in *gag*. The fluorophores are coded between MA and CA. After HIV-1 protease cleavage of MA and CA, the fluorophore is trapped inside the virion [8, 10].
3. The vector pCMV-VSV-G that codes for the G-protein of vesicular stomatitis virus. This protein is used to pseudotype the viral particles with an envelope protein capable of infecting a wide range of cells through the interaction with LDL receptor, therefore mimicking VSV tropism [11].
4. pGFPVpr/pCherryVpr—HIV-1 Vpr protein fusions can be used to track HIV-1 RTCs. These plasmids provide a fusion protein between either GFP or mCherry and Vpr [1, 3].
5. (*Optional*) pSPAX2 or pCMV-dR8.2 dVpr. Second- or third-generation lentiviral packaging plasmid (*gag-pol*).

2.3 Wide-Field Imaging Components

1. The protocol below was optimized for a DeltaVision wide-field microscope equipped with an EMCCD camera, a SSI light path, and a 100× Olympus Lens. The system must be located within the appropriate biocontainment environment to maintain safe experimental conditions.
2. Delta T Culture Dish Controller (Bioptechs).
3. Delta TPG Culture Dishes 0.17 mm thick (Bioptechs).
4. Lens heater system: Objective Heater Controller (Bioptechs) and an Objective Heater adapted to the diameter of the objective (Bioptechs).
5. CO_2 system with blood gas mixture tank (5 % CO_2, 20 % oxygen).
6. Light-Duty Tissue Wipers.
7. (*Optional*) OxyFluor (OXYRASE) at a 1:200 dilution supplemented with 15 mM sodium DL-lactate.
8. (*Optional*) DRAQ5 for nuclear staining.

2.4 Data Analysis Software

Many data analysis software are available (Imaris, ImageJ/Fiji, and IDL or python libraries for Crocker and Grier algorithms). The analysis described below was performed with the TrackMate Plugin for ImageJ according to the author's description [12].

3 Methods

Carry out all procedures that involve cell lines at 37 °C—5 % CO_2 unless otherwise specified.

3.1 Dual-Labeled HIV Production

Day 1: Plate 1.5×10^6 HEK-293 T cells into 10 cm diameter cell culture plates.

Day 0: *Transfect cells*:

In a 1.5 ml Eppendorf tube, mix:

1. 6 μg of either HIV-Gag-iGFPΔEnv or HIV-Gag-iCherryΔEnv plasmid (for hybrid viruses containing WT *gag* with higher viral titer mix 3 μg of pSPAX2 with 3 μg of HIV-Gag-iGFPΔEnv/HIV-Gag-iCherryΔEnvplasmid).
2. 4 μg of pCMV-VSVg (to pseudotype the virions with G-protein from vesicular stomatitis virus).
3. 1.5 μg of pCMV-CherryVpr/pCMV-GFPVpr (Vpr accompanies the virus through the process of fusion, uncoating, and reverse transcription [4]). If using iGFP, complement with pCMV-CherryVpr (or vice versa for fluorescent protein tag).
4. 1000 μl serum-free DMEM/OptiMEM.
5. Add 40 μl of PEI.

6. Shake and incubate for 15 min. (Do not vortex since it might cause DNA shearing.)
7. Apply the solution drop-by-drop to the 10 cm HEK-293 T cell culture plate.

   Day 1 (14–16 h post-transfection): Change the medium with prewarmed DMEM.

   Day 2 (36–48 h post-transfection):

   1. Recover the supernatant with an appropriate-sized syringe and filter through a 0.45 μm filter.
   2. Aliquot into Cryovials and store at −80 °C. Titer the viruses to determine the infectivity of your stocks. A virus with a titer higher than 1×10^4 TU/ml (transducing units per ml) is highly recommended for an efficient experimentation (*see* **Note 2**).

3.2 Preparing CHO-pgsA-745 Cells for Imaging

Day 2: Plate 40×10^3 CHO-pgsA-745 cells on a DeltaT dish diluted with appropriate DMEM medium (DMEM supplemented with 10 % FBS, NEAA, and L-glutamine) up to a volume of 1.5 ml.

Day 0:

1. Change the DMEM medium with 1.5 ml of prewarmed *20 % FBS*-FluoroBrite DMEM Media (or phenol red-free DMEM) complemented with MEM-NEAA and L-glutamine.
2. Add polybrene to a final concentration of 5 μg/μl.

If nuclear staining is required for cell or nuclear identification (*see* **Note 3**).

If photobleaching and phototoxicity occur (*see* **Note 4**).

3.3 Setting Up the Imaging System

1. Install an appropriate DeltaT plate holder into the microscope.
2. Turn on the microscope heating system several hours prior to the experiment (overnight if possible), allowing the system temperature to stabilize at 37 °C. Turn on both the environmental chamber and the lens warmer. Both temperature-regulating systems are necessary for temperature stability.
3. Carefully, apply a drop of imaging oil to the objective.
4. In case of the use of a non-sealed lid: minutes prior to the imaging process and without compromising the microscope integrity, humidify the area around the DeltaT holder in order to avoid evaporation to the fullest, and, optionally, place tissue wipers soaked with deionized water around the culture plate.
5. Set up the blood gas mixture with a cover on top of the DeltaT dish holder in order to provide CO_2 to stabilize the pH level. Start diffusing the system several minutes before imaging.

6. Place the DeltaT dish containing the cells in the appropriate DeltaT dish holder.
7. Cover the plate with the included lid to avoid evaporation to the fullest. Preferably, utilize a transparent lid with the DeltaT, so that manual eye focus is possible. In the case of the requirement of differential interference contrast (DIC, white light), the use of a clear DeltaT lid is absolutely required (*see* **Note 5**).
8. (*Optional*) Focus at the bottom of the plate in order to optimize the acquisition to the whole cell. Configure the microscope so that the software recognizes the bottom of the plate as the setup point.
9. Add multiple points to the visit list (*see* **Note 6** for details on multiple visits points).
10. Utilize the ultimate focus system (or similar focus maintaining system) to maintain focus throughout the whole acquisition (*see* **Note 7** for details).
11. Set up the acquisition thickness according to the cell type (number of z's), in order to image the whole cell from top to bottom. CHO-pgSA-745 cells usually have a thickness from 6 to 9 μm. Set up the Z-stacking spacing between 0.4 and 0.6 μm.
12. Set up the time-lapse settings: the time between acquisitions per cell should depend on the study at hand. A quick process with multiple steps, several intensity changes, and a high number of particles and/or high movement of viral particles requires a higher rate of acquired frames/minute. A slow process with particles that have a low displacement rate requires a lower rate of acquired frames/minute. For example, the settings for a good measurement of HIV-VSVg membrane fusion would be 1 min per z-stack acquisition for a total duration of 45–60 mins.
13. Add viruses to the medium in order to have approximately 10–15 particles per field of view (empirical assessment is required; a typical volume for the production referred above can vary from 10 to 50 μl).
14. (*Optional*) Check if the selected "visit points" maintained focus; if not, reset the correct focus of the previously selected visit points. Maintaining focus over extended periods is necessary for a successful time-lapse experiment. If problems arise, return to **step 8** and begin again.

3.4 Setting Up the System: Choosing the Right Amount of Light to Correctly Detect Dual-Labeled HIV-1 Particles

1. Set up transmission and exposure for every required wavelength so that the particles have a signal-to-noise ratio that will allow post-acquisition analyses. An increase on the amount of light transmission increases photobleaching, while a lower transmission and higher exposure time might result in spatial disparities to the particles between acquisition wavelengths, causing a "tail-chase" effect (*see* **Note 8**). Optimize according

to your system. The optimal amount of light is highly dependent on the particular microscope; therefore, it should be empirically assessed according to the signal-to-noise ratio needed for detection and analysis.

2. Start acquisition.

3.5 Signal-to-Noise Ratio Optimization

1. Deconvolve the image files in order to increase signal-to-noise ratio.
2. Z project the files using "max intensity" method (if 2D analysis is preferred).
3. Assure yourself that you are able to perform the required analysis with the present signal-to-noise ratio with the software of your choice. If it is not possible to correctly analyze the expected phenotype with the current settings, a higher exposure time or transmission percentage settings might be required.

   An example of acquired time-lapses and analysis of deconvolved Z projections is shown in Fig. 1.

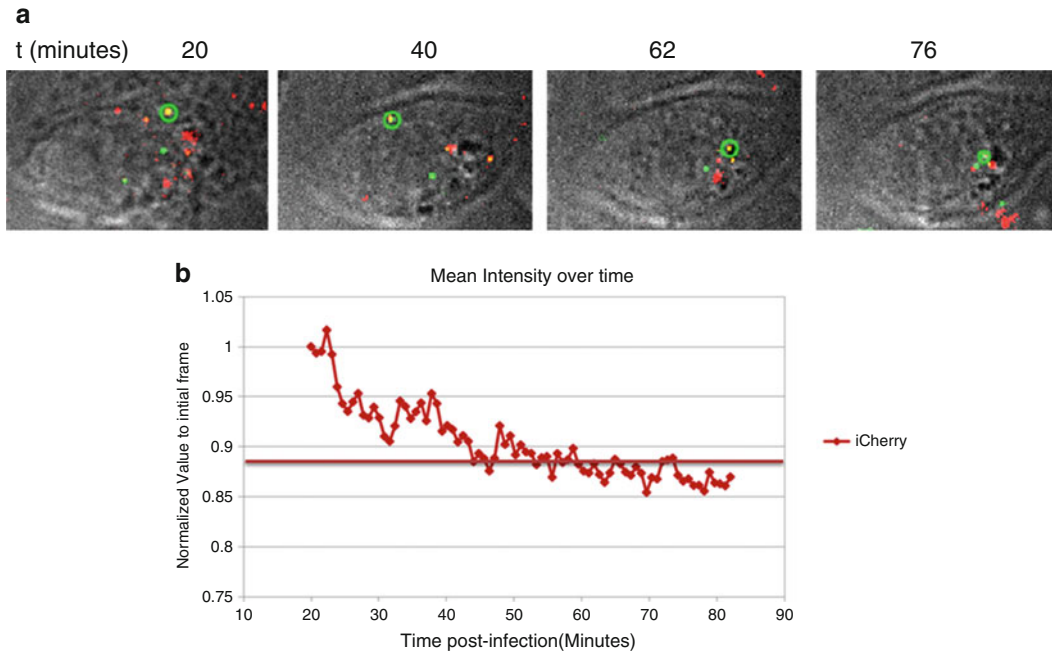

Fig. 1 Time-lapse wide-field imaging of dual-labeled iCherry/GFPVpr HIV-1 particles. (**a**) CHO-pgsA-745 cells were imaged for 60 min (starting 20 min post-infection); the snapshots represent different time points. GFP-tagged Vpr (emission at 528 nm) is represented in green; iCherry is represented in red (emission at 608 nm); and DIC acquisition is represented in gray. The images were Deconvolved and Z-projected operating Softworks software from DeltaVision. The tracked particle of interest is encircled in green. (**b**) GFPVpr particles were tracked with TrackMate plugin for ImageJ, and the mean intensities for the acquisition at 608 nm (mCherry) of the particle of interest are represented. An initial fusion event is observed around 22 min post-infection, and a second drop of signal is observed around 40 minutes, which is believed to be uncoating. Horizontal bar represent the limit of detection to the given wavelength.

4. Be sure that you are able to detect all the desired particles. For instance, while employing the iGFP/iCherry system, there is a first drop of intensity at the moment of membrane fusion; if the level of light and exposure are not properly set, a perception of full loss of signal might occur despite the remaining of fluorophore inside a given number of particles.

   (For an example of how to set up the exposure/transmission values, *see* **Note 9**.)

5. Repeat the setting-up process with cells that have not been infected with fluorescent viral particles. For this comparison with infected cells, the same transmission and exposure conditions have to be used. This control is crucial to ascertain that autofluorescence events are not being confused with real particle events.

3.6 Setting Up the System: Reducing Photobleaching and Phototoxicity

Two of the biggest challenges to live cell imaging are photobleaching and phototoxicity. While performing live cell imaging experiments, there is a need of fast acquisition of multiple xy "snapshots" to produce a z-stack that encompasses the whole cell. For a single time point, it is not uncommon to take 30–50 snapshots to a given cell. The amount of light that is applied to the sample might have the undesired effects of photobleaching and phototoxicity. Even though these processes are interconnected and the steps that are taken to prevent them are frequently the same, these are two distinct phenomena. Photobleaching is the process of the irreversible destruction of a fluorophore or dye upon light exposure, while phototoxicity is the process where continuous or repetitive imaging leads to a deregulation of the cell (or other biological processes sensitive to light), resulting in cell death or the incapacity to image the desired phenotype. For an extended review and further study, read Diaspro et al. and Tinevez et al. [13, 14]. Here we will report several procedures that might be taken to reduce problems arising due to both of these phenomena.

The measures that are taken to reduce photobleaching are generally effective in reducing phototoxicity, and vice versa, since both optimizations rely on both the reduction of the light that is applied to the sample and the reduction of toxic species in the sample.

1. Reducing the amount of acquisitions.
   While performing live imaging experiments, the experimenter has to adapt their settings to the specifics of the experiment at hand. For example, if the phenotype that is meant to be observed is in the order of minutes with particles that are relatively static in the field of view, it might be futile to acquire an image every 200 ms. If a longer time interval between acquisitions is possible, this will reduce the amount of light that is applied to the sample, therefore reducing both photobleaching and phototoxicity.

2. Binning
   Binning is a process that sums the result of pixel signals at the level of the camera.

   Augmenting the binning from 1×1 to 2×2, or higher, results in an increase of signal-to-noise ratio while sacrificing resolution. Image binning sums the values of pixel intensities (4 pixels in a 2×2 setting), while leaving the noise relatively the same as the value of one pixel, thereby increasing the signal-to-noise ratio (up to 8:1 in a 2×2 setting). This higher signal-to-noise ratio will allow us to decrease the amount of light that is applied to the sample and therefore protect the fluorophores.

3. Z-stack spacing.
   Yet another optimization that can diminish the total amount of light applied to a cell is to increase the spacing between z's (z-stack spacing). Again, this will always depend on the experiment at hand. Regarding the experiment portrayed in this text, the major goal is to measure the timing of viral particles fusion or uncoating; therefore, resolution in z is not an absolute priority. Throughout optimization experiments, it was observed that a stacking of 0.55 μm would be enough for the study at hand. Again, reducing the spacing between z's will reduce the number of acquisitions and exposures to the sample and consequently reduce the amount of light applied to the sample.

4. Oxygen scavengers.
   The repetitive and intense amount of light that is used to detect fluorescence results in the production of oxygen free radicals. Production of these species results in a reduction of fluorescence duration and fluorescence intensity. Moreover, oxygen free radicals might also lead to a toxic environment to both the cell and the viral particles that often result in the loss of the biological function under study (phototoxicity). Oxyrase/OxyFluor (www.oxyrase.com) is an enzyme system that removes dissolved oxygen from the cell environment, therefore protecting the fluorophores from photobleaching and cells from oxygen free radicals.

4 Notes

1. This cell line was derived from CHO-K1 cells. It was screened for deficiency in proteoglycan synthesis, resulting in a lower level of particles that are lost due to deleterious endocytosis [15].

2. Calculate transducing units/ml with the following equation:

$$\text{Titer}\left(\frac{\text{Transducing units}}{\text{ml}}\right) = \frac{\text{Number of target cells} \times \frac{\%\ \text{infected cells}}{100}}{\text{Volume of supernatant (ml)}}$$

3. Add DRAQ5 if nuclear staining is desired. DRAQ5 is preferred over live-Hoechst since the presence of UV light results in significant photobleaching. Other dyes might be added for cell tracing, such as the lipophilic tracers, Dil, DiO, DiD, DiA, and DiR.
4. In case of a high level of photobleaching and phototoxicity, add an oxygen scavenger, such as OxyFluor at 100x dilution complemented with 15 mM of sodium DL-lactate. This will decrease photobleaching and phototoxicity.
5. If differential interference contrast (DIC) will be used during acquisition, for instance, to detect cell position, clear dishes are required. If only fluorescence-based acquisition is required, the black version will allow a lower interference from the environmental light in the room.
6. In order to acquire as much data as possible, multiple visit points should be selected. The areas of acquisition should be as distant as possible to each other to avoid photobleaching/phototoxicity effects. The chosen amount of points should take into account the time it takes to acquire one cell in every wavelength and the full z-stack and the desired frame-rate per cell.
7. Regarding the example in Fig. 1, the ultimate focus settings used were move threshold = 300 nm, number of iterations = 2, and performed in every time point = 2. Note that performing higher numbers of iterations in between time points will increase the acquisition time.
8. In order to minimize "tail-chase" spatial effects to the acquired particles, set up the microscope to acquire every wavelength first and then z, possibly sacrificing some acquisition speed per cell.
9. In order to access the correct amount of light that is needed to detect HIV particles, an accumulation of fused viral cores has to be performed. It is possible to accumulate HIV-1 viral cores containing GFP/mCherry using cells expressing TRIM5 proteins (TRIM5α or TRIMcypA), in the presence of MG132 [9]. With this system, a certain amount of fused particles will accumulate in TRIM5 bodies since a high number of intact viral cones contain GFP/mCherry proteins.

References

1. Fassati A, Goff SP (2001) Characterization of intracellular reverse transcription complexes of human immunodeficiency virus type 1. J Virol 75:3626–3635. doi:10.1128/JVI.75.8.3626-3635.2001
2. Goff SP (2001) Intracellular trafficking of retroviral genomes during the early phase of infection: viral exploitation of cellular pathways. J Gene Med 3:517–528. doi:10.1002/1521-2254(200111)3:6<517::AID-JGM234>3.0.CO;2-E
3. McDonald D, Vodicka MA, Lucero G, Svitkina TM, Borisy GG, Emerman M, Hope TJ (2002) Visualization of the intracellular behavior of HIV in living cells. J Cell Biol 159:441–452. doi:10.1083/jcb.200203150
4. Hulme AE, Perez O, Hope TJ (2011) Complementary assays reveal a relationship between HIV-1 uncoating and reverse transcription. Proc Natl Acad Sci U S A 108:9975–9980. doi:10.1073/pnas.1014522108
5. Nermut MV, Fassati A (2003) Structural analyses of purified human immunodeficiency virus type 1 intracellular reverse transcription complexes. J Virol 77:8196–8206
6. Warrilow D, Tachedjian G, Harrich D (2009) Maturation of the HIV reverse transcription complex: putting the jigsaw together. Rev Med Virol 19:324–337. doi:10.1002/rmv.627
7. Xu H, Franks T, Gibson G, Huber K, Rahm N, De Castillia CS, Luban J, Aiken C, Watkins S, Sluis-Cremer N, Ambrose Z (2013) Evidence for biphasic uncoating during HIV-1 infection from a novel imaging assay. Retrovirology 10:70. doi:10.1186/1742-4690-10-70
8. Hübner W, Chen P, Portillo AD, Liu Y, Gordon RE, Chen BK (2007) Sequence of human immunodeficiency virus type 1 (HIV-1) gag localization and oligomerization monitored with live confocal imaging of a replication-competent, fluorescently tagged HIV-1. J Virol 81:12596–12607. doi:10.1128/JVI.01088-07
9. Yu Z, Dobro MJ, Woodward CL, Levandovsky A, Danielson CM, Sandrin V, Shi J, Aiken C, Zandi R, Hope TJ, Jensen GJ (2013) Unclosed HIV-1 capsids suggest a curled sheet model of assembly. J Mol Biol 425:112–123. doi:10.1016/j.jmb.2012.10.006
10. Padilla-Parra S, Marin M, Gahlaut N, Suter R, Kondo N, Melikyan GB (2013) Fusion of mature HIV-1 particles leads to complete release of a Gag-GFP-based content marker and raises the intraviral pH. PLoS One 8, e71002. doi:10.1371/journal.pone.0071002
11. Finkelshtein D, Werman A, Novick D, Barak S, Rubinstein M (2013) LDL receptor and its family members serve as the cellular receptors for vesicular stomatitis virus. Proc Natl Acad Sci U S A 110:7306–7311. doi:10.1073/pnas.1214441110
12. Jaqaman K, Loerke D, Mettlen M, Kuwata H, Grinstein S, Schmid SL, Danuser G (2008) Robust single-particle tracking in live-cell time-lapse sequences. Nat Methods 5:695–702. doi:10.1038/nmeth.1237
13. Diaspro, A., Chirico, G., Usai, C., Ramoino, P., and Dobrucki, J. (2006) Photobleaching. In: Pawley JB (ed) Handb. Biol. Confocal Microsc. Springer US, pp 690–702
14. Tinevez J-Y, Dragavon J, Baba-Aissa L, Roux P, Perret E, Canivet A, Galy V, Shorte S (2012) Chapter fifteen—a quantitative method for measuring phototoxicity of a live cell imaging microscope. In: Conn M (ed) Methods enzymol. Academic, New York, pp 291–309
15. Zhang Y, Hatziioannou T, Zang T, Braaten D, Luban J, Goff SP, Bieniasz PD (2002) Envelope-dependent, cyclophilin-independent effects of glycosaminoglycans on human immunodeficiency virus type 1 attachment and infection. J Virol 76:6332–6343. doi:10.1128/JVI.76.12.6332-6343.2002

Chapter 5

HIV-1 Reverse Transcriptase-Based Assay to Determine Cellular dNTP Concentrations

Joseph A. Hollenbaugh and Baek Kim

Abstract

Deoxynucleoside triphosphates (dNTPs) are the building blocks of DNA and their biosynthesis is tightly regulated in the cell. HPLC-MS and enzyme-based methods are currently employed to determine dNTP concentrations from cellular extracts. Here, we describe a highly efficient, HIV-1 reverse transcriptase (RT)-based assay to quantitate dNTP concentrations. The assay is based on the ability of HIV-1 RT to function at very low dNTP concentrations, thus providing for the high sensitivity of detection.

Key words dNTP concentration, HIV-1, Reverse transcriptase, Deoxynucleoside triphosphates

1 Introduction

DNA polymerases use deoxynucleoside triphosphates (dNTPs) as substrates during DNA replication. dNTPs are generated by either the de novo pathway using ribonucleotide reductase or by the deoxynucleoside salvage pathway. The functional activities of DNA polymerases are dependent on cellular dNTP concentrations, meaning that enzymes with high steady-state *Km* and presteady-state *Kd* values (low dNTP binding affinity) require high dNTP concentrations in order to function efficiently. In normal replicating cells, chromosomal DNA synthesis by DNA polymerase occurs during the S phase of cell division, when dNTP biosynthesis is most active and cellular dNTP concentrations are highest. For cancer cells and transformed cell lines, cellular dNTP concentrations are increased due to their uncontrolled cell division. In primary, terminally differentiated, nondividing cells, such as macrophages or neurons, have very low dNTP concentrations due to their lack of robust dNTP biosynthesis. Measuring the cellular dNTP concentrations in these cell types requires a highly sensitive and reliable assay to accurately detect the small quantities of dNTPs present. Indeed, high-performance liquid chromatography-mass

Vinayaka R. Prasad and Ganjam V. Kalpana (eds.), *HIV Protocols*, Methods in Molecular Biology, vol. 1354,
DOI 10.1007/978-1-4939-3046-3_5,

spectrometry (HPLC-MS) and polymerase-based dNTP assay have been developed to determine cellular dNTP concentrations, which will be described in this section. For HPLC-MS, a standard curve for each dNTP needs to be routinely generated to validate the assay and then be used to quantitate dNTP concentrations for samples. Although HPLC-MS is very accurate and quantitative, major drawbacks of the method are (1) the requirement of enough biomass to detect dNTPs over background noise, (2) the time required for sample collection on the machine, (3) matrix effect (contaminants may change the profile), and (4) time required for data analysis. Several polymerase-based dNTP assays have been developed using DNA polymerase I (Klenow fragment) [1], *Taq* DNA polymerase [2], or human immunodeficiency virus type 1 (HIV-1) reverse transcriptase (RT) [3]. The ability to detect very low concentrations of dNTPs will depend upon the *Kd* for the particular enzyme used in a given assay. Klenow has a *Kd* of 18 μM [4], whereas the *Kd* of HIV-1 RT ranges between 0.3 and 3.9 μM [5], allowing it to function under low substrate conditions.

2 Materials

2.1 Cell Lysis

1. Prepare 65 % v/v methanol and store at −20 °C before use.
2. PBS without magnesium chloride or calcium chloride.

2.2 Primer and Template Labeling

1. DNA primer sequence is 5′-GTCCCTCTTCGGGCGCCA-3′.
2. DNA template sequences are 5′-ATGGCGCCCGAACAG GGAC-3′, 5′-TTGGCGCCCGAACAGGGAC-3′, 5′-GTG GCGCCCGAACAGGGAC-3′, and 5′-CTGGCGCCCGAA CAGGGAC-3′.
3. T4 polynucleotide kinase (PNK) enzyme (10,000 units/ml).
4. 10× PNK buffer: (700 mM Tris–HCl, 100 mM $MgCl_2$, and 50 mM dithiothreitol, pH at 25 °C: 7.6).
5. Gamma-[^{32}P] ATP (*see* **Note 1**).
6. Sodium chloride-Tris-EDTA (STE) buffer (10×): 5 M NaCl, 1 M Tris–HCl (pH 7.5), and 0.5 M EDTA.
7. Geiger counter.
8. Pipettes (P20 and P1000) and tips.

2.3 Reverse Transcription

1. Reconstitute the 18-mer oligo dT at 200 μM in buffer: 10 mM Tris–HCl (pH 7.5) and 1 mM EDTA.
2. RT reaction buffer (4×): 100 mM Tris–HCl (pH 8.0), 400 mM KCl, 8 mM dithiothreitol, 20 mM $MgCl_2$, and 0.4 mg/ml bovine serum albumin.
3. Recombinant HIV-1 reverse transcriptase (RT) (*see* **Note 2**).

4. Dialysis buffer (5×): 1 M Tris–HCl (pH 7.5), 0.5 M EDTA, 5 M NaCl, 50 % glycerol.
5. 50 μM dNTPs (positive control)—dilute the 100 mM stocks from commercial supplier in water.
6. Stop dye: 99 % formamide, 40 mM EDTA, 0.003 g/ml bromophenol blue, and 0.003 g/ml xylene cyanol.

2.4 Urea Polyacrylamide Gel

1. Part A reagent: 20 % acrylamide/bis-solution (19:1), 8 M urea, 0.1 M Tris, 0.08 M borate, 1 mM EDTA, and 0.075 % TEMED.
2. Part B diluent: 8 M urea, 0.1 M Tris, 0.08 M borate, 1 mM EDTA, and 0.075 % TEMED.
3. Ammonium persulfate—10 % solution in water.
4. 10× Tris-Borate-EDTA (TBE) buffer (890 mM Tris, 890 mM boric acid, 20 mM EDTA. pH at 25 °C: 8.0).
5. Whatman filter paper (No 1) (46 × 57 cm sheets).
6. Plastic wrap (18 in. wide).
7. Gel dryer.
8. Radioactive waste containers—liquid and dry.
9. Protective beta radiation shielding.
10. Beta radiation microcentrifuge tube rack.

2.5 Data Capture and Analysis

1. Phosphorimager screen.
2. Phosphorimager instrument.
3. Data analysis software such as QuantityOne from BioRad Imagine.

3 Methods

3.1 Processing Cells for dNTPs

3.1.1 Working with Nonadherent Cells

1. Determine the number of cells/ml and resuspend cells at a final concentration of 2×10^6 cells/ml (*see* **Note 3**).
2. Transfer 2×10^6 cells to a 1.5 ml Eppendorf tube and close the top.
3. Microcentrifuge the Eppendorf tube at 2000 × *g* for 15 s.
4. Remove supernatant and wash cell pellet with 1 ml of PBS.
5. Pellet cells by centrifugation the tube at 2000 × *g* for 15 s.
6. Carefully remove PBS and do not disrupt the cell pellet.
7. The cells are lysed by quickly adding 200 μl of ice-cold 65 % methanol to the tube.
8. Vigorously vortex sample for 2 min.

9. Completely lyse the cells by incubating the tube at 95 °C for 3 min. Make sure an Eppendorf tube lid lock is securely in place to prevent the lid from opening during the 95 °C incubation. Do not use Parafilm M to seal the tube since it may melt at 95 °C.
10. Chill the tube on ice for 1 min to prevent burning your hands and loss of material due to lid opening.
11. The tube is centrifuged for 3 min at 18,000 × *g*. Next, the 65 % methanol solution is transferred to a new labeled tube. Discard the tube with the cell pellet in proper waste receptacle.
12. Speed vacuum the tube until the liquid is completely evaporated. This process usually takes 1–2 h at 55 °C.
13. Store the tube at −80 °C until you are ready to perform the HIV-1 RT-based dNTP assay (*see* **Note 4**).

3.1.2 Working with Adherent Cells

1. Wash cell monolayer twice with PBS (*see* **Note 5**).
2. Lyse the cells by quickly adding 200 µl of ice-cold 65 % methanol for a six-well plate. Larger volumes of methanol can be used for Petri dishes; however, try and keep the volumes under 1.5 ml to fit into an Eppendorf tube.
3. Use a cell scraper to remove cells from plate. Wash the six-well plate by adding another 200 µl of ice-cold 65 % methanol in order to recover all the biomaterial. Place all the materials into one tube. (Place the tubes on ice if processing multiple samples.)
4. Follow **steps 8–13** as indicated for the nonadherent cell protocol above.

3.2 Primer Labeling

To determine the concentration of each dNTP, four separate primer-template combinations are needed. The template provides specificity by having one additional nucleotide (Subheading 2.2). Therefore, we ^{32}P-radiolabel the primer in four separate tubes and then add one of the four templates to the tube.

1. In four 1.5 ml Eppendorf tubes, combine 4 µl of 20 µM primer, 23 µl of water, and 4 µl of 10× PNK buffer. This can be done at the bench. If only one of the four dNTPs will be evaluated, then only one tube with reaction components is needed.
2. Next, move the tubes behind a beta shield. While wearing proper protective equipment, open the radiation container and add 5 µl of gamma-[^{32}P] ATP to the first tube. Discard pipette tip in the solid radioactive waste. Move to the next tube and repeat until all the tubes have radiation added.
3. Add 2 µl of PNK enzyme to each tube. Change the pipette tip between tubes.

4. Incubate the tubes in a heating block at 37 °C for 30 min.
5. Add an additional 2 μl of PNK enzyme to each tube. Remember to change the pipette tip between tubes and discard the tips in the solid radioactive waste container. Incubate the tubes for another 30 min at 37 °C.
6. Stop the PNK enzyme reaction by placing the tubes in a heating block set at 95 °C for 10 min.
7. Removed tubes from the 95 °C heating block. Allow the tubes to cool to room temperature behind beat radiation shielding. Cooling usually takes about 5 min.
8. Add 12 μl of 20 μM of template to the tube. Each tube with ^{32}P-labeled primer will have a different template added to it. Make sure to identify the template used and the date of ^{32}P-labeling on the tubes.
9. Add 10 μl of 10× STE, 38 μl of water, and 700 μl of 1× STE.
10. To anneal the different primer/templates, place a lid lock on the tubes and then incubate tubes in a heating block set at 95 °C for 10 min.
11. Remove the block from the heating apparatus. Allow the block with the tubes in it to cool to room temperature. This usually takes about 1 h to cool down to room temperature.
12. The different primer/templates are now ready to be used in the HIV-1 RT-based dNTP assay (*see* **Note 6**). Place the tubes containing the ^{32}P-labeled primer/templates in a beta radiation microcentrifuge tube rack. Store the radioisotope as per your institute radiation safety guidelines.
13. Clear up your area using the Geiger counter to detect any radioactive contamination.

3.3 HIV-1 RT-Based dNTP Assay

1. If the sample tubes were stored at −80 °C (Subheading 3.1), allow the tubes to equilibrate to room temperature for 5 min before adding 20 μl of RNase-/DNase-free water to each tube. Vortex the tube for 30 s to suspend the pellet. Next, microcentrifuge the tube for 1 min at 18,000×*g* to pellet cellular debris—dNTPs will be in the solution. Small batches of tubes (1–20 tubes) can be kept at room temperature on the bench if the reactions are done that day; otherwise, store them at −80 °C (*see* **Note 4**).
2. Mark reaction tubes for samples, and include both positive and negative control tubes for each ^{32}P-labeled primer/template.
3. Prepare reaction master mix. Calculate the appropriate volumes for each of the components below, while have enough for two additional reactions. The reaction master mix for one sample volume is 5 μl of 4× RT reaction buffer, 1 μl of oligonucleotide dT, 6 μl of water, and 2 μl of ^{32}P-radiolabeled

primer/template. Remember to work behind protective shielding and wear proper protective equipment when handling the ^{32}P-radiolabeled primer/templates.

4. Aliquot 14 μl of the reaction master mix into each of the marked tubes. Next, add 2 μl of the sample to the proper tube. The negative control tube has 2 μl of water added, while the positive control has 2 μl of 50 nM dNTPs added to it. The next set is to prepare for the enzymatic reaction. Set a timer for 5 min. To the first tube, add 4 μl of HIV-1 RT enzyme (*see* **Note 2**) and place the tube at 37 °C. Discard the pipette tip in the solid radiation waste and then start the timer. Move to the second tube and allow a 5 s interval before adding the enzyme. Place the tube in the heating block. Repeat the process until all the sample reactions have enzyme added.
5. At the end of 5 min, stop the reactions by adding 10 μl of stop buffer and then place the tube in a heating block set at 95 °C. Stop the reaction in the order in which they were started. After 5 min, remove the tubes from the heating block and allow them to cool to room temperature behind proper shielding. Samples are now ready to be resolved on a 14 % urea-PAGE. Alternatively, reactions can be stored at 4 °C for several weeks in a beta radiation microcentrifuge tube rack, but remember the decay of the radioisotope is occurring and this will lead to longer imaging screen exposure times.

3.4 Urea-PAGE

1. Clean both the large and the small glass plates with ethanol for the apparatus. Treat the small plate with a thin layer of silicone-based rain repellent and assemble PAGE apparatus.
2. Cast a 14 % urea-PAGE. Volumes of Part A reagent and Part B diluent will depend on apparatus size. Refer to manufactures recommendations for total volume required. Wait 30 min for gel polymerization to occur.
3. Remove the comb and place the glass plates into the gel apparatus. Add 1× TBE running buffer to the top and bottom reservoirs. Flush the wells out with running buffer using a 20 ml syringe with an 18-gauge needle. Then prewarm the gel (100 W) for 10 min. Next, flush the wells again with running buffer. Count the number of wells needed and position your samples in the middle of the gel. The first and last wells should contain 4 μl of stop reaction buffer, with 4 μl of the samples loaded in between. Run the urea-PAGE until the bromophenol blue dye runs into the lower reservoir (15 in. from the bottom of the comb well), to provide enough separation between the primer and the primer +1 product (extended product).
4. Carefully disassemble the apparatus to remove the glass plates. Use a plastic wedge to separate the two plates, being careful to keep the gel intact on one plate (usually the large, non-silicone-

based treated plate). The plate should be on the counter top with the gel on top. To remove the gel from the glass plate, cover the gel with seal wrap and fold over the edges back onto the seal wrap. Turn the plate over, and using the plastic wedge, carefully remove the gel from the plate, which should be sticking to the plastic wrap.

5. Detect where the radiation is using a handheld Geiger counter. Cut a piece of Whatman paper lengthwise so it is longer than the first and last stop dyes about 3 in. wide. One can use the xylene cyanol dye as a reference point in order help position the Whatman paper. Press the Whatman paper on the gel. Use scissors to cut the edge of the Whatman paper, removing the remaining nonradioactive gel to be discarded in the dry radioactive waste container. Dry the gel using a vacuum gel dryer for at least 45 min. A very large gel can take up to 3 h to dry.
6. Clean up area by discarding the remaining gel in the solid radioactive waste and the running buffer in the liquid radioactive waste. Clean the PAGE apparatus with water and allow it to air-dry.

3.5 Phosphoimaging and Data Analysis

1. After the gel has dried onto the Whatman paper, expose a phosphorimaging screen. The duration of time for exposure will be dependent on the amount of radioactivity. When using freshly ^{32}P-labeled primer/template, screen exposure time will be for 1–2 h to prevent oversaturation. Capture the data using phosphorimager instrument. We use the program software to ensure that the screen is not oversaturated; otherwise, a shorter exposure is required. Figure 1 shows a typical gel.

Fig. 1 HIV RT-based dNTP urea-PAGE analysis. Sample reactions were resolved on a 14 % urea-PAGE. Imaging Screen K (BioRad) was exposed to the dried gel. The image data were captured using PharosFX Plus Molecular Imager (BioRad). Data analysis was accomplished by using QuantityOne software (BioRad). The unextended primer (primer) and the extended primer (primer +1) are shown. *Lanes 1* and *2* are the negative and positive controls, respectively. *Lane 3* was left empty. *Lanes 4–8* were the samples to be quantitated. A quantity box was set to capture the raw data. U1, negative control (primer +1 area), was used to subtract background. *Boxes U2–U6* were for the unextended primer values, whereas *boxes U7–U11* captured data for extended primer +1 values.

2. Data analysis for dNTPs is done using the vendor's software. As depicted in Fig. 1, a rectangle is set and then applied to the negative control primer +1. This accounts for the amount of background noise. Apply this same rectangle to primer and primer +1 bands for the samples. The densities allow for determining the amount of extension over the total amount of primer in that lane. Table 1 shows how the dNTP concentrations are calculated. As shown in Table 1, a box is set in the negative control primer +1 region, which is used for an internal blank to be subtracted from all the samples (Table 1, Column D). The amount of extension is calculated by primer +1/(primer +1 and primer) (Column E). This is converted to a percentage (Column F). Values below 2 % are below the linear range of the assay and need to be discarded. Extensions over 36 % require additional dilution of that sample [3] (*see* **Note 7**). Column G is the amount of volume the sample was suspended in, which is typically 20 μl. Column H is the determined cell number at the time of dNTP harvesting. The fmol/reaction is calculated using the following formula: ((200 fmol of primer × % extension × volume suspended cell pellet × dilution)/(volume added to the reaction)) and displayed in Column K. The fmol/cell number is then calculated by dividing the fmol/Rxn by the cell count (Column L). If the cell volume is known, then the molar concentration can be determined as depicted in Column M. The cell volumes for macrophage, resting $CD4^+$ T cells, and activated $CD4^+$ T cells are 2660 μm^3, 186 μm^3, and 320 μm^3, respectively [3]. For dendritic cells [6] and HeLa cells [7], the cell volumes are 1000 μm^3 and 2600 μm^3, respectively (*see* **Note 8**).

4 Notes

1. Institutional radiation training using radioactive isotopes should be completed before starting any experiments. Radiation safety procedures should be followed at all times. Proper personally protective equipment to limit exposure to radioactive materials should be worn at all times.
2. Recombinant HIV-1 reverse transcriptase can be obtained by commercial sources such as Chimerx and EMD Millipore. We overexpress the His-tagged p66 subunit from HIV-1 strain HXB2 in *E. coli* and purify it using a nickel column chromatography.
3. If using cancer cell lines, 600,000 cells can be used since the dNTP concentrations are very high. Importantly, empirical analysis may be required to determine the minimum number of cells needed for a given cell type. For examine, primary

Table 1
Calculating dNTP concentrations

		C	D	E	F	G	H	I	J	K	L	M
A	B	CNT*mm2	(–) Blank	Extended	Percent extended	Volume resuspended (µl)	Cell number	Vol/Rxn	Dilution	fmol/Rxn	fmol/cell number	nM
	Neg. control	17681										
Sample 1	Primer	1138268	1120587	0.01	1.4	20	2000000	2	1	28.7	1.4E-05	5.5
Sample 2	Primer	1015468	997787	0.11	11.2	20	2000000	2	1	223.3	1.1E-04	42.9
Sample 3	Primer	97371	79690	0.93	92.9	20	2000000	2	1	1858.0	9.3E-04	357.3
Sample 4	Primer	981895	964214	0.13	13.0	20	2000000	2	1	260.8	1.3E-04	50.2
Sample 5	Primer	1033627	1015946	0.15	14.6	20	2000000	2	1	292.3	1.5E-04	56.2
Sample 1	Primer +1	34020	16339									
Sample 2	Primer +1	143072	125391									
Sample 3	Primer +1	1060461	1042780									
Sample 4	Primer +1	162278	144597									
Sample 5	Primer +1	191546	173865									

Extended: (primer +1/(primer + primer +1))
fmole/rxn: ((200 × extended × volume resuspended × dilution)/(volume/Rxn))
fmol/cell number: ((fmol/Rxn)/cell number)
nM: (fmol/cell number)/cell volume

human monocytes have very low dNTPs, and even 5 million cells are just at the level of detection for this assay. Therefore, we recommend 2×10^6 cells/ml to provide enough biomaterial for dNTP analysis for most cell types.

4. Dried sample pellets can be stored indefinitely at −80 °C.
5. Cell count is required in order to calculate the concentration of dNTPs per cell. Always have an extra experimental well for adherent cells to do cell counts for each experimental group.
6. One can store the primer/template at room temperature for several weeks. If one freezes the ^{32}P-labeled primer/template, reannealing it is required. This is accomplished by heating the tube, with a lid lock on, in a heating block to 95 °C for 5 min. Next, remove the block from the apparatus and allow it to slowly cool to room temperature, which usually takes about 1 h.
7. Samples will over 36 % extension require sample diluted and retested in order to bring them within the linear range of the assay.
8. Conversion of literature reported cell volumes (μm^3). 1.0 μm^3 = 1×10^{-15} l.

Acknowledgement

This work was supported by National Institutes of Health grants AI049781 and GM104198 (B.K.).

References

1. Ferraro P, Franzolin E, Pontarin G, Reichard P, Bianchi V (2010) Quantitation of cellular deoxynucleoside triphosphates. Nuc Acids Res 38, e85
2. Wilson PM, Labonte MJ, Russell J, Louie S, Ghobrial AA, Ladner RD (2011) A novel fluorescence-based assay for the rapid detection and quantification of cellular deoxyribonucleoside triphosphates. Nuc Acids Res 39, e112
3. Diamond TL, Roshal M, Jamburuthugoda VK, Reynolds HM, Merriam AR, Lee KY, Balakrishnan M, Bambara RA, Planelles V, Dewhurst S, Kim B (2004) Macrophage tropism of HIV-1 depends on efficient cellular dNTP utilization by reverse transcriptase. J Biol Chem 279:51545–51553
4. Reineks EZ, Berdis AJ (2004) Evaluating the contribution of base stacking during translesion DNA replication. Biochemistry 43:393–404
5. Santos-Velazquez J, Kim B (2008) Deoxynucleoside triphosphate incorporation mechanism of foamy virus (FV) reverse transcriptase: implications for cell tropism of FV. J Virol 82:8235–8238
6. de Baey A, Lanzavecchia A (2000) The role of aquaporins in dendritic cell macropinocytosis. J Exp Med 191:743–748
7. Zhao L, Kroenke CD, Song J, Piwnica-Worms D, Ackerman JJ, Neil JJ (2008) Intracellular water-specific MR of microbead-adherent cells: the HeLa cell intracellular water exchange lifetime. NMR Biomed 21:159–164

Chapter 6

Rapid Determination of HIV-1 Mutant Frequencies and Mutation Spectra Using an mCherry/EGFP Dual-Reporter Viral Vector

Jonathan M.O. Rawson, Christine L. Clouser, and Louis M. Mansky

Abstract

The high mutation rate of human immunodeficiency virus type-1 (HIV-1) has been a pivotal factor in its evolutionary success as a human pathogen, driving the emergence of drug resistance, immune system escape, and invasion of distinct anatomical compartments. Extensive research has focused on understanding how various cellular and viral factors alter the rates and types of mutations produced during viral replication. Here, we describe a single-cycle dual-reporter vector assay that relies upon the detection of mutations that eliminate either expression of mCherry or enhanced green fluorescent protein (EGFP). The reporter-based method can be used to efficiently quantify changes in mutant frequencies and mutation spectra that arise due to a variety of factors, including viral mutagens, drug resistance mutations, cellular physiology, and APOBEC3 proteins.

Key words Retrovirus, Lentivirus, Retroviral vector, Reverse transcription, Evolution, Diversity, Mutagenesis

1 Introduction

Human immunodeficiency virus type-1 (HIV-1) mutates at a rate of ~3.6×10^{-5} mutations/base pair (bp)/cycle (average across all studies; range of $1.4–8.5 \times 10^{-5}$), corresponding to about one mutation per three genomes synthesized [1–8]. The rapid mutation rate, in conjunction with high rates of recombination and replication [9, 10], drives viral evolution within infected individuals and poses a significant barrier to the development of effective vaccines and drug regimens. Several studies have demonstrated that a variety of factors can affect the frequency and/or types of mutations that arise during viral replication, thus potentially altering the evolutionary path of the virus within infected individuals. These factors include experimental and approved antiviral therapeutics

Vinayaka R. Prasad and Ganjam V. Kalpana (eds.), *HIV Protocols*, Methods in Molecular Biology, vol. 1354,
DOI 10.1007/978-1-4939-3046-3_6,

(e.g., nucleoside analogs that cause chain termination or altered base-pairing) [11–19], cell type [20], drug resistance-associated mutations in reverse transcriptase [8, 11, 13, 14, 21], viral accessory proteins (Vif and Vpr) [3, 13, 22], and host proteins of the APOBEC3 family [23, 24]. The examination of factors influencing the mutagenesis of HIV-1 remains an area of active investigation, necessitating the development of improved vectors and methodologies for quantifying and characterizing viral mutants.

Several methods have been used to determine mutant frequencies, mutation rates, and mutation spectra in HIV-1, most of which rely on reporter genes that confer a phenotype that can be easily scored, such as *lacZα* [1, 6], *egfp* [15, 16], and *thymidine kinase* [5]. Direct amplification and sequencing of viral genes have also been used to determine HIV-1 mutation rates and spectra [7, 25], but Sanger sequencing of viral genes is relatively inefficient (as most sequences lack mutations) and next-generation sequencing methods are currently too error-prone (error rates of 10^{-2}–10^{-4} mutations/bp depending on how the data is processed) to be of much utility [26–28]. Using reporter genes, both the restoration of defective reporter gene phenotypes (reversion assays) and the elimination of functional reporter gene phenotypes (forward mutation assays) can be detected. Forward mutation assays have generally been preferred because they allow for the detection of numerous types of mutations at many different positions within the reporter sequence. Using these assays, forward mutant frequencies can be calculated by determining the ratio of mutant proviruses (i.e., those lacking LacZα or EGFP expression) to all proviruses. As these assays rely on the detection of mutations that eliminate reporter gene expression, silent mutations will typically not be detected, and thus the calculated mutant frequencies underestimate the intrinsic mutation rates. In the case of *lacZα*, mutant frequencies can be converted to mutation rates, as saturation mutagenesis has determined the target bases at which substitutions or frameshifts can be detected within the *lacZα* gene region [29, 30]. Currently, other reporter genes have not yet been characterized to the same extent such that this type of conversion is not possible. In addition to mutant frequencies, these mutation assays enable targeted Sanger sequencing of defective reporter genes for the characterization of mutation spectra.

Here, we describe a replication-defective mCherry/EGFP dual-reporter vector that has been used in single-cycle assays for determination of HIV-1 mutant frequencies and mutation spectra [18, 19]. Recently, a similar vector based on HIV type-2 (HIV-2) has been engineered, enabling comparative analyses between HIV-1 and HIV-2 [31]. The vector does not express Env and must be complemented *in trans* with an envelope gene to produce infectious virus. Within *nef*, a cassette containing *mCherry* and *egfp* has been inserted, separated by an internal ribosome entry

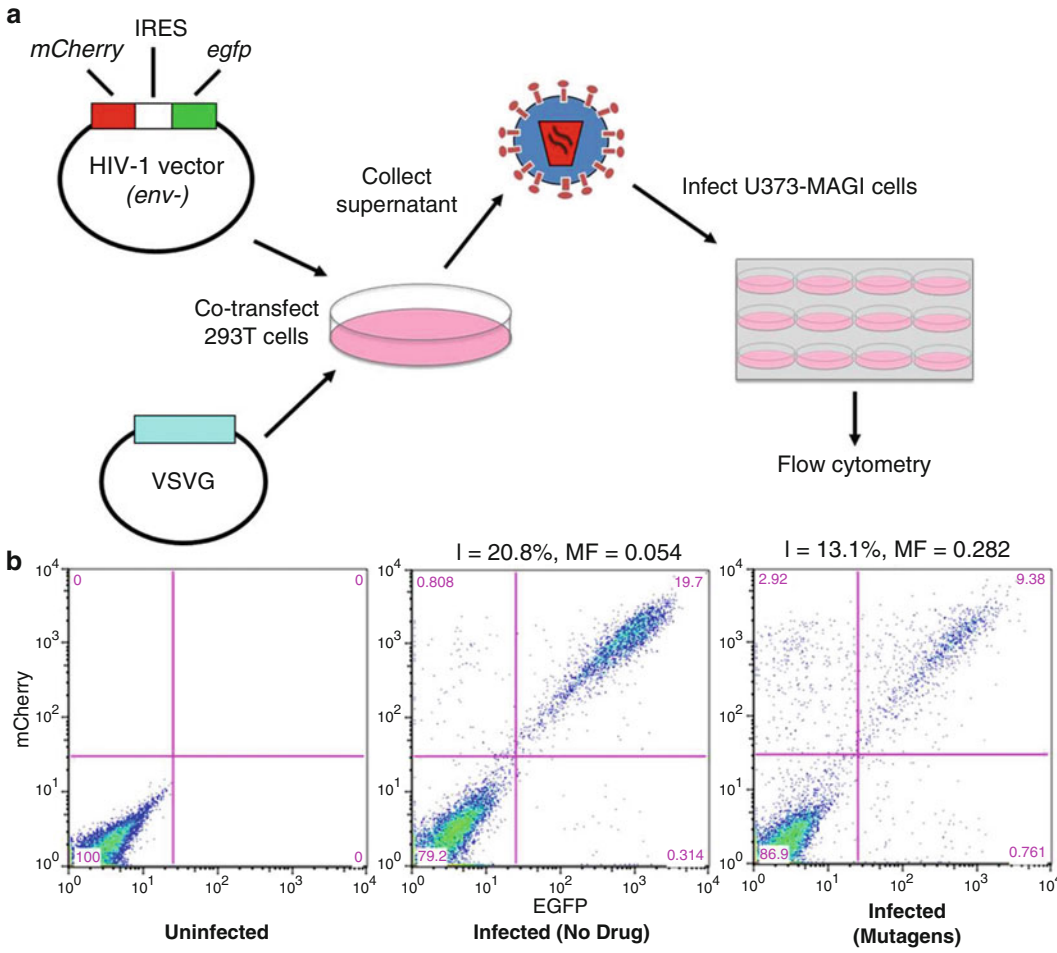

Fig. 1 Vector and assay design for rapid determination of HIV-1 infectivities and mutant frequencies. (**a**) An HIV-1 vector expressing mCherry and EGFP (pNL4-3 MIG) was co-transfected with VSVG to produce infectious virus. The supernatant was used to infect U373-MAGI-CXCR4 target cells. Cells were collected 72 h post-infection for analysis of infectivity and mutant frequency via flow cytometry. Reprinted in adapted form from Rawson, J. M. et al. 2013 [18] with permission from Elsevier. (**b**) Examples of representative flow cytometry data (EGFP vs. mCherry) from uninfected cells, infected untreated cells, and infected cells treated with a mutagenic drug combination (50 μM resveratrol + 200 μM KP-1212). The infectivities (I) were calculated by adding the percentages of cells in all three positive quadrants, whereas mutant frequencies (MF) were calculated by adding the single-positive quadrants ($mCherry^+/EGFP^-$ + $mCherry^-/EGFP^+$) and dividing by the infectivities.

site necessary for translation of EGFP. Thus, the final molecular clone has functional open reading frames for all genes except *env* and *nef*. The resulting vector, called pNL4-3 MIG, can be used to determine viral mutant frequencies as follows: first, infectious viral stocks are produced by co-transfecting the vector and the vesicular stomatitis virus envelope glycoprotein (VSVG) into 293T cells (Fig. 1a). The supernatants are collected, filtered, DNase I-treated, and titered to determine infectivity. Next, viral stocks are used to

infect U373-MAGI-CXCR4 cells, which are then analyzed by flow cytometry to measure mCherry and EGFP expression. Mutant frequencies are calculated by dividing the number of cells expressing only mCherry or EGFP by all infected cells. Lastly, the mutation spectra can be analyzed by sorting out single-positive cells ($mCherry^+/EGFP^-$ and/or $mCherry^-/EGFP^+$), isolating genomic DNA, performing PCR, and sequencing the mutated reporter gene(s). The entire assay can be performed in approximately 2–3 weeks, permitting rapid evaluation of the impact of mutations in reverse transcriptase, APOBEC3 proteins, viral mutagens, or alterations in cell physiology on HIV-1 mutant frequencies and mutation spectra.

2 Materials

2.1 Cell Culture, Production of Viral Stocks, Infections

1. Cells: 293T and U373-MAGI-CXCR4 [32]. In addition to U373-MAGI-CXCR4, many other cell lines can successfully be used as target cells in this assay (*see* **Note 1**).
2. 293T Medium: Dulbecco's modified Eagle's medium (DMEM) supplemented with 10 % fetal bovine serum (FBS) and 1 % penicillin/streptomycin.
3. U373-MAGI-CXCR4 Medium (MAGI Medium): DMEM supplemented with 10 % FBS, 1 % penicillin/streptomycin, 0.2 mg/mL G418, 0.1 mg/mL hygromycin B, and 1.0 μg/mL puromycin.
4. Dulbecco's phosphate-buffered saline (DPBS) without Ca^{2+} or Mg^{2+}.
5. FACS buffer: DPBS, 2 % FC3, 10 mM HEPES (pH 7.2), 10 U/mL DNase I, 5 mM $MgCl_2$.
6. Trypsin-EDTA.
7. Serum-free DMEM.
8. Poly-L-lysine (10×): Dilute 1:10 in sterile water and store at 4 °C. Stocks can be reused up to five times.
9. Polyethylenimine: Other transfection reagents can also be used (*see* **Note 2**). Prepare liquid stocks by dissolving the PEI in sterile water to a final concentration of 1 mg/mL, adjusting the pH to 7.0 with 1 M HCl, and filtering through a 0.2 μM filter. Divide stocks into 1 mL aliquots and freeze at −80 °C. Maintain thawed stocks at 4 °C; stocks should retain full activity for up to 3 weeks.
10. Plasmids: pNL4-3 MIG (available upon request) and pHCMV-G (a kind gift from J. Burns, University of California, San Diego) or a comparable plasmid, such as pHEF-VSVG. HIV-1 Env constructs may be used in place of VSVG (*see* **Note 3**).

11. DNase I.
12. Syringes: 10, 20, or 60 mL, depending on the volume of virus to be produced.
13. 0.2 μm filters.
14. Hemocytometer.
15. 96-Well polystyrene plates.
16. Polystyrene round-bottom tubes with strainer caps.

2.2 DNA Isolation and PCR

1. Dpn I.
2. Genomic DNA purification kit, such as the High Pure PCR Template Preparation Kit.
3. High-fidelity amplification system, such as Phusion Hot Start II.
4. Taq DNA polymerase.
5. dNTPs.
6. Primers: EGFP-forward (5′-TCAAGCGTATTCAACAAGG-3′) and EGFP-reverse (5′-CATTGTTAGCTGCTGTATTGC-3′).
7. Gel extraction kit.
8. T/A cloning kit, such as the pGEM-T Vector Kit II.
9. LB plates with ampicillin/IPTG/X-Gal: LB-agar, 100 μg/mL ampicillin, 0.5 mM IPTG, and 80 μg/mL X-Gal.
10. LB broth with ampicillin: LB-broth, 100 μg/mL ampicillin.
11. Standard DNA miniprep kit or 96-well miniprep kit, depending on the desired throughput.
12. Sequencing primers: T7 promoter (5′-TAATACGACTCACTATAGGG-3′) and SP6 upstream (5′-ATTTAGGTGACACTATAG-3′). Sequencing facilities often provide these primers at no additional cost.

2.3 Equipment and Software

1. Flow cytometer capable of simultaneously detecting and separating mCherry and EGFP signals (*see* **Note 4**), preferably attached to a high-throughput sample (HTS) unit.
2. Access to a flow cytometer capable of fluorescence-activated cell sorting (FACS); this cytometer must also be able to simultaneously detect and separate mCherry and EGFP signals.
3. FlowJo (Tree Star Inc.; Ashland, OR) or similar program for analyzing flow cytometry data.
4. GraphPad Prism or similar program for data analysis.
5. Program capable of assembling many Sanger sequences, such as SeqMan Pro (Lasergene Core Suite; DNASTAR, Inc.; Madison, WI) or Vector NTI (Life Technologies; Carlsbad, CA).

3 Methods

3.1 Production of Viral Stocks

1. Plate four million 293T cells/10 cm plate ~24 h before transfection. Optional: Pre-coat plates with poly-L-lysine to minimize cell detachment during the transfection procedure. Pre-coat plates by adding sufficient poly-L-lysine to cover the plates (~5 mL/plate), waiting for 5–10 min, aspirating or pipetting off the poly-L-lysine, and drying the plates for ~1 h in a certified biosafety cabinet. Plates should be ~90–95 % confluent at the time of transfection.
2. Begin the transfection procedure ~24 h after plating the cells by preparing the transfection mixture. For each 10 cm plate, mix 10 μg pNL4-3 MIG, 1 μg pHCMV-G, and serum-free DMEM to a final volume of 0.5 mL in a microcentrifuge tube. Mix 33 μL 1 mg/mL PEI (3:1 ratio of μL PEI to μg of DNA) and 467 μL serum-free DMEM in a separate microcentrifuge tube. Add the DNA/DMEM all at once to the PEI/DMEM, mix by pipetting, and incubate for 15–20 min.
3. Replace the medium on the 293T cells (10 mL/plate).
4. Add the DNA-PEI transfection mixture dropwise to the plates of 293T cells; mix with gentle swirling.
5. Replace the medium again ~12–16 h post-transfection (7–10 mL/plate).
6. Collect viral stocks ~36–48 h post-transfection by filtering the supernatants through 0.2 μm filters. Treat viral stocks with 10 U/mL of DNase I (in 1× DNase I buffer) at 37 °C for 3 h to reduce plasmid contamination (*see* **Note 5**). Freeze stocks in 0.5–1.0 mL aliquots at −80 °C until the time of infection. If desired, the transfected cells can be collected for analysis of transfection efficiency by flow cytometry.

3.2 Titering Viral Stocks

1. Plate 31,250 U373-MAGI-CXCR4 cells/well in a 24-well plate ~24 h before infection, using 1 mL MAGI medium/well.
2. At the time of infection, aspirate the medium and replace with variable volumes of the viral stock to be titered and 293T medium, keeping a total volume in each well of 1 mL (*see* **Note 6**). Note that 293T medium is used to avoid any effect that the selection compounds in the MAGI medium could have on infectivity. Perform all infections in triplicate and include uninfected controls.
3. Replace the medium 24 h post-infection.
4. Collect the cells for flow cytometry 72 h post-infection. Aspirate the medium and add 0.2 mL trypsin-EDTA/well. Transfer the trypsinized cells to a 96-well plate and centrifuge at 500 × *g* for 5 min at 4 °C. Remove the trypsin-EDTA and

wash the samples with 0.2 mL DPBS/2 % FBS/well before centrifuging the cells for a second time. Remove the DBPS/2 % FBS and again add 0.2 mL DPBS/2 % FBS/well, wrap in parafilm film, and store at 4 °C until samples are assessed by flow cytometry.

5. Perform flow cytometry to quantify the number of cells expressing mCherry and/or EGFP. Optimize flow cytometer settings before recording data (*see* **Note 7**). Analyze a minimum of 10,000 gated cells/sample. Gates should be consistent across all samples. Determine the percent infection in each sample by taking the sum of the following quadrants: $mCherry^+/EGFP^-$, $mCherry^-/EGFP^+$, and $mCherry^+/EGFP^+$. Alternatively, subtract the double-negative population ($mCherry^-/EGFP^-$) from 100.
6. Using GraphPad Prism, plot the volume of virus (in μL) against the percent infection. The relationship between the volume of virus and the percent infection should be linear up to ~40 %, and we recommend excluding data above this value (*see* **Note 8**). If less than five data points are below 40 % infectivity, repeat the titer using less virus. Fit a trend line to the data using linear regression; the r^2 value should be >0.99. The equation of the trend line allows calculation of predicted volumes of viral stocks to achieve targeted infectivities in future experiments. Although not necessary for this protocol, one can also calculate infectious titers from the data, though these titers likely underestimate true infectious titers (*see* **Note 9**).

3.3 Small-Scale Infections to Determine Viral Mutant Frequencies

1. Plate 31,250 U373-MAGI-CXCR4 cells/well in a 24-well plate ~24 h before infection, using 1 mL MAGI medium/well.
2. At the time of infection, replace the medium with 293T medium and the amount of virus predicted to result in 20 % infection based upon the viral titer (*see* **Note 10**). Include uninfected controls. If testing the impact of small molecules on viral mutant frequency, add variable amounts of the compounds 2 h before infection (*see* **Note 11**).
3. Replace the medium 24 h post-infection.
4. Collect the cells for analysis by flow cytometry 72 h post-infection as described before.
5. Perform flow cytometry to quantify the number of cells expressing mCherry and/or EGFP. Determine viral infectivity to ensure that it is close to the targeted 20 % infection. Determine mutant frequency by adding the single-positive cell populations and dividing by all infected cells: $(mCherry^+/EGFP^- + mCherry^-/EGFP^+)/(100 - mCherry^-/EGFP^-)$. Examples of flow cytometry data with corresponding infectivities and mutant frequencies are illustrated in Fig. 1b.

HIV-1 wild-type mutant frequencies typically fall within the range of 0.04–0.06 in this assay. Using the length of the entire cassette (mCherry-IRES-EGFP; 2072 bp) as the size of the mutational target (a conservative means of estimating viral mutation rates), these mutant frequencies correspond to mutation rates of $1.9–2.9 \times 10^{-5}$ mutations/bp/cycle.

6. In GraphPad Prism, graph the infectivity and mutant frequency of the infected control (i.e., untreated wild-type virus) against the other samples (e.g., cells treated with compounds of interest or infected with mutant viruses), as shown in Fig. 2a. Perform at least three independent experiments and graph the means ± standard deviations. Although absolute infectivities and mutant frequencies can be graphed, we prefer to normalize the data relative to the control virus (set to 100 % for infectivity or 1 for mutant frequency) to simplify data interpretation.
7. Perform statistical analysis to assess significance of differences in mutant frequencies between samples. One-way ANOVA followed by Tukey's posttest using GraphPad Prism or similar software is usually sufficient to examine differences in mutant frequencies across multiple treatment groups. ANOVA should be performed using absolute (rather than normalized) mutant frequencies. As ANOVA tests rely upon certain assumptions, the data should ideally be transformed prior to one-way ANOVA (*see* **Note 12**). Other types of ANOVAs may be ideal for more complex comparisons of treatment groups (*see* **Note 13**).

3.4 Large-Scale Infections to Determine Viral Mutation Spectra

1. Plate 1.2 million U373-MAGI-CXCR4 cells/10 cm plate ~24 h before infection, using 10 mL MAGI medium/plate. Prepare two plates/treatment and include uninfected controls.
2. At the time of infection, replace the medium with fresh 293T medium and the amount of virus predicted to result in 20 % infection based upon the viral titer (*see* **Note 14**). If examining the impact of small molecules on viral mutant frequency, add the compounds 2 h before infection.
3. Replace the medium 24 h after infection.
4. Collect the cells for FACS 72 h post-infection. Before collecting samples, we advise discussing the procedure with the operator of the FACS instrument, as they may suggest modifications to this protocol. Begin by aspirating the medium and adding 3 mL trypsin-EDTA/plate. Neutralize the trypsin with 7 mL 293T medium/plate and centrifuge in 15 or 50 mL conical tubes for 5 min at 500 × *g* and 4 °C. Aspirate the trypsin-EDTA/medium.
5. Wash the cells twice with 10 mL DPBS/2 % FBS/plate. Resuspend the final cell pellet in 1 mL FACS buffer/plate of cells and transfer to 5 mL polystyrene tubes.

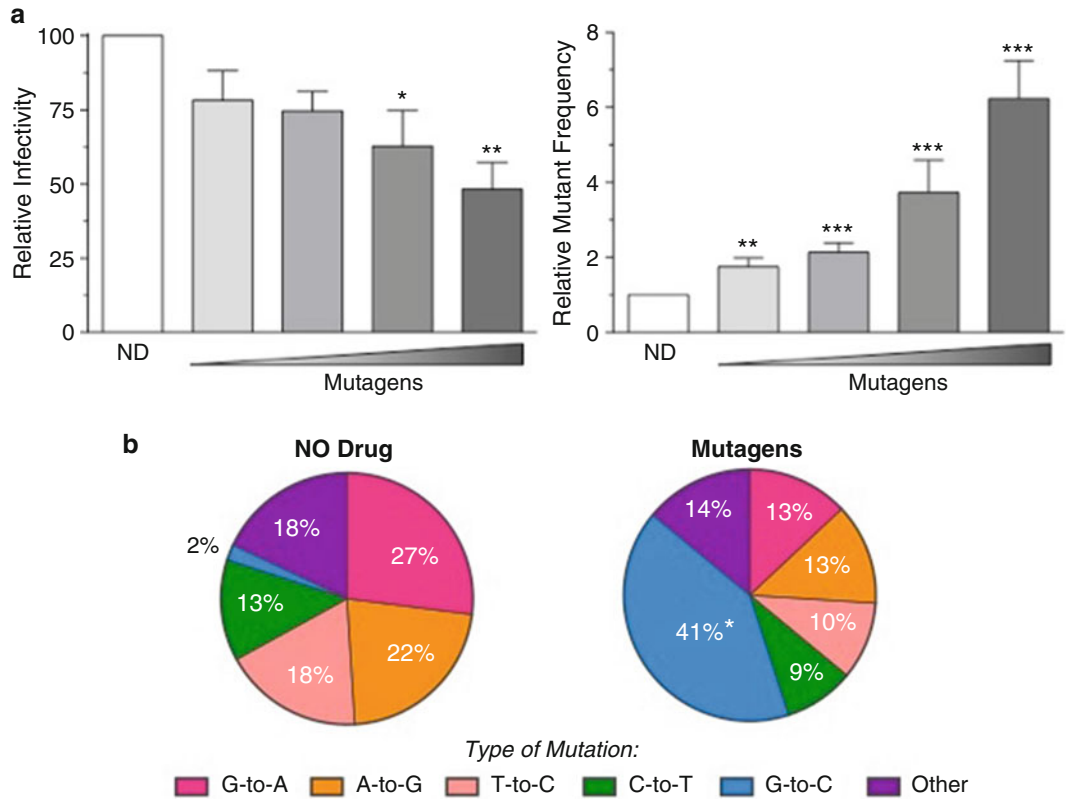

Fig. 2 Use of the dual-reporter HIV-1 vector to analyze viral infectivities, mutant frequencies, and mutation spectra. (**a**) The impact of a mutagenic drug combination (50 μM resveratrol + 0, 5, 50, or 200 μM KP-1212) on viral infectivities and mutant frequencies was determined. The data were normalized to the no-drug (ND) control, which was set to 100 (infectivity) or 1 (mutant frequency). The data represent the means of three independent experiments ± standard deviations. One-way ANOVA with Dunnett's posttest was performed on the un-normalized data to assess statistical significance. *p-value <0.05, **p-value <0.01, ***p-value <0.001. (**b**) To examine mutation spectra, mCherry$^+$/EGFP$^-$ cells were isolated by fluorescence-activated cell sorting (FACS). Genomic DNA was extracted, and *egfp* from the proviral DNA was amplified, cloned, and analyzed by Sanger sequencing. After alignments and identification of mutations, the percentage of mutations belonging to each class was determined for the no-drug (ND) control and cells treated with a mutagenic drug combination (50 μM resveratrol + 200 μM KP-1212). The drug combination caused an increase in G-to-C mutations from 2 to 41 % of total mutations, which was statistically significant (p-value <0.0001). Total mutations analyzed: 45 (no drug) and 69 (drug combination). Reprinted in adapted form from Rawson, J. M. et al. 2013 [18] with permission from Elsevier.

6. Bring the following to the FACS instrument: samples for analysis, FACS buffer (~10 mL in a 15 mL conical tube), polystyrene tubes with strainer caps (one/sample), and collection tubes (microcentrifuge tubes with 0.1 mL DPBS/2 % FBS/tube; bring two/sample).

7. Subject samples to FACS to sort out the mCherry$^+$/EGFP$^-$ and mCherry$^-$/EGFP$^+$ cell populations (*see* **Note 15**). Each sample should be filtered into a polystyrene tube through a strainer cap immediately before FACS to remove cell aggregates. The speed and efficiency of sorting can vary widely depending on numerous factors (infectivity, degree of cell death, etc.). We typically collect at least 2000 mCherry$^+$/EGFP$^-$ cells per sample, though the ideal number depends on the amount of sequencing data required for analysis (*see* **Note 16**).

3.5 Extraction of Genomic DNA, PCR, and Sequencing

1. Purify genomic DNA from infected cells using Roche's High Pure PCR Template Preparation Kit (or a similar kit), following the manufacturer's instructions. Elute in 50 μL sterile water/sample. Isolate genomic DNA from uninfected cells as a negative control for the PCR reaction.
2. Treat genomic DNA with 0.2 U/μL DpnI in 1× DpnI buffer at 37 °C for 2 h to degrade any residual plasmid DNA.
3. Perform PCR amplification of *egfp* using a high-fidelity amplification system that is based on a proofreading polymerase, such as Phusion Hot Start II. Proofreading polymerases are recommended because they exhibit much lower error rates than Taq polymerase, which lacks proofreading activity (error rates of 10^{-6}–10^{-7} mutations/bp/cycle or 10^{-4}–10^{-5} mutations/bp/cycle, respectively). High-fidelity polymerases minimize background errors that could otherwise contribute to the mutation spectra data (*see* **Note 17** for further discussion). Using Phusion Hot Start II, set up the PCR reactions with 28.5 μL nuclease-free water, 10 μL 5× HF buffer, 1 μL dNTPs (10 mM), 2.5 μL of each primer (EGFP-forward and EGFP-reverse primers; 10 μM stocks), 5 μL genomic DNA, and 0.5 μL Phusion Hot Start II. We advise performing the PCR reactions from each sample in triplicate and pooling the resulting products in order to increase the number of unique mutations that can be observed by sequencing. The *egfp* gene from the pNL4-3 MIG plasmid should be amplified as a positive control reaction. Use water and genomic DNA from uninfected cells as negative control reactions.
4. Perform PCR using the following cycling parameters: 98 °C for 30 s, 40 cycles of 98 °C 10 s/60 °C 30 s/72 °C 30 s, and a final extension of 72 °C for 10 min. In some cases, the number of PCR cycles can be reduced to 30 or 35 in order to further decrease PCR-mediated background errors, but in general this is not recommended because (1) the benefit in terms of reducing background errors is relatively small (*see* **Note 17**), and (2) the PCR product may not be sufficiently visible on a gel to allow for DNA purification.

5. Gel-purify the PCR products (981 bp in length) to remove any nonspecific products or primer dimers. Gel extraction also removes the proofreading polymerase (i.e., Phusion Hot Start II), which is crucial for efficient A-tailing of PCR products.
6. Add A-tails to the blunt-end PCR products by mixing 6 μL purified PCR product, 1 μL 10× Taq buffer, 2 μL dATP (1 mM), and 1 μL (5 U) Taq polymerase. Incubate at 72 °C for 20 min.
7. Ligate the A-tailed PCR products into a T/A cloning vector such as pGEM-T following the manufacturer's instructions. Use 3 μL of PCR product in each ligation reaction and ligate overnight at 4 °C for maximum efficiency.
8. Transform 5 μL of each ligation reaction into JM109 cells. Other high-efficiency competent cells ($\geq 10^8$ colony forming units/μg) can be used as well, provided that they are compatible with blue-white color screening. Plate several different volumes (e.g., 50, 200, 500 μL) onto LB-amp plates containing IPTG and X-Gal for blue-white color screening.
9. Start 1.5 mL liquid cultures in LB broth with ampicillin from white colonies (i.e., those that contain an insert disrupting the *lacZα* reading frame in pGEM-T) the following day.
10. Purify plasmid DNA from the liquid cultures the next day. For smaller numbers of cultures (<48), we recommend using standard miniprep kits. For larger numbers of cultures (≥48), use 96-well high-throughput miniprep kits.
11. Submit the samples for Sanger sequencing using primers that flank the ligated insert, such as the T7 promoter and/or SP6 upstream primers (*see* **Note 18**).
12. Align resulting sequences to the wild-type *egfp* sequence (this will exclude the primer sequences from analysis, as the primers anneal outside of *egfp*) using a program like SeqMan Pro (part of the Lasergene Core Suite) or Vector NTI. Perform trimming to remove low-quality sequence data.
13. Use the program to identify all putative mutations within the assembled sequences. Verify each mutation by viewing the chromatogram. Compile a list of information about each mutation—sequence identifier, position, and mutation type. Exclude identical mutations that are found in multiple clones from the same sample, as these may have arisen due to sequencing of amplified products from the same original provirus. It is important to note that even if the identical mutations occur in distinct sequences (e.g., with different co-occurring mutations), they may still have arisen from one initial provirus, as recombination can occur during PCR. Occasional G-to-A hypermutants (likely due to the activity of APOBEC3 proteins) may be identified, and the mutation spectra should

be analyzed both in the presence and absence of these G-to-A hypermutants (*see* **Note 19**).

14. From the list of verified mutations, compile the mutation spectra by determining the absolute numbers and relative percentages that each mutational type contributes to the total. The mutation spectra data can be presented in table or pie chart format (as shown in Fig. 2b). Mutation spectra can be compiled both for total mutations and for specific classes of mutations, such as substitutions. While insertions and deletions can be observed in this assay, we have found that they occur much less frequently than substitutions, and therefore it is difficult to make meaningful comparisons of their frequencies between samples.
15. Analyze statistical significance of differences in mutation spectra using the Cochran-Mantel-Haenszel test or Fisher's Exact test (*see* **Note 20**). These analyses should be performed on the absolute numbers of mutants from each class, rather than relative percentages of the total.

4 Notes

1. Many other cell lines may successfully be used as targets for infection, particularly when viral stocks are pseudotyped with VSVG. Besides U373-MAGI-CXCR4, we have successfully used immortalized T-cell lines, such as CEM and SupT1. Infectivity of viral stocks can vary widely between cell lines, such that they must be titered in each target cell line.
2. We have also produced viral stocks using standard calcium phosphate protocols and lipid-based reagents (such as GenJet and Lipofectamine 2000), but the PEI method has provided the best balance between cost, efficiency, and speed. If viral titers are insufficient, lipid-based methods are recommended. Alternatively, larger volumes of virus may be produced by PEI transfection and then concentrated.
3. VSVG is usually preferable for pseudotyping the HIV-1 vector as it results in high-titer viral stocks that can infect a variety of cell lines. However, when using VSVG, it is possible for the virus to re-infect the producer cells (293T). While this may elevate the absolute mutant frequency, it should not affect relative mutant frequency comparisons between samples. In place of VSVG, constructs expressing CXCR4-tropic HIV-1 Env may be utilized. While the use of these constructs prevents re-infection of producer cells, infectivity of viral stocks will likely be reduced.
4. For our experiments, we have used a BD LSR II flow cytometer equipped with 488, 561, and 640 nm lasers. EGFP is excited by the standard 488 nm laser and detected with 505LP and 525/50 filters, while mCherry is excited with the 561 nm

laser and detected with 595LP and 610/20 filters. With this particular setup, no fluorescence compensation was necessary. We recommend optimizing the flow cytometer setup with single-color controls (such as 293T cells transfected with EGFP or mCherry) before using the pNL4-3 MIG construct. If the mCherry and EGFP signals cannot be satisfactorily separated (even with compensation), a similar molecular clone of HIV-1 (pNL4-3 HIG) that expresses the mouse heat stable antigen (HSA) and EGFP can be used instead [15, 16]. In this case, an additional step must be performed in which HSA is stained with a phycoerythrin (PE)-conjugated anti-HSA antibody.

5. DNase I treatment of viral stocks is highly recommended to reduce plasmid contamination of genomic DNA used for PCR and sequencing. Perform this step before freezing and titering viral stocks, as the DNase I treatment itself may somewhat reduce viral titers. If viral stocks will only be used to determine mutant frequencies by flow cytometry, DNase I treatment is unnecessary.
6. For NL4-3 MIG-VSVG, infect with 1.25–80 μL of virus (two-fold dilution series). For NL4-3 MIG complemented with NL4-3 Env, infect with 31.25–500 μL of virus. These ranges should comfortably span the target of 20 % infection for further experiments. Titers may vary considerably if other target cell lines or envelopes are used.
7. When initially performing flow cytometry of infected cells, include several extra samples (uninfected and infected) for optimization of flow settings (voltages and thresholds). We suggest optimizing the settings in tube mode and then proceeding with the analysis of all remaining samples in HTS mode. After gaining familiarity with the procedure, these extra samples can be omitted.
8. Within this assay, cells infected by a single virus or by multiple viruses cannot reliably be distinguished. However, at low infectivities, the probability of co-infection is small such that the relationship between the volume of virus added and percent infection is highly linear. We have found that linearity is maintained up to ~40 % infection.
9. Calculate the titer (infectious units/mL) as follows: $(F \times N \times 1000)/V$, where F is the percentage of fluorescent cells (expressed in decimal form), N is the number of cells at the time of infection, and V is the volume (μL) of virus stock added. Determine the titer for each volume of virus within the linear range of infection and average the resulting values. These titers may underestimate true infectious titers because (1) some cells may be co-infected, and (2) some cells may be infected but fail to express mCherry or EGFP (due to mutations in

both *mCherry* and *egfp*, mutations in *tat*, or integration into a transcriptionally repressive region of the genome).

10. We highly recommend performing experiments within the range of 15–30 % infection (for the untreated control) whenever possible. At lower infectivities, mutant frequencies become noticeably more variable due to the low number of mutants detected. At higher infectivities, changes in mutant frequencies become harder to detect due to high levels of co-infection (in which case wild-type proviruses can mask mutant proviruses).
11. When testing the impact of small molecules on viral mutant frequencies, we generally preincubate the cells with the compounds of interest for 2 h prior to infection. However, some compounds may require longer activation periods, necessitating optimization of the time of compound addition. At the desired time point, replace the medium and add the compounds of interest (typically 1–2 μL) to a final volume of 0.5 mL/well. Test a range that spans at least six concentrations of each compound. Include equivalent volumes of the compound solvent in the untreated (infected and uninfected) controls. At the time of infection, add virus and medium to bring the final volume to 1 mL/well. Compound concentrations are based on the final volume of 1 mL/well; thus, adding 1 μL of compound results in a 1000-fold dilution of the compound stock.
12. ANOVA tests assume that all treatment groups are normally distributed and that all treatment groups have equal variance. The small fractions obtained using this reporter assay can invalidate these assumptions and therefore invalidate the ANOVA. Variance stabilization can be performed to account for unequal variance among treatment groups that may arise from small fractions. Arcsin transformation is one method of variance stabilization that does not require specialized software for statistical analysis. To analyze the data by this method, first transform mutant frequencies (arcsin(square root of mutant frequency)) prior to analysis by ANOVA with Tukey's posttest. We have used ANOVA to evaluate both transformed and untransformed data and found little difference in the statistical results, suggesting that the ANOVA is a fairly robust procedure.
13. To compare samples with two factors (e.g., a drug combination) against samples with a single factor (e.g., single-drug treatments), first transform the data using the arcsin square root equation (as described in **Note 12**) and then perform either a one-way or a two-way ANOVA. Although both the one-way and two-way ANOVA are valid methods for evaluating the data, the two-way ANOVA is a more powerful method for estimating interactions. To compare multiple treatment groups to an untreated control, perform one-way ANOVA with Dunnett's multiple comparison test.

14. Assay results are typically highly comparable across different plate formats as long as the numbers of cells and volumes of viruses are scaled based on surface area differences. The scaling factor between 10 cm plates and 24-well plates is 39.27, though this may vary depending on the manufacturer. Therefore, one can calculate the amount of virus necessary per 10 cm plate by taking the amount needed per well of a 24-well plate and multiplying by 39.27.
15. Although previous analyses have only included sequences from the mCherry$^+$/EGFP$^-$ population, other populations (typically up to four total) can be sorted without adding any additional time or expense to the experiment. Thus, we suggest isolating the mCherry$^-$/EGFP$^+$ cell population as well. Genomic DNA from these cells can be used to identify additional unique mutations in *mCherry*, which may be useful in cases where mCherry$^+$/EGFP$^-$ genomic DNA is exhausted.
16. The number of cells isolated by FACS should be maximized such that the chance of re-sampling identical mutants is low. Re-sampling of sequences can be minimized by increasing the number of cells sorted and/or by decreasing the number of colonies selected. For example, very little, if any, re-sampling would be expected if 100 colonies were sequenced from 2000 cells. Increasing the number of colonies screened to 200 would increase the probability of re-sampling, but still less than 10 % of the sequences would be expected to be identical due to re-sampling.
17. The frequency of background errors in this assay due to PCR can be estimated based on the published fidelities of thermostable DNA polymerases. While error rates vary considerably depending on the specific polymerase, reaction conditions, and template sequence, error rates for Taq generally range from 10^{-4} to 10^{-5} mutations/bp/cycle [33–38] while error rates for proofreading polymerases range from 10^{-6} to 10^{-7} mutations/bp/cycle [36, 37, 39]. Phusion Hot Start II exhibits an error rate of 4.4×10^{-7} mutations/bp/cycle according to the manufacturer, while published estimates of its error rate range from 4.2×10^{-7} to 2.6×10^{-6} mutations/bp/cycle [36, 37, 39]. Based on these error rates, the size of the mutational target (*egfp*-720 bp), and 40 cycles of amplification, the use of Phusion should result in ~0.02–0.07 errors/sequence. As we typically observe an average of ~1 mutation/sequence, these calculations suggest that PCR-mediated errors would contribute <10 % of the resulting data. In contrast, Taq would be expected to result in ~0.3–3.0 errors/sequence, and PCR errors would thus substantially contribute to resulting mutational spectra data. PCR errors can also be reduced by limiting the number of cycles to 30 or 35, but the benefit is marginal (e.g., 30 cycles with Phusion would lower expected errors to

0.01–0.06 errors/sequence), and the resulting products may not be readily visible by gel electrophoresis.

18. Most of the mutations in the PCR products can be identified by single-sequencing reactions with primers that anneal to regions of the vector flanking the insert, such as the T7 and SP6 promoters. However, as the PCR product is 981 bp in length, both sequencing reactions are necessary to cover the entire 981 bp region. The overlapping region of these sequences can also be used to ensure that the same mutation is identified in both directions.
19. In this assay, we have observed occasional G-to-A hypermutants, characterized by 2–20 G-to-A mutations in a single-sequencing read [18, 20]. The high numbers of G-to-A mutations as well as their dinucleotide context (heavily biased toward GA dinucleotides) suggest that these hypermutants result from the activity of APOBEC3 proteins. Although these sequences are relatively rare, they can contain many G-to-A mutations and thus substantially skew the mutation spectra. Therefore, we suggest compiling and comparing mutation spectra with and without the G-to-A hypermutants from each sample.
20. If three independent experiments were performed, analyze the data using the Cochran-Mantel-Haenszel test, as this procedure can assess differences in mutation types and also account for differences among the independent experiments. If the experiment was not performed three independent times, evaluate the data using Fisher's exact test. While these analyses are useful, they may not be powerful enough to detect small differences between treatment groups. To increase the likelihood of detecting differences in mutation types, it is always preferable to have a hypothesis that focuses on one specific mutation type. For example, studies focused on APOBEC3 proteins may only require detecting differences in the G-to-A mutations rather than identifying differences in all types of mutations.

Acknowledgements

This work was supported by NIH grant R01 GM105876. J.M.O.R. was supported by NIH grant T32 AI083196 and a University of Minnesota Doctoral Dissertation Fellowship. We are grateful to Cavan Reilly and James Hodges for advice on statistical procedures.

References

1. Mansky LM, Temin HM (1995) Lower in vivo mutation rate of human immunodeficiency virus type 1 than that predicted from the fidelity of purified reverse transcriptase. J Virol 69:5087–5094
2. Mansky LM (1996) Forward mutation rate of human immunodeficiency virus type 1 in a T lymphoid cell line. AIDS Res Hum Retroviruses 12:307–314
3. Mansky LM (1996) The mutation rate of human immunodeficiency virus type 1 is influenced by the vpr gene. Virology 222:391–400. doi:10.1006/viro.1996.0436
4. O'Neil PK, Sun G, Yu H, Ron Y, Dougherty JP, Preston BD (2002) Mutational analysis of HIV-1 long terminal repeats to explore the relative contribution of reverse transcriptase and RNA polymerase II to viral mutagenesis. J Biol Chem 277:38053–38061. doi:10.1074/jbc.M204774200
5. Huang KJ, Wooley DP (2005) A new cell-based assay for measuring the forward mutation rate of HIV-1. J Virol Methods 124:95–104. doi:10.1016/j.jviromet.2004.11.010
6. Abram ME, Ferris AL, Shao W, Alvord WG, Hughes SH (2010) Nature, position, and frequency of mutations made in a single cycle of HIV-1 replication. J Virol 84:9864–9878. doi:10.1128/JVI.00915-10
7. Schlub TE, Grimm AJ, Smyth RP, Cromer D, Chopra A, Mallal S, Venturi V, Waugh C, Mak J, Davenport MP (2014) 15-20% of HIV substitution mutations are associated with recombination. J Virol 88:3837. doi:10.1128/JVI.03136-13
8. Abram ME, Ferris AL, Das K, Quinones O, Shao W, Tuske S, Alvord WG, Arnold E, Hughes SH (2014) Mutations in HIV-1 reverse transcriptase affect the errors made in a single cycle of viral replication. J Virol 88:7589–7601. doi:10.1128/JVI.00302-14
9. Smyth RP, Davenport MP, Mak J (2012) The origin of genetic diversity in HIV-1. Virus Res 169:415–429. doi:10.1016/j.virusres.2012.06.015
10. Delviks-Frankenberry K, Galli A, Nikolaitchik O, Mens H, Pathak VK, Hu WS (2011) Mechanisms and factors that influence high frequency retroviral recombination. Viruses 3:1650–1680. doi:10.3390/v3091650
11. Mansky LM, Bernard LC (2000) 3′-Azido-3′-deoxythymidine (AZT) and AZT-resistant reverse transcriptase can increase the in vivo mutation rate of human immunodeficiency virus type 1. J Virol 74:9532–9539
12. Mansky LM (2003) Mutagenic outcome of combined antiviral drug treatment during human immunodeficiency virus type 1 replication. Virology 307:116–121
13. Mansky LM, Le Rouzic E, Benichou S, Gajary LC (2003) Influence of reverse transcriptase variants, drugs, and Vpr on human immunodeficiency virus type 1 mutant frequencies. J Virol 77:2071–2080
14. Chen R, Yokoyama M, Sato H, Reilly C, Mansky LM (2005) Human immunodeficiency virus mutagenesis during antiviral therapy: impact of drug-resistant reverse transcriptase and nucleoside and nonnucleoside reverse transcriptase inhibitors on human immunodeficiency virus type 1 mutation frequencies. J Virol 79:12045–12057. doi:10.1128/JVI.79.18.12045-12057.2005
15. Dapp MJ, Clouser CL, Patterson S, Mansky LM (2009) 5-Azacytidine can induce lethal mutagenesis in human immunodeficiency virus type 1. J Virol 83:11950–11958. doi:10.1128/JVI.01406-09
16. Clouser CL, Patterson SE, Mansky LM (2010) Exploiting drug repositioning for discovery of a novel HIV combination therapy. J Virol 84:9301–9309. doi:10.1128/JVI.01006-10
17. Clouser CL, Chauhan J, Bess MA, van Oploo JL, Zhou D, Dimick-Gray S, Mansky LM, Patterson SE (2012) Anti-HIV-1 activity of resveratrol derivatives and synergistic inhibition of HIV-1 by the combination of resveratrol and decitabine. Bioorg Med Chem Lett 22:6642–6646. doi:10.1016/j.bmcl.2012.08.108
18. Rawson JM, Heineman RH, Beach LB, Martin JL, Schnettler EK, Dapp MJ, Patterson SE, Mansky LM (2013) 5,6-Dihydro-5-aza-2′-deoxycytidine potentiates the anti-HIV-1 activity of ribonucleotide reductase inhibitors. Bioorg Med Chem 21:7222–7228. doi:10.1016/j.bmc.2013.08.023
19. Dapp MJ, Bonnac L, Patterson SE, Mansky LM (2014) Discovery of novel ribonucleoside analogs with activity against human immunodeficiency virus type 1. J Virol 88:354–363. doi:10.1128/JVI.02444-13
20. Holtz CM, Mansky LM (2013) Variation of HIV-1 mutation spectra among cell types. J Virol 87:5296–5299. doi:10.1128/JVI.03576-12
21. Dapp MJ, Heineman RH, Mansky LM (2013) Interrelationship between HIV-1 fitness and mutation rate. J Mol Biol 425:41–53. doi:10.1016/j.jmb.2012.10.009

22. Chen R, Le Rouzic E, Kearney JA, Mansky LM, Benichou S (2004) Vpr-mediated incorporation of UNG2 into HIV-1 particles is required to modulate the virus mutation rate and for replication in macrophages. J Biol Chem 279:28419–28425. doi:10.1074/jbc.M403875200
23. Refsland EW, Harris RS (2013) The APOBEC3 family of retroelement restriction factors. Curr Top Microbiol Immunol 371:1–27. doi:10.1007/978-3-642-37765-5_1
24. Munk C, Jensen BE, Zielonka J, Haussinger D, Kamp C (2012) Running loose or getting lost: how HIV-1 counters and capitalizes on APOBEC3-induced mutagenesis through its Vif protein. Viruses 4:3132–3161. doi:10.3390/v4113132
25. Gao F, Chen Y, Levy DN, Conway JA, Kepler TB, Hui H (2004) Unselected mutations in the human immunodeficiency virus type 1 genome are mostly nonsynonymous and often deleterious. J Virol 78:2426–2433
26. Dohm JC, Lottaz C, Borodina T, Himmelbauer H (2008) Substantial biases in ultra-short read data sets from high-throughput DNA sequencing. Nucleic Acids Res 36:e105. doi:10.1093/nar/gkn425
27. Minoche AE, Dohm JC, Himmelbauer H (2011) Evaluation of genomic high-throughput sequencing data generated on Illumina HiSeq and genome analyzer systems. Genome Biol 12:R112. doi:10.1186/gb-2011-12-11-r112
28. Nakamura K, Oshima T, Morimoto T, Ikeda S, Yoshikawa H, Shiwa Y, Ishikawa S, Linak MC, Hirai A, Takahashi H, Altaf-Ul-Amin M, Ogasawara N, Kanaya S (2011) Sequence-specific error profile of Illumina sequencers. Nucleic Acids Res 39:e90. doi:10.1093/nar/gkr344
29. Bebenek K, Kunkel TA (1995) Analyzing fidelity of DNA polymerases. Methods Enzymol 262:217–232
30. Boyer JC, Bebenek K, Kunkel TA (1996) Analyzing the fidelity of reverse transcription and transcription. Methods Enzymol 275:523–537
31. Beach LB, Rawson JM, Kim B, Patterson SE, Mansky LM (2014) Novel inhibitors of human immunodeficiency virus type 2 infectivity. J Gen Virol 95:2778. doi:10.1099/vir.0.069864-0
32. Vodicka MA, Goh WC, Wu LI, Rogel ME, Bartz SR, Schweickart VL, Raport CJ, Emerman M (1997) Indicator cell lines for detection of primary strains of human and simian immunodeficiency viruses. Virology 233:193–198. doi:10.1006/viro.1997.8606
33. Cline J, Braman JC, Hogrefe HH (1996) PCR fidelity of pfu DNA polymerase and other thermostable DNA polymerases. Nucleic Acids Res 24:3546–3551
34. Flaman JM, Frebourg T, Moreau V, Charbonnier F, Martin C, Ishioka C, Friend SH, Iggo R (1994) A rapid PCR fidelity assay. Nucleic Acids Res 22(15):3259–3260
35. Keohavong P, Thilly WG (1989) Fidelity of DNA polymerases in DNA amplification. Proc Natl Acad Sci U S A 86:9253–9257
36. Li M, Diehl F, Dressman D, Vogelstein B, Kinzler KW (2006) BEAMing up for detection and quantification of rare sequence variants. Nat Methods 3:95–97. doi:10.1038/nmeth850
37. McInerney P, Adams P, Hadi MZ (2014) Error rate comparison during polymerase chain reaction by DNA polymerase. Mol Biol Int 2014:287430. doi:10.1155/2014/287430
38. Tindall KR, Kunkel TA (1988) Fidelity of DNA synthesis by the Thermus aquaticus DNA polymerase. Biochemistry 27:6008–6013
39. Kinde I, Wu J, Papadopoulos N, Kinzler KW, Vogelstein B (2011) Detection and quantification of rare mutations with massively parallel sequencing. Proc Natl Acad Sci U S A 108:9530–9535. doi:10.1073/pnas.1105422108

Part II

HIV-1 RNA Structure and RNA-Protein Interactions

Chapter 7

Novel Biochemical Tools for Probing HIV RNA Structure

Jason W. Rausch, Joanna Sztuba-Solinska, Sabrina Lusvarghi, and Stuart F.J. Le Grice

Abstract

Functional analysis of viral RNA requires knowledge of secondary structure arrangements and tertiary base interactions. Thus, high-throughput and comprehensive methods for assessing RNA structure are highly desirable. Selective 2′-hydroxyl acylation analyzed by primer extension (SHAPE) has proven highly useful for modeling the secondary structures of HIV and other retroviral RNAs in recent years. This technology is not without its limitations however, as SHAPE data can be severely compromised when the RNA under study is structurally heterogeneous. In addition, the method reveals little information regarding the three-dimensional (3D) organization of an RNA. This chapter outlines four detailed SHAPE-related methodologies that circumvent these limitations. "Ensemble" and "in-gel" variations of SHAPE permit structural analysis of individual conformers within structurally heterogeneous mixtures of RNA, while probing strategies that utilize "through-space" cleavage reagents such as methidiumpropyl-EDTA (MPE) and peptides appended with an ATCUN (amino terminal copper/nickel binding motif) can provide insight into 3D organization. Combinational application of these techniques provides a formidable arsenal for exploring the structures of HIV RNAs and associated nucleoprotein complexes.

Key words Ensemble SHAPE, In-gel SHAPE, Methidiumpropyl-EDTA, ATCUN, Chemical probing, HIV RNA

Abbreviations

ATCUN	Amino terminal copper- and nickel-binding motif
MPE	Methidiumpropyl-EDTA
ND	Non-denaturing
PAGE	Polyacrylamide gel electrophoresis
RRE	Rev response element
SHAPE	Selective 2′-hydroxyl acylation analyzed by primer extension
TAR	Trans-activation response element

Jason W. Rausch and Joanna Sztuba-Solinska have equally contributed to this chapter.

Vinayaka R. Prasad and Ganjam V. Kalpana (eds.), *HIV Protocols*, Methods in Molecular Biology, vol. 1354,
DOI 10.1007/978-1-4939-3046-3_7,

1 Introduction

SHAPE, or selective 2′-OH acylation analyzed by primer extension, is a biochemical method that has been used to obtain secondary structural models for segments of HIV RNA including the 5′ untranslated region (5′ UTR; [1]) and the Rev response element (HIV-1 RRE; [2]), as well as the HIV-1 RNA genome in its entirety, both in vitro and in virio [3]. Unlike traditional chemical probing techniques, SHAPE reagents are non-hazardous and exhibit minimal nucleotide reactivity bias. Moreover, SHAPE can be adapted for use with high-throughput capillary electrophoresis, making it the method of choice for biochemical RNA structure probing.

The defining feature of SHAPE is exposure of RNA to a probing reagent that selectively acylates unpaired ribonucleotides at the 2′-OH position. The sites and frequencies of RNA acylation are then recorded by reverse transcription, where cDNA synthesis prematurely terminates at RNA acylation sites. The resulting cDNA library is fractionated by denaturing polyacrylamide gel or capillary electrophoresis and detected/quantified as described herein and previously [4]. Raw cDNA quantities obtained by fractionating reverse transcription products are subjected to mathematical transformations such as signal decay correction, background subtraction and internal normalization to produce "reactivity values" attributable to individual template ribonucleotides. Collectively, a set of reactivity values obtained for a given RNA is referred to as the reactivity profile of that RNA. This metric may be inputted into RNAstructure software [5] to obtain the most energetically favorable secondary structural model(s) for the RNA in question. Alternatively, in the event that RNAstructure software is unavailable or does not meet the user's needs, a reactivity profile may be overlaid onto a secondary structural model generated by other methods, and the fit between the profile and model evaluated subjectively.

One shortcoming of SHAPE is that it has required the RNA under evaluation to be structurally homogeneous throughout the course of the acylation reaction. Failure to meet this requirement can produce an "averaged" structure model that fails to match any of the RNA conformers present in solution. However, two variations of the methodology have recently been developed that circumvent the requirement for RNA structural homogeneity: ensemble SHAPE and in-gel SHAPE. These variations enable assignment of RNA secondary structures to individual conformers present in a mixture, provided that these can be segregated by non-denaturing polyacrylamide gel electrophoresis. Although related, the SHAPE variations differ significantly in the manner in which reactivity data is obtained and processed.

The guiding concept of ensemble SHAPE is that experimentally determined reactivity values are actually composite values comprised of contributions from each of the individual RNA conformers present in a mixture. In addition, conformer contributions to the ensemble reactivity value are in proportion to their molar fractions in solution. As described herein, these principles can be expressed algebraically, thus allowing for mathematical extraction of theoretical reactivity values and profiles, and therefore structures, attributable to individual RNA conformers. Experimentally, ensemble SHAPE resembles conventional SHAPE except that the former additionally requires fractionation and quantitation of RNA conformers by non-denaturing polyacrylamide gel electrophoresis. SHAPE experiments must also be repeated under conditions that produce differing conformer distributions; specifically, at least one unique distribution is required per conformer in order for the resulting algebraic formulae to be solved. Ensemble SHAPE has been experimentally validated using in vitro-transcribed model RNAs derived from the HIV-1 5′ UTR, and subsequently to identify intermediate structures assumed upon folding of the HIV-2 RRE [6].

Data acquisition and analysis are more straightforward for in-gel SHAPE, although this approach is more labor intensive and typically requires more RNA than ensemble SHAPE. During in-gel SHAPE, conformeric mixtures of RNA are fractionated by non-denaturing gel electrophoresis, bands comprised of individual conformers are excised from the gel, and acylating reagent is soaked into the slices. Modified RNAs are extracted by electroelution, precipitated, and subjected to the same reverse transcription and downstream procedures required in standard SHAPE. Like ensemble SHAPE, in-gel SHAPE is suitable for examining conformeric mixtures of RNA, particularly when the RNA is abundant and individual conformers can be completely separated by non-denaturing PAGE. In-gel probing is also theoretically applicable to footprinting of RNA-protein complexes, provided that these complexes are stable throughout the course of non-denaturing gel electrophoresis. In-gel SHAPE has been used to identify structural transitions that occur during dimerization of the HIV-1 5′UTR [7], as well as to define alternative conformations of the HIV-1 RRE (Rausch, J. W., unpublished observations).

While SHAPE is a simple and elegant tool for determining and refining RNA secondary structural models, none of its variations can be used to directly explore the 3D organization of an RNA. This information can be revealed using “through space” probing reagents, i.e., reagents that bind within defined motifs in an RNA and cleave or modify ribonucleotides in spatial proximity—including those not within or adjacent to the reagent binding site(s). Methidiumpropyl-EDTA (MPE) is one such reagent and has been used to validate the computer-generated three-dimensional

structure of HIV-2 RRE RNA [6]. MPE comprises two functional groups: methidium, which has been reported to intercalate between adjacent ribonucleotides within defined RNA structural motifs such as CpG islands [8], and EDTA, which chelates Fe(II). When activated, tethered iron ions generate hydroxyl radicals that diffuse to and damage/cleave RNA near the MPE binding site(s). Nucleotides thus modified are identified by reverse transcription, and cDNAs are fractionated and quantified as in standard SHAPE. Such experiments, together with control experiments to identify specific methidium-binding sites, can provide useful insights into the 3D organization of an RNA.

Finally, in some instances, it is useful to tether a cross-linking or chemical cleavage agent to a protein or peptide component of a nucleoprotein complex in order to directly probe the ligand binding site(s) of an RNA. ATCUNs, or amino-terminal Cu^{2+}/Ni^{2+} binding motifs, are 3-amino acid sequences (typically NH_2-Xaa-Xaa-His, where X is any amino acid) that have been shown to chelate these metal ions and consequently, when activated, damage or cleave proximal RNA. When incorporated into RNA-binding peptides, the modification patterns produced by these peptides correlate with and allow for definition of ligand-binding sites. We have generated peptides linking an ATCUN with the arginine-rich nucleic acid-binding motif of either HIV-1 or HIV-2 Rev (ARM1 or ARM2), and used these Rev-ATCUN peptides to probe Rev binding sites on their respective RREs. After being exposed to/modified by these peptides, RRE RNAs were subjected to reverse transcription and the subsequent processing of conventional SHAPE.

Together, ensemble SHAPE, in-gel SHAPE, MPE-Fe(II), and peptide-ATCUN probing constitute a formidable arsenal for exploring the structures of HIV RNAs and nucleoprotein complexes—even when the RNAs/complexes are not structurally homogeneous. These methods are presented together here both because of their related applications and because they share a common backbone protocol of RNA modification, reverse transcription, cDNA fractionation and data processing/analysis. An additional method, i.e., three-dimensional modeling of RNAs using the recently developed RNAComposer software [9], is also briefly discussed.

2 Materials

Take precautions working with RNA to prevent non-specific degradation. Use molecular biology-grade chemicals and reagents and ultrapure water for preparation of all solutions.

1. RNA.

   Extract RNA from biological samples or transcribe in vitro. It is often preferable to purify RNAs prior to probing, i.e., via denaturing polyacrylamide gel electrophoresis [10] or using commercially available kits, but this is not always essential. Shorter RNAs (<400 nt) are generally best suited for the applications presented here and may be engineered to contain a 3′ structure cassette [4] to maximize the amount of native sequence that is readable. Store frozen, in low salt buffer such as TE light: 10 mM Tris-Cl, pH 7.6; 0.1 mM EDTA.

2. RNA folding.

   10× RNA folding buffer: 500 mM Tris–HCl, pH 8.0, 50 mM $MgCl_2$, 1.0 M NaCl.

   2× ND gel RNA folding buffer: 70 mM Tris–HCl, pH 8.0, 180 mM KCl, 0.3 mM EDTA, 8 mM $MgCl_2$, 10 % glycerol.

3. Non-denaturing polyacrylamide gel electrophoresis (ND PAGE) and RNA detection/quantitation.

   10× TBE: 0.89 M Tris-borate, pH 8.3, 20 mM Na_2EDTA.

   40 % acrylamide/bis-acrylamide (19:1).

   10 % ammonium persulfate (store at 4 °C).

   Tetramethylethylenediamine (TEMED).

   10× ND gel loading buffer: 50 % glycerol, 0.025 % bromophenol blue.

   Electrophoresis equipment (power supply, gel box, gel plates, combs, spacers).

   SYBR Green II RNA gel stain (Life Technologies).

   Fluorescent TLC plate.

   Clear plastic wrap or plastic bag.

   Fluorescence scanner.

4. RNA modification.

   N-methylisatoic anhydride (NMIA) (store desiccated at ambient temperature).

   1-Methyl-7-nitroisatoic anhydride (1M7) (*see* **Note 1**).

   Dimethyl sulfoxide (DMSO).

   5× TBE reaction buffer: 5× TBE, 25 mM $MgCl_2$.

5. Precipitation.

   100 % ethanol (used to make 95 % ethanol).

   3 M NaOAc, pH 5.5.

   10 mg/mL glycogen.

6. MPE cleavage.

   Methidiumpropyl-EDTA (*see* **Note 2**).

   Methidium carboxylate TFA salt (*see* **Note 2**).

   10 mM sodium ascorbate (prepare fresh with each use, protect from light).

   0.3 % hydrogen peroxide (prepare fresh with each use).

   $Fe(SO_4)_2$ $(NH_4)_2 \cdot 6H_2O$.

7. ATCUN-peptide RNA modification.

   Peptides containing the ATCUN motif (N-terminus-aa1-aa2-His) can be synthesized in-house using solid-phase synthesis or purchased commercially. Peptides should be HPLC purified and stored in water at −20 °C.

   RNA buffer: 50 mM Tris–HCl, pH 8.0, 100 mM NaCl, 5 mM $MgCl_2$.

   $NiCl_2$.

8. Reverse transcription.

   SuperScript™ III Reverse Transcriptase (Life Technologies; *see* **Note 3**).

   10 mM dNTP Mix, PCR grade.

   Primers 5′end-labeled with Cy5 or Cy5.5 (*see* **Note 4**).

9. Preparation of sequencing ladders.

   Primers 5′end-labeled with WellRed D2 or Licor IR800 (*see* **Note 4**).

   USB Cycle Sequencing kit (*see* **Note 5**).

10. Capillary electrophoresis (*see* **Note 6**).

    Deionized formamide.

    Beckman-Coulter CEQ 8000 Genetic Analyzer.

    96-Well sample microtiter plate.

    Thermowell® 96 well PCR plate.

    CEQ™ Separation Buffer (Beckman Coulter).

    LPA-1 gel (Beckman Coulter).

11. RNA modeling.

    ShapeFinder software: To obtain this software, contact Morgan C. Giddings (http://giddingslab.org/welcome).

    RNAstructure software: http://rna.urmc.rochester.edu/RNAstructure.html

    VARNA RNA folding software: http://varna.lri.fr/

3 Methods

3.1 Ensemble SHAPE

Ensemble SHAPE is useful for studying RNAs that assume more than one conformational state in solution. While the differences between ensemble and conventional SHAPE relate primarily to data processing, two conditions must be met before an RNA may be analyzed using the former method. First, it must be possible to segregate RNA conformers by electrophoretic mobility on a non-denaturing polyacrylamide gel. This in turn requires that conformer interconversion occurs only slowly or not at all during electrophoresis. Second, at least one distinct mixture of conformers—each with a unique conformer distribution—must be evaluated for every conformer observed. This requirement relates to the algebraic relationships among the reactivity values measured for each mixture, the distribution of conformers in each mixture, and the theoretical reactivity values calculated for each conformer. This algebraic relationship is discussed in more detail below.

Ensemble SHAPE was used to determine the structures of transient folding intermediates of the HIV-2 RRE (Fig. 1) [6]. In this case, three distinct conformers could be segregated by non-denaturing gel electrophoresis, and the distribution of conformers in the mixture was found to vary with RNA folding time (i.e., the amount of time the RNA was incubated at 37 °C in the presence

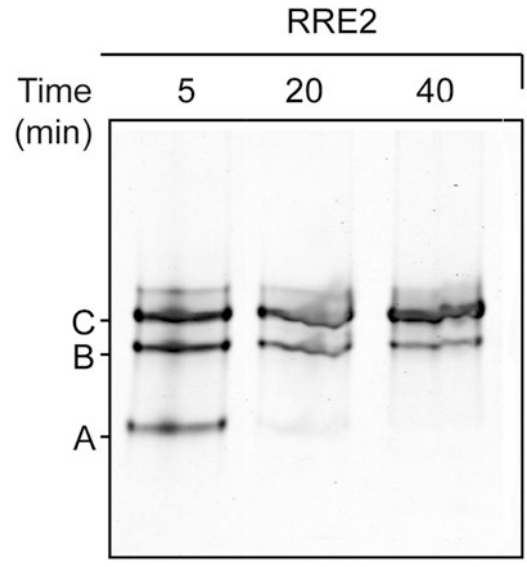

Fig. 1 Non-denaturing gel migration and distribution of HIV-2 RRE conformers as a function of RNA folding time (artistic depiction). During the early stages of RNA folding, the HIV-2 RRE exists as a mixture of three conformers designated A, B, and C. The relative abundance of these conformers varies with RNA folding time, with the most stable conformer C ultimately predominating.

of 5 mM $MgCl_2$ after heating/cooling). As folding time increased, the less stable conformations were increasingly converted into the most stable form. We were able to evaluate five different conformer distributions, one each at 5, 10, 20, 40, and 100 min of RNA folding, thus satisfying both of the aforementioned requirements for using ensemble SHAPE.

3.1.1 RNA Folding

Parameters that must be considered in an RNA folding procedure include (1) RNA quantity and concentration, (2) reaction volume, (3) salt concentration, (4) Mg^{2+} ion concentration, and (5) folding duration. Although specific optimization goals may vary, it is generally desirable to establish conditions that are close to physiological and/or produce a structurally homogeneous RNA. Conditions used to fold HIV-2 RRE RNA are given below.

For ensemble SHAPE, RNA mixtures must be evaluated by non-denaturing gel electrophoresis (to determine the fractional contribution of each conformer) as well as by SHAPE. However, provided a given set of folding conditions consistently produces the same conformer distribution, it is not essential that the two experiments be conducted using portions of the same RNA sample. For the HIV-2 RRE, conformer distributions were the same regardless of RNA concentration. Hence, differing amounts of RNA (4 pmol or 40 pmol, respectively) were used for non-denaturing gel electrophoresis and for SHAPE. A typical HIV-2 RRE RNA folding procedure is described here:

1. Dissolve or dilute 4 (40) pmol RNA in 36 μL of water.
2. Heat to 95 °C for 3 min and then immediately cool on ice for at least 5 min.
3. Add 4 μL of 10× RNA folding buffer. Mix.
4. Incubate at 37 °C.
5. At 5, 10, and 20 min, transfer 10 μL folding mix to precooled 0.5 mL microfuge tubes on ice to arrest RNA folding.
6. Analytical ND gel samples: Add 1 μL 10× ND gel loading buffer and fractionate by ND PAGE (Subheading 3.1.2).
7. SHAPE samples: Dilute with 30 μL 1× RNA folding buffer (40 μL total, each) and divide mixture into 20 μL modified (+) and control (−) aliquots. Continue with RNA modification (Subheading 3.1.4).

3.1.2 RNA Fractionation by ND PAGE

Prior to conducting a SHAPE experiment, the structural homo- or heterogeneity of the RNA being studied should first be assessed on an analytical scale by non-denaturing polyacrylamide gel electrophoresis (ND PAGE) [11]. In-gel detection of RNA by SYBR Green staining typically requires loading of 25–100 ng RNA per well, depending on the length of the RNA in question, the number

and distribution of conformers in the mixture, well width, and other parameters that must be empirically optimized. If the RNA is found to be heterogeneous, ensemble or in-gel SHAPE may then be used to determine the structures of individual conformers. However, these methods require additional analytical scale ND gel electrophoresis followed by quantification of RNA conformers or preparative-scale ND PAGE, respectively.

Because the conditions required for ND PAGE vary considerably according to the RNA probing methodology being used, the RNA being fractionated, electrophoresis equipment and a number of other factors, we are unable to provide a definitive protocol for this technique that is suitable for all of the applications presented here. However, the following procedure provides general guidelines for ND-PAGE that may be modified to suit a specific application:

1. Pouring the gel: We typically pour gels containing 5–8 % polyacrylamide (19:1 acrylamide:bis-acrylamide), 1× TBE ± 4–5 mM $MgCl_2$ to fractionate RNAs from 100 to 400 nt in length. Gel plate dimensions are approximately 15 cm × 15 cm and spacers/combs are typically 0.8 or 1.6 mm thick. Polymerization of gel solution is activated prior to pouring by mixing in of 1/100th volume 10 % ammonium persulfate and 1/1000th volume tetramethylethylenediamine (TEMED).
2. Pre-running the gel: Clamp gel into the gel tank and add buffer. Remove comb and clean out the wells out with a syringe/needle. Gels are typically pre-run for 30–60 min in 1× TBE (±5 mM $MgCl_2$) at 150–200 V and 4 °C prior to sample loading.
3. Sample loading: Sample volumes and RNA concentrations vary widely by method. Typically, 5–20 μL samples containing a total of 25–100 ng RNA are loaded in each well for analytical ND PAGE and ensemble SHAPE, while 40–200 μL samples of 10 μg RNA or more may be required for in-gel SHAPE. Unless glycerol was already present in the RNA folding buffer, add 1/10th volume of 10× ND gel loading buffer to the samples, so they layer evenly at the bottoms of the wells.
4. Running the gel: Gels are run under conditions matching the pre-run, i.e., typically at 150–200 V and 4 °C. It is important that the RNA remains cool both immediately prior to and during the gel run to minimize interconversion among conformers and smearing of the associated bands.

3.1.3 Detection and Quantitation of RNA

Small quantities of RNAs that have been fractionated by ND PAGE are detected using the fluorescent dye SYBR Green, and quantified as necessary for ensemble SHAPE.

1. Remove gel sandwich from gel box and place flat on workbench. Carefully remove top plate using spacers and/or spatulas.

Pour or wick away with a paper towel any pooled buffer on the surface of the gel.

2. Dilute 1 μL SYBR Green dye in 10 mL water and pour solution evenly over gel surface. Use roller where necessary to ensure complete coverage. Wait for 5 min to allow dye to soak into gel and bind RNA.
3. Pour off or wick away SYBR Green solution from the gel. Carefully place clear plastic wrap over the gel surface and around the bottom plate to seal in residual liquid.
4. Scan gel in fluorescence scanner at 520 nm and quantify fractionated conformers using appropriate software.

3.1.4 RNA Modification and Recovery

1M7 and NMIA are the best-characterized SHAPE reagents, with half-lives in aqueous solution of ~70 s and ~8 min, respectively [12]. However, in order to minimize the opportunity for RNA conformers to interconvert during the course of the acylation reaction, the more reactive 1M7 reagent is generally preferred for use in ensemble SHAPE experiments.

1. Prepare a 30 mM solution of 1M7 by adding small amounts of reagent to a 1.5 mL microfuge tube and then adding an appropriate volume of DMSO (*see* **Note 7**).
2. Add 2 μL 1M7 solution or DMSO, respectively, to the 20 μL (+) and (−) aliquots produced in the RNA folding step (Subheading 3.1.1).
3. Incubate reactions at 37 °C for 5 min (*see* **Note 8**).
4. Precipitate RNA. Add 52.5 μL cold 100 % ethanol, 2.1 μL 3 M NaOAc (pH 5.5) and 0.2 μL glycogen (10 mg/mL). Mix gently. Incubate at −20 °C for 2 h.
5. Collect precipitated RNA by centrifugation at 14,000 × *g* for 30 min, carefully remove supernatant, and air-dry the pellet for 1–5 min (*see* **Note 9**).
6. Dissolve RNA in 10 μL of TE buffer. Proceed to reverse transcription (Subheading 3.1.5), or store at −20 °C.

3.1.5 Reverse Transcription

This step generates cDNA products that indirectly identify the degree to which RNA nucleotides have been modified by 1M7 or NMIA. If reverse transcription reactions are primed with fluorescently tagged oligonucleotides, the relative abundance of each cDNA fragment can be assessed via capillary electrophoresis (CE). Oligonucleotides labeled with Cy5 and Cy5.5 are used to prime the (+) and (−) reactions, respectively. These primers should be stored in small aliquots in amber microfuge tubes at −20 °C. Note that 5′ ^{32}P-labeled primers (5′-RP) may be used as an alternative to fluorescent primers in the reverse transcription reactions, in which case lower concentrations of both primer and template may be

used. Additional comments addressing the use of radiolabeled primers are designated 5′-RP below.

1. Prepare (+) and (−) RNA samples for reverse transcription in 0.5 mL microfuge tubes. Transfer 5 μL of (+) and (−) samples from modification step (~2.5 pmol RNA each) into 0.5 mL microfuge tubes. Store the unused portion at −20 °C. For the (+) RT reaction, add 6 μL of water and 1 μL Cy5-labeled primer (10 μM); for the (−) RT reaction, add 6 μL water and 1 μL Cy5.5-labeled primer (10 μM).
2. Thaw the RT mix reagents (5× RT buffer, 100 mM DTT, RNase-free water, and 10 mM dNTPs) and place on ice.
3. Place (+) and (−) reaction tubes in a thermal cycler and initiate the following program: 85 °C, 1 min; 60 °C, 5 min; 35 °C, 5 min and 50 °C, 50 min (*see* **Note 10**).
4. During annealing, prepare 2.5× RT mix by combining 4 μL 5× RT buffer, 1 μL 100 mM DTT, 1.5 μL water, 1 μL 10 mM dNTPs and 0.5 μL SuperScript™ III reverse transcriptase for each RT reaction. Mix well and incubate at 37 °C for 5 min.
5. Once the temperature of the annealing reactions reaches 50 °C, add 8 μL of 2.5× RT mix to each and continue incubation at 50 °C for 50 min (*see* **Note 11**).
6. Add 1 μL 4 M NaOH to each RT reaction and incubate at 95 °C for 3 min to hydrolyze the RNA. Cool the tubes on ice and neutralize with 2 μL of 2 M HCl (*see* **Note 12**).
7. Combine (+) and (−) reactions in a single tube and precipitate by adding 54 μL water, 10 μL 3 M NaOAc, 0.8 μL glycogen (10 mg/mL), and 300 μL 100 % ethanol. Incubate at −20 °C for 2 h. Pellet cDNA by centrifugation at 13,000 × *g* for 30 min, 4 °C.
8. Wash pellet(s) twice with 400 μL of cold 70 % ethanol and centrifuge immediately at 13,000 × *g* for 5 min (*see* **Note 13**).
9. Remove supernatant and dry pellet for 3 min by centrifugal vacuum evaporation (*see* **Note 14**).
10. Dissolve DNA in 40 μL of deionized formamide (*see* **Note 15**).

3.1.6 Preparation of Sequencing Ladder

5′-end-labeled sequencing ladders generated by cycle sequencing (USB cycle sequencing kit, product #78500) are co-fractionated with (+) and (−) reverse transcription products by CE in order to map the 3′ termini of modified cDNAs. PCR-generated transcription templates can serve as sequencing templates, provided that they are purified from PCR primers and dNTPs prior to use. Due to the relatively low fluorescence of WellRed D2 and IRDye800, sequencing reactions must be scaled up severalfold to ensure sufficient yield for detection by capillary electrophoresis. In the example below, ddA and ddC are used as chain terminating nucleotides.

However, any combination of dideoxynucleotide triphosphates may be used to generate sequencing ladders. 5′-RP: Use the USB cycle sequencing kit protocols for 5′ end-labeling and cycle sequencing.

1. Mix 16 μL ddA termination mix, 0.5 pmol of DNA template, 1.8 μL 10× Sequenase buffer, 2.0 μL WellRed D2 labeled primer (5 μM) in a 0.5 mL thin-walled microfuge tube. Add water to bring the total volume to 30 μL, mix, add 2.0 μL Sequenase, and mix again. Store on ice until cycling.
2. Prepare a second, parallel sequencing reaction including primer labeled with IRDye800 and ddC termination mix.
3. Cycle both sequencing mixes according to the program recommended by the kit manufacturer.
4. Combine the ddA and ddC sequencing reactions into one 1.5 mL microfuge tube (64 μL)
5. Precipitate sequencing products by adding 6.4 μL 3 M NaOAc (pH 5.5), 6.4 μL 100 mM EDTA, 0.5 μL 10 mg/mL glycogen, and 192 μL 95 % ethanol. Mix well, incubate at 4 °C for 2 h, and centrifuge at 13,000 × *g* for 30 min at 4 °C.
6. Remove supernatant by pipetting and dry pellet by vacuum centrifugation for 5 min.
7. Resuspend pelleted DNA in 100 μL of deionized formamide by heating to 65 °C for 10 min, followed by vortexing for at least 30 min.
8. Mix 10 μL pooled sequencing reactions with 40 μL pooled (+) and (−) RT reactions. Store the remaining sequencing reaction mix at −20 °C.

3.1.7 Capillary Electrophoresis

High-throughput capillary electrophoresis with fluorescence detection allows simultaneous fractionation and detection of four differently labeled DNA products in a single sample. The Beckman-Coulter CEQ 8000 Genetic Analyzer can fractionate as many as eight sets of pooled reactions simultaneously, while as many as 96 samples can be fractionated consecutively in a single program.

1. Load 40 μL of the pooled reactions (i.e., (+) Cy5-labeled cDNAs, (−) Cy5.5-labeled cDNAs, and two sequencing ladders labeled with WellRed D2 and IRDye800) into a single well in a 96-well sample plate. Repeat as necessary for additional pooled reactions, making sure to load them into the same row.
2. Program and prepare capillary electrophoresis instrument according to the previously published capillary automated footprinting analysis (CAFA) method parameters [13] and initiate run as per the manufacturer's instructions.
3. Export raw fluorescence traces into ShapeFinder.

5′-RP: Radioactive reverse transcription and cycle sequencing products can be fractionated over a denaturing slab gel (5–8 % 19:1 polyacrylamide:bis-acrylamide, 1× TBE, 7 M urea). Typically, samples are loaded in adjacent wells, and loading is staggered to maximize the amount of readable sequence. Gels are dried and exposed to a phosphorimaging cassette.

3.1.8 Data Analysis by ShapeFinder

ShapeFinder is free available software that allows the user to mathematically transform and graphically visualize CE migration data. To acquire ShapeFinder software, contact the Giddings lab (http://www.giddingslab.org). We provide here an overview of how SHAPE data are transformed to obtain an RNA reactivity profile. Detailed instructions for data handling in ShapeFinder are provided with the software documentation.

1. Adjust raw data to account for (1) fluorescent background, (2) spectral overlap between fluorescent traces, (3) differential mobility of equivalent DNAs labeled with different fluorophores, and (4) signal decay resulting from the imperfect processivity of reverse transcriptase (*see* **Note 16**).
2. Correlate peaks in the adjusted electropherogram to specific ribonucleotides in the RNA sequence using the "Setup" function of the "Align and Integrate" tool. Errors in initial assignments can be corrected manually using the "Modify" function of the same tool.
3. Calculate the areas under the aligned (+) and (−) reaction peaks using the "Fit" function. These values are automatically tabulated in a tab-delimited text file readable in Microsoft Excel or other spreadsheet software.

5′-RP: Bands corresponding to individual cDNAs are detected by phosphorimaging and quantified using software such as ImageQuant TL (GE Healthcare Life Sciences). Band volumes for (−) reaction products are subtracted from the corresponding (+) reaction products to generate raw reactivity values. Note that while cDNAs co-migrate with chain-terminated sequencing products of the same length, reactivity values should be attributed to ribonucleotides in the RNA sequence one position 5′ to the complementary cDNA stop position. Also, unlike ShapeFinder, ImageQuant TL cannot systematically correct for signal decay or band overlap as slower migrating products become less intense and closer together. For this, SAFA, or semiautomated footprinting analysis software, has proven useful [14]. This software is free and can be downloaded from http://ribosnitch.bio.unc.edu/The_Laederach_Lab/Software.html.

3.1.9 Data Normalization

Before raw reactivity values can be used for secondary structure modeling, SHAPE data must be normalized according to the "2–8 % rule" described previously [15, 16]. After this transformation,

reactivity values of <0.2 and >0.8 (for example) are deemed to reflect highly or minimally constrained nucleotide bases that are most likely base-paired or single-stranded, respectively. Extreme values (i.e., those <−0.2 or >1.5) must be interpreted with caution, as they are often indicative of natural RT pause sites ("stops") or are artificially produced by imperfect signal decay correction and/or data scaling. Because they typically represent <1 % of the data, excluding outliers from the reactivity profile inputted into the RNAstructure software is often the most prudent course of action. A general summary of the data normalization process follows:

1. In a new column in Microsoft Excel, order raw reactivity values and identify quartiles (Q1, Q2, and Q3).
2. Identify "outlier" values; i.e., values greater than $Q3 + 1.5 \times (Q3 - Q1)$.
3. Excluding outliers, calculate the average of the highest 8 % of the remaining values. This average is defined as the "effective maximum" of the data.
4. Normalize the original, unsorted reactivity data by dividing all values (including outliers) by the effective maximum, thereby producing normalized reactivity values for all nucleotides for which SHAPE data was obtained.
5. For ensemble SHAPE, proceed to "Mathematical Deconvolution" below (Subheading 3.1.10), after which **steps 6** and **7** here should be followed to eliminate bad values and to format conformer-specific reactivity profiles for use with RNAstructure. For the other three methods, proceed directly to **steps 6** and **7** below.
6. Eliminate values less than −0.09 and those associated with unusually strong natural pause sites (i.e., "stops"). Replace omitted values with "−999", the preferred skipped-value indicator in the RNAstructure software.
7. Save the paired nucleotide numbers and associated, normalized reactivity data as tab-delimited pairs arranged in adjacent columns as a text file with the suffix ".shape". This file provides the "SHAPE reactivity values" used to generate pseudoenergy constraints in RNAstructure software.

3.1.10 Mathematical Deconvolution (Ensemble SHAPE Only)

Normalized reactivity values obtained in ensemble SHAPE are comprised of contributions from all RNA conformers in a mixture. Because these are averaged values, they cannot be used to direct the secondary structural prediction of any single conformational variation of the RNA being probed. In order to obtain a reactivity profile attributable to an individual RNA conformer, theoretical reactivity values must be mathematically extracted from the experimentally obtained ensemble values, as described below. The resulting profile(s) may be inputted into RNAstructure software in the same manner as a profile generated by conventional SHAPE. In this

case, however, the set of theoretical reactivity values will be used by the software to generate pseudoenergy constraints that reflect the structure of the respective RNA conformation exclusively.

For an RNA that can assume any of the conformations A, B, or C (and perhaps others), and for each nucleotide position probed by SHAPE, the following mathematical relationship applies:

$$R_T = p_A R_A + p_B R_B + p_C R_C \ldots$$

In this equation, R_T is the experimentally determined, normalized ensemble reactivity value for a specific nucleotide position, and p_A, p_B, and p_C are the fractional contributions of individual conformers to total RNA, as determined by quantitative ND gel electrophoresis. R_A, R_B, and R_C are the theoretical reactivity values for the same nucleotide in the respective conformers; these values are calculated, and should remain constant regardless of the conformer distribution established in a given set of experimental conditions.

In the simplest possible example for which ensemble SHAPE may be applied, two RNA conformers are differently distributed under two distinct folding/solution conditions 1 and 2. Given the experimentally established mathematical relationship presented above, a two-variable, two-equation system may be established for this scenario as follows:

$$\text{Conditions—1: } R_{T1} = p_{A1} R_A + p_{B1} R_B$$

$$\text{Conditions—2: } R_{T2} = p_{A2} R_{A+} p_{B2} R_B$$

Variable assignments are the same as in the general case above except that the subscript "1" or "2" indicates the value in question was measured using RNA folded under the specified set of conditions. Also, for the system of equations to be soluble in all but the trivial instance in which $R_{T1} = R_{T2}$, conformer distributions must differ under the two sets of conditions (i.e., so that $p_{A1} \neq p_{A2}$ and $p_{B1} \neq p_{B2}$). Note that the theoretical reactivity values R_A and R_B are inherent to the respective conformers and do not vary with differing folding conditions. The system may be solved for R_A and R_B using conventional algebraic techniques and/or matrix mathematics, and the process repeated for all nucleotides for which normalized ensemble reactivity values have been determined. This is most easily accomplished using Microsoft Excel or other spreadsheet software. The theoretical reactivity profiles obtained in this manner may be used to generate secondary structural models for individual RNA conformers as in conventional SHAPE.

3.1.11 RNA 2D Modeling

Prediction of experimentally supported RNA secondary structure requires RNAstructure, a stand-alone application that converts SHAPE-derived reactivity values into pseudo-free energy constraints which are then incorporated into the RNA folding

algorithm [5]. The software generates 2D representations of RNA structures both in graphical format and dot-bracket notation. The latter can be inputted into RNA structure viewers such as PseudoViewer [17] or Varna [18] to produce publication-quality images.

1. RNAstructure software is available at: http://rna.urmc.rochester.edu/RNAstructure.html.
2. Input the RNA sequence and SHAPE data as formatted text files containing ".seq" and ".shape" suffixes, respectively. Sequence data may also be inputted manually.
3. The user may alter "slope" and "intercept" parameters in the linear function that defines the relationship between reactivity and pseudo-free energy [15]. We generally do not find it necessary to adjust the default settings of 2.6 kcal/mol and −0.8 kcal/mol for slope and intercept, respectively.
4. RNAstructure ranks the models it produces by pseudo free energy, where the structure having the lowest energy is the one that best matches (1) the empirically determined thermodynamics rules for base-pairing embedded in the folding algorithm and (2) the pseudoenergy constraints imposed by the SHAPE reactivity profile. To facilitate qualitative analysis of the match between reactivity values and base pairing predictions, the software permits addition of a color-coded overlay of the reactivity profile onto the graphical representations. In a high-quality structure, weakly or unreactive and highly reactive nucleotides should generally be found in base-paired and unpaired regions, respectively.

One drawback to using RNAstructure as the exclusive means of predicting base pairing interactions is the inability of the software to predict the existence of pseudoknots, kissing loops, or other complex tertiary interactions. These must either be detected manually or through use of alternative RNA structure prediction software that, while useful, cannot optimize their models to match experimentally determined reactivity values. To address this shortcoming, a modification of the conventional SHAPE methodology, designated antisense-interfered or aiSHAPE, was developed to interrogate long-range tertiary interactions. In brief, a short oligonucleotide containing a combination of locked nucleic acid and 2′-*O*-methyl substitutions is site-specifically hybridized to a site within such a putative structural motif. Hybridization of the interfering oligonucleotide disrupts native base-pairing, with the consequence that the displaced complement is rendered susceptible to acylation. Reactivity profiles obtained in the presence and absence of the oligonucleotide are then compared, and a determination is made as to whether the differences between the two reactivity profiles are consistent with the existence of the predicted tertiary

interaction. aiSHAPE has been used to verify the existence of pseudoknot and kissing loop interactions within the MusD RNA transport element MTE [19], as well as the Dengue virus [20] and HIV RNA genomes [21], and should be appropriate for use with the ensemble and in-gel SHAPE methods presented here. A more detailed summary of the aiSHAPE methodology has been presented elsewhere [22].

3.1.12 3D Modeling: RNAComposer

RNAComposer is a server-based modeling program that generates 3D models of RNA structure from inputted RNA sequences of up to 500 nts in length, the corresponding secondary structure(s) and, when available, atomic distance constraints [9]. Sequence and secondary structure information is provided as strings of text—the latter formatted into dot-bracket notation. Other formatting requirements are described in detail on the hosting website. In brief 3D RNA structure models are generated as follows: (1) the secondary structure is fragmented into small pieces; (2) the algorithm searches FRABASE, a comprehensive database of RNA structures that have been solved in three dimensions, for motifs matching or near-matching the secondary structure of each fragment; (3) the 3D structures of the best-matching motifs are selected for assembly; (4) a second algorithm assembles the motifs into a complete, intact structural model; and (5) the model is subjected to multiple rounds of energy minimization and, where possible, fit into conserved folding patterns. RNAComposer is available at http://rnacomposer.cs.put.poznan.pl/.

3.2 In-Gel SHAPE

3.2.1 RNA Folding

Because in-gel SHAPE requires recovery of RNA fractionated by ND PAGE, more starting material is required than for any of the other techniques presented here. This preparative scale folding protocol was optimized for analysis of a truncated HIV-1 RRE RNA construct by in-gel SHAPE (Fig. 2) (Rausch, J. W., unpublished observations). In general, it is assumed that prior to preparative scale RNA folding, folding and fractionation conditions will have been optimized on an analytical scale.

1. Mix RNA (100 pmol), water, and 2 μL 10× RNA folding buffer to a final volume of 20 μL on ice.
2. Heat to 85 °C for 3 min, and then cool to 25 °C at a rate of 0.1 °C/s.
3. Add 20 μL of 2× ND gel RNA folding buffer. Mix.
4. Incubate at 37 °C for 20 min, then immediately place on ice prior to fractionation by ND PAGE.

3.2.2 RNA Fractionation by ND PAGE

For in-gel SHAPE, RNA samples should be evenly distributed over several lanes to facilitate even division into modified (+) and control (−) samples during gel excision. It is assumed that conformers

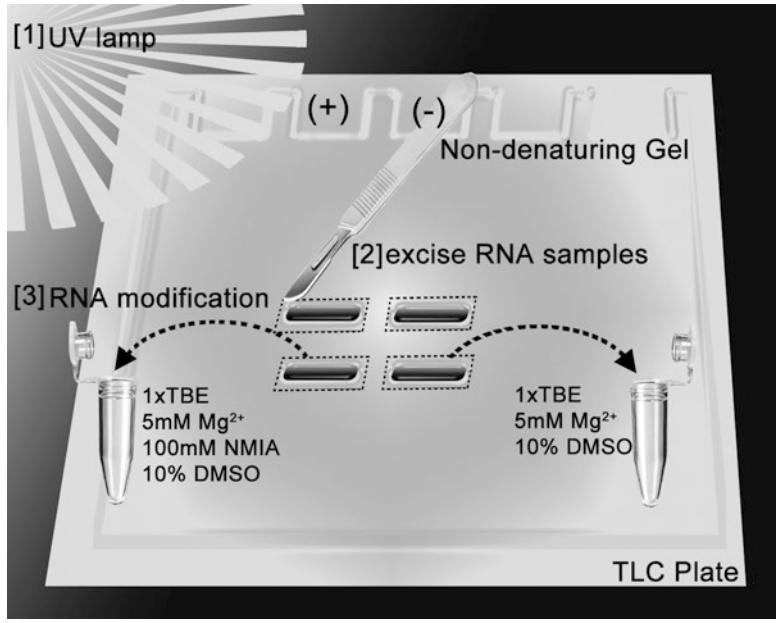

Fig. 2 In-gel RNA detection and probing. [1] Illuminate ND gel TLC plate overlay with UV lamp (254 or 300 nm). [2] Locate RNA bands and excise them with a clean scalpel. [3] Submerge (+) and (–) gel slices in NMIA and DMSO solutions, respectively.

of the RNA in question migrate differently and are distinguishable following electrophoresis. Other ND PAGE guidelines can be found in Subheading 3.1.2.

3.2.3 Detection, Quantitation, and Isolation of RNA by UV Shadowing (Preparative Scale)

It is impractical to detect large quantities of fractionated RNA using SYBR Green as background fluorescence produced during preparative scale ND PAGE is too high. Moreover, intercalation of SYBR Green into the RNA may alter its reactivity to NMIA or other probing reagents. As a consequence, an indirect detection method [7] or UV shadowing is preferable. The latter approach was used to detect HIV-1 RRE conformers (Rausch, J. W., unpublished observations) and is presented here.

1. Remove gel plate or gel sandwich from gel box and place flat on workbench. Remove top plate using spacers and/or spatulas. Pour off or blot any pooled buffer from the gel with a paper towel.
2. Wrap an appropriately sized fluorescent TLC plate in clear plastic wrap, minimizing wrinkles over the silica-coated surface. Alternatively, the TLC plate may be placed inside a smooth, clear plastic bag. Place wrapped or bagged TLC plate silica-side down on the gel surface. Invert gel sandwich and use a spatula to carefully remove the glass plate.

3. Wearing eye protection and covering exposed skin, use a handheld short-wave UV lamp (254–300 nm) to illuminate the TLC plate. RNA bands will be evident as "shadows" of UV absorption amidst a background of white fluorescence.
4. Using a clean spatula, excise gel slices containing the fractionated conformers, segregating equivalent modified (+) and control (–) RNA conformer samples. Work quickly to minimize UV damage to RNA.

3.2.4 RNA Modification with NMIA

For in-gel SHAPE, it is essential that the acylating reagent have a half-life in solution sufficient to allow it to soak into the gel before being hydrolyzed. Consequently, a relatively slow-acting reagent such as NMIA is best suited for these experiments. The protocol below was used to chemically modify two distinct HIV-1 RRE RNA conformers.

1. Prepare 50 mL each of 5× TBE reaction buffer and 1× TBE. Store at 4 °C.
2. For each conformer to be probed, mix 1050 μL water and 300 μL 5× TBE reaction buffer in each of two 2 mL microfuge tubes labeled NMIA(+) and DMSO(–). Heat to 37 °C.
3. Prepare 100 mM NMIA solution in DMSO. Keep desiccated and protected from light until use.
4. Submerge the (+) and (–) gel slices obtained from UV shadowing and gel excision in the corresponding labeled tube.
5. Immediately add 150 μL NMIA solution to the NMIA(+) reaction. Add 150 μL DMSO to the control reaction. Mix both reactions well.
6. Incubate all reactions at 37 °C for 50 min, then cool to 4 °C, and remove reaction solution.
7. Wash gel slices by adding 1.5 mL wash buffer (1× TBE), inverting 3–4 times, and then centrifuging briefly at ~2500 × *g* on a tabletop centrifuge. Repeat twice to completely remove NMIA hydrolysis byproducts.
8. Recover RNA by electroelution in 1× TBE buffer according to the manufacturer's recommendations.
9. Add 0.1 volumes 3 M NaOAc (pH 5.5), 3 volumes 95 % EtOH, and 0.5 μL 10 mg/mL glycogen to recovered RNA solutions.
10. Centrifuge 20 min at 13,000 × *g* in refrigerated tabletop centrifuge. Decant supernatant, and wash with ice-cold 70 % EtOH.
11. Centrifuge an additional 5 min to recover RNA pellet. Decant supernatant, and air-dry for 10 min. Resuspend in 12 μL TE light.

12. Determine concentration of recovered RNA by UV absorption.
13. Determine the molar concentration of each RNA, and dilute in TE light to a concentration suitable for reverse transcription (e.g., 0.5 pmol/μL). Proceed to reverse transcription, or store samples at −20 °C.

3.2.5 Further Processing and Data Analysis

Once RNA has been modified and electroeluted from the gel, subsequent processing and data analysis closely resembles that required for ensemble SHAPE. Accordingly, proceed with reverse transcription (Subheading 3.1.5), preparation of sequencing ladder (Subheading 3.1.6), capillary electrophoresis (Subheading 3.1.7), ShapeFinder data analysis (Subheading 3.1.8), Data Normalization (Subheading 3.1.9), RNA 2D Modeling (Subheading 3.1.11), and RNA 3D Modeling (Subheading 3.1.12) as appropriate.

3.3 Probing RNA with MPE-Fe(II)

MPE is a bifunctional reagent composed of methidium, an intercalator reported to site-bind RNA at select sites, and EDTA, a chelator of metal ions such as Fe^{2+} (Fig. 3). Under oxidizing conditions, the MPE-Fe(II) complex generates highly reactive hydroxyl radical species inducing strand scission at the MPE-binding site(s) as well as in neighboring regions of RNA. MPE cleavage can therefore provide information on RNA nucleotides that are proximal to the

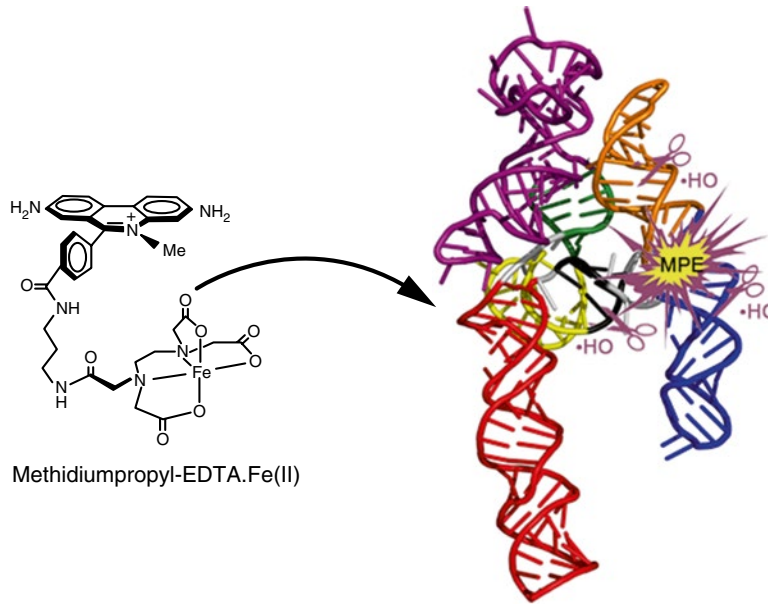

Fig. 3 Examining RNA tertiary interactions by through-space hydroxyl radical cleavage (•OH) with the threading intercalator MPE. Once the secondary structure of the studied RNA is experimentally determined, an MPE cleavage experiment can be performed to provide clues regarding its 3D organization.

reagent binding site, even when these nucleotides and the binding site are separated in primary sequence.

MPE-Fe(II) has been used to probe the 3D structure of tRNA containing engineered CpG islands [23]. In a separate study, however, binding of MPE-Fe(II) to RNA was considered to be nonspecific, and the reagent was used to map solvent accessibility throughout the RNAs of interest [8]. The following protocol describes the application of MPE-Fe(II) to validate the two-dimensional models generated for RRE2 and provide clues regarding the 3D organization of RRE2 substructures [6].

3.3.1 RNA Folding: MPE

The following protocol was optimized for MPE and Rev-ATCUN probing of the HIV-2 RRE [6]. As with all protocols presented here, RNA heterogeneity should be verified by analytical scale folding and ND PAGE.

1. Working on ice, bring RNA (20 pmol) to a total volume of 36 μL in water.
2. Heat RNA to 85 °C for 3 min and then cool to 25 °C at a rate of 0.1 °C/s.
3. Add 4 μL of 10× RNA folding buffer. Mix.
4. Incubate at 37 °C for 20 min, and then immediately place on ice.

3.3.2 MPE Binding and Cleavage

The activated metal ion chelated by MPE (Fe^{2+}) is responsible for RNA damage.

1. Transfer 18 μL folded RNA (Subheading 3.3.1) into each of the two 0.5 mL microfuge tubes labeled (+) and (−), respectively.
2. Prepare fresh solutions of 10 mM sodium ascorbate and 0.03 % hydrogen peroxide (H_2O_2).
3. Form the MPE–Fe(II) complex by mixing equal volumes of 20 μM MPE and 8 μM $Fe(SO_4)_2$ $(NH_4)_2 \cdot 6H_2O$ solutions to achieve final concentrations of 10 μM MPE and 4 μM Fe(II) (1:0.4 ratio). Incubate for 10 min at room temperature. This solution is 10× relative to the binding and cleavage reaction, so 2 μL is required per 20 μL reaction. Prepare enough for all experiments.
4. For use in the (−) control reactions, mix equal volumes of 20 μM MPE and water to generate the 10× MPE control solution. Again, prepare enough for all (−) control reactions (2 μL required per reaction).
5. Add 2 μL 10× MPE–Fe(II) complex and 10× MPE control to the (+) and (−) RNA solutions, respectively. Incubate for 1 min at room temperature to allow methidium to bind RNA.

6. Initiate cleavage by adding sodium ascorbate and hydrogen peroxide solutions (final concentrations of 1 mM and 0.003 %, respectively) to both the (+) and (−) reactions. Incubate at room temperature for 15 s.
7. Quench reactions by adding 2 μL 3 M NaOAc, 1 μL of 10 mg/mL glycogen, and 50 μL ice-cold 95 % ethanol.
8. Pellet RNA by centrifugation at 14,000 × *g* for 30 min. Carefully remove supernatant and air dry the pellet for 1–5 min.
9. Dissolve the RNA in 10 μL of H_2O and proceed to reverse transcription (Subheadings 3.3.3 and 3.3.4).

3.3.3 Determining Methidium-Binding Site by Hydroxyl Radical Cleavage

Hydroxyl radical footprinting can be used to indirectly identify methidium-binding sites. In brief, RNA is incubated with methidiumpropyl compound devoid of the EDTA moiety and the resulting complex probed by exogenous Fe^{2+}-EDTA. In contrast to MPE probing, hydroxyl radical footprinting target nucleotides that are not protected by methidium binding, thus revealing the methidium footprint(s). Once methidium-binding sites have been identified, comparing these sites with those targeted by MPE reveals which cleavages are produced by diffusion of hydroxyl radicals to nearby sites in the RNA that do not directly contact MPE.

1. An additional 20 pmol RNA must be folded in the same manner as described in Subheading 3.3.1.
2. Transfer 9 μL folded RNA (Subheading 3.3.1) into each of the two 0.5 mL microfuge tubes labeled (+) and (−).
3. Prepare fresh 10 μM methidium carboxylate solution in double-distilled water.
4. Add 1 μL of 10 μM methidium carboxylate solution to the (+) reaction and 1 μL of H_2O to the (−) reaction. Incubate for 10 min at room temperature.
5. Perform hydroxyl radical footprinting according to previously published procedures [24]. Briefly, prepare Fe(II)-EDTA solution (10 mM Fe(II), 20 mM EDTA), 0.6 % H_2O_2 and 10 mM sodium ascorbate. Carefully place 1 μL of each reagent in separate droplets on the inside wall of the (+)-labeled microfuge tube containing folded RNA. Centrifuge the tube to mix the reagents and initiate the footprinting reaction. Incubate the reaction mixture for 30 s at room temperature. A control experiment should be performed in the same manner, except add water rather than methidium carboxylate to the reaction.
6. Quench as described above for the MPE experiment (**step 6**).
7. Proceed to reverse transcription (Subheading 3.3.4), or store at −20 °C.

3.3.4 Further Processing and Data Analysis

Once MPE and methidium-binding/cleavage reactions have been performed, subsequent processing and data analysis closely resembles that required for ensemble SHAPE. Accordingly, proceed with reverse transcription (Subheading 3.1.5), preparation of sequencing ladder (Subheading 3.1.6), capillary electrophoresis (Subheading 3.1.7), ShapeFinder data analysis (Subheading 3.1.8), and Data Normalization (Subheading 3.1.9).

3.3.5 RNA 2D Modeling

After modification data have been normalized, values can be overlaid onto RNA secondary structure maps in RNAstructure by color-coding. This means of viewing the data can be helpful for discerning patterns or groupings among affected nucleotides. However, the secondary structure maps themselves must be generated using SHAPE or other methods. MPE or methidium footprinting data cannot be used directly to generate RNA secondary structural models.

3.3.6 RNA 3D Modeling: RNAComposer

Values obtained by MPE probing or methidium footprinting indicate sites damaged by MPE and/or bound by methidium. As such, they may be used to help validate 3D RNA structural models such as those obtained for RRE2 folding intermediates [6]. It might also be possible to use MPE probing data to generate atomic distance constraints useful for modeling in RNAComposer [9]. More information on RNAComposer and imposing distance constraints during 3D modeling can be found in Subheading 3.1.12, the RNAComposer website (http://rnacomposer.cs.put.poznan.pl/), and the original RNAComposer ref. 9.

3.4 ATCUN Probing

Much like MPE, ATCUN-peptides can be used to damage or cleave RNA in the vicinity of the peptide binding site(s) (Fig. 4). The method presented here was adapted from previous work in which ATCUN-peptides containing the arginine rich motif (ARM) of Rev1 were incubated with RRE RNA and activated to cleave the HIV-1 RRE [25], These peptides were developed as antiviral agents, and bound $\underline{Cu}^{2+}$ rather than $\underline{Ni}^{2+}$ as described here. In our experiments, ATCUN-ARM peptides derived from HIV-1 or HIV-2 Rev were complexed with Ni^{2+}, activated with the oxidizing reagent MMPP and used to map the binding sites of Rev1 and Rev2 on their respective RREs (Lusvarghi, S., unpublished observations). This approach also offers the potential to map Tat, Gag, NC, and/or other HIV-related protein-binding sites on HIV RNAs.

3.4.1 RNA Folding: ATCUN

RNA is folded during setup for the ATCUN-binding/cleavage reaction (Subheading 3.4.2).

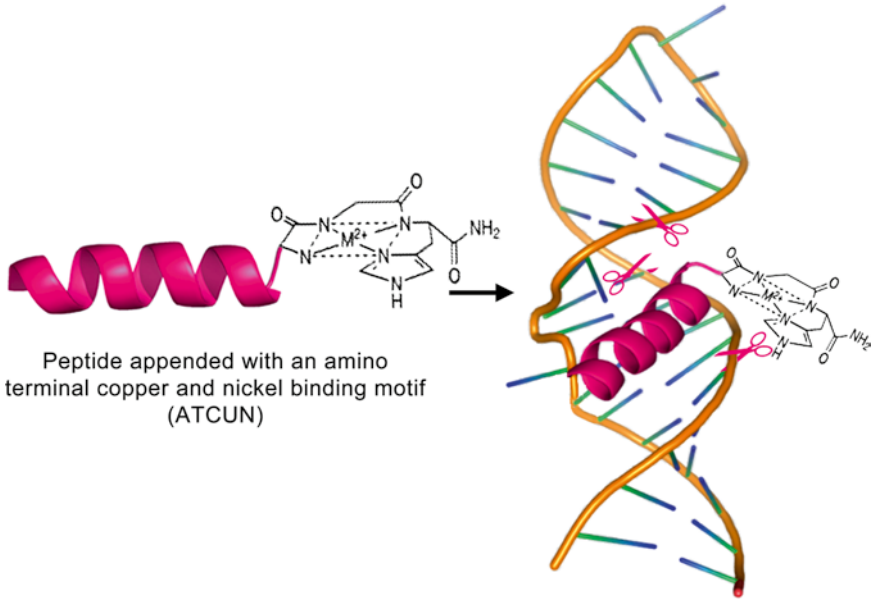

Fig. 4 Peptides containing the amino terminal copper- and nickel-binding motif (ATCUN) can be used to map specific sites of metallopeptide-RNA interactions.

3.4.2 ATCUN Peptide Binding/RNA Modification

1. Prepare experimental (+) (400 pmol peptide, 360 pmol $NiCl_2$) and control (−) (400 pmol peptide only) peptide solutions in 20 μL of 1× RNA folding buffer (50 mM Tris–HCl, pH 8.0, 100 mM NaCl, 5 mM $MgCl_2$). Incubate peptide solutions for 20 min at 37 °C prior to mixing with RNA. Solutions may be stored at −20 °C for later use.
2. Heat 10 μL aliquots of RNA (4 μM in water) to 95 °C for 3 min, and then immediately place on ice for 3 min.
3. To complete RNA folding, add 2 μL of 10× RNA folding buffer and 8 μL water to the RNA sample, mix, and incubate at 37 °C for 20 min.
4. Divide RNA solutions evenly between experimental (+) and control (−) reactions (10 μL each). Mix RNA solutions with ATCUN peptide solutions with (+) or without (−) Ni^{2+}, respectively, at the different peptide:RNA ratios (e.g., 0.5:1, 1:1, or 2:1). The final volume of each reaction should be adjusted to 20 μL with 1× RNA folding buffer. Incubate samples for 20 min at 37 °C to allow peptide binding. The peptide:RNA ratio yielding optimal levels of RNA modification must be empirically determined.
5. Add 1 μL freshly prepared 20 mM magnesium monoperoxyphthalate (MMPP) solution to each sample. Incubate an additional 20 min at 37 °C.

6. Terminate reaction and desalt RNA samples by spin-chromatography through Sephadex-G50 columns or ethanol precipitation.
7. Use 2–10 pmol of the recovered RNA for reverse transcription.

3.4.3 Further Processing and Data Analysis

Once exposed to the activated ATCUN peptide and recovered, treated RNA is ready for subsequent processing as required for ensemble SHAPE. Therefore, proceed with reverse transcription (Subheading 3.1.5), preparation of sequencing ladder (Subheading 3.1.6), capillary electrophoresis (Subheading 3.1.7), ShapeFinder data analysis (Subheading 3.1.8), and Data Normalization (Subheading 3.1.9).

3.4.4 RNA 2D Modeling

As with MPE-Fe(II) probing data, normalized ATCUN-peptide data can be overlaid onto RNA secondary structure maps in RNAstructure. This means of viewing the data can be helpful for identifying ATCUN-peptide-binding sites. Secondary structure maps must be generated using SHAPE or other methods.

4 Notes

1. 1M7 was synthesized according to previously published procedure [12].
2. These reagents were synthesized according to previously published procedure [26].
3. Of the RT variants we have tested, SuperScript III works best for SHAPE-related applications.
4. 5′ fluorescently labeled primers can be either purchased or synthesized in-house. Primers 5′-labeled with Cy5, Cy5.5, WellRedD2 (Beckman Coulter), and IRDye800 (LI-COR) (Beckman Coulter) are best suited for the Beckman Coulter 8000 CEQ. Primers should be designed to hybridize near the RNA 3′ terminus or within the structure cassette in order to maximize the number of nucleotides for which SHAPE data can be obtained. Store in amber test tubes in water at −20 °C in 10 μM aliquots.
5. Of the commercial kits we have tested, the USB Cycle Sequencing kit works best for this application.
6. All equipment, accessories and reagents are supported by Beckman Coulter for use with their CEQ 8000 Genetic Analyzer. We have tried using other accessories and reagents with equipment, but have generally found the results to be inferior.
7. 1M7 should be stored in a desiccator at 4 °C and allowed to warm gradually to room temperature prior to use.

8. Precision in reaction time duration is not absolutely essential here, as 1M7 is over 90 % reacted with RNA or hydrolyzed after 5 min.
9. Do not dry the RNA by vacuum centrifugation. Over-drying the pellet may make it difficult to resuspend.
10. The first three steps of the program serve to anneal the labeled primers to the RNA template.
11. It is our experience that incubation for longer than 50 min can result in aberrant cDNA products.
12. Omitting this step results in poor separation of cDNA products.
13. Centrifugation at a higher speed or for a longer period may result in difficulties in resuspending the pellet(s) and/or coprecipitation of salt, which can adversely affect capillary electrophoresis.
14. Always vacuum dry DNA pellets and avoid over-drying.
15. Pellets may require prolonged vortexing and/or gentle heating (e.g., 65 °C for 5 min) to dissolve. Failure to adequately dissolve the pellet at this stage may result in a lack of signal or weak signal during capillary electrophoresis.
16. In order to analyze the data from SHAPE experiment, two initial calibration reactions are necessary: (1) matrixing—to correct for fluorescent overlaps in multifluor runs, necessary only if you use older Beckman capillary electrophoresis instruments; (2) mobility shift—to correct for small differences in the electrophoretic mobility between fluorescent dyes.

Acknowledgements

This work was funded by the Intramural Research Program of the National Cancer Institute, National Institutes of Health, Department of Health and Human Services. The authors would like to thank Jennifer Miller for critical reading of the manuscript.

References

1. Deforges J, Chamond N, Sargueil B (2012) Structural investigation of HIV-1 genomic RNA dimerization process reveals a role for the Major Splice-site Donor stem loop. Biochimie 94:1481–1489
2. Legiewicz M et al (2008) Resistance to RevM10 inhibition reflects a conformational switch in the HIV-1 Rev response element. Proc Natl Acad Sci U S A 105: 14365–14370
3. Wilkinson KA et al (2008) High-throughput SHAPE analysis reveals structures in HIV-1 genomic RNA strongly conserved across distinct biological states. PLoS Biol 6:e96
4. Merino EJ, Wilkinson KA, Coughlan JL, Weeks KM (2005) RNA structure analysis at

single nucleotide resolution by selective 2′-hydroxyl acylation and primer extension (SHAPE). J Am Chem Soc 127:4223–4231

5. Reuter JS, Mathews DH (2010) RNAstructure: software for RNA secondary structure prediction and analysis. BMC Bioinform 11:129
6. Lusvarghi S et al (2013) The HIV-2 Rev-response element: determining secondary structure and defining folding intermediates. Nucleic Acids Res 41:6637–6649
7. Kenyon JC, Prestwood LJ, Le Grice SF, Lever AM (2013) In-gel probing of individual RNA conformers within a mixed population reveals a dimerization structural switch in the HIV-1 leader. Nucleic Acids Res 41:e174. doi:10.1093/nar/gkt690
8. Han H, Schepartz A, Pellegrini M, Dervan PB (1994) Mapping RNA regions in eukaryotic ribosomes that are accessible to methidiumpropyl-EDTA.Fe(II) and EDTA.Fe(II). Biochemistry 33:9831–9844
9. Popenda M et al (2012) Automated 3D structure composition for large RNAs. Nucleic Acids Res 40:e112
10. McGookin R (1988) Electrophoresis of DNA in nondenaturing polyacrylamide gels. Methods Mol Biol 4:75–79
11. Rio DC, Ares M Jr, Hannon GJ, Nilsen TW (2010) Nondenaturing agarose gel electrophoresis of RNA. Cold Spring Harb Protoc 2010:pdb.prot5445
12. Mortimer SA, Weeks KM (2007) A fast-acting reagent for accurate analysis of RNA secondary and tertiary structure by SHAPE chemistry. J Am Chem Soc 129:4144–4145
13. Mitra S, Shcherbakova IV, Altman RB, Brenowitz M, Laederach A (2008) High-throughput single-nucleotide structural mapping by capillary automated footprinting analysis. Nucleic Acids Res 36:e63
14. Das R, Laederach A, Pearlman SM, Herschlag D, Altman RB (2005) SAFA: semi-automated footprinting analysis software for high-throughput quantification of nucleic acid footprinting experiments. RNA 11:344–354
15. Deigan KE, Li TW, Mathews DH, Weeks KM (2009) Accurate SHAPE-directed RNA structure determination. Proc Natl Acad Sci U S A 106:97–102
16. McGinnis JL, Dunkle JA, Cate JH, Weeks KM (2012) The mechanisms of RNA SHAPE chemistry. J Am Chem Soc 134:6617–6624
17. Byun Y, Han K (2006) PseudoViewer: web application and web service for visualizing RNA pseudoknots and secondary structures. Nucleic Acids Res 34:W416–W422
18. Darty K, Denise A, Ponty Y (2009) VARNA: interactive drawing and editing of the RNA secondary structure. Bioinformatics 25: 1974–1975
19. Legiewicz M et al (2010) The RNA transport element of the murine musD retrotransposon requires long-range intramolecular interactions for function. J Biol Chem 285: 42097–42104
20. Sztuba-Solinska J et al (2013) Structural complexity of Dengue virus untranslated regions: cis-acting RNA motifs and pseudoknot interactions modulating functionality of the viral genome. Nucleic Acids Res 41:5075–5089
21. Stephenson JD et al (2013) Three-dimensional RNA structure of the major HIV-1 packaging signal region. Structure 21:951–962
22. Sztuba-Solinska J, Le Grice SF (2014) Insights into secondary and tertiary interactions of dengue virus RNA by SHAPE. Methods Mol Biol 1138:225–239
23. Gherghe CM, Leonard CW, Ding F, Dokholyan NV, Weeks KM (2009) Native-like RNA tertiary structures using a sequence-encoded cleavage agent and refinement by discrete molecular dynamics. J Am Chem Soc 131:2541–2546
24. Celander DW (2001) Probing RNA structures with hydroxyl radicals. Curr Protoc Nucleic Acid Chem Chapter 6: Unit 6.5
25. Jin Y, Cowan JA (2007) Cellular activity of Rev response element RNA targeting metallopeptides. J Biol Inorg Chem 12:637–644
26. Hertzberg RP, Dervan PB (1984) Cleavage of DNA with methidiumpropyl-EDTA-iron(II): reaction conditions and product analyses. Biochemistry 23(17):3934-45.

Chapter 8

Analysis of HIV-1 Gag-RNA Interactions in Cells and Virions by CLIP-seq

Sebla B. Kutluay and Paul D. Bieniasz

Abstract

Next-generation sequencing-based methodologies have revolutionized the analysis of protein-nucleic acid complexes; yet these novel approaches have rarely been applied in virology. Because it has an RNA genome, RNA-protein interactions play critical roles in human immunodeficiency virus type 1 (HIV-1) replication. In many cases, the binding sites of proteins on HIV-1 RNA molecules in physiologically relevant settings are not known. Cross-linking-immunoprecipitation sequencing (CLIP-seq) methodologies, which combine immunoprecipitation of covalently crosslinked protein-RNA complexes with high-throughput sequencing, is a powerful technique that can be applied to such questions as it provides a global account of RNA sequences bound by a RNA-binding protein of interest in physiological settings at near-nucleotide resolution. Here, we describe the application of the CLIP-seq methodology to identify the RNA molecules that are bound by the HIV-1 Gag protein in cells and in virions. This protocol can easily be applied to other viral and cellular RNA-binding proteins that influence HIV-1 replication.

Key words HIV-1, Gag, RNA packaging, RNA-binding protein, Protein–RNA interaction, CLIP-seq, UV cross-linking, Next-generation sequencing, Cells, Virions, Bioinformatics

1 Introduction

Viral and host RNA-binding proteins regulate all major stages of HIV-1 replication, including transcription, splicing and export of viral mRNAs, assembly of infectious virions, and reverse transcription. HIV-1 Gag is one such viral RNA-binding protein that coordinates all major steps in virion assembly, including the selective packaging of the dimeric, unspliced viral RNA genome [1–3].

HIV-1 genomic RNA packaging has long been thought to be driven by the binding of the nucleocapsid (NC) domain of Gag to a *cis*-acting packaging element, psi (Ψ), located within the 5′ leader of the viral genome [4–7]. However, several lines of evidence indicate that Gag-Ψ interaction is not sufficient for packaging and that Gag-RNA interactions are more complex. First, knowledge of the viral RNA sequences that are directly bound by Gag has largely

Vinayaka R. Prasad and Ganjam V. Kalpana (eds.), *HIV Protocols*, Methods in Molecular Biology, vol. 1354,
DOI 10.1007/978-1-4939-3046-3_8,

been inferred from genetic studies and limited in vitro data. To date, no assay has been able to demonstrate a direct and specific interaction between Ψ and Gag protein in a relevant context, i.e., in live cells and in virions. Second, deletion of Ψ does not completely abolish genome encapsidation [8–10], suggesting that other regions within the viral genome may contribute. Third, Gag undergoes several changes in localization [11, 12] and multimerization state [12] and is proteolytically processed during particle genesis. It is completely unknown how these changes affect the RNA-binding properties of Gag. Fourth, Gag is also thought to promiscuously bind to and package cellular RNAs in proportion to their abundance in the cytosol [13, 14]. Whether these interactions take place within cells and virions, and if so, how they change during the genesis of viral particles is largely unknown.

To identify the RNA molecules directly bound by Gag in physiological settings, we have recently applied CLIP-seq methodologies [15, 16] to various stages of particle genesis [17]. One CLIP-seq approach that is referred to as photoactivatable-ribonucleoside-enhanced-CLIP (PAR-CLIP) relies on the incorporation of photoreactive ribonucleoside analogs, such as 4-thiouridine (4-SU) and 6-thioguanosine (6-SG), into nascent RNAs in live cells. Exposure of cells to UV light at 365 nm wavelength prior to cell lysis induces the covalent cross-linking of the RNA-binding proteins to their target RNA molecules primarily at these 4-SU and 6-SG-modified sites. Following cell lysis and limited RNase digestion, protein-RNA adducts are immunopurified and the RNA molecules, often about 15–50 nucleotides long, are isolated. Following sequential adapter ligations, RNA is reverse-transcribed, the resulting cDNA is PCR amplified and deep sequenced using the Solexa technology. One distinct advantage of the PAR-CLIP methodology is the introduction of T-to-C (for 4-SU) or G-to-A (for 6-SG) mutations during reverse-transcription, which defines the precise sites within target RNA molecules that are cross-linked to the RNA-binding protein of interest.

As 4-SU/6-SG-mediated cross-linking is more efficient than conventional UV cross-linking, PAR-CLIP yields more abundant protein-RNA complexes, which can be critical for the success (i.e., high signal-to-background ratios) of a given CLIP-seq experiment. However, one potential disadvantage of the PAR-CLIP approach is the potential for alteration of RNA structure by incorporation of the ribonucleoside analogs. Therefore, it is worthwhile to perform CLIP-seq experiments in which protein-RNA cross-links are induced by conventional UV cross-linking for confirmatory purposes (i.e., HITS-CLIP). In addition, it is important to validate results obtained from a given experiment by using a different immunoprecipitating antibodies, varying the ribonucleoside analog and the RNase. Overall, we think that this protocol will not only provide a useful tool for analysis of HIV-1 Gag-RNA interactions, but that it can also be adapted to other viral and cellular RNA-binding proteins that regulate viral replication.

2 Materials

2.1 UV Cross-Linking, Lysis, and RNase Treatment Components

1. 4-Thiouridine (Sigma-Aldrich Chemical Company, St. Louis, MO, USA): Dissolve in water to a final concentration of 100 μM.
2. Stratalinker 1800/2400 or an equivalent UV-cross-linking chamber equipped with UV365nm bulbs.
3. Phosphate-buffered saline (PBS), without calcium and magnesium.
4. Ultracentrifuge tubes.
5. 20 % sucrose solution (w/v): Prepare in 1× PBS, filter, and store at 4 °C.
6. Protease inhibitor cocktail.
7. NP-40 lysis buffer: 50 mM HEPES, pH 7.5, 150 mM KCl, 2 mM EDTA, 0.5 % NP-40, supplemented with 0.5 mM DTT and protease inhibitor cocktail (*see* **Note 1**).
8. RIPA buffer: 50 mM Tris pH 7.4, 1 % NP-40, 0.25 % Na-deoxycholate, 0.1 % SDS, 150 mM NaCl, 1 mM EDTA, supplemented with 0.5 mM DTT and protease inhibitor cocktail.
9. RNase A.
10. DNase I.

2.2 Immunoprecipitation, Alkaline Phosphatase Treatment and End-Labeling Components

1. Citrate-phosphate buffer: 4.7 g/L citric acid, 9.2 g/L Na_2HPO_4, pH 5.0.
2. Protein G magnetic beads.
3. Magnetic stand.
4. Calf intestinal alkaline phosphatase.
5. T4 polynucleotide kinase.
6. ATP, [γ-^{32}P], 3000 Ci/mmol, 10 mCi/mL.
7. ATP.
8. Low-retention microcentrifuge tubes.
9. IP wash buffer: 50 mM HEPES-KOH, pH 7.5, 300 mM KCl, 0.05 % NP-40, supplemented with 0.5 mM DTT.
10. LiCl buffer: 250 mM LiCl, 10 mM Tris pH 8.0, 1 mM EDTA, 0.5 % NP-40, 0.5 % Na-deoxycholate, supplemented with 0.5 mM DTT.
11. NaCl buffer: 50 mM Tris pH 7.4, 1 M NaCl, 1 mM EDTA, 0.1 % SDS, 0.5 % Na-deoxycholate, 1 % NP-40, supplemented with 0.5 mM DTT.
12. KCl buffer: 50 mM HEPES-KOH, pH 7.5, 500 mM KCl, 0.05 % NP-40, supplemented with 0.5 mM DTT.
13. Dephosphorylation buffer: 50 mM Tris–HCl, pH 7.9, 100 mM NaCl, 10 mM $MgCl_2$, supplemented with 1 mM DTT.

14. Phosphatase wash buffer: 50 mM Tris–HCl, pH 7.5, 20 mM EGTA, 0.5 % NP-40, supplemented with 1 mM DTT.
15. PNK buffer: 50 mM Tris–HCl, pH 7.5, 50 mM NaCl, 10 mM $MgCl_2$, supplemented with 1 mM DTT.
16. Protein sample buffer (4×): 0.5 M Tris, 1.6 mM EDTA, 8 % SDS, 40 % glycerol, 0.002 % bromophenol blue. Adjust pH to 8.5.
17. Thermal mixer.

2.3 RNA Purification Components

1. 4–12 % Bis-Tris protein gels.
2. MOPS SDS running buffer (20×): 50 mM MOPS, 50 mM Tris base, 0.1 % SDS, 1 mM EDTA. Adjust pH to 7.7.
3. Nitrocellulose membrane.
4. Tris-glycine transfer buffer (10×): 250 mM Tris, 1.92 M glycine. Prepare 1× buffer containing 20 % ethanol.
5. Autoradiography cassettes and film.
6. Proteinase K, recombinant, PCR grade.
7. Proteinase K buffer (2×): 200 mM Tris–HCl, pH 7.5, 100 mM NaCl, 20 mM EDTA, 2 % SDS.
8. Glycoblue co-precipitant (Life Technologies, Carlsbad, CA, USA).
9. 3 M sodium acetate, pH 5.2.
10. Ethanol:isopropanol (1:1).
11. Acid phenol:chlorofom:isoamyl alcohol (125:24:1).

2.4 Adapter Ligations and Library Preparation Components

1. 80% ethanol.
2. Nuclease-free water.
3. RNase inhibitor.
4. Pure BSA.
5. DMSO.
6. 50 % PEG8000.
7. T4 RNA ligase 2, truncated K227Q (New England Biolabs, Ipswich, MA, USA).
8. T4 RNA Ligase 1 (New England Biolabs).
9. 6 and 15 % TBE-urea gels.
10. TBE-urea sample buffer (2×): 45 mM Tris, 45 mM boric acid, 1 mM EDTA (free acid), 6 % Ficoll type 400, 3.5 M urea, 0.005 % bromophenol blue, 0.025 % xylene cyanol.
11. TBE running buffer (10×): 890 mM Tris, 890 mM boric acid, 20 mM EDTA, pH 8.3.

12. Sterile centrifuge tube filters with cellulose acetate membrane (pore size 0.22 μm).
13. Low-molecular-weight marker (range of 10–100 nt).
14. SuperScript® III First-Strand Synthesis System (Life Technologies).
15. High-fidelity DNA polymerase.
16. Low-molecular-weight DNA ladder (range of 50–500 nt).
17. Diffusion buffer: 0.5 M ammonium acetate, 10 mM magnesium acetate, 1 mM EDTA, pH 8.0, 0.1 % SDS.
18. DNA gel extraction kit.
19. *Adapters and primer pairs*:

    3′ adapter: 5′adenylated/TCG TAT GCC GTC TTC TGC TTG-3′dideoxyC

    5′ barcoded adapters:

    5′-rGUU CAG AGU UCU ACA GUC CGA CGA UC AGU NNN UC-3′

    5′-rGUU CAG AGU UCU ACA GUC CGA CGA UC GAU NNN UC-3′

    5′-rGUU CAG AGU UCU ACA GUC CGA CGA UC GUG NNN UC-3′

    5′-rGUU CAG AGU UCU ACA GUC CGA CGA UC ACG NNN UC-3′

    5′-rGUU CAG AGU UCU ACA GUC CGA CGA UC UAG NNN UC-3′

    5′-rGUU CAG AGU UCU ACA GUC CGA CGA UC AUC NNN UC-3′

    Positive control RNA oligo: 5′-rAUAGCUACGAUUGCA-3′

    RT/ReversePCRprimer:5′-CAAGCAGAAGACGGCATACGA-3′

    Forward PCR primer:

    5′-AATGATACGGCGACCACCGACAGGTTCAGA GTTCTACAGTCCGA-3′

All adapters used in ligation are HPLC purified. PCR reactions can be performed with standard desalted primers.

3 Methods

3.1 UV Cross-Linking, Lysis, and RNase Treatment

1. 2 days prior to UV cross-linking, transfect HEK293T cells with proviral plasmid DNAs. For each CLIP-seq experiment, use six 10 cm dishes, each transfected with 10 μg of proviral plasmid DNA (*see* **Note 2**).

2. One day post-transfection and 14 h prior to UV cross-linking, change media on plates with 100 μM 4-SU containing media (*see* **Note 3**).
3. On the day of UV cross-linking, collect cell culture supernatants containing virions and set aside for processing as detailed in **steps 8–12**.
4. Wash cells with 10 mL of ice-cold PBS, aspirate and irradiate the dish containing cells uncovered at an energy setting of 0.15 J/cm^2 in a Stratalinker UV-cross-linking chamber equipped with UV365 nm bulbs (*see* **Note 4**).
5. Add 3 mL of PBS to each plate and collect cells using a rubber policeman. Pellet cells by centrifugation at 500 × *g* for 5 min and discard the PBS. Cells can be flash-frozen and stored at this stage.
6. Lyse cells in 2.5 mL of NP40-lysis buffer and keep on ice for 10 min (*see* **Note 5**).
7. Transfer lysates to microcentrifuge tubes. Clear lysates by centrifugation at 20817 × *g* at 4 °C for 10 min and collect the supernatants.
8. In parallel, process cell culture supernatants containing virions. Pellet cellular debris by centrifugation at 500 × *g* for 5 min and filter the supernatant through a 0.2 μM filter.
9. Add 13 mL of 20 % sucrose solution in ultracentrifuge tubes and layer 25 mL of cleared cell culture supernatant on top. Pellet the virions by ultracentrifugation at 131218 × *g*, 4 °C, for 90 min.
10. Aspirate the supernatant and resuspend the virions in a total of volume of 500 μL PBS.
11. In a six-well cell-culture dish UV-cross-link the virions twice as above at an energy setting of 0.15 J/cm^2. Mix between two irradiations.
12. Collect the virions and add 125 μL of 5× NP40 lysis buffer (*see* **Note 6**).
13. Add RNase A and DNase I to lysates at a final concentration of 20 U/mL and 60 U/mL, respectively. Incubate samples at 37 °C for 5 min and transfer to ice (*see* **Note 7**).

3.2 Immunoprecipitation, Alkaline Phosphatase Treatment and End-Labeling

1. For each cell and virion lysate, prepare 60 μL and 40 μL of protein G magnetic beads, respectively. Wash beads twice with 1 mL and resuspend in two bead volumes of citrate-phosphate buffer.
2. Add 5–10 μg of antibody per 100 μL of beads. Incubate on a rotating wheel at room temperature for 45 min (*see* **Note 8**).

3. Wash beads twice with 1 mL and resuspend in one bead volume of citrate-phosphate buffer.
4. Add the proper amount of antibody-conjugated magnetic beads to cell and virion lysates and incubate on a rotating wheel at 4 °C for 1 h.
5. Collect beads on a magnetic stand in low-retention microcentrifuge tubes. Wash beads twice each with 1 mL of IP wash buffer, LiCl buffer, NaCl buffer, KCl buffer, and dephosphorylation buffer. Briefly spin the beads and remove the remaining buffer.
6. Resuspend beads in one bead volume of dephosphorylation buffer containing calf intestinal alkaline phosphatase at a final concentration of 0.5 U/μL. Incubate for 10 min at 37 °C in a thermal mixer programmed to mix at 1400 rpm for 20 s every 2 min.
7. Wash beads twice with 1 mL of phosphatase wash buffer. Incubate on a rotating wheel for 5 min between washes.
8. Wash beads twice with 1 mL of PNK buffer. Briefly spin the beads and remove the remaining wash buffer.
9. Resuspend beads in one bead volume of 1× PNK buffer containing 0.5 μCi/μL γ-^{32}P-ATP and 1 U/μL T4 PNK. Incubate at 37 °C for 40 min in a thermal mixer programmed to mix at 1400 rpm for 20 s every 2 min.
10. Add nonradioactive ATP at a final concentration of 100 μM and incubate as above at 37 °C for an additional 10 min.
11. Wash beads once each with 1 mL of PNK Buffer, LiCl buffer, KCl buffer, and NaCl buffer as described above. Briefly spin the beads and remove the remaining wash buffer.
12. Resuspend beads in 50 μL of 1× SDS-PAGE loading buffer and elute protein-RNA complexes by incubation at 72 °C for 10 min in a thermal mixer set to constantly mix at 1400 rpm. Collect the eluates.

3.3 Separation of Protein-RNA Adducts and Purification of RNA

1. Run 45 μL of the eluate on a 4–12 % Bis-Tris polyacrylamide gel and transfer to a nitrocellulose membrane. Use the remaining eluate to test for the efficiency of immunoprecipitation by western blotting.
2. Place the membrane in a plastic wrap and expose to autoradiography film until the protein-RNA adducts can be visualized (*see* **Note 9**).
3. Using a clean scalpel or razor blade, cut a region of the membrane directly above the expected molecular weight of the protein of interest. Cut the membrane further into smaller pieces and place in low-retention microcentrifuge tubes.

4. Add 400 μL of 1× Proteinase K buffer containing 2 mg/mL Proteinase K to each sample. Incubate for 30 min in a thermal mixer set to 55 °C with constant agitation at 1100 rpm.
5. Supplement with an additional 400 μg Proteinase K and incubate for 15 min as above (*see* **Note 10**).
6. Lower the temperature to 37 °C and add one volume of phenol:chlorofom:isoamyl alcohol. Vortex and incubate at 37 °C in a thermal mixer as above for 10 min.
7. Centrifuge samples at 14,000 rpm, 3 min, RT.
8. Collect the supernatants and add 100 μL 3 M sodium acetate, 1 μL glycoblue, and 1 mL ethanol:isopropanol (1:1). Mix well and place samples at −20 °C overnight.

3.4 Adapter Ligations

1. Pellet RNA by centrifugation at 20817 × *g*, 4 °C for 30 min.
2. Wash with 500 μL 80 % ethanol. Centrifuge as above for 5 min.
3. Air-dry RNA pellet and resuspend in 8 μL water.
4. In parallel, bring 1 pmole of the end-labeled positive control RNA up to 8 μL with water.
5. Add 100 pmoles of 3′ adapter (1 μL of 100 μM stock), 2 μL DMSO and 5 μL PEG8000 (50 %). Mix well and denature RNA by incubation at 72 °C for 2 min. Place samples immediately on ice.
6. To each sample add 2 μL 10× T4 RNA ligase 2 buffer without ATP, 20 U of RNase inhibitor, 1 μL 2 mg/mL BSA, and 1 μL of T4 RNA ligase 2, truncated K227Q (200 U/μL). Mix well.
7. Incubate samples overnight at 16 °C.
8. Add 20 μL of 2× TBE-urea loading buffer to each sample and incubate at 72 °C for 2 min. Transfer samples to ice.
9. Load samples on a 15 % TBE-urea gel, while leaving at least one empty well between each sample to avoid cross-contamination. Run at 180 V, 70 min.
10. Place gel in plastic wrap and expose to autoradiography film.
11. Cut a gel piece corresponding to the ligated RNA products, including the ligated positive control RNA. Crush the gel into smaller pieces (*see* **Note 11**).
12. Add three volumes of 0.4 M NaCl supplemented with 200 U/mL of RNase inhibitor.
13. Incubate samples overnight in a thermal mixer set to constant shaking at 1400 rpm, 4 °C.
14. Pass gel slurry through a spin column with cellulose acetate filter. Add 1 μL glycoblue and 2.5 V of ethanol:isopropanol (1:1). Place samples on ice for 20 min.
15. Precipitate RNA as above and resuspend in 10 μL of ultrapure water. Add 20 pmoles (1 μL of 20 μM stock) of barcoded 5′

adapter and 2 μL DMSO. Incubate samples at 72 °C for 2 min and immediately transfer to ice.

16. To each sample add ligation mix containing 2 μL 10× T4 RNA ligase 1 buffer, 20 U of RNase inhibitor, 1 μL of 2 mg/mL BSA, 2 μL ATP (10 mM), and 1 μL T4 RNA Ligase 1 (10 U/μL).
17. Incubate samples overnight at 16 °C.
18. If barcoded adapters are used, samples can be pooled at this stage. After adding 20 μL of 2× TBE-Urea loading buffer to each sample, incubate at 72 °C for 5 min. Transfer samples on ice and combine them as desired (*see* **Note 12**).
19. Process samples as described in **steps 9–15**. Resuspend pelleted RNA in 10 μL of ultrapure water.

3.5 Reverse Transcription and PCR Amplification of CLIP Library

1. Use the SuperScript III First Strand Synthesis System as detailed by the manufacturer. To 8 μL of RNA, add 1 μL of reverse transcription primer (10 μM) and 1 μL of dNTP (10 mM). Incubate at 65 °C for 5 min. Transfer samples on ice.
2. Add 4 μL $MgCl_2$ (25 mM), 2 μL 10× reverse transcription buffer, 2 μL DTT (0.1 M), 1 μL RNaseOUT (40 U/μL), and 1 μL SSIII RTase (200 U/μL).
3. Reverse transcribe according to the manufacturer's instructions.
4. Set up a 100 μL PCR reaction containing 10 μL of cDNA, 50 pmoles of forward and reverse primers, 20 μL 5× high-fidelity buffer, 2 μL dNTPs (10 mM), and 2 μL high-fidelity polymerase (2 U/μL). Run PCR for a total of 15 cycles programmed at 98 °C 15 s, 55 °C 30 s, and 72 °C 15 s. Take 20 μL aliquots at the end of PCR cycle 6, 9, 12, and 15.
5. Run samples on a 6 % TBE-urea gel. Stain with EtBr in 1× TBE buffer and excise a region corresponding to the CLIP library (*see* **Note 13**).
6. Weigh the gel and add one to two volumes of diffusion buffer.
7. Incubate at 50 °C for 30 min in a thermal mixer set to constant agitation at 1400 rpm.
8. Collect the supernatant and extract CLIP DNA library using a gel extraction kit.
9. As CLIP libraries are derived from short RNA sequences, they can be sequenced on an Illumina platform for 50 cycles.

3.6 Bioinformatics Analyses

Despite the astounding progress in the development and accessibility of next-generation sequencing-based experimental approaches, data analysis still remains the major limiting step in many laboratories and institutions. Several tools have been developed and are publicly available for data analyses. We perform our data analysis by running these programs from the command line

on our local Linux server, for which a basic knowledge of UNIX operating system and other programming languages is necessary. Below we outline the basic analysis of the CLIP-seq data, including sample command line instructions:

1. Raw reads obtained from the sequencing facility can be processed prior to mapping to human or viral genomes using the FASTX toolkit (http://hannonlab.cshl.edu/fastx_toolkit/).
2. Discard reads that contain ambiguous nucleotides, did not contain the 3′ adapter sequence, or are shorter than 15 nucleotides: fastx_clipper –c –a TCGTATGC –l 23 –i INFILE.fastq –o OUTFILE (*see* **Note 14**).
3. Separate reads based on their 5′ barcode sequences: cat OUTFILE | /usr/local/bin/fastx_barcode_splitter.pl --bcfile barcodes.txt --bol --mismatches 0 --prefix OUTFILE_split.
4. Collapse reads to generate a set of unique sequences: fastx_collapser -i OUTFILE_split -o OUTFILE_collapsed.
5. Trim the 5′ adapter sequence: fastx_trimmer -f 9 -v -i OUTFILE_collapsed -o OUTFILE_trimmed.
6. After the reads are "cleaned up" they can be aligned to the appropriate viral and human genomes using several short-read aligners (i.e., Bowtie, BWA). For alignment to the human genome, we typically allow up to two mismatches and report locations for reads with the minimum number of observed mismatches for each read (Bowtie criteria: -m 10 -v 2 --best --strata for mapping to hg19, and - m 1 -v 2 for mapping to the viral genomes).
7. Following the alignment, SAMtools [18] and BEDtools [19] can be used to further process the data.
8. Clusters, which represent binding sites derived from overlapping mapped reads, can be generated using the PARalyzer algorithm [20].
9. The generated clusters can be annotated by in-house scripts using publicly available databases (i.e., ENSEMBL, UCSC) as reference.
10. Following annotation, motif searches within clusters can be performed by the cERMIT algorithm [21].

4 Notes

1. Sigma-Aldrich has replaced NP-40 with Igepal-CA 630, which works equally well in our hands.
2. As an alternate to transfection, infected HEK293T cells or other cell types (i.e., suspension cells) can be used in CLIP assays.

3. 6-Thioguanosine (6-SG, Sigma-Aldrich) at a final concentration of 100 μM can be used as an alternative ribonucleoside analog, which yields G-to-A mutations in the sequenced reads. However, the efficiency of UV cross-linking with 6-SG and the resulting mutation rates are significantly lower than 4SU-mediated cross-linking.
4. If CLIP is done on suspension cells, resuspend cells in 10 mL PBS and spread on a 15-cm cell culture dish. Perform UV cross-linking twice, mixing cells in between.
5. Following UV cross-linking, subcellular fractionation can be performed prior to immunoprecipitation. To this end, we found out that a commercially available fractionation kit (Minute plasma membrane isolation kit (Invent Biotechnologies)) works quite well. As has been observed before [22] immunoprecipitation of Gag from the plasma membrane fraction requires harsher detergent conditions (i.e., RIPA buffer). On the other hand, fractionation of cells by membrane flotation on sucrose cushions followed by immunoprecipitation does not yield sufficient Gag-RNA complexes, likely due to the presence of high concentrations of sucrose and increased immunoprecipitation volumes.
6. Although immunoprecipitation of Gag from immature virions was very efficient in 1× NP40-lysis buffer, immunoprecipitation of NC from mature particles required harsher detergent conditions (i.e., 1× RIPA buffer).
7. RNase T1 can be used as an alternative to RNase A. The concentration of RNase for each protein and stock of RNase shall be determined separately. We suggest trying several dilutions of RNases in pilot experiments and move forward with the RNase concentration that yields protein-RNA complexes migrating ~5–10 kDa above the expected molecular weight of the protein of interest in SDS-PAGE. The goal is to obtain RNA molecules that are short enough to be sequenced on an Illumina platform but long enough to be unambiguously mapped to the viral and human genomes.
8. To facilitate the purification of Gag-RNA adducts, we typically utilize proviral clones carrying three consecutive copies of a HA-tag within the stalk region of matrix domain and perform immunoprecipitations using a mouse monoclonal anti-HA antibody (HA.11, Covance). This approach yields abundant and fairly pure Gag-RNA adducts [17].
9. If protein-RNA complexes cannot be visualized following 4–5 h of exposure, we think it is critical to optimize the preceding steps to obtain more abundant crosslinked protein-RNA complexes, which is critical for obtaining meaningful results from a given CLIP-seq experiment.

10. The goal at this step is to maximize the amount of RNA recovered from the nitrocellulose membrane. If sufficient RNA is recovered after the initial round of Proteinase K digestion, this step can be omitted.
11. To crush gel pieces, poke four holes on the bottom of a 0.5 mL microcentrifuge tube and place it in a 1.5 mL low-retention microcentrifuge tube. Place the gel piece in the 0.5 mL tube and centrifuge at 20817 × *g*, RT for 3 min. Alternatively, a Teflon pestle can be used.
12. If RNA abundance varies significantly between samples, it is preferable to pool them at equimolar concentrations to obtain relatively similar number of sequencing reads from each sample.
13. We usually observe two bands, one corresponding to adapter-adapter ligations that migrate at ~75 nt and the CLIP library that migrate at 90–150 nt. From the smallest number of PCR cycle (typically 9–12) that yields a visible library, carefully cut the region that corresponds to the CLIP library from the gel. If necessary, repeat the PCR using the purified CLIP library as template.
14. Length filter at this step is 23 nucleotides (-l 23) as this includes the length of the 5′ adapter (8 nucleotides).

Acknowledgements

This work was supported by NIH grants R01AI501111 and P50GM103297. S.B.K. was supported in part by an AmFAR Mathilde Krim Postdoctoral Fellowship.

References

1. Kuzembayeva M, Dilley K, Sardo L et al (2014) Life of psi: how full-length HIV-1 RNAs become packaged genomes in the viral particles. Virology 454–455:362–370
2. Lu K, Heng X, Summers MF (2011) Structural determinants and mechanism of HIV-1 genome packaging. J Mol Biol 410: 609–633
3. Rein A, Datta SA, Jones CP et al (2011) Diverse interactions of retroviral Gag proteins with RNAs. Trends Biochem Sci 36:373–380
4. Aldovini A, Young RA (1990) Mutations of RNA and protein sequences involved in human immunodeficiency virus type 1 packaging result in production of noninfectious virus. J Virol 64:1920–1926
5. Clavel F, Orenstein JM (1990) A mutant of human immunodeficiency virus with reduced RNA packaging and abnormal particle morphology. J Virol 64:5230–5234
6. Lever A, Gottlinger H, Haseltine W et al (1989) Identification of a sequence required for efficient packaging of human immunodeficiency virus type 1 RNA into virions. J Virol 63:4085–4087
7. Luban J, Goff SP (1994) Mutational analysis of cis-acting packaging signals in human immunodeficiency virus type 1 RNA. J Virol 68:3784–3793
8. Clever JL, Parslow TG (1997) Mutant human immunodeficiency virus type 1 genomes with defects in RNA dimerization or encapsidation. J Virol 71:3407–3414
9. Laham-Karam N, Bacharach E (2007) Transduction of human immunodeficiency virus type 1 vectors lacking encapsidation and dimerization signals. J Virol 81:10687–10698

10. McBride MS, Schwartz MD, Panganiban AT (1997) Efficient encapsidation of human immunodeficiency virus type 1 vectors and further characterization of cis elements required for encapsidation. J Virol 71:4544–4554
11. Jouvenet N, Simon SM, Bieniasz PD (2009) Imaging the interaction of HIV-1 genomes and Gag during assembly of individual viral particles. Proc Natl Acad Sci U S A 106:19114–19119
12. Kutluay SB, Bieniasz PD (2010) Analysis of the initiating events in HIV-1 particle assembly and genome packaging. PLoS Pathog 6, e1001200
13. Rulli SJ Jr, Hibbert CS, Mirro J et al (2007) Selective and nonselective packaging of cellular RNAs in retrovirus particles. J Virol 81:6623–6631
14. Muriaux D, Mirro J, Harvin D et al (2001) RNA is a structural element in retrovirus particles. Proc Natl Acad Sci U S A 98:5246–5251
15. Hafner M, Landthaler M, Burger L et al (2010) Transcriptome-wide identification of RNA-binding protein and microRNA target sites by PAR-CLIP. Cell 141:129–141
16. Licatalosi DD, Mele A, Fak JJ et al (2008) HITS-CLIP yields genome-wide insights into brain alternative RNA processing. Nature 456:464–469
17. Kutluay SB, Zang T, Blanco-Melo D et al (2014) Global changes in the RNA binding specificity of HIV-1 Gag regulate virion genesis. Cell 159:1096–1109
18. Li H, Handsaker B, Wysoker A et al (2009) The sequence alignment/map format and SAMtools. Bioinformatics 25:2078–2079
19. Quinlan AR, Hall IM (2010) BEDTools: a flexible suite of utilities for comparing genomic features. Bioinformatics 26:841–842
20. Corcoran DL, Georgiev S, Mukherjee N et al (2011) PARalyzer: definition of RNA binding sites from PAR-CLIP short-read sequence data. Genome Biol 12:R79
21. Georgiev S, Boyle AP, Jayasurya K et al (2010) Evidence-ranked motif identification. Genome Biol 11:R19
22. Ono A, Waheed AA, Joshi A et al (2005) Association of human immunodeficiency virus type 1 gag with membrane does not require highly basic sequences in the nucleocapsid: use of a novel Gag multimerization assay. J Virol 79:14131–14140

Chapter 9

Isolation of Cognate Cellular and Viral Ribonucleoprotein Complexes of HIV-1 RNA Applicable to Proteomic Discovery and Molecular Investigations

Deepali Singh, Ioana Boeras, Gatikrushna Singh, and Kathleen Boris-Lawrie

Abstract

All decisions affecting the life cycle of human immunodeficiency virus (HIV-1) RNA are executed by ribonucleoprotein complexes (RNPs). HIV-1 RNA cycles through a progression of host RNPs composed of RNA-binding proteins regulating all stages of synthesis, processing, nuclear transport, translation, decay, and co-localization with assembling virions. RNA affinity chromatography is a versatile method to identify RNA-binding proteins to investigate the molecular basis of viral and cellular posttranscriptional control of gene expression. The bait is a HIV-1 RNA motif immobilized on a solid support, typically magnetic or Sepharose beads. The prey is pre-formed RNPs admixed in lysate from cells or concentrated virus particles. The methodology distinguishes high-affinity RNA-protein interactions from low-affinity complexes by increases in ionic strength during progressive elution cycles. Here, we describe RNA affinity chromatography of the 5′ untranslated region of HIV-1, obtaining mixtures of high-affinity RNA binding proteins suitable for mass spectrometry and proteome identification.

Key words High-affinity RNA–protein interaction, Ribonucleoprotein particle (RNP), Streptavidin-biotin affinity, Isotype-specific antibody, Immunoprecipitation, Magnetic beads, Cis-acting RNA element, Posttranscriptional control of gene expression

1 Introduction

RNA affinity isolation has been a valuable tool to discover cellular cofactors of retroviruses, and their investigation consistently provides fundamental insights into cell biology [1, 2]. The combination of RNA affinity isolation with subsequent mass spectrometry is a powerful discovery tool [2, 3] and is producing a genome-wide view of RNP components on HIV-1 RNA [4].

Every step in the life cycle of HIV-1 is dependent upon cellular machineries composed of RNA-binding proteins and noncoding RNA [5]. HIV-1-bound ribonucleoprotein particles (RNPs) are the molecular basis for balanced expression of all viral gene products

Vinayaka R. Prasad and Ganjam V. Kalpana (eds.), *HIV Protocols*, Methods in Molecular Biology, vol. 1354,
DOI 10.1007/978-1-4939-3046-3_9,

and the trafficking of HIV-1 unspliced RNA that becomes packaged into progeny virions [6]. Distinct HIV-1 RNP components are isolated by cis-acting RNA elements: Tat trans-activation responsive (TAR) sequence, 5′ UTR posttranscriptional control element (PCE), 5′ splice site, and packaging signal (psi) [2, 7–9]. Distinct RNP components and cognate cis-acting elements work in common purpose to produce over a dozen mRNA templates for viral proteins and to balance an appropriate reserve of virion precursor RNA [10]. A variety of cellular RNA-binding proteins enable the immense utility of HIV-1 RNA and their identification is necessary to fully elucidate HIV-1 biology.

The premise of RNA affinity chromatography is the ability to isolate a cognate RNA and its partners from a complex mixture of RNPs, along the lines of retrieving a needle in a haystack. The RNA bait is secured to streptavidin-coated magnetic or Sepharose beads, which are efficiently collected by a magnet or centrifugation. The RNA bait is tagged with UTP-11-biotin by in vitro transcription of HIV-1 sequences (Fig. 1a); or by ligation of CTP-11-biotin to oligonucleotides complementary to HIV-1 RNA (Fig. 1b). The strong affinity of biotin to streptavidin on solid support implements collection of the HIV-1 RNA and associated RNP components from cell lysate or virion preparation. The captured RNPs are subject to stringent washes and are collected in progressive elution cycles. The samples are suitable for peptide sequencing using mass spectrometry or molecular analyses.

The following procedures direct UTP-11-biotin-labeled RNA labeling, cell lysate preparation, RNP collection, and preparative analysis suitable for mass spectrometry with subsequent proteomic identification. Versatility is inherent to this method by varying the cognate RNA bait or providing different sources of RNPs. Here we describe the isolation of HIV-1 RNP components from both cells and HIV-1 particles.

2 Materials

2.1 RNA Affinity Isolation of Cell-Associated HIV-1 RNPs

2.1.1 Synthesis of Body-Labeled Biotinylated HIV-1 RNA

1. RiboMAX Large Scale RNA Production System.
2. T7 RNA polymerase (included in the Ribomax system).
3. Biotin-labeled UTP (bio-11-UTP).
4. DNase I (included in the Ribomax system).

2.1.2 Design of Complementary RNA Oligonucleotides

This approach enables capture of HIV-1 RNPs formed under native conditions in live cells. One or a small collection of oligonucleotides complementary to unpaired RNA segments are end-labeled with CTP-11-biotin (Fig. 1b). To facilitate sequence-specific

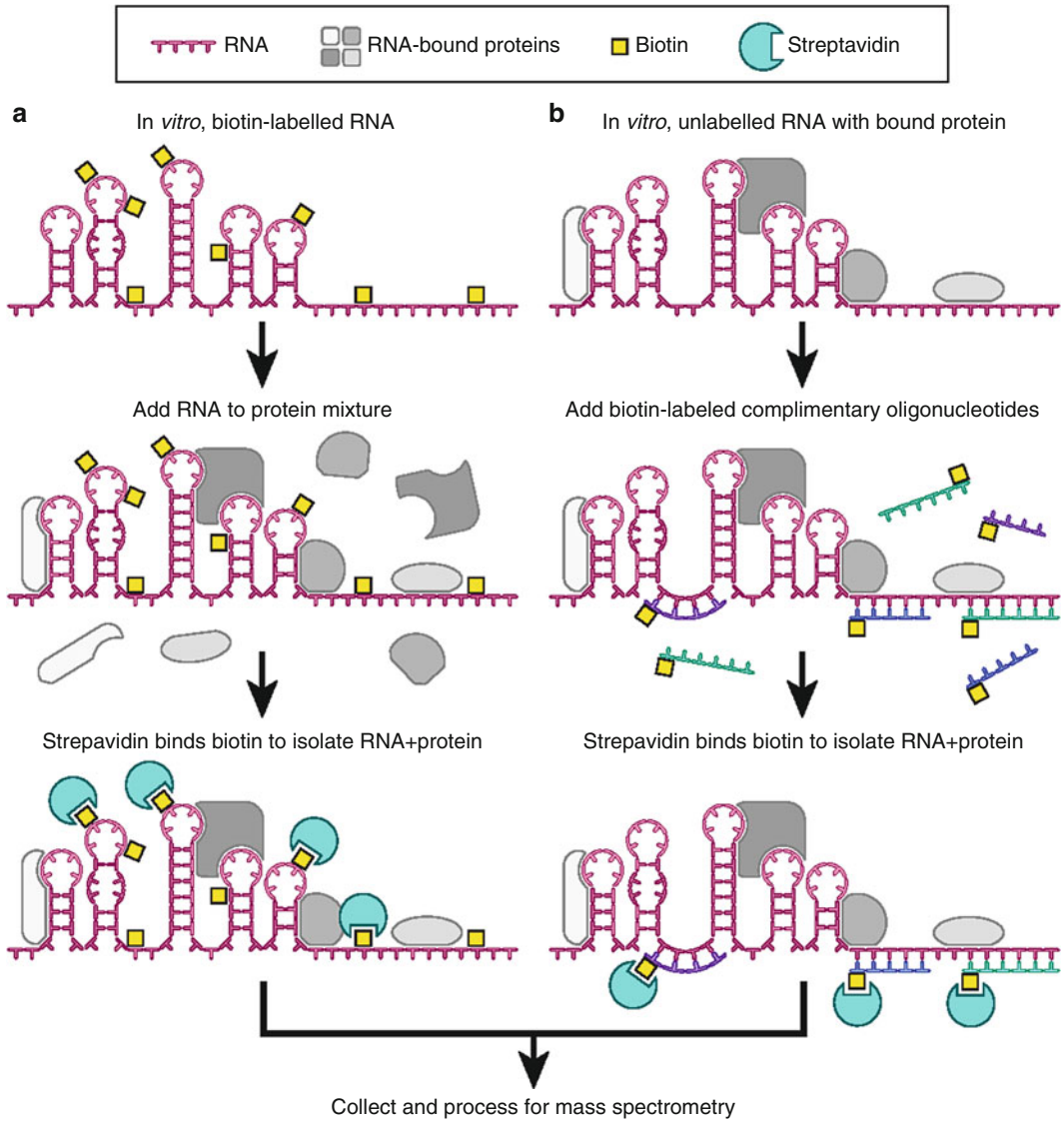

Fig. 1 Isolation of HIV-1 RNA-protein complexes from a mixture of heterogeneous RNPs. (**a**) The HIV-1 5′ UTR (1–350 nt) incorporated biotin-UTP during in vitro transcription; following incubation in cell lysate or virion lysate, the biotin-RNPs are captured by biotin-streptavidin affinity column. (**b**) Oligonucleotides complementary to HIV-1 5′ UTR sequences are 3′ end-labeled with biotin-11-CTP and mixed with HIV-1-infected cell lysate and hybridized by sequence complementarity. The biotin-HIV-1 RNPs are collected on streptavidin beads and subject to elution cycles. HIV-1 RNA bait, *dashed blue line*; complementary RNA oligonucleotides, *thick black line*; biotin, *orange asterisks*; RNA-binding proteins, *various spheres*.

hybridization with the HIV-1 RNA, avoid RNA regions with known secondary structures that may preclude complementary base pairing with the oligonucleotides. HIV-1 RNPs associated with the biotin-labeled oligonucleotides are captured on the streptavidin beads.

2.1.3 The 3′ Biotinylation of HIV-1 RNA Bait

RNA 3′ End biotinylation reagents include:

1. 10× T4 RNA ligase buffer.
2. T4 RNA ligase (20 U/μl).
3. Biotinylated cytidine (Bis)phosphate (1 mM).
4. RNase inhibitor (40 U/μl).
5. PEG 30 %, and nuclease-free water.
6. RNA ligation reaction mix: 10× RNA ligation buffer 3 μl, RNase inhibitor 1 μl (final concentration—1.33 U/μl), RNA oligonucleotide 5 μl (final concentration—50 pmol), biotin-cytidine (bis)-phosphate 1 μl (final concentration—1 nmol), T4 RNA ligase 2 μl (final concentration 1.33 U/μl), 30 % PEG 15 μl (final concentration—15 %), and nuclease-free water 3 μl.

2.1.4 Isolation of Biotin-Labeled RNA Oligonucleotides

1. Dynabeads M-280 Streptavidin
2. 1× binding buffer and washing: DEPC-treated 10 mM Tris–HCl (pH 7.5), 1 mM EDTA, 500 mM NaCl.
3. Solution A: DEPC-treated 0.1 M NaOH and DEPC-treated 0.05 M NaCl.
4. Solution B: DEPC-treated 0.1 M NaCl.
5. Magnetic stand.

2.1.5 Cell Lysate Preparation

1. HIV-1 infected cells.
2. PBS.
3. 1× lysis buffer: 25 mM Tris–HCl (pH 7.5), 150 mM NaCl, 1 mM EDTA, 1 % NP40, 5 % glycerol prepared in autoclaved DEPC water.

2.1.6 Incubation for RNP Affinity and Isolation

1. Rotating tabletop platform.
2. Magnetic stand.
3. 1× binding buffer and washing buffer: DEPC-treated 10 mM Tris–HCl (pH 7.5), 1 mM EDTA, 500 mM NaCl.
4. Sepharose-bound streptavidin or magnetic Dynabeads M-280-bound streptavidin.

2.1.7 Preparative PAGE and Protein Visualization

1. SDS-PAGE running apparatus.
2. 1× SDS-PAGE buffer.
3. 4–20 % SDS-PAGE gel.
4. 4 % SDS sample buffer.
5. Silver-stain Plus or Coomassie Brilliant Blue.

2.2 Preparation of Particle-Associated RNP Mixtures

2.2.1 Propagation of HIV-1 Infected Lymphocytes

1. RPMI medium supplemented with 10 % FBS and 1× antibiotic–antimycotic.
2. CEM×174 lymphocytes.
3. T125 tissue culture flasks.
4. Stock of infectious HIV-1 of $\geq 10^5$ IU/ml.
5. Tissue culture incubator at 37 °C and 5 % CO_2 that contains an oscillating platform.

2.2.2 Monitoring the HIV-1 Infection by Intracellular Gag Detection

1. Cell fixation/permeabilization solution.
2. FITC-conjugated HIV-1 Gag p24 antibody.
3. Guava flow cytometer.

2.2.3 Collecting the Virus for Lysate Preparation

1. Beckman ultracentrifuge.
2. Beckman SW28 swinging bucket rotor and ultra-clear tubes.
3. 45 μm filters.
4. 20 % sucrose solution in TNE: 50 mM Tris, 100 mM NaCl, 1 mM EDTA.
5. RIPA buffer use to resuspend virion preparation: 50 mM Tris, 150 mM NaCl, 1 % NP40, 0.25 % deoxycholic acid, 1 mM EDTA.

2.2.4 Isolation of Select RNA-Binding Proteins from Virion Preparations (See **Notes 1** and **2**)

1. Magnetic beads that have been conjugated with either protein A or protein G.
2. Appropriate antibody and isotype-matched IgG control (*see* **Note 3**).
3. NETN-150 buffer: 20 mM Tris, 150 mM NaCl, 0.5 % NP40, 0.1 mM EDTA.
4. 1× wash buffer: 50 mM Tris, 150 mM NaCl.
5. Magnet stand.
6. Antibodies used in the immunoprecipitation process [11]: Rabbit IgG, Mouse IgG, CBP80, eIF4E, and DHX9/RNA helicase A. Use 10 μg per immunoprecipitation.

2.2.5 Extraction of RNA from Coprecipitated RNA-Binding Protein

1. TRIZOL LS reagent.
2. Chloroform.
3. Isopropanol.
4. Ultrapure RNase-free water.
5. RNAeasy clean-up Kit.

2.2.6 Reverse Transcription of RNA

1. Omniscript RT.
2. Random hexamers or RNA-specific antisense primers.

(a) Reverse transcription mix (total volume 20 µl): RNA 13 µl (*see* **Note 4**), buffer 10 × 2 µl, dNTP (5 mM) 2 µl, random hexamer (100 µM) 2 µl, RNase Out 0.25 µl, and Omniscript reverse transcriptase 1 µl.

2.2.7 Amplification of Target Sequence from cDNA Template

1. Taq polymerase.
2. Specific primers.
3. dNTPs.
4. Thermocycler.
5. PCR reaction mix: cDNA 2–4 µl, 10× buffer 2 µl, dNTP (10 mM stock) 0.5 µl, forward primer 1 µl, reverse primer 1 µl, Taq polymerase 0.25 µl, and water 13.25 µl.

2.2.8 Protein Analysis

1. 4× Laemmli sample buffer.
2. SDS-PAGE reagents.
3. Transfer reagents.
4. Immunoblot antibody that is raised in an alternative species from the antibody used for IP in order to avoid cross-reactivity on the immunoblot.

HIV-1_{NL4-3}-specific primers (*see* **Note 5**):

gag - Forward—5′ GTAAGAAAAAGGCACAGCAA GCAGC3′

Reverse—5′ CATTTGCCCCTGGAGGTTCTG3′

(yields 94 bp product)

env - Forward—5′ GGGCGGCGACTGGAAGAAG3′

Reverse—5′ GGACCACACAACTATTGCTATT ATTATTGC3′

(yields 150 bp product)

nef - Forward—5′ CGGCGACTGGAAGAAGCG3′

Reverse—3′ CTCGGGATTGGGAGGTGGGTC3′

(yields 200 bp product)

rev - Forward—5′ CTCGGGATTGGGAGGTGGGTC3′

Reverse—5′ CGGCGACTGCCTTAGGCATC3′

(yields 120 bp product)

tat - Forward—5′ GGAACCACCCGGGAAGTCAG3′

Reverse—5′ CTTCTTCTTCGATTCTTTCGGGC3′

(yields 240 bp product)

3 Methods

3.1 Isolation of HIV-1 RNPs from Infected Lymphocytes

3.1.1 Isolation of RNA Oligonucleotides on Streptavidin-Conjugated Magnetic Beads

1. Resuspend Dynabeads M-280 Streptavidin in the supplier's tube by gentle mixing.
2. Aliquot 30 μl Dynabeads M-280 Streptavidin to a nuclease-free tube.
3. Place the tube on magnetic stand to collect the beads and carefully pipet to decant the liquid.
4. Add 500 μl of 1× binding buffer to the beads and rotate for 5 min on the tabletop platform. Place the tube on magnetic stand to collect the beads and decant the liquid.
5. Repeat **steps 4** and **5** twice.
6. Add 200 μl Solution A to the tube and mix by gentle pipetting.
7. Place the tube on the magnetic stand to collect the beads and decant the liquid.
8. Repeat **steps 6** and 7 twice.
9. Add 200 μl Solution B to the tube and mix by gentle pipetting.
10. Place the tube on the magnetic stand and decant the liquid.
11. Add 500 μl 1× binding buffer to the tube and rotate for 5 min on the tabletop platform.
12. Transfer the RNA ligation reaction to the Dynabeads M-280 Streptavidin tube and rotate on the tabletop platform for 1 h at room temperature.
13. Place the tube on magnetic stand and decant the liquid.
14. Wash the beads with 500 μl 1× washing buffer twice as described in **steps 6** and 7.

3.1.2 In Vitro Transcription of Biotin-Labeled HIV-1 RNA

1. Thaw all reagents on ice including the RiboMAX Large Scale RNA Production System, biotin-labeled UTP (bio-11-UTP), and template DNA.
2. In a nuclease-free tube, combine the manufacturer's recommended volumes of reagents and incubate at 37 °C for 4 h.
3. Add 1 unit of DNase 1 and incubate the reaction for 30 min at 37 °C to digest template DNA.
4. Add 500 μl DEPC-treated water and 0.1 volume of 3 M NaOAc; mix with an equivalent volume of phenol:chloroform:isoamyl alcohol (25:24:1) and vigorously vortex. Centrifuge the tube for 3 min at 9,300 × *g* in a microcentrifuge.

5. Decant the aqueous phase to fresh nuclease-free tube and add 1 μl glycogen and 2.5 volumes of cold ethanol (stored at −20 °C). Incubate the mixture at −80 °C for 30 min.
6. Centrifuge the tube for 15 min at 9,300 × *g* in a refrigerated microcentrifuge.
7. Decant the supernatant using a fine-tipped pipet. Resuspend the pellet in 30 μl RNase-free water.
8. Pipet the entire 30 μl sample to the side of a G25 Sepharose spin column, which captures residual unincorporated dNTPs. Place the column in a 15 ml adaptor tube of a swinging bucket rotor of a tabletop centrifuge and run for one min at 800 × *g*.
9. Collect the solution with a fine-tipped pipet and place in a new labeled tube.
10. Perform PAGE on an aliquot of the RNA sample, typically 10 %, stain the sample with ethidium bromide and view to verify the appropriate size and homogeneity of the biotin-labeled RNA (*see* **Note 6**).
11. Determine the concentration of RNA in the sample by placing 1 μl on a NanoDrop spectrometer. Store the biotin-labeled RNA at −80 °C for up to 3 months.

3.1.3 Preparation of RNA Oligonucleotide Labeled with Biotin at 3′ Terminus

This procedure ligates biotin-labeled cytidine (bis) phosphate nucleotide that contains a 3′, 5′ phosphate on the ribose ring to accommodate ligation of the cytidine with the biotin linker. The ligation should be performed in a nuclease-free tube on a nuclease-free lab bench while wearing sterile latex gloves and a lab coat.

1. Reagents are thawed on ice and remain on ice throughout the procedure with the exception of the 30 % PEG, which is thawed at room temperature.
2. Dilute the RNA oligonucleotide in nuclease-free water to final concentration 10 pmol/μl.
3. Transfer 6 μl to a sterile microfuge tube and incubate at 85 °C for 5 min.
4. Promptly move the tube onto ice and incubate for 5 min.
5. In the meantime, prepare the RNA ligation reaction mix.
6. Combine the mix and the RNA oligonucleotide and incubate the RNA ligation reaction overnight at 4 °C.

3.1.4 Cell Lysate Preparation

Adequate collection of HIV-1 from infected cells is a vital parameter in this experimental procedure. Cell culture and cell harvesting are executed in a Bio-safety level 2 (BSL-2) laminar flow hood wearing gloves and lab coat and minimizing aerosols.

1. Collect cells by centrifugation at 800 × *g* for 3 min in a tabletop centrifuge. Decant the culture medium and wash the cells twice by resuspension in 1/5th volume of 1× PBS (*see* **Note 7**).

2. Prepare the lysis buffer immediately prior to use by the addition of protease inhibitor and RNase inhibitor.
3. Add 200 µl lysis buffer per aliquot of 1×10^6 cells, mix by pipetting, and incubate on an orbital shaker for 5 min.
4. Collect the cell lysate in a nuclease-free tube and microfuge at $9{,}300 \times g$ for 2 min.
5. Transfer the supernatant to a fresh nuclease-free tube.
6. Warm the cell lysate at 60 °C for 10 min and place the tube on ice (*see* **Note 8**).

3.1.5 Preparation of Streptavidin Beads Bound to Biotinylated RNAs

1. In a nuclease-free tube, prepare a slurry of streptavidin-coated agarose beads in 5 volumes of binding buffer; gently mix by inverting the tube five times. Each treatment group requires a 25 µl aliquot of beads.
2. Centrifuge the tube at $1200 \times g$ for 1 min. Decant the supernatant.
3. Resuspend the beads in 5 volumes of binding buffer; invert the tube five times. Repeat **steps 2** and **3** twice.
4. Resuspend the streptavidin beads in 300 µl of binding buffer and supplement the preparation with 8 µg of biotin-labeled RNA (bait); gently rock the tube on table top rotator at 4 °C for 1 h. In addition to each RNA-streptavidin treatment group, prepare a duplicate tube deficient in biotin-labeled RNA (bait); this reaction will be used to benchmark proteins binding beads relative to those binding the RNA bait.
5. Collect the complexes by centrifuging at $1200 \times g$ for 1 min at 4 °C. Decant the supernatant.
6. Resuspend the beads in 1 ml of binding buffer. Gently rock the tube at room temperature for 5 min with buffer coating the beads.
7. Centrifuge the slurry at $1200 \times g$ for 1 min at 4 °C. Decant the supernatant, which eliminates residual biotin in solution.
8. Resuspend the beads in 1 ml binding buffer and incubate with gentle rocking at 4 °C for 5 min.
9. Repeat **step 7**.

3.1.6 RNA Affinity Chromatography on Sepharose Beads

1. Resuspend the bead preparations in 200 µl binding buffer and add 300 µg of cell protein and binding buffer to generate 0.5 ml reaction volume. Incubate at 4 °C for 2 h with gentle rocking.
2. Collect the beads using $1200 \times g$ for 1 min. Decant the supernatant.
3. Resuspend the beads in 1 ml of elution buffer at 4 °C.

4. Supplement the elution buffer to 40 mM washes, which serve to release low-affinity RNA-binding proteins. Mix by inverting the tube five times, incubate at room temperature for 5 min, and centrifuge at 1200 × *g* for 1 min. Decant the supernatant. Repeat **steps 12** and **13** three times with 100 mM KCl, 200 mM KCl, and 400 mM KCl in each of the three progressive washes.
5. Supplement the elution buffer to 2 M KCl and use 200 μl to resuspend the beads. Mix by inverting the tube five times, incubate at room temperature for 5 min, and centrifuge at 1200 × *g* for 1 min. Decant the supernatant.
6. Collect the 200 μl sample and dialyze overnight at 4 °C against binding buffer.

3.1.7 RNA Affinity Chromatography on Magnetic Beads

1. Resuspend the beads in 100 μl binding buffer and then add 300 μg of cell lysate in 200–500 μl binding buffer. Incubate with gentle rocking at 4 °C for 2 h.
2. Place the tube on magnetic stand to collect the beads and decant the binding buffer.
3. Wash the beads thrice with 500 μl washing buffer by collections on the magnetic stand.
4. Remove washing buffer and add 100 μl of 1× SDS-PAGE sample buffer.
5. Boil the reactions for 5 min to elute complexes from the beads. Allow the tube to cool to room temperature.
6. Collect the eluent at 9,300 × *g* for 2 min. Transfer the aqueous material a fresh labeled tube and store at –20 °C.

3.1.8 Preparative SDS-PAGE and Visualization of Protein

1. Use 80 % of the collected protein sample for SDS-PAGE with 8 % acrylamide (*see* **Note 9**).
2. Stain the gel with Coomassie Brilliant Blue or Silver stain to visualize protein content.
3. Harvest the entire lane in one gel slice. Submit for protease digestion, typically using trypsin, and peptide mass spectro photometry.

3.2 Isolation of Virion-Associated RNPs

3.2.1 Cell-Free Infection and Propagation of HIV-1NL4-3 Producer Cells

1. In a volume of 1–2 ml, mix in a sterile 15 ml tube 1×10^6 naïve CEM × 174 cells and supernatant medium containing 1×10^6 IU/ml HIV-1^{NL4-3}.
2. Incubate for 3 h in 5 % CO_2 incubator at 37 °C with rotation at ~600 rpm.
3. Move to a flask containing 8 ml RPMI and continue incubation at 37 °C for 2–3 days.

4. Monitor infection by intracellular staining with Gag p24 antibody in 24-h intervals until the intracellular staining indicates 50 % of the cells are infected. Designate this culture—the producer cells.

3.2.2 Propagation of Infected Cells by Coculture with Producer Cells

1. In a 15 ml tube, mix 1×10^6 producer cells and 9×10^6 naive CEM×174 cells in 1 ml medium; the producer:naive cell ratio is 1:10.
2. Incubate for 3 h in 5 % CO_2 incubator with rotation at ~600 rpm at 37 °C.
3. Add 28 ml fresh RPMI and incubate the culture for 36–42 h at 37 °C.
4. Discard media and replace with fresh medium.
5. Incubate 18–24 h and collect supernatant medium that contains the HIV-1 particles (*see* **Note 10**).

3.2.3 Collect HIV-1 Particles to Be Subject to RNA IP

1. Pellet CEM×174 cells at 1000×*g* for 5 min and collect the supernatant. The cells may be conserved for coculture expansion.
2. Pass the supernatant through a 0.45 μm filter.
3. Overlay the filtrate to a 0.5 ml of 20 % sucrose placed in 15 ml ultracentrifuge tube.
4. Place the tubes in the SW28 rotor and centrifuge at 100,000×*g* for 2 h at 4 °C in Beckman Optima ultracentrifuge.
5. Remove supernatant by decanting.
6. Add 300 μl of cell lysis buffer.
7. Reserve 10 μl as protein input and designate 100 μl as RNP input.
8. Use the rest for RNA affinity isolation (*see* **Note 11**).

3.2.4 RNA Immunoprecipitation (RIP)

1. Aliquot to a 1.5 ml Eppendorf tube 50 μl protein A or G beads into 900 μl NENT-150.
2. Invert the tube several times to wash the beads, add tube to the magnet and decant the NETN-150 buffer with a pipetman.
3. Add 500 μl 1× wash buffer to the tube and gently resuspend the beads.
4. Label the tubes, accordingly add antibodies and place on rotator for 1 h at 4 °C.
5. Place tubes on the magnet stand and decant the supernatant.
6. Add 500 μl of the virion preparation and 500 μl 1× wash buffer.
7. Rotate at 4 °C for 3 h.

8. Apply to magnet. Retain first supernatant and label as flow-through. Freeze for future quality control by immunoblotting (using 20 µl).
9. Execute repeated buffer exchanges using ice-cold wash buffer as follows:
   (a) Three washes with 1 ml NETN-150 wash buffer.
   (b) Two washes with 1 ml wash buffer.
10. Resuspend the beads in 1 ml wash buffer and aliquot 100 µl and 900 µl to separate tubes.
11. Collect the beads in each tube using the magnet, decant the wash buffer and remove residual buffer using a fine-tipped pipet.
12. Resuspend the beads as follows:
    (a) Vortex the 100 µl aliquot with 30 µl 2× Laemmli buffer (*see* **Note 12**).
    (b) Vortex 900 µl aliquot with 250 µl wash buffer, supplement with 750 µl Trizol LS and vortex; incubate at room temperature for 5 min.
13. Retrieve the input lysate from –80 freezer and add 150 µl 1× wash buffer, vortex, supplement with 750 µl Trizol LS, vortex, and incubate at room temperature for 5 min.

3.2.5 Extraction of RNA from the Immunoprecipitate

1. To each tube, add 100 µl chloroform, vortex, and incubate for another 3 min.
2. Collect at 13,400×*g* for 15 min in a refrigerated microcentrifuge.
3. Decant the aqueous supernatant to a new tube and mix with an equal volume of isopropanol. Repeat **step 2**.
4. Discard supernatant and add 100 µl RNase-free water to the tube and vortex to resuspend the precipitate that is typically invisible.
5. Apply the Qiagen RNAeasy Clean-up protocol to the 100 µl sample.
6. Resuspend RNA in a final volume of 30 µl of RNase-free water and store at –80 °C.

*3.2.6 Reverse Transcription of RNA to cDNA (See **Note 13**)*

1. Prepare the reverse transcription reaction mix.
2. Incubate for 1 h at 37 °C.

3.2.7 PCR to Amplify cDNA

1. Prepare the PCR reaction mix.
2. Program the thermocycler and incubate the PCR reaction: **Step 1**—initial denaturation, 5 min at 94 °C; **step 2**—denaturation, 5 min at 94 °C; **step 3**—annealing, 30 s at 60 °C; **step 4**—Extension 1 min at 72 °C; **step 5**—final extension, 3 min at 72 °C; step 6—hold at 4 °C.

4 Notes

1. The abundance of RNA in the IP reactions is minimal and great care must be taken to preserve the integrity of the samples. The lab bench and all pipets should be treated with an RNase removal agent. Maintenance of RNase-free tubes, tips and reagents is critical to successful isolation and detection of the immunoprecipitated RNA.
2. RNase-free water and containers are used to make every buffer in this protocol.
3. We strongly recommend pilot experimentation to establish that the IP antibody exhibits sufficient specificity and avidity for effective RNA coprecipitation.
4. Equivalent volumes of RNA preparations are used for reverse transcription given that RNA quantity is insufficient for spectrophotometry and productive reverse transcription.
5. The primer pairs that can distinguish between spliced and unspliced viral RNA were previously described [10].
6. A critical parameter is the homogeneity of the biotinylated RNA. The preparative gel electrophoresis of the RNA sample may be used to isolate the appropriately sized transcript by gel elution [2].
7. General guidelines for lysate preparation are to start with 1×10^8 cells in logarithmic growth and 16–20 h after medium exchange.
8. The purpose of warming the cell lysate at 60 °C for 10 min is to reduce nonspecific RNA–protein interactions and promote isolation of higher affinity RNPs.
9. The preparative SDS-PAGE partitions RNA binding proteins by size, but to engage an unbiased screen, proceed with ~80 % protein sample and conduct in-solution digestion prior to the mass spectrometry.
10. Virions sufficient for RNP isolation are released over a 24-h period from culture of 50 % HIV-1-positive cells (MOI = 1).
11. It is advisable for HIV-1 virions to be extracted immediately after collection and freeze/thaw cycles may reduce yield of RNPs.
12. The reserved protein samples will enable comparison of IP efficiency; the immunoblots are loaded with 10 μl input sample, 20 μl flow-through sample, and 15 μl of the IP protein sample.
13. The detection limit for the immunoprecipitated RNA warrants use of RT-qPCR rather than less sensitive approaches.

Acknowledgements

This work was supported by the National Institutes of Health's National Cancer Institute RO1CA10888 and National Institutes of General Medical Sciences P30CA740300.

References

1. Grüter P, Tabernero C, von Kobbe C, Schmitt C, Saavedra C, Bachi A, Wilm M, Felber BK, Izaurralde E (1998) TAP, the human homolog of Mex67p, mediates CTE-dependent RNA export from the nucleus. Mol Cell 5:649–659
2. Hartman TR, Qian S, Bolinger C, Fernandez S, Schoenberg DR, Boris-Lawrie K (2006) RNA helicase A is necessary for translation of selected messenger RNAs. Nat Struct Mol Biol 13:509–516
3. Tacheny A, Dieu M, Arnould T, Renard PJ (2013) Mass spectrometry-based identification of proteins interacting with nucleic acids. Proteomics 6:89–109
4. Stake M, Singh D, Singh G, Hernandez JM, Kaddis R, Parent LJ, Boris-Lawrie K (2015) HIV-1 and two avian retroviral 5' untranslated regions bind orthologous human and chicken RNA binding proteins. Virology. NIHMS ID: 709312 (In Press)
5. Leblanc J, Weil J, Beemon K (2013) Posttranscriptional regulation of retroviral gene expression: primary RNA transcripts play three roles as pre-mRNA, mRNA, and genomic RNA. Wiley Interdiscip Rev RNA 4:567–580
6. Butsch M, Boris-Lawrie K (2002) Destiny of unspliced retroviral RNA: ribosome and/or virion? J Virol 76:3089–3094
7. Wei P, Garber ME, Fang SM, Fischer WH, Jones KA (1998) A novel CDK9-associated C-type cyclin interacts directly with HIV-1 Tat and mediates its high-affinity, loop-specific binding to TAR RNA. Cell 92:451–462
8. Bell NM, Kenyon JC, Balasubramanian S, Lever AM (2012) Comparative structural effects of HIV-1 Gag and nucleocapsid proteins in binding to and unwinding of the viral RNA packaging signal. Biochemistry 51:3162–3169
9. Amarasinghe GK, Zhou J, Miskimon M, Chancellor KJ, McDonald JA, Matthews AG, Miller RR, Rouse MD, Summers MF (2001) Stem-loop SL4 of the HIV-1 psi RNA packaging signal exhibits weak affinity for the nucleocapsid protein, structural studies and implications for genome recognition. J Mol Biol 314:961–970
10. Purcell DF, Martin MA (1993) Alternative splicing of human immunodeficiency virus type 1 mRNA modulates viral protein expression, replication, and infectivity. J Virol 67:6365–6378
11. Sharma A, Yilmaz A, Marsh K, Cochrane A, Boris-Lawrie K (2012) Thriving under stress: selective translation of HIV-1 structural protein mRNA during Vpr-mediated impairment of eIF4E translation activity. PLoS Pathog. doi:10.1371/journal.ppat.1002612

Part III

HIV-1 Replication—Post-integration Events

Chapter 10

Methods for the Analyses of Inhibitor-Induced Aberrant Multimerization of HIV-1 Integrase

Jacques J. Kessl, Amit Sharma, and Mamuka Kvaratskhelia

Abstract

HIV-1 integrase (IN) is an important therapeutic target as its function is essential for the viral lifecycle. The discovery of multifunctional allosteric IN inhibitors or ALLINIs, which potently impair viral replication by promoting aberrant, higher order IN multimerization as well as inhibit IN interactions with its cellular cofactor, LEDGF/p75, has opened new venues to exploit IN multimerization as a therapeutic target. Furthermore, the recent discovery of multimerization selective IN inhibitors or MINIs, has provided new investigational probes to study the direct effects of aberrant IN multimerization in vitro and in infected cells. Here we describe three complementary methods designed to detect and quantify the effects of these new classes of inhibitors on IN multimerization. These methods include a homogenous time-resolved fluorescence-based assay which allows for measuring EC_{50} values for the inhibitor-induced aberrant IN multimerization, a dynamic light scattering-based assay which allows for monitoring the formation and sizes of oligomeric IN particles in a time-dependent manner, and a chemical cross-linking-based assay of interacting IN subunits which allows for the determination of IN oligomers in viral particles.

Key words HIV-1 integrase, Protein multimerization, Homogenous time-resolved fluorescence, Dynamic light scattering, Chemical cross-linking

1 Introduction

A tetramer of HIV-1 integrase (IN) assembles on the reverse-transcribed viral DNA ends, forming the stable synaptic complex (SSC) or intasome, and catalyzes integration of viral DNA into the host chromatin [1]. In this two-step reaction, IN first removes a GT dinucleotide from the 3′ end of each viral DNA (termed 3′ processing), and subsequently catalyzes the concerted trans-esterification reactions (termed DNA strand transfer) to join the recessed viral DNA ends into the host target DNA. Cellular chromatin-associated protein LEDGF/p75 engages the IN tetramer as part of the preintegration complex [2–8], which in addition

Vinayaka R. Prasad and Ganjam V. Kalpana (eds.), *HIV Protocols*, Methods in Molecular Biology, vol. 1354,
DOI 10.1007/978-1-4939-3046-3_10,

to the intasome contains viral and cellular proteins. Through a bimodal interaction with chromatin and viral IN, LEDGF/p75 is able to target HIV-1 integration to active genes.

The catalytic activity of HIV-1 IN has been successfully exploited as a therapeutic target in the clinic. The first generation of HIV-1 IN strand transfer inhibitors (INSTIs) raltegravir (RAL) and elvitegravir (EVG) engage the SSC following the 3′ processing reaction and inhibit the subsequent DNA strand transfer activity [9–11]. Escape mutations in HIV-1 IN that were initially detected in cell culture have also emerged in patients receiving INSTI-based treatment [12–14]. While a second generation INSTI, dolutegravir (DTG), similarly impairs the strand transfer activity, a significantly higher genetic barrier for resistance to this inhibitor has been observed as compared with its first generation counterparts. Yet, substitutions in the IN coding region that confer low-level resistance to DTG have also been identified [15]. Therefore, the development of novel small-molecule inhibitors that impair IN function with distinct mechanisms of action while retaining potency against current INSTI resistant mutants is an important goal.

One such potential mechanism is to modulate the ordered multimerization of HIV-1 IN. For example, dynamically interacting IN subunits could be prematurely stabilized by a small molecule that binds and bridges between interacting IN subunits to induce aberrant IN multimerization (the term "aberrant IN multimerization" refers here to formation of IN multimers, which are significantly higher than the functional tetramer required for its catalytic function) (Fig. 1). Initial proof-of-concept studies have shown that IN activity can be compromised by small-molecule tetra-acetylated chicoric acid binding at the IN dimer interface and stabilizing interacting IN subunits into incorrectly assembled multimeric states [16, 17]. This concept has been significantly extended by the recent discovery of quinoline-based allosteric IN inhibitors (ALLINIs) that potently impair HIV-1 replication (reviewed in ref. 18–21). ALLINIs are multifunctional in nature

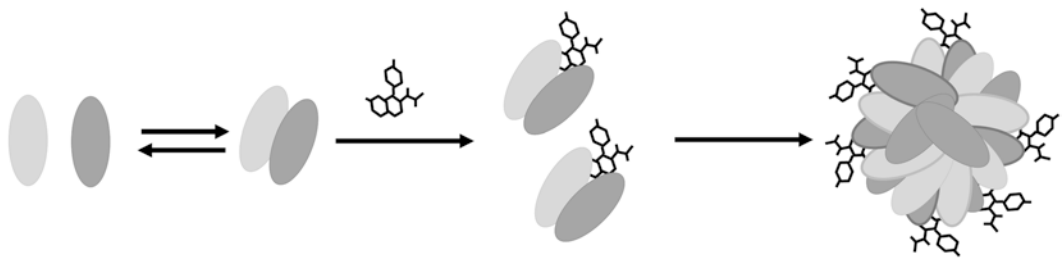

Fig. 1 Schematics of the inhibitor-induced aberrant IN multimerization. Unliganded IN exists in a dynamic equilibrium between monomeric, dimeric, and tetrameric species (for clarity only monomers and dimers are shown). The addition of active compound stabilizes interactive species and consequently induces the formation of aberrant, higher order multimerization of IN.

as they bind at the IN dimer interface in the LEDGF/p75 binding pocket and thus inhibit IN-LEDGF/p75 binding as well as promote aberrant IN multimerization. While ALLINI IC_{50} values for inhibiting IN-LEDGF/p75 binding and EC_{50} values for inducing aberrant IN multimerization are comparable in vitro, in infected cells the primary mechanism of action of this class of inhibitors is through promoting aberrant, higher order IN multimerization [22–25]. Strikingly, ALLINIs are more potent when added to virus producer cells than in target cells [23, 25–28]. It was observed that during the late stage of virus replication, ALLINIs induce aberrant, higher order IN multimerization, which results in eccentric viral particles that are impaired for the subsequent round of reverse transcription. The recent discovery of multimerization selective IN inhibitors (MINIs) further underscores IN multimerization as a plausible therapeutic target [29]. Collectively, these findings have prompted a strong interest in better understanding the structural and mechanistic foundations for IN multimerization as a therapeutic target.

Accordingly, new methods had to be developed to allow for monitoring the inhibitor-induced changes of IN multimeric states. In this chapter, we describe three complementary methods designed in our laboratory to detect and quantify the effects of ALLINIs, MINIs, and related compounds on aberrant IN multimerization both in vitro and within viral particles [29, 30]. These methods include homogeneous time-resolved fluorescence (HTRF) resonance energy transfer, dynamic light scattering (DLS), and chemical cross-linking in the virion.

The HTRF-based assay allows for the determination of EC_{50} values for inhibitor-induced formation of higher order HIV-1 IN multimers (Fig. 2). In this assay, we use two recombinant INs containing either a hexahistidine (6xHis) tag or the FLAG epitope at the protein's N-terminus. Commercially available anti-6xHis-XL665- and anti-FLAG-EuCryptate-conjugated antibodies, which bind to the 6xHis and FLAG tags, respectively, are added to measure time-resolved fluorescence resonance energy transfer between the XL665 and EuCryptate fluorophores upon IN multimerization. In the assay, compounds that induce IN multimerization result in a corresponding increase in the FRET signal. Additionally, the titration of a test compound into the assay will yield the EC_{50} value for IN multimerization. Because of the simplicity of the HTRF-based assay (add reagents, mix, incubate, and measure) and the need for only minute amount of reagents, this method can also be adapted to automated handling and used in a high-throughput screening format.

The DLS-based method allows for measuring sizes of the large IN particles, which are formed upon addition of the inhibitor, in a concentration- and time-dependent manner. DLS measures fluctuations in intensity of light scattered from a sample irradiated by a laser.

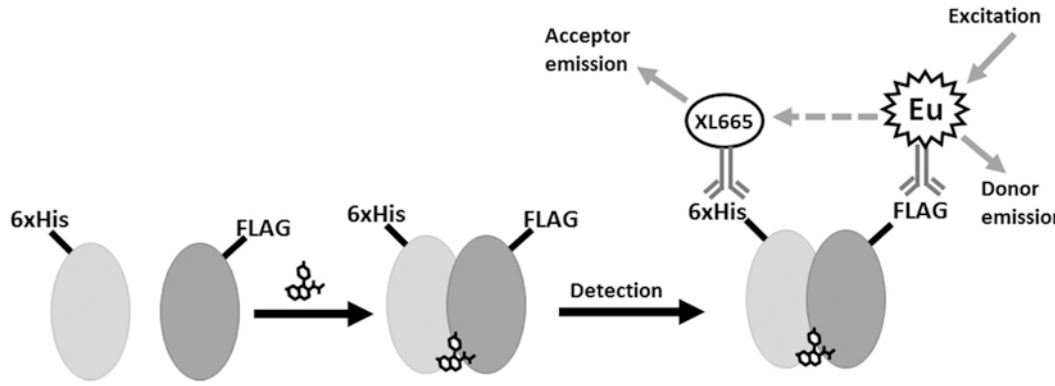

Fig. 2 Schematics of the HTRF-based IN multimerization assay. The assay monitors the interaction between two IN molecules tagged at the N-terminus: one containing 6xHis tag and the other containing the FLAG epitope. The antibodies conjugated with europium cryptate (Eu) and XL665 fluorophores yield HTRF signal upon protein-protein interaction. Europium cryptate is excited at 320 nm, and emissions at 665 and 620 nm are measured. The HTRF signal is calculated from the 665:620 nm emission ratio. While dimeric IN is shown for simplicity, drug-induced aberrant IN multimerization produces large multimeric species resulting in significant increase in the HTRF signal.

These fluctuations contain information about the motion of the scattering particles, thus allowing for the determination of diffusion coefficients of the particles in the sample solution. The diffusion coefficients depend on particle size and shape and can be affected by inter-particle interactions. The ability to monitor the temporal evolution of these parameters makes DLS a useful tool for studying particle aggregation and protein assembly [31]. When recombinant full length IN is maintained in a fully soluble state by a high ionic strength buffer, dynamically interacting individual IN subunits are not detected by DLS due to their small sizes. Upon addition of a multimerization-inducing compound the reaction equilibrium shifts towards the higher order IN multimers, resulting in corresponding increases in particle sizes in a time-dependent manner, which can be monitored by DLS.

The chemical cross-linking-based method allows for the detection of HIV-1 IN multimeric states within the virus particles. This method uses the cross-linking reagent BS^3, which contains an amine-reactive N-hydroxysulfosuccinimide (NHS) ester at each end of an 8-carbon spacer arm. The NHS esters react with the primary amines present within IN to form intra- and intermolecular stable amide bonds. This allows for the covalent bridging between interacting IN subunits and the determination of its oligomeric species in the virion, which can then be detected by immunoblotting. Using this methodology, one can monitor the relative variations in quantities of monomeric, dimeric, as well as higher order oligomeric species of IN within viral particles that are produced in the presence or the absence of the test compound.

2 Materials

2.1 HTRF-Based HIV-1 IN Multimerization Assay

2.1.1 HTRF Reagents and Proteins

1. Recombinant full-length HIV-1 IN tagged at the N-terminus with hexahistidine (6xHis-HIV-1 IN) from frozen concentrated stock at −80 °C (*see* **Note 1**).
2. Recombinant full-length HIV-1 IN tagged at the N-terminus with FLAG epitope (FLAG-HIV-1 IN) from frozen concentrated stock at −80 °C (also *see* **Note 1**).
3. Commercially available anti-FLAG EuCryptate antibody reconstituted to 0.2 μM in H_2O (according to the manufacturer's guidelines), aliquoted in small volumes, and stored in the dark at −20 °C.
4. Commercially available anti-6xHis XL665 antibody reconstituted to 2.6 μM in H_2O (according to the manufacturer's guidelines), aliquoted in small volumes, and stored in the dark at −80 °C.
5. HTRF buffer: 25 mM Tris pH 7.4, 150 mM NaCl, 2 mM $MgCl_2$, 0.1 % Nonidet P40, 1 mg/ml bovine serum albumin (BSA) (*see* **Note 2**) prepared on the day of the experiment and stored on ice.
6. 1 M KF solution in H_2O prepared on the day of the experiment and stored on ice.
7. The "Ab MIX" is prepared by diluting together anti-FLAG EuCryptate antibody to 1.8 nM, anti-6xHis XL665 antibody to 40 nM and KF to 200 μM in HTRF buffer. The volume of Ab MIX required for the experiment is obtained by multiplying 20 μl by the number of assays. Equilibrate the mixture to RT in the dark for 30 min before use.
8. Dimethyl sulfoxide (DMSO) (HPLC grade).
9. BI-1001 or related compound capable of inducing IN multimerization (*see* **Note 3**) is used as a positive control, whereas RAL or another small compound that does not affect IN multimerization is used as a negative control. The test and control compounds are dissolved in DMSO.

2.1.2 HTRF Microplates and Instrument

1. 386-Well polypropylene V-bottom microplates.
2. 386-Well low-volume high-base white microplates.
3. Plate reader instrument equipped with a time-resolved fluorescence (TRF) module and filters (*see* **Note 4**).
4. Data analysis software for curve fitting.

2.2 DLS-Based IN Multimerization Assay

2.2.1 DLS Reagents and Proteins

1. Recombinant full-length 6xHis tagged HIV-1 IN from frozen concentrated stock at −80 °C (*see* **Note 5**).
2. DLS buffer: 1 M NaCl, 2 mM $MgCl_2$, 2 mM DTT, 50 mM HEPES pH 7.4 (*see* **Note 6**) prepared on the day of the experiment and stored on ice.
3. DMSO (HPLC grade).
4. Compounds to be tested are dissolved in DMSO.
5. Milli-Q grade water.
6. Methanol (HPLC grade).

2.2.2 DLS Instrument and Software

1. Malvern Zetasizer Nano S90 (dynamic light scattering instrument).
2. Malvern Low Volume Microcuvette.
3. Cuvette washer with vacuum flask.
4. Microsoft Excel software.

2.3 IN Multimerization in Viral Particles

2.3.1 Plasmid, Mammalian Cell Culture, and Transfection Reagents

1. Replication competent full-length HIV-1 molecular clone pNL4-3.
2. Dulbecco's modified Eagle's medium (DMEM), fetal bovine serum (FBS), antibiotic-antimycotic.
3. Complete medium: DMEM + 10 % FBS + 1 % antibiotic-antimycotic.
4. Reduced serum media.
5. DNA transfection reagent: We routinely use X-tremeGENE HP DNA transfection reagent.
6. HIV-1 p24 antigen ELISA.

2.3.2 Virion Pelleting

1. 25 % (w/v) sucrose solution prepared in 1× phosphate-buffered saline (PBS).
2. 13.2 ml ultracentrifuge tubes.
3. Swinging bucket ultracentrifuge rotor.
4. L-80 ultracentrifuge (Beckman).

2.3.3 IN Cross-Linking

1. Virion lysis buffer: PBS + 0.25 % (v/v) Triton X-100.
2. Bis(sulfosuccinimidyl)suberate (BS^3) cross-linking reagent.
3. Conjugation buffer: 20 mM HEPES, pH 7.5.
4. Quenching buffer: 0.5 M Tris–HCl, pH 7.5.

2.3.4 Immunoblotting

1. Polyacrylamide gel 4–12 % Bis-Tris precast gel, 1.0 mm, 10 well.
2. 4× sample loading buffer.
3. Pre-stained molecular weight marker.

4. SDS gel running buffer 20×.
5. Nitrocellulose membrane 0.45 μm.
6. Semidry transfer cell.
7. 20× transfer buffer.
8. PBS-T solution: PBS + 0.1 % (v/v) Tween® 20.
9. Blocking solution: 5 % (w/v) nonfat milk in PBS-T.
10. Primary antibody: Mouse monoclonal anti-HIV-1 IN antibody.
11. Secondary antibody: Anti-mouse horseradish peroxidase (HRP)-linked antibody.
12. Chemiluminescence-based HRP antibody detection reagent.

3 Methods

3.1 HTRF-Based IN Multimerization Assay

3.1.1 HTRF Reagent Preparation

1. Slowly thaw on ice 6xHis-HIV-1 IN and FLAG-HIV-1 IN aliquots from −80 °C frozen stocks.
2. Perform a serial dilution of the compound to be tested in DMSO. Include additional control setup with DMSO alone, RAL as a negative control, and BI-1001 as a positive control.
3. Prepare the "IN MIX" by mixing together 6xHis-HIV-1 IN and FLAG-HIV-1 IN to a final concentration of 30 nM (for each protein) in the HTRF buffer. Calculate the volume of the IN MIX required for the experiment by multiplying 40 μl by the number of assays. Typically, each data point/drug concentration must be measured in triplicate. Allow the IN MIX to reach room temperature (~30 min) before going to the next step.

3.1.2 HTRF-Based Assay and Incubations

1. Add 40 μl/well of the IN MIX equilibrated at room temperature in a 386-well polypropylene V-bottom plate.
2. To the 40 μl IN MIX, add and mix thoroughly 1.2 μl of DMSO or tested compound dissolved in DMSO (*see* **Note 7**). Avoid the formation of bubbles by carefully controlling the pipetting speed.
3. Incubate the plate containing the IN MIX with compounds for 3 h at room temperature.
4. To the 40 μl IN MIX with test compound, add 20 μl of Ab MIX and mix. Avoid the formation of bubbles by carefully controlling the pipetting speed.
5. Incubate the assay plate in the dark for 2 h at room temperature.

3.1.3 HTRF Signal Detection and Data Analysis

1. Transfer 20 µl/well from the assay plate to a 386-well low-volume white plate. Avoid the formation of bubbles by carefully controlling the pipetting speed.
2. Insert the plate in the instrument and perform the HTRF measurement (*see* **Note 8**) three times on the same plate.
3. Average the HTRF signal of the three measurements to minimize instrument reading deviation. Calculate the average and standard deviation of each triplicate data point. Plot the HTRF signal versus compound concentration and perform a computational nonlinear curve fitting using the Hill equation (Fig. 3):

$$y = \frac{x^n}{k^n + x^n}$$

where x is the compound concentration, y is the HTRF signal, k is the inhibitor IC_{50}, and n is the Hill slope.

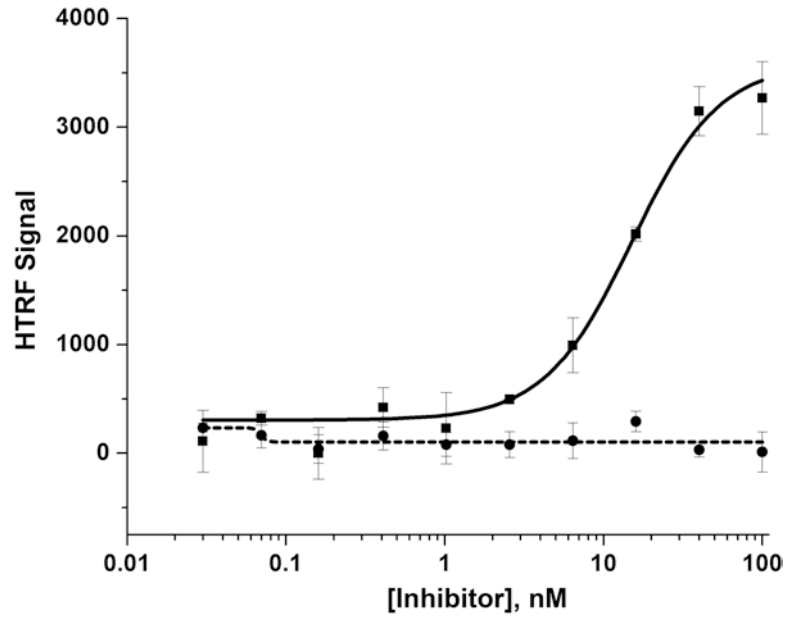

Fig. 3 Example data set for HTRF-based IN multimerization assay. HTRF data obtained with increasing concentration of BI-1001 *(black squares)* and RAL (*black circles*). Each data point represents the mean of three independent reactions with standard deviations shown. The curve fitting of dose–response effects of ALLINI BI-1001 on IN multimerization is shown. The sharp HTRF signal increase observed with BI-1001 is typical with compounds that promote aberrant IN multimerization. The INSTI RAL (negative control) does not induce any signal variation.

3.2 DLS-Based IN Multimerization Assay

3.2.1 DLS Reagent Preparation

1. Take out and slowly thaw on ice full-length 6xHis-tagged HIV-1 IN aliquots from −80 °C frozen stocks.
2. Calculate the volume of IN dilution required for the experiment by multiplying 500 μl by the number of assays. Typically, each data point must be measured in triplicate.
3. Divide IN dilutions into 500 μl aliquots and maintain them on ice until ready.

3.2.2 DLS Measurements

1. Set the DLS instrument for size distribution recording (*see* **Note 9**).
2. Equilibrate 500 μl IN dilution aliquots to room temperature for 30 min.
3. To a 500 μl IN dilution aliquot, add and mix thoroughly 0.5 μl of DMSO or test compound dissolved in DMSO (*see* **Note 10**). Avoid the formation of bubbles by carefully controlling the pipetting speed.
4. Immediately transfer 100 μl of the mixture into the microcuvette and record the size distribution using the DLS instrument.
5. Measure additional size distribution of the mixture at regular time intervals until it reaches a total time of 30 min incubation (leave the microcuvette in the instrument).
6. Between measurements of different samples, thoroughly wash the microcuvette with Milli-Q-grade water and then rinse it with methanol.
7. Using the same procedure, record the size distributions of negative controls (DLS buffer, DLS buffer with 0.5 μl of test compound).

3.2.3 DLS Data Analysis

1. Transfer size versus number distribution data from Malvern measuring software into Microsoft Excel.
2. Using Excel, plot the particle diameter in nm size versus the number distribution at different incubation time (Fig. 4). Signal detected below the 1 nm diameter threshold should be regarded as background noise.

3.3 IN Multimerization in Viral Particles

3.3.1 Generation, Isolation, and Lysis of Viral Particles

1. Seed 2×10^6 HEK293 cells in 10 ml complete medium in a 100 mm tissue-culture dish and culture overnight at 37 °C and 5 % CO_2.
2. Next day, transfect cells with HIV-1 proviral plasmid (*see* **Note 11**). Take 500 μl of reduced serum media in an Eppendorf tube, add 10 μg of pNL4-3 plasmid DNA, and incubate at room temperature for 5 min. Next, add 30 μl of DNA transfection reagent (*see* **Note 12**) directly into the reduced serum media-DNA mixture without touching the sides of the tube and

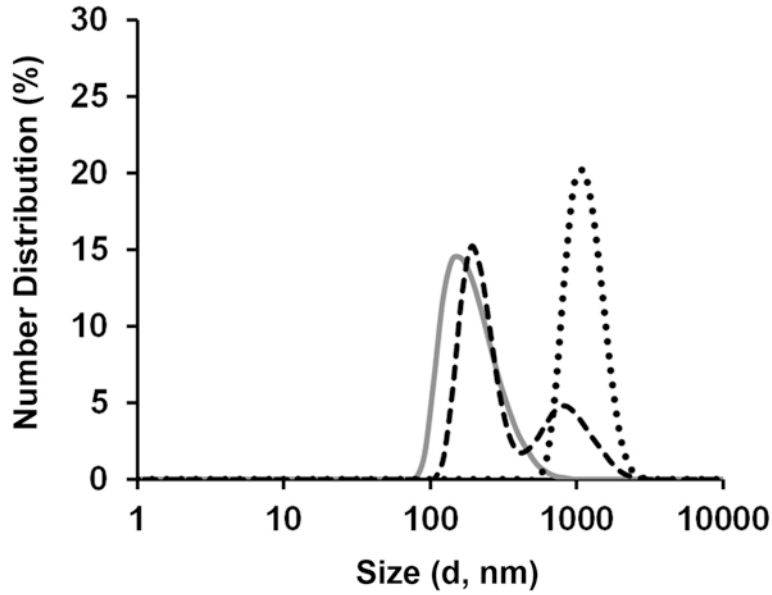

Fig. 4 Example data set of DLS-based IN multimerization assay. Size distribution of IN at 2 min (*grey*), 8 min (*black*, *dashed*), and 30 min (*black*, *dotted*) after addition of MINI KF116. Recorded signals indicate an equilibrium shift toward higher order oligomers in a time-dependent manner. Of note, these particle sizes are significantly larger than functional HIV-1 IN tetramers (which has a diameter of ~7.5 nm) seen by atomic force microscopy analysis of in vitro-assembled HIV-1 intasomes [32]. No detectable signal above 1 nm diameter was recorded with buffer alone, buffer with DMSO, buffer with compound, and IN with DMSO incubated for up to 30 min.

incubate at room temperature for 15 min. Add the transfection complex to the cells in a dropwise manner. Culture the cells for 24 h at 37 °C and 5 % CO_2.

3. Twenty-four hours post-transfection, wash the cells once with complete medium by gently removing the culture supernatant and replacing with 5 ml of complete medium. Next, replace the complete medium with 5 ml of complete medium containing the desired concentration of tested compound or diluent control (*see* **Note 13**). Culture the cells for 1 h at 37 °C and 5 % CO_2.
4. After 1 h, replace the culture supernatant again with fresh 10 ml of complete medium containing the tested compound or diluent control. Culture the cells for 24 h at 37 °C and 5 % CO_2.
5. Harvest the virus-containing culture supernatant in a 15 ml tube. Centrifuge at 2000 × *g* for 5 min at room temperature to pellet the cell debris. Collect the cell-free virus-containing

supernatant and filter it through 0.45 μm sterile filter. Aliquot 25 μl of virus-containing, filtered supernatant in an Eppendorf tube and store the rest at 4 °C.

6. Use 25 μl of virus-containing, filtered supernatant to perform HIV-1 p24 ELISA using the manufacturer's kit and protocol. Generate the standard curve in the range of 7.8–125 pg/ml of HIV-1 p24 using HIV-1 p24 antigen supplied with the kit.
7. Calculate the volume of virus-containing, filtered supernatant equivalent to 1000–1500 ng of HIV-1 p24 using the HIV-1 p24 standard curve. Aliquot the calculated volume of virus-containing, filtered supernatant in a new 15 ml tube and bring the volume up to 12 ml with complete medium.
8. Load 12 ml of virus-containing, filtered supernatant in a 13.2 ml ultracentrifuge tube. Gently underlay 1 ml of 25 % sucrose solution using a Pasteur pipette. Load the ultracentrifuge tube in the swinging bucket rotor. Ultracentrifuge at 135,000 × *g* for 2 h at 4 °C.
9. Decant the supernatant and carefully wipe the inside of the tube with rolled-up Kimwipes to remove traces of supernatant and sucrose. Avoid touching the bottom of the tube.
10. Add virion lysis buffer to adjust the concentration of virions to 15 ng/μl of HIV-1 p24. For example, if supernatant equivalent to 1500 ng of HIV-1 p24 was pelleted then add 150 μl of virion lysis buffer. Incubate the tube at 37 °C for 15 min, briefly vortex the tube to dislodge the viral pellet, and resuspend by pipetting. Collect the lysed virions in a new Eppendorf tube.

3.3.2 Virion-Associated IN Cross-Linking Reaction

1. In an Eppendorf tube add lysed virions equivalent to 50 ng of HIV-1 p24 and the calculated volume of conjugation buffer.
2. Prepare 200 μM BS^3 cross-linking solution (*see* **Note 14**).
3. Add BS^3 cross-linking agent to a final concentration of 50 μM in a final reaction volume of 12 μl.
4. Incubate the reaction mixture at room temperature for 20 min.
5. Quench the reaction by adding quenching buffer to a final concentration of 50 mM.
6. Incubate the quenching reaction mixture at room temperature for 20 min.

3.3.3 Immunoblotting to Detect Cross-Linked Reaction Products

1. Add sample loading buffer, to a final concentration of 1×, to the cross-linked reaction products. Heat at 90 °C for 3 min.
2. Load the cross-linked reaction products into the wells of a 4–12 % gradient polyacrylamide gel. Also load 10 μl of molecular weight marker in one well.
3. Run the gel at 200 V for 40 min in 1× SDS gel running buffer.

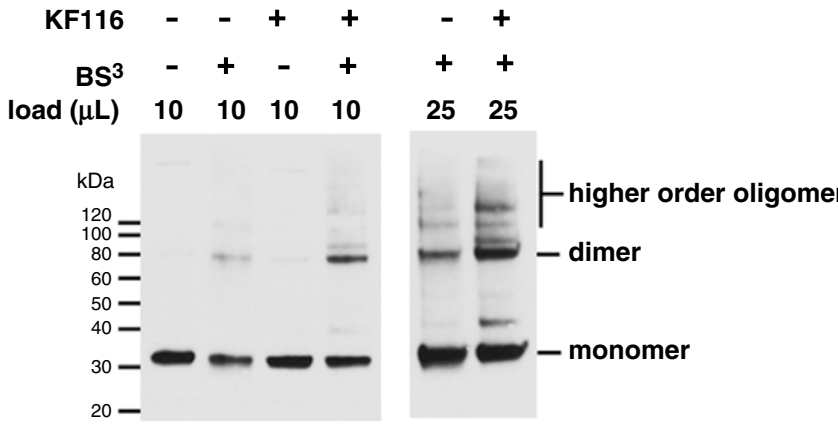

Fig. 5 Example of inhibitor-induced IN multimerization in HIV-1 viral particles. HIV-1 virions were produced in the presence of DMSO or the inhibitor, cell-free virions were harvested, detergent-lysed, and treated with BS^3 cross-linking reagent. The indicated volumes of cross-linked reaction products were resolved by SDS-PAGE and immunoblotted with HIV-1 IN antibody. The bands corresponding to IN "monomer," "dimer," and "higher order oligomers" are indicated. When virions were produced in the presence of MINI KF116, the levels of IN dimers increased as well as the appearance of new higher molecular weight bands, which likely to correspond to higher oligomeric states of IN. Adapted and reprinted from Sharma et al. [29].

4. Transfer the resolved proteins onto a nitrocellulose membrane in 1× transfer buffer using a semidry transfer cell. Transfer at 15 V for 50 min.
5. Post-transfer, block the membrane for 1 h at room temperature in blocking solution.
6. Incubate the membrane with the primary antibody diluted 1:2000 in blocking solution overnight at 4 °C.
7. Wash the membrane three times in PBS-T solution for 5 min each time.
8. Incubate the membrane with the secondary antibody diluted 1:2000 in blocking solution for 1 h at 4 °C.
9. Wash the membrane four times in PBS-T solution for 5 min each time.
10. Detect proteins using HRP antibody detection reagent and expose on X-ray film.
11. Scan the exposed X-ray film and analyze signal with an imaging software (Fig. 5).

4 Notes

1. The recombinant 6xHis-HIV-1 IN and FLAG-HIV-1 IN are purified from *E. coli* as previously described [22]. The concentration of the purified proteins must be maintained between 10 and 30 µM in the storage buffer (50 mM HEPES pH 7.5, 1 M

NaCl, 7.5 mM CHAPS, 2 mM β-mercaptoethanol, and 10 % glycerol) to avoid auto-aggregation. Purified recombinant INs are aliquoted into small volumes, flash-frozen by liquid N_2 immersion, and stored at −80 °C. Importantly, once thawed the protein aliquot must be used immediately or discarded.

2. The BSA must be of TRF grade (Perkin Elmer #CR84-100) and free from trace amounts of heavy metals to minimize critical interference with the donor EuCryptate fluorophore label conjugated on the anti-FLAG antibody.
3. RAL can be obtained from the NIH AIDS Reagent program. The complete step-by-step synthesis of BI-1001 has been previously described [22].
4. We recommend using PerkinElmer Enspire plate reader instrument with Time Resolved Fluorescence module installed and mounted with 320 nm excitation filters. The Molecular Devices plate reader M1 instrument was also successfully tested and used for this assay.
5. The recombinant 6xHis-HIV-1 IN was purified from *E. coli* as previously described [22]. The 6xHis tag does not interfere with the assay and can be left to simplify the IN purification procedure.
6. The DLS buffer must be prepared using Milli-Q grade water and thoroughly filtered using syringe-mounted 0.2 μm filter units.
7. The HTRF-based multimerization assay has been successfully tested with DMSO at final concentrations between 0.2 and 4 %.
8. The following plate reader instrument settings in time-resolved fluorescence mode have been optimized for the use of the CISBIO reagent pair EuCryptate/XL665:
   - Measurement A: excitation 320 nm, emission 665 nm, number of flashes 100, delay 50 μs, window time 450 μs.
   - Measurement B: excitation 320 nm, emission 620 nm, number of flashes 100, delay 50 μs, window time 450 μs.
   - HTRF signal is defined as: measurement A/measurement B × 10,000.
9. DLS instrument settings are size mode, measurement recorded in number distribution (not intensity or percentage), and average of ten measurements.
10. The DLS-based multimerization has been successfully tested with DMSO at final concentration up to 0.5 %.
11. The virion-associated IN cross-linking assay can also be performed on single-cycle, pseudotyped HIV-1 virions. For this, transfect cells with 10 μg of envelope-defective HIV-1 clone

with firefly luciferase gene inserted into the nef gene pNL4-3. Luc.Env$^-$ and 5 μg of vesicular stomatitis virus G glycoprotein (VSV-G) eukaryotic expression vector pMD.G.

12. We routinely use X-tremeGENE HP DNA transfection reagent to get higher transfection efficiency. We recommend using X-tremeGENE HP at 1:3 ratio (volume: μg of total DNA transfected). Other transfection reagents and methods such as calcium-phosphate, lipofection, or polyethylenimine can also be used.
13. Always set up control treatment in which the volume of diluent (for example DMSO) is equal to the test IN inhibitor that is added to the cells.
14. Always prepare BS^3 cross-linking solution immediately before use. Do not prepare and store stock solutions of BS^3 cross-linking reagent as the *N*-hydroxysuccinimide ester moiety of BS^3 undergoes rapid hydrolysis making the cross-linking reagent nonreactive. We also recommend using the no-weigh microtube format of BS^3 cross-linking reagent in which pre-weighed 2 mg BS^3 aliquots are supplied in the ready-to-use microtubes.

Acknowledgments

We thank Dr. Ross C. Larue for critical reading of the manuscript and valuable suggestions. The present study was supported by the National Institutes of Health (grants AI110270 to J.J.K., AI062520 and AI110310 to M.K.).

References

1. Li M, Mizuuchi M, Burke TR Jr, Craigie R (2006) Retroviral DNA integration: reaction pathway and critical intermediates. EMBO J 25:1295–1304
2. Cherepanov P, Maertens G, Proost P, Devreese B, Van Beeumen J, Engelborghs Y, De Clercq E, Debyser Z (2003) HIV-1 integrase forms stable tetramers and associates with LEDGF/p75 protein in human cells. J Biol Chem 278:372–381. doi:10.1074/jbc.M209278200
3. Ciuffi A, Llano M, Poeschla E, Hoffmann C, Leipzig J, Shinn P, Ecker JR, Bushman F (2005) A role for LEDGF/p75 in targeting HIV DNA integration. Nat Med 11:1287–1289. doi:10.1038/nm1329
4. Llano M, Saenz DT, Meehan A, Wongthida P, Peretz M, Walker WH, Teo W, Poeschla EM (2006) An essential role for LEDGF/p75 in HIV integration. Science 314:461–464. doi:10.1126/science.1132319
5. Shun MC, Raghavendra NK, Vandegraaff N, Daigle JE, Hughes S, Kellam P, Cherepanov P, Engelman A (2007) LEDGF/p75 functions downstream from preintegration complex formation to effect gene-specific HIV-1 integration. Genes Dev 21:1767–1778. doi:10.1101/gad.1565107
6. Ferris AL, Wu X, Hughes CM, Stewart C, Smith SJ, Milne TA, Wang GG, Shun MC, Allis CD, Engelman A, Hughes SH (2010) Lens epithelium-derived growth factor fusion proteins redirect HIV-1 DNA integration. Proc Natl Acad Sci U S A 107:3135–3140. doi:10.1073/pnas.0914142107

7. Busschots K, Vercammen J, Emiliani S, Benarous R, Engelborghs Y, Christ F, Debyser Z (2005) The interaction of LEDGF/p75 with integrase is lentivirus-specific and promotes DNA binding. J Biol Chem 280:17841–17847
8. Cherepanov P, Ambrosio AL, Rahman S, Ellenberger T, Engelman A (2005) Structural basis for the recognition between HIV-1 integrase and transcriptional coactivator p75. Proc Natl Acad Sci U S A 102:17308–17313
9. Hazuda DJ, Felock P, Witmer M, Wolfe A, Stillmock K, Grobler JA, Espeseth A, Gabryelski L, Schleif W, Blau C, Miller MD (2000) Inhibitors of strand transfer that prevent integration and inhibit HIV- 1 replication in cells. Science 287:646–650
10. Johnson AA, Marchand C, Pommier Y (2004) HIV-1 integrase inhibitors: a decade of research and two drugs in clinical trial. Curr Top Med Chem 4:1059–1077
11. Hazuda DJ (2012) HIV integrase as a target for antiretroviral therapy. Curr Opin HIV AIDS 7:383–389. doi:10.1097/COH.0b013e3283567309
12. Sichtig N, Sierra S, Kaiser R, Daumer M, Reuter S, Schulter E, Altmann A, Fatkenheuer G, Dittmer U, Pfister H, Esser S (2009) Evolution of raltegravir resistance during therapy. J Antimicrob Chemother 64:25–32. doi:10.1093/jac/dkp153
13. Steigbigel RT, Cooper DA, Kumar PN, Eron JE, Schechter M, Markowitz M, Loutfy MR, Lennox JL, Gatell JM, Rockstroh JK, Katlama C, Yeni P, Lazzarin A, Clotet B, Zhao J, Chen J, Ryan DM, Rhodes RR, Killar JA, Gilde LR, Strohmaier KM, Meibohm AR, Miller MD, Hazuda DJ, Nessly ML, DiNubile MJ, Isaacs RD, Nguyen BY, Teppler H, Teams BS (2008) Raltegravir with optimized background therapy for resistant HIV-1 infection. N Engl J Med 359:339–354. doi:10.1056/NEJMoa0708975
14. Metifiot M, Vandegraaff N, Maddali K, Naumova A, Zhang X, Rhodes D, Marchand C, Pommier Y (2011) Elvitegravir overcomes resistance to raltegravir induced by integrase mutation Y143. AIDS 25:1175–1178. doi:10.1097/QAD.0b013e3283473599
15. Wares M, Mesplede T, Quashie PK, Osman N, Han Y, Wainberg MA (2014) The M50I polymorphic substitution in association with the R263K mutation in HIV-1 subtype B integrase increases drug resistance but does not restore viral replicative fitness. Retrovirology 11:7. doi:10.1186/1742-4690-11-7
16. Shkriabai N, Patil SS, Hess S, Budihas SR, Craigie R, Burke TR Jr, Le Grice SF, Kvaratskhelia M (2004) Identification of an inhibitor-binding site to HIV-1 integrase with affinity acetylation and mass spectrometry. Proc Natl Acad Sci U S A 101:6894–6899
17. Kessl JJ, Eidahl JO, Shkriabai N, Zhao Z, McKee CJ, Hess S, Burke TR Jr, Kvaratskhelia M (2009) An allosteric mechanism for inhibiting HIV-1 integrase with a small molecule. Mol Pharmacol 76:824–832
18. Jurado KA, Engelman A (2013) Multimodal mechanism of action of allosteric HIV-1 integrase inhibitors. Expert Rev Mol Med 15:e14. doi:10.1017/erm.2013.15
19. Engelman A, Kessl JJ, Kvaratskhelia M (2013) Allosteric inhibition of HIV-1 integrase activity. Curr Opin Chem Biol 17:339–345. doi:10.1016/j.cbpa.2013.04.010
20. Demeulemeester J, Chaltin P, Marchand A, De Maeyer M, Debyser Z, Christ F (2014) LEDGINs, non-catalytic site inhibitors of HIV-1 integrase: a patent review (2006–2014). Expert Opin Ther Pat. doi:10.1517/13543776.2014.898753
21. Fader LD, Malenfant E, Parisien M, Carson R, Bilodeau F, Landry S, Pesant M, Brochu C, Morin S, Chabot C, Halmos T, Bousquet Y, Bailey MD, Kawai SH, Coulombe R, LaPlante S, Jakalian A, Bhardwaj PK, Wernic D, Schroeder P, Amad M, Edwards P, Garneau M, Duan J, Cordingley M, Bethell R, Mason SW, Bos M, Bonneau P, Poupart MA, Faucher AM, Simoneau B, Fenwick C, Yoakim C, Tsantrizos Y (2014) Discovery of BI 224436, a noncatalytic site integrase inhibitor (NCINI) of HIV-1. ACS Med Chem Lett 5:422–427. doi:10.1021/ml500002n
22. Kessl JJ, Jena N, Koh Y, Taskent-Sezgin H, Slaughter A, Feng L, de Silva S, Wu L, Le Grice SF, Engelman A, Fuchs JR, Kvaratskhelia M (2012) Multimode, cooperative mechanism of action of allosteric HIV-1 integrase inhibitors. J Biol Chem 287:16801–16811. doi:10.1074/jbc.M112.354373
23. Jurado KA, Wang H, Slaughter A, Feng L, Kessl JJ, Koh Y, Wang W, Ballandras-Colas A, Patel PA, Fuchs JR, Kvaratskhelia M, Engelman A (2013) Allosteric integrase inhibitor potency is determined through the inhibition of HIV-1 particle maturation. Proc Natl Acad Sci U S A 110:8690–8695. doi:10.1073/pnas.1300703110
24. Feng L, Sharma A, Slaughter A, Jena N, Koh Y, Shkriabai N, Larue RC, Patel PA, Mitsuya H, Kessl JJ, Engelman A, Fuchs JR, Kvaratskhelia M (2013) The A128T resistance mutation reveals aberrant protein multimerization as the primary mechanism of action of allosteric HIV-1 integrase inhibitors. J Biol Chem 288:15813–15820. doi:10.1074/jbc.M112.443390

25. Gupta K, Brady T, Dyer BM, Malani N, Hwang Y, Male F, Nolte RT, Wang L, Velthuisen E, Jeffrey J, Van Duyne GD, Bushman FD (2014) Allosteric inhibition of human immunodeficiency virus integrase: late block during viral replication and abnormal multimerization involving specific protein domains. J Biol Chem. doi:10.1074/jbc.M114.551119
26. Balakrishnan M, Yant SR, Tsai L, O'Sullivan C, Bam RA, Tsai A, Niedziela-Majka A, Stray KM, Sakowicz R, Cihlar T (2013) Non-catalytic site HIV-1 integrase inhibitors disrupt core maturation and induce a reverse transcription block in target cells. PLoS One 8:e74163. doi:10.1371/journal.pone.0074163
27. Desimmie BA, Schrijvers R, Demeulemeester J, Borrenberghs D, Weydert C, Thys W, Vets S, Van Remoortel B, Hofkens J, De Rijck J, Hendrix J, Bannert N, Gijsbers R, Christ F, Debyser Z (2013) LEDGINs inhibit late stage HIV-1 replication by modulating integrase multimerization in the virions. Retrovirology 10:57. doi:10.1186/1742-4690-10-57
28. Le Rouzic E, Bonnard D, Chasset S, Bruneau JM, Chevreuil F, Le Strat F, Nguyen J, Beauvoir R, Amadori C, Brias J, Vomscheid S, Eiler S, Levy N, Delelis O, Deprez E, Saib A, Zamborlini A, Emiliani S, Ruff M, Ledoussal B, Moreau F, Benarous R (2013) Dual inhibition of HIV-1 replication by integrase-LEDGF allosteric inhibitors is predominant at the post-integration stage. Retrovirology 10:144. doi:10.1186/1742-4690-10-144
29. Sharma A, Slaughter A, Jena N, Feng L, Kessl JJ, Fadel HJ, Malani N, Male F, Wu L, Poeschla E, Bushman FD, Fuchs JR, Kvaratskhelia M (2014) A new class of multimerization selective inhibitors of HIV-1 integrase. PLoS Pathog 10:e1004171. doi:10.1371/journal.ppat.1004171
30. Kessl JJ, Jena N, Koh Y, Taskent-Sezgin H, Slaughter A, Feng L, de Silva S, Wu L, Le Grice SF, Engelman A, Fuchs JR, Kvaratskhelia M (2012) A multimode, cooperative mechanism of action of allosteric HIV-1 integrase inhibitors. J Biol Chem 287:16801–16811
31. Serriere J, Fenel D, Schoehn G, Gouet P, Guillon C (2013) Biophysical characterization of the feline immunodeficiency virus p24 capsid protein conformation and in vitro capsid assembly. PLoS One 8:e56424. doi:10.1371/journal.pone.0056424
32. Kotova S, Li M, Dimitriadis EK, Craigie R (2010) Nucleoprotein intermediates in HIV-1 DNA integration visualized by atomic force microscopy. J Mol Biol 399:491–500. doi:10.1016/j.jmb.2010.04.026

Chapter 11

Quantification of HIV-1 Gag Localization Within Virus Producer Cells

Annalena La Porte and Ganjam V. Kalpana

Abstract

Trafficking of newly synthesized Gag protein to the plasma membrane is one of the important steps during HIV-1 assembly. It requires participation of both viral and cellular determinants. Several techniques have been used to measure the amount of Gag that is associated with plasma membrane. Here we describe a microscopy-based method to estimate the distribution of Gag protein within the producer cell. This method can be used in conjunction with other biochemical techniques to quantify the distribution of Gag within a virus-producing cell and its accumulation at the plasma membrane. Since this method is microscopy based, it allows one to quantitate Gag across the cytoplasm, from the nuclear periphery to plasma membrane, at the single-cell level.

Key words HIV-1 Gag, Quantitating Gag protein, Gag trafficking

1 Introduction

The late events of HIV-1 replication involve several steps including transcription of the provirus, nuclear export of singly and multiply spliced RNAs, translation of viral RNAs to produce viral proteins, and the trafficking of these proteins to the plasma membrane, where these proteins are assembled to produce infectious particles [1–4]. While Envelope protein (Env) is synthesized on the rough endoplasmic reticulum (ER) and gets transported through the Golgi and trans-Golgi network, the Gag ($pr55^{Gag}$) and Gag-Pol polyproteins are synthesized on the cytoplasmic ribosomes and traffic through the cytoplasm to the plasma membrane for assembly [2]. The process by which Gag traffics through the cytoplasm is not well understood. Both viral and cellular determinants are involved in this process [2, 4]. Several methods, described elsewhere, have been used to determine the trafficking of Gag to the plasma membrane including cell fractionation and membrane flotation assays [5–7]. In this protocol, we describe a simple microscopy-based method to quantify the trafficking of the Gag

Vinayaka R. Prasad and Ganjam V. Kalpana (eds.), *HIV Protocols*, Methods in Molecular Biology, vol. 1354,
DOI 10.1007/978-1-4939-3046-3_11,

protein by measuring the density of the protein across the cytoplasm from the site of synthesis to the plasma membrane within the cells, by visualizing Gag by immunoflourescence microscopy and by quantifying the intensity of signals using image analysis software. Using this method, the gradient of Gag levels from the nucleus to the plasma membrane can be determined to characterize the pattern of Gag distribution. A clear accumulation of the Gag protein at the plasma membrane can be seen in a producer cell infected with wild type HIV-1. However, factors that affect Gag trafficking may influence this distribution and hence the localization of Gag within these cells can be seen as diffuse (both nuclear and cytoplasmic), nuclear, cytoplasmic or perinuclear.

To quantitate Gag distribution, typically, HIV-infected cells are stained by using α-p24 antibody, the cells are imaged using confocal microscopy, and z-stacks of the cell are obtained to visualize the protein distribution at various planes. The saved images are analyzed and pixel intensity of the images representing the protein in question (such as Gag) within the cell is quantitated using analysis programs such as ImageJ. The immunofluorescence signals are analyzed to obtain intensities or gray value of each pixel within a given area (*see* **Note 1**). By plotting the intensities or gray values/pixel as a function of distance (in pixels) across the cytoplasm, a quantitative measure of the protein distribution is obtained. If a line is drawn from the nucleus to the plasma membrane, then one can obtain an estimation of the intensity of the protein distribution from the plasma membrane to the nucleus within the area covered by the line. There are many advantages to using this method of quantification using microscopy. (1) The method allows the quantification of proteins within the single cells and hence cell-cell variation can be assessed within a given population. (2) If there is limited amount of sample (as with the clinical specimen), this is the method of choice, as biochemical methods require large quantities of the proteins. (3) If there are variations within a subcellular compartment (for example within the cytoplasm), then the microscopy-based methods will allow the determination of distribution in these subcellular regions. However, the disadvantage may be that the cells are of different size and shape and in some cells (such as T-cells) there may be very little cytoplasm present. One can overcome these disadvantages by imaging and quantitating a large number of cells, as well as by noting different patterns of distribution within the cells. Quantifying 50–100 cells per given sample provides sufficient information, where the mean of the values across the drawn line can be plotted as a function of distance from a fixed point in the image. For example, the starting point could be plasma membrane or the nuclear periphery and the distribution of the protein going inwards/outwards from this point for about 50 pixels can be plotted. This method is best when used in conjunction with other biochemical methods to establish the distribution of the proteins within the cells.

Here we provide an example to illustrate the quantitation of Gag within the producer cells under conditions that affect its trafficking to the membrane. It is well established that MA protein is responsible for targeting Gag polyprotein to the plasma membrane [5]. Accumulating evidence suggest that in addition to MA, cellular proteins influence the trafficking of Gag protein to the membrane. We have demonstrated that the expression of a dominant negative mutant derived from a cellular protein inhibits trafficking of Gag to the plasma membrane [8]. INI1 (integrase-interacting protein 1) is an IN-binding cellular protein. The expression of a INI1 fragment harboring a minimal IN-binding domain [termed S6(Rpt1)] has been shown to inhibit particle production in part by affecting the trafficking of Gag/Gag-Pol to the plasma membrane [8, 9]. Furthermore, it has been demonstrated that sub-cellular localization of S6 affects the distribution of Gag [8]. While S6(Rpt1) is diffusely distributed both in nucleus and cytoplasmic, NLS-S6(Rpt1) is exclusively localized in the nucleus. While the presence of S6(Rpt1) in the cytoplasm inhibits HIV-1 particle production and Gag trafficking, relocation of S6(Rpt1) into the nucleus by fusing it to a strong NLS prevents its inhibitory effect on Gag/Gag-Pol trafficking and particle production. Examples of Gag distribution pattern in cells expressing CFP-S6(Rpt1) that inhibits Gag trafficking or CFP-NLS-S6(Rpt1) that does not inhibit trafficking, are provided in Fig. 1. This figure illustrates the difference in distribution patterns of Gag/Gag-Pol expressed from HIV-1_{NL4-3}, when detected by immunofluorescence using α-p24 antibodies (Fig. 1). Analysis of pixel intensities of the immunofluorescence signal across the cytoplasm from large number of cells, and plotting the results as a function of distance in pixels, indicates the distribution pattern of Gag/Gag-Pol within these cells (Fig. 1). While cells expressing HIV-1_{NL4-3} and CFP-NLS-S6(Rpt1) show a clear peak of accumulation of Gag/Gag-Pol at the plasma membrane (Fig. 1a), cells expressing CFP-S6 show a diffuse pattern of Gag/Gag-Pol distribution without a peak of accumulation at the membrane (Fig. 1a). Plotting mean gray intensities of p24 staining in multiple cells, graphed as a function of distance in pixels, illustrates the difference in Gag/Gag-Pol accumulation in two different cells (Fig. 1b). These results suggest that the presence of cytoplasmic CFP-S6(Rpt1) affects Gag membrane targeting. However, nuclear CFP-NLS-S6(Rpt1) allows Gag trafficking and accumulation of Gag/Gag-Pol at the membrane.

2 Materials

2.1 General Laboratory Equipment

1. Humidified CO_2 tissue culture incubator.
2. BSL-2 tissue culture facility.

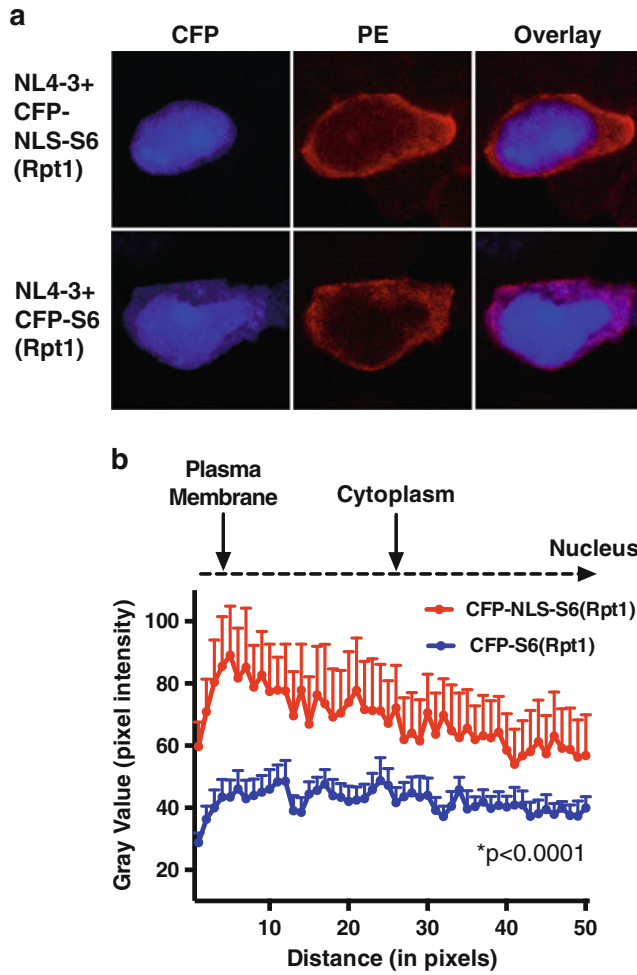

Fig. 1 Quantification of subcellular distribution of Gag/Gag-Pol in cells expressing variants (with or without NLS) of S6. (**a**) Confocal images illustrating subcellular distribution of Gag/Gag-Pol in cells expressing CFP fusions of S6(Rpt1) or NLS-S6(Rpt1) along with HIV-1_{NL4-3}. Confocal images (63× with 6× zoom) of cells were captured as described. The images illustrate the representative z-section of the cells. *Left most column*, CFP fluorescence indicating expression of CFP-fusion proteins; *middle column*, PE fluorescence indicating expression of p24; *right column*, the merge of the two. Plasmids pECFP-S6(Rpt1), pECFP-NLS-S6(Rpt1), and pNL4-3 were transfected into 293T cells in 4-chambered wells. Transfected cells were subjected to immunoflourescence analysis using α-p24 antibodies and secondary antibodies conjugated to PE, as described. (**b**) Graphic representation of differential distribution of Gag/Gag-Pol in the cells expressing CFP-S6(Rpt1) or CFP-NLSS6(Rpt1). Cells transfected either with CFP-S6(Rpt1) or CFP-NLS-S6(Rpt1) along with pNL4-3, were subjected to quantification using ImageJ as described. Mean pixel intensities, or gray value of the pixels representing intensities of p24 staining from the plasma membrane towards the nucleus across the cytoplasm, were plotted as a function of distance in pixels. The graph represents the mean of measurements taken from eight different transfected cells each (+/− SEM). The statistical difference in the distribution pattern was determined by performing two-way ANOVA to obtain the *p* value using Graphpad Prism.

2.2 Cell Culture Media

1. Cell culture medium: DMEM high glucose supplemented with 10 % heat-inactivated FBS, 100 U/ml penicillin-streptomycin and 2 mM l-glutamine.
2. Wash buffer: DPBS (1×).

2.3 Tissue Culture Plasticware and Materials

1. 4-chambered culture slides.
2. Serological pipettes (1 ml, 10 ml).
3. Syringe filter 0.2 μm.
4. 10 ml syringe.

2.4 Immunofluorescence Materials

1. Cover slips.
2. Nail polish—instant-dry type.

2.5 Immunofluorescence Buffers and Fixing Reagents

1. Fixing solution (Eddy fix): 3.65 % formaldehyde, 0.1 % glutaraldehyde, and 0.15 mg of saponin.
2. Permeabilization (Triton) solution: 0.5 % Triton ×100 in DPBS.
3. Blocking solution: 2.5 % BSA in DPBS.
4. Primary antibody: 1:500 dilution of goat α-p24 antibody, 1.5 % BSA in DPBS.
5. Secondary antibody: 1:133 dilution of bovine α-goat IgG-PE (phycoerythrin) and 1.5 % BSA in DPBS.
6. Mounting medium for fluorescence with DAPI.

2.6 Imaging Materials

1. Confocal microscope (Leica SP5) with the capacity of lasers at 405 and 543 nm wavelengths for detecting DAPI and PE fluorescence, respectively.
2. A computer with Leica Confocal Software Leica Microsystems LAS AF (Leica Application Suite, Advanced Fluorescence).
3. 95 % ethanol.
4. Immersion oil.

2.7 Image Analysis Software for Quantification

1. ImageJsoftware (http://rsb.info.nih.gov/ij/download.html).

2.8 Reagent Preparation

2.8.1 Preparation of Fixing Solution

1. Prepare 50 mg/ml stock solution of saponin by adding 50 mg of saponin to 1 ml of water in a 15 ml conical tube. Gently rotate the tube for 30 min at room temperature. Do not vortex. Vortexing may result in foaming. Discard the solution after one time use.
2. Prepare an 8 % glutaraldehyde working solution from a stock. This working solution can be kept at 4 °C for several months.

3. To prepare the fixing solution take 8.845 ml of DPBS in a 15 ml conical tube, add 125 μl of 8 % glutaraldehyde, 1 ml of 36.5 % formaldehyde, and 30 μl of 50 mg/ml saponin. The fixing solution should be made fresh.

2.8.2 Preparation of Blocking Solution

1. Make enough blocking buffer. You need 200 μl of blocking buffer/chamber well.
2. The blocking buffer (2.5 % BSA in DPBS) should be passed through 0.2 μm syringe filter using a 10 ml syringe.

2.8.3 Preparation of Primary and Secondary Antibody Solutions

1. Make enough antibody solution. You need 200 μl/chamber well.
2. Prepare 1.5 % BSA in DPBS, and mix until fully dissolved.
3. Pass solution through 0.2 μm syringe filter using a 10 ml syringe.
4. Dilute goat α-p24 antibody to 1:500 in the above BSA solution to prepare primary antibody solution.
5. Dilute bovine α-goat antibody conjugated to PE to 1:133 in the above BSA solution to make secondary antibody solution.

3 Methods

3.1 Transfection of 293T Cells

1. Plate 293T cells in a 4-chamber well culture slide the day before transfection at 15–20 % confluency to achieve 35–40 % confluency the next day, at the time of transfection (*see* **Note 2**).
2. Transfect the cells with HIV-1 DNA such as pNL4-3 or other viral DNAs encoding *gag* (*see* **Note 3**).
3. Incubate the cells at 37 °C for 24 h post media switch.
4. Proceed with staining protocol.

3.2 Immunofluorescence Staining of Cells Expressing HIV-1 Gag Protein (See Note 4)

1. Wash the cells using 200 μl DPBS/chamber well for 5 min at room temperature. Aspirate after each subsequent step.
2. Fix the cells for 15 min using 200 μl Eddy fix/chamber well for 15 min at room temperature in the dark. Keep chamber well culture slides in the dark from here on. For this purpose, you can work in the hood with very little light. Or when working on the bench, you can use a box covered with alluminium foil to covert the slide.
3. Wash the cells using 200 μl DPBS/chamber well for 5 min at room temperature.
4. Permeabilize the cells by adding 200 μl Triton solution/chamber well for 10 min at room temperature.
5. Wash the cells twice using 200 μl DPBS/chamber well for 5 min at room temperature.
6. Block samples using 200 μl blocking solution/chamber well for 1 h at 37 °C.

7. Wash the cells using 200 μl DPBS/chamber well for 5 min at room temperature.
8. Incubate samples with 200 μl of the primary antibody solution/chamber well for 3 h at 37 °C. For the no-primary antibody control, incubate samples with DPBS + 1.5 % BSA solution.
9. Wash cells three times using 200 μl DPBS/chamber well for 5 min at room temperature.
10. Incubate samples with 200 μl of the secondary antibody solution/chamber well for 1 h at 37 °C.
11. Wash the cells three times using 200 μl DPBS/chamber well each for 5 min at room temperature.
12. Detach the chambers from the slides using the tool provided with the chamber well slide packet.
13. Aspirate the remaining liquid at the edges.
14. Add one drop of mounting media with DAPI solution/chamber.
15. Mount cover slip and let settle for 20 min or overnight at room temperature (or at 4 °C) in the dark.
16. Adhere cover slip to slide using nail polish, gently applying around all sides of the cover slip.
17. Store slides at 4 °C in the dark.

3.3 Imaging of HIV-1 Gag Protein

1. Turn on the computer attached to microscope.
2. In the following order, turn on the scanner power, the laser power, and the external light source for the Leica SP5 microscope. For easy visualization by eye, increase the intensity of the external light source to the second highest intensity setting (indicated by second largest circle along dial).
3. Log in and open Leica Microsystems LAS AF software. Do not initialize the DM1600 stage (when prompted).
4. Acquisition mode should be set to xyz.
5. Change objective to 63× oil objective.
6. Check “Pinhole” and select “Airy1” as your unit.
7. Turn on the 405 laser for DAPI staining and the 543 laser for the α-p24-PE staining by entering the “configuration” panel, selecting “laser” and checking the boxes next to the lasers shown.
8. Clean the slide gently using 95 % ethanol and add a drop of immersion oil directly onto 63× objective.
9. Place clean slide with the cover slip facing down onto the 63× objective.
10. Open the shutter on the microscope, press the blue button (to visualize your DAPI or CFP), and adjust the focus until DAPI-stained nuclei become clearly visible.

11. Turn on the "live" button in the software to visualize DAPI-stained nuclei on the screen.
12. To select your lasers using the software follow these instructions. In the "Acquire" mode, select the "acquisition" panel. Set up lasers for your experiment by selecting "sequ" (the sequential scan settings). To set up the DAPI channel, double click PM1, enter your spectral range from 380 to 478, adjust the 405 laser intensity to 15 %, pick blue from the color scheme, check the "active" box by clicking, and save the laser setting as "DAPI." To set up the PE channel, click the "+" button, double-click PM3 as your PE setting, enter your spectral range from 553 to 623, adjust the 543 laser intensity to 25 %, pick Red from the color scheme (or preferred color), check the "UV," "visible" options, as well as the "active" box, and save the laser setting as "PE." You can select CFP channel instead of DAPI if you are visualizing the CFP fusion protein.
13. To adjust the gain and offset settings for image acquisition follow these instructions. Click the "quick LUT (Look Up Table)" button on the top left of the scanning screen to turn on the heatmap mode. This mode uses a heat map to show staining intensity levels. Increase the gain to just below oversaturated levels. Oversaturation is indicated by blue color, so increase the gain until the blue color becomes visible and then reduce the gain just enough for the blue color to disappear. Increase the offset until a speckled appearance of green color is visible. These settings should be ideal for visualization and quantification of the different ranges of Gag protein staining, since they allow for maximum signal intensity but are still quantifiable.
14. To reduce background signal, set the line average to four. This allows four images to be taken and pixels in these images are counted only if they appear in all four images. This reduces non-specific signal.
15. Select a field of image in which the p24-Gag staining is present within transfected cells and increase the zoom by 6.5×.
16. If using single cell images for quantitation, focus to the middle of the cell and capture the image.
17. If are taking z-stacks for quantitation, click open the "z-stack" window and focus to the top of the desired cell and set it as z-stack starting point (*see* **Note 5**). Then focus to the bottom of the cell and set it as z-stack endpoint. Determine the number and thickness of stacks you would like to image and click "Start" to obtain the stack.
18. Save the raw "*.lif*" files by clicking "save all" button and designate the storage location.

19. Export all images by right-clicking the folders and saving them as *.tiff* files. Click the "export LUT" box to save the images in color. Overlays can be saved separately by clicking the "overlay channels" box.
20. Shut off the microscope.

3.4 Quantitation of HIV-1 Gag Protein

1. Open ImageJ software on your computer.
2. Drop selected .tiff files of the images/stack into the opened software window. Images will open automatically.
3. In the "Analyze" panel select "select scale" and change scale to 1 pixel/unit by typing "pixel" into the "unit of length" description box.
4. Draw a line on one of the cell images, then select "edit," "options," and "line width" and change the line width to 8 pixels. This is the thickness of the line used. You can chose to select thicker lines.
5. Then draw a line from the plasma membrane towards the nucleus, fixing the length of the line to desired pixel length (for example, 50 pixels).
6. After each line drawn, select "Analyze," and then "Plot Profile" to obtain the gray value. The gray value indicates the pixel intensity of the staining across the line drawn.
7. A new window will pop up labeled "Plot of Image x." This window will display the histoplot of the pixel intensity detected as a function of distance from the beginning to the end of the line. The histoplot represents the distribution of Gag from plasma membrane towards the nucleus along the line.
8. To obtain the individual gray values/pixel intensity of the line drawn, click "list." The list provides individual gray values depending on pixel location along the line. These values indicate the intensity of Gag staining from the plasma membrane towards the nucleus within the cytoplasm.
9. Since cell shapes are variable, collect plot profiles from as many cells as required for analysis to determine the localization of Gag staining intensity.
10. Here we have provided a representative analysis using a line width of 8 pixels. This can be increased depending on the cell type or the requirement for the experiment.

4 Notes

1. The gray value indicates the brightness of a pixel and is an arbitrary unit. This method is not intended to obtain absolute quantification of Gag proteins and therefore is best used in comparative settings, such as when assessing Gag distribution

within the cytoplasm in the presence and absence of inhibitors or with and without a dominant-negative mutant.

2. The method described here can be used to analyze the Gag distribution in infected or transfected cells.
3. Transfection of cells with HIV molecular clones and maintenance of HIV-producer cells should be done within a BSL2+ facility.
4. Here we have used HIV Gag as an example to quantify the proteins within the cells, but the localization of other proteins can be quantified using this method.
5. Depending on the type of analysis desired, either single images or z-stacks can be analyzed. The type of data generated from a z-stack vs. a single image will likely be correlative in this type of analysis. In order to reduce bias of lines drawn by the user, a commonality of the line drawing itself, such as only using horizontal or vertical lines can be implemented. However, since cell shape varies and this might not always be possible, bias can also be reduced by using more than one line drawn from the nucleus to the plasma membrane from various starting points on the plasma membrane within a single cell and averaging the values.

Acknowledgements

This work was supported by NIH R01 GM112520 (to G.V.K.) and in part by Center for AIDS Research (CFAR) at the Albert Einstein College of Medicine funded by the NIH AI-051519. A.L. Was supported by the NIH funded Institutional AIDS training grant, T32-AI007501. We thank Dr. Jennifer Cano for initially optimizing the technique and Rosiris Leon for help with the experiment that generated the figure included in this chapter.

References

1. Sundquist WI, Krausslich HG (2012) HIV-1 assembly, budding, and maturation. Cold Spring Harb Perspect Med 2(7):a006924
2. Balasubramaniam M, Freed EO (2011) New insights into HIV assembly and trafficking. Physiology (Bethesda) 26(4):236–251
3. Martin-Serrano J, Neil SJ (2011) Host factors involved in retroviral budding and release. Nat Rev Microbiol 9(7):519–531
4. Klein KC, Reed JC, Lingappa JR (2007) Intracellular destinies: degradation, targeting, assembly, and endocytosis of HIV Gag. AIDS Rev 9(3):150–161
5. Ono A (2009) HIV-1 assembly at the plasma membrane: Gag trafficking and localization. Future Virol 4(3):241–257
6. Ono A, Ablan SD, Lockett SJ, Nagashima K, Freed EO (2004) Phosphatidylinositol (4,5) bisphosphate regulates HIV-1 Gag targeting to the plasma membrane. Proc Natl Acad Sci U S A 101(41):14889–14894
7. Waheed AA, Ono A, Freed EO (2009) Methods for the study of HIV-1 assembly. Methods Mol Biol 485:163–184
8. Cano J, Kalpana GV (2011) Inhibition of early stages of HIV-1 assembly by INI1/hSNF5 transdominant negative mutant S6. J Virol 85(5):2254–2265
9. Kalpana GV, Marmon S, Wang W, Crabtree GR, Goff SP (1994) Binding and stimulation of HIV-1 integrase by a human homolog of yeast transcription factor SNF5 [see comments]. Science 266(5193):2002–2006

Chapter 12

Methods to Study Determinants for Membrane Targeting of HIV-1 Gag In Vitro

Gabrielle C. Todd and Akira Ono

Abstract

Assembly of HIV-1 viral particles is a critical step of the HIV-1 life cycle; yet many details of this complex process are unknown. The Gag polyprotein drives viral particle assembly at the plasma membrane via three different types of interactions: protein-protein, protein-RNA, and protein-membrane interactions. As an approach to tease apart the importance of these interactions during viral particle assembly, in particular at the step of Gag membrane binding, we have developed an in vitro liposome-binding assay. Below we describe how to prepare liposomes, which serve as model membranes, and how to assess their interaction with Gag by liposome flotation centrifugation. Additionally, we outline extensions of this basic assay that can be used to address the role of RNA in regulating Gag-membrane interactions.

Key words HIV-1 assembly, Gag, RNA, Membrane binding, Liposome flotation centrifugation

1 Introduction

Assembly of HIV-1 particles is choreographed by the Gag polyprotein, which uses each of its four major domains to carry out different roles in the assembly process [1, 2]. The matrix domain (MA) recruits Gag to the plasma membrane (PM), the capsid domain (CA) is involved in Gag multimerization, the nucleocapsid domain (NC) packages a dimer of genomic RNA, and the p6 domain recruits cellular factors to pinch off completed particles from the cell surface.

Of particular interest is the initial targeting of Gag to the PM, which is directed by MA [1–4]. MA has an N-terminal myristoyl group that is sequestered in a hydrophobic binding pocket in MA and exposed upon Gag-membrane binding [5]. A second important feature of MA is a concentrated region of basic amino acids between residues 17 and 31 known as the highly basic region (HBR). These residues enable Gag to specifically recognize the phospholipid, phosphatidylinositol (4,5) bisphosphate, or PI(4,5)P_2 [6–9]. PI(4,5)P_2 is enriched in the inner leaflet of the PM; thus specific recognition of this lipid by Gag promotes productive viral

Vinayaka R. Prasad and Ganjam V. Kalpana (eds.), *HIV Protocols*, Methods in Molecular Biology, vol. 1354,
DOI 10.1007/978-1-4939-3046-3_12,

particle assembly at the PM rather than unproductive assembly on other intracellular membranes [10].

MA also binds to RNA [11–13], presumably via the HBR [11, 13], and the presence of RNA inhibits interactions between Gag and membranes lacking PI(4,5)P_2 [8, 14–16]. Thus RNA-MA interactions appear to provide an additional layer of regulation for Gag-membrane association. To study the interplay among Gag, RNA, and membranes we have developed an in vitro liposome flotation assay to monitor relative membrane binding of Gag under various conditions [7, 8, 16, 17].

2 Materials

2.1 Liposome Preparation

1. Lipids from Avanti Polar Lipids, Inc.
   (a) POPC—[1-palmitoyl-2-oleoyl-*sn*-glycero-3-phosphocholine].
   MW 760.076 g/mol, can be stored for 6 months at −20 °C.
   (b) POPS—[1-palmitoyl-2-oleoyl-*sn*-glycero-3-phospho-L-serine (sodium salt)].
   MW 783.988 g/mol, can be stored for 6 months at −20 °C.
   (c) Brain PI(4,5)P_2—[L-α-phosphatidylinositol-4,5-bisphosphate (Brain, Porcine) (ammonium salt)].
   $MW_{(ave)}$ 1096.385 g/mol, can be stored for 3 months at −20 °C.
2. 250 μl Hamilton syringe.
3. Glass vials (0.5–1 ml).
4. Chloroform, methanol, water for rinsing Hamilton syringes.
5. N_2(g) tank or house nitrogen.
6. Vacuum source.
7. 20 mM Hepes pH 7.0.
8. Dry ice and acetone bath.
9. Mini Extruder, Avanti Polar Lipids, Inc.
10. Membranes, Avanti Polar Lipids, Inc., of the desired pore size (100 nm).
11. Filter Supports, Avanti Polar Lipids, Inc.
12. Forceps.
13. Sonicating water bath.

2.2 TNT Rabbit Reticulocyte Lysate

1. Plasmid containing the *gag* gene downstream of either a T7, T3, or SP6 phage transcription promoter. In our experiments, a fragment from the pNL4-3 strain of HIV-1 from nucleotides 639–5748 (*gag* is 790–2292) is oriented downstream of an SP6 promoter in a pGEM vector backbone.

2. Promega TnT® Coupled Reticulocyte Lysate Systems (we use the kit with SP6 RNA polymerase, L4600, but other variations are also available).
3. *Optional*: Homemade 1 mM amino acid mix (-Met) in 10 mM Hepes pH 7.0.
4. RNasin (Promega).
5. EXPRE^{35}S^{35}S Protein Labeling Mix (Perkin Elmer).
6. RNase A (Thermo Fisher).
7. 10× Rabbit reticulocyte lysate (RRL) buffer [18]: 200 mM Hepes-KOH pH 7.0, 1 M KCl, 5 mM $MgCl_2$.
8. Yeast total tRNA (Ambion).

2.3 Liposome Flotation

1. Prepare solutions of 85.5, 65, and 10 % (w/v) sucrose in 20 mM Hepes pH 7.0.
2. Centrifuge tubes (Beckman Coulter).
3. Rotor AH-650, or equivalent *swinging bucket rotor*.
4. Ultracentrifuge.

2.4 SDS-PAGE

1. 4× Resolving gel buffer: 1.5 M Tris–HCl pH 8.8, 0.4 % sodium dodecyl sulfate (SDS).
2. 4× Stacking gel buffer: 500 mM Tris–HCl pH 6.8, 0.4 % SDS.
3. 3× SDS loading buffer: 188 mM Tris–HCl pH 6.8, 30 % (v/v) glycerol, 15.2 % (v/v) β-mercaptoethanol, 9.4 % (w/v) SDS, 0.02 % (w/v) bromophenol blue.
4. 10× Running buffer: 248 mM Tris base, 1.92 M glycine, 35 mM SDS.
5. Gels (29:1 acrylamide:bis-acrylamide): 10 % resolving, 4 % stacking.
6. Rotator platform.
7. Fixing solution: 40 % methanol, 10 % acetic acid.
8. Soaking solution: 1 M salicylic acid, 2 % (v/v) glycerol.
9. Whatmann paper (3 mm).
10. Slab gel dryer.
11. Phosphor storage screen.
12. ImageQuant software.

3 Methods

3.1 Preparing Liposomes

To study Gag-membrane interactions, we prepare liposomes that have a 20 mM final lipid concentration with a 2:1 ratio of POPC:POPS. When $PI(4,5)P_2$ is incorporated, it typically

Table 1
Required lipid quantities for liposome preparation

Lipid	Stock concentration (μg/μl)	2:1 POPC:POPS (μl)	2:1 POPC:POPS + 7.25 % $PI(4,5)P_2$ (μl)
POPC	10	152	141
POPS	10	78	73
$PI(4,5)P_2$	1	–	239

Quantities of each lipid needed for 20 mM final total lipid concentration in 150 μl of liposomes

comprises 7.25 mol %; the remaining mol % of lipid is divided in a 2:1 ratio of POPC:POPS [4, 8, 16]. We generally prepare 150 μl of each liposome solution using the volumes listed in Table 1 below for ease of extrusion. Detailed instructions and theory about liposome preparation can also be found on the website of Avanti Polar Lipid, Inc. (http://avantilipids.com/).

There are two types of liposomes that can be used to study Gag-membrane interactions. Unilamellar liposomes prepared by extrusion are composed of a single bilayer while multilamellar liposomes prepared by sonication consist of several concentric bilayers similar to the layers of an onion. The advantages of unilamellar liposomes are that they have well-defined diameters of varying sizes depending on the pore size of the membrane used during extrusion, and the amount of liposome surface available for protein binding is consistent between each liposome preparation. Multilamellar liposomes, however, are advantageous in that they are less dense than unilamellar liposomes and therefore flotation levels are somewhat higher. Thus different types of liposomes can be used depending on the desired application.

1. Before and after measuring out each type of lipid, rinse the Hamilton syringe five times using the same solvent in which the lipid is dissolved. Removing trace amounts of lipid with a good solvent is critical to prevent clogging of the syringe with precipitated lipid (*see* **Note 1**).
   (a) For POPC and POPS, rinse the syringe with chloroform.
   (b) For $PI(4,5)P_2$, rinse the syringe with a chloroform/methanol/water mixture (20:9:1).
2. Combine the desired amount of each lipid (Table 1) into a small glass vial. Vortex gently to mix the lipids.
3. Remove the solvent with a gentle stream of $N_2(g)$ until the lipids form a milky film on the sides of the glass vial (*see* **Note 2**).

4. Once all of the bulk solvent is removed, place the uncapped vials under vacuum for 4 h or overnight to remove any trace amount of solvent.

3.1.1 Unilamellar Liposomes: Extrusion

1. Resuspend the lipid film in 150 µl of 20 mM Hepes pH 7.0 and vortex for 1 min. The solution should be cloudy (*see* **Note 3**).
2. Let the liposome suspension stand for 1 h at room temperature (RT) to hydrate.
3. Disrupt the nonuniform, multilamellar liposomes by ten cycles of freeze-thaw between an acetone-dry ice bath and a water bath set above the transition temperature (for rapid thawing we use a water bath set to 50 °C).
4. Assemble the extruder according to the instructions on the website of Avanti Polar Lipids, Inc. Briefly:
   (a) In the retainer nut (side B), place the Teflon bearing followed by the internal membrane support, O-ring side up.
   (b) Inside of the O-ring, place a filter support.
   (c) Place a polycarbonate membrane with the desired pore size over the filter support such that it covers the internal membrane support O-ring completely. We use membranes with a pore size of 100 nm for our experiments.
   (d) Place a second filter support in the center of the polycarbonate membrane (*see* **Note 4**).
   (e) Place the second internal membrane support on top of the stack, O-ring side down.
   (f) Slide the extruder outer casing (side A) over the top internal membrane support and screw it into the retainer nut. Tighten by hand, making sure that the apexes of the outer casing and retainer nut line up.
5. Rinse the extruder syringes three times with water and three times with 20 mM Hepes pH 7.0.
6. To reduce the dead volume in the extruder, pass one to three syringe volumes worth of 20 mM Hepes pH 7.0 through the extruder and discard.
7. Take up the liposome solution into syringe A and insert it into side A of the extruder set up. Remove any excess buffer that is pushed out of side B with a Kim wipe.
8. Insert an empty syringe B into side B of the extruder setup.
9. Place the assembly in the holder (*see* **Note 5**).
10. Gently push the liposome solution from syringe A to syringe B and back again, repeating 10–60 times.
11. Push the liposome solution into syringe B and remove the assembly from the holder. Holding the assembly vertically with

syringe B on the bottom, remove syringe A, and pull down on the plunger in syringe B to remove all of the liposome solution from the chamber. Transfer the extruded liposome solution from syringe B into an Eppendorf tube and store at RT (or above the transition temperature) until use (*see* **Note 6**).

12. Clean the extruder syringes three times with 20 mM Hepes pH 7.0, three times with water, and once with 100 % ethanol (*see* **Note 7**).
13. Disassemble the extruder and discard the membrane and filter supports. Rinse all of the components with milli-Q water.

3.1.2 Multilamellar Liposomes: Sonication

1. Resuspend the lipid film in 150 μl (or adjusted volume) of 20 mM Hepes pH 7.0 and vortex for 1 min to mix. The solution should be cloudy.
2. Let the liposome suspension stand for 1 h at room temperature (RT) to hydrate.
3. Transfer the liposomes to a plastic Eppendorf tube and sonicate the liposomes for 30 min.
4. Shake the liposome solution overnight at 4 °C.

3.2 In Vitro Transcription/ Translation of Gag Polyprotein

Preparation of recombinant full-length, myristoylated Gag using bacterial expression systems is often challenging due to poor solubility and proteolytic degradation. Therefore, to obtain full-length myristoylated Gag, we generate it by in vitro transcription/translation (TNT) in either rabbit reticulocyte lysates or wheat germ extracts, both of which can be purchased as kits from Promega. Below, we give a brief description of a typical experiment using rabbit reticulocyte lysate which can be altered as desired to use wheat germ extract [19], purified full-length Gag [20], purified Gag domains [5], or cell-derived Gag [16] (*see* **Note 8**).

3.2.1 Rabbit Reticulocyte Lysate Transcription/ Translation Reaction

1. Combine the components listed in Table 2, adding the DNA template last.
2. Incubate the reaction for 90 min at 30 °C for optimal synthesis of Gag protein.
3. Follow the steps for the liposome flotation assay (see below).

3.2.2 Monitoring the Gag-Membrane Interactions in the Absence of RNA

1. Prepare a master mix of the TNT reaction with enough for two 25 μl reactions.
2. Incubate the master mix pool for 90 min at 30 °C for optimal synthesis of Gag protein.
3. Dilute RNase A (10 μg/μl) 1:10 in 20 mM Hepes pH 7.0.
4. For a negative control, remove 25 μl of the Gag TNT reaction from the pool and add 1.5 μl of 20 mM Hepes pH 7.0.

Table 2
Recipe for rabbit reticulocyte lysate transcription/translation assay

Component	Volume (μl)
Milli-Q H_2O	8
25× TNT reaction buffer	1
TNT rabbit reticulocyte lysate	12.5
RNasin	0.5
SP6 RNA polymerase	0.5
1 mM amino acid mixture (-Met)*	0.5
^{35}S Met/Cys (10 μCi/μl)	1
DNA template (1 μg/μl)	1
	25

*Composition of a standard TNT reaction (*see* **Note 9**)

5. For the RNase-treated condition, remove 25 μl of the Gag TNT reaction from the pool and add 1.5 μl of the diluted RNase A (1.5 μg RNase A per reaction).
6. Incubate the negative control and RNase-treated reaction at 37 °C for 20 min.
7. Follow the steps for the liposome flotation assay (see below).

3.2.3 Testing the Effect of Specific RNAs on Gag-Membrane Interactions: RNA Add-Back Assay

1. Prepare a master mix of the TNT reaction with enough for three 25 μl reactions.
2. Incubate the master mix pool for 90 min at 30 °C for optimal synthesis of Gag protein.
3. Dilute RNase A (10 μg/μl) 1:10 in 20 mM Hepes pH 7.0.
4. For a negative control, remove 25 μl of the Gag TNT reaction from the pool and add 1.5 μl of 20 mM Hepes pH 7.0.
5. For the rest of the pool, add the diluted RNase A (1.5 μl per reaction).
6. Incubate the negative control and RNase-treated reaction at 37 °C for 20 min.
7. Inactivate the RNase A by addition of RNasin, 8 μl to the negative control reaction and 8 μl per reaction to the RNase A-treated pool. Incubate for 10 min at 37 °C.
8. Add 8 μl of 1× RRL buffer to the negative control reaction.
9. Remove 34.5 μl from the RNase A-treated pool as the RNase control and add 8 μl of 1× RRL buffer.

10. Remove 34.5 μl from the RNase A-treated pool and add 8 μl of RNA, refolded in RRL buffer (*see* the Refolding RNA section).
11. Incubate negative control, RNase control, and RNA add-back reaction(s) at 37 °C for 30 min.
12. Follow the steps for the liposome flotation assay (see below) adding 7.5 μl of liposomes (the final reaction volume should be 50 μl).

3.2.4 Refolding RNA

To test the impact of various RNAs on Gag-membrane interactions, RNAs can be chemically synthesized or prepared by in vitro transcription and purified using standard techniques [21]. Prior to adding these RNAs to our Gag protein, they should be refolded. If refolding conditions for a particular RNA species are known, they can be used. If no specific conditions have been established, we recommend refolding in a buffer similar to that of the rabbit reticulocyte lysate. Although the exact composition of Promega's rabbit reticulocyte reaction buffer is proprietary information, the literature from which Promega's protocol is derived is known [18]. Thus we refold under these buffer conditions.

Yeast total tRNA can be used as a positive control. At 1 μg/μl final concentration in our 50 μl add-back reaction, yeast tRNA can completely inhibit Gag binding to PC + PS liposomes, but has no impact on Gag binding to PC + PS + $PI(4,5)P_2$ liposomes. At 100 ng/μl yeast tRNA, Gag binding to PC + PS liposome is inhibited by ~50 % relative to the RNase-treated condition. Thus the desired final concentration of your RNA of interest may need to be titrated to optimally discern its impact on Gag-membrane binding.

1. To maintain a 50 μl final reaction volume, 8 μl of RNA stock can be added.
2. For refolding, mix the desired amount of RNA with water to a final volume of 7.2 μl.
3. Heat the RNA for 1 min at 95 °C to denature and snap cool on ice.
4. Add 0.8 μl of 10× RRL buffer, mix well, and incubate at 37 °C for 15 min (*see* **Note 10**).
5. Keep the refolded RNA on ice until use.

3.2.5 Liposome Flotation Assay

1. Following Gag synthesis (and possible RNase treatment and/or RNA add-back), add 7.5 μl of liposomes and incubate at 37 °C for 15 min (*see* **Note 11**).
2. Bring the final reaction volume up to 200 μl with 20 mM Hepes pH 7.0.
3. In a 5 ml ultracentrifuge tube add 1 ml of 85.5 % sucrose.

4. Add the 200 µl reaction to the 85.5 % sucrose solution and vortex *gently* for 5 s.
5. Carefully layer on 2.8 ml of the 65 % sucrose solution.
6. Carefully layer on 1 ml of the 10 % sucrose solution.
7. Balance pairs of tubes with additional 10 % sucrose solution if necessary.
8. Centrifuge for 16 h at 35,000 rpm (100,000 × *g*) at 4 °C.
9. Collect five 1 ml fractions from the top of the gradient by pipetting.
10. Vortex each fraction thoroughly. Then mix 100 µl of each fraction with 50 µl of 3× SDS loading buffer.
11. Boil samples for 5 min and resolve on a 10 % gel by standard SDS-PAGE techniques (*see* Subheading 2 for our buffer compositions).
12. Remove the stacking gel and incubate the resolving gel in fixing solution for 30–60 min on a rotating platform.
13. Rinse the gel twice briefly with water.
14. Incubate the gel in soaking solution for 30–60 min.
15. Dry the gel onto a piece of Whatman paper at 80 °C for 2 h.
16. Expose the gel to a Phosphor Storage screen overnight, scan, and quantify Gag bands (~55 kDa) using ImageQuant software. We consider the top two fractions of each gradient to contain all floated liposomes and therefore membrane-bound Gag. Unbound Gag will remain at the bottom of the gradient. The proportion of liposome-bound Gag can be quantified as the sum of Gag signal in fractions 1 and 2 over the total amount of Gag present in fractions 1–5. For representative data, please see previously published results [7, 8, 16, 17].

4 Notes

1. Avoid using plastic pipette tips or storage vessels when working with chloroform. Chloroform can dissolve some plastics leading to contamination of your liposomes with unknown quantities and types of hydrophobic compounds.
2. For solutions containing $PI(4,5)P_2$, the dried film may form large white chunks as the water component of the solvent from this lipid will be the slowest to evaporate. Once all of the water is removed by $N_2(g)$, resuspend the lipids in ~100 µl of chloroform with gentle vortexing and dry once more with $N_2(g)$. The lipids should now dry in a smooth film.
3. Care must be taken to ensure that liposomes are resuspended and extruded at temperatures above the gel-liquid crystal tem-

perature of the lipid with the highest transition temperature. The liposomes described in this chapter all have transition temperatures well below room temperature; thus we perform all subsequent extrusion steps at room temperature. More information about the transition temperatures of lipids can be found on the Avanti Polar Lipids, Inc. website.

4. If having difficulty placing the filter supports or membrane due to static electricity, place a droplet of water between each layer.
5. If the transition temperature of the lipid mixture is above room temperature, the extruder holder can be placed on a heat block set to the desired temperature so that extrusion can be carried out at elevated temperatures.
6. Liposomes can be extruded starting from either side of the assembly. However, it is critical that liposomes are removed from the apparatus in the syringe opposite the one from which they entered the extruder to ensure that all liposomes have passed through the membrane. Thus we find it easiest to label the sides A and B and always input from side A and extract from side B.
7. It is important that organic solvents other than alcohols are not used with the extruder syringes because organic solvents can dissolve the glue holding on the Teflon plunger tip.
8. These protocols involve radiolabeling of the Gag protein. Specific protocols for handling radioactive samples and for collecting radioactive waste vary among institutions. *Be sure to follow the standard procedures outlined by your institution.*
9. We used a homemade preparation of amino acids (-Met) because several lots of amino acids (-Met) prepared by Promega were mislabeled and actually contained Met, resulting in very low levels of ^{35}S Met incorporation.
10. Do not heat RNA in the presence of divalent ions! This will result in degradation of your RNA. Therefore it is important to add the stock buffer containing Mg^{2+} *after* the RNA has cooled.
11. The amount of liposomes needed to obtain good levels of flotation may need to be titrated for specific applications.

Acknowledgments

We would like to thank the past and present members of our laboratory for their contributions to development of the methods described here. The methods described here were developed in the studies supported by the National Institutes of Health grant R01 AI071727 (to A.O.).

References

1. Adamson CS, Freed EO (2007) Human immunodeficiency virus type 1 assembly, release, and maturation. Adv Pharmacol 55:347–387. doi:10.1016/S1054-3589(07)55010-6
2. Adamson CS, Jones IM (2004) The molecular basis of HIV capsid assembly--five years of progress. Rev Med Virol 14:107–121. doi:10.1002/rmv.418
3. Alfadhli A, Barklis E (2014) The roles of lipids and nucleic acids in HIV-1 assembly. Front Microbiol 5:253. doi:10.3389/fmicb.2014.00253
4. Chukkapalli V, Ono A (2011) Molecular determinants that regulate plasma membrane association of HIV-1 Gag. J Mol Biol 410:512–524. doi:10.1016/j.jmb.2011.04.015
5. Tang C, Loeliger E, Luncsford P, Kinde I, Beckett D, Summers MF (2004) Entropic switch regulates myristate exposure in the HIV-1 matrix protein. Proc Natl Acad Sci U S A 101:517–522. doi:10.1073/pnas.0305665101
6. Saad JS, Miller J, Tai J, Kim A, Ghanam RH, Summers MF (2006) Structural basis for targeting HIV-1 Gag proteins to the plasma membrane for virus assembly. Proc Natl Acad Sci U S A 103:11364–11369. doi:10.1073/pnas.0602818103
7. Chukkapalli V, Hogue IB, Boyko V, Hu WS, Ono A (2008) Interaction between the human immunodeficiency virus type 1 Gag matrix domain and phosphatidylinositol-(4,5)-bisphosphate is essential for efficient gag membrane binding. J Virol 82:2405–2417. doi:10.1128/JVI.01614-07
8. Chukkapalli V, Oh SJ, Ono A (2010) Opposing mechanisms involving RNA and lipids regulate HIV-1 Gag membrane binding through the highly basic region of the matrix domain. Proc Natl Acad Sci U S A 107:1600–1605. doi:10.1073/pnas.0908661107
9. Shkriabai N, Datta SA, Zhao Z, Hess S, Rein A, Kvaratskhelia M (2006) Interactions of HIV-1 Gag with assembly cofactors. Biochemistry 45:4077–4083. doi:10.1021/bi052308e
10. Ono A, Ablan SD, Lockett SJ, Nagashima K, Freed EO (2004) Phosphatidylinositol (4,5) bisphosphate regulates HIV-1 Gag targeting to the plasma membrane. Proc Natl Acad Sci U S A 101:14889–14894. doi:10.1073/pnas.0405596101
11. Purohit P, Dupont S, Stevenson M, Green MR (2001) Sequence-specific interaction between HIV-1 matrix protein and viral genomic RNA revealed by in vitro genetic selection. RNA 7:576–584
12. Lochrie MA, Waugh S, Pratt DG Jr, Clever J, Parslow TG, Polisky B (1997) In vitro selection of RNAs that bind to the human immunodeficiency virus type-1 gag polyprotein. Nucleic Acids Res 25:2902–2910
13. Ramalingam D, Duclair S, Datta SA, Ellington A, Rein A, Prasad VR (2011) RNA aptamers directed to human immunodeficiency virus type 1 Gag polyprotein bind to the matrix and nucleocapsid domains and inhibit virus production. J Virol 85:305–314. doi:10.1128/JVI.02626-09
14. Alfadhli A, McNett H, Tsagli S, Bachinger HP, Peyton DH, Barklis E (2011) HIV-1 matrix protein binding to RNA. J Mol Biol 410:653–666. doi:10.1016/j.jmb.2011.04.063
15. Alfadhli A, Still A, Barklis E (2009) Analysis of human immunodeficiency virus type 1 matrix binding to membranes and nucleic acids. J Virol 83:12196–12203. doi:10.1128/JVI.01197-09
16. Chukkapalli V, Inlora J, Todd GC, Ono A (2013) Evidence in support of RNA-mediated inhibition of phosphatidylserine-dependent HIV-1 Gag membrane binding in cells. J Virol 87:7155–7159. doi:10.1128/JVI.00075-13
17. Inlora J, Chukkapalli V, Derse D, Ono A (2011) Gag localization and virus-like particle release mediated by the matrix domain of human T-lymphotropic virus type 1 Gag are less dependent on phosphatidylinositol-(4,5)-bisphosphate than those mediated by the matrix domain of HIV-1 Gag. J Virol 85:3802–3810. doi:10.1128/JVI.02383-10
18. Jackson RJ, Hunt T (1983) Preparation and use of nuclease-treated rabbit reticulocyte lysates for the translation of eukaryotic messenger RNA. Methods Enzymol 96:50–74
19. Lingappa JR, Hill RL, Wong ML, Hegde RS (1997) A multistep, ATP-dependent pathway for assembly of human immunodeficiency virus capsids in a cell-free system. J Cell Biol 136:567–581
20. Carlson LA, Hurley JH (2012) In vitro reconstitution of the ordered assembly of the endosomal sorting complex required for transport at membrane-bound HIV-1 Gag clusters. Proc Natl Acad Sci U S A 109:16928–16933. doi:10.1073/pnas.1211759109
21. Beckert B, Masquida B (2011) Synthesis of RNA by in vitro transcription. Methods Mol Biol 703:29–41. doi:2

Part IV

Studying HIV-1 Replication and Pathogenesis in Animal Models

Chapter 13

Visualizing the Behavior of HIV-Infected T Cells In Vivo Using Multiphoton Intravital Microscopy

Radwa Sharaf, Thorsten R. Mempel, and Thomas T. Murooka

Abstract

The introduction of multiphoton microscopy has dramatically broadened the scope of intravital imaging studies and has allowed researchers to validate and refine basic mechanistic concepts in many areas of biology within the context of physiologically relevant tissue microenvironments. This has also led to new insights into the behavior of immune cells at steady state, and how their behaviors are altered during an immune response. At the same time, advances in the humanized mouse model have allowed for in vivo studies of strictly human pathogens, such as HIV-1. Here, we describe in detail an intravital microscopy approach to visualize the dynamic behavior of HIV-infected T cells within the lymph nodes of live, anesthetized humanized mice.

Key words Multiphoton intravital microscopy, In vivo imaging, Popliteal lymph node, Lymphocyte motility, HIV-1, Humanized mice, Fluorescent protein, Mean track velocity

1 Introduction

Multiphoton intravital microscopy (MP-IVM) is a powerful imaging modality that allows for the direct dynamic observation of biological processes in their physiological tissue environment at cellular and subcellular resolution. The physical principle of multiphoton excitation allows for deeper optical penetration into tissues, compared to conventional fluorescence techniques, as well as for prolonged, continuous observations due to minimized phototoxicity and photobleaching [1, 2]. The study of the migratory behavior and function of immune cells, especially in the context of a developing immune response, is particularly amenable to this technology [3, 4].

Current humanized mouse models of HIV infection closely recapitulate several key aspects of HIV-1 infection in humans, including high viral loads upon vaginal [5–7] and rectal transmission [8], $CD4^+$ T cell depletion in the peripheral blood and mucosal

Vinayaka R. Prasad and Ganjam V. Kalpana (eds.), *HIV Protocols*, Methods in Molecular Biology, vol. 1354,
DOI 10.1007/978-1-4939-3046-3_13,

tissues [5, 9], the generation of functional CTL responses [10], and viral latency [11]. Accordingly, the mouse models have been used to evaluate the efficacy of several preclinical vaccine and anti-retroviral strategies. Here, we describe a new in vivo imaging approach that utilizes fluorescent HIV reporter strains to visually track and characterize the dynamic behavior of infected cells in lymph nodes of humanized mice. The technique can be adapted to understand the cellular and molecular mechanisms that govern the efficient spread of HIV within lymphoid and non-lymphoid organs in real time.

2 Materials

2.1 Construction and Preparation of Fluorescent Reporter HIV

1. DNA plasmid containing a fluorescent protein-expressing, full-length HIV-1 proviral cDNA, such as the CCR5-using, NL4-3 IRES GFP reporter strain (HIV-GFP) [7] (*see* **Note 1**).
2. HEK 293T cell line (human embryonic kidney cells expressing SV40 T antigen).
3. MAGI-CCR5 cell line (NIH AIDS Reagent Program).
4. DMEM supplemented with 10 % FCS, 2 mM L-glutamine, 1 mM sodium pyruvate, and 10 mM HEPES.
5. Calcium phosphate transfection kit.
6. 150 mm tissue culture plates.
7. Ultracentrifuge with a swinging bucket rotor and buckets (e.g., sw32Ti).
8. Ultraclear ultracentrifuge tubes (e.g., 38.7 mL capacity tubes).
9. 20 % sucrose solution in phosphate-buffered saline.
10. 50 mL conical tube.

2.2 Human CD4+ T Cell Isolation and Expansion into Central Memory-Like T Cells (Tcm)

1. Spleen and lymph node cells harvested from humanized mice.
2. Immunomagnetic human $CD4^+$ T cell-positive selection kit.
3. Anti-human CD3ε/CD28 antibody-conjugated Dynabeads.
4. Human recombinant IL-2.
5. RPMI medium supplemented with 10 % FCS, 2 mM L-glutamine, 1 mM sodium pyruvate, and 10 mM HEPES.
6. CellTracker Orange (CMTMR; 5-(and-6-)-(((4-chloromethyl) benzoyl)amino) tetramethylrhodamine).
7. PBS supplemented with 1 % FCS.

2.3 In Vitro Infection of CD4+ Tcm with a Fluorescent Reporter HIV Strain

1. 96-well, flat-bottom culture plates.
2. Polybrene (hexadimethrine bromide).
3. 25 cm^2 tissue culture flask.

2.4 Surgical Anesthesia

1. Ketamine HCl solution, 100 mg/mL (e.g., Ketaset).
2. Xylazine HCl solution, 20 mg/mL (e.g. Rompun).
3. NaCl 0.9 % for injection.
4. Insulin syringe (19G).

2.5 Microsurgical Preparation of the Mouse Popliteal Lymph Node for Intravital Microscopy

1. Custom-built microscope stage (*see* Fig. 1b, *see* **Note 2**).
2. Small animal clipper (e.g., Pocket Pro pet trimmer).
3. Depilation crème (e.g., Nair).
4. Cotton tip applicators.
5. 2×2 in. gauze sponges.

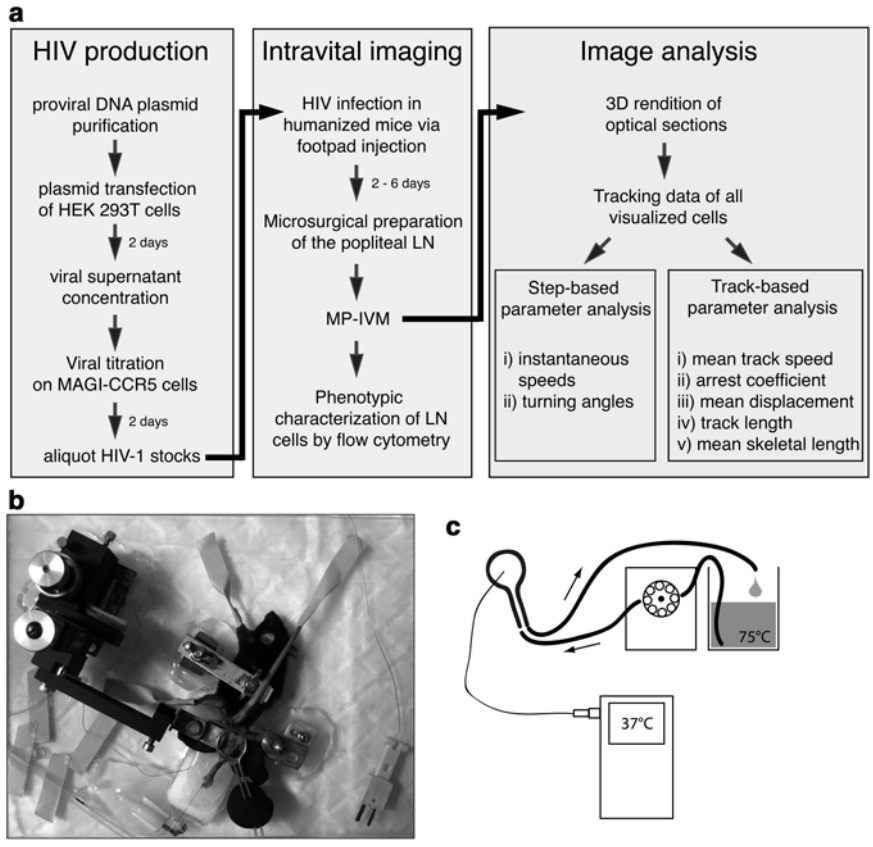

Fig. 1 General overview of the methodological steps required to visualize HIV-infected cells in the lymph node. (**a**) Flowchart view of (1) HIV production, (2) intravital imaging, and (3) image analysis. (**b**) Fully assembled popliteal LN preparation. (**c**) Schematic of the temperature control system.

6. Surgical instruments: Straight "tough-cut" iris scissors (1), Vannas spring scissors with 3–5 mm blades (1), Dumont #5 Forceps standard tip, straight, 0.1 mm × 0.6 mm, Inox, 11 cm total length (2), Dumont #5 Forceps, Biologie tip, 0.05 mm × 0.02 mm, Inox, 11 cm total length (2).
7. 18 mm #1 round cover glasses.
8. Ethyl-2-cyanoacrylate glue (e.g., Crazyglue).
9. Adhesive tape.
10. Suture material (e.g., 5-0 braided silk).
11. High-viscosity vacuum grease.
12. Plasticine modeling clay.
13. Miniature K type thermocouple.

2.6 Multiphoton Intravital Microscopy of the Mouse Popliteal Lymph Node (See Note 3)

1. Upright multiphoton microscope equipped with (a) at least three non-descanned PMT detectors (e.g., Ultima IV, Bruker Corporation; TriMScope, LaVision Biotec; TCS SP8, Leica; LSM 7 MP Zeiss; FluoView MPE-RS, Olympus); (b) a high numerical aperture objective lens (e.g., Olympus XLUMPLFL20XW 20×, 0.95 NA, water immersion, 2 mm working distance); and (c) a femtosecond-pulsed infrared laser (e.g., Insight DS$^+$, Spectra-Physics/Newport or Chameleon Vision II, Coherent).
2. Small water bath.
3. Roller pump (e.g., Masterflex L/S with Easyload II).
4. Digital thermometer (e.g., model 710, BK).
5. Polyethylene tubing (e.g., Intramedic PE160).

2.7 Image Processing and Quantitative Analysis of HIV-Infected Cell Motility

1. Image analysis computer workstation with high graphics processing capability.
2. Image analysis software that allows processing and analysis of 4-dimensional (3-D and time) data sets (e.g., Volocity or Imaris). As a more cost-effective alternative to these commercial products, the freeware program ImageJ with its wide array of freely available plug-ins (http://rsb.info.nih.gov/ij/) can substitute for some of the most relevant functions of image processing and analysis.

3 Methods

We describe two approaches to visualize the behavior of HIV-infected cells in the lymph node of live, anesthetized humanized mice: (1) footpad injection with reporter HIV to visualize in situ-infected cells (*see* Fig. 2a), and (2) footpad injection with HIV-infected, CD4$^+$ central memory-like T cells (Tcm) to visualize

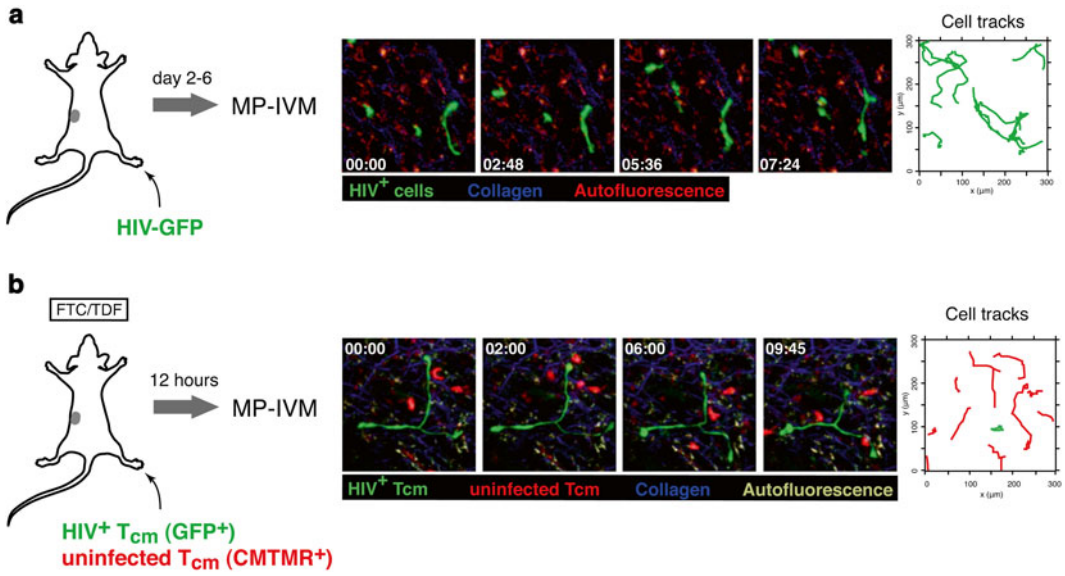

Fig. 2 Intravital microscopy of HIV-infected cells in lymph nodes. (**a**) Visualization of in situ HIV-infected lymph node cells. The popliteal LN was prepared for microscopy at day 4 after footpad injection with HIV-GFP. Elapsed time in minutes:seconds. Migratory tracks are shown on the *right*. (**b**) Visualization of adoptively transferred uninfected and HIV-infected Tcm in the lymph node. The popliteal LN was prepared at 12 h after adoptive transfer of Tcm. Selected intravital micrographs of infected (GFP^+; *green*) and uninfected ($CMTMR^+$; *red*) in the lymph node show differences in the morphologies that these two populations adopt in the LN. Elapsed time in minutes:seconds. T cell migratory tracks are shown on the *right*.

adoptively transferred cells (*see* Fig. 2b). Each protocol is designed to address distinct questions, and the investigator can choose the approach that best suits their study objectives. The generation of humanized *b*one marrow/*l*iver/*t*hymus "BLT" mice is not discussed in this chapter; a detailed description of how to generate these mice has been previously reported [9]. Notably, imaging studies were conducted using BLT mice reconstituted on the NOD.scid genetic background, where skin-draining lymph nodes (e.g., popliteal LNs) are well developed and suitable for intravital imaging. We found that mice with a minimum human peripheral blood reconstitution of >50 % human $CD45^+$ cells, and >30 % T cells within the $CD45^+$ gate, worked best for T cell imaging studies. A flowchart illustrating the overall methods described below is shown in Fig. 1a.

3.1 Preparation of High-Titer Reporter HIV for Footpad Injection

1. The day before transfection, seed 7×10^6 HEK 293T cells in a 150 mm tissue culture plate in complete DMEM.
2. Referring to Table 1, add plasmid DNA (e.g., HIV-GFP) to nuclease-free water in a 50 mL conical tube and gently mix by pipetting.

Table 1
Reagents and volumes required for calcium phosphate transfection

Reagent	Volume per 150 mm culture dish
HIV plasmid	36 μg
2 M $CaCl_2$	174 μL
Nuclease-free water	Up to 1400 μL
2× HBS, pH 7.05	1400 μL
Total	2800 μL

3. Again referring to Table 1, add the appropriate amount of 2 M $CaCl_2$ to the DNA/water mixture and thoroughly mix.
4. While gently vortexing the tube containing the DNA/water/$CaCl_2$ mixture, add 2× HBS dropwise. Incubate the mixture for 3 min at room temperature.
5. Gently vortex the mixture and add dropwise directly onto the medium and gently rock the tissue culture plates. Incubate the cells at 37 °C.
6. Replace the medium at 16–18 h post-transfection after a single wash with PBS.
7. At 40–42 h post-transfection, harvest the viral supernatant and centrifuge for 5 min at 400 × *g*. This will remove cellular debris that may be present in the viral supernatant. An additional collection may be performed after incubating for another 24 h with 20 mL of fresh complete DMEM.
8. Fill 32 mL of clarified viral supernatant into a 38.7 mL capacity ultracentrifuge tube, and underlay with 4 mL of 20 % sucrose solution.
9. Centrifuge the viral supernatant at 90,000 × *g* for 2 h at 4 °C. Set the deceleration rate on low to avoid disruption of the viral pellet.
10. Decant the supernatant and resuspend the pellet with 32 μL of PBS to achieve a concentration of approximately 1000× from the starting material.
11. Aliquot viral stocks into cryovials and keep in a −80 °C or −152 °C freezer for long-term storage. Repeated freeze-thaw cycles will result in reduced infectivity and should be avoided.

12. Viral titers are measured using MAGI-CCR5 cell lines, as described previously [12]. HIV titers obtained using this method are typically 5×10^6–5×10^7 infectious units/mL.
13. Inject HIV (typically 50,000–150,000 infectious particles) into the right footpad of humanized mice using an insulin syringe. The right popliteal lymph node is then prepared for intravital imaging at days 2–6 post-infection.

3.2 Human CD4+ Central Memory T Cell Expansion, Infection, and Adoptive Transfer into Humanized Mice

1. Spleen and lymph node cells are harvested from a humanized mouse (*see* **Note 4**). Naïve $CD4^+$ T cells are isolated using an anti-CD4 microbead separation kit.
2. T cells are washed and resuspended at 1×10^6 cells/mL in complete RPMI medium. Plate one million cells into each well in a 24-well tissue culture plate and incubate with 75 μL of anti-CD3ε/CD28 antibody-conjugated Dynabeads to achieve a 3:1 ratio of beads to cells. Incubate at 37 °C.
3. At day 2, remove the Dynabeads by running the cell suspension through a magnetic column, and reseed T cells at 2×10^5 cells/mL in complete RPMI medium supplemented with 50 IU/mL human recombinant IL-2. At days 4 and 6, centrifuge T cells again and reseed at 2×10^5 cells/mL in fresh complete RPMI medium supplemented with 50 IU/mL IL-2 to gradually increase cell numbers.
4. At day 8, analyze T cell cultures for CD4, CCR7, CD45RO, and CD62L cell surface expression. Central memory $CD4^+$ T cells are $CCR7^+$ $CD45RO^+$ $CD62L^+$, as described previously [7].
5. Pellet five million cells by centrifugation at $400 \times g$ and resuspend in a mixture of concentrated HIV-GFP viral stocks and complete RPMI medium to reach a final volume of 200 μL. Add polybrene to a final concentration of 8 μg/mL and plate the T cell/HIV suspension into a 96-well, flat-bottom tissue culture plate. Typically, a multiplicity of infection (MOI) of 0.5–1 is used to infect T cells.
6. Seal the lid onto the plate with paraffin wax and centrifuge the plate at $1200 \times g$ for 2 h at 37 °C.
7. After the spin, remove T cells, add 5 mL of complete RPMI 1640 supplemented with 50 IU/mL hrIL-2, and plate in a 25 cm^2 tissue culture flask, standing up.
8. At day 2 post-infection, T cells are collected and the proportion of GFP^+ infected T cells is enumerated by flow cytometry.
9. Recipient humanized mice are given daily intraperitoneal injections of emtricitabine (FTC, 100 mg/kg) and tenofovir (TDF, 150 mg/kg) for 2 days prior to T cell transfer (*see* **Note 5**).

10. Resuspend T cells in 50 μL (or less) of PBS and inject into the right footpad of humanized mice using an insulin syringe. Injection of 250,000–500,000 GFP^+ T cells typically seeds the draining lymph node with sufficient cell numbers for intravital imaging.
11. (Optional) Prepare and label one million uninfected T cells with 10 μM CMTMR for 15 min in PBS + 1 % FCS and wash with equal volume of 100 % FCS. Adoptively transfer $CMTMR^+$ T cells into the same right footpad to seed the draining popliteal lymph node with an uninfected, control T cell population.
12. Prepare the right popliteal lymph node for intravital microscopy 10–12 h after adoptive cell transfer.

3.3 Surgical Anesthesia

1. Mice are anesthetized by initially intraperitoneal injection of a mixture of ketamine, xylazine, and NaCl 0.9 % (to achieve a dose of 100 mg/kg body weight for ketamine and 10 mg/kg for xylazine). A surgical plane of anesthesia is achieved if the mouse does not react to firm pinching of the footpad. Repeat injections during the surgical procedure and later on during the imaging session can be carried out intramuscularly to achieve slower release and more even plasma levels.

3.4 Microsurgical Preparation of the Mouse Popliteal Lymph Node for Intravital Microscopy (See Note 6)

We have previously described a detailed protocol for the lymph node preparation, which will not be discussed in this chapter [13] (Fig. 1b). Notably, we found no differences in the positioning and size of the popliteal LN between conventional C57BL/6 and humanized mice. When performing surgeries on HIV-infected mice, biosafety measures approved by the relevant institutional agency must be strictly followed. Standard personal protective equipment in BSL 2^+ facilities typically includes Tyvek coveralls, hairnet, protective mask, goggles, shoe covers, and double gloves. Additional safety measures such as the use of syringes with retractable needles, puncture-proof gloves, and DecapiCone mouse restrainers are recommended.

3.5 Multiphoton Intravital Microscopy of the Mouse Popliteal Lymph Node

1. Through the eyepieces of the microscope, the popLN can be distinguished from the surrounding tissue structures by its oval shape and its green autofluorescence under mercury arc lamp illumination (*see* **Note 7**). Flow in negatively contrasted blood vessels can be assessed for robustness of perfusion. Any residual movement of the specimen that is noticeable at this point will preclude acquisition of high-resolution 3D image stacks and should be corrected by readjustment of the preparation under the dissecting microscope.
2. T cell migration is highly temperature dependent [14]. Since the water immersion objective lens functions as a heat sink, the ambient popLN temperature must be actively maintained

close to 37 °C. Perfusing the circular metal tube overlying the cover glass is a cost-effective and convenient approach, since the temperature can be quickly adjusted by changing the flow rate (Fig. 1c).

3. The laser source is tuned to 920 nm and the microscope equipped with appropriate filter combinations to detect blue, green, and orange-red fluorescence emission (e.g., using 455/50, 525/50, and 590/50 nm bandpass filters). After switching to viewing by multiphoton fluorescence excitation, back-scattered second harmonic signals from the collagen-rich organ capsule and the lymph node reticulum are visible in the blue channel and serve as convenient landmark structures to assess the current location within the popLN. The green channel will show fluorescence of eGFP, and the red channel will show fluorescence of CMTMR. Any autofluorescence will be detected in all channels.
4. To test the viability of the preparation, the baseline migratory behavior of labeled lymphocytes is recorded. To this end, a field of view containing the T cell area (typically 150–200 μm away from the LN capsule) is chosen and a stack of optical sections (e.g., 11 sections spaced 4 μm apart in the *z*-axis, corresponding to 40 μm of depth) repetitively recorded (e.g., at 15-s intervals) for 15 min without optical zoom (when using a 20× lens this typically results in a field size of 500–700 μm). Most commercial image acquisition software allows subsequent browsing through the acquired image sequence along the time axis to visually assess cell motility. At this point, attention should also be paid to the stability of the preparation. In particular, movement artifacts caused by the respiratory movement of the mouse or the pulsation of a nearby arterial vessel as well as a gradual drift of the specimen need to be corrected by readjustment of the preparation under the dissection microscope. At this point, the optimal microscope settings (laser power, PMT gain, offset, etc.) to obtain balanced signals of GFP and CMTMR are determined and loaded.
5. Once a representative location with a sufficient number of fluorescently labeled cells is identified, begin image acquisition. Ideally, a continuous recording of several hours should be generated, but because of practical limitations, typically multiple sequential recordings have to be obtained (*see* **Note 8**).

3.6 Image Processing and Quantitative Analysis of Cell Migration Behavior

Image analysis software that allows for processing and analysis of 4-dimensional (3-D and time) data sets is used (e.g., Volocity, Improvision or Imaris, Bitplane). Each lymphocyte track is visually inspected, and those that track artifacts (e.g., autofluorescent structures) are manually deleted from the analysis (*see* **Note 9**). Information on the calibrated spatial position in the *x*, *y*, and *z*

dimension and on the green (infected) and red (uninfected) integrated fluorescence for all individual time points of measured T lymphocyte tracks is exported as tab-delimited .txt files. These can then be computed to obtain parameters describing cell motility (e.g., instantaneous migratory velocity, turning angles) in a spreadsheet calculation program such as Excel (Microsoft corporation) or a matrix-based computing environment such as Matlab (Mathworks). The speed of cellular movement is a useful parameter describing cell motility, and is often reported. The instantaneous migratory velocity is measured by dividing the distance traveled between two subsequent time frames by the time between frames, and provides information on the short-term fluctuations of cell motility of individual cells. Track velocity, on the other hand, describes the average velocity of individual cells. Finally, the arrest coefficient describes the fraction of time an individual cell is "arrested" (defined as velocities below an arbitrarily defined threshold velocity, e.g., 4 μm/min). Only determining the mean arrest coefficient or track velocity of a population can obscure the behavior of minor but biological relevant subpopulations, which may be revealed by analyzing the distribution of these parameters. The turning angle is also an important feature describing the directional persistence or bias of migrating cells and can be used to detect subtle changes in movement behavior. A cell displaying random migration would exhibit an even distribution of turning angles, whereas a preferred range of turning angles may be overrepresented in biased random or nonrandom movement. It is important to note that the speed and turning angle are dependent on the acquisition parameters, and larger time intervals between frames will generally lead to a larger error. We refer readers to a comprehensive review on the analysis of these and additional parameters of cellular migration [15]. Taken together, the speed, turning angle, and mean displacement of a cell population are all powerful measures to describe cell motility and to characterize subtle changes in movement behavior in vivo.

4 Notes

1. HIV encodes only a small number of genes, whose open reading frames overlap. This makes it difficult to insert fluorescent reporter genes or tags within the genome without negatively affecting multiple genes or critical regulatory elements required for viral infection and replication. The R5-tropic HIV-GFP reporter used in our experiments expresses Nef and GFP from a single bicistronic RNA via an IRES element, and had comparable in vivo infection kinetics when compared to the parental, non-GFP-encoding strain [7].

All newly constructed reporters must be rigorously validated to ensure that the introduced reporter sequence does not negatively impact the infectivity, replication kinetics, and budding/release of HIV in primary cells. If a fluorescent protein-based reporter is used [7, 16, 17], additional considerations including the brightness, photostability, oligomerization property and maturation time of the fluorescent protein (FP), the impact of FP fusions on the function of the protein they are fused to, and whether the FP used is optimally excited and detected by the imaging setup being employed [18] need to be taken into account. When non-fluorescent protein-based reporters are used [19, 20], potential toxicity of the labeling procedure and the low signal-to-noise ratio in many tissues must be considered.

2. Our microscope stage is manufactured using a Plexiglas plate as the base, onto which various elements for the fixation of the mouse are mounted. These elements for the most part consist of materials available in any hardware store that are shaped to suit their particular function. We found small steel corner brackets, angle-style steel shelf support pegs, screws and nuts of various calibers, silicone-based windshield sealer, and the casting resin to be very useful items. The only expensive element is a 3-D micromanipulator, which allows for the controlled positioning of the cover glass on the popLN.
3. The microscope must be situated in the appropriate biosafety containment-level facility for the handling of HIV-infected mice. All required biosafety and animal care protocols must be approved by the relevant institutional agencies in order to conduct all imaging studies described in this chapter.
4. Typically, 10–20 humanized mice are implanted with tissue/cells from a single human donor and are immunologically tolerant to each other within the same "batch." Donor (source of T cells) and recipient (host receiving adoptive T cell transfers) humanized mice from the same batch are used to prevent immune rejection and/or inappropriate alloreactivity of transferred T cells in all experiments.
5. The pretreatment of recipient mice with a combination of antiretroviral drugs prevents the infection of recipient mice to ensure that only the transferred HIV-infected T cells are visualized.
6. Our choice of the popLN for MP-IVM studies over other skin-draining LNs was based on two observations: (1) The quantity of footpad-injected reagents that drains to the LN can be controlled more accurately with the popLN than with other skin-draining LNs. (2) Due to the popLN's remote location to the animal's trunk, the respiratory movements, which would inevitably cause motion artifacts during the slow

image acquisition achieved by laser-scanning microscopy, could be shielded off effectively without applying pressure to the surrounding tissues.

7. If a conventional epifluorescence unit is unavailable, marking the position of the lymph node by drawing a circle around it on the dry cover glass with a fine marker pen can help with locating and focusing of the tissue under the multiphoton microscope. Oblique bright-field epi-illumination with a handheld flashlight then allows viewing of the specimen through the eyepieces of the microscope.
8. The duration of the recording is limited by (1) the requirement to obtain access to the animal in order to maintain surgical anesthesia, (2) evaporation of the immersion water, and (3) restrictions of either the acquisition software or the computer hardware on the maximum size of the recorded data files. Besides the total length of the recording, the file size can typically be adjusted through the pixel resolution, the number of z planes, and the cycle time. We typically use a pixel resolution of 512×512, 11 optical sections, and a cycle time of 15 s, since this provides us with a good compromise between file size, image detail, and the ability to follow individual motile cells for sufficient time to obtain meaningful data.
9. Specific points to consider when visually inspecting tracks: (1) Tracks with very low meandering indices (large displacement values between the first and last track despite a low length of distance travelled) may indicate noncellular artifacts, (2) tracks that contain few time points may indicate cells leaving the field of view (FOV) and possibly not suitable for analysis (this should be recorded and kept constant for the entire data set), (3) tracks with low displacement values may be indicative of non-motile autofluorescent artifacts, (4) two intersecting tracks leading to a switching of the two tracks should be manually corrected, and (5) tracks that border the FOV where only a portion of the cell is visible should be deleted. It is important to note that these are guidelines, and manual inspection of all tracks is essential not to over/underestimate cellular motility.

References

1. Denk W, Strickler JH, Webb WW (1990) Two-photon laser scanning fluorescence microscopy. Science 248:73–76
2. Helmchen F, Denk W (2005) Deep tissue two-photon microscopy. Nat Methods 2:932–940
3. Cahalan MD, Parker I, Wei SH, Miller MJ (2002) Two-photon tissue imaging: seeing the immune system in a fresh light. Nat Rev Immunol 2:872–880
4. Pittet MJ, Mempel TR (2008) Regulation of T-cell migration and effector functions: insights from in vivo imaging studies. Immunol Rev 221:107–129
5. Denton PW, Estes JD, Sun Z, Othieno FA, Wei BL, Wege AK, Powell DA, Payne D, Haase AT, Garcia JV (2008) Antiretroviral pre-exposure prophylaxis prevents vaginal transmission of HIV-1 in humanized BLT mice. PLoS Med 5, e16

6. Denton PW, Othieno F, Martinez-Torres F, Zou W, Krisko JF, Fleming E, Zein S, Powell DA, Wahl A, Kwak YT, Welch BD, Kay MS, Payne DA, Gallay P, Appella E, Estes JD, Lu M, Garcia JV (2011) One percent tenofovir applied topically to humanized BLT mice and used according to the CAPRISA 004 experimental design demonstrates partial protection from vaginal HIV infection, validating the BLT model for evaluation of new microbicide candidates. J Virol 85:7582–7593
7. Murooka TT, Deruaz M, Marangoni F, Vrbanac VD, Seung E, von Andrian UH, Tager AM, Luster AD, Mempel TR (2012) HIV-infected T cells are migratory vehicles for viral dissemination. Nature 490:283–287
8. Sun Z, Denton PW, Estes JD, Othieno FA, Wei BL, Wege AK, Melkus MW, Padgett-Thomas A, Zupancic M, Haase AT, Garcia JV (2007) Intrarectal transmission, systemic infection, and CD4+ T cell depletion in humanized mice infected with HIV-1. J Exp Med 204:705–714
9. Brainard DM, Seung E, Frahm N, Cariappa A, Bailey CC, Hart WK, Shin HS, Brooks SF, Knight HL, Eichbaum Q, Yang YG, Sykes M, Walker BD, Freeman GJ, Pillai S, Westmoreland SV, Brander C, Luster AD, Tager AM (2009) Induction of robust cellular and humoral virus-specific adaptive immune responses in human immunodeficiency virus-infected humanized BLT mice. J Virol 83:7305–7321
10. Dudek TE, No DC, Seung E, Vrbanac VD, Fadda L, Bhoumik P, Boutwell CL, Power KA, Gladden AD, Battis L, Mellors EF, Tivey TR, Gao X, Altfeld M, Luster AD, Tager AM, Allen TM (2012) Rapid evolution of HIV-1 to functional CD8(+) T cell responses in humanized BLT mice. Sci Transl Med 4:143ra198. doi:10.1126/scitranslmed.3003984, 4/143/143ra98 [pii]
11. Denton PW, Olesen R, Choudhary SK, Archin NM, Wahl A, Swanson MD, Chateau M, Nochi T, Krisko JF, Spagnuolo RA, Margolis DM, Garcia JV (2012) Generation of HIV latency in humanized BLT mice. J Virol 86:630–634
12. Pirounaki M, Heyden NA, Arens M, Ratner L (2000) Rapid phenotypic drug susceptibility assay for HIV-1 with a CCR5 expressing indicator cell line. J Virol Methods 85:151–161
13. Murooka TT, Mempel TR (2012) Multiphoton intravital microscopy to study lymphocyte motility in lymph nodes. Methods Mol Biol 757:247–257
14. Miller MJ, Wei SH, Parker I, Cahalan MD (2002) Two-photon imaging of lymphocyte motility and antigen response in intact lymph node. Science 296:1869–1873
15. Beltman JB, Maree AF, de Boer RJ (2009) Analysing immune cell migration. Nat Rev Immunol 9:789–798
16. Gelderblom HC, Vatakis DN, Burke SA, Lawrie SD, Bristol GC, Levy DN (2008) Viral complementation allows HIV-1 replication without integration. Retrovirology 5:60. doi:10.1186/1742-4690-5-60, 1742-4690-5-60 [pii]
17. Brown A, Gartner S, Kawano T, Benoit N, Cheng-Mayer C (2005) HLA-A2 down-regulation on primary human macrophages infected with an M-tropic EGFP-tagged HIV-1 reporter virus. J Leukoc Biol 78:675–685
18. Shaner NC, Steinbach PA, Tsien RY (2005) A guide to choosing fluorescent proteins. Nat Methods 2:905–909
19. Arhel N, Genovesio A, Kim KA, Miko S, Perret E, Olivo-Marin JC, Shorte S, Charneau P (2006) Quantitative four-dimensional tracking of cytoplasmic and nuclear HIV-1 complexes. Nat Methods 3:817–824. doi:10.1038/nmeth928, nmeth928 [pii]
20. Eckhardt M, Anders M, Muranyi W, Heilemann M, Krijnse-Locker J, Muller BA (2011) SNAP-tagged derivative of HIV-1: a versatile tool to study virus-cell interactions. PLoS One 6:e22007. doi:10.1371/journal.pone.0022007, PONE-D-11-06412 [pii]

Chapter 14

Modeling HIV-1 Mucosal Transmission and Prevention in Humanized Mice

Milena Veselinovic, Paige Charlins, and Ramesh Akkina

Abstract

The new generation humanized mice (hu-mice) that permit continuous de novo generation of human hematopoietic cells have led to novel strategies in studying HIV-1 pathogenesis, prevention and therapies. HIV-1 infection of hu-mice results in chronic viremia and CD4+ T cell loss, thus mimicking key aspects of the disease progression. In addition, the new generation hu-mice are permissive for HIV-1 sexual transmission by vaginal and rectal routes thus allowing in vivo efficacy testing of new anti-HIV-1 drugs for prevention. Two leading models are currently being used, namely the hu-HSC mice and the BLT mice. Here we describe the methodology for generating both hu-HSC and BLT mice and their use in the study of HIV-1 transmission and prevention of infection by topical and oral administration of anti-retroviral drugs. Practical aspects of the methodologies are emphasized.

Key words Modeling HIV transmission and prevention, HIV pre-exposure prophylaxis, HIV-1 PrEP, HIV-1 animal models, Preparation of humanized mice, Hu-HSC and BLT mice, HIV infection in humanized mice, HIV mucosal transmission, HIV vaginal and rectal transmission, PK-PD in HIV-1 PrEP

1 Introduction

As HIV-1 is a human pathogen, conventional animal models are not suitable to study its pathogenesis, prevention and therapeutic strategies. To overcome this limitation, immunodeficient mice engrafted with human cells that are permissible for HIV-1 infection (hu-mice) have been developed. Hu-mouse models have undergone progressive improvements during the last two decades and the new models have proven to be far superior to earlier models [1]. The early hu-mice versions, namely the hu-PBL-SCID mice and SCID-hu mice, while susceptible to HIV-1 infection, do not permit de novo generation of all hematopoietic lineages and thus have drawbacks. The advent of new generation immunodeficient mice that also harbor IL-2 gamma chain mutation permit higher levels of human cell reconstitution and more robust human

Vinayaka R. Prasad and Ganjam V. Kalpana (eds.), *HIV Protocols*, Methods in Molecular Biology, vol. 1354,
DOI 10.1007/978-1-4939-3046-3_14,

hematopoiesis [2]. These mice, after reconstitution with human hematopoietic stem cells (HSC) generate human T cells, B cells, monocytes/macrophages, NK cells as well as dendritic cells, which are principal components of both innate and adaptive immune responses. Infection of these mice with HIV-1 results in chronic viremia and CD4+ T cell depletion which are hallmarks of HIV-1 infection and AIDS. In contrast to the early hu-mouse models, there is also an HIV-1 specific immune response. Two new generation hu-mouse models are currently used. The hu-HSC model (sometimes referred to as RAG-hu mice in the literature) employs engraftment of human CD34+ HSC whereas the BLT mouse model is generated by transplantation of human fetal thymic and liver tissues under the kidney capsule in addition to engraftment of CD34+ HSC [3, 4]. While both models support HIV-1 infection and immune responses, an advantage with the BLT mouse model is the maturation of human T cells occurring in the autologous human thymus and thus permitting human HLA restricted human T cell responses to antigens.

The primary mode of HIV-1 transmission is by sexual routes via the vaginal or rectal mucosa. To prevent HIV-1 infection through these routes, strong and sustained mucosal immune responses are necessary. However, currently no vaccine has been successful to impart such protective immunity [5]. Therefore, other alternative methods are urgently needed. In this regard, pre-exposure prophylaxis (PrEP) approaches that encompass either oral or topical administration of anti-HIV-1 retroviral drugs have shown considerable promise and many clinical trials are currently underway [6–8].

Due to the lack of an ideal in vivo model for HIV-1 mucosal transmission until recently, the SIV/SHIV-1 model had been used extensively to study the viral transmission and its prevention in non-human primates (NHP) [9]. However, among the limitations with using NHPs are high cost and the inability to use HIV-1 itself for challenge studies. These disadvantages are now overcome by the recent demonstration that hu-mice can be infected by HIV-1 by both vaginal and rectal mucosal routes since both hu-HSC and BLT models were shown to harbor HIV-1 susceptible cells in the vaginal and rectal mucosa [1]. Viremia is detected within 1–3 weeks after mucosal HIV-1 challenge with either CCR5 or CXCR4-tropic HIV. Using these models, both oral and topical PrEP strategies were shown to be successful and a number of antiretroviral drugs were shown to be effective [1, 3]. The stage is now set to evaluate a number of new anti-HIV-1 compounds in the current anti-retroviral drug pipeline.

Here we describe the methodologies of how to prepare hu-mice, infection by parenteral (intraperitoneal) and mucosal routes, assessment of HIV-1 viremia, CD4+ T cell loss, efficacy testing of anti-retroviral drugs administered either by topical or oral routes

and collection of mucosal tissues after drug administration (*see* **Notes 1** and **2**). While both the hu-HSC and BLT mice can be used for these purposes, the hu-HSC mice have some advantages in terms of lower cost, little or no graft versus host disease, no surgery involved and the capacity to generate larger number of animals in a single cohort using tissues from one donor. A major question in the PrEP field currently is what concentration of the drug is necessary in the mucosal tissues to afford full protection [10]. Thus, detailed PK-PD studies are necessary to establish protective concentration of various anti-HIV-1 drugs. Recent data from our laboratory have demonstrated the utility of hu-HSC mice in this regard as detailed below [11].

2 Materials

2.1 General Laboratory Materials and Equipment

1. BSL-2 laboratory with biosafety cabinet.
2. Personal protective equipment (PPE)—lab coat, gloves, face mask, protective glasses.
3. Disposable protective absorbent pads.
4. Petri dishes (100 mm).
5. 20 ml syringe.
6. 1.5 ml microcentrifuge tubes.
7. 15 and 50 ml conical vials.
8. 5, 10 and 25 ml serological pipettes.
9. 1× phosphate buffered saline (PBS).
10. Microcentrifuge.
11. Bench top centrifuge.
12. Single channel manual pipettes and tips p20, p200, and p1000.

2.2 Isolation and Maintenance of Human CD34+ HSC

1. Human fetal liver tissue.
2. 2× AB/AM AIMs media: AIM-V media + AlbuMAX (BSA) supplemented with 0.5 μg/ml amphotericin B, 200 μg/ml streptomycin, and 200 units/ml penicillin.
3. DNase—322 Kunitz/ml, hyaluronidase—1 mg/ml, collagenase type IV—1 mg/ml—(for making a concentrated 100× stock *see* **Note 3**).
4. Ficoll-Paque PLUS.
5. CD34+ cell isolation buffer: 1× PBS with 0.5 % BSA and 2 mM EDTA, sterilized by vacuum filtration (*see* **Note 4**).
6. MACS magnetic bead separation system: Pre-separation filters, Midi MACS separation magnets, MACS separation multistand, LS columns, FcR human blocking reagent, CD34+ (human) microbeads.

7. CD34+ cell media: Iscove's Modified Dulbecco's Media supplemented with 0.5 μg/ml amphotericin B, 200 μg/ml streptomycin, and 200 units/ml penicillin, 10 % fetal bovine serum, 25 ng/ml of IL-3, IL-6, and SCF, sterilized by vacuum filtration (*see* **Note 5**).
8. Stainless steel disposable scalpels.
9. 40 μm cell strainer.
10. Mouse anti-human CD34-PE.
11. Stem cell cryopreservation media.
12. Flow cytometer.

2.3 Preparation of hu-HSC Mice

1. 1–4 day old neonate *BALB/c-Rag1*$^{null}\gamma c^{null}$, *BALB/c-Rag2*^{null} γc^{null} or NOD-*scid* IL2Rγ^{null} (NSG) mice.
2. Sterile ½ cc U-100 Insulin syringe.
3. CD34+ cell media: Iscove's Modified Dulbecco's Media (IMDM) with 0.5 μg/ml amphotericin B, 200 μg/ml streptomycin, and 200 units/ml penicillin, 10 % fetal bovine serum, 25 ng/ml of IL-3, IL-6, and SCF, sterilized by vacuum filtration (*see* **Note 5**).
4. Isolated human CD34+ HSC (*see* **Note 6**).
5. Gamma irradiation source.

2.4 Preparation of BLT Mice

1. 7–10 week old *BALB/c-Rag1*$^{null}\gamma c^{null}$, *BALB/c-Rag2*$^{null}\gamma c^{null}$, or NOD-*scid* IL2Rγ^{null} (NSG) mice.
2. Human fetal liver and thymus (*see* **Note 7**).
3. Autologous isolated CD34+ HSC (*see* **Note 7**).
4. Electric shaver.
5. Banamine 2.5 mg/kg.
6. Buprenorphine (slow release formulation) 0.6 mg/kg.
7. Anesthesia apparatus.
8. 2 % Isoflurane in O_2.
9. Surgical instruments: SWISS jeweler style forceps, utility forceps, KELLY forceps 5 1/2″ curved, Iris scissors straight 4″, 9 mm Autoclip Applier, 9 mm Autoclips, trochar (laboratory animal cancer implant needle 16 gauge 8.3 cm), needle holder forceps, sutures size 4-0, C-13 size needle (*see* **Note 8**).
10. Sterile ½ cc U-100 Insulin syringe.
11. Betadine.
12. 70 % alcohol swabs.
13. Cotton gauze.
14. Gamma irradiation source.

2.5 Screening of hu-Mice for Engraftment Levels

1. Heparinized micro-hematocrit capillary tubes.
2. Human erythrocyte lysing kit.
3. Mouse blocking buffer: Normal mouse serum (Jackson Immuno Research Labs), Rat anti-mouse CD16/CD32 (Mouse FC Receptor Monoclonal), Human gamma globulin (Jackson Immuno Research Labs).
4. Mouse anti-human CD45-PE.
5. 1 % v/v Paraformaldehyde: paraformaldehyde in PBS without Ca^{2+} and Mg^{2+}.
6. 12 × 75 mm 5 ml polystyrene round-bottom tubes.
7. Flow cytometer.

2.6 HIV-1 Infection by Vaginal or Rectal Mucosal Route

1. 22 gauge 1.25 mm straight gavage needle (*see* **Note 8**).
2. HIV-1 viral stock, titer $\geq 10^6$ IU/ml.
3. Anesthesia apparatus.
4. 2 % Isoflurane in O_2.
5. Gauze.
6. Dry ice.
7. Ice Bucket.
8. Timer.
9. Sterile 1 ml syringe.

2.7 HIV-1 Infection by Parenteral (Intraperitoneal) Routes

1. Sterile ½ cc U-100 Insulin syringe.
2. HIV-1 viral stock, titer $\geq 10^6$ IU/ml.
3. Ice bucket.

2.8 Monitoring of HIV-1 Viremia by qRT-PCR

1. Micro-hematocrit capillary tubes.
2. Microtainer tubes with EDTA.
3. PBS without Ca^{2+} and Mg^{2+}.
4. E.Z.N.A Viral RNA Kit.
5. iTaq Universal Probes One-Step Kit.
6. HIV-1 LTR Forward Primer-5′GCCTCAATAAAGCTTGC CTTGA 3′
7. HIV-1 LTR Reverse Primer-5′GGCGCCACTGCTAGAGA TTTT3′
8. HIV-1 LTR Probe-5′FAM/AAGTAGTGTGTGCCCGTC TGTTRTKTGACT 3′
9. HIV-1 RNA standard (NIH AIDS Reagent Program).
10. Low 96-well clear plate.

11. Microseal 'B' seal.
12. Bio-Rad C1000 Thermal Cycler with a CFX96 Real-Time System.

2.9 Monitoring of CD4+ T Cell Levels by FACS

1. Heparinized micro-hematocrit capillary tubes.
2. Mouse blocking buffer: Normal mouse serum, Rat anti-mouse CD16/CD32 (Mouse FC Receptor Monoclonal), Human gamma globulin.
3. Human erythrocyte lysing kit.
4. Mouse anti-human CD45-FITC.
5. Mouse anti-human CD4-PE-Cy5.
6. Mouse anti-human CD3-PE.
7. 1 % v/v Paraformaldehyde: paraformaldehyde, PBS without Ca^{2+} and Mg^{2+}.
8. 12 × 75 mm 5 ml polystyrene round-bottom tubes.
9. Flow cytometer.

2.10 Antiretroviral Drug Preparation and Administration of Oral PrEP

1. Antiretroviral pharmaceutical tablets, such as Selzentry™ (maraviraoc) 150 mg tablets, Isentress™ (raltegravir) 400 mg tablets, Viread® (tenofovir disoproxil fumarate) 300 mg tablets, or pure compounds in powder form.
2. Mortar and pestle.
3. Sterile PBS.
4. 70 % alcohol swabs.
5. 20 gauge 2.25 mm curved gavage needle (*see* **Note 8**).
6. Sterile 1 ml syringes.

2.11 Topical Microbicide PrEP: Antiretroviral Drug Preparation and Administration

1. Antiretroviral pharmaceutical tablets or pure powder compounds.
2. 2.2 % hydroxyethylcellulose (HEC) vehicle.

2.12 Blood and Tissue Sampling for Pharmacokinetic Analysis

1. CO_2 euthanasia chamber.
2. Surgical instruments (scissors, tweezers) (*see* **Note 8**).
3. Heparinized micro-hematocrit capillary tubes.
4. Micro-hematocrit capillary tubes.
5. Microtainer tubes with EDTA.
6. 2 ml cryovials.
7. 70 % ethanol.
8. Digital scale.
9. Liquid nitrogen container.

3 Methods

3.1 Isolation and Culturing of Human CD34+ HSC from Fetal Liver

CD34+ HSC are employed to engraft immunocompromised mice to generate hu-mice that support multilineage human hematopoiesis [12].

Day 1

1. Wash the tissue two to three times at room temperature with 1× PBS in a 100 mm dish. Aspirate final wash and weigh the tissue under sterile conditions (*see* **Note 6**).
2. Use 100× stock aliquots of DNase, hyaluronidase, and collagenase and add to create 50 ml of the 2× AB/AM AIMs media with digestive enzymes. Add serum free 2× AB/AM AIMs media containing the digestive enzymes to the washed and weighed tissue. Use 35 ml media to add to the dish with the tissue and save 15 ml media for **step 5** (*see* **Note 3**).
3. Mince the tissue into small pieces using two scalpels, and then use a 20 ml syringe to disperse the tissue until all visible clumps are gone.
4. Dispense into 3–4 100 mm plates depending on the size of the tissue and incubate 3–5 h at 37 °C.
5. After 30–60 min of incubation add 5 ml fresh enzyme media to each plate, resuspend well and split into more plates if necessary.
6. Mix suspension every 40–45 min by pipetting until a single cell suspension is obtained as seen under the light microscope (*see* **Note 9**).
7. Pipette the solution one last time and filter through a 40 μm cell strainer into a 50 ml conical tube.
8. Distribute the solution evenly between 4 and 8 50 ml tubes for Ficoll prep. Add fresh 2× AB/AM AIMs media (no digestive enzymes) to make 25 ml in each tube.
9. Take 12 ml of Ficoll-Paque and underlay by slowly pipetting out the Ficoll-Paque creating a distinct layer between the tissue solution and the Ficoll-Paque (*see* **Note 10**).
10. Centrifuge at 530×*g* at room temperature with NO BRAKE in a swinging bucket rotor for 30 min.
11. Aspirate off the top layer and collect the interphase. Dispose of the rest.
12. Dilute collection at least 1:2 with CD34+ cell isolation buffer; use as many 50 ml conical as needed here.
13. Centrifuge tubes at 1200×*g* with brake for 10 min at room temperature.

14. Carefully vacuum off the supernatant (leave 2–3 ml in the conical) and resuspend and combine the pellets in a total volume of 50 ml isolation buffer. Take a sample to determine cell count and spin again at 1200×*g* with brake for 10 min (*see* **Notes 6** and **11**).
15. After centrifugation and cell count, resuspend pellet in 300 µl isolation buffer per 10^8 total cells.
16. Add 100 µl FcR human blocking reagent per 10^8 total cells to inhibit nonspecific binding of the magnetic beads.
17. Label cells by adding 100 µl CD34+ human Microbeads per 10^8 total cells, mix well and incubate at 4 °C for 30 min.
18. Wash cells one time—add isolation buffer to 50 ml, spin 1200×*g* for 10 min. After the spin resuspend in the isolation buffer (2×10^8 cells per ml buffer—10 ml max).
19. Set-up the magnetic separation stage using the Midi MACS separation magnet and MACS separation multistand. Place LS column with a pre-separation filter into the magnet. Place a collection tube under the LS column (50 ml conical).
20. Rinse column with 3 ml isolation buffer and allow it to flow through into the collection tube (*see* **Note 4**).
21. Rinse pre-separation filter with 1 ml isolation buffer prior to passing cells through filter and allow the wash to flow through the LS column.
22. Pass cells through pre-separation filter and allow cells to pass through the column.
23. Wash three times with 3 ml isolation buffer. Allow for each wash to flow through before applying the next one.
24. Remove column from magnet and place in a sterile collection tube (15 ml conical). Add 5 ml of isolation buffer to the column and plunge the column into the 15 ml conical vial.
25. Repeat **steps 20–24** with a fresh magnetic column without a pre-separation filter.
26. After the final elution step from the second column, centrifuge cell suspension at 360×*g* for 5 min at room temperature.
27. Resuspend cells in CD34+ cell culture media with cytokines and plate in a 6 well plate (*see* **Note 12**).
28. Incubate cells overnight in the CD34+ cell culture media at 37 °C and 5 % CO_2.

Day 2

29. Change the CD34+ cell culture media—take two samples of cell suspension to count the cells and determine the CD34+ cell purity.

30. Determine CD34+ cell purity by following **steps 31–37**.
31. Take 1–3 × 10^5 cells from the CD34+ cell suspension—wash 1× PBS, resuspend in 200 μl 1× PBS.
32. Separate into two 100 μl samples (*see* **Note 13**).
33. Add 2 μl FcR human blocking reagent to both samples.
34. Add 2 μl CD34-PE to one sample (label as positive).
35. Incubate 20 min in the dark (room temperature).
36. Wash 1× PBS.
37. Resuspend in 300 μl PBS and transfer to 12 × 75 mm polystyrene round-bottom tubes for analysis on the flow cytometer for CD34+ cell percentage.

3.2 Preparation of hu-HSC Mice

CD34+ HSC are used to reconstitute immunocompromised mice to generate hu-mice capable of multilineage human hematopoiesis [13–15].

1. Following the cell count, centrifuge 0.2–1 × 10^6 CD34+ cells per pup at 360 × *g* for 5 min. Resuspend the CD34+ cells in CD34+ media at 30–50 μl media per injection. Keep cells on ice and inject immediately (*see* **Note 14**).
2. Using a sterile ½ cc Insulin syringe, inject 30–50 μl of CD34+ cell suspension intrahepatically into pups that have been preconditioned by irradiation (*see* **Note 15**).

3.3 Preparation of BLT Mice

Fetal liver and thymus tissue fragments are transplanted under the kidney capsule of immunodeficient mice together with injection of autologous CD34+ HSC to prepare BLT mice [3, 16, 17].

1. Irradiate mice with 350 rads from a gamma source on the day of surgery prior to the tissue implantation.
2. Conduct all manipulations using aseptic techniques.
3. Prepare the surgical site by shaving the left flank region.
4. Administer Banamine subcutaneously and then anesthetize the mouse with 2 % Isoflurane by inhalation (*see* **Note 16**).
5. Disinfect surgical region by scrubbing with betadine scrub for 2–3 min, and rinsing with 70 % alcohol swabs.
6. Make an incision along the left lateral flank of the mouse to expose the kidney and the kidney capsule.
7. Implant small pieces of human fetal thymus and liver (1–2 mm) under the left kidney capsule by use of the trochar (laboratory animal cancer implant needle) (*see* **Note 17**).
8. After insertion of the tissues under the kidney capsule, suture together the inside muscle layer with 1–2 stitches and staple the outer skin with wound clips. Remove the wound clips 10 days later.

9. To alleviate pain following surgery, immediately administer buprenorphine subcutaneously (*see* **Note 18**).
10. Allow implants to grow for 2–4 months prior to engraftment screen and experimental use of BLT mice.

3.4 Screening of hu-Mice for Engraftment Levels

1. Collect one heparin capillary tube via tail vein bleed from each hu-mouse and place into a labeled 1.5 ml microcentrifuge tube at room temperature (*see* **Note 19**).
2. Add 5 μl of mouse blocking buffer to each sample, briefly vortex and incubate 10 min at room temperature.
3. Add 2 μl of mouse anti-human CD45-PE to each sample and gently vortex. Incubate samples for 20–30 min at room temperature in the dark.
4. Place 2 ml of 1× erythrocyte lysis buffer into labeled 15 ml conical vials.
5. When staining is complete, add 1 ml lysis buffer to each sample, pipette to mix, then transfer to corresponding 15 ml conical vial containing the additional 2 ml of lysis buffer and vortex briefly to mix.
6. Incubate samples for 12 min at room temperature in the dark.
7. Add 11 ml of wash buffer to each vial, mix by inversion, and then centrifuge at 650 × *g* at room temperature for 5 min.
8. Aspirate supernatant and resuspend pellet in 1 ml wash buffer and transfer to a new labeled 1.5 ml microcentrifuge tube. Centrifuge at 450 × *g* at room temperature for 5 min.
9. Aspirate supernatant and resuspend pellet in appropriate volume of 1 % paraformaldehyde, transfer to 12 × 75 mm 5 ml round-bottom tubes for CD45+ cell population analysis by flow cytometry.

3.5 HIV-1 Infection by Vaginal or Rectal Mucosal Route

Humanized mice are susceptible to HIV-1 infection by vaginal and rectal mucosal routes [13, 18, 19].

1. For the duration of the procedure (up to 10 min), anesthetize mice by 2 % Isoflurane inhalation.
2. Thaw HIV-1 virus stock and keep on ice throughout the procedure to ensure viability of the virus.
3. Take a sample of the viral stock for each individual challenge (keep the syringe cold throughout the procedure).
4. Anesthetized mice are placed on their back, with the head/nose underneath the inhalational anesthesia tube outlet.
5. Using a blunt end needle to ensure no trauma/abrasions of the vaginal mucosa, apply the virus (20–30 μl) to the vaginal cavity.

6. Following virus application, hold anesthetized mice with pelvis and lower extremities elevated for 5 min post-inoculation to prevent immediate discharge of virus.

3.6 HIV-1 Infection by Parenteral (Intraperitoneal) Route

1. Thaw HIV-1 virus on ice prior to injection.
2. Restrain mice with their stomach exposed and head pointed downward.
3. Aspirate 100–150 μl of virus into a sterile ½ cc Insulin syringe. Insert the needle into the peritoneal cavity in the lower right quadrant of the abdomen at an approximately 15–20° angle directing the needle towards the head. Prior to injection, aspirate the syringe to ensure no vital organs or blood vessels have been penetrated.

3.7 Monitoring of HIV-1 Viremia by qRT-PCR

HIV-1 plasma viral loads can be quantitatively measured by qRT-PCR [15, 20].

1. Collect two micro-hematocrit capillary tubes via tail vein bleed from each hu-mouse and place into microtainer tubes with EDTA and keep on ice (*see* **Note 19**).
2. Add 90 μl PBS without Ca^{2+} and Mg^{2+} to each tube. Centrifuge tubes at 1700 × *g* for 5 min at room temperature.
3. Transfer 150 μl of plasma from each tube to a nuclease free 1.5 ml microcentrifuge tube (*see* **Note 20**).
4. Extract RNA from the entire plasma sample following E.Z.N.A Viral RNA Kit protocol. Elute in 60 μl DEPC water. Store samples on ice for immediate qRT-PCR analysis or store at −80 °C.
5. Prepare qRT-PCR reaction mixes following the iTaq Universal Probes One-Step Kit for a 20 μl final reaction volume. In brief, iTaq Universal Probes Reaction Mix, HIV-1 LTR Forward Primer at a final concentration of 500 nM, HIV-1 LTR Reverse Primer at a final concentration of 500 nM, HIV-1 LTR Probe at a final concentration of 100 nM, Reverse Transcriptase, and water are mixed together on ice to create a master mix.
6. Pipette 15 μl of the master mix into a low 96-well clear plate and add 5 μl of the extracted RNA to each well and mix by carefully pipetting to achieve a final reaction volume of 20 μl.
7. HIV-1 LTR RNA based standards are used to quantify samples.
8. After the samples and standards are added to the PCR plate, cover the plate with a Microseal 'B' seal.
9. Run samples in a Bio-Rad C1000 Thermal Cycler with a CFX96 Real-Time System using the following thermocycler protocol: 10 min 50 °C Reverse Transcriptase step, 2 min

95 °C Taq activation and DNA denaturation step, 40 cycles of 10 s 95 °C denaturation and 30 s 64 °C anneal/extend/plate read.

10. After generating a standard curve with the known HIV-1 LTR standards, plasma samples can be analyzed for HIV-1 viral copies/ml of plasma.

3.8 Monitoring of CD4+ T Cell Levels by FACS

HIV-1 disease progression can be monitored by FACS analysis of CD4+ T cell levels [13–15].

1. Collect two heparin capillary tubes via tail vein bleed from each hu-mouse and place into a labeled 1.5 ml microcentrifuge tube at room temperature (*see* **Note 19**).
2. Add 7 μl of mouse blocking buffer to each sample, briefly vortex and incubate 10 min at room temperature.
3. Prepare an antibody master mix on ice with 2 μl per sample human anti-CD45 FITC, 4 μl per sample human anti-CD4 PE-Cy5 and 4 μl per sample human anti-CD3 PE. Add 10 μl of the master mix to each sample and gently vortex. Incubate samples for 30 min at room temperature in the dark.
4. Place 2 ml of 1× erythrocyte lysis buffer into labeled 15 ml conical vials.
5. When staining is complete, add 1 ml lysis buffer to each sample, pipette to mix, then transfer to corresponding 15 ml conical vial containing the additional 2 ml lysis buffer and vortex briefly to mix.
6. Incubate samples for 12 min at room temperature in the dark (*see* **Note 21**).
7. Add 11 ml of wash buffer to each vial, mix by inversion, and then centrifuge at 650 × *g* at room temperature for 5 min.
8. Aspirate supernatant and resuspend pellet in 1 ml wash buffer and transfer to a new labeled 1.5 ml microcentrifuge tube. Centrifuge at 450 × *g* at room temperature for 5 min.
9. Aspirate supernatant and resuspend pellet in appropriate volume of 1 % paraformaldehyde and transfer to 12 × 75 mm round-bottom tube for flow cytometry analysis.
10. Determine CD4+ T cell levels by calculating the CD4+ to CD3+ ratio of human CD45+ cell population (CD45 + CD3 + CD4+).

3.9 Antiretroviral Drug Preparation and Administration of Oral PrEP

Humanized mice can be used as a model for evaluating oral PrEP strategies [11, 21].

1. Calculate the mouse-equivalent of the human drug dose using the interspecies scaling factor 12.3 for a standard 20 × *g* RAG-hu mouse (*see* **Note 22**).

2. Pulverize the appropriate amount of the drug using mortar and pestle, and then dissolve in sterile 1× PBS.
3. Aliquot drug solution into 2 ml cryovials and store at −80 °C (*see* **Note 23**).
4. Resuspend drug aliquots after thawing and load individual dose into syringe for each mouse. Gavage the mice (oral administration) according to the dosing schedule. Wipe gavage needle with 70 % alcohol swab between individual mice.

3.10 Antiretroviral Drug Preparation and Administration of Topical PrEP

Humanized mice can be used as a model for evaluating topical PrEP strategies [22–24].

1. Dissolve Hydroxyethylcellulose (HEC) in sterile water to arrive at a 2.2 % final HEC concentration when prepared with antiretroviral drug(s). Sterilize HEC gel by autoclaving and cool to room temperature prior to addition of the drug(s) (*see* **Note 24**).
2. Prepare antiretroviral gels by dissolving appropriate amount of the drug in HEC.
3. Antiretroviral gels are applied as the first step in the intravaginal mucosal HIV-1 challenge protocol, described in Subheading 3.5. Prior to the HIV-1 mucosal challenge, apply gels (20–30 μl) intravaginally or intrarectally to the anesthetized mice using blunt-end needles. The time of the viral challenge after gel application is determined by the experimental protocol (*see* **Note 25**).

3.11 Pharmacokinetic (PK) Analysis-Blood and Tissue Sample Collection

Humanized mice allow for pharmacokinetic analysis of antiretroviral drugs in various tissues [11, 23].

1. PK analysis includes oral or topical application of antiretrovirals following Subheadings 3.9 and 3.10 and blood and tissue collections following the protocol below.
2. Euthanize the mouse using appropriate protocol for CO_2 euthanasia chamber and cervical dislocation to ensure proper euthanasia.
3. Open the thoracic cavity and collect the blood from the heart, using heparinized capillary tubes or micro-hematocrit capillary tubes in combination with microtainer tubes with EDTA, depending on the drug(s) being analyzed. Collection should be done efficiently and rapidly, to minimize the loss of blood collected due to coagulation.
4. Transfer collected blood to 1.5 ml microcentrifuge tubes, spin at 2700 × *g* for 10 min at 4 °C and collect the upper phase (blood plasma) for PK analysis. Certain protocols might require PK analysis in PBMCs, in which case cellular fraction should also be saved following plasma isolation. Both plasma

and cellular blood fractions should be stored at −80 °C immediately after isolation.

5. Isolate tissues based on the study design. For PK analysis, tissues to be isolated include vaginal, rectal and intestinal tissue. Vaginal tissue is collected as a whole and separated from the surrounding muscle and fat tissue. Rectal tissue is also collected as a whole, and proximal to it the intestinal tissue sample is collected. Both rectal and intestinal tissue samples must be properly cleaned of fecal matter with a quick saline flush, due to potential presence of the drug in the excrement.
6. Following tissue isolation, weigh the tissues and record the weight on the cryovial.
7. Snap freeze the tissue samples in liquid nitrogen within a couple of minutes from the time of collection. Minimize the time between tissue collections and snap freezing as much as possible and store the samples at −80 °C until HPLC analysis.

3.12 Pharmacodynamic (PD) Analysis

Humanized mice can be utilized to conduct pharmacodynamic analysis of antiretroviral drugs to determine their protective efficacy against HIV-1 challenge [21–26].

1. PD analysis includes oral or topical application of antiretrovirals, HIV-1 mucosal challenge (Day 0) and assays for HIV-1 infection analysis in humanized mice, following protocols in Subheadings 3.5 and 3.7–3.10.
2. Follow mice for 10–12 weeks post-challenge, for the detection of HIV-1 infection, indicated by positive viral load and CD4+ T cell depletion.

4 Notes

1. Working with hu-mice is a laborious process that requires patience, skill and proper training in animal handing, especially when working with live HIV-1. Experiments are time consuming and expensive, therefore careful planning is necessary.
2. HIV-1 infections of hu-mice involve handling live virus, thus posing exposure risks. Care must be taken by the researcher during all aspects of experimentation where live HIV-1 is present. Proper PPE must be worn at all times and contaminated materials need to be disposed of properly.
3. Prepare tissue digestive enzymes as 100× stock solutions: DNase I 32,200 Kunitz/ml, hyaluronidase 100 mg/ml, collagenase type IV 100 mg/ml, store at −20 °C.
4. De-gas CD34+ cell isolation buffer each time before use.
5. Cytokines are stable in media at 4 °C up to 14 days. The combination described here has been routinely used in our lab

with success; other labs may use a different combination of cytokines with similar success.

6. Tissue size as supplied can vary from 1 to 15 × *g*, yielding approximately 1×10^6–30×10^6 CD34+ cells. The final CD34+ cell yield is around 2–3 % of total cell count after Ficoll separation (*see* **step 14** in CD34+ cell isolation protocol—Subheading 3.1). CD34+ cells should be used within 24 h of isolation or frozen for later use. Up to 20 % cell death is expected following overnight incubation due to isolation procedure. If frozen CD34+ cells are to be used, allow for the cells to recover overnight prior to injection and increase CD34+ injection cell number to 0.5–1.0×10^6 per pup.
7. Autologous donor tissue must be used for BLT mice preparation.
8. All instruments are sterilized by autoclaving prior to use.
9. Ensure single cell suspension has been achieved prior to proceeding. Insufficient tissue digestion decreases CD34+ cell yield. Check sample under the light microscope prior to proceeding.
10. Prevent Ficoll and cell suspension from mixing by maintaining slow expulsion of the Ficoll onto the bottom of the tube. Mixing will cause insufficient gradient separation.
11. Obtain cell count using hemacytometer or cell counter. Depending on the size of pellet, dilute cell suspension with isolation buffer and then again with trypan blue. Final dilution range is typically between 1:20 and 1:40.
12. Resuspend CD34+ cells in appropriate media volume to yield 1×10^6 cells in 3–4 ml of media. Approximate media volume is based on the pre-column cell count and tissue size.
13. Use the unstained (negative) sample to set the Forward versus Side Scatter (FSC/SSC) gate each time.
14. On day 2 of CD34+ cell isolation, CD34+ cells not used for pup injections can be frozen down in stem cell cryopreservation media at 2×10^6 cells per milliliter in cryovials.
15. Mouse pups (1–4 days old) are preconditioned prior to CD34+ cell injection by sublethal irradiation at a dose of 350 rads. Pup injections should be performed within 24 h post-irradiation directly into the liver, which can be seen through the skin on the right side of the abdomen—presents as a dark red region (liver) above the belly which is usually filled with milk (white region). Carefully place the pup on its back and control it gently with the index and middle finger above and below the region for injection. Insert the insulin syringe very shallow (up to 1 mm) and holding the needle in the same position, inject the cells.

16. Administer Isoflurane by inhalation to anesthetize mouse. Eye ointment is applied in each eye during the anesthesia to protect against corneal ulceration.
17. Tissues are washed two to three times with sterile 1× PBS, placed into 2× AB/AM AIMs media and cut into small pieces (approximately 1 mm in length, which can fit into implant needle) using two scalpels. Tissues are loaded into the trochar creating a liver–thymus–liver sandwich.
18. After surgery, mice need to be closely monitored for the next 2 weeks for any signs of infection.
19. Screen mice at 12 weeks post engraftment. Prior to blood collection, allow mice to warm up under a heat lamp for 2 min. Watch for overheating by both feel and animal behavior. Ensure that blood collection for flow cytometry is done with heparinized capillary tubes and that blood for qRT-PCR is collected into non-heparinized capillaries and transferred to EDTA tubes.
20. Plasma samples can be frozen at −80 °C until processing. Plasma samples should be thawed on ice and brought up to room temperature just prior to RNA extraction.
21. It is necessary to achieve near complete erythrocyte lysis to obtain reliable results.
22. The allometric interspecies scaling factor of 12.3 is applied for the conversion of drug dosage from human to mouse (multiply the human dose by 12.3 to arrive at the equivalent mouse dose) [27]. Maximum volume for a single gavage in RAG-hu mice should not exceed 150 μl.
23. Drugs should be thawed on the day of gavages and only a single freeze/thaw cycle is allowed to ensure drug stability.
24. Final concentration of the HEC gel vehicle is 2.2 %. All antiretroviral-based gels should be prepared on the day of the experiment and only used that day.
25. Usual time for topical antiretroviral gel application is 1 h before the viral challenge.

Acknowledgements

Work reported here was supported by NIH grants RO1AI100845, R56AI095101, and RO1AI111891. We thank the NIH AIDS Research and Reference Reagents Program for supplying some of the reagents outlined in this protocol.

References

1. Akkina R (2013) New generation humanized mice for virus research: comparative aspects and future prospects. Virology 435:14–28. doi:10.1016/j.virol.2012.10.007
2. Brehm MA, Wiles MV, Greiner DL, Shultz LD (2014) Generation of improved humanized mouse models for human infectious diseases. J Immunol Methods 410C:3–17. doi:10.1016/j.jim.2014.02.011
3. Denton PW, Garcia JV (2011) Humanized mouse models of HIV infection. AIDS Rev 13(3):135–148
4. Garcia S, Freitas AA (2012) Humanized mice: current states and perspectives. Immunol Lett 146:1–7. doi:10.1016/j.imlet.2012.03.009
5. Maartens G, Celum C, Lewin SR (2014) HIV infection: epidemiology, pathogenesis, treatment, and prevention. Lancet 384:258–271. doi:10.1016/S0140-6736(14)60164-1
6. Romano J, Kashuba A, Becker S, Cummins J, Turpin J, Veronese F, Antiretroviral Pharmacology In HIVPTTP (2013) Pharmacokinetics and pharmacodynamics in HIV prevention; current status and future directions: a summary of the DAIDS and BMGF sponsored think tank on pharmacokinetics (PK)/pharmacodynamics (PD) in HIV prevention. AIDS Res Hum Retroviruses 29:1418–1427. doi:10.1089/AID.2013.0122
7. Baeten JM, Celum C (2013) Antiretroviral preexposure prophylaxis for HIV prevention. N Engl J Med 368:83–84
8. Hankins CA, Dybul MR (2013) The promise of pre-exposure prophylaxis with antiretroviral drugs to prevent HIV transmission: a review. Curr Opin HIV AIDS 8:50–58. doi:10.1097/COH.0b013e32835b809d
9. Veazey RS (2013) Animal models for microbicide safety and efficacy testing. Curr Opin HIV AIDS 8:295–303. doi:10.1097/COH.0b013e328361d096
10. Trezza CR, Kashuba AD (2014) Pharmacokinetics of antiretrovirals in genital secretions and anatomic sites of HIV transmission: implications for HIV prevention. Clin Pharmacokinet 53:611–624. doi:10.1007/s40262-014-0148-z
11. Veselinovic M, Yang KH, LeCureux J, Sykes C, Remling-Mulder L, Kashuba AD, Akkina R (2014) HIV pre-exposure prophylaxis: mucosal tissue drug distribution of RT inhibitor Tenofovir and entry inhibitor Maraviroc in a humanized mouse model. Virology 464–465:253–263. doi:10.1016/j.virol.2014.07.008
12. Akkina RK, Rosenblatt JD, Campbell AG, Chen IS, Zack JA (1994) Modeling human lymphoid precursor cell gene therapy in the SCID-hu mouse. Blood 84:1393–1398
13. Berges BK, Akkina SR, Folkvord JM, Connick E, Akkina R (2008) Mucosal transmission of R5 and X4 tropic HIV-1 via vaginal and rectal routes in humanized Rag2-/- gammac -/- (RAG-hu) mice. Virology 373:342–351. doi:10.1016/j.virol.2007.11.020
14. Berges BK, Akkina SR, Remling L, Akkina R (2010) Humanized Rag2(-/-)gammac(-/-) (RAG-hu) mice can sustain long-term chronic HIV-1 infection lasting more than a year. Virology 397:100–103. doi:10.1016/j.virol.2009.10.034
15. Berges BK, Wheat WH, Palmer BE, Connick E, Akkina R (2006) HIV-1 infection and CD4 T cell depletion in the humanized Rag2-/-gamma c-/- (RAG-hu) mouse model. Retrovirology 3:76. doi:10.1186/1742-4690-3-76
16. Lan P, Tonomura N, Shimizu A, Wang S, Yang YG (2006) Reconstitution of a functional human immune system in immunodeficient mice through combined human fetal thymus/liver and CD34+ cell transplantation. Blood 108:487–492. doi:10.1182/blood-2005-11-4388
17. Bristol GC, Gao LY, Zack JA (1997) Preparation and maintenance of SCID-hu mice for HIV research. Methods 12:343–347
18. Denton PW, Estes JD, Sun Z, Othieno FA, Wei BL, Wege AK, Powell DA, Payne D, Haase AT, Garcia JV (2008) Antiretroviral pre-exposure prophylaxis prevents vaginal transmission of HIV-1 in humanized BLT mice. PLoS Med 5:e16. doi:10.1371/journal.pmed.0050016
19. Denton PW, Garcia JV (2012) Mucosal HIV-1 transmission and prevention strategies in BLT humanized mice. Trends Microbiol 20:268–274. doi:10.1016/j.tim.2012.03.007
20. Rouet F, Ekouevi DK, Chaix ML, Burgard M, Inwoley A, Tony TD, Danel C, Anglaret X, Leroy V, Msellati P, Dabis F, Rouzioux C (2005) Transfer and evaluation of an automated, low-cost real-time reverse transcription-PCR test for diagnosis and monitoring of human immunodeficiency virus type 1 infection in a West African resource-limited setting. J Clin Microbiol 43:2709–2717. doi:10.1128/JCM.43.6.2709-2717.2005
21. Neff CP, Ndolo T, Tandon A, Habu Y, Akkina R (2010) Oral pre-exposure prophylaxis by anti-retrovirals raltegravir and maraviroc protects against HIV-1 vaginal transmission in a humanized mouse model. PLoS One 5:e15257. doi:10.1371/journal.pone.0015257
22. Neff CP, Kurisu T, Ndolo T, Fox K, Akkina R (2011) A topical microbicide gel formulation

of CCR5 antagonist maraviroc prevents HIV-1 vaginal transmission in humanized RAG-hu mice. PLoS One 6:e20209. doi:10.1371/journal.pone.0020209

23. Denton PW, Othieno F, Martinez-Torres F, Zou W, Krisko JF, Fleming E, Zein S, Powell DA, Wahl A, Kwak YT, Welch BD, Kay MS, Payne DA, Gallay P, Appella E, Estes JD, Lu M, Garcia JV (2011) One percent tenofovir applied topically to humanized BLT mice and used according to the CAPRISA 004 experimental design demonstrates partial protection from vaginal HIV infection, validating the BLT model for evaluation of new microbicide candidates. J Virol 85:7582–7593. doi:10.1128/JVI.00537-11
24. Chateau ML, Denton PW, Swanson MD, McGowan I, Garcia JV (2013) Rectal transmission of transmitted/founder HIV-1 is efficiently prevented by topical 1% tenofovir in BLT humanized mice. PLoS One 8:e60024. doi:10.1371/journal.pone.0060024
25. Denton PW, Long JM, Wietgrefe SW, Sykes C, Spagnuolo RA, Snyder OD, Perkey K, Archin NM, Choudhary SK, Yang K, Hudgens MG, Pastan I, Haase AT, Kashuba AD, Berger EA, Margolis DM, Garcia JV (2014) Targeted cytotoxic therapy kills persisting HIV infected cells during ART. PLoS Pathog 10:e1003872. doi:10.1371/journal.ppat.1003872
26. Choudhary SK, Rezk NL, Ince WL, Cheema M, Zhang L, Su L, Swanstrom R, Kashuba AD, Margolis DM (2009) Suppression of human immunodeficiency virus type 1 (HIV-1) viremia with reverse transcriptase and integrase inhibitors, CD4+ T-cell recovery, and viral rebound upon interruption of therapy in a new model for HIV treatment in the humanized Rag2-/-{gamma}c-/- mouse. J Virol 83:8254–8258. doi:10.1128/JVI.00580-09
27. Stoddart CA, Bales CA, Bare JC, Chkhenkeli G, Galkina SA, Kinkade AN, Moreno ME, Rivera JM, Ronquillo RE, Sloan B, Black PL (2007) Validation of the SCID-hu Thy/Liv mouse model with four classes of licensed antiretrovirals. PLoS One 2:e655. doi:10.1371/journal.pone.0000655

Chapter 15

High-Throughput Humanized Mouse Models for Evaluation of HIV-1 Therapeutics and Pathogenesis

Tynisha Thomas, Kieran Seay, Jian Hua Zheng, Cong Zhang, Christina Ochsenbauer, John C. Kappes, and Harris Goldstein

Abstract

Mice cannot be used as a model to evaluate HIV-1 therapeutics because they do not become infected by HIV-1 due to structural differences between several human and mouse proteins required for HIV-1 replication. This has limited their use for in vivo assessment of anti-HIV-1 therapeutics and the mechanism by which cofactors, such as illicit drug use accelerate HIV-1 replication and disease course in substance abusers. Here, we describe the development and application of two in vivo humanized mouse models that are highly sensitive and useful models for the in vivo evaluation of candidate anti-HIV therapeutics. The first model, hu-spl-PBMC-NSG mice, uses NOD-SCID IL2rγ$^{-/-}$ (NSG) mice intrasplenically injected with human peripheral blood mononuclear cells (PBMC) which develop productive splenic HIV-1 infection after intrasplenic inoculation with a replication-competent HIV-1 expressing *Renilla reniformis* luciferase (HIV-LucR) and enables investigators to use bioluminescence to visualize and quantitate the temporal effects of therapeutics on HIV-1 infection. The second model, hCD4/R5/cT1 mice, consists of transgenic mice carrying human CD4, CCR5 and cyclin T1 genes, which enables murine CD4-expressing cells to support HIV-1 entry, Tat-mediated LTR transcription and consequently develop productive infection. The hCD4/R5/cT1 mice develop disseminated infection of tissues including the spleen, small intestine, lymph nodes and lungs after intravenous injection with HIV-1-LucR. Because these mice can be infected with HIV-LucR expressing transmitted/founder and clade A/E and C Envs, these mouse models can also be used to evaluate the in vivo efficacy of broadly neutralizing antibodies and antibodies induced by candidate HIV-1 vaccines. Furthermore, because hCD4/R5/cT1 mice can be infected by vaginal inoculation with replication-competent HIV-1 expressing NanoLuc (HIV-nLucR)-, this mouse model can be used to evaluate the mechanisms by which substance abuse and other factors enhance mucosal transmission of HIV-1.

Key words HIV-1, Mouse model, Antiretroviral treatment

1 Introduction

HIV-1 does not infect mice because many restrictions prevent HIV-1 from replicating in mouse T cells and macrophages including the inability of HIV-1 to enter mouse cells because HIV's envelope

Tynisha Thomas and Kieran Seay have equally contributed to this chapter.

Vinayaka R. Prasad and Ganjam V. Kalpana (eds.), *HIV Protocols*, Methods in Molecular Biology, vol. 1354,
DOI 10.1007/978-1-4939-3046-3_15,

(Env) glycoprotein, gp120, does not engage mouse CD4 and CCR5 [1] and mouse cyclin T1 does not bind to HIV-1 Tat—preventing recruitment of transcription elongation factor b (P-TEFb) complex to the HIV-1 TAR RNA element and efficient transcription [2–4]. Humanized mouse models for HIV-1 investigation have been developed using severe combined immunodeficient (SCID) mice implanted under their renal capsules with human fetal thymus and liver [5], Rag2$^{-/-}\gamma_c^{-/-}$ mice injected with human hematopoietic stem cells (hHSC) [6, 7], NOD/SCID/IL2Rγ^{null} mice injected with hHSC [8] or NOD/SCID mice transplanted with human fetal thymus and liver tissue and injected with syngeneic hHSC [9]. However, the construction of these humanized mice is technically challenging and time-consuming as it requires access to fetal tissue or cord blood, may necessitate irradiation of the mice and requires several months of passage for sufficient engraftment of the bone marrow with human hematopoietic cells to populate the mouse lymphoid tissues with human leukocytes.

We have developed a new high throughput humanized mouse model, hu-spl-PBMC-NSG mice, that enables the in vivo monitoring of HIV-1 infection and the temporal response to treatment which employs highly immunodeficient NOD-SCID IL2r$\gamma^{-/-}$ (NSG) mice intrasplenically injected with human peripheral blood mononuclear cells (PBMC) (~10×10^6 PBMC). These mice can be immediately infected with HIV-1 and used for the evaluation of candidate therapeutics or to study pathogenesis. Using a donor leukopack containing ~5–10×10^8 PBMCs, over 50 mice can be generated from the same donor for experiments, which enables highly reproducible results. Continued localization of the human PBMCs to the spleen for several weeks enables visualization of the course of in vivo HIV infection and evaluation of candidate therapies over several weeks in lymphoid tissues, the predominant location for HIV-1 replication in HIV-1 infected individuals. HIV-1 infection in these mice can be monitored by in vivo visualization because they are infected with HIV-LucR reporter viruses over multiple cycles of replication [10], which correlates with active replication because of the short cellular half-life of LucR (~3 h) [11]. HIV-1 replication at different time points in a single mouse can be monitored by quantifying LucR activity in the splenocytes by imaging the bioluminescence signals in the spleens captured with an IVS Spectrum photon-detection imaging system at any time point, facilitating the study of anti-HIV therapeutic efficacy or the impact of drug abuse on HIV-1 replication. One can express a diverse range of HIV-1 Env sequences in HIV-LucR [10], allowing the use of this mouse model to evaluate antiviral efficacy of broadly neutralizing anti-HIV-1 antibodies and those induced by candidate HIV-1 vaccines to prevent intravenous HIV-1 infection.

A limitation of this humanized NSG mouse model is that each mouse must be constructed individually by intrasplenic injection

with PBMCs, the HIV-1 infection is limited to the spleen, and investigators must have access to the infrastructure required to house the mice in specialized biocontainment facilities to protect them from nosocomial infections. To circumvent this limitation, we developed a second mouse model constructed using a CD4 promoter/enhancer cassette to express human CD4, CCR5, and cyclin T1 transgenes in CD4 T lymphocytes, macrophages, and monocytes thereby overcoming the HIV-1 entry and Tat-dependent replication blocks in mouse cells. The hCD4/R5/cT1 mice carry the three human genes as tightly linked transgenes that are transmitted as a single allele, enabling efficient breeding and screening of the transgenic mice that develop acute systemic HIV-1 infection after intravenous injection of HIV-LucR. These mice provide the HIV-1 research community with a new in vivo infection model that is highly reproducible, inexpensive and easy to use for the evaluation of the inhibitory capacity of candidate antiretroviral therapeutics and the delineation of the mechanisms by which factors such as illicit drugs enhance HIV-1 replication and transmission.

2 Materials

2.1 Cells and Cell Culture

1. The TZM-bl reporter cell line was obtained through the NIH AIDS Reagent Program, Division of AIDS, NIAID, NIH: from Dr. John C. Kappes, Dr. Xiaoyun Wu, and Tranzyme Inc. [12].
2. 293T cells optimized for the production of lentivirus can be obtained from the ATCC.
3. Complete RPMI: RPMI 1640 supplemented with 10 % heat inactivated FCS, penicillin (100 U/ml), streptomycin (10 μg/ml), glutamine (2 mM) and HEPES (10 mM).
4. Fetal calf serum.
5. Cellular Isolation media: RPMI 1640 medium supplemented with penicillin (100 U/ml), streptomycin (100 mg/ml), L-glutamine (2 mM), 2-mercaptoethanol (5×10^{-5} M), sodium pyruvate (2 mM), HEPES buffer (20 mM), and 5 % heat-inactivated FCS.
6. Phytohemagglutinin (PHA).
7. Interleukin-2 (IL-2).

2.2 Mice

1. NOD-SCID IL2rγ$^{-/-}$ (NSG) mice are obtained from Jackson Laboratories (Bar Harbor, ME). If large numbers of mice are required, a local breeding colony can be established and maintained under biocontainment conditions as described [13].
2. hCD4/R5/cT1 mice are transgenic for the expression of the human CD4, CCR5 and cyclin T1 genes under the control of a

CD4 enhancer/promoter as described [14] and can be obtained from the authors. To completely link transmission of the human CD4 and CCR5 transgenes in the transgenic line, we constructed a vector expressing human CD4 and CCR5 as a single transcript linked by the self-cleaving picornavirus-derived 2A peptide sequence (CD4-2A-CCR5) as described [14]. To tightly link transmission of the human cyclinT1 gene with the CD4-2A-CCR5 transgene, the human cyclinT1 construct was microinjected together with the human CD4-2A-CCR5 construct into fertilized oocytes from C57BL/6 mice and transgenic hCD4/R5/cT1 mouse founders expressing these three genes and who displayed tight linkage transmission of human CD4, CCR5, and cyclin T1 genes to their progeny were identified. The hCD4/R5/cT1 mice carrying the transgenes are identified by screening tail DNA samples from the progeny by PCR analysis using human-specific internal primer sets for CD4 (5′ primer: 5′GTGGAGTTCAAAATAGACATCGTG3′, 3′ primer: 5′CAGCACCCACACCGCCTTCTCCCGCTT3′), CCR5 (5′ primer: 5′CACCTGCAGCTCTCATTTTCC3′, 3′ primer: 5′TTGTAGGGAGCCCAGAAGAG3′) and cyclin T1 (5′ primer: 5′TCCCAACTTCCAGTTGGTACT3′ 3′ primer: 5′TCCACCAGACCGAGGATTCAG3′).

2.3 Plasmids, Transfection, and Infection

1. The NL-LucR.T2A-Bal.ecto and NL-LucR.T2A-JR-CSF.ecto plasmids encode HIV-LucR whose Env protein sequences are derived from HIV-1_{Bal} or HIV-$1_{JR\text{-}CSF}$, respectively, and express the *Renilla reniformis* luciferase (LucR) gene linked with a "self-cleaving" 2A peptide to Nef and titered as previously described [10, 15].
2. The NLENG1i-Bal.ecto plasmid was derived from the *gfp-expressing* NLENG1-IRES clone [16–18] and was modified to encode the HIV-1 BaL *env* sequence [19] to produce HIV-GFP, replication competent HIV-1 which expresses all of the HIV genes including Nef R5 HIV-1_{Bal} envelope and the reporter gene GFP, after transfection of 293T cells [14].
3. DNA Transfection reagent Fugene 6.
4. DEAE-Dextran (10 μg/ml).

2.4 Measuring HIV-p24 Antigen Levels and Luciferase Reporter Gene Expression

1. A commercial enzyme-linked immunosorbent assay (ELISA) for quantifying HIV-1 p24 antigen concentration was obtained from Perkin-Elmer.
2. Commercial assays were used to measure the activities of firefly luciferase (Luciferase Assay System E1501), Renilla luciferase (Renilla Luciferase Assay System E2810), and NanoLuc luciferase (Nano-Glo™ Luciferase Assay N1120).
3. A Berthold LB-953 tube luminometer (Berthold Technologies, Bad Wildbad, Germany) was used to measure light emission

mediated by luciferase activity in cells after lysis and the addition of substrate.

4. RediJect Coelenterazine h (Caliper Life Sciences, Hopkinton, MA) is intravenously injected as a substrate for the detection of in vivo luciferase activity according to the manufacturer's instruction.
5. An IVIS Spectrum imager (Caliper Life Sciences) is used to quantify light emission mediated by in vivo luciferase activity.

3 Methods

3.1 Generation and Titration of Infectious HIV-1

Virus stocks are generated by transient transfection of 293T cells with the infectious molecular clone NL-LucR.T2A-JR-CSF.ecto, which generates HIV-LucR expressing the JR-CSF Env and the *Renilla reniformis* luciferase (LucR) gene as previously described [10, 15]. Briefly, 293T cells are transfected with the NL-LucR.T2A-JR-CSF.ecto plasmid. Sixty hours after transfection, culture supernatants containing the virus are harvested, centrifuged at $1800 \times g$ for 10 min to remove cells and cell debris, filtered through a 0.45 μm pore size filter and frozen at –80 °C. The concentration of the virus is determined by quantifying the HIV-1 p24 and the infectious titer of the virus is obtained by limiting dilution titration using a modification of a previously described technique [12]. Briefly, 96-well plates are seeded at a density of 5×10^5 TZM-bl cells/well 1 day prior to infection in Dulbecco-modified Eagle medium containing 10 % fetal bovine serum. The next day, media is removed and serial twofold dilutions of the viral stocks are added to the cultures in the presence of DEAE-dextran. After 2 days of culture at 37 °C in 5 % CO_2, the cell monolayers were washed with PBS, lysed with 1× firefly lysis buffer and frozen for at least 60 min at –80 °C. HIV-1-infection in each well is determined by measuring luciferase activity in 20 μl of cellular lysate incubated in 96-well white plates with substrate from the Firefly Luciferase Assay System. The lowest virus dilution that generated productive infection was used to calculate the number of HIV-1 infectious units/milliliter of the virus stock (*see* **Note 1**).

3.2 Construction and Use of Humanized Mice to Evaluate HIV-1 Infection and Therapeutic Efficacy

1. PBMCs are isolated from an HIV naïve donor by Hypaque-Ficoll density centrifugation and activated by culturing the cells (10^6 cells/ml) in Complete RPMI with PHA (3–4 μg/ml) and IL-2 (50 U/ml) for 24–48 h. The cells are then washed and resuspended (5×10^8 cells/ml) in sterile cold PBS.
2. NSG mice (10–12 weeks old) are anesthetized with ketamine (80–100 mg/kg) and xylazine (8–10 mg/kg) injected intraperitoneally, the skin is prepped with alcohol and betadine and a scissors is used to make an ~1 cm incision in the skin on the

left mouse flank to reveal the underlying peritoneal membrane. A forceps is inserted through the skin incision and is used to bluntly dissect and free the peritoneal membrane. While gripping the peritoneal membrane with a forceps, the peritoneal cavity is accessed by using a scissors to cut an ~0.5 cm incision in the membrane which is used as an opening to insert a second forceps into the peritoneal cavity to grasp and gently pull the splenic fat pad to exteriorize the entire spleen out of the peritoneal cavity. While applying traction on the spleen by continuing to pull on the fat pad attached to the spleen with the forceps, an insulin syringe using a 28 g needle is used to slowly inject 50 μl of the suspension of cells alone (~10^7 activated human PBMC cells) or cells mixed with LucR-HIV (~10^7 infectious units (IU)/ml) into the spleen. After injection, the spleen is gently slipped back through the incisions into the peritoneal cavity, the peritoneal membrane is closed with a 7-0 absorbable suture using a purse-string suture and the skin incision is closed with an AUTOCLIP (Clay Adams, Parsippany, NJ). All surgical procedures are performed in a laminar flow hood using sterile technique (*see* **Note 2**).

3. Mice may be treated with an intravenous injection of an antibody whose in vivo neutralizing capacity is being evaluated, immunostimulants being evaluated for in vivo anti-HIV activity or by treatment with antiretrovirals administered parenterally or in drinking water at a concentration that provides therapeutic levels of the drugs as described [13].
4. To determine the role of subpopulations of cells such as $CD8^+$ T cells, macrophages, dendritic cells or NK cells in the in vivo progression of HIV-1 infection or their role in facilitating the clinical response to therapeutics such as neutralizing antibodies, the PBMC can be selectively depleted of these subpopulation prior to injection into the mice by incubating the PBMCs with commercially available microbeads expressing the appropriate phenotypic marker, followed by immunomagnetic sorting.
5. The level of HIV-1 infection that develops in the transferred human PBMCs can be quantified in vivo at multiple time points after infection by bioluminescent imaging. The bioluminescence substrate RediJect Coelenterazine h is intravenously injected (5 μg) into the mice followed by measurement of the luciferase activity in the spleen by imaging the mice with the IVIS Spectrum imager using the Wizard bioluminescent selection tool for automatic wavelength and exposure detection. The bioluminescent and gray-scale images are overlaid using the LivingImage 4.0 software package and a pseudocolor image is created representing bioluminescence intensity, which can be quantified as photon counts/second.

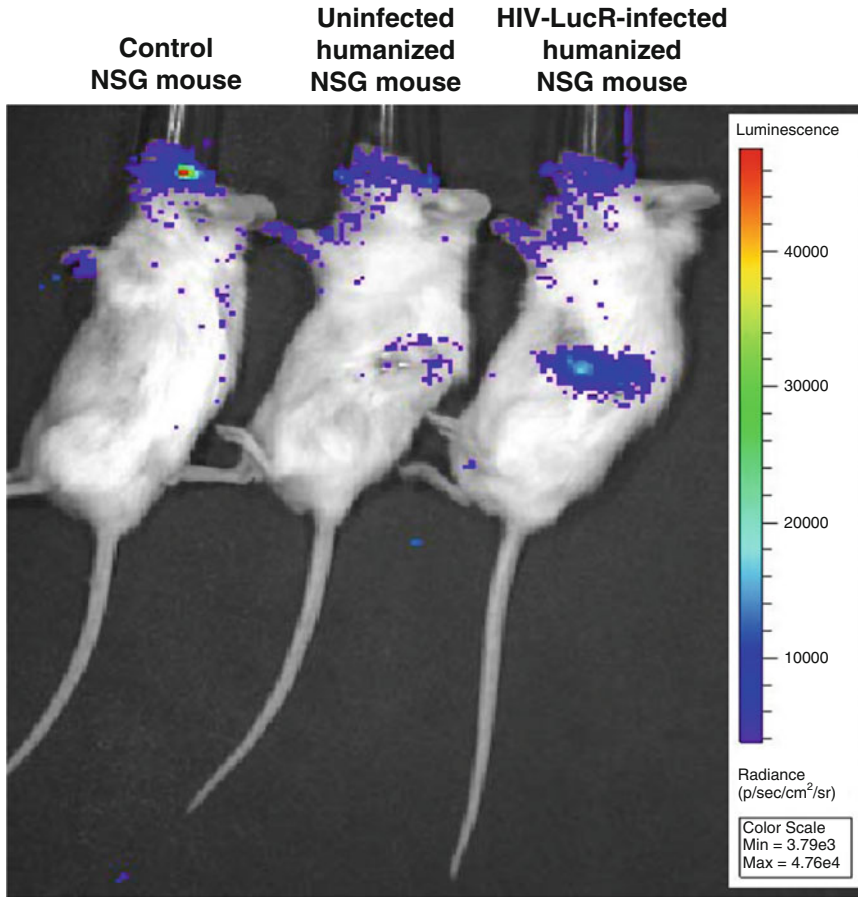

Fig. 1 In vivo imaging of HIV-1 infection humanized NSG mice. NSG mice were intrasplenically co-injected with human PBMC alone or with NL4-LucR.T2A-JRCSF.ecto HIV. Five days later the mice were evaluated for HIV-1 infection in the spleen by injecting with the bioluminescence substrate RediJect Coelenterazine h and capturing bioluminescent and gray-scale images of an NSG mouse, a humanized NSG mouse and a humanized NSG mouse intrasplenically injected with the NL4-LucR.T2A-JRCSF.ecto HIV with the IVIS Spectrum imager with bioluminescence intensity represented in a pseudocolor image indicating photon counts/second.

6. An example of using this model to visualize HIV-1 infection is shown in Fig. 1. An NSG mouse, NSG mouse intrasplenically injected with human PBMC and NSG mouse intrasplenically injected with human PBMC and 5 days post-infection with LucR were intravenously injected with the bioluminescence substrate and imaged as described above. While the control NSG mouse and uninfected humanized NSG mouse show some background signal, the HIV-LucR injected humanized NSG mouse displayed a clear and intense signal localized to the spleen, which could be readily quantitated.
7. At the conclusion of the study or if only a final endpoint is needed to the study, HIV-1 infection in the spleen is quantified by measuring the LucR activity in the mouse splenic lysates

using the Renilla Luciferase Assay System. Briefly, the cells are washed once with PBS containing Ca^{2+} and Mg^{2+}, lysed with 350 μl 1× *Renilla* luciferase assay lysis buffer and frozen at −70 °C. Samples are frozen and then thawed and 20 μl of each cell lysate is analyzed for LucR activity. Samples are analyzed using the luminometer programmed to inject 100 μl of Luciferase Assay Reagent per tube with an exposure time of 10 s/well. Results are reported as relative light units (RLU)/second (*see* **Note 3**).

3.3 Humanized NSG Mice for Studying the Acquisition and Dissemination of HIV Infection in the Lymphoid Environment and How It Is Affected by Substance Abuse

Abuse of recreational drugs such as opioids or meth are well-established risk-factors for HIV infection potentially due to the direct effect of these drugs on compromising host immunity and facilitating HIV replication [17, 20]. The availability of a mouse model populated with human cells capable of being infected with HIV-1 helps delineate the mechanisms by which opioids and meth facilitate the establishment of HIV infection after transmission.

1. PBMCs are isolated from an HIV naïve donor by Hypaque-Ficoll density centrifugation and resuspended (4×10^8 cells/ml) in sterile cold PBS.
2. NSG mice (8–10 weeks old) are anesthetized and injected intrasplenically with human PBMC cells alone in PBS or mixed with HIV-GFP (~10^7 infectious units (IU)/ml) in a total volume of 50 μl, as outlined in Subheading 2.3, **item 3** (*see* **Note 4**).
3. One day post-surgery, the mice are treated for six consecutive days by i.p injection with escalating doses of meth: 5 mg/kg for the first 3 days, 6 mg/kg for day 4, 6.5 mg/kg for day 5 and 7 mg/kg for day 6 [21] (*see* **Note 5**).
4. One can use this model to evaluate the impact of substance abuse on selective infection and depletion of human T cell subpopulations. Mice are infected with HIV-GFP which expresses the HIV-1_{Bal} envelope [14] and the phenotype of the HIV-infected and uninfected cells is determined by multiparameter flow cytometric analysis of GFP-positive and GFP-negative human T cells using an LSRII. HIV-infected cells can be identified by the expression of the GFP reporter gene and phenotypic markers for human T cells (for example, hCD45+). Results are analyzed using FlowJo software.
5. One can use this system to determine the in vivo capacity of meth treatment to increase HIV-1 infection and the impact of meth on the CD4 T cell subpopulations uninfected and infected with HIV-1. Humanized NSG mice constructed as described above are intrasplenically injected with unactivated human PBMCs (10×10^6) and HIV-GFP expressing the R5 HIV-1_{Bal} envelope. Although using unactivated PBMC to populate the mice leads to a low fraction of infected cells, we feel

that it reflects the in vivo physiological state of HIV-infected CD4+ T cells. One group of NSG mice should be untreated and the other group treated with daily i.p. doses of meth increasing from 5 to 7 mg/kg over a 6 day period. This dose of meth has been shown to provide serum levels similar to those detected in heavy users of meth [21]. On day 7, harvest spleens, isolate mononuclear cells and evaluate HIV infection by flow cytometry by quantifying the fraction of human CD45+ cells that express the GFP-reporter. Representative dot plots from this type of experiment (Fig. 2) show analysis of GFP expression by human CD45+ cells in the spleens from two HIV-infected mice treated with PBS (lower panels) and from two mice both HIV-infected and treated with meth (upper panels). There is a clear increase in the number of HIV-

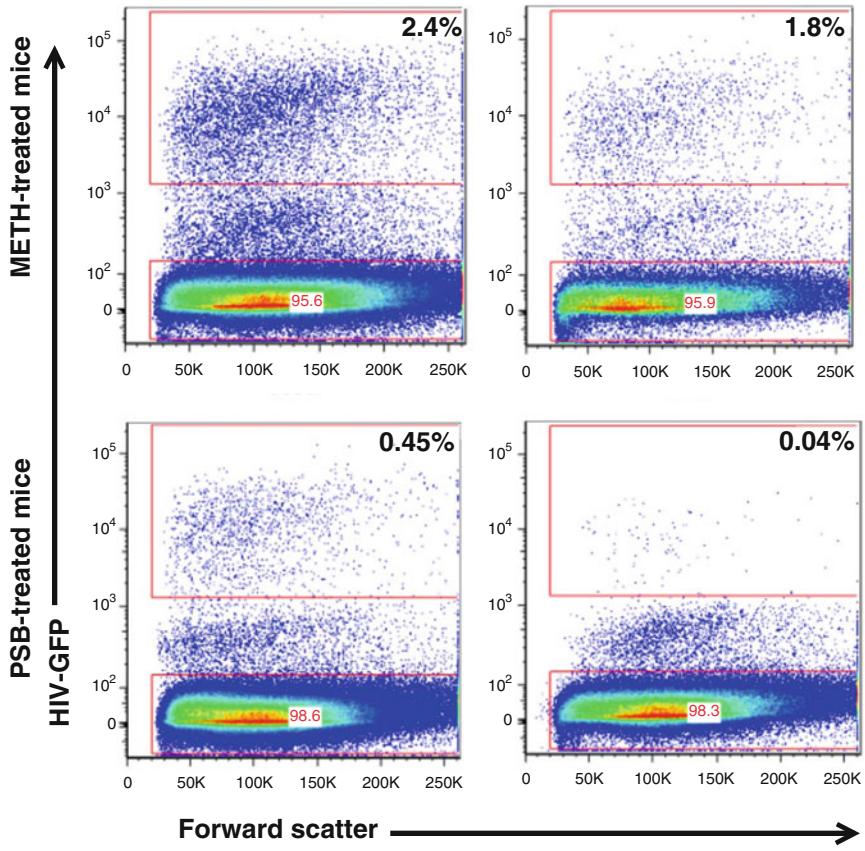

Fig. 2 Meth treatment increases in vivo HIV-1 infection in humanized mice. NSG mice were injected with HIV-GFP and one group ($n=5$ mice) was untreated and the other group ($n=5$ mice) was treated with 6 days of meth. Seven days after infection, HIV-1-infected cells in the spleen were isolated and analyzed by flow cytometry. Representative dot plots of GFP expression by splenocytes from two PBS-treated mice and two meth-treated mice after gating for expression of human CD45 are shown.

1-infected cells expressing the reporter GFP gene in the spleens of meth-treated mice (2.4 and 1.8 %) compared to control mice treated with PBS (0.45 and 0.04 %).

6. The effects of illicit drugs on HIV-1 infection can also be evaluated using humanized NSG mice infected with LucR. The temporal effects of illicit drugs on HIV-1 infection can be determined by monitoring the level of HIV-1 infection in the spleens in vivo at multiple time points after infection by bioluminescent imaging. At the conclusion of the study, HIV-1 infection in the spleen can be quantified by measuring the LucR activity in the mouse splenic lysates as described above and compared to that of untreated mice (Subheading 3.2).

3.4 Human CD4, CCR5, and Cyclin T1 Transgenic Mice (hCD4/R5/cT1 Mice) for Evaluation of Anti-HIV Therapeutics and the Impact of Substance Abuse on HIV-1 Infection and Transmission

1. *Intravenous HIV-1 infection of the mice.* To infect hCD4/R5/cT1 mice, HIV-LucR ($1–2 \times 10^7$ IU) is intravenously injected into the mice and 5–7 days later HIV-1 infection is quantified by measurement of LucR activity in splenic lysates as described above (Subheading 3.3). The effect on in vivo infection by neutralizing antibodies, antiretroviral therapy or immunomodulators can be evaluated by treating the mice and then comparing the level of infection in the spleen and other tissues to untreated mice [13].
2. *Use of hCD4/R5/cT1 mice to evaluate the effect of meth treatment on the acquisition of HIV-1 infection after intravenous inoculation.* One can use these mice to evaluate the effect of meth on the establishment of HIV-1 infection after intravenous injection, a frequent route of infection in illicit drug users [22]. CD4/R5/cT1 mice are untreated, or treated with meth starting 1 day prior to infection at a dosage of 1 mg/kg/day for 3 days, followed by a dosage of 2.5 mg/kg/day for 5 days until sacrificing the mice. Intravenously inject untreated and meth-treated mice with HIV-LucR expressing the BaL envelope ($1–2 \times 10^7$ IU) and determine the level of HIV-1 infection at day 7 after injection by quantification of LucR activity in splenic lysates as described above. In our own experiments, 7 days after inoculation, meth-treated hCD4/R5/cT1 mice exposed to HIV-1 by intravenous injection displayed fivefold higher levels of infection in their spleens as compared to untreated mice (Fig. 3). This indicated that meth was enhancing HIV-1 replication during the initial stages of acquisition and thereby facilitating HIV-1 transmission. This model should be helpful to investigators investigating the underlying mechanisms by which meth and other intravenously administered illicit drugs increase HIV-1 infection and acquisition after intravenous exposure.
3. *Use of hCD4/R5/cT1 mice to evaluate inhibitors of vaginal infection.* The capacity of microbicides, neutralizing antibodies, antiretroviral therapy or immunomodulators to inhibit or

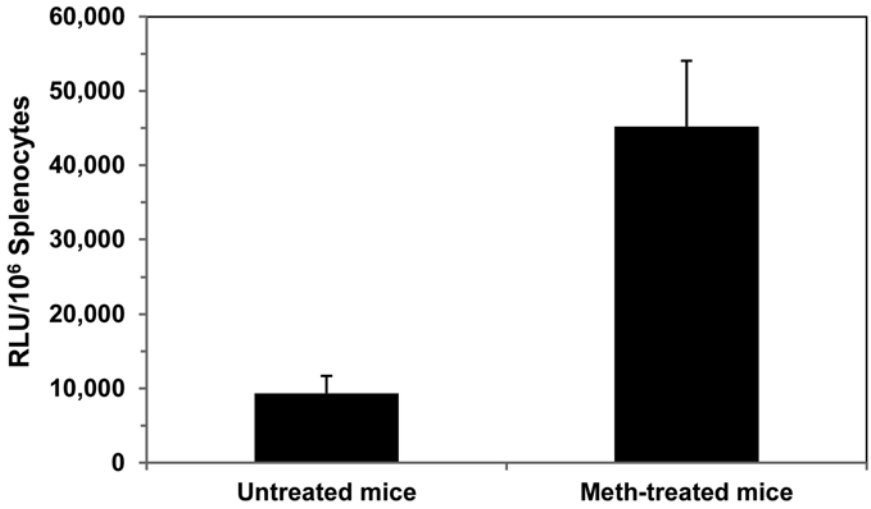

Fig. 3 Meth treatment increases in vivo HIV-1 infection in hCD4/R5/cT1 mice after intravenous inoculation. hCD4/R5/cT1 mice were either treated ($n=4$) or not treated ($n=4$) with meth starting 1 day prior to inoculation at a dose of 1 mg/kg/day. The mice were intravenously injected with NL-LucR.T2A-BaL.ecto ($1–2 \times 10^7$ IU) and the treated mice were continued on meth for two more days at a dose of 1 mg/kg/day and then increased to a dose of 2.5 mg/kg/day until the spleen was harvested. One week later, HIV-1 infection was quantified by measuring LucR activity in the splenic lysates. The average LucR activity for the mice in each group +/– STE is shown.

enhance in vivo HIV-1 infection by the mucosal route can be evaluated by comparing the level of infection after mucosal exposure to HIV-1 in the treated mice to that of the untreated mice. To examine vaginal transmission, treat hCD4/R5/cT1 mice with one subcutaneous injection with Depo-Provera (2.5 mg). Five days later, introduce HIV-nLuc (30 μl containing ~10^5 IU) atraumatically into the vagina by using a micropipette (*see* **Notes 6** and **7**). One week later, isolate vaginal mucosal leukocytes as described [23, 24]. Briefly, vaginal cells are isolated by mincing the excised vagina using a sterile scalpel in Cellular Isolation media. Digest the vaginal tissue in Cellular Isolation media with added 0.425 mg/ml collagenase D and 30 μg/ml DNase I for 45 min at 37 °C. Add EDTA to a final concentration of 5 mM to stop the enzymatic reaction. After removing cellular debris by passing the dissociated tissue suspension through sterile nylon mesh (70 μm pore size), harvest the lymphoid cell-enriched cells by centrifugation ($800 \times g$) for 10 min, wash twice in Hanks balanced salt solution (HBSS), and count after staining with trypan blue dye to identify viable cells. Quantify the HIV-1 infection of these cells by measuring the NanoLuc activity in the lysed cells using the Nano-Glo™ Luciferase Assay (Promega) according to manufacturer's instructions.

4. *Use of hCD4/R5/cT1 mice to evaluate the effect of meth treatment on the acquisition of HIV-1 infection after vaginal inoculation*. It is difficult to determine the relative contributions of the direct effect of illicit drugs on compromising host immunity and stimulating HIV replication from the behavior associated with illicit drug use such as increased promiscuity and risk taking behavior that cause the increased incidence of HIV infection [25]. These mice can be used to determine the effect of illicit drugs on the establishment of HIV-1 infection by mucosal exposure. As an example, we used this mouse model to evaluate the effect of meth on the establishment of HIV-1 infection after vaginal exposure. We described above the vaginal inoculation of hCD4/R5/cT1 mice by atraumatically introducing HIV-NanoLuc expressing the C.DU151.2 envelope (4.5×10^5 IU) into the vagina 5 days after subcutaneous injection with Depo-Provera (2.5 mg). In the same manner, treat one group of mice with meth 1 day prior to infection at a dose of 1 mg/kg/day for 3 days, followed by 2.5 mg/kg/day for 3 days until the mice are evaluated for HIV-1 infection. Five days after inoculation, isolate vaginal mucosal leukocytes from untreated mice and meth-treated mice and quantify HIV-1 infection by measuring NanoLuc activity in the cellular lysate as described above. In our own experience, mice infected intravaginally and treated with meth ($n = 4$ mice) display eight-fold higher levels of HIV-1 infection in cervical-vaginal mucosal leukocytes as compared to untreated mice ($n = 4$ mice) (Fig. 4). This indicates that meth enhances HIV-1 acquisition through the mucosal route and may thereby facilitate HIV-1 transmission. This model should be helpful to investigate the underlying mechanisms by which meth increases HIV-1 infection and acquisition after mucosal exposure.

4 Notes

1. Low passage, healthy 293T cells are critical for quality virus production. Overgrown cells or cells that float during the process will not produce high titer virus. Freeze virus in small, "1-time thaw" working aliquots to avoid multiple freeze–thaws as this will compromise the virus titer.
2. It is important not to grasp the spleen directly with the forceps as this may lacerate the spleen and cause fatal bleeding. Instead, the fat tissue that is attached to the spleen should be grasped and used to pull the spleen out of the peritoneal cavity and to apply traction to the spleen for intrasplenic injections. After the human PBMC's have been injected into the spleen, the spleen is closely scrutinized to ensure that the cells are properly injected by observing that the spleen swells during the injection, that

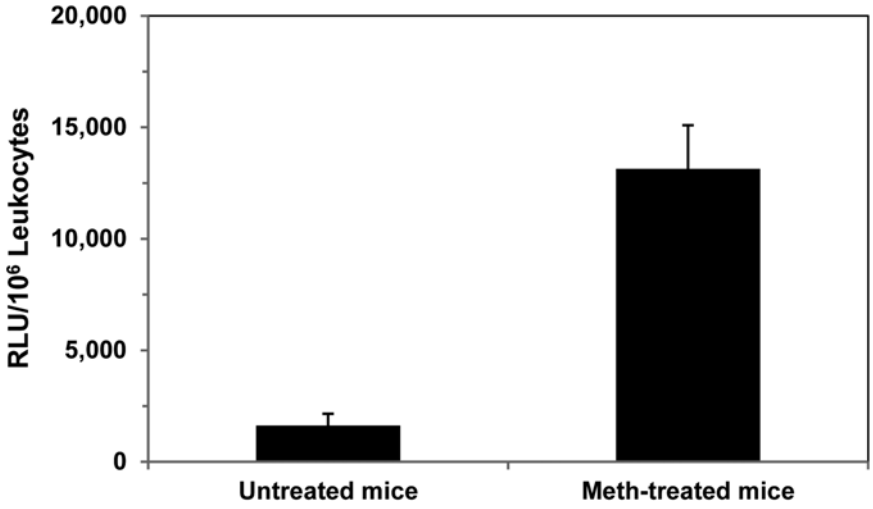

Fig. 4 Meth treatment increases in vivo HIV-1 infection in hCD4/R5/cT1 mice after intravaginal inoculation. hCD4/R5/cT1 mice were either treated ($n=4$) or untreated ($n=4$) with meth starting 1 day prior to infection at a dosage of 1 mg/kg/day. The mice were vaginally infected by atraumatically introducing HIV-1-NLucR (NL-nLuc.T2A-C.DU151.2.ecto) (4.5×10^5 IU) into the vagina 5 days after subcutaneous injection with Depo-Provera (2.5 mg). The treated mice were continued on meth for two more days at a dosage of 1 mg/kg/day and then increased to a dose of 2.5 mg/kg/day. Five days after infection, vaginal mucosal leukocytes were isolated from untreated mice ($n=4$) and treated mice ($n=4$) and NanoLuc activity in the cellular lysate was determined. The average NanoLuc activity for the mice in each group +/− STE is shown.

the cellular suspension diffuses into the splenic tissue and that no cell suspension leaks out.

3. We have found the Berthold LB-953 tube luminometer provides extremely sensitive and reproducible detection of light with extremely low background counts and a high dynamic range as compared to microplate-based readers. According to the manufacturer, the sensitivity of detection of firefly luciferase is 1 zmol (~600 molecules) and the dynamic range is greater than 6 orders of magnitude.
4. It has been observed that male mice tolerate meth better than female mice. When using female mice, the minimum weight recommended is ≥30 g (0.030 kg). The minimum weight recommended for male mice is ≥28 g (0.028 kg). Mice should be monitored daily to monitor dose tolerance.
5. Mice should be dosed around the same time daily to ensure comfort and increase the rate of survival, especially at higher doses.
6. To atraumatically infect the mice, we hold the mice upside down and carefully and gently insert the micropipette tip less than 10 mm into the vaginal canal and slowly pipette out the virus. Insertion of the micropipette tip further than 10 mm into the vaginal canal could damage the intravaginal epithelial

layer thus facilitating HIV transmission directly through the blood and not by the mucosal route.

7. It is important to keep the mouse completely vertical for 5 min after microinjecting the NanoLuc HIV-1 virus into the vaginal canal to prevent the loss of virus through leakage.

References

1. Deng H, Liu R, Ellmeier W, Choe S, Unutmaz D, Burkhart M, Di Marzio P, Marmon S, Sutton RE, Hill CM, Davis CB, Peiper SC, Schall TJ, Littman DR, Landau NR (1996) Identification of a major co-receptor for primary isolates of HIV-1. Nature 381:661–666
2. Imai K, Asamitsu K, Victoriano AF, Cueno ME, Fujinaga K, Okamoto T (2009) Cyclin T1 stabilizes expression levels of HIV-1 Tat in cells. FEBS J 276:7124–7133
3. Wei P, Garber ME, Fang SM, Fischer WH, Jones KA (1998) A novel CDK9-associated C-type cyclin interacts directly with HIV-1 Tat and mediates its high-affinity, loop-specific binding to TAR RNA. Cell 92:451–462
4. Wimmer J, Fujinaga K, Taube R, Cujec TP, Zhu Y, Peng J, Price DH, Peterlin BM (1999) Interactions between Tat and TAR and human immunodeficiency virus replication are facilitated by human cyclin T1 but not cyclins T2a or T2b. Virology 255:182–189
5. McCune JM, Namikawa R, Kaneshima H, Shultz LD, Lieberman M, Weissman IL (1988) The SCID-hu mouse: murine model for the analysis of human hematolymphoid differentiation and function. Science 241:1632–1639
6. Baenziger S, Tussiwand R, Schlaepfer E, Mazzucchelli L, Heikenwalder M, Kurrer MO, Behnke S, Frey J, Oxenius A, Joller H, Aguzzi A, Manz MG, Speck RF (2006) Disseminated and sustained HIV infection in CD34+ cord blood cell-transplanted Rag2-/-gamma c-/- mice. Proc Natl Acad Sci U S A 103:15951–15956
7. Ince WL, Zhang L, Jiang Q, Arrildt K, Su L, Swanstrom R (2010) Evolution of the HIV-1 env gene in the Rag2-/- gammaC-/- humanized mouse model. J Virol 84:2740–2752
8. Watanabe S, Ohta S, Yajima M, Terashima K, Ito M, Mugishima H, Fujiwara S, Shimizu K, Honda M, Shimizu N, Yamamoto N (2007) Humanized NOD/SCID/IL2Rgamma(null) mice transplanted with hematopoietic stem cells under nonmyeloablative conditions show prolonged life spans and allow detailed analysis of human immunodeficiency virus type 1 pathogenesis. J Virol 81:13259–13264
9. Wege AK, Melkus MW, Denton PW, Estes JD, Garcia JV (2008) Functional and phenotypic characterization of the humanized BLT mouse model. Curr Top Microbiol Immunol 324: 149–165
10. Edmonds TG, Ding H, Yuan X, Wei Q, Smith KS, Conway JA, Wieczorek L, Brown B, Polonis V, West JT, Montefiori DC, Kappes JC, Ochsenbauer C (2010) Replication competent molecular clones of HIV-1 expressing Renilla luciferase facilitate the analysis of antibody inhibition in PBMC. Virology 408:1–13
11. Miyawaki A (2007) Bringing bioluminescence into the picture. Nat Methods 4:616–617
12. Wei X, Decker JM, Liu H, Zhang Z, Arani RB, Kilby JM, Saag MS, Wu X, Shaw GM, Kappes JC (2002) Emergence of resistant human immunodeficiency virus type 1 in patients receiving fusion inhibitor (T-20) monotherapy. Antimicrob Agents Chemother 46:1896–1905
13. Sango K, Joseph A, Patel M, Osiecki K, Dutta M, Goldstein H (2010) Highly active antiretroviral therapy potently suppresses HIV infection in humanized Rag2-/-gammac-/- mice. AIDS Res Hum Retrovir 26:735–746
14. Seay K, Qi X, Zheng JH, Zhang C, Chen K, Dutta M, Deneroff K, Ochsenbauer C, Kappes JC, Littman DR, Goldstein H (2013) Mice transgenic for CD4-specific human CD4, CCR5 and cyclin T1 expression: a new model for investigating HIV-1 transmission and treatment efficacy. PLoS One 8:e63537
15. Ochsenbauer C, Kappes JC (2009) New virologic reagents for neutralizing antibody assays. Curr Opin HIV AIDS 4:418–425
16. Gelderblom HC, Vatakis DN, Burke SA, Lawrie SD, Bristol GC, Levy DN (2008) Viral complementation allows HIV-1 replication without integration. Retrovirology 5:60
17. Kutsch O, Benveniste EN, Shaw GM, Levy DN (2002) Direct and quantitative single-cell analysis of human immunodeficiency virus type 1 reactivation from latency. J Virol 76:8776–8786
18. Levy DN, Aldrovandi GM, Kutsch O, Shaw GM (2004) Dynamics of HIV-1 recombination in its natural target cells. Proc Natl Acad Sci U S A 101:4204–4209
19. Ochiel DO, Ochsenbauer C, Kappes JC, Ghosh M, Fahey JV, Wira CR (2010) Uterine epithelial cell regulation of DC-SIGN expression

inhibits transmitted/founder HIV-1 trans infection by immature dendritic cells. PLoS One 5:e14306

20. Wang X, Ho WZ (2011) Drugs of abuse and HIV infection/replication: implications for mother-fetus transmission. Life Sci 88:972–979
21. Toussi SS, Joseph A, Zheng JH, Dutta M, Santambrogio L, Goldstein H (2009) Short communication: methamphetamine treatment increases in vitro and in vivo HIV replication. AIDS Res Hum Retrovir 25:1117–1121
22. Suntharasamai P, Martin M, Vanichseni S, van Griensven F, Mock PA, Pitisuttithum P, Tappero JW, Sangkum U, Kitayaporn D, Gurwith M, Choopanya K (2009) Factors associated with incarceration and incident human immunodeficiency virus (HIV) infection among injection drug users participating in an HIV vaccine trial in Bangkok, Thailand, 1999-2003. Addiction 104:235–242
23. Fidel PL Jr, Wolf NA, KuKuruga MA (1996) T lymphocytes in the murine vaginal mucosa are phenotypically distinct from those in the periphery. Infect Immun 64:3793–3799
24. Iijima N, Mattei LM, Iwasaki A (2011) Recruited inflammatory monocytes stimulate antiviral Th1 immunity in infected tissue. Proc Natl Acad Sci U S A 108:284–289
25. Patterson TL, Semple SJ, Staines H, Lozada R, Orozovich P, Bucardo J, Philbin MM, Pu M, Fraga M, Amaro H, Torre Ade L, Martinez G, Magis-Rodriguez C, Strathdee SA (2008) Prevalence and correlates of HIV infection among female sex workers in 2 Mexico-US border cities. J Infect Dis 197: 728–732

Part V

Tools to Study HIV-1 Latency and Pathogenesis

Chapter 16

Measuring the Frequency of Latent HIV-1 in Resting CD4+ T Cells Using a Limiting Dilution Coculture Assay

Gregory M. Laird, Daniel I.S. Rosenbloom, Jun Lai, Robert F. Siliciano, and Janet D. Siliciano

Abstract

Combination antiretroviral therapy (cART) can reduce HIV-1 viremia to clinically undetectable levels. However, replication competent virus persists in a long-lived latent reservoir in resting, memory CD4+ T cells. The latent reservoir in resting CD4+ T cells is the major barrier to curing HIV-1 infection. The recent case of the Berlin patient has suggested that it may be possible to cure HIV-1 infection in certain situations. As efforts to cure HIV-1 infection progress, it will become critical to measure the latent reservoir in patients participating in clinical trials of eradication strategies. Our laboratory has developed a limiting dilution virus outgrowth assay that can be used to demonstrate the presence and persistence of latent HIV-1 in patients. Here we describe both the original and a simplified version of the quantitative virus outgrowth assay (QVOA) to measure the frequency of latently infected resting CD4+ T cells with replication competent provirus in patients on suppressive cART.

Key words HIV-1, Latency, Latent reservoir, Viral outgrowth assay

1 Introduction

Despite the success of cART in halting viral replication in HIV-1 infected patients, the infection cannot be cured by cART alone. HIV-1 can persist in a latent state that arises as a consequence of the normal physiology of CD4+ T cells. HIV-1 preferentially infects activated CD4+ lymphoblasts in infected individuals. While the majority of infected CD4+ T lymphoblasts die rapidly [1, 2], a small fraction of these infected cells are not eliminated and transition to a resting state to persist as long-lived memory CD4+ T cells [3–7]. In these infected resting CD4+ T cells, key transcription factors and other cellular components necessary for efficient HIV-1 gene expression are down regulated while additional chromatin changes occur that may further hinder HIV-1 transcription (reviewed previously [8–10]). As a result, HIV-1 gene expression largely ceases in these resting CD4+ T cells [11], and the integrated

Vinayaka R. Prasad and Ganjam V. Kalpana (eds.), *HIV Protocols*, Methods in Molecular Biology, vol. 1354,
DOI 10.1007/978-1-4939-3046-3_16,

replication competent HIV-1 provirus persists in a latent state. Notably, HIV-1 latency can be reversed by activation of latently infected CD4+ T cells [3–7], though recent work suggests that a single round of T cell activation may not reactivate all latent proviruses [12, 13]. HIV-1 latency is defined by the absence of productive HIV-1 gene expression or virion production.

Latent infection of resting CD4+ T cells was demonstrated definitively for the first time using a limiting dilution viral outgrowth assay [6, 14], which has since been modified [15] and is presented in this protocol (Fig. 1). Using this assay, we have shown that latently infected cells are rare; latent proviruses can be found at a frequency of roughly 1 per 10^6 resting CD4+ T cells [3, 6]. Longitudinal studies have examined the decay rate of the HIV-1 latent reservoir using this viral outgrowth assay [16, 17], and have concluded that the slow decay rate of the reservoir (~44 months) guarantees lifetime persistence of the virus, even in

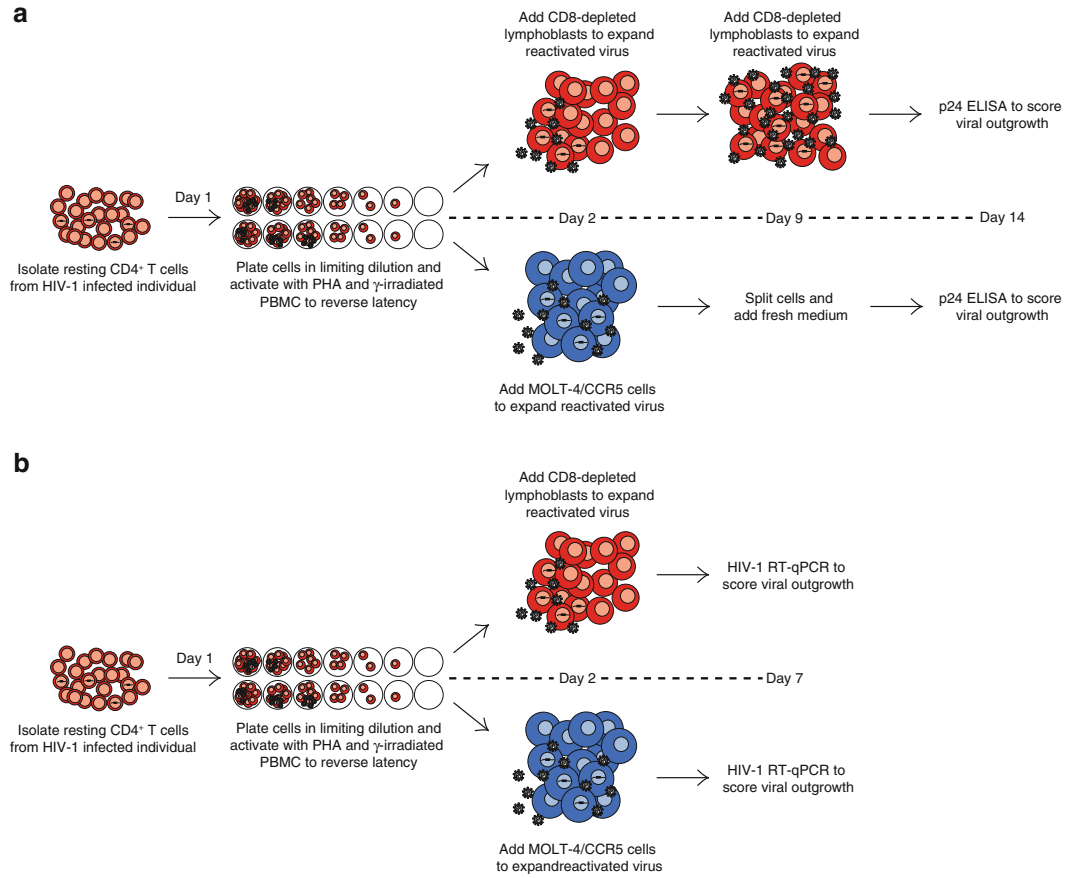

Fig. 1 Schematic of limiting dilution viral outgrowth assay. The limiting dilution viral outgrowth assay can be performed using either MOLT-4/CCR5 cells or healthy donor lymphoblasts as target cells, with outgrowth scored (**a**) after 14 days using HIV-1 p24 ELISA or (**b**) after 7 days using HIV-1 RT-qPCR.

infected individuals on suppressive antiretroviral therapy [16–18]. This virus outgrowth assay (VOA) remains a gold-standard measurement in the study of HIV-1 latency [19] and provides a definitive minimal estimate of the frequency of latently infected cells.

The quantitative viral outgrowth assay begins with the isolation of resting $CD4^+$ T cells from HIV-1 infected donors who have been on suppressive antiretroviral therapy for at least 6 months [20]. During the initial 6 months of suppression on cART, the frequency of latently infected cells identified by the quantitative viral outgrowth assay will decay significantly due to the clearance of a more labile population of cells containing non-integrated HIV-1 proviruses. This labile state is distinct from the stable post-integration latency, which is being quantitated in the VOA in suppressed patients. Resting $CD4^+$ T cells are plated in limiting dilution and activated by the mitogen phytohemagglutinin (PHA) in the presence of irradiated allogeneic peripheral blood mononuclear cells (PBMCs). T cell activation reverses latency in these cells, resulting in the production of replication-competent HIV-1. This step results in 100 % of the resting cells to become activated as assessed by CFSE dilution and cell surface expression of activation markers (CD25 and CD69) [12]. Virus released into the supernatant of the culture wells is amplified by adding target cells that support robust replication. Outgrowth of replication-competent virus is then scored, and maximum likelihood statistics are used to determine the frequency of latent infection. This frequency is presented as infectious units per million input resting $CD4^+$ cells, or IUPM. Typically, HIV-1-infected individuals on suppressive antiretroviral therapy will have IUPM values between 0.03 and 3, with an average approximately 1 IUPM [6, 16, 18]. In this protocol, two target cell options for virus expansion are presented: MOLT-4/CCR5 T cell line or CD8-depleted lymphoblasts from uninfected donors [15]. Both target cells support robust replication of CCR5-tropic and CXCR4-tropic HIV-1 (*see* **Note 1**). The use of the MOLT-4/CCR5 cell line is advantageous because these cells can be continuously cultured in large numbers without the need for additional uninfected donors or cell purification and activation. Additionally, the MOLT-4/CCR5 target cells need only be added once in the assay. Finally, the use of the MOLT-4/CCR5 cell line reduces variability inherent to uninfected donor derived target cells. Two readout measures have been developed to score the outgrowth of replication-competent HIV-1: p24 ELISA or RT-qPCR [15]. Both assays quantitate the frequency of cells with replication competent virus. The p24 ELISA is used on day 14 of the assay to score outgrowth (Fig. 1a), while the RT-qPCR assay can be used as early as day 7 of the assay [15] (Fig. 1b). An outgrowth-scoring assay can be chosen on the basis of time constraints and instrument availability.

2 Materials

2.1 General Laboratory Equipment

1. Humidified CO_2 tissue culture incubator.
2. Centrifuges, both refrigerated and non-refrigerated, with rotors and adaptors for 15 and 50 mL conical tubes.
3. Light microscope and hemocytometer (or other cell counter).
4. BSL-2 tissue culture facility.

2.2 Cell Culture Media

1. Wash medium (WM): phosphate-buffered saline, pH 7.4, 2 % heat-inactivated newborn calf serum, 0.1 % dextrose; 1× penicillin–streptomycin, 12 mM HEPES, pH 7.2.
2. Super T cell medium (STCM): RPMI 1640 with GlutaMAX, 10 % heat-inactivated fetal bovine serum, 100 U/mL recombinant human IL-2, 1× penicillin–streptomycin, 1 % T cell growth factor (TCGF, see below for preparation).
3. T Cell Growth Factor (TCGF): human serum type AB, phorbol 12-myristate 13-acetate (PMA), colorimetric MTS cell proliferation assay, phytohemagglutinin (PHA), leukopaks from HIV negative donors.

2.3 Preparation of Human Primary Resting CD4+ T Cells

1. Ficoll-Paque Plus.
2. Heparin, sodium salt: dissolve in phosphate buffered saline, filter-sterilize and store aliquots at 4 °C.
3. Human $CD4^+$ T Cell Isolation Kit.
4. Human CD25 MicroBeads.
5. Human CD69 MicroBead Kit II.
6. Human Anti-HLA-DR MicroBeads.
7. LS columns.
8. MACS Separator magnets and stand.
9. Cs-source irradiator (e.g., Gammacell 3000 Elan; MDS Nordion).
10. Recombinant human IL-2, 22×10^6 U/vial.
11. Phytohemagglutinin (PHA); 150 μg/mL in WM, filter-sterilized; stock solution stored at −80 °C.
12. 1× penicillin–streptomycin.
13. Heat-inactivated fetal bovine serum (*see* **Note 2**).
14. RPMI 1640 medium with GlutaMAX.

2.4 Preparation of Human CD8+ Depleted Lymphoblasts (If Chosen as Target Cell)

1. Dynabeads CD8 magnetic beads.
2. Dynal MPC-1 magnetic particle concentrator.

2.5 Culturing MOLT-4/CCR5 Cells (If Chosen as Target Cell)

1. MOLT-4/CCR5 T cell line.
2. Geneticin (G418).
3. Spinner flasks may be used for high-density MOLT-4/CCR5 culture (*see* **Note 3**).

2.6 Tissue Culture Materials

1. Multi-well 6-well and 24-well sterile tissue culture plates with flat bottom and low evaporation lid.
2. T-25, T-75, and T-150 sterile tissue culture flasks.

2.7 Endpoint Measurement of Viral Outgrowth

1. For p24 ELISA endpoint at 14 days:
   (a) Alliance HIV-1 P24 ANTIGEN ELISA Kit.
   (b) Absorbance microplate reader capable of reading absorbance at 490 nm with >600 nm reference.
2. For RT-qPCR endpoint at 7 days:
   (a) Appropriate reagents for RNA isolation from supernatant.
   (b) cDNA synthesis reagents.
   (c) Quantitative PCR Reagents.
      - Master mix (e.g., TaqMan Fast Advanced Master Mix, Life Technologies).
      - Forward Primer VQA forward (5′ → 3′): CAGATGCTGCATATAAGCAGCTG
      - VQA reverse (5′ → 3′):
      - TTTTTTTTTTTTTTTTTTTTTTTTGAAGCAC
      - VQA probe (5′ → 3′; 6′FAM/MGB):
      - CCTGTACTGGGTCTCTCTGG
      - pVQA plasmid standard (NIH AIDS Reagent Program, catalog # 12666).
   (d) Thermal cycler for cDNA synthesis.
   (e) Quantitative PCR machine.

2.8 Reagent Preparation

2.8.1 Preparation of T Cell Growth Factor (TCGF)

1. Need four HIV negative leukopaks.
2. Isolate PBMCs from leukopaks by Ficoll density centrifugation using manufacturer's protocol. Perform cell washes with WM. Approximately $1–2 \times 10^9$ PBMCs are obtained from four leukopaks.
3. Resuspend isolated PBMCs at ~5×10^6 mL^{-1} and culture together in RPMI + 2.5 % heat-inactivated human AB serum with 1× penicillin–streptomycin in T150 tissue culture flasks. A total of 70 mL medium is added to each flask. Incubate overnight in a humidified incubator at 37 °C, 5 % CO_2 with flasks lying flat.

4. The following day, activate cells by adding PHA to a final concentration of 2 μg/mL and PMA to a final concentration of 5 ng/mL. Incubate 4 h at 37 °C, 5 % CO_2.
5. After incubation, carefully remove the culture supernatant from the activated cells and gently wash settled PBMCs with 15 mL pre-warmed WM. Repeat this wash to remove residual PHA and PMA. Take care not to lose cells attached to the surface of the culture flasks.
6. Add back 70 mL fresh RPMI + 2.5 % heat-inactivated human AB serum + 1× penicillin–streptomycin. Incubate for 40 h at 37 °C, 5 % CO_2.
7. Collect the conditioned culture supernatant from the activated PBMCs and transfer to fresh conical tubes. Centrifuge at ~400 × *g* for 10 min to remove cell debris.
8. Filter–sterilize the conditioned culture supernatant using a 0.45 μm filter unit. This filtered culture medium is now TCGF.
9. Freeze the TCGF in 40 mL aliquots at −20 °C.

2.8.2 Testing TCGF

1. The efficacy of TCGF can be evaluated using a colorimetric MTS cell proliferation assay to determine the minimum amount of TCGF needed to stimulate maximal cell growth. For first-batch analysis, add TCGF to RPMI + 10 % FBS + 100 U/mL IL-2, titrating the TCGF concentration from ~1 to 2 % of the final volume. For later batches of TCGF, compare new batch to previous batch of TCGF. This test media will be used in the evaluation of TCGF.
2. Isolated PBMCs from healthy donors by Ficoll density centrifugation. Approximately 3×10^5 PBMCs are needed per TCGF titration.
3. In triplicate, add 1×10^5 PBMCs in 100 μL of each test media titration to a 96 well plate. Incubate for 2–3 days at 37 °C, 5 % CO_2. Plate can be loosely wrapped in foil to minimize evaporation.
4. Perform the colorimetric MTS proliferation assay to determine the minimal TCGF percentage required to stimulate maximal proliferation without assay saturation. Typically, no more than 2 % TCGF is required to stimulate maximal proliferation (*see* **Note 4**).

2.8.3 Preparation of T Cell Medium (STCM)

RPMI + 10 % heat-inactivated FBS, 100 U/mL IL-2, TCGF (percent determined by cell proliferation assay; *see* **Note 4**) and 1× penicillin–streptomycin.

2.8.4 Culturing MOLT-4/CCR5 Cell Line

MOLT-4/CCR5 is a T-lymphoblastoid cell line established by Baba and colleagues [21]. These cells were derived from the $CD4^+CXCR4^+$ MOLT-4 cell line, and have been engineered to

stably express CCR5. The cell line can be obtained from the NIH AIDS Reagent program and should be cultured in suspension in RPMI + 10 % FBS + 0.2 mg/mL G-418. For increased culture density, cells are cultured in spinner flasks. G418 should not be included during the coculture of MOLT-4/CCR5 cells with patient resting $CD4^+$ T cells.

3 Methods

3.1 Selection of Target Cells for Virus Expansion

If MOLT-4/CCR5 cells are chosen, ensure that ~75×10^6 cells are available for each standard assay.

If CD8-depleted lymphoblasts are chosen, draw 120 mL blood from a healthy, HIV negative donor into heparinized syringes 1 day before beginning the assay. Syringes should be inverted several times to prevent clotting of blood. Isolate PBMCs by Ficoll density centrifugation, resuspend washed PBMCs in 30 mL STCM in a T75 tissue culture flask and add PHA to a final concentration of 0.5 μg/mL. Incubate flask at 37 °C, 5 % CO_2 for 2–3 days so that cells are fully permissive for infection when added to the cultures. After this incubation, $CD8^+$ T cells must be removed by negative bead depletion, described below (*see* **Note 5**).

3.2 Day 1: Resting $CD4^+$ T Cell Isolation, Plating, and Activation

3.2.1 Preparation of Irradiated Allogeneic PBMC from Healthy Donors

1. Draw 120–180 mL blood from healthy donor into heparinized syringes.
2. Inactivate by γ irradiation (5000R in Cs-source irradiator).
3. Isolate PBMCs by Ficoll density centrifugation per manufacturer's protocols. Perform cell washes with WM.
4. Resuspend washed PBMCs in STCM at 2.5×10^6 cells/mL.
5. Add PHA at a final concentration of 1 μg/mL. Place irradiated, washed PBMCs on ice immediately to prevent cell adhesion to tube. Store on ice until use. Irradiated PBMCs must be used the same day that they are prepared.

3.2.2 Isolation and Purification of Resting $CD4^+$ T-Cells from HIV-1 Infected Donor

1. Isolate patient PBMCs from 120 to 180 mL freshly donated whole blood by Ficoll density gradient centrifugation per manufacturer's protocols. Perform cell washes with WM.
2. Isolate $CD4^+$ T-cells by depletion using Miltenyi $CD4^+$ T-cell isolation kit.
   (a) Resuspend PBMCs in 4 μL of cold WM per 10^6 cells.
   (b) Add 1 μL of supplied $CD4^+$ T-cell Biotin-Antibody Cocktail per 10^6 cells.
   (c) Incubate cells for 5 min at 4 °C.
   (d) Add 3 μL of additional cold wash media and 2 μL of supplied $CD4^+$ T-cell MicroBead Cocktail per 10^6 cells.

(e) Incubate cells for 10 min at 4 °C.

(f) Apply cells to pre-equilibrated Miltenyi LS columns (10^8 cells per column) in no less than 500 µL per 10^8 cells and collect flow-through, containing negatively selected $CD4^+$ T-cells.

(g) Wash each column once with 3 mL cold wash media. Count the eluted $CD4^+$ T-cells and pellet cells.

3. Isolate resting $CD4^+$ T-cells ($CD69^-$, $CD25^-$, HLA-DR^-) by depletion.

(a) Resuspend $CD4^+$ T-cells in 9 µL cold WM per 10^6 cells.

(b) Add 1 µL of anti-CD69 Biotin antibody per 10^6 cells.

(c) Incubate for 15 min at 4 °C.

(d) Add 2 µL of anti-Biotin MicroBeads, 2 µL of CD25 MicroBeads II, and 2 µL of anti-HLA-DR MicroBeads per 10^6 cells.

(e) Incubate for 15 min at 4 °C.

(f) Add 1–2 mL cold WM per 10^8 cells to wash and pellet cells.

(g) Resuspend cells in cold WM, apply to a pre-equilibrated LS column (10^8 cells per column) in no less than 500 µL per 10^8 cells, and collect flow-through.

(h) Wash each column three times with 3 mL cold WM. Count the eluted resting $CD4^+$ T-cells and pellet cells. Resuspend in STCM at 1×10^6 mL^{-1}. This is considered tube A in the dilution series outlined below.

*3.2.3 Setting Up Well Dilutions and Plating Cells (See **Note 6**)*

1. Set up serial dilutions of resting $CD4^+$ cells in STCM (Table 1). Note that the maximum number of resting $CD4^+$ cells in one well of a 6-well plate is 1×10^6. For maximum activation, a tenfold excess of irradiated allogeneic PBMCs from uninfected donors are added to each well.
2. Plate setup: leave one empty well between each well containing patient cells to avoid inter-well contamination.

(a) 6-well plate: two wells with 1×10^6 resting $CD4^+$ T cells each (A1 and A2) (*see* Table 2).

(b) 24-well plates: label plates 1 and 2, label wells B1–G1 and B2–G2 (*see* Table 3).

3. Stack plates, two plates per stack, wrap loosely in aluminum foil to minimize evaporation, and incubate at 37 °C, 5 % CO_2.

3.3 Day 2 of the Assay: Addition of HIV-1 Target Cells (See Note 7)

1. The PHA must be removed from the culture to minimize toxicity. Thus, carefully remove 6 mL of culture media without removing cells from the large A wells and 1.5 mL of culture media from the small B–G wells and discard. Replace with an

Table 1
Resting CD4+ T cell dilution scheme

Tube	Volume of previous tube (μL)	Volume of STCM (mL)	Cell concentration	Volume into culture assay (mL)
A	–	–	1×10^6 cells/mL	1
B	550	2.2	200,000 cells/mL	1
C	550	2.2	40,000 cells/mL	1
D	550	2.2	8000 cells/mL	1
E	550	2.2	1600 cells/mL	1
F	550	2.2	320 cells/mL	1

Table 2
Setup of large volume assay wells

Well	Volume resting CD4+ cells from appropriate tube (mL)	Volume irradiated PBMC + PHA (mL)	Volume STCM (mL)	Final volume (mL)
A1	1 (1×10^6 cells)	4 (1×10^7 cells)	3	8
A2	1 (1×10^6 cells)	4 (1×10^7 cells)	3	8

Table 3
Setup of small volume assay wells

Well	Volume resting CD4+ cells from appropriate tube (mL)	Volume irradiated PBMC + PHA (mL)	Volume STCM (mL)	Final volume (mL)
B1	1 (200,000 cells)	1 (2.5×10^6 cells)	–	2
C1	1 (40,000 cells)	1 (2.5×10^6 cells)	–	2
D1	1 (8000 cells)	1 (2.5×10^6 cells)	–	2
E1	1 (1600 cells)	1 (2.5×10^6 cells)	–	2
F1	1 (320 cells)	1 (2.5×10^6 cells)	–	2
G1	–	1 (2.5×10^6 cells)	1	2

equal volume of fresh, STCM. Incubate at 37 °C, 5 % CO_2 for at least 3 h to allow cells to settle.

2. (a) If MOLT-4/CCR5 cells are chosen as the target cells:

   Carefully remove 6 mL of culture media from the large A wells and 1.5 mL of culture media from the small B–G wells

and discard. Replace with and equal volume of MOLT-4/CCR5 cells in fresh, pre-warmed STCM at 6.7×10^5 cells/mL. Incubate at 37 °C, 5 % CO_2.

(b) If CD8-depleted lymphoblasts are chosen as the target cells:

Using CD8 DynaBeads, deplete $CD8^+$ T cells from healthy donor PBMCs activated prior to beginning the assay. Resuspend these CD8 depleted lymphoblasts in fresh, pre-warmed STCM at 6.7×10^5 cells/mL. Next, carefully remove 6 mL of culture media from the large A wells and 1.5 mL of culture media from the small B–G wells and discard. Replace with and equal volume of the resuspended CD8-depleted lymphoblasts. Incubate at 37 °C, 5 % CO_2.

3.3.1 Selection of Endpoint HIV-1 Outgrowth-Scoring Assay

The remaining steps in the viral outgrowth assay protocol are dependent on which outgrowth-scoring assay is chosen.

3.4 Using RT-qPCR to Score Viral Outgrowth

*3.4.1 Day 5 of the Assay: Splitting of the Cultures (Optional, See **Note 8**)*

1. Carefully remove 3 mL culture media from the large A wells and 0.75 mL culture media from the small B–G wells and discard.
2. Thoroughly resuspend the cells.
3. Remove 1 mL of the resuspended cells from the large A wells and 0.25 mL of the resuspended cells from the small B–G wells and discard.
4. Replace with an equal volume of fresh STCM. Incubate at 37 °C, 5 % CO_2.

3.4.2 Day 7 of the Assay: RNA Isolation, cDNA Synthesis, and qPCR for Outgrowth

1. Perform RNA isolation on maximum amount of supernatant per the manufacturer's instructions.
2. Perform cDNA synthesis per the manufacturer's instructions.
3. Perform qPCR per the manufacturer's instructions. Using a 20 μL TaqMan Fast Advanced PCR Master Mix, we employ the following conditions: 10 μM each primer, 250 nM probe, 6 μL cDNA template; T_m 60 °C.

3.5 Using p24 ELISA to Score Viral Outgrowth

3.5.1 Day 5 of the Assay: Split the Cultures

1. Carefully remove 3 mL culture media from the large A wells and 0.75 mL culture media from the small B–G wells and discard.
2. Thoroughly resuspend the cells.
3. Remove 1 mL of the resuspended cells from the large A wells and 0.25 mL of the resuspended cells from the small B–G wells and discard.

4. Replace with an equal volume of fresh. Incubate at 37 °C, 5 % CO_2.

3.5.2 Day 7 of the Assay (If $CD8^+$ Depleted Lymphoblasts Were Chosen as HIV-1 Target Cells)

Draw 120 mL blood from a healthy, HIV-negative donor into heparinized syringes 1 day before setting up the virus outgrowth assay. Syringes should be inverted several times to prevent clotting of blood. Isolate PBMCs by Ficoll density centrifugation, resuspend washed PBMCs in 30 mL STCM in a T75 tissue culture flask and add PHA to a final concentration of 0.5 μg/mL. Incubate flask at 37 °C, 5 % CO_2 for 2–3 days. After this incubation, $CD8^+$ T cells are then removed by negative bead depletion as described below (*see* **Note 5**).

3.5.3 Day 9 of the Assay: Split the Cultures

1. Thoroughly resuspend the cells.
2. Carefully remove 4 mL culture media from the large A wells and 1 mL culture media from the small B–G wells and discard.
3. (a) If MOLT-4/CCR5 cells were chosen as HIV-1 target cells: replace media with an equal volume of fresh STCM. Incubate at 37 °C, 5 % CO_2.

   (b) If CD8-depleted lymphoblasts were chosen as HIV-1 target cells:

   Using CD8 DynaBeads, deplete $CD8^+$ T cells from healthy donor PBMCs activated on day 7 of the assay. Resuspend these CD8 depleted lymphoblasts in fresh STCM at 1×10^6 cells/mL. Next, carefully remove 4 mL of culture media from the large A wells and 1 mL of culture media from the small B–G wells and discard. Replace with and equal volume of the resuspended CD8-depleted lymphoblasts. Incubate at 37 °C, 5 % CO_2.

3.5.4 Day 14 of the Assay: Assay Wells for Viral Outgrowth

1. Perform p24 ELISA per the manufacturer's protocol using 200 μL of culture supernatant from each well (*see* **Note 7**). Score wells positive for outgrowth if absorbance in the well is greater than or equal to that of the lowest p24 standard (3.25 pg/mL).

3.6 Calculation of the Frequency of Latent HIV-1 Infection

Infection frequency can be determined by maximum likelihood statistics. An application to perform this calculation is provided online at http://silicianolab.johnshopkins.edu. Input required for this calculation is:

1. Size of each well in assay (# of input cells from infected individuals).
2. Number of wells of each size.

3. Number of wells of each size which were scored positive for outgrowth.

The application uses this input to compute the following:

1. Estimated infection frequency in IUPM.
2. 95 % confidence interval for infection frequency.
3. *p*-value of the null hypothesis that each cell collected in the assay represents an independent and identically distributed binary random variable (infected/not infected).
4. "Most likely data": Prediction of the most likely scoring of positive/negative wells that would result if the assay were performed again under the same conditions. Often, but not always, the same as the scoring inputted.

Any deviation from the limiting dilution described in Table 1 above, should be accurately recorded; e.g., use of a single well containing five million cells should be recorded as such, and not as five separate wells containing one million cells each. The statistical analysis is valid for any collection of well sizes.

The *p*-value is calculated using a χ^2 test. A very small *p*-value suggests that one or more assumptions underlying the analysis fail to hold: either cross-well contamination occurred, well sizes were recorded incorrectly, or cells were not sufficiently mixed such that each well contains a representative sample.

There are two special cases in which the interpretation of program output differs from that given above:

1. All-positive wells. In this case, analysis cannot proceed and smaller wells must be used.
2. All-negative wells. In this case, the maximum likelihood estimate of infection frequency is formally zero. To provide a meaningful estimate, the application instead uses Bayesian analysis, assuming a uniform prior distribution of infection frequency on the interval [0, 1]. The median of the posterior distribution is provided as the primary estimate (i.e., this value exceeds the true frequency with 50 % probability). Additionally, a 95 % upper bound is provided (i.e., this value exceeds the true frequency with 95 % probability). Neither a lower bound nor a *p*-value is meaningful in this case.

4 Notes

1. Target cells can be chosen on the basis of availability to the investigator. Many labs do not have access to large numbers of healthy donor lymphoblasts. MOLT-4/CCR5 cells provide an effective alternative.

2. Multiple lots of fetal bovine serum should be tested to find the lot that will support optimal growth of human T cells. A proliferation assay with PBMCs and media containing the 10 % FBS to be tested is set up as follows. Cells are resuspended in STCM at a concentration of 1×10^6 cells/mL. Using a multichannel pipette, 0.1 mL of cells is added to the wells of a 96-well round bottom tissue culture plate. Next, add 0.1 mL of RPMI 1640 + 20 % of the FBS lots to be tested to each well. Plate in triplicate for each lot of FBS to be tested. Incubate plate at 37 °C with 5 % CO_2 for 48 h. A colorimetric assay (Promega CellTiter 96 Aqueous One Solution Cell Proliferation Assay) is used to quantitate the number of proliferating cells according to the manufacturer's protocol.
3. Cells in the spinner flask should only be kept in culture for 6–8 weeks after which time a new stock vial should be thawed. Typically, when cells are initially obtained, they are grown to sufficient quantity in a spinner flask. Aliquots of 20×10^6 cells are frozen viably in 90 % fetal bovine serum/10 % DMSO in a prechilled Mr. Frosty cooler, placed at −80 °C for a day and then transferred to liquid nitrogen for long-term storage.
4. At higher concentrations of TCGF exceeding the typical 2 % v/v, the introduction of higher amounts of chemokines from activated $CD8^+$ T cells in the preparation can inhibit viral replication.
5. Depletion of activated $CD8^+$ T cells is required for efficient viral replication as chemokines secreted by $CD8^+$ T cells can inhibit viral replication.
6. The resting $CD4^+$ T cell dilutions recommended in this protocol can be modified. If additional resting $CD4^+$ T cells are available, additional "A wells" can be plated to increase both the sensitivity and precision of the assay. The IUPM can be calculated for any dilution scheme using the calculator described in this protocol.
7. After addition of PHA on day 1 of the assay, it is imperative that a different pipette tip or serological pipette be used for each well to avoid cross contamination of wells with either virus or cells from another well.
8. When RT-qPCR is used as a readout for viral outgrowth on day 7 of the assay, the splitting of cells and addition of fresh media on day 5 may be optional. Splitting on day 5 may decrease the concentration of replicating HIV-1 virions detected on day 7. However, the cell split and fresh media addition may support better cell viability.

References

1. Ho DD, Neumann AU, Perelson AS, Chen W, Leonard JM, Markowitz M (1995) Rapid turnover of plasma virions and CD4 lymphocytes in HIV-1 infection. Nature 373:123–126. doi:10.1038/373123a0
2. Wei X, Ghosh SK, Taylor ME, Johnson VA, Emini EA, Deutsch P, Lifson JD, Bonhoeffer S, Nowak MA, Hahn BH et al (1995) Viral dynamics in human immunodeficiency virus type 1 infection. Nature 373:117–122. doi:10.1038/373117a0
3. Chun TW, Carruth L, Finzi D, Shen X, DiGiuseppe JA, Taylor H, Hermankova M, Chadwick K, Margolick J, Quinn TC, Kuo YH, Brookmeyer R, Zeiger MA, Barditch-Crovo P, Siliciano RF (1997) Quantification of latent tissue reservoirs and total body viral load in HIV-1 infection. Nature 387:183–188. doi:10.1038/387183a0
4. Chun TW, Finzi D, Margolick J, Chadwick K, Schwartz D, Siliciano RF (1995) In vivo fate of HIV-1-infected T cells: quantitative analysis of the transition to stable latency. Nat Med 1:1284–1290
5. Chun TW, Stuyver L, Mizell SB, Ehler LA, Mican JA, Baseler M, Lloyd AL, Nowak MA, Fauci AS (1997) Presence of an inducible HIV-1 latent reservoir during highly active antiretroviral therapy. Proc Natl Acad Sci U S A 94:13193–13197
6. Finzi D, Hermankova M, Pierson T, Carruth LM, Buck C, Chaisson RE, Quinn TC, Chadwick K, Margolick J, Brookmeyer R, Gallant J, Markowitz M, Ho DD, Richman DD, Siliciano RF (1997) Identification of a reservoir for HIV-1 in patients on highly active antiretroviral therapy. Science 278:1295–1300
7. Wong JK, Hezareh M, Gunthard HF, Havlir DV, Ignacio CC, Spina CA, Richman DD (1997) Recovery of replication-competent HIV despite prolonged suppression of plasma viremia. Science 278:1291–1295
8. Karn J (2011) The molecular biology of HIV latency: breaking and restoring the Tat-dependent transcriptional circuit. Curr Opin HIV AIDS 6:4–11. doi:10.1097/COH.0b013e328340ffbb
9. Richman DD, Margolis DM, Delaney M, Greene WC, Hazuda D, Pomerantz RJ (2009) The challenge of finding a cure for HIV infection. Science 323:1304–1307. doi:10.1126/science.1165706
10. Siliciano RF, Greene WC (2011) HIV latency. Cold Spring Harb Perspect Med 1:a007096. doi:10.1101/cshperspect.a007096
11. Hermankova M, Siliciano JD, Zhou Y, Monie D, Chadwick K, Margolick JB, Quinn TC, Siliciano RF (2003) Analysis of human immunodeficiency virus type 1 gene expression in latently infected resting CD4+ T lymphocytes in vivo. J Virol 77:7383–7392
12. Ho YC, Shan L, Hosmane NN, Wang J, Laskey SB, Rosenbloom DI, Lai J, Blankson JN, Siliciano JD, Siliciano RF (2013) Replication-competent noninduced proviruses in the latent reservoir increase barrier to HIV-1 cure. Cell 155:540–551. doi:10.1016/j.cell.2013.09.020
13. Cillo AR, Sobolewski MD, Bosch RJ, Fyne E, Piatak M Jr, Coffin JM, Mellors JW (2014) Quantification of HIV-1 latency reversal in resting CD4+ T cells from patients on suppressive antiretroviral therapy. Proc Natl Acad Sci U S A 111:7078. doi:10.1073/pnas.1402873111
14. Siliciano JD, Siliciano RF (2005) Enhanced culture assay for detection and quantitation of latently infected, resting CD4+ T-cells carrying replication-competent virus in HIV-1-infected individuals. Methods Mol Biol 304:3–15. doi:10.1385/1-59259-907-9:003
15. Laird GM, Eisele EE, Rabi SA, Lai J, Chioma S, Blankson JN, Siliciano JD, Siliciano RF (2013) Rapid quantification of the latent reservoir for HIV-1 using a viral outgrowth assay. PLoS Path 9:e1003398. doi:10.1371/journal.ppat.1003398
16. Siliciano JD, Kajdas J, Finzi D, Quinn TC, Chadwick K, Margolick JB, Kovacs C, Gange SJ, Siliciano RF (2003) Long-term follow-up studies confirm the stability of the latent reservoir for HIV-1 in resting CD4+ T cells. Nat Med 9:727–728. doi:10.1038/nm880
17. Strain MC, Gunthard HF, Havlir DV, Ignacio CC, Smith DM, Leigh-Brown AJ, Macaranas TR, Lam RY, Daly OA, Fischer M, Opravil M, Levine H, Bacheler L, Spina CA, Richman DD, Wong JK (2003) Heterogeneous clearance rates of long-lived lymphocytes infected with HIV: intrinsic stability predicts lifelong persistence. Proc Natl Acad Sci U S A 100:4819–4824. doi:10.1073/pnas.0736332100
18. Finzi D, Blankson J, Siliciano JD, Margolick JB, Chadwick K, Pierson T, Smith K, Lisziewicz

J, Lori F, Flexner C, Quinn TC, Chaisson RE, Rosenberg E, Walker B, Gange S, Gallant J, Siliciano RF (1999) Latent infection of CD4+ T cells provides a mechanism for lifelong persistence of HIV-1, even in patients on effective combination therapy. Nat Med 5:512–517. doi:10.1038/8394

19. Eriksson S, Graf EH, Dahl V, Strain MC, Yukl SA, Lysenko ES, Bosch RJ, Lai J, Chioma S, Emad F, Abdel-Mohsen M, Hoh R, Hecht F, Hunt P, Somsouk M, Wong J, Johnston R, Siliciano RF, Richman DD, O'Doherty U, Palmer S, Deeks SG, Siliciano JD (2013) Comparative analysis of measures of viral reservoirs in HIV-1 eradication studies. PLoS Path 9:e1003174. doi:10.1371/journal.ppat.1003174
20. Blankson JN, Finzi D, Pierson TC, Sabundayo BP, Chadwick K, Margolick JB, Quinn TC, Siliciano RF (2000) Biphasic decay of latently infected CD4+ T cells in acute human immunodeficiency virus type 1 infection. J Infect Dis 182:1636–1642. doi:10.1086/317615
21. Baba M, Miyake H, Okamoto M, Iizawa Y, Okonogi K (2000) Establishment of a CCR5-expressing T-lymphoblastoid cell line highly susceptible to R5 HIV type 1. AIDS Res Hum Retroviruses 16:935–941. doi:10.1089/08892220050058344

Chapter 17

LGIT In Vitro Latency Model in Primary and T Cell Lines to Test HIV-1 Reactivation Compounds

Ulrike Jung, Mayumi Takahashi, John J. Rossi, and John C. Burnett

Abstract

Persistent latent HIV-1 reservoirs pose a major barrier for combinatorial antiretroviral therapy (cART) to achieve eradication of the virus. A variety of mechanisms likely contribute to HIV-1 persistence, including establishment of post-integration latency in resting CD4+ T-lymphocytes, the proliferation of these latently infected cells, and the induced or spontaneous reactivation of latent virus. To elucidate the mechanisms of latency and to investigate therapeutic strategies for reactivating and purging the latent reservoir, investigators have developed in vitro models of HIV-1 latency using primary CD4+ T-lymphocytes and CD4+ T-cell lines. Several types of in vitro latency models range from replication-competent to single-round, replication-deficient viruses exhibiting different degrees of viral genomic deletion. Working under the hypothesis that HIV-1 post-integration latency is directly linked to HIV-1 promoter activity, which can be obscured by additional proteins expressed during replication, we focus here on the creation of latently infected primary human T-cells and cell lines through the single-round, replication deficient HIV-1 LGIT model. In this model the long terminal repeat (LTR) of the HIV-1 virus drives a cassette of *GFP-IRES-Tat* that allows testing of reactivating components and initiates a positive feedback loop through Tat expression.

Key words HIV, Latency, Reactivation, T-cell line, Primary T-cells, LGIT, LTR

1 Introduction

The current gold standard of HIV-1 therapy, the drug based combinatorial antiretroviral therapy (cART), can suppress plasma viremia below detection limits. However, no eradiation is achieved as interruption of the therapy usually causes a rebound of virus in the plasma. A primary reason for viral persistence is a non-productive state of infection in individual cells with stably integrated provirus, known as HIV latency. Latently infected cells, which are established early in acute infection [1], demonstrate only minimal or no translation of viral proteins and maintain only a low level of transcripts [2, 3]. Although plasma viremia remains suppressed by cART, latently infected cells are not susceptible to cART and due

Vinayaka R. Prasad and Ganjam V. Kalpana (eds.), *HIV Protocols*, Methods in Molecular Biology, vol. 1354,
DOI 10.1007/978-1-4939-3046-3_17,

to the long-lived nature of resting memory CD4+ T cells (a major proportion of the latent reservoir), it is estimated that it would require over 70 years to completely deplete these cells by natural eradication [4]. This is not possible with current therapies and therefore a primary barrier to a cure. A potential strategy for HIV eradication is activating latently infected cells under cART as non-quiescent cells have a relatively short half-life. HIV-1 expression is closely tied to cellular activation stage as it depends mostly on host transcription factors. There is a wide range of in vitro models to understand HIV-1 latency. These include primary human CD4+ T-cells infected by spinoculation with a single-cycle infection reporter virus [5], the infection of primary human, pre-activated CD4+ T-cells with replication-competent HIV to establish latency through coculture with an astrocytoma feeder cell line [6] or a Jurkat-based stable, latently infected cell line with *Env*-deficient integrated provirus where *GFP* replaced *Nef* (J-Lat) [7]. Owing to these different models, changes in chromatin structure, DNA methylation, transcription elongation restriction, as well as interaction of various host transcription factors with numerous *cis*-regulatory elements in the viral 5′-LTR were identified as possible mechanisms and potent targets of reactivation [5, 6, 8–12]. Adding to the complexity of the latency phenomenon, the viral sequence/subtype impacts significantly the efficacy of a reactivation approach [13]. To allow screening for reactivating compounds without restriction to HIV subtypes the *LTR-GFP-IRES-Tat* (LGIT) latency model was developed. It allows testing of unique LTR sequences in Jurkat and primary CD4+ T-cells and demonstrates that subtype specific variability of Sp1 and NF-κB binding sites in the LTR U3 region has a major impact on emergence of latency [13].

Weinberger et al. [14] first constructed the LGIT HIV latency system to understand how stochastic fluctuations in Tat can lead to bifurcating phenotypes, in which cells with the same proviral integration site can exhibit either very high or near zero GFP expression. The LGIT vector is similar to the Jurkat-based LTR-Tat-IRES-GFP (LTIG) construct developed by the Verdin lab [7, 15, 16]. However, by swapping the positions of the *GFP* and *Tat* genes relative to IRES, the LGIT construct yielded higher expression of the GFP signal and lower expression of Tat, as the IRES-dependent translation of the downstream genes is known to be significantly less efficient than the cap-dependent translation of the upstream gene [17]. By emulating HIV-1 expression at HIV-1 integration sites having low basal expression [14], the LGIT vector produces low levels of Tat that are susceptible to random fluctuations that can result in bifurcating clonal populations—'Off' and 'Bright' [18, 19]. The LGIT vector has subsequently been used to study how chromatin and related factors [18, 20] and transcriptional pulsing [21] contribute to the stochastic behavior of HIV gene expression and to construct mathematical models of the

Tat-feedback circuit [19, 22]. It has also been used to study novel shRNA targets against HIV [23], to characterize the functionality of coevolving Tat mutations [24], and to analyze the reactivation of latency using pharmacological agents [13].

As mentioned above, the LGIT vector encodes a strong Tat-mediated positive feedback loop that yields strong 'Off' and 'Bright' phenotypes that correspond to latent and active HIV-1 infections, respectively. This system is highly sensitive to noise and has been used extensively in CD4+ Jurkat and CEM cell lines to investigate the molecular mechanisms involved in HIV latency. Furthermore, in an effort to model the physiological conditions of HIV-1 latency in resting CD4+ T cells, we have also developed a method to utilize the LGIT reporter system in human CD4+ primary cells [13]. This model is similar to the primary CD4+ T cells system developed by the Planelles lab [5, 25], which uses a defective HIV (DHIV) vector that undergoes a single round of infection, like LGIT. Using both Jurkat and the primary CD4+ T cell models, we have used the LGIT vector to study the mechanisms of latency and the therapeutic reactivation with pharmacological agents [13, 18]. We have also constructed variants of the LGIT vector that contain the entire U3 enhancer region from HIV-1 subtypes A, A2, B, C, and F and circulating recombinant forms A/G, B/C, and B/F [13]. In the protocol below, we describe the procedures for packaging and titering LGIT lentivirus (Subheadings 3.3 and 3.4) and for establishing the LGIT HIV-1 latency system in Jurkat and CEM cell lines (Subheading 3.5) as well as in resting memory CD4+ T cells (Subheading 3.6).

2 Materials

2.1 Culture Media

1. D10 medium, Dulbecco's Modified Eagle's Medium (DMEM) supplemented with 2 mM L-glutamine, 10 % fetal bovine serum, and 100 U/ml penicillin–streptomycin.
2. R10 medium, RPMI1640 supplemented with 12.5 mM L-glutamine, 25 mM sodium pyruvate, 10 % fetal bovine serum, and 100 U/ml penicillin–streptomycin.

2.2 Cell Lines

1. HEK 293T cells maintained in D10 medium under 5 % CO_2 at 37 °C.
2. Jurkat cells, maintained at 1×10^5–5×10^5 cells/ml in R10 medium under 5 % CO_2 at 37 °C.
3. CEM cells, maintained at 1×10^5–5×10^5 cells/ml in R10 medium under 5 % CO_2 at 37 °C.

2.3 Primary Cell Isolation and Culture

2.3.1 Isolation of PBMCs

1. 1.077 g/ml Ficoll density centrifugation reagents, sterile-filtered.
2. Human peripheral blood from healthy donors (for experiment verification, using blood from ≥3 different donors is desirable). Blood-bank buffy coat or apheresis cones are ideal.
3. 1× Phosphate Buffered Saline without calcium and magnesium (1× PBS).
4. Centrifuge, swinging bucket for 50 ml tubes, maximum velocity 400 × *g* (1400 rpm).
5. 50 ml tubes.
6. Trypan Blue.
7. Red blood cell (RBC) lysis buffer: 0.8 % ammonium chloride, 0.1 mM EDTA, buffered with $KHCO_3$ to pH of 7.2–7.6, 0.22-μm filtered.
8. 200 μl non-barrier pipette tips, sterilized.
9. Scissors, cleaned with 70 % EtOH.
10. Bleach for waste.

2.3.2 Isolation of Naïve CD4+ T Cells from PBMCs

1. Naïve CD4+ T Cell Isolation Kit II, human, containing Naïve CD4 T cell Biotin-Antibody Cocktail II and Anti-Biotin MicroBeads.
2. autoMACS Rinsing Solution.
3. MACS BSA Stock Solution.
4. MACS LS Columns, for $>10^8$ cells.
5. Separator (magnet and stand) for the appropriate columns.
6. Tube rack and 15 ml tubes.
7. 0.1 % BSA in 1× PBS (BPBS).

2.4 Activation and Expansion of T Cells

1. Dynabeads Human T-Activator CD3/CD28 activator beads (Life Technologies).
2. PEB buffer (2 mM EDTA, 0.1 % BSA, pH 7.4).
3. Recombinant human Interleukin-2 (rIL-2).
4. Flat bottom tissue culture plates or tissue culture flasks.

2.5 Lentivirus Packaging

1. pMDLg/pRRE (*Gag/Pol* expressing plasmid) [26]: 1 μg/μl.
2. pCMV-VSV-G (VSV-glycoprotein envelope expressing plasmid) [27]: 1 μg/μl (*see* **Note 1**).
3. pRSV-Rev (*Rev* expressing plasmid) [26]: 1 μg/μl.
4. Transgene vector (pLGIT plasmid) [13, 14, 18] 1 μg/μl.
5. 2× HEPES-Buffered Saline (HBS): 50 mM HEPES, 0.28 M NaCl, 1.4 mM Na_2HPO_4, pH 7.05 (*see* **Note 2**), 0.22-μm filtered.

6. 2.5 M $CaCl_2$, 0.22-μm filtered.
7. Distilled water.
8. 10 cm tissue culture dishes or 6-well plates.

2.6 Virus Purification and Titration

1. 0.45 μm sterilized syringe filters.
2. Luer-Lok syringes.
3. 15 ml/50 ml tubes.
4. 20 % sucrose in 1× PBS (20SPBS).
5. Ultracentrifuge and ultracentrifuge tubes (e.g., Beckman Coulter, Thinwall, Polypropylene, 38.5 ml, 25 × 89 mm).
6. PBS without calcium and magnesium.
7. 1.5 ml sterilized tubes for the long-term storage at −80 °C.
8. *N*,*N*′-Hexamethylene bis(acetamide) (HMBA).
9. Tumor necrosis factor alpha (TNF-α).
10. Trichostatin A (TSA).
11. HIV-1 Tat protein.

2.7 Flow Cytometry Analysis

1. 0.1 % BSA in 1× PBS (BPBS).
2. DAPI.
3. CD4 antibody-Pacific Blue conjugate.
4. CD27 antibody-APC-Alexa Fluor 750 conjugate.
5. CD45RA antibody-APC conjugate.
6. CD45RO antibody-PerCP conjugate.
7. 5 ml tubes for flow cytometry.
8. Flow cytometer.

2.8 Reactivation

1. Tumor necrosis factor alpha (TNF-α).
2. Prostratin.
3. Suberoylanilide Hydroxamic Acid (SAHA).
4. Trichostatin A (TSA).

3 Methods

This section describes the procedures to generate the HIV-1 LGIT latency model in primary CD4+ T-cells and Jurkat and CEM CD4+ cell lines. This protocol contains information regarding the production, purification, and titering of the LGIT reporter virus. It also explains the isolation of naïve CD4+ T-cells from PBMCs in whole blood and the steps required to generate latently infected resting CD4+ T-cells. Refer to Subheading 2 for the reagents and materials required for this protocol.

3.1 Purification of Primary Naïve CD4+ T-Cells

1. Adjust 10 ml human peripheral blood with PBS to 25 ml (*see* **Note 3**). Carefully layer 12.5 ml Ficoll to the bottom of each 50 ml tube. Immediately centrifuge the tubes at 1400 rpm (400 × *g*) for 30–40 min at room temperature (24 °C). After centrifugation there should be a clear top layer of plasma and PBS fluid, a thin white layer of PBMCs, a pink Ficoll layer, and a red bottom layer of erythrocytes. Carefully remove and discard the PBS fluid to within 0.5 ml of the PBMC. Quickly transfer the PBMC from this layer, using a transfer pipette, to a new 50 ml tube.
2. Adjust 500 μl of PBMC suspension with PBS to 45 ml and centrifuge again at 400 × *g* for 10 min at room temperature.
3. Lyse the erythrocytes by resuspending the pellet in 4 ml PBS with 36 ml of RBC lysis buffer (ammonium chloride) on ice for 10 min.
4. Pellet the PBMC at 400 × *g* for 10 min at room temperature.
5. Wash PBMC in 10 ml PBS and centrifuge again at 400 × *g*.
6. Count PBMCs using a hemocytometer and Trypan Blue.
7. Purify naïve T-cells according to manufacturer protocol for Naïve CD4+ T Cell Isolation Kit II, human; (Miltenyi Biotec, Cat# 130-094-131) from 10^8 PBMC on LS columns.
8. Transfer 10^5 cells in 1.5 ml tube and centrifuge at 300 × *g* for 5 min. Then resuspend the pellet in 100 μl BPBS.
9. Add 2 μl each of antibody (CD4, CD27, CD45RA, and CD45RO) to the cell suspensions and incubate at room temperature for 20 min.
10. Wash the antibody-stained cells twice with BPBS and resuspend in 500 μl BPBS to analyze by flow cytometry.
11. Wash cells (repeat **step 10**). Resuspend with BPBS buffer to a final volume of 40 μl of buffer per 10^7 cells. (Note: you only need 10^8 PBMCs per LS column, so there might be extra PBMCs. These can be frozen or used for other applications.)
12. Follow manufacturer's instructions for Naïve CD4 T cell Biotin-Antibody Cocktail II (MACS Miltenyi Biotec, https://www.miltenyibiotec.com/).
13. Proceed to Dynabeads expansion protocol in Subheading 3.3.

3.2 Expansion with CD3/CD28 Dynabeads

1. Prepare PEB buffer for washing of Dynabeads.
2. Follow manufacturer's instructions for activating naïve CD4+ T-cells with Dynabeads Human T-Activator CD3/CD28 (Life Technologies, http://www.lifetechnologies.com/). The protocol also requires rIL-2 and BPBS.
3. For full activation, incubate the cells with Dynabeads more than 3 days (*see* **Note 4**).
4. Proceed to Subheading 3.7 for transduction with LGIT lentivirus.

3.3 Lentivirus Packaging

1. Twenty to twenty-four hour prior to packaging seed HEK 293T cells to have 50–70 % confluency at the time point of transfection (5×10^6 HEK 293T per 10 cm dish or 10^6 cells for 6-well plate).
2. Combine 10 μg pLGIT, 5 μg pMDLg/pRRE, 1.5 μg pRSV-Rev, and 3.5 μg pVSV-G and 0.3 M $CaCl_2$ in 1 ml volume (*see* **Note 5**).
3. Add the mix dropwise into 1 ml 2× HBS while vortexing, incubate 25–30 min at room temperature and add dropwise to cells.
4. Incubate the cells at 37 °C, 5 % CO_2 for 6–8 h, exchange the media with 10 ml fresh D10 and allow cells to produce virus for 36–48 more hours.

3.4 Purification of Lentivirus and Titration on Jurkat T-Cells

1. Collect viral supernatant in 15 ml tubes at 48 h post transfection.
2. Centrifuge at $1000 \times g$ for 5 min to pellet cell debris and filter with 0.45 μm filter using a Luer-Lok syringe. Use the virus as is or proceed to the concentration/purification step.
3. Ultracentrifuge the virus supernatant on a sucrose cushion for 90 min at $104{,}000 \times g$ and 4 °C (*see* **Note 6**).
4. Resuspend the pellet in 50–100 μl PBS.
5. Seed Jurkat cells at 5×10^5 cells/ml in R10 media in 24-well plate. For titering of lentivirus, infect cells by adding 0.1–10 μl of purified virus per well.
6. Six days after lentiviral transduction, incubate Jurkat cells with 5 mM HMBA, 20 ng/ml TNF-α, and 400 nM TSA and incubate for 18 h. This combination of agents is used to stimulate the promoter via P-TEFb, NF-κB, and Sp1-dependent mechanisms, as previously described [18].
7. Wash cells three times with 1× PBS and determine percentage of GFP positive cells by FACS (*see* **Note 7**). Proceed to Subheading 3.5 with the virus concentration that yielded ~5–10 % GFP+ cells after maximum stimulation, which corresponds to a MOI of ~0.05–0.10.

3.5 LGIT Latency Model in Jurkat/CEM Cells

1. Seed 5×10^5 cells/ml for Jurkat and CEM cells in R10 medium in a 6-well plate.
2. Add MOI of 0.05 and 0.1 and incubate 24–48 h 5 % CO_2 at 37 °C or for spinoculation centrifuge at $1200 \times g$ for 2 h at room temperature prior 24–48 h incubation.
3. Wash cells with 1× PBS three times to remove unbound virus.
4. Culture cells in R10 medium at $1–2 \times 10^5$ cells/ml and incubate in 5 % CO_2 at 37 °C.

5. Six days after transduction, add 5 mM HMBA and 12.5 μg Tat protein to activate LGIT expression in infected cells and incubate for 18 h, as previously described [18].
6. Wash cells twice with 1× PBS. Sort cells based on GFP expression and culture the GFP positive population in R10 medium (1×10^5 cells/ml) for 2 weeks to allow GFP positive cells switch to latent stage (GFP-off) mode (*see* **Note 8**).
7. Re-sort cells for GFP expression and culture GFP-off populations in R10 medium in 5 % CO_2 at 37 °C for 1 week to expand for subsequent experiments (Jurkat, JLGIT latency model; CEM, CLGIT latency model, *see* **Note 9**).

3.6 LGIT Latency Model in Primary Human CD4+ T Cells

1. Add Human T-Activator CD3/CD28 Dynabeads at a bead-to-cell ratio of 25 μl beads for 10^6 human naïve or resting primary CD4+ T-cells (from Subheading 3.4) in R10 medium and incubate for 3 days.
2. After activation, analyze expression of cell surface marker by flow cytometry (**step 9**, Subheading 3.1).
3. Culture cells with 30 U/ml rIL-2 at 5 % CO_2 and 37 °C for 1 week.
4. Seed 1×10^6 cells/ml in R10 medium in a 6-well plate.
5. Add MOI of 0.05 and 0.1 and 30 U/ml rIL-2 and incubate 24–48 h 5 % CO_2 at 37 °C while maintaining density of 10^6 cells/ml for 1 week.
6. Wash cells with 1× PBS three times to remove unbound virus.
7. Culture cells in R10 medium at 1×10^6 cells/ml with 1 ng/ml IL-7 and 10 U/ml IL-2 to maintain cell viability under resting conditions and incubate in 5 % CO_2 at 37 °C for 2 weeks.
8. Use the cells (CD4TLGIT latency model) for subsequent experiments (*see* **Note 9**).

3.7 Analysis and Reactivation of Latent Infection

1. Seed 4×10^5 JLGIT cells or CD4TLGIT cells in 400 μl R10 medium per well in a 24-well plate.
2. Add single drugs (20 ng/ml TNF-α, 1 μM prostratin, 4 μM SAHA or 400 nM TSA) or combinations of drugs (TNF-α + TSA and prostratin + SAHA) to the cells and incubate for 24 h. GFP expression might be seen as early as 6 h after drug treatment (*see* **Note 10**).
3. Wash the cells twice with PBS and analyze GFP expression by FACS. Determine percentage of reactivated cells to cells that harbor latently integrated provirus. In case of CD4TLGIT, the total latently integrated provirus can be determined by strong activation using CD3/CD28 Dynabeads. This percentage can be set as the baseline to normalize the latency reactivation by drugs.

4 Notes

1. While the HIV-1 gp160 envelope can be used instead of VSV-G to pseudotype the vectors, no ultracentrifugation is possible for purification in that case. For gp160 pseudotyped viruses, use 10 μg gp160 plasmid.
2. Adjust the pH of 2× HBS exactly to 7.05 at 25 °C. This is crucial for the transfection efficiency.
3. Blood from anonymous healthy donors is screened for infectious pathogens, including HIV. However, for your own safety, treat the blood sample as if it were infectious. This means to sterilize everything that contacts the blood (tubes, tips, pipettes) with 10 % bleach before disposal.
4. Activation conditions of primary naïve T-cells can be adjusted to specific experimental needs.
5. High quality, purified DNA should be used for transfection.
6. Polypropylene ultracentrifuge tubes must be sterile for use and can be autoclaved.
7. For titration, use only the data that give you between 1 and 20 % GFP positive cells to determine titer. Because cells that show greater than 20 % are likely to have multiple infections in a single cell.
8. After relaxation of the cells from GFP sorting many GFP-off cells will be visible after 2 weeks. In these cells, integrated provirus could be in a latent state and does not express GFP but it is not clear if they can be re-activated.
9. Optional step: single clone isolation and determination of integration site.
10. Procedure of reactivations using a NF-κB activator (TNF-α), a protein kinase C (PKC) activator (prostratin), and HDAC inhibitors (suberanilohydroxamic acid (SAHA)) and Trichostatin A (TSA) were described but other means of reactivation can of course be used as well.

References

1. Chun TW, Engel D, Berrey MM, Shea T, Corey L, Fauci AS (1998) Early establishment of a pool of latently infected, resting CD4(+) T cells during primary HIV-1 infection. Proc Natl Acad Sci U S A 95:8869–8873
2. Malim MH, Cullen BR (1991) HIV-1 structural gene expression requires the binding of multiple Rev monomers to the viral RRE: implications for HIV-1 latency. Cell 65:241–248
3. Lassen KG, Ramyar KX, Bailey JR, Zhou Y, Siliciano RF (2006) Nuclear retention of multiply spliced HIV-1 RNA in resting CD4+ T cells. PLoS Pathog 2:e68. doi:10.1371/journal.ppat.0020068
4. Siliciano JD, Siliciano RF (2000) Latency and viral persistence in HIV-1 infection. J Clin Invest 106:823–825. doi:10.1172/JCI11246
5. Bosque A, Planelles V (2009) Induction of HIV-1 latency and reactivation in primary memory CD4+ T cells. Blood 113:58–65. doi:10.1182/blood-2008-07-168393

6. Sahu GK, Lee K, Ji J, Braciale V, Baron S, Cloyd MW (2006) A novel in vitro system to generate and study latently HIV-infected long-lived normal CD4+ T-lymphocytes. Virology 355:127–137. doi:10.1016/j.virol.2006.07.020
7. Jordan A, Bisgrove D, Verdin E (2003) HIV reproducibly establishes a latent infection after acute infection of T cells in vitro. EMBO J 22:1868–1877. doi:10.1093/emboj/cdg188
8. Burke B, Brown HJ, Marsden MD, Bristol G, Vatakis DN, Zack JA (2007) Primary cell model for activation-inducible human immunodeficiency virus. J Virol 81:7424–7434. doi:10.1128/JVI.02838-06
9. Marini A, Harper JM, Romerio F (2008) An in vitro system to model the establishment and reactivation of HIV-1 latency. J Immunol 181:7713–7720
10. Swiggard WJ, Baytop C, Yu JJ, Dai J, Li C, Schretzenmair R, Theodosopoulos T, O'Doherty U (2005) Human immunodeficiency virus type 1 can establish latent infection in resting CD4+ T cells in the absence of activating stimuli. J Virol 79:14179–14188. doi:10.1128/JVI.79.22.14179-14188.2005
11. Tyagi M, Pearson RJ, Karn J (2010) Establishment of HIV latency in primary CD4+ cells is due to epigenetic transcriptional silencing and P-TEFb restriction. J Virol 84:6425–6437. doi:10.1128/JVI.01519-09
12. Yang HC, Xing S, Shan L, O'Connell K, Dinoso J, Shen A, Zhou Y, Shrum CK, Han Y, Liu JO, Zhang H, Margolick JB, Siliciano RF (2009) Small-molecule screening using a human primary cell model of HIV latency identifies compounds that reverse latency without cellular activation. J Clin Invest 119:3473–3486. doi:10.1172/JCI39199
13. Burnett JC, Lim KI, Calafi A, Rossi JJ, Schaffer DV, Arkin AP (2010) Combinatorial latency reactivation for HIV-1 subtypes and variants. J Virol 84:5958–5974. doi:10.1128/JVI.00161-10
14. Weinberger LS, Burnett JC, Toettcher JE, Arkin AP, Schaffer DV (2005) Stochastic gene expression in a lentiviral positive-feedback loop: HIV-1 Tat fluctuations drive phenotypic diversity. Cell 122:169–182. doi:10.1016/j.cell.2005.06.006
15. Jordan A, Defechereux P, Verdin E (2001) The site of HIV-1 integration in the human genome determines basal transcriptional activity and response to Tat transactivation. EMBO J 20:1726–1738. doi:10.1093/emboj/20.7.1726
16. Pion M, Jordan A, Biancotto A, Dequiedt F, Gondois-Rey F, Rondeau S, Vigne R, Hejnar J, Verdin E, Hirsch I (2003) Transcriptional suppression of in vitro-integrated human immunodeficiency virus type 1 does not correlate with proviral DNA methylation. J Virol 77:4025–4032
17. Mizuguchi H, Xu Z, Ishii-Watabe A, Uchida E, Hayakawa T (2000) IRES-dependent second gene expression is significantly lower than cap-dependent first gene expression in a bicistronic vector. Mol Ther 1:376–382. doi:10.1006/mthe.2000.0050
18. Burnett JC, Miller-Jensen K, Shah PS, Arkin AP, Schaffer DV (2009) Control of stochastic gene expression by host factors at the HIV promoter. PLoS Pathog 5:e1000260. doi:10.1371/journal.ppat.1000260
19. Weinberger LS, Shenk T (2007) An HIV feedback resistor: auto-regulatory circuit deactivator and noise buffer. PLoS Biol 5:e9. doi:10.1371/journal.pbio.0050009
20. Miller-Jensen K, Dey SS, Pham N, Foley JE, Arkin AP, Schaffer DV (2012) Chromatin accessibility at the HIV LTR promoter sets a threshold for NF-kappaB mediated viral gene expression. Integr Biol (Camb) 4:661–671. doi:10.1039/c2ib20009k
21. Weinberger LS, Dar RD, Simpson ML (2008) Transient-mediated fate determination in a transcriptional circuit of HIV. Nat Genet 40:466–470. doi:10.1038/ng.116
22. Razooky BS, Weinberger LS (2011) Mapping the architecture of the HIV-1 Tat circuit: a decision-making circuit that lacks bistability and exploits stochastic noise. Methods 53:68–77. doi:10.1016/j.ymeth.2010.12.006
23. Leonard JN, Shah PS, Burnett JC, Schaffer DV (2008) HIV evades RNA interference directed at TAR by an indirect compensatory mechanism. Cell Host Microbe 4:484–494. doi:10.1016/j.chom.2008.09.008
24. Dey SS, Xue Y, Joachimiak MP, Friedland GD, Burnett JC, Zhou Q, Arkin AP, Schaffer DV (2012) Mutual information analysis reveals coevolving residues in Tat that compensate for two distinct functions in HIV-1 gene expression. J Biol Chem 287:7945–7955. doi:10.1074/jbc.M111.302653
25. Bosque A, Planelles V (2011) Studies of HIV-1 latency in an ex vivo model that uses primary central memory T cells. Methods 53:54–61. doi:10.1016/j.ymeth.2010.10.002
26. Dull T, Zufferey R, Kelly M, Mandel RJ, Nguyen M, Trono D, Naldini L (1998) A third-generation lentivirus vector with a conditional packaging system. J Virol 72:8463–8471
27. Stewart SA, Dykxhoorn DM, Palliser D, Mizuno H, Yu EY, An DS, Sabatini DM, Chen IS, Hahn WC, Sharp PA, Weinberg RA, Novina CD (2003) Lentivirus-delivered stable gene silencing by RNAi in primary cells. RNA 9:493–501

Chapter 18

Improved Methods to Detect Low Levels of HIV Using Antibody-Based Technologies

Eliseo A. Eugenin and Joan W. Berman

Abstract

Persistence of latent virus represents a major barrier to eradicating HIV even in the current antiretroviral therapy era. A critical limitation to eliminating these viral reservoirs is the lack of reliable methods to detect, quantify, and characterize cells harboring low levels of virus. However, recent work of several laboratories indicates that PCR and viral amplification based technologies underestimate or overestimate the size of the reservoirs. Thus, new technologies and methodologies to detect, quantify, and characterize these viral reservoirs are necessary to monitor and eradicate HIV. Recent developments in imaging technologies have enabled the development or improvement of detection protocols and have facilitated the identification and quantification of several markers with exquisite resolution. In the context of HIV, we developed new protocols for the detection of low amounts of viral proteins. In this chapter, we describe several antibody-based technologies for signal amplification to improve and detect low amounts of HIV proteins in cells, tissues, and other biological samples. The improvement in these techniques is essential to detect viral reservoirs and to design strategies to eliminate them.

Key words HIV, Reservoirs, Eradication, AIDS, QVOA, Detection

1 Introduction

HIV has become a chronic disease and despite the reduction in viremia to often to undetectable levels by antiretroviral therapy (ART), treatment is still not curative. A major obstacle to complete HIV eradication is the generation of viral reservoirs that sequester the virus in infected individuals [1–3]. The best characterized HIV reservoir is a small population of resting $CD4^+$ memory and naïve T cells [1, 2, 4], but other reservoirs in macrophages and astrocytes [3–5] also have been described. Currently, identification and quantification of viral reservoirs is mainly performed by PCR or cell reactivation based technologies, but both detection systems have interpretation and technical difficulties, including the need for large amounts of blood, extensive time allocation, high cost, and significant differences in assay sensitivity [6–8].

Vinayaka R. Prasad and Ganjam V. Kalpana (eds.), *HIV Protocols*, Methods in Molecular Biology, vol. 1354,
DOI 10.1007/978-1-4939-3046-3_18,

We have developed several comprehensive, integrated, and highly sensitive assays to analyze viral reservoirs by simultaneously examining integrated HIV DNA (sensitivity equal to one copy of HIV DNA per cell) or HIV mRNAs (sensitivity for few molecules) and viral proteins (sensitivity of few proteins, protocols described below). Because the detection is by imaging techniques, it does not require cell purification or amplification of the HIV components for the identification of a small number of viral reservoirs among millions of uninfected cells. We achieved this sensitivity using highly specific signal amplification systems as well as improved microscopy and optic devices as described recently [9, 10]. In addition to the HIV products, we are able to detect several cellular/molecular markers to analyze further viral trafficking, cellular activation, compartmentalization, and HIV interacting proteins including histone acetylates, apolipoproteins, and others (up to 5–6 colors). Our approach enables improved techniques of antigen recovery, staining, and confocal analysis resulting in outstanding identification and quantification of viral reservoirs. By using these methods, we are able to analyze millions of cells and focus only on the cells positive for viral HIV DNA/mRNA/protein using confocal microscopy, improved equipment, and imaging software. In this chapter, we focus on two methods of detection of low levels of HIV proteins in cells. These methods can then be combined with assays for detection of HIV DNA and/or mRNA in the same samples, to obtain the most sensitive and reliable detection of viral reservoirs.

Some of the technical improvements described here include: (1) *Improved cell and tissue preparation* to conserve antigens and nuclei acids during the processing of the sample even in archival materials; (2) *The use of larger pieces of tissue or numbers of cells to analyze millions of cells* using big pinholes to generate large optical sections to detect any positive signal; (3) *The development of novel protocols* to enable signal amplification for antibodies. (4) *The use of state of the art confocal systems and the automation of microscopes* to allows one to perform fast scanning of large areas in three dimensions to identify the few HIV-infected cells by 3D reconstructions and deconvolution; (5) *The use of a spectrum detection and unmixing system* to detect extremely narrow wavelengths and to eliminate autofluorescence; (6) *Improved detection systems* that include cameras with recovery of 90 % of photons per frame unlike the high resolution microscopy cameras that only recover ~50 % of photons and (7) Lastly, *improved software and algorithms* to detect and quantify the signals generated by the different viral components (see details using other latent pathogens in refs. [10, 11]).

The combination of all these factors enables us to detect, quantify, and localize specific signals from HIV reservoirs.

2 Materials

2.1 Tissue Sections

1. Any tissue section can be analyzed for viral reservoirs. The important point is the preservation and size of the section (10–300 μm) to allow analysis of millions of cells.
2. Alcohol/Xylenes.
3. Phosphate buffered saline (PBS) and Tris buffered saline (TBS).
4. Citrate.
5. Fish Gelatin.
6. Horse serum.
7. Sudan Black.
8. Sodium borohydrate.
9. Pontamine sky blue and 6.6′-[(3,3′-dimethoxy[1,1′-biphenyl]-4,4′-diyl)bis(azo)]bis[4-aminuteso-5-hydroxy-1,3-naphthalenedisulfonic acid], tetrasodium.
10. Toluidine blue.
11. Triton X.
12. Biotin blocking reagents.
13. Streptavidin conjugated to different fluorochromes or beads.
14. Alexa conjugated secondary antibody—Goat Anti-Rabbit IgG.
15. Prolong Gold anti-fade agent with DAPI.

2.2 Leukocytes

1. Whole blood or leukopacks from HIV infected or uninfected individuals.
2. HIV-p24 ELISA (Perkin Elmer, Boston, MA; sensitivity: 12.5 pg/ml) or by COBAS Roche Amplicor v 1.5 (Roche, Germany; sensitivity 20 RNA copies/ml) to detect HIV infection.
3. Lysis buffer.
4. Ficoll Paque plus.
5. Poly-lysine glass slides.
6. Phorbol myristate acetate (PMA).
7. ACH-2 and OM-10 cell lines [11–14].
8. HeLa cells.
9. Paraformaldehyde (PFA).

3 Methods

3.1 Equipment

Several types of confocal microscopes can be used depending on the brand. In our case we used an A1 Nikon confocal microscope with spectrum detection and unmixing separation systems. The configuration of the system is described in Fig. 1. Using these configurations in addition to better protocols for staining and identification of dim signals, we are able to detect several latent pathogens, including low levels of HIV [9, 10].

3.2 Quantification of HIV Replication by ELISA

Viral replication was quantified by measuring HIV-1 p24 concentrations by ELISA using a commercial kit or by PCR.

3.3 Positive and Negative Controls and Sample Fixation

1. ACH2 (a human lymphoid) or OM-10 cells (a monocytic cell line) were used as positive controls because each cell has only one integrated copy of HIV-1 DNA and produces significant amounts of viral proteins when stimulated with phorbol myristate acetate (PMA) or TNF-α.
2. HeLa cells are used as a negative control representing uninfected cells.
3. For tissue sections, we use human lymph nodes obtained from individuals with high or undetectable replication, as well as uninfected tissues, as positive and negative controls, respectively.

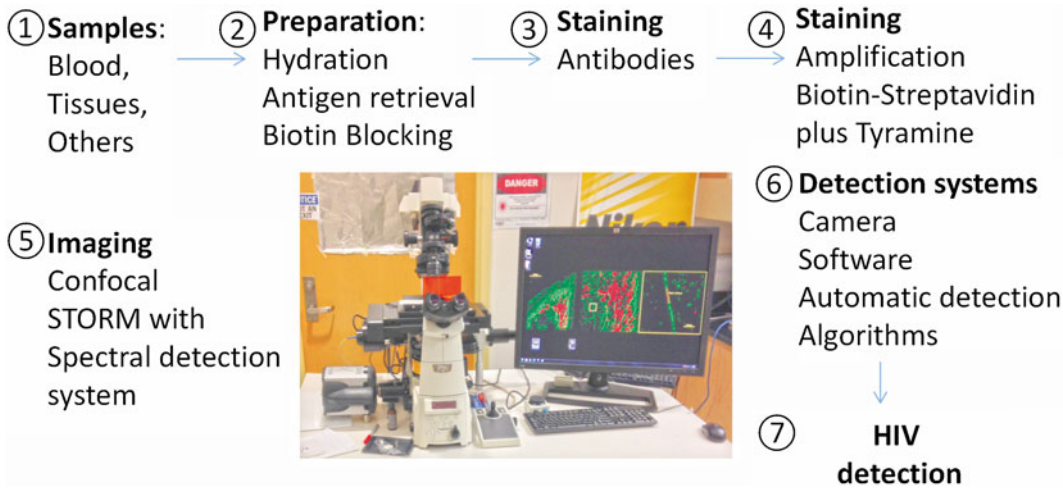

Fig. 1 Description of the improved sample and microscopy technology to detect low levels of HIV proteins. Every step has been optimized to achieve outstanding resolution. (*1*) and (*2*), correspond to improved techniques for tissue preservation. (*3*) and (*4*), correspond to the use of new or improved techniques for signal amplification. (*5*) and (*6*), correspond to improved imaging and detection systems as well as to software analysis. These improvements result in maximal sensitivity to detect HIV proteins in viral reservoirs (*7*) as well as in HIV replicating cells.

3.4 Sample Preparation

Multiple fixatives can be used for tissues, cells, or fluids including:

1. 70 % cold Ethanol (−20 °C for 20 min).
2. Acetone.
3. 20 % buffered formalin and subsequent permeabilization using 0.1 % Triton X for 3 min.
4. Four percent paraformaldehyde (PFA) containing 0.1 M sodium phosphate buffer, pH 7.4, and subsequent permeabilization using 0.1 % Triton X for 3 min.

3.5 Deparaffinization

After fixation, and mounting into paraffin blocks, tissue sections from 10 to 300 μm in thickness are deparaffinized using Ethanol–Xylene in the following order: Ethanol 30, 50, 60, 70, 80, 90, and 100 %, Xylene 1 and 2 (two separate solutions), and then Ethanol 100, 90, 80, 70, 60, 50, and 30 %, and then PBS for 10 min. It is important to include all of the steps to assure the slow and efficient elimination of paraffin. The thickness of the section is also extremely important due to the large numbers and optical sections required for identification of viral reservoirs. Many companies and facilities only prepare sections of 5–10 μm; thus, a special request to the company or training of personnel is required to obtain these types of sections.

3.6 Antigen Retrieval

There are several techniques of antigen retrieval depending on the application. For a comprehensive list of antigen retrieval methods visit, www.ihcworld.com/epitope_retrieval.htm. For our applications, we use the boiling citrate buffer method for 15 min (pH 6.0) for thicker tissue sections (10–300 μm), but we have also obtained good results with microwave-based techniques.

3.7 Leukocyte Analysis

To analyze a significant number of circulating leukocytes, whole blood, isolated PBMCs, leukopacks or specific populations of cells isolated using magnetics beads, are isolated, pelleted, and subjected to confocal analysis. The pellets can be generated directly on the glass slide or the centrifuged pellet can be fixed and cut with a cryostat. By doing this protocol, we can reduce the size and volume of cells analyzed such that millions of cells can be evaluated with a better chance of detecting viral reservoirs.

The following five points are critical in protocols for the detection of low levels of HIV proteins using minimal amplification, because high autofluorescence can result in false positives. Most of these protocols apply to archival tissues.

3.7.1 Elimination of Lipofuscins Fluorescence

Natural autofluorescence is due to flavins, porphyrins, and chlorophyll (mostly in plants). The main problem with these compounds present in tissues and cells is that during cutting and solvent treatments, they become redistributed, resulting in background fluorescence.

However, new optical configurations to perform unmixing and spectrum detection can significantly reduce this problem. In addition, treatment of the sample with Sudan Back (0.3 % in 70 % Ethanol) stirred in the dark for 2 h, will significantly reduce the autofluorescence produced by lipofuscins.

3.7.2 Elimination of Elastin and Collagen Autofluorescence

This artifact is mainly found in blood vessel walls. Elastin contains several potential fluorophores when there is cross-linking of tricarboxylic amino acid with a pyridinium rings [15, 16]. In small vessels detection of these products is minimal, but in large vessels it is a significant problem. To eliminate autofluorescence from elastin products, incubate your samples in 0.5 % pontamine sky blue and 6.6′-[(3,3′-dimethoxy[1,1′-biphenyl]-4,4′-diyl)bis(azo)]bis[4-aminuteso-5-hydroxy-1,3-naphthalenedisulfonic acid], tetrasodium salt dissolved in 50 mM Tris buffer before mounting the samples. However, the use of both compounds requires extensive calibration, because pontamine sky blue fluoresces in the red channels. However, if the red channel is not to be used, it is an excellent choice.

An alternative solution is 0.1 % toluidine blue for 3 min before mounting the samples, but this does not work in all vessels and the interpretation of the fluorescence can become complicated.

3.7.3 Elimination of Fixative-Induced Fluorescence

Aldehydes react with amines and proteins to generate fluorescent products, especially in samples incubated for a long time in fixatives. This problem occurs most often in fixatives such as glutaraldehyde and formaldehyde. For tissue sections 10–300 μm, incubate them five times for 15 min each in a solution of fresh borohydrate (1 mg/ml dissolved in PBS and prepared on ice). After this process, wash in PBS three times and discard the leftover sodium borohydrate.

3.7.4 Bleaching Treatment

Currently there is no company that sells appropriate light boxes, but it is relatively easy to construct. To build a specific wavelength light box (like the one used to detect ethidium bromide in agarose gels), fluorescent tubes, especially for blue, green, red, and far red channels can be purchased from several companies. These can be used to "burn" the autofluorescence in the tissue sections before the staining process.

3.7.5 Endogenous Biotin Blocking

If the tissue has endogenous biotin activity, biotin blocking is suggested using a Biotin blocking kit. First, incubate the tissue sections or pelleted leukocytes with avidin solution for 10–30 min and then wash in TBST three times for 5 min. Next, incubate with biotin solution for 10–30 min and then wash in TBST three times for 5 min.

3.8 Antibodies and Biotinylation of Antibodies

All antibodies for staining of multiple colors are described below. IgG biotinylation is performed using commercial Biotin labeling kits.

3.9 Data Analysis

Mean differences are tested by nonparametric Kruskal–Wallis analysis. If a significant *F*-value is obtained, means are compared with the Bonferroni–Dunn multiple comparison test. A value of $p < 0.05$ is considered significant.

3.10 Multiple Methods of Signal Amplification to Detect Viral Reservoirs

Normally immune detection of proteins requires either a single antibody conjugated to a fluorescent dye or a primary antibody with a secondary antibody that amplifies the fluorescent signal. Most of the times these protocols are inefficient in detecting viral reservoirs or low HIV replication in multiple systems, and only high viral replication can be detected [17, 18]. As described in Fig. 2, the combination of better protocols for fixation, antigen recovery, staining, and detection, enables exquisite identification and resolution of HIV proteins, despite minimal to undetectable replication as assayed by ELISA or PCR. A critical component in optimizing these protocols is to determine the expected level of expression of HIV proteins, because most protocols described here are designed to amplify low signals (*see* **Note 1** to decide the best protocol for your application).

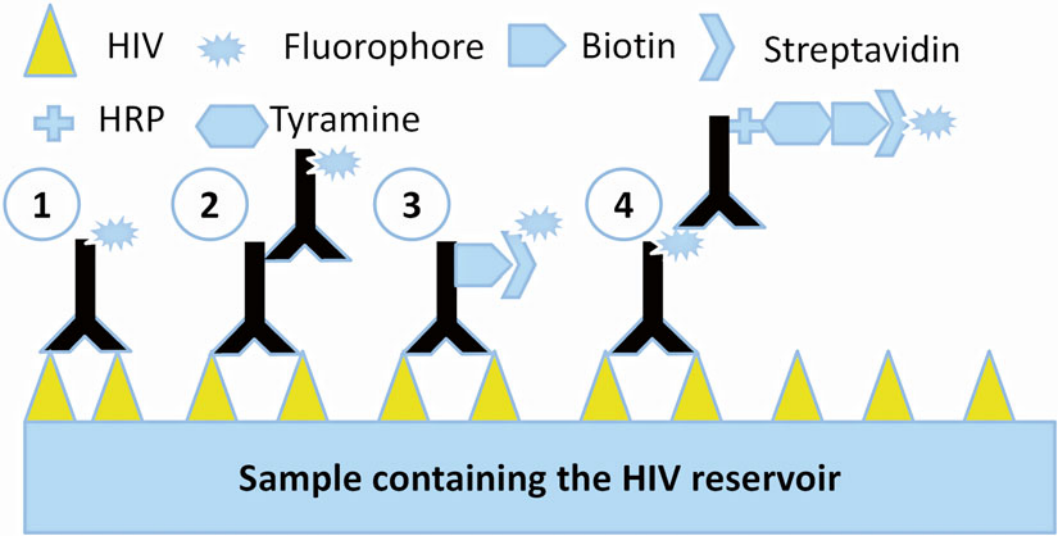

Fig. 2 Schematic of four different methods of immune staining. Method 1 illustrates an antibody directly conjugated to a fluorophore. This technique is commonly used in FACS analysis and also in immunohistochemistry and cytochemistry. Method 2 represents a method providing additional amplification of the signal. Method 3 demonstrates antibodies labeled with biotin and detection is by biotin–streptavidin interactions. Our system, method 4, uses a multistep process that amplifies the number of fluorophores binding to the antigen, resulting in high sensitivity and amplification. Methods 3 and 4 are most appropriate for detection of HIV reservoirs depending on the cells and tissues being analyzed.

3.11 Staining Process

As described above and in Figs. 1 and 2, fixation, sample preparation, staining, signal amplification, and detection systems are essential for identifying and quantifying low amounts of HIV proteins. Some improvements of detection and imaging components are recently described in detail [9, 10]. For viral reservoirs, standard staining using directly conjugated antibodies (Fig. 2, method 1) and secondary conjugated antibodies (Fig. 2, method 2) is not sufficient to detect low levels of proteins. Thus, the methods using antibody–biotin–streptavidin–fluorophore (Fig. 2, method 3) and antibody–fluorophore–antibody to fluorophore conjugated to HRP–tyramide–biotin–streptavidin–fluorophore (Fig. 2, method 4) are highly sensitive and adaptable to determine localization, quantification, and trafficking of HIV proteins in cells, tissues, and fluids.

3.11.1 Approach 1: Antibody Conjugated to Biotin–Streptavidin–Fluorophore Amplification

(*see* Fig. 2, third method):

1. Samples are fixed, and prepared as described above (antigen retrieval, and elimination of autofluorescence) according to the sample used, tissue sections or pelleted leukocytes (go to **step 4** below).
2. If tissue sections are used from paraffin blocks, heat the slides to remove excess paraffin in an oven at 60 °C for 15 min and dry at 37 °C overnight.
3. Deparaffinize the sections as described above using sequential alcohols and xylenes to eliminate the paraffin slowly.
4. Proceed with either antigen retrieval or blocking endogenous biotin as described above, depending upon the tissue or cells being analyzed and the staining process performed. Liver, spleen, and brain are tissues with endogenous biotin.
5. Using the set up described in Fig. 1, we are able to detect several colors (up to 5–6 colors). We can probe for nucleic acids (DAPI), HIV/SIV proteins (e.g., HIV p24, p17, gp120, Tat, Integrase, or Nef), in combination with different cellular markers including CD4, CD8, GFAP (an astrocyte marker), NeuN or MAP-2 (a neuronal markers), or Iba1 (a microglia/macrophage marker). For pelleted leukocytes, several cellular markers such as CD3, CD4, CD11b, CD11c, CD14, CD16, CD68, and CD163 can also be included in the same staining protocol.
6. Tissue sections or pelleted leukocytes are blocked for at least 60 min to overnight using blocking solution (0.5 M EDTA, 1 % horse serum, 1 % Ig free BSA, 4 % human serum and 1 % fish gelatin in PBS).
7. Samples are incubated overnight in primary antibody at 4 °C. A critical point is to determine how many antibodies can be

used concomitantly based on antibody species and isotypes. Several combinations can be used. Some examples are:

(a) HIV biotinylated antibodies (monoclonal, IgG_1) + CD4 (rabbit antibodies) + Iba 1 (macrophage marker) + nuclei acid staining (DAPI).

(b) HIV biotinylated antibodies (monoclonal, IgG_1) + CD4 (rabbit antibodies) + Iba 1 (macrophage marker) + actin staining + nuclei acid staining (DAPI).

A critical point of these experimental approaches is the determination of appropriate negative controls. For the examples described above the following controls are used:

(c) Purified IgG_1 (same concentration as the HIV antibodies) + rabbit serum or rabbit purified IgG (same concentration as the serum or of the immune IgG) and non-immune goat serum or IgG (same concentration of the Iba-1 IgGs) (*see* **Note 2** to identify the best negative controls for your experiments).

(d) Several tissues express low levels of endogenous biotin; therefore a control for this expression is required, despite inhibition of biotin binding as described above.

Importantly, negative controls using no primary antibodies or only secondary antibodies are not accurate controls. As described above, by using non-immune IgGs or serum, we consider the possibility of nonspecific binding to several proteins such as Fc receptors, especially in immune and inflamed tissues. All cells, tissues, and fluids to some degree have nonspecific binding that is necessary to consider, especially in cases of detection of low amounts of proteins, such as found in HIV reservoirs. Thus, specificity of the antibodies must be confirmed by replacing the primary antibody with the appropriate isotype-matched control reagent, anti-IgG_1, IgG_{2A}, IgG_{2B} or the IgG fraction of normal rabbit serum depending on the primary antibody being used (*see* **Note 2**).

8. After incubation with the primary antibodies, at least five washes with PBS every 10 min are required to eliminate the unbounded antibodies to the antigen.

9. To detect antibodies conjugated to biotin, streptavidin conjugated to a fluorophore is necessary. In addition, other streptavidin-conjugated reagents can be used such as beads or gold. Detection of low levels of HIV proteins requires at least 3 h of incubation.

10. After incubation with the secondary antibody or conjugated streptavidin, at least five washes with PBS are required to eliminate the unbounded streptavidin or secondary antibodies. Our confocal equipment has unmixing and spectrum detection

systems that enable the separation of extremely narrow wavelengths (up to 2.5 nm) to separate multiple colors without overlay (some examples in refs. [9, 10])

11. After several washes to eliminate unbounded antibodies or dyes, samples are mounted using Prolong Gold anti-fade reagent with DAPI. If beads are used, we suggest using Prolong Diamond anti-fade reagent with DAPI.
12. After staining, keep samples in the dark.
13. The analysis of thick samples (tissues and pelleted leukocytes) is performed first using a large pinhole just to detect HIV positive signals. After we detect the positive optical section, we perform confocal microscopy in the specific XYZ positive axis with a regular pinhole and good resolution to detect and quantify the localization of viral proteins using 3D reconstructions and deconvolution (*see* **Note 3** for details).

3.11.2 Approach 2: Antibody–Fluorophore–Antibody to Fluorophore Conjugated to HRP–Tyramide–Biotin–Streptavidin–Fluorophore

(*see* Fig. 2, fourth method) (*see* **Note 4** for potential problems):

This method is essentially similar to method 1, but uses additional amplification steps.

1. Sample fixation, antigen retrieval, biotin blocking, and tissue preparation are similar to what is described for method 1 as well as described in Fig. 2.
2. This method includes antibodies conjugated to a fluorophore to target any HIV protein in a similar manner described above. However, the main difference is that an anti-fluorophore secondary antibody conjugated to HRP (dilutions 1:600–1:2000) is used by adding biotinyl-tyramide for 15 min in the presence of 0.3 % H_2O_2 for 20 min to amplify the binding of the new fluorophores.
3. Wash the slides in PBS twice for 10 min each.
4. Incubate in 0.25 mg/ml streptavidin conjugated to any fluorophore for 30 min–3 h in the dark.
5. Wash three times in PBS every 10 min in the dark.
6. Incubate the slides in water for 10 min.
7. Mount using prolong with DAPI as described above.

   It is important to note that for all of these protocols it is essential to use pure solutions, because any contamination can be amplified and result in false positive signals (*see* **Note 5**).

3.12 Improved Microscopic Analysis to Detect Low Levels of HIV Proteins in HIV Reservoirs

New confocal systems, including the Nikon A1, have an improved spectral detector and unmixing systems, PMT, and cameras to improve detection and reduce potential cross contamination amount different colors. These systems allow a critical reduction in signal to noise ratio, improving the detection of specific staining.

The spectral detector is the mechanism responsible for emitting light through a high-efficiency gate into its individual components, similar to how a prism separates white light into its individual "rainbow" components. The improved spectral detector allows for precise separation of emission wavelengths that are then passed through a 32-photomultiplier tube (PMT) array detector that enables distinction between wavelengths as small as 2.5 nm apart. This precise detection system allows the researcher to separate and analyze specific wavelengths or eliminate autofluorescence. This technology enables the identification of signals that would be impossible to detect with wide-field fluorescence or standard confocal microscopy (for details of these improved technologies *see* refs.[11, 19–21]).

Example 1: As demonstrated in Fig. 3, isolated CD4⁺ T lymphocytes from individuals with undetectable HIV replication as determined by ELISA (<15 pg/ml) and PCR (<20 copies/ml) were negative for HIV-p24 staining using regular immune staining (Fig. 4, top panel). Using the staining and microscopy techniques

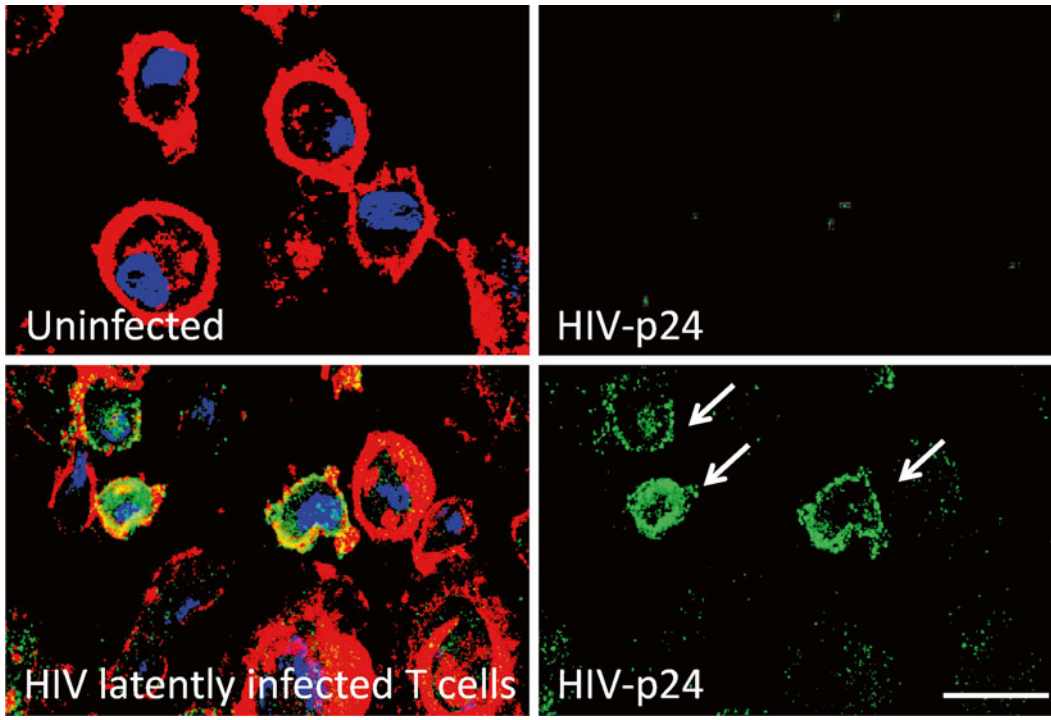

Fig. 3 Detection of latent HIV in human CD4⁺ T lymphocytes using enhanced HIV-p24 staining. Merged images are presented on the *right side* of the figure. HIV-p24 staining (HIV-p24, *green*), actin (phalloidin conjugated to Texas red, *red*), and nuclei (DAPI, *blue*) detection were performed. Uninfected cells did not show any HIV-p24 staining. Conventional staining without amplification did not result in reliable staining. Enhanced staining using the protocols described above resulted in reliable and reproducible detection of HIV-p24. Bar: 30 μm.

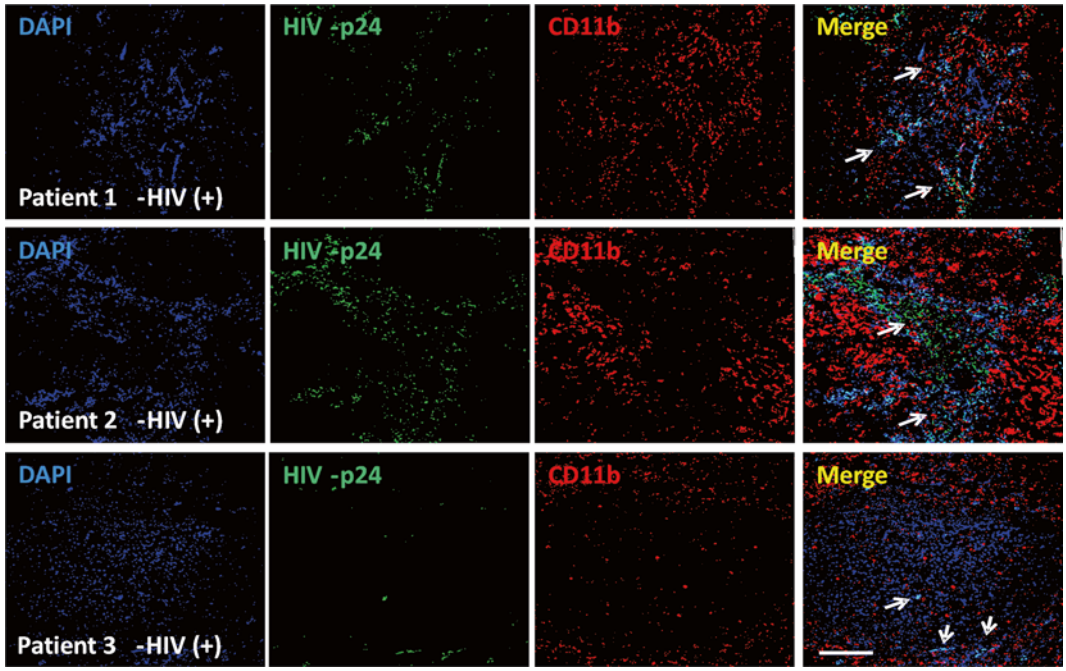

Fig. 4 $CD4^+$ T lymphocytes and a population of macrophages present in human lymph nodes serve as viral reservoirs. Using thicker lymph node tissue sections (200 μm) obtained from HIV infected individuals with undetectable viral replication (for at least 1 year), tissue staining for Nuclei (DAPI, *blue*), CD4, Iba-1, or CD11b (*red* staining), and HIV-p24 viral protein was performed. Using the protocols described above we performed confocal microscopy and subsequent 3D reconstructions. No staining was observed using IgG1 or preimmune sera controls. Quantification of HIV infected cells was performed using the total number of cells (DAPI staining), versus the total number of HIV positive cells. Bar: 40 μm.

described above, we identified the few latently HIV infected cells, without viral reactivation (Fig. 3, lower panel).

Example 2: Human lymph nodes were obtained from HIV infected individuals with undetectable viral replication for at least 1 year. Using our signal amplification techniques, we were able to detect HIV proteins (Fig. 4) in all cases analyzed ($n=9$). No signal was detected in uninfected tissues (data not shown). We identified viral reservoirs not only in $CD4^+$ T lymphocytes (data not shown) but also in dendritic cells (CD11b positive cells, Fig. 4) as well as in a small population of macrophages (Iba-1 positive cells, data not shown). The tissue distribution of these infected cells was donor dependent. Some donors have diffuse presence of HIV cells while others have well compartmentalized HIV infection.

Most of these techniques also can be combined with detection of HIV DNA and mRNA as described in **Note 6**. Thus, it is possible to detect HIV DNA or mRNA, viral proteins, and cellular markers at the same time in the same sample.

3.13 Summary of Detection Properties with Different Systems and Conditions

HIV protein staining: We are able to detect several HIV proteins including HIV-p24, Nef, Vif, and integrase in one latently infected cell among 10^6–10^8 uninfected cells in blood smears and isolated PBMCs (pelleted preparations) from HIV infected individuals on ART with no detectable viral replication. In tissue sections obtained from HIV infected individuals with no detectable replication at the time of death, we are able to detect 1.6 ± 1.2 % of T cells in lymph nodes. In brains obtained from individuals with minimal replication, we detected 5–8 % of astrocytes and 3–6 % of microglia/macrophages infected with HIV.

4 Notes

The protocols described above are mostly dependent upon the quality of the starting tissue, cell separation, area of the tissue examined, and degree of viral replication. Most of the problems are due to:

1. *Levels of expression and amplification*: This is an essential consideration before you start the experiment. How much staining is expected? The amplification system described in Fig. 2, method 4, is extremely sensitive; thus, it is not recommended to samples that are expected to have high expression of HIV proteins. In cases for which viral replication is detected by ELISA and PCR, we suggest the use of the technique described in Fig. 2, method 2 or 3 instead of method 4. If your detected fluorescence is too strong, leave the stained samples at 4 °C for 1–2 weeks to allow reduction of the signal or repeat the experiment using the same samples using protocol 1 (antibody conjugated to biotin–streptavidin–fluorophore amplification, Fig. 2, third method).
2. *Negative controls*: Problems with negative control antibodies, endogenous biotin, and Fc receptor expression are also common, resulting in increased background staining. If the background is uniform, changes in gain or unmixing systems in the confocal microscope may be enough to detect specific staining. If the background is nonuniform, repeat the experiment, because uneven staining is not reliable, especially by confocal microscopy. Most of the uneven staining occurs in inflamed, activated tissues that were in formalin for long periods of time. Activated cells expressing high levels of Fc receptors that can bind nonspecifically to the Fc region of the immunoglobulin being used for detection [22].
3. *3D reconstruction*: Most of our techniques involve 3D reconstructions and thicker tissue sections. Conventional microscopes are not able to detect specific signals. Analysis by confocal microscopy allows the quantification of thick tissue sections, serial optimal sections, and 3D reconstructions to

quantify accurately the total numbers of HIV positive cells. Thus, the use of specific programs to perform 3D reconstruction is required such as Image J from the NIH, or others such as NIS imaging (Nikon, Japan) or Metamorph (Molecular devices, CA) [11, 23–26].

4. *Amplification problems*: The tyramine amplification method is based on the binding reaction of biotinylated tyramine to phenol derivatives of a protein by peroxidase. This reaction gives nonspecific signals; therefore, it is important to pretreat specimens with methanol containing 0.3 % H_2O_2 to reduce endogenous peroxidase activity.
5. *Purity of the solutions*: Due to the high amplification, any cross contamination between samples by using contaminated PBS will generate nonspecific signals. Thus, use different containers for each slide.
6. *Combination of protein and other HIV markers*: The described techniques could be combined with detection of HIV DNA and mRNA, resulting in a multicomponent detection system of viral reservoirs. Detection of only viral proteins is not sufficient to demonstrate viral reservoirs, because HIV proteins can be released and taken up by phagocytosis or nonspecific uptake.

Acknowledgements

This work was supported by the National Institute of Mental Health grants MH075679, MH090958, and MH102113 (to J.W.B.), and MH096625 (to E.A.E.). NIH Centers for AIDS Research (CFAR) Grant AI-051519. We would like to thank the Analytical Imaging Facility at PHRI and Nikon Instruments for microscopy support (http://www.phri.org/facilities/facil_imaging.asp).

References

1. Richman DD, Margolis DM, Delaney M, Greene WC, Hazuda D, Pomerantz RJ (2009) The challenge of finding a cure for HIV infection. Science 323:1304–1307
2. Chomont N et al (2009) HIV reservoir size and persistence are driven by T cell survival and homeostatic proliferation. Nat Med 15:893–900
3. Bagasra O, Lavi E, Bobroski L, Khalili K, Pestaner JP, Tawadros R, Pomerantz RJ (1996) Cellular reservoirs of HIV-1 in the central nervous system of infected individuals: identification by the combination of in situ polymerase chain reaction and immunohistochemistry. AIDS 10:573–585
4. Mahlknecht U, Deng C, Lu MC, Greenough TC, Sullivan JL, O'Brien WA, Herbein G (2000) Resistance to apoptosis in HIV-infected CD4+ T lymphocytes is mediated by macrophages: role for Nef and immune activation in viral persistence. J Immunol 165:6437–6446
5. Coleman CM, Wu L (2009) HIV interactions with monocytes and dendritic cells: viral latency and reservoirs. Retrovirology 6:51
6. Durand CM, Blankson JN, Siliciano RF (2012) Developing strategies for HIV-1 eradication. Trends Immunol 33:554–562
7. Eriksson S et al (2013) Comparative analysis of measures of viral reservoirs in HIV-1 eradication studies. PLoS Pathog 9:e1003174
8. Spina CA et al (2013) An in-depth comparison of latent HIV-1 reactivation in multiple cell model systems and resting CD4+ T cells from aviremic patients. PLoS Pathog 9:e1003834

9. Rella CE, Ruel N, Eugenin EA (2014) Development of imaging techniques to study the pathogenesis of biosafety level 2/3 infectious agents. Pathog Dis 72:167–173
10. Subbian S, Eugenin E, Kaplan G (2014) Detection of Mycobacterium tuberculosis in Latently Infected Lungs by Immunohistochemistry and Confocal Microscopy. J Med Microbiol 63:1432–1435
11. Folks TM, Clouse KA, Justement J, Rabson A, Duh E, Kehrl JH, Fauci AS (1989) Tumor necrosis factor alpha induces expression of human immunodeficiency virus in a chronically infected T-cell clone. Proc Natl Acad Sci U S A 86:2365–2368
12. Harrer T, Jassoy C, Harrer E, Johnson RP, Walker BD (1993) Induction of HIV-1 replication in a chronically infected T-cell line by cytotoxic T lymphocytes. J Acquir Immune Defic Syndr 6:865–871
13. Butera ST, Roberts BD, Leung K, Nabel GJ, Folks TM (1993) Tumor necrosis factor receptor expression and signal transduction in HIV-1-infected cells. AIDS 7:911–918
14. Okamoto M, Makino M, Kitajima I, Maruyama I, Baba M (1997) HIV-1-infected myelomonocytic cells are resistant to Fas-mediated apoptosis: effect of tumor necrosis factor-alpha on their Fas expression and apoptosis. Med Microbiol Immunol 186:11–17
15. Deyl Z, Horakova M, Vancikova O (1981) Changes in pyridinoline content of elastin during ontogeny. Mech Ageing Dev 17:321–325
16. Deyl Z, Macek K, Adam M, Vancikova O (1980) Studies on the chemical nature of elastin fluorescence. Biochim Biophys Acta 625: 248–254
17. Orellana JA, Saez JC, Bennett MV, Berman JW, Morgello S, Eugenin EA (2014) HIV increases the release of dickkopf-1 protein from human astrocytes by a Cx43 hemichannel-dependent mechanism. J Neurochem 128: 752–763
18. Hazleton JE, Berman JW, Eugenin EA (2012) Purinergic receptors are required for HIV-1 infection of primary human macrophages. J Immunol 188:4488–4495
19. Murooka TT, Mempel TR (2013) Intravital microscopy in BLT-humanized mice to study cellular dynamics in HIV infection. J Infect Dis 208(Suppl 2):S137–S144
20. Paddock SW, Eliceiri KW (2014) Laser scanning confocal microscopy: history, applications, and related optical sectioning techniques. Methods Mol Biol 1075:9–47
21. Shaner NC (2014) Fluorescent proteins for quantitative microscopy: important properties and practical evaluation. Methods Cell Biol 123:95–111
22. Buchwalow I, Samoilova V, Boecker W, Tiemann M (2011) Non-specific binding of antibodies in immunohistochemistry: fallacies and facts. Sci Rep 1:28
23. Amat F, Lemon W, Mossing DP, McDole K, Wan Y, Branson K, Myers EW, Keller PJ (2014) Fast, accurate reconstruction of cell lineages from large-scale fluorescence microscopy data. Nat Methods 11:951–958
24. Ellefsen KL, Settle B, Parker I, Smith IF (2014) An algorithm for automated detection, localization and measurement of local calcium signals from camera-based imaging. Cell Calcium 56:147–156
25. Maska M et al (2014) A benchmark for comparison of cell tracking algorithms. Bioinformatics 30:1609–1617
26. Song W, Liu W, Niu X, Wang Q, Sun L, Liu M, Fan Y (2013) Three-dimensional morphometric comparison of normal and apoptotic endothelial cells based on laser scanning confocal microscopy observation. Microsc Res Tech 76:1154–1162

Chapter 19

Analysis of ABCA1 and Cholesterol Efflux in HIV-Infected Cells

Nigora Mukhamedova, Beda Brichacek, Christina Darwish, Anastas Popratiloff, Dmitri Sviridov, and Michael Bukrinsky

Abstract

Cholesterol is an essential component of the cellular membranes and, by extension, of the HIV envelope membrane, which is derived from the host cell plasma membrane. Depletion of the cellular cholesterol has an inhibitory effect on HIV assembly, reduces infectivity of the produced virions, and makes the cell less susceptible to HIV infection. It is not surprising that the virus has evolved to gain access to cellular proteins regulating cholesterol metabolism. One of the key mechanisms used by HIV to maintain high levels of cholesterol in infected cells is Nef-mediated inhibition of cholesterol efflux and the cholesterol transporter responsible for this process, ABCA1. In this chapter, we describe methods to investigate these effects of HIV-1 infection.

Key words HIV-1, Nef, Cholesterol efflux, ABCA1, Confocal microscopy, Image analysis

1 Introduction

Replication of enveloped viruses assembling at the plasma membrane of infected cells, such as HIV, critically depends on cholesterol, and depletion of cholesterol in HIV-infected cell affects viral production and infectivity [1]. HIV assembles at the plasma membrane domains enriched in cholesterol and sphingolipids called lipid rafts [2]. Lipid rafts are also used by HIV as entry gates into the target cells [3]. In general, high levels of lipid rafts on the plasma membrane are beneficial for HIV replication. It is not surprising that HIV evolved to regulate the abundance of lipid rafts. The mechanism used by the virus for this purpose is inhibition of the cellular ATP binding cassette transporter A1 (ABCA1), which controls cholesterol efflux from cells to apoA-I acceptor in the blood. Activity of ABCA1 is inversely correlated to the abundance of lipid rafts on the plasma membrane: stimulation of ABCA1 expression reduces the number of lipid rafts, whereas inhibition of ABCA1 activity increases lipid raft abundance [4, 5]. To inhibit

Vinayaka R. Prasad and Ganjam V. Kalpana (eds.), *HIV Protocols*, Methods in Molecular Biology, vol. 1354,
DOI 10.1007/978-1-4939-3046-3_19,

ABCA1 activity, HIV relies on Nef protein, which blocks ABCA1 exit from the endoplasmic reticulum (ER) and stimulates its degradation [6, 7]. To accomplish this effect, Nef interacts with ER chaperone calnexin, which regulates folding and maturation of glycosylated proteins, and disrupts the interaction between calnexin and ABCA1, thus abrogating the processing of ABCA1 in ER [8]. Importantly, this activity of Nef affects not only infected cells, but also bystander cells, which take up Nef released from infected cells into the bloodstream [9, 10]. The side effect of this viral activity is increased risk of atherosclerosis and cardiovascular disease in HIV-infected patients [11]. The protocols described in this chapter provide effective and reliable methods to analyze and visualize ABCA1 and measure the rate of cholesterol efflux from HIV-infected cells.

2 Materials

Prepare all solutions using deionized water and analytical grade reagents. Prepare and store all reagents at room temperature (unless indicated otherwise).

2.1 Cholesterol Efflux

1. Human monocytic cell line THP-1.
2. 24-well plates.
3. RPMI-1640. Store at 4 °C.
4. Fetal Bovine Serum (FBS). Store at –20 °C.
5. Pen/Strep. Store at –20 °C.
6. L-glutamine. Store at –20 °C.
7. Phorbol 12-myristate-13-acetate (PMA). Prepare 10 mg/ml stock solution in DMSO, aliquot and store at –20 °C. Prepare working solution by diluting the stock solution in PBS to 100 μg/ml; it can be stored at –20 °C for 1–2 months.
8. [^{3}H]cholesterol. Store at –20 °C.
9. Purified ApoA-I, store at –20 °C (*see* **Note 1**).
10. Ultrapure water.
11. Ethanol.
12. LXR agonist TO-901317. Prepare 100 mg/ml (200 mM) stock solution in EtOH, store at –70 °C; working solution is prepared by diluting stock solution in PBS to 100 μM.
13. PBS.
14. Lysis buffer (1 % Triton X-100 in RPMI-1640).
15. Scintillation fluid.

2.2 Confocal Microscopy and Image Analysis

1. HeLa-ABCA1-GFP cell line (a kind gift of Dr. A. Remaley [12]).
2. Nef expression vector pT7consnefhis6 (NIH AIDS Research and Reference Reagent Program).
3. Dulbecco's Modified Eagle's Medium (DMEM). Store at 4 °C.
4. Selective DMEM medium: DMEM supplemented with 10 % FBS, 100-fold diluted pen/strep, 100-fold diluted L-Glu, 0.15 mg/ml G418, and 0.2 mg/ml Hygromycin B. Store at 4 °C.
5. Fetal Bovine Serum (FBS). Store at –20 °C.
6. Pen/Strep. Store at –20 °C.
7. L-glutamine (L-Glu). Store at –20 °C.
8. G418 Sulfate (G418) (50 mg/ml solution). Store at 4 °C.
9. Hygromycin B (50 mg/ml solution). Store at 4 °C.
10. PBS.
11. Polyclonal rabbit anti-Nef antisera. Store at 4 °C.
12. Mouse monoclonal anti-Calnexin-ER membrane marker antibody. Store at 4 °C.
13. Alexa Fluor® 647 Goat Anti-Rabbit IgG (H + L) Antibody. Store at 4 °C.
14. DyLight 550 Goat Anti-Mouse IgG Antibody. Store at 4 °C.
15. DAPI dilactate. Store at 4 °C.
16. Goat IgG. Store at 4 °C.
17. Albumin, from bovine serum (BSA). Store at 4 °C.
18. Formaldehyde Solution.
19. Triton X-100.
20. Ethanol.
21. Ultrapure water.
22. 6-well plates.
23. Coverslips (cover glasses; thickness no. 1½).
24. Microscope Slides (3″ × 1″ × 1 mm).
25. Mounting medium Fluoromount-G.
26. Blocking solution: 20 μl Goat IgG per milliliter of 1 % BSA in PBS (filtered through 0.2 μm filter). Prepare fresh before use.

3 Methods

3.1 Cholesterol Efflux Analysis

This protocol describes measurement of cholesterol efflux from human monocytic cell line, THP-1, differentiated into macrophage-like cells by PMA treatment. The format we usually use is the

24-well plate format, but it can be formatted to 12 or 48-well plates and the assay can be adapted for different cell types. The assay measures efflux of radioactively labeled cholesterol pre-loaded into the target cells to the apoA1 acceptor. This process is controlled by ABCA1, which is induced in cells by stimulation with LXR agonist TO-901317 (*see* **Note 2**). The procedure allows one to measure either the capacity of *cells* to release cholesterol to extracellular acceptors or the capacity of the *acceptor* to accept cholesterol released from cells. For the former, the acceptor should be added in saturating concentration, for the latter, the concentration of the acceptor should be approximately half of the saturating concentration. The assay consists of the following steps: (1) loading cells with labeled cholesterol; (2) equilibrating labeled cholesterol among all intracellular cholesterol pools; and (3) quantitating the transfer of labeled cholesterol from cells to the acceptor.

1. Resuspend cells from stock culture and count them. Plate cells into 24-well plates (*see* **Note 3**) at the final density of 0.3×10^6 cells per well in 1 ml of complete RPMI-1640 supplemented with 10 % FBS, 1 % Pen/Strep, and 2 mM L-glutamine. The density can be adjusted to accommodate requirements of treatment prior to the efflux assay (e.g., transfections, treatment with an inhibitor or activator, infection with a virus).
2. Dispense the required amount of [^{3}H]cholesterol into a 1.5 ml microfuge tube (0.5 μCi or 19 kBq per well is required for a typical assay) (*see* **Note 4**). Dilute [^{3}H]cholesterol solution in complete media to the final concentration 5 μCi/ml and add labeled cholesterol into each well (100 μl/well, final volume per well is 1 ml). Add PMA to a final concentration of 100 ng/ml, and incubate cells for 72 h in cell culture incubator (37 °C, 5 % CO_2).
3. Remove media containing [^{3}H]cholesterol. Wash cells gently with PBS. Repeat washing three times.
4. Prepare serum-free medium with 1 μM TO-901317, add 1 ml to each well. Incubate for 18 h in the cell culture incubator.
5. Wash cells gently with PBS.
6. Add 500 μl of apoA-I solution in serum-free medium (final apoA-I concentration—30 μg/ml for saturating efflux, or 15 μg/ml for non-saturating) (*see* **Note 5**).
7. One set of wells is used to determine background efflux; add to these wells serum-free medium without apoA-I.
8. Incubate cells for 2 h in cell culture incubator (37 °C, 5 % CO_2). Duration of the efflux incubation may vary from 30 min to 8 h if required, but for shorter incubations the amount of radioactivity and/or number of cells may need to be increased.

9. After incubation, collect media into 1.5 ml microfuge tubes. Spin at 10,000 × *g* for 5–10 min at room temperature to remove cellular debris.
10. Transfer 100 μl of media into 7 ml scintillation vial. Add 5 ml of Insta-gel Plus and vortex mixture. Store remaining samples at 4 °C.
11. Add 1 ml of lysis buffer to each well, shake the plate on a shaker, and collect the lysate. Check cells under microscope to ensure that all cells have been removed. If some cells remain, add 100 μl of lysis buffer and scrape the wells.
12. Transfer 100 μl of cell lysates into 7 ml scintillation vials. Add 5 ml of Insta-gel Plus and vortex the mixture.
13. Count radioactivity in the media collected and the cells on a scintillation counter for dpm of [^{3}H] cholesterol.
14. The rate of cholesterol efflux is usually expressed as a proportion of cholesterol moved from cells to the acceptor. The following formula is used:

$$\text{Efflux}\ (\%) = \frac{\text{media counts} \times \text{dilution factor}}{(\text{media counts} \times \text{dilution factor}) + (\text{cell counts} \times \text{dilution factor})} \times 100\%.$$

15. The specific efflux is calculated as a difference between the efflux in the presence and absence of an acceptor (blank): *Specific cholesterol efflux* (%) = Cholesterol efflux to the acceptor (%) – Cholesterol efflux without acceptor (%).

3.2 Confocal Microscopy and Image Analysis

This protocol describes the technique for visualization of ABCA1 by fluorescent microscopy in HeLa cells stably expressing ABCA1-GFP [12] and transfected with HIV-1 Nef, but can be used for any HIV-infected or transfected cells (*see* **Note 6**). The analysis described involves staining for Nef and calnexin (an ER chaperone), and counterstaining of the nuclei. The procedure helps to identify cellular components interacting with ABCA1 and allows to follow and to analyze changes in ABCA1 distribution upon such interactions. The presented example elucidates changes in the interaction of ABCA1 with one of its cellular counterparts—calnexin—when HIV Nef is expressed. Since calnexin also serves as a marker for Endoplasmatic Reticulum (ER), the altered ABCA1 distribution and its retention in ER can be demonstrated.

Confocal microscope can generate either 2D or 3D images. Both serve as valuable tools for analysis of events on cellular and subcellular levels. Creation of a tile-scan image using 2D imaging allows one to analyze a large area in a single optical plane and to choose a representative section for presentation and further analysis. An example of such a section is in Fig. 1 where a cell expressing HIV Nef (white) is surrounded by Nef negative cells. ABCA1

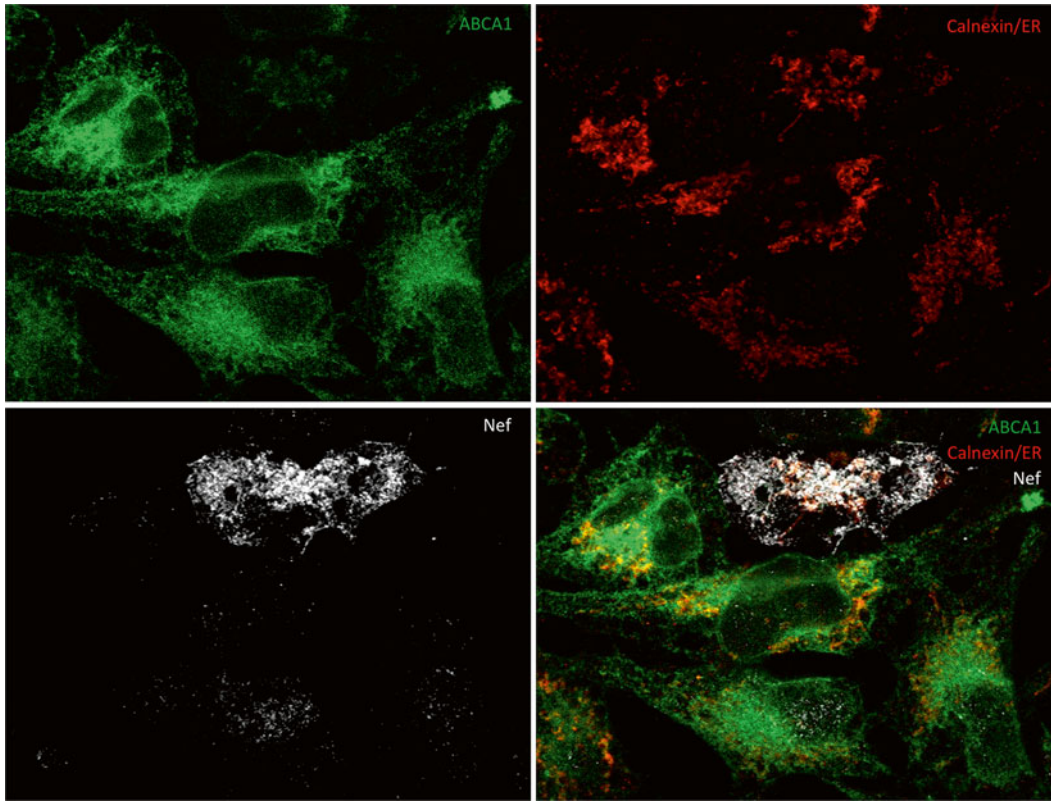

Fig. 1 A 2D image of HeLa-ABCA1-GFP cells transfected with HIV-1 Nef. Calnexin and HIV-1 Nef were visualized using anti-Calnexin-ER membrane marker mouse monoclonal antibody followed by goat anti-mouse DyLight 550 antibody (*red*), and by anti-Nef rabbit serum followed by goat anti-rabbit Alexa Fluor 647 antibody (*white*), respectively. Cellular nuclei were stained by DAPI dilactate (*blue*). ABCA1 is co-expressed with GFP (*green*). Co-localization of ABCA1 and calnexin in Nef-negative cells is visualized as yellow/orange colored areas in the overlay. ABCA1 abundance is greatly reduced in the Nef-positive cell, reflecting the inhibitory effect of Nef on this cholesterol transporter.

(green) is markedly suppressed in the Nef positive cell and remaining ABCA1 is almost exclusively localized in the areas positive for calnexin (red). In the surrounding cells not expressing Nef, only a smaller fraction of ABCA1 is co-localizing (yellow to orange) with calnexin, while a substantial proportion of ABCA1 is localized outside of ER, mainly on the cellular membrane, where it can perform its functions associated with cholesterol efflux. A better understanding of subcellular localization of molecules of interest is provided by a 3D image (Fig. 2). Using appropriate software, a 3D image can be rotated into positions that best reveal relationships between molecules of interest.

1. Clean and sterilize the coverslips by dipping them into 70 % ethanol.
2. Air dry the coverslips (remove the majority of ethanol by vacuum).

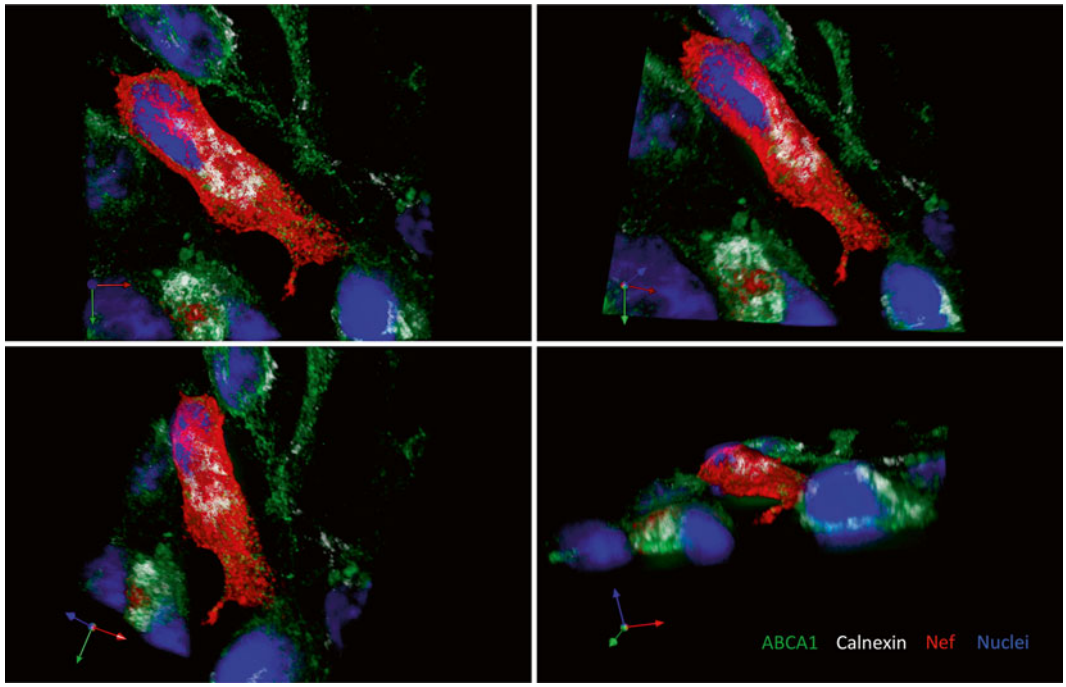

Fig. 2 A 3D image of HeLa-ABCA1-GFP cells transfected with HIV-1 Nef. Calnexin and HIV-1 Nef were visualized using anti-Calnexin-ER membrane marker mouse monoclonal antibody followed by goat anti-mouse DyLight 550 antibody (*white*), and by anti-Nef rabbit serum followed by goat anti-rabbit Alexa Fluor 647 antibody (*red*), respectively. Cellular nuclei were stained by DAPI dilactate (*blue*). ABCA1 is co-expressed with GFP (*green*). Analysis of the 3D image was performed in Volocity allowing for precise spatial determination of localization of molecules of interest within a cell.

3. Place the sterilized coverslips into 6 well plates.
4. Plate HeLa-ABCA1-GFP cells to approximately 40 % confluency in selective DMEM medium.
5. Incubate the seeded plates in CO_2 incubator at 37 °C overnight. Optimal cell culture confluency for transfection is 60–80 %.
6. Prepare Transfection Mix 1 (100 μl per well) by adding Nef-expressing plasmid DNA (2 μg per well) to DMEM media (no FBS, antibiotics or supplements added) in an Eppendorf tube. Pipette twice up and down.
7. Prepare Transfection Mix 2 (100 μl per well) by adding 6 μl of Metafectene into 94 μl of DMEM media (no FBS, antibiotics or supplements added) in an Eppendorf tube. Pipette twice up and down.
8. Add Transfection Mix 1 into Transfection Mix 2 moving the pipette throughout the flask (do not vortex the solution after Mix 1 and 2 are combined since it may destroy the DNA/lipid complex).

9. Incubate 20 min at room temperature.
10. During the incubation time, replace culture medium in 6-well plates with cells with 3 ml of fresh selective DMEM medium/well.
11. Transfer 200 μl of DNA/lipid complex drop-wise to each well using a 200 μl tip with its sharp end cut off. Target the drops over the area of the coverslip.
12. Incubate the plates with transfected cells in CO_2 incubator at 37 °C overnight.
13. The next day, replace culture medium with 3 ml of fresh selective DMEM medium/well and continue incubation in CO_2 incubator at 37 °C.
14. 48 h (*see* **Note 7**) post-transfection, aspirate the culture medium and wash the cultures twice with warm PBS (37 °C).
15. Fix cells with 3.5 % formaldehyde solution (formaldehyde solution prepared in PBS from the 37 % concentrate) for 10 min at room temperature.
16. Wash the fixed cells three times with PBS. The plates can be stored at 4 °C overnight.
17. Permeabilize fixed cells with 0.1 % Triton X-100 (in PBS) for 5 min using 2 ml Triton solution/well.
18. Wash the permeabilized cells three times with PBS.
19. Block with 2 ml of Blocking solution/well for 30 min at room temperature (cover plates with aluminum foil). The plates can be left with blocking solution at +4 °C overnight.
20. Drain the coverslips (on the paper towel and using vacuum) and transfer them on the Parafilm in a large Petri dish (use syringe needle and flat end forceps to manipulate the coverslips).
21. Incubate with 200 μl (for 18 mm × 18 mm coverslip) of primary antibody (mixture of anti-Nef rabbit serum and anti-Calnexin-ER membrane marker mouse monoclonal antibody, both diluted 1:750 in PBS, and ChromPure Goat IgG diluted 1:30 in PBS) at room temperature for 60 min (use wet paper towel to keep humid conditions in the Petri dish; perform incubation in the dark).
22. Wash three times with PBS in a 6-well plate.
23. Drain the coverslips and transfer them back on the Parafilm in a large petri dish.
24. Incubate with 200 μl (for 18 mm × 18 mm coverslip) of secondary antibody (goat anti-rabbit Alexa Fluor 647 antibody and goat anti-mouse DyLight 550 antibody, both diluted 1:500 in PBS, and ChromPure Goat IgG diluted 1:30 in PBS)

at room temperature for 30 min (use wet paper towel to keep humid conditions in the Petri dish; perform incubation in the dark).

25. Wash three times with PBS in a 6-well plate.
26. Stain with DAPI (diluted 1:10,000 from the stock solution; 2 ml/well) for 5 min.
27. Wash three times with PBS in a 6-well plate. At this step, it is possible to leave coverslips in the plates with PBS at +4 °C overnight.
28. Drain the coverslips (on the paper towel and using vacuum).
29. Mount the coverslips on microscope slides with mounting medium.
30. Leave the slides to settle in the dark at room temperature overnight.
31. Use the slides for imaging or store them in the dark at +4 °C.
32. High-content and three-dimensional image data acquisition is performed on a Zeiss Cell Observer Spinning Disk Confocal instrument, equipped with two Photometrics Evolve Delta high-speed (512×512) EM CCD cameras on Axio Observer Z1 microscope equipped with scanning stage with piezo z-motor, which ensures generation of highly reliable 3D image sets. Stitching and multi-position modules are part of the Zen Blue software.
33. 3D image sets are acquired with Plan Apochromat 150×/1.35 objective lens, allowing generation of 512×512 images at pixel resolution of 0.089 μm. 16-bit image format is used for intensity registration, as pixel integration within 25 % or above of the available dynamic range is considered satisfactory. This approach allows for detection efficiency of GFP/ABCA1, not possible even on advanced point-scan confocal microscopes.
34. For 3D analyses, the z-step is set at 0.250 μm to optimize for the z-point spread and optical section thickness. Multiple positions are selected and memorized. The instrument then executes capturing of image sets channel by channel for each individual position in *z*-dimension (Fig. 2).
35. For 2D analyses, single optical plane is captured but large squared area is selected, to produce tile-scan image set with overlap between adjacent image frames at 15–25 %. This overlap is used for subsequent stitching using precise correlation in the overlapping areas.
36. Four channels are generated using the following parameters: (1) channel 1, representing Alexa Fluor 568, encoding for calnexin is generated by excitation with 561 nm diode laser and the emission filtered by 629/62 nm band filter; (2) channel 2,

representing GFP/ABCA1 is created by excitation with 488 nm diode laser while the emission is filtered by 535/30 nm band emission filter; (3) channel 3, representing nuclear stain DAPI is recorded using excitation of 405 nm diode laser and the emission is filtered with 450/50 nm emission filter; (4) channel 4, representing the Alexa Fluor 647 encoding Nef is generated by 633 nm diode laser excitation and the emission filtered with 690/50 nm emission filter. The entire z-stack is captured channel by channel (Fig. 2).

37. Image analysis is performed using Volocity software from 2D or 3D image sets.
38. For visualization of the co-localization, voxel overlap is first determined by establishing legitimate intensity threshold for each channel. Using interactive stepwise threshold and false color feedback, elimination of the dark currents serves as a threshold point. Intersecting the thresholds of the two channels determines the voxel overlap. For voxel co-localization the so-called positive co-localization is used, which is the overlap of the voxels that bear an intensity value larger than the mean value (over threshold) of the given channel. The co-localized voxels are visualized as a separate channel. Visualization is achieved by 3D rendering using transparency mode. The co-localization is compared by plotting the co-localization co-efficiency.
39. For two 2D analyses the cells having high and no Nef expression are selected by free hand tool from a large tiled and stitched image. The large size of these images allows extraction of several hundred cells for each group. The average intensity for Nef, ABCA1, and calnexin can be plotted and compared.

4 Notes

1. As acceptors for cholesterol efflux, one can use isolated HDL, plasma, and serum (human or other species). However, apoA-I is a specific acceptor for ABCA1-mediated efflux, whereas HDL, plasma, and serum accept cholesterol delivered by a variety of transporters.
2. When the experiment is performed to evaluate ABCA1 activity, TO-901317 stimulation can be omitted. However, cholesterol efflux may be too low in such cases, and one may need to titrate the dose of TO-901317. No TO-901317 stimulation is needed when working with cells transfected with ABCA1-expressing vector.
3. The number of wells should be sufficient for quadruplicate determinations for each experimental condition.

4. Commercially available [^{3}H]cholesterol comes as a solution in either toluene or ethanol. If [^{3}H]cholesterol is a toluene solution, dry it completely with N_2 in a toluene-resistant tube and resuspend in absolute ethanol at a final concentration of 1 μCi/μl. Vortex and mix well. If [^{3}H]cholesterol is an ethanol solution, it can be used immediately.
5. Other acceptors that can be used are high density lipoprotein (HDL) (final concentration 50 μg/ml saturating, or 25–30 μg/ml non-saturating), plasma or serum (final concentration 5 % saturating, 1–2 % non-saturating).
6. Other cell types, infected with HIV or transfected with vectors expressing HIV proteins, can be analyzed by this method. An example is presented in Fig. 3, which shows monocyte-derived macrophages infected with HIV-1. HIV-1 Env was stained using anti-HIV gp120 sheep serum as a primary and Alexa Fluor® 488 conjugated donkey anti-sheep IgG as a secondary

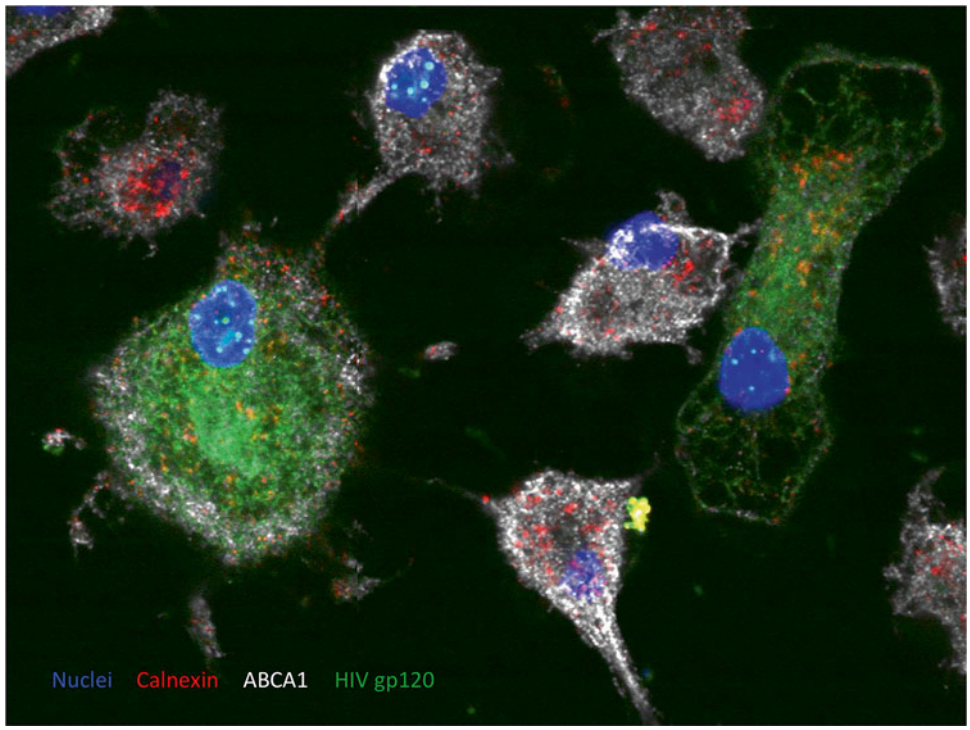

Fig. 3 A 2D image of monocyte-derived macrophages infected with HIV-1. Peripheral blood monocytes were differentiated into the macrophages and infected with VSV-G pseudotyped HIV-1 NL4-3. HIV-1 envelope protein was stained using anti-HIV gp120 sheep serum followed by Alexa Fluor® 488 Donkey Anti-Sheep IgG (H + L) Antibody (*green*). Cellular proteins Calnexin and ABCA1 were visualized using mouse monoclonal anti-Calnexin-ER membrane marker antibody followed by goat anti-mouse DyLight 550 antibody (*red*) and by anti-ABCA1 rabbit polyclonal antibody followed by goat anti-rabbit Alexa Fluor 647 antibody (*white*), respectively. Cellular nuclei were stained by DAPI dilactate (*blue*). Abundance of ABCA1 is reduced in HIV-infected macrophages.

antibody, ABCA1 was stained using anti-ABCA1 rabbit polyclonal antibody as a primary and Alexa Fluor® 647 conjugated goat anti-rabbit IgG as a secondary antibody and the endoplasmic reticulum (ER) chaperone calnexin was stained using mouse monoclonal anti-calnexin-ER membrane marker antibody as primary and goat anti-mouse DyLight 550 conjugated antibody as secondary. Calnexin regulates folding and maturation of glycosylated proteins, including ABCA1 and gp160, in the ER. Nuclei were counterstained with DAPI.

7. Transfected cells can be incubated for 72 h in some cases to obtain better expression.

Acknowledgments

This study was supported by NIH grants R01HL093818, R01HL101274, R21AI108533, P30AI087714, P30HD040677, S10OD010710, 1S10RR025565.

References

1. Waheed AA, Freed EO (2009) Lipids and membrane microdomains in HIV-1 replication. Virus Res 143:162–176
2. Ono A, Freed EO (2001) Plasma membrane rafts play a critical role in HIV-1 assembly and release. Proc Natl Acad Sci U S A 98: 13925–13930
3. Manes S, del Real G, Lacalle RA et al (2000) Membrane raft microdomains mediate lateral assemblies required for HIV-1 infection. EMBO Rep 1:190–196
4. Koseki M, Hirano K-i, Masuda D et al (2007) Increased lipid rafts and accelerated lipopolysaccharide-induced tumor necrosis factor-{alpha} secretion in Abca1-deficient macrophages. J Lipid Res 48:299–306
5. Landry YD, Denis M, Nandi S et al (2006) ATP-binding cassette transporter A1 expression disrupts raft membrane microdomains through its ATPase-related functions. J Biol Chem 281:36091–36101
6. Cui HL, Grant A, Mukhamedova N et al (2012) HIV-1 Nef mobilizes lipid rafts in macrophages through a pathway that competes with ABCA1-dependent cholesterol efflux. J Lipid Res 53:696–708
7. Brichacek B, Darwish C, Popratiloff A et al (2014) HIV-1 Infection of macrophages induces retention of cholesterol transporter ABCA1 in the endoplasmic reticulum. AIDS Res Hum Retroviruses 30:947
8. Jennelle L, Hunegnaw R, Dubrovsky L et al (2014) HIV-1 protein nef inhibits activity of ATP binding cassette transporter A1 by targeting endoplasmic reticulum chaperone calnexin. J Biol Chem 289:28870
9. Asztalos BF, Mujawar Z, Morrow MP et al (2010) Circulating Nef induces dyslipidemia in simian immunodeficiency virus-infected macaques by suppressing cholesterol efflux. J Infect Dis 202:614–623
10. Cui HL, Ditiatkovski M, Kesani R et al (2014) HIV protein Nef causes dyslipidemia and formation of foam cells in mouse models of atherosclerosis. FASEB J 28:2828–2839
11. Crowe SM, Westhorpe CL, Mukhamedova N et al (2010) The macrophage: the intersection between HIV infection and atherosclerosis. J Leukoc Biol 87:589–598
12. Neufeld EB, Remaley AT, Demosky SJ et al (2001) Cellular localization and trafficking of the human ABCA1 transporter. J Biol Chem 276:27584–27590

Chapter 20

The Proteomic Characterization of Plasma or Serum from HIV-Infected Patients

Nicole A. Haverland, Lance M. Villeneuve, Pawel Ciborowski, and Howard S. Fox

Abstract

Proteomics holds great promise for uncovering disease-related markers and mechanisms in human disorders. Recent advances have led to efficient, sensitive, and reproducible methods to quantitate the proteome in biological samples. Here we describe the techniques for processing, running, and analyzing samples from HIV-infected plasma or serum through quantitative mass spectroscopy.

Key words Mass spectroscopy, SWATH-MS, HIV, Proteomics, Serum, Plasma, Bayesian, Z-score

1 Introduction

Plasma/serum proteomics holds a vast potential for new biomarker discovery [1, 2]. Blood, which can repeatedly be harvested from patients with relatively low invasion and at a relatively low cost, is an attractive clinical material. Although blood contains a vast assortment of proteins and metabolites, numerous issues, such as reproducibility and sensitivity, have plagued plasma proteomics, thereby limited successes in the field. With the development of new mass spectrometry techniques and technologies, comprehensive, replicable analysis of the plasma proteome has become feasible.

Mass spectrometry-based quantitative techniques have been at the forefront of analytical approaches in biomarker discovery from the very beginning of proteomics [3, 4]. During one and a half decades of blood/plasma/serum/CSF proteomics, researchers have attempted to identify and quantify these proteomes using various methods including in vitro labeling techniques (such as iTRAQ, TMT, ICAT, super-SILAC) as well as label-free

Nicole A. Haverland and Lance M. Villeneuve have equally contributed to this chapter.

Vinayaka R. Prasad and Ganjam V. Kalpana (eds.), *HIV Protocols*, Methods in Molecular Biology, vol. 1354,
DOI 10.1007/978-1-4939-3046-3_20,

techniques, often using shotgun proteomics [5]. However, while each method has provided insight into various disorders, reproducibility and broad validation remains an unresolved issue. Each of these techniques suffers from various limiting factors with one common underlying limitation being data-dependent acquisition (DDA). The application of data-independent acquisition (DIA), in which all molecular species are recorded, opens new avenue in mass spectrometry-based, body fluid-based biomarker discovery. Sequential Window data-independent Acquisition of the Total High-resolution Mass Spectra (SWATH-MS) platform offers higher dynamic range of linearity of recorded ion intensities vastly improving precision and accuracy of quantification and sensitivity [6]. SWATH-MS uses DIA to generate the experimental data, which is searched against a library constructed of DDA acquired samples. In addition, the DIA data collected for the experimental samples creates a permanent spectral record that can be utilized to extract additional information in future analyses with other DDA libraries. Although at this time only a limited number of peer-reviewed studies employing SWATH-MS platform have been published, initial results are highly promising in the prospects of contribution to biomarker discovery.

SWATH-based proteomic analysis offers additional benefits compared to previous proteomic approaches. Using SWATH, additional fractionation is commonly unnecessary and detection of low abundance peptides is possible. However, to gain the most out of SWATH mass spectrometry (as with any experiment), optimization is necessary. Here we present our optimized methods for four critical steps of SWATH-MS: DDA for the building of the library, DIA for running of the experimental samples, data processing, and statistical analysis. In addition to their use for plasma/serum samples, these steps also apply to other applications of SWATH-MS.

2 Materials and Equipment

2.1 Sample Processing

1. Protease inhibitor cocktail.
2. Sodium dodecyl sulfate (SDS).
3. Seppro IgY14 Column (Sigma-Aldrich).
4. VIVASPIN 15R with 5000 MWCO.
5. Centrifuge with swinging bucket rotor.
6. HRM Calibration kit Standard Peptides (Biognosys).

2.2 Instrumentation

1. Centrifugal vacuum concentrator with rotor for 1.5–2.0 mL microcentrifuge tubes.
2. cHiPLC-nanoflex system (Eksigent).
3. TripleTOF 5600 Mass Spectrometer equipped with a NanoSpray III Ion Source (AB SCIEX).

2.3 Supplies

1. Nano-cHiPLC column 75 μm × 15 cm ChromXp C18-CL 3 μm 300 Å (Eksigent).
2. Nano-cHiPLC Trap column 200 μm × 0.5 mm ChromXp C18-CL 3 μm 300 Å (Eksigent).
3. Oasis MCX 1 cm^3 column (Waters).
4. Trap-elute jumper chip (Eksigent).
5. 0.1 % Formic Acid in Water.
6. Solution A: 0 % Aqueous Solution with 0.1 % Formic Acid.
7. Solution B: 100 % Acetonitrile with 0.1 % Formic Acid.
8. National Limited Volume Wide Opening Plastic Crimp Top Autosampler Vials; 450 μL capacity (Thermo Scientific).
9. 11 mm Snap-It Cap for Autosampler Vials, 6 mm hole (Thermo Scientific).

2.4 Data Processing: Generating the Spectral Library

1. 8-core computer with ProteinPilot installed and licensed (AB SCIEX).

2.5 Data Processing: Targeted Data Extraction

1. Computer with PeakView v. 2.1 Software installed and licensed (AB SCIEX) and the add-on, Protein Quantitation 1.0 MicroApp, installed and licensed.

3 Methods

3.1 Sample Processing for SWATH-MS Designed Experiments

1. Obtain plasma or serum sample from patients or biobanks (*see* **Notes 1** and **2**).
2. If samples are frozen, thaw, and immediately upon thawing add 50 μL of 20× Protease Inhibitors per milliliter of the sample to prevent protein degradation. Samples are mixed with the inhibitors by inversion or gentle vortexing and then immediately placed on ice. To delipidate, the samples should be centrifuged at 18,000 × *g* at 4 °C for 15 min and the middle layer of the cleared plasma/serum collected.
3. Deplete samples of highly abundant proteins using a commercial mix of immobilized antibodies (*see* **Note 3**). The standard manufacturer protocol for immunodepletion should be followed for the Seppro IgY14 columns. This kit is available in a spin column format or as HPLC columns of different sizes depending on the volume of sample to be depleted, and contains all necessary buffers. Concentrate the flow-through depleted samples using a VIVASPIN 15R spin concentrator, centrifuging at 4000 × *g* for approximately 1.5 h. Samples may be frozen at this stage if desired.

4. Bring samples to 4 % sodium dodecyl sulfate (SDS) (*see* **Note 4**). Centrifuge at 400 × *g* to pellet any debris. Transfer supernatant to a clean sample container. Quantify the protein concentration within the sample using the Pierce 660 protein quantification kit (*see* **Note 5**).
5. Digest the samples using trypsin and using filter-assisted sample preparation (FASP; http://www.nature.com/nmeth/journal/v6/n5/extref/nmeth.1322-S1.pdf) protocol. FASP is compatible with SDS and has many benefits over in-gel or in-solution approaches [7] (*see* **Note 6**). We recommend digesting 50 μg of protein using a protein:enzyme ratio of <1:50.
6. Desalt the digested samples using an Oasis mixed cation exchange column following manufacturer's protocols. Desiccate the desalted sample using a vacuum concentrator.
7. Resuspend the peptides in a minimal volume of 0.1 % formic acid in HPLC-grade water (*see* **Note 7**). Perform peptide quantification based on spectral absorbance at 205 nm on a NanoDrop 2000 [8] (*see* **Note 8**). Remove an aliquot (2 μg or less; keep this consistent across biological and technical replicates) of cleaned peptides from each sample and transfer to a clean autosampler vial (*see* **Note 9**). If the total volume is >6 μL, dessicate the sample and resuspend in 6 μL 0.1 % formic acid in HPLC-grade water. If the total volume is <6 μL, bring the solution to a total volume of 6 μL.
8. (Optional for DIA) Spiking-in peptides: Peptide spiking-in is a process whereby artificial peptides are added to the database and to each experimental sample. These artificial peptides have various predicted elution times. After determining the change in experimental elution times from predicted elution times, the elution profile can be shifted to enable better matching of the SWATH library reference spectra to the experimentally obtained DIA spectra. Add an equal amount of artificial peptides from the HRM calibration kit to each DIA sample.

3.2 Mass Spectrometry

1. Replace nano-cHiPLC columns if necessary (*see* **Note 10**). The Eksigent cHiPLC system requires three chips: the cHiPLC column that is used for elution, the trap column that is used during sample loading, and a trap-and-elute jumper chip.
2. *See* Table 1 for the LC method for LC-MS/MS analyses of tryptic digested peptides (*see* **Note 11**). Equilibrate cHiPLC columns. If the Eksigent LC system is used, insert pre-run flush for 0.1 min using 100 % initial flow rate into the LC in the second tab of Eksigent method.
3. *See* Table 2 to prepare mass spectrometry data acquisition methods for DDA and DIA experiments. For both methods, the mass spectrometer will be operated in high sensitivity mode.

Table 1
LC method

Sample loading			
Flow mode	Independent		
Time (min)	Flow Soln. A (μL/min)	Flow Soln. B (μL/min)	Event
0	10	0	
8.5	10	0	
9	2	0	
10	2	0	
Elution			
Flow mode	Conserved. Total flow rate = 0.3 μL/min		
Time (min)	% Soln. A	% Soln. B	Event (*see* **Note 26**)
0	95	5	AUX3 TTL Low
0	95	5	AUX4 TTL High
1	95	5	AUX3 TTL High
180	65	35	
182	10	90	
192	10	90	
193	95	5	AUX4 TTL Low
200	95	5	

Samples for the library must be run using the DDA method, while experimental samples for SWATH-MS analysis must be run using DIA method. For information on samples for library construction, *see* **Note 12**.

4. Retrieve the autosampler vial(s) prepared in **step 7**, which contain the resuspended peptides. Transfer the vials to the autosampler and assign the samples to queue accordingly (*see* **Note 13**). Ensure that the autosampler lids are on flush and the tubes are not crooked, as this may result in breaking the autosampler needle or unequal sample uptake.
5. Start queue. Each sample will take approximately 3.5 h for completion using the LC methods provided in Table 1. The total ion current (TIC) chromatogram can be used to monitor sample elution during the run within the Analyst program (*see* **Note 14**).
6. As samples finish mass spectrometry analysis, the TICs can be overlaid in the PeakView software using the open multiple

Table 2
Mass spectrometry methods

DDA	
Charge state	From +2 to +5
Intensity threshold	>100 counts
Switch after	50 spectra
Advanced settings	True
Always exclude	True
Exclude for	15 s
Mass tolerance units	mDa
Mass tolerance	50
Use inclusion list	False
Use exclusion list	False
Ignore peaks within	6 Da
Real time	None
Dynamic collision energy	True
Fragment intensity multiplier	2
Maximum accumulation	2 s
Allow standard filters for smart IDA	True
Number of cycles	7615
Polarity	Positive
Period cycle time	2798 ms
Pulser frequency	14.170 kHz
ISVF (IonSpray voltage floating)	2400 V
Pulser frequency	14.170 kHz
Precursor scan (MS1) experiment type	TOF MS
MS1 accumulation time	250.0 ms
MS1 start mass	400.0 Da
MS1 end mass	1800.0 Da
Precursor fragmentation (MS2) experiment type (50 selections)	TOF MS^2
MS2 accumulation time	50.0 ms
MS2 start mass	100.0 Da
MS2 end mass	1800.0 Da

(continued)

Table 2
(continued**)**

DDA	
DIA	
Number of cycles	3555
Polarity	Positive
Period cycle time	3363 ms
Pulser frequency	14.170 kHz
ISVF (IonSpray voltage floating)	2400 V
Pulser frequency	14.170 kHz
Precursor scan (MS1) experiment type	TOF MS
MS1 accumulation time	50.0 ms
MS1 start mass	400.0 Da
MS1 end mass	1250.0 Da
SWATH-MS (MS2) experiment type	TOF MS^2
MS2 accumulation time	96.0 ms
MS2 start mass	100.0 Da
MS2 end mass	1800.0 Da
SWATH-MS experiment mass window	25 + 1 Da overlap
Fragment conditions	Rolling collision energy, charge state +2, collision energy spread of 15 V

WIFF tool to compare the chromatograms and evaluate differences between samples (*see* **Note 15**).

7. Following completion of all mass spectrometry, transfer all files to the hard drive of the computer that will be used for database searching of library samples and targeted data extraction of SWATH-MS files (*see* **Note 16**).

3.3 Data Processing: Generating the Spectral Library

1. If not already performed, transfer all DDA-generated files that will be used for creating the spectral library to the computer hard drive. The computer must have ProteinPilot installed.
2. Compile the FASTA file that will be used for database searching (*see* **Note 17**). For this step, we use the UniProt-SwissProt (www.uniprot.org) database to export the reference proteomes for *Homo sapiens* (search "organism:9606 AND reviewed:yes AND keyword:1185") and for HIV-1 (search: "taxonomy:11706 AND reviewed:yes AND keyword:1185"). A word processor,

such as notepad, can be used to merge the files and add any additional FASTA sequences, such as the file with common laboratory contaminants provided by the AB SCIEX. Transfer the newly generated FASTA file to the databases folder within the AB SCIEX ProteinPilot Application folder.

3. (Optional for DIA) Inclusion of artificial peptides in the FASTA database. Information on the spiked-in peptides must be added to the FASTA database manually (*see* **Note 18**). Open the FASTA database in Notepad. Provide an entry for each artificial peptide. The sequence and name (Artificial names are ok) must be provided for each peptide (*see* **Note 19**).
4. Launch ProteinPilot. In the workflow tasks panel, click "LC…" under the "Identify Proteins" tab. Use the "Add…" button to add DDA samples to the search file. Process the file using a new paragon method (Table 3) and save the method using the "Save As…" button. Back in the "Identify Proteins" dialog box, save the results file and assign its location using the "Save As…" button. Click the "Process" button to begin the search. The file that is generated is a .group file, which will be uploaded as the reference spectral library during targeted data extraction.

Table 3
Paragon method

Describe sample	
Sample type	Unlabeled
Cys alkylation	Iodoacetamide
Digestion	Trypsin
Instrument	TripleTOF 5600
Special factors	None selected
Species	None
Specify processing	
Quantitate, bias correction, background correction	Not able to be selected
ID Focus	Biological modifications, amino acid substitutions
Database	FASTA database compiled in Data Processing: Generating the Spectral Library **Step 2**.
Search effort	Thorough ID
Results quality	Detected protein Threshold >0.05 (10 %)
Run false discovery rate analysis	Checked

3.4 Data Processing: Targeted Data Extraction

1. If not already performed, transfer all DIA-generated files that will be used for targeted data extraction to the computer hard drive. The computer must have PeakView installed and licensed with the Protein Quantitation MicroApp installed.
2. Launch PeakView. Under the "Quantitation" menu, click "Import Ion Library." Select the group file that was generated in Data Processing: Generating the Spectral Libary **step 4** (*see* **Note 20**). The upload time will vary from minutes to hours and is dependent on the size of the .group file and computer processor speed. After the library has successfully been loaded, a dialog box will automatically appear and request selection of the SWATH-MS files that will be used for targeted data extraction. Select all the files that will be used for export.
3. If applicable, select the peptides that will be used for retention time (RT) correction, using either the spiked-in peptides or selecting high-abundance endogenous peptides (*see* **Note 21**). To do this, search for the protein of interest and click the peptides that will be used for correction so that a check mark is apparent next to the peptide sequence. Next, click the "Add RT-Cal" button to add selected peptides to the RT calibration set. To edit the set of peptides used for RT calibration, click the "Edit RT-Cal" button and select peptides for deletion. In addition, use the "Edit RT-Cal" tool to calculate RT fit and apply RT modifications.
4. Following RT correction, click the processing settings button under the SWATH Processing dialog box. Set the processing settings accordingly. We use the following parameters: Up to 30 peptides, 6 transitions, 95 % peptide confidence threshold, 1 % false discovery rate threshold, exclude shared peptides, XIC window of 12 min, and XIC width of 75 ppm. These settings will likely require optimization dependent on the samples used for mass spectrometry (*see* **Note 22**).
5. Click process to perform targeted data extraction. Following processing, export all information using the Quantitation menu → SWATH processing → Export → All. The file that is generated is an .xlsx and can be opened in a database application or alternative statistical platforms capable of importing .xlsx files.

3.5 Data Processing: Normalization of Data and Statistical Analysis

We use one of two distinct approaches for normalization and statistical analysis of SWATH-MS data.

3.5.1 Normalization in MarkerView and Statistical analysis

When investigating any proteomic data, there is a necessity to normalize to correct for any error in preparation. To compensate for this error, we recommend normalization in MarkerView.

MarkerView offers a wide variety of normalization parameters that may be chosen dependent on the experimental design. Using MarkerView normalization in conjunction with a Bayesian analysis, a probabilistic statistical approach, offers additional benefits. Bayesian analysis can analyze data of high dimensionality by demonstrating the data must follow the rules of probability introduced by the Bayes theorem [9]. By following these rules, Bayesian analysis is able to correctly analyze data with fewer biological replicates than a simple *t*-test. This can be performed in eight steps:

Step 1. Export the area under curve data from PeakView as a MarkerView file.

Step 2. Open the extracted ion chromatogram (XIC) data in MarkerView.

Step 3. Normalize the data choosing the best normalization method based upon the design of the experiment (*see* **Note 23**).

Step 4. Statistical analysis of mass spectrometry data is necessary to draw strong conclusions from the data. Unfortunately, when comparing multiple proteins in multiple samples, common multiple testing corrections (e.g., Bonferroni) render everything insignificant. To combat these problems, Bayesian analysis followed our multiple testing correction is a viable method to analyze data.

Step 5. CyberT (http://cybert.ics.uci.edu or http://molgen51.biol.rug.nl/cybert/), an online Bayesian analysis calculator, can be used for analyzing high dimension mass spectrometry data [9, 10].

Step 6. Format the data for upload into CyberT in accordance with the recommendations provided by the online calculator.

Step 7. Select the correct analysis parameters.

For normalization, CyberT can perform normalizations but is limited in number of normalization methods. We recommend loading MarkerView normalized data.

For the Bayesian analysis parameters, we recommend following CyberT instructions for Sliding window size. For the Bayesian confidence value, we recommend multiplying the number of replicates by 3 and using the corresponding value.

For multiple testing correction, multiple methods may be calculated through a single analysis by selecting to "Compute multiple test corrections" under "Standard Multiple Hypothesis Testing Corrections."

We recommend computing the Posterior Probability of Differential Expression (PPDE). PPDE gives the prob-

ability of observing a real change. Cumulative PPDE is the best method for determining statistical significance because it corrects the PPDE to a false discovery rate of 0.05.

Proteins with a p-value <0.05 and a Cumulative PPDE >0.95 are considered to be significantly altered between samples.

Step 8. Export the data to Excel or other data formats for further analysis.

3.5.2 Normalization by Relative Abundance and Parametric Statistical Testing

Normalization by relative abundance uses the z-score to assign a value that represents the relative distribution of each protein within a given dataset/condition. This value is then used to measure alterations in the relative abundance of a given protein between conditions. An advantage of the z-score transformation is that normalization of the dataset to the standard normal distribution can be performed independently for each dataset, which allows for the rapid inclusion of multiple conditions, replicates, and comparisons. The change in relative abundance between conditions for any given protein is termed z-difference, and this measure can be used for parametric statistical testing, including the z-test [11, 12] and even other parametric tests, such as the ANOVA for multiple conditions and comparisons. The methods below provide a step-by-step procedure for normalization and statistical testing, including the paired and unpaired z-test.

1. Open the targeted data extraction file that was exported from PeakView and move (as a copy) the protein data to a new Excel spreadsheet. In this manner, the original export retains its integrity if the raw data is requested.
2. In the new spreadsheet, transform the raw intensity data using the natural log (ln). This transformation will normalize the data so that the entire dataset better approaches a normal distribution that is required for statistical testing (*see* **Note 24**).
3. Z-transformation of the data requires calculation of the mean and standard deviation of all proteins within a single dataset (one replicate, one condition). The z-score is a quantitative representation of the relative abundance of a protein and can be calculated using the following equation:

$$z = \frac{x - \mu}{\sigma}$$

where x is the natural log transformed raw intensity value for a given protein, μ is the overall average of natural log transformed raw intensity values for all proteins within a single dataset, and σ is the standard deviation of the natural log transformed raw intensity values for all proteins within a single dataset.

4. Based on the experimental design, choose the appropriate statistical test: the paired samples or independent samples z-test. For multiple comparisons/conditions, consider using a statistical test such as an ANOVA. The paired samples z-test is the more appropriate statistical test when comparing the expression of a protein before and after a condition within the same donor whereas the independent samples z-test is the more appropriate statistical test when comparing the overall expression of a given protein within a cohort of control subjects as compared to the overall expression of a given protein within a cohort of subjects with a defined disease or condition. The paired and independent samples z-tests are conceptually equivalent to the paired and independent samples Student's *t*-tests, respectively.
5. For paired samples, use the following formula to calculate the z-test statistic [12]:

$$\text{ztest}_{\text{paired}} = \frac{\bar{d} - D}{\sigma_d / \sqrt{n}}$$

where $\bar{d}$ is the mean value of pairwise differences across all replicates, D is the hypothesized mean of the pairwise differences across all replicates (most often 0), σ_d is the standard deviation of the pairwise differences across all replicates, and n is the total number of pairwise comparisons (replicates).

6. For independent samples, use the following formula to calculate the z-test statistic [11]:
7. After the z-test statistic is calculated, determine the *p*-value using the standard normal distribution for a two-tailed test (e.g., a test statistic of 1.96 = 95 % confidence or $p = 0.05$) (*see* **Note 25**)

$$\text{ztest}_{\text{ind}} = \frac{\overline{x_{\text{exp}}} - \overline{x_{\text{cont}}}}{\sqrt{\frac{\sigma_{\text{exp}}^2}{n_{\text{exp}}} + \frac{\sigma_{\text{cont}}^2}{n_{\text{cont}}}}}$$

where $\overline{x_{\text{exp}}}$ is the mean value of a given protein across all replicates in the "experimental condition," $\overline{x_{\text{cont}}}$ is the mean value of a given protein across all replicates in the "control condition," σ_{exp}^2 is the variance of the protein expression across all replicates in the "experimental condition," σ_{cont}^2 is the variance of the protein expression across all replicates in the "control condition," and n is the total number of samples for each condition.

3.6 Limitations of Proteomics

Despite unquestionable progress in acquisition of mass spectra, a major limitation of quantitative proteomics is the very high dynamic range of protein concentrations in highly complex mixtures of proteins and peptides generated by any method of controlled (i.e., enzymatic) fragmentation. This limitation applies to all methods: label free, chemical labeling, or metabolic labeling methods and researchers are advised to look for potential systemic bias. Approaches of extensive fractionation leading to reduction of complexity of samples have been used and will be refined in the future. These approaches help to reduce the impact of the high dynamic range of concentrations by providing high quality spectra for low abundant proteins as well as remove suppressive effect of many spectra from highly abundant proteins. For plasma, an immunodepletion of highly abundant proteins as described in Sample Processing for SWATH-MS Designed Experiments **Step 3** has been widely used to reduce interference from highly abundant proteins and is recommended.

No matter how refined and advanced the proteomics technology becomes, nothing can make up for problems in experimental design. In addition to the issues in **Note 1**, adequate group sizes, proper controls, consistency in specimen acquisition, processing and storage, and other aspects important in studies of biospecimens from diverse human populations apply to proteomic experiments.

4 Notes

1. People with HIV infection offer interesting problems for performing serum/plasma biomarker studies. People with HIV-1 infection have a high incidence of comorbidities including hepatitis C co-infection [13], cardiovascular, liver, and kidney disease [14], and all these factors may influence serum/plasma protein composition. When performing biomarker studies, these confounding issues have the potential to confound experimental results. Therefore, additional effort should be focused on obtaining a thorough background on each patient to identify and account for confounding variables.
2. All work on patients as well as specimens derived from patients must be done under approval from the proper regulatory bodies such as Institutional Review Boards. In addition, working with human samples (and here with known infectious agents) must be done under appropriate safety standards (in general, BSL-2). Both of these aspects should be done following your institutional requirements. Samples should be drawn, processed, and stored under standardized conditions.
3. Immunodepletion will reduce the concentration of high-abundance serum/plasma proteins and in doing so will help

improve the detection and quantification of other lower abundance proteins that may have otherwise been masked. However how many most abundant proteins should be removed to facilitate analysis, and the best means to do this, is still an open question. We currently recommend using the Seppro IgY14 column (with avian antibodies targeting the following proteins: albumin, α_1-antitrypsin, IgM, haptoglobin, fibrinogen, α_1-acid glycoprotein, apolipoprotein A-I and A-III, apolipoprotein B, IgG, IgA, transferrin, α_2-macroglobulin, and complement C3) from Sigma-Aldrich.

4. SDS inactivates HIV-1 [15]; depending on one's institutional biosafety requirements the safety precautions may differ following viral inactivation.
5. We suggest using the Pierce 660 protein quantification methods because of the rapidity of analysis. Alternative methods (Bradford, BCA, etc.) can also be used if desired. However, we do not recommend using spectral absorbance for quantification as this measure is dependent on the presence of aromatic amino acids and can lead to a mistaken representation for protein concentration.
6. Numerous digest procedures are available online and provided in the literature and through protease manufacturer websites. In addition to trypsin, other enzymes may also be used, such as LysC; however these enzymes will require additional optimization. As an alternate to SDS treatment followed by FASP, samples may also be digested using a standard in-gel or in-solution tryptic digest protocol without the use of SDS; however remain aware of biosafety considerations.
7. For a sample with approximately 50 μg of starting protein, we recommend resuspending the sample in no more than 25 μL. Using this volume will allow for accurate analysis of peptide quantification by using a minimal amount of sample. In our experience, peptide quantity is usually 20–50 % of the amount of protein measured in Sample Processing for SWATH-MS Designed Experiments, **step 4**.
8. Using absorbance at a wavelength of 205 nm will quantify peptides by measuring at level of peptide bonds, rather than by inclusion of aromatic rings (measured at 280 nm). To customize the detection method, visit: http://www.nanodrop.com/Library/A205%20Proteins%20&%20Peptides%20Custom%20Method.pdf.
9. Peptide quantity to be loaded on the LC column is dependent on the type of cHiPLC columns being used. A variety of cHiPLC columns with different lengths, diameters, pore size, and resin are available, but will require additional optimization.
10. We recommend using the same cHiPLC columns for the duration of the project. Multiple columns are available and differ in

pore size and column length. Use of alternative columns will require additional optimization (also *see* **Note 9**).

11. Although Table 1 gives a suggested LC protocol (with a 180 min gradient from 5 to 35 % acetonitrile), optimization is necessary, and depending on the experimental setup, the gradient may be shortened or lengthen as necessary. However, it is important that all DIA and DDA for an experiment are performed with the same gradient.
12. When performing a SWATH-MS experiment, generation of the spectral library in DDA mode is important. Three methods are available to generate a library: (1) use a preconstructed library, (2) generate a library from experimental samples, or (3) generate a library from a variety of cell lines or other suitable samples containing proteins covering the range of those found in the experimental samples. Each method has benefits, but if limits on the sample availability exist the generation of a library through cell lines is an enticing option. We have previously performed such an analysis [16]. Until issues of alignment of elution times are resolved, we do not recommend using a preconstructed library.
13. At this step, we separate our samples into library or SWATH-MS runs and randomize the samples within each group. In this way, the mass spectrometry methods will only be changed once when transitioning from samples used for the library to SWATH-MS (or vice versa).
14. In our experience, peptides will begin eluting at approximately 30 min and maximum intensity readings occur between 70 and 110 min. However, elution times will change based on the elution gradient and will be influenced by sample composition. It can also be influenced by type of resin used for the reverse phase HPLC.
15. While some differences are expected between samples, TICs that are markedly dissimilar may indicate impurities in the sample, problems with the cHiPLC system, or issues with the mass spectrometry methods. We recommend testing all the procedures using a comparable sample to the experimental samples, but can be discarded in the event of procedural shortcomings.
16. Because of the processor intensive demands for searching and for targeted data analysis, we recommend using a computer distinct from the computer that is loaded with Analyst and operates the mass spectrometer.
17. The SwissProt section of UniProtKB is a high quality, manually curated database of protein sequences that eliminates redundancy. In contrast, the TrEMBL section contains computationally analyzed records that are obtained from the translation of annotated coding sequences of the EMBL-bank/

GenBank/DDBJ nucleotide databases. Although TrEMBL contains more information, this section of UniProtKB is limited in experimental validation of sequences and the use of TrEMBL sequences during database searching may increase the risk of inappropriate spectral assignment during targeted data extraction of SWATH-MS files.

18. Artificial peptides are added to the SWATH library in the same fashion as contaminants (*see* Data Processing: Generating the Spectral Libary, **step 2**).
19. FASTA files for artificial peptides listed in the Materials and Equipment can be found on the manufacturer's website. http://www.biognosys.ch/fileadmin/Uploads/iRT/iRT_Peptides_Fusion.FASTA. An alternative to using spiked-in peptide standards to correct for retention time drift is to select peptide(s) from abundant proteins (actin, keratin, etc.) in the PeakView software during data analysis.
20. Although proteins with a lower confidence are being imported to PeakView for targeted data extraction, lower confidence proteins will be filtered out during targeted data extraction within the PeakView software (FDR, Score) and can also be filtered manually after export (e.g., filtered by number or peptides per protein ≥2).
21. When selecting spiked-in or endogenous peptides for RT correction, be sure to select only those peptides with high intensity readings, overlapping transition states, those that are free of background noise, and cumulatively have adequate coverage across the entire elution gradient.
22. Low confidence assignment of spectra for a number of given samples *may* impact the quality of the export for all samples if exported in unison. For this reason, perform targeted data extraction only for samples that will be used for direct comparison to one another. The processing settings will need to be optimized for each individual experiment with a particular emphasis on the extraction window. Using the RT correction tool will likely improve RT variability between samples and allow for narrowing of the extraction window. Additionally, setting a stringent FDR threshold (e.g., 1 %) will improve the quality of the exported data (as assessed by manual review of the overlay of transition states in the XIC pane and the alignment of the SWATH spectra to the library spectra in the spectra pane). It should be noted, however, that this stringency comes with the cost of decreasing the total number of proteins exported and will likely impact the number of peptides used for quantification. Also discussed in [6].
23. Four normalization methods are available in MarkerView: (1) Selected peak, (2) Total peak intensity, (3) median peak intensity,

and (4) manual scale factor. Additional information on the normalization can be obtained in the MarkerView program.

24. In some cases, such as working with supernatants or whole cell lysates from cell lines, the means and standard deviations between replicates and conditions will be comparable and as such, no further transformation is necessary. In these cases, it is suggested to perform statistical testing using the *t*-test (for two comparisons) or a variation of the ANOVA for multiple comparisons. However, when working with biological fluids obtained from primary donors, it should be expected that the mean intensity and standard deviations between donors is not comparable, and as such, the z-transformation can be applied in order to allow for parametric statistical testing.
25. If desired, multiple comparisons corrections can be employed, but it may limit the robustness and utility of continued analyses, including bioinformatic analysis.
26. "Event" describes the programming that is used to direct the sample path within the trap and column and is provided for reference. For additional information on this subject, please contact Eksigent.

References

1. Pernemalm M, Lehtio J (2014) Mass spectrometry-based plasma proteomics: state of the art and future outlook. Expert Rev Proteomics 11(4):431–448
2. Anderson L (2014) Six decades searching for meaning in the proteome. J Proteomics 107C:24–30
3. Burkhard PR, Rodrigo N, May D, Sztajzel R, Sanchez JC, Hochstrasser DF, Schiffer E, Reverdin A, Lacroix JS (2001) Assessing cerebrospinal fluid rhinorrhea: a two-dimensional electrophoresis approach. Electrophoresis 22(9):1826–1833
4. Vejda S, Posovszky C, Zelzer S, Peter B, Bayer E, Gelbmann D, Schulte-Hermann R, Gerner C (2002) Plasma from cancer patients featuring a characteristic protein composition mediates protection against apoptosis. Mol Cell Proteomics 1(5):387–393
5. DeSouza LV, Siu KW (2013) Mass spectrometry-based quantification. Clin Biochem 46(6):421–431
6. Gillet LC, Navarro P, Tate S, Rost H, Selevsek N, Reiter L, Bonner R, Aebersold R (2012) Targeted data extraction of the MS/MS spectra generated by data-independent acquisition: a new concept for consistent and accurate proteome analysis. Mol Cell Proteomics 11(6): O111.016717
7. Wisniewski JR, Zougman A, Nagaraj N, Mann M (2009) Universal sample preparation method for proteome analysis. Nat Methods 6(5):359–362
8. Scopes RK (1974) Measurement of protein by spectrophotometry at 205 nm. Anal Biochem 59(1):277–282
9. Baldi P, Long AD (2001) A Bayesian framework for the analysis of microarray expression data: regularized t -test and statistical inferences of gene changes. Bioinformatics 17(6): 509–519
10. Kayala MA, Baldi P (2012) Cyber-T web server: differential analysis of high-throughput data. Nucleic Acids Res 40(Web Server issue):W553–W559
11. Cheadle C, Vawter MP, Freed WJ, Becker KG (2003) Analysis of microarray data using Z score transformation. J Mol Diagn 5(2):73–81
12. Haverland NA, Fox HS, Ciborowski P (2014) Quantitative proteomics by SWATH-MS reveals altered expression of nucleic acid binding and regulatory proteins in HIV-1-infected macrophages. J Proteome Res 13(4): 2109–2119

13. Taylor LE, Swan T, Mayer KH (2012) HIV coinfection with hepatitis C virus: evolving epidemiology and treatment paradigms. Clin Infect Dis 55(Suppl 1):S33–S42
14. Deeks SG, Lewin SR, Havlir DV (2013) The end of AIDS: HIV infection as a chronic disease. Lancet 382(9903):1525–1533
15. Krebs FC, Miller SR, Malamud D, Howett MK, Wigdahl B (1999) Inactivation of human immunodeficiency virus type 1 by nonoxynol-9, C31G, or an alkyl sulfate, sodium dodecyl sulfate. Antiviral Res 43(3):157–173
16. Villeneuve LM, Stauch KL, Fox HS (2014) Proteomic analysis of the mitochondria from embryonic and postnatal rat brains reveals response to developmental changes in energy demands. J Proteomics 109C: 228–239

Chapter 21

Proteomic Characterization of Exosomes from HIV-1-Infected Cells

Ming Li and Bharat Ramratnam

Abstract

Proteomics has increasingly become an invaluable tool to characterize proteomes from various subcellular compartments. Here, we describe a quantitative proteomics method using the technique of Stable Isotope Labeling by Amino acids in Cell culture (SILAC) to analyze the effects of HIV infection on host exosomal proteomes. The procedure, described below, involves differential isotope labeling of cells, exosome purification, mass spectrometric quantification, and various bioinformatic analyses/verifications. Although this chapter focuses on analyzing the effects of HIV-1 infection on the exosomal proteome, the protocol can easily be adapted to other subcellular compartments under different stress conditions.

Key words HIV-1, Exosome, Proteomics, Mass spectrometry, SILAC

1 Introduction

HIV-1 buds from the host plasma membrane in order to complete its life cycle [1, 2]. Exosomes, 30–100 nm vesicles secreted by a wide range of cell types [3–5], have been shown to play crucial roles during this process [6, 7]. As exosomes are largely composed of various proteins [8], characterizing these proteins may allow us to better understand how HIV-1 influences exosomal cargo and the host secretion machinery.

Numerous quantitative proteomics methods have been developed in recent years. These include the commonly used metabolic labeling based SILAC technique [9]. Other examples include chemical labeling based iTRAQ (isobaric Tags for Relative and Absolute Quantification), an isobaric labeling method that can be used to determine the amount of proteins from multiple sources in a single experiment [10]. A label-free MRM (Multiple Reaction Monitoring) method has been commonly used for the targeted quantitation of proteins/peptides in biological samples [11, 12]. However, a detailed comparison (Table 1) shows that SILAC is an excellent choice for HIV-1/exosomal proteome study in cultured cells.

Vinayaka R. Prasad and Ganjam V. Kalpana (eds.), *HIV Protocols*, Methods in Molecular Biology, vol. 1354,
DOI 10.1007/978-1-4939-3046-3_21,

Table 1
The comparison among three commonly used quantitative proteomics methods

	Labeling	Samples	Cost	Analysis	Small change measurement	Technical variability
SILAC	Metabolic	Mainly for cultured cells	Relatively low	Relatively straightforward	Reliable	Low
iTRAQ	Chemical	Wide ranges of samples	Moderate	Moderate	Relatively reliable	Relatively low
MRM	No labeling	Mainly for clinical samples	Relatively high	Time-consuming	Less reliable	Relatively high

The differences of SILAC, iTRAQ, and MRM are compared in the category of labeling principle, sample application scope, experimental cost, easiness of doing analysis, ability to detect small changes, and technical variability

For a majority of biomedical laboratories, the whole procedure is quite straightforward and the cost is relatively low. The principle of SILAC labeling is based on metabolic incorporation of given nonradioactive isotopic forms of an amino acid in the culture media into cellular proteins. Typically, SILAC experiments start with two cell populations: one is labeled in the culture medium composed of heavy isotopic $^{13}C_6$ L-lysine and/or $^{13}C_6{}^{15}N_4$ L-arginine for 6 doublings, while the other is maintained in the same medium but with normal L-lysine and/or L-arginine for the same period. Protein is extracted from the two cellular populations mixed at equal proportions and subjected to mass spectrometry. The relative intensities of mass spectrometric peak(s) generated from a protein reflect its relative abundance [13]. As seen in Fig. 1, we adapted SILAC-based proteomics to determine the effects of HIV-1 infection on host exosomal proteome using the following procedure. Initially, HIV-1 uninfected and infected cells are differentially isotope labeled. Then, the labeled exosomes are purified and subjected to total protein extraction. Next, liquid chromatography-tandem mass spectrometry is employed to analyze the exosomal proteome. Finally, the resulting mass spectrometry data and potential candidates are subjected to statistical, bioinformatics analyses as well as vigorous biochemical verification.

2 Materials

Prepare solutions using ultrapure water and store reagents according to their specific requirements as stated below. Strictly follow all waste disposal regulations when disposing of waste materials, especially HIV-1 infected samples.

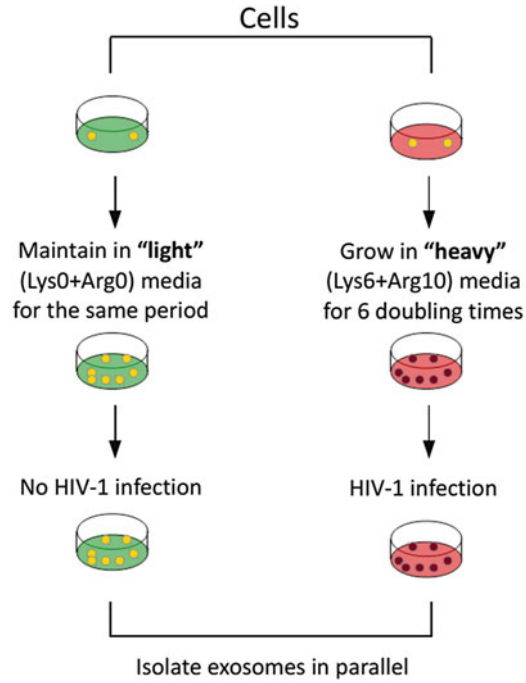

Fig. 1 Overall experimental schema for SILAC labeling. Ready to be labeled cells are divided into two batches. One batch is expanded in "heavy" medium for six doublings to achieve complete labeling. The other batch is independently maintained for the same periods. When the cells are completely labeled, the heavy cells are infected with HIV-1, while light cells receive no infection. At the end of infection, heavy (infected) and light (uninfected) are subjected to exosome isolation in parallel.

1. Cells: In order to be effectively labeled by SILAC, the cells chosen need to be in an actively proliferative stage (*see* **Note 1**). Depending on specific experimental settings, cells are also often required to be susceptible to HIV-1 infection. Some examples of cell lines that meet these two criteria are: HeLa $T4^+$ cells, a human cervical epithelial carcinoma modified to stably express $CD4^+$; H9 cells and CCRF-CEM cells, both suspension cell lines derived from acute lymphoblastic leukemia.
2. Reagents for checking cell survival and proliferation rate: Trypan blue and MTT [3-(4,5-dimethylthiazol-2-yl)-2,5-diphenyltetrazolium bromide] assay kit are commercially available.
3. Dialyzed fetal bovine serum (FBS) (*see* **Note 2**).
4. Medium: Standard DMEM, RPMI, or other medium of choice deficient in Arginine and Lysine. Please refer to http://www.atcc.org/ for detailed composition. Store it at 4 °C.

5. Amino acids: Normal light L-Lysine and L-Arginine; Heavy isotopical Lysine ($^{13}C_6$ L-lysine) and Arginine ($^{13}C_6{}^{15}N_4$ L-arginine) (*see* **Note 3**). All amino acids are commercially available.
6. Facilities for HIV-1 related research: class II biological safety cabinets and a BSL-2+ environment.
7. Refrigerated ultracentrifuge or super-speed centrifuge: it is necessary that the centrifuge chosen can reach at least $100{,}000 \times g$ (*see* **Note 4**).
8. Centrifuge tubes: Tubes that can withstand ultracentrifugation and are compatible with rotors.
9. Phosphate-buffered saline (PBS): 144.0 mg/L of Potassium Phosphate monobasic (KH_2PO_4), 795.0 mg/L of Sodium Phosphate dibasic ($Na_2HPO_4 \cdot 7H_2O$), and 9.0 g/L of Sodium Chloride (NaCl) pH 7.4. Store at 4 °C.
10. RIPA (Radio Immuno Precipitation Assay) buffer: 50 mM Tris-HCl, 150 mM NaCl, 1.0 % NP-40, 0.5 % sodium deoxycholate, and 0.1 % SDS (sodium dodecyl sulfate), pH 8.0.
11. Protease inhibitor cocktails: Commercially available.
12. Microcentrifuge shaker: A shaker with speed and temperature control is recommended.
13. Platform rocker with circular motion.
14. Benchtop microcentrifuge: Centrifuge with cooling feature is recommended.
15. Spectrophotometer: Fluorometer can be an alternative.
16. SDS-PAGE (PolyAcrylamide Gel Electrophoresis) gel running apparatus and a quality power supply (*see* **Note 5**).
17. Gel running reagents: Refer to specific literature for detailed procedures on how to prepare gel casting reagents, running buffers and sample buffers. Alternatively, precast gels and proprietary reagents can be purchased.
18. Gel staining and destaining reagents: Staining solution: 15 % methanol, 10 % acetic acid, and 2 g Coomassie Brilliant Blue in water; Destaining solution: 15 % methanol and 10 % glacial acetic acid in water.
19. Gel wash buffer: 25 mM ammonium bicarbonate (NH_4HCO_3) prepared in HPLC (High-Performance Liquid Chromatography) grade water; 25 mM ammonium bicarbonate (NH_4HCO_3) dissolved in 50 % acetonitrile (1:1 ACN/H_2O).
20. Reduction and alkylation reagents: 10 mM Dithiothreitol (DTT) in 25 mM NH_4HCO_3 and 55 mM iodoacetamide in 25 mM NH_4HCO_3. Prepare freshly.

21. Digestion buffer: 12.5 ng/μl mass spectrometry grade modified trypsin dissolved in freshly prepared 25 mM NH_4HCO_3.
22. Peptide recovery buffer: 5 % formic acid in 50 % ACN.
23. Vacuum concentrator.
24. HPLC buffers: Buffer A: 0.9 % acetonitrile and 0.1 % formic acid in HPLC grade water; Buffer B: 100 % acetonitrile.
25. Nanoflow HPLC and Mass spectrometer: Contact proteomics core facilities in your institution or send your samples to outside institutions that have experience in SILAC-based quantitative proteomic analysis (*see* **Note 6**).
26. Protein/peptide identification software: Open-source Andromeda available at http://www.andromeda-search.org/ or Mascot, commercially available from MatrixScience.
27. Quantitation software: MaxQuant, freely available at http://www.maxquant.org/ or other software from mass spectrometer instrument vendors.
28. Western blotting reagents: Related buffer and reagents are commercially available or can be prepared in the lab. Refer to western blotting-specific manual for details.
29. Software and databases: ImageStudio® lite can be downloaded from http://www.licor.com/bio/products/software/image_studio_lite/ with registration; Silacratioanalyser is available at http://proteome.moffitt.org/proteomics/silacratioanalyser/silacratioanalyser.jnlp; STRAP (Software Tool for Rapid Annotation of Proteins) can be downloaded from http://www.bumc.bu.edu/cardiovascularproteomics/cpctools/strap/. Exosome database can be accessed at http://www.exocarta.org; the URL of the HIV-1 Human Interaction Database is http://www.ncbi.nlm.nih.gov/genome/viruses/retroviruses/hiv-1/interactions/; DAVID (Database for Annotation, Visualization and Integrated Discovery) can be accessed at http://david.abcc.ncifcrf.gov; the URL of STRING (Search Tool for the Retrieval of Interacting Genes/Proteins) is http://string-db.org/

3 Methods

3.1 Cell Culture (Labeling) and HIV-1 Infection

SILAC medium should be freshly prepared (follow manufacturer's manual closely) before use. Medium can be stored at 4 °C for up to about 3 months. To assure healthy and highly proliferative cells, the use of trypan blue staining (to measure cell viability) and MTT assay (to check cell proliferation) is recommended before conducting actual metabolic labeling.

1. Seed and culture two batches of cells in 10 cm cell culture dishes in parallel. One is in "heavy" labeling medium, which contains 10 % dialyzed FBS supplemented with 100 mg/L $^{13}C_6$ L-lysine and 100 mg/L $^{13}C_6{}^{15}N_4$ L-arginine, the other one is in "light" medium (containing 10 % dialyzed FBS supplemented with 100 mg/L L-Lysine and 100 mg/L L-Arginine) (*see* **Note 7**).
2. Expand cells in the heavy medium for six doublings to achieve complete (>99 %) labeling of cellular proteins with heavy amino acids, while independently maintain cells in light medium for the same number of doublings (*see* **Note 8**).
3. Change media regularly (depending on specific cell type, normally every 2–3 days) during the labeling period.
4. After complete labeling, infect cells grown in heavy labeling medium ("Heavy") with HIV-1 (e.g., NL4-3 HIV-1 strain, *see* **Note 9**) by following standard HIV infection protocol [14]. During the same period, maintain cells grown in light labeling medium ("Light") in parallel without infection.
5. Harvest both "Light" (uninfected) and "Heavy" (infected) supernatants independently at the end of infection (*see* **Note 10**).

3.2 Exosome Isolation

Using sequential ultrahigh centrifugation, exosomal fractions are independently enriched from culture supernatants from both infected and uninfected cells [15]. All of the followings steps are performed at 4 °C (Fig. 2).

1. Collect culture supernatants, not cells, into proper sized centrifuge tubes and centrifuge at 300 × *g* for 10 min to remove residual cells.
2. Transfer the cleared supernatants to new centrifuge tubes and centrifuge at 2000 × *g* for 10 min to remove dead cells. Pipet supernatants carefully, do not touch pellets as they can contaminate supernatants.
3. Transfer the supernatants to ultracentrifugation tubes and centrifuge (make sure tubes are well balanced) at 10,000 × *g* for 30 min to remove cell debris. Similar to **step 2**, do not touch pellets while collecting supernatants.
4. Transfer the resulting supernatants to fresh ultracentrifugation tubes and centrifuge at 100,000 × *g* for 70 min. Remove the supernatants completely and discard. Unlike previous steps, starting from this step, remove supernatants and save pellets.
5. Resuspend the pellets, containing exosomes, in 5 ml fresh PBS, transfer the suspensions to clean ultracentrifugation tubes and centrifuge again at 100,000 × *g* for 70 min.
6. Remove the supernatants and discard, resuspend the resulting pellets, in 50 μl PBS (*see* **Note 11**) for long-term storage (at −80 °C freezer) or proceed directly to protein extraction.

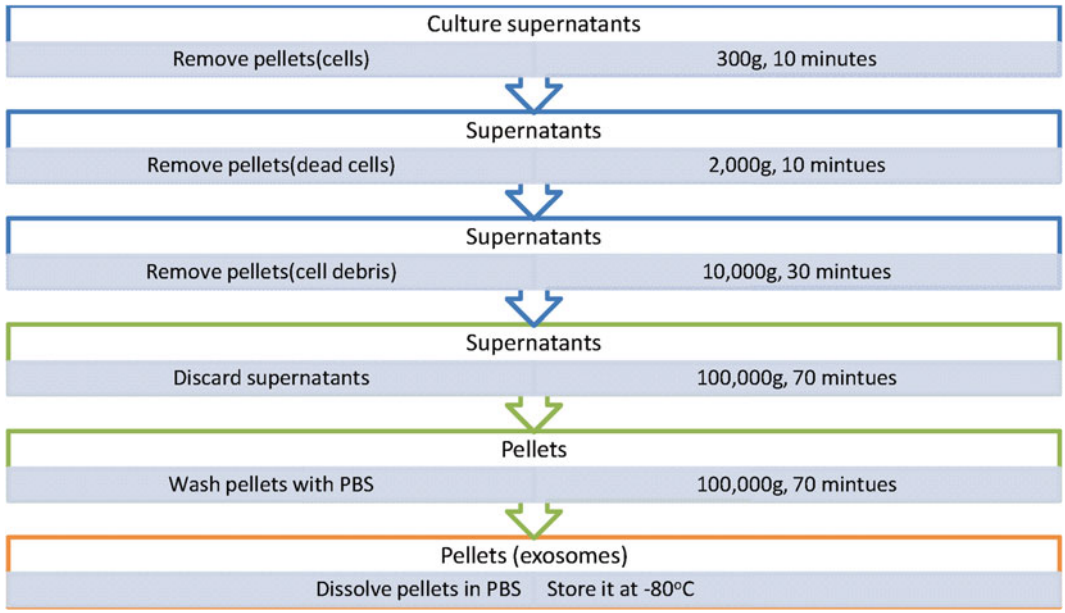

Fig. 2 Flow chart of exosome purification procedure based on differential ultracentrifugation. For each step, samples need to be processed are listed in the *middle* of chart. Fractions to be discarded in each step are indicated on the *left*. The speed and length of each centrifugation are shown on the *right*. Need to note, for the first three centrifugations, pellets are discarded and the supernatants are saved for the next step. However, for the last two ultracentrifugation steps, pellets are saved and supernatants are discarded.

3.3 Protein Extraction and Preparation

1. Add 50–200 μl of RIPA buffer supplemented with protease inhibitor cocktails to the tubes containing the purified exosomal pellets. Vortex the tubes vigorously to completely dissolve the pellets.
2. Transfer the dissolved protein solutions to new 1.5 ml microcentrifuge tubes. Shake the tubes vigorously (e.g., 400 rpm) for 5 min on a microcentrifuge shaker.
3. Centrifuge the mixtures for 10 min at 13,000 × *g*.
4. Transfer the resulting supernatants, which contain extracted exosomal proteins, to new microcentrifuge tubes for storage or continue to the next step.
5. Quantify protein concentration from the "Light" (uninfected) and "Heavy" (infected) exosomal samples respectively by employing a standard protein quantification assay, such as bicinchoninic acid (BCA) or Bradford-based method.
6. Based on the concentrations determined from previous step, calculate and mix the right volumes of light and heavy protein extracts to form a mixture that contains equal proportions (1:1) of total protein from "Light" and "Heavy" samples. Load the single mixture on an SDS-PAGE gel and run electrophoresis. 2–10 μg of total protein per gel lane is recommended.

7. Transfer the finished gel to a square petri dish and stain it with Coomassie blue for 1 h with gentle orbital shaking.
8. Destain the gel for a few hours to overnight.
9. Cut the entire sample lane from the destained gel into 10–15 equal gel pieces with a clean razor blade. Further slice each gel piece into smaller (e.g., 1×1 mm) cubes and transfer them into a new 1.5 ml microcentrifuge tube.
10. In each tube, add enough 25 mM NH_4HCO_3 in 50 % ACN to fully immerse the gel cubes and vortex for 10 min. Remove the supernatants and discard. Repeat this step twice.
11. Dry the gel cubes in a vacuum concentrator for 20 min.
12. Rehydrate gel cubes with enough 10 mM DTT, vortex and centrifuge briefly. Allow reaction to proceed at 56 °C for 1 h.
13. Remove the supernatant. Add enough 55 mM iodoacetamide to fully immerse the gel cubes. Vortex and spin briefly. Incubate in the dark at room temperature for 45 min.
14. Remove the supernatant. Add enough 25 mM NH_4HCO_3 to immerse the gel pieces. Vortex and centrifuge briefly.
15. Remove the supernatant. Add 25 mM NH_4HCO_3 in 50 % ACN to immerse the gel pieces. Vortex and centrifuge briefly.
16. Repeat **steps 14** and **15** once.
17. Dry the gel cubes in a vacuum concentrator.
18. Add 25 μl trypsin in 25 mM NH_4HCO_3 to the dried gel cubes and incubate at 4 °C for 30 min. Remove excess solution and discard. Add a minimum amount of 25 mM NH_4HCO_3 without trypsin to keep gel pieces immersed throughout digestion. Incubate overnight at 37 °C.
19. To recover peptides from the gel: Spin down briefly and transfer extract to a new tube. Add 30 μl of 5 % formic acid in 50 % ACN to the original gel cubes, vortex for 30 min and spin. Transfer the supernatant and combine with the extract obtained initially.
20. Dry down the combined peptide extracts by a vacuum concentrator to less than 5 μl and resuspend with 20 μl HPLC buffer A before proceeding to next step.

3.4 Mass Spectrometry Identification and Quantitation

Duplicate runs of samples are required; triplicates are recommended to minimize variation and to achieve a high fidelity of proteomic analysis. Your mass spectrometry core facilities are likely to perform all the steps in this section for you. We list brief steps here as a reference.

1. Apply the resulting peptide mixtures from each gel piece to microcapillary reversed phase liquid chromatography-tandem mass spectrometry (LC-MS/MS) separately.

2. Perform HPLC using a nanoflow HPLC with a self-packed 75 μm id × 15 cm C^{18} column in buffer A. The LC gradient is produced over 60 min from 2 to 38 % HPLC buffer B.
3. Set mass spectrometer (MS) at following settings: Operate in data-dependent acquisition (DDA)/positive ion mode; Acquire the full scan range between 390 and 1500 m/z at 30,000 resolution using a Top5 DDA method via collision-induced dissociation (CID); Exclude precursor ions for a duration of 2 min; Use Nano-ESI spray voltage of +3 kV without sheath or auxiliary flow gas; Set the ion count threshold for MS/MS selection at 700 counts; Use default settings for activation time and Q values.
4. Search the generated MS/MS spectra against the reversed and concatenated non-redundant Human IPI database by using the program Mascot with the following parameters: use the fixed modification of carbamidomethyl Cys and variable modifications of oxidation of Met and acetylation of protein N-terminus; allow two missed cleavages and Trypsin with Pro restriction; require a match of at least six amino acid residues; set MS tolerance at 30 ppm and MS/MS tolerance at 0.08 Da; allow the peptide and protein false discovery rate (FDR) ≤ 1 %.
5. Achieve protein quantitation by MaxQuant software [16], which is set to require at least two peptides per protein (one razor and one unique) for quantitation. Normalized SILAC ratios are used for all subsequent interpretation.

   Various information, including protein IDs, names, descriptions, and heavy/light ratios, of the identified proteins can be exported and saved as spreadsheet format for detailed downstream analysis.

3.5 Western Blotting Verification

Western blotting is recommended to verify protein quantification as determined by mass spectrometry. Standard western blotting procedures should be followed. Please refer to specific protocols for details. It is important to ensure that equal amounts of protein (can use aforementioned protein quantification method) are loaded from the control and experimental arms. In order to obtain robust quantitative verification, it is also recommended to develop blots with a digital imaging system and to analyze acquired image with analysis software (e.g., ImageStudio®).

3.6 Proteomic Data Analysis

The data quality assessment, data pretreatment, and calculation steps are carried out for each mass spectrometric replicate independently before merging data from all replicates for final inspections (Fig. 3).

1. Data quality assessment: (1) Log2 transform heavy/light ratios of all quantified proteins; (2) Group the transformed ratios into multiple (40–100) ratio bins; (3) Use statistical software

Fig. 3 Flow chart for determining significant candidates from proteomic analysis. Four successive steps of analysis and verification are implemented to ensure finding reliable, significant candidates. First step of plotting SILAC ratio histogram is to ensure the global data integrity. Second step is to make whole dataset less noisy by removing less ideal candidates. By employing unbiased statistical tools, the third step defines the significant thresholds for potential candidates. The last step finalizes the list of significant candidates by merging and analyzing the replicate data for each candidate from previous step.

to plot the number of detected ratios per bin. The resulting histogram of SILAC ratio distribution should follow normal distribution (*see* **Note 12**) [17].

2. Data pretreatment: To ensure greater confidence in the accuracy of the mass spectrometry-derived peptide (protein) ratios, a given protein needs at least two quantifiable peptides in order to be included in candidate selection (*see* **Note 13**).
3. Determination of significant threshold: To determine significantly up- and downregulated protein candidates, conservative cut-off values are calculated as followings: (1) Log2 transform the original SILAC protein ratios; (2) Calculate the median and standard deviation (σ) of the transformed ratios by using a statistical or spreadsheet software; (3) Calculate the cut-off of value (median $\pm 2\sigma$) in log space initially and then transform back into linear space. Candidates having ratios above median $+ 2\sigma$ or less than median $- 2\sigma$ are considered to be significant. In most cases, a small percent of candidates on both extreme ends will be assigned as significant.
4. Data comparison and inspection: The resulting significant candidates are compared across all replicates. A three-step workflow is carried out to identify potential candidates: (1) Only select the candidate(s) consistently shown in all replicates;

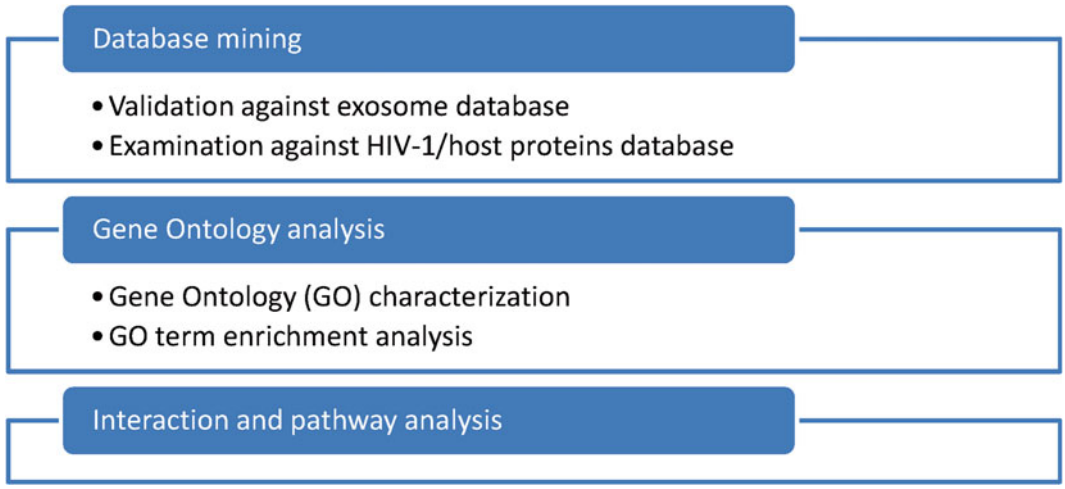

Fig. 4 Overall bioinformatics analysis procedures for HIEP candidates. To gain insights into HIEP candidates, data mining and bioinformatics analysis are implemented. Current exosome database and HIV-1/host interactome database are mined to verify the exosomal origins and the known interactions with HIV-1. Gene ontology characterization and enrichment analysis are performed to narrow down research scope and point out potential direction. Interaction and pathway analysis are also carried out to find potential binding or interacting partners.

(2) For each candidate, manually inspect all identification and quantitation, remove candidates that do not have the same direction among the replicates (up- or downregulated) and/or similar expression ratios. (3) Finalize data for the selected candidates by merging their data from all replicates.

3.7 Bioinformatics Verification and Characterization of HIV-1 Impacted Exosomal Protein (HIEP) Candidates

To take advantage of abundant (genomic, proteomic, and bioinformatic) existing information for almost every single protein, data mining and bioinformatics analysis are carried out to gain insights into HIEP candidates (Fig. 4). Several relevant databases and software programs are described below.

1. *Validation against exosome database*: To further verify a given candidate protein's assignment to the exosomal compartment, search HIEP candidates using their name or UniProt IDs against the current exosome database, which is a manually curated database that is integrated from both published and unpublished exosomal studies, by using "query" function [18, 19] (*see* **Note 14**).
2. *Examination against HIV-1/host proteins database*: To find potential known associations between HIV-1 and HIEP candidates, search the HIEP candidates (using the search boxes) against the HIV-1 and Human Protein Interaction Database [20] in order to identify proteins shared by the database and HIEP candidates (*see* **Note 15**).

3. *Gene Ontology (GO) characterization*: To get representation of GO terms: (1) Save UniProt IDs of HIEP candidates on txt file; (2) Import the txt file to STRAP software [21] and run the software to search against UniprotKB, EBI, and GO databases; (3) Visualize GO analysis results (e.g., in the form of pie chart) through a spreadsheet software by using analyzed data from STRAP (*see* **Note 16**).
4. *GO term enrichment analysis*: To find statistically significant overrepresented gene ontology (GO) terms: (1) Submit the HIEP candidate list to DAVID via its web interface by using "Functional Annotation Tool" [22]; (2) On the page of "Annotation Summary Results," choose the "Gene_Ontology" category, the enriched GO terms, *p*-value, and other associated parameters will be reported there (*see* **Note 17**).
5. *Interaction and pathway analysis*: To help downstream biochemical analysis and pathway discovery, it is worthwhile to find the known and predicted associations of HIEP candidates beforehand. A representative tool, STRING, is employed to provide direct (physical) and indirect (functional) associations [23]. This process is done by inputting protein ID or sequence in designated search box, choosing the right species and searching the database. The top ten known partners associated with each exosomal candidate will be shown as a part of the results (*see* **Note 18**).

   With all above mentioned analyses, a wealth of information of HIEP candidates will be analyzed. The most significant candidate(s) will be selected and subjected to downstream molecular and biochemical analysis.

4 Notes

1. For SILAC labeling, try to avoid using cells that have been propagated for an extended period. It is preferable to use early passage cells to achieve high labeling efficiency.
2. Dialyzed fetal bovine serum (FBS), not regular FBS, needs to be added to SILAC media to make the complete labeling medium. The Dialyzed FBS contains no or few free amino acids and peptides, which may interfere with SILAC labeling.
3. Usually, a SILAC labeling kit comes with only a single heavy isotope $^{13}C_6$ L-lysine. In order to improve coverage in mass spectrometry analysis, double "heavy" isotope labeling using $^{13}C_6$ L-lysine and $^{13}C_6{}^{15}N_4$ L-arginine is recommended. In which case, "heavy" $^{13}C_6{}^{15}N_4$ L-arginine should be obtained and added to labeling media (final concentration at 100 mg/L) accordingly.

4. The classical way of isolating exosomes involves ultra high-speed centrifugation. Currently, there are a few commercially available reagents that permit exosome isolation without ultra high-speed centrifugation and related equipment. These alternative methods may be carried out at the reader's discretion.
5. An alternative way to perform trypsin digestion is to do it directly in the protein extract without running a gel. However, conditions, such as buffer and digestion time, will have to be optimized for complete digestion.
6. Each proteomics core may have their own specific procedures and requirements for sample preparation and mass spectrometry analysis; consult them first to determine the best strategy and procedure.
7. Many factors, such as the sensitivity of mass spectrometer, goal of analysis (whole proteome or post-translational modification), and mass per cell, affect the minimum amount of protein (thereby minimum number of cells) needed for downstream analysis. We found ten million cells can be a good starting point to determine the optimal number of cells for proteomic analysis.
8. For a specific cell type, the exact cell doubling time needs to be determined. Fast growing cells obviously need less time to be completely labeled than slow growing cells.
9. HIV-1 infection should be monitored. One way of doing this is via p24 quantification in culture supernatants.
10. For adherent cells, the supernatants can be used directly for exosome isolation. For suspension cells, a pre-clearing step of centrifugation at $200 \times g$ for 10 min is needed to remove excess cells.
11. As HIV-1 virions are similar in size to exosomes, the purified exosomes from HIV-1 infected samples may be contaminated with HIV-1 virions. In proteomic screen, potential viral contaminants can be filtered out by limiting search database only to human. However, if further downstream experiments are expected, readers should employ established methodologies to separate HIV-1 virions from exosomes, if necessary [24].
12. If the SILAC ratio distribution is heavily skewed in one direction, the reader needs to determine the causes before continuing data analysis. Possible cause(s) may be due to unequal mix of "light" and "heavy" samples.
13. Although some proteins may have multiple (≥ 2) identified peptides; however, not all peptides come with heavy/light (SILAC) ratio values. Those proteins are recommended to be excluded if they have one or no peptide bearing SILAC values.

14. One way of verifying the success of exosomal purification and proteomic identification is to search the top 25 exosomal marker proteins listed at ExoCarta against HIEP candidates. A successful experiment usually finds a majority of the 25 exosome maker proteins in the SILAC list.
15. The database contains extensive HIV-1/host protein interactions that have been reported. The detailed interactions between HIEP candidates and HIV-1 are recommended to be mined.
16. There are many other (either standalone or web-based) GO term analysis software (e.g., GoMiner® [25] or PANTHER (Protein ANalysis THrough Evolutionary Relationships) [26]) available. It is up to reader's judgment to choose which software suits their needs.
17. Another alternative tool to DAVID is GORILLA (Gene Ontology enRIchment anaLysis and visuaLizAtion, http://cbl-gorilla.cs.technion.ac.il/) [27].
18. There are also quite a few software that can do pathway analysis. A proprietary Ingenuity IPA from Qiagen and a public accessible ConsensusPathDB (http://cpdb.molgen.mpg.de/) [28] are good examples.

Acknowledgements

This work was supported by an ARRA supplement to the Lifespan/Tufts/Brown CFAR, P30AI042853-13S1, NIH P20GM103421, P01AA019072, R01HD072693 to BR. This work was also supported by Lifespan Pilot Research Fund (#701-5857), Rhode Island Foundation Medical Research Grant (#20133969), and NIH COBRE URI/RIH Pilot Research Grant (P20GM104317) to ML.

References

1. Ivanchenko S, Godinez WJ, Lampe M, Krausslich HG, Eils R, Rohr K, Brauchle C, Muller B, Lamb DC (2009) Dynamics of HIV-1 assembly and release. PLoS Pathog 5:e1000652. doi:10.1371/journal.ppat.1000652
2. Sundquist WI, Krausslich HG (2012) HIV-1 assembly, budding, and maturation. Cold Spring Harb Perspect Med 2:a006924. doi:10.1101/cshperspect.a006924
3. Keller S, Sanderson MP, Stoeck A, Altevogt P (2006) Exosomes: from biogenesis and secretion to biological function. Immunol Lett 107:102–108. doi:10.1016/j.imlet.2006.09.005, S0165-2478(06)00228-8 [pii]
4. Schorey JS, Bhatnagar S (2008) Exosome function: from tumor immunology to pathogen biology. Traffic 9:871–881. doi:10.1111/j.1600-0854.2008.00734.x, TRA734 [pii]
5. Thery C, Ostrowski M, Segura E (2009) Membrane vesicles as conveyors of immune responses. Nat Rev Immunol 9:581–593. doi:10.1038/nri2567, nri2567 [pii]
6. Booth AM, Fang Y, Fallon JK, Yang JM, Hildreth JE, Gould SJ (2006) Exosomes and HIV Gag bud from endosome-like domains of the T cell plasma membrane. J Cell Biol 172:923–935. doi:10.1083/jcb.200508014

7. Van Engelenburg SB, Shtengel G, Sengupta P, Waki K, Jarnik M, Ablan SD, Freed EO, Hess HF, Lippincott-Schwartz J (2014) Distribution of ESCRT machinery at HIV assembly sites reveals virus scaffolding of ESCRT subunits. Science 343:653–656. doi:10.1126/science.1247786
8. Thery C, Zitvogel L, Amigorena S (2002) Exosomes: composition, biogenesis and function. Nat Rev Immunol 2:569–579. doi:10.1038/nri855, nri855 [pii]
9. Ong SE, Blagoev B, Kratchmarova I, Kristensen DB, Steen H, Pandey A, Mann M (2002) Stable isotope labeling by amino acids in cell culture, SILAC, as a simple and accurate approach to expression proteomics. Mol Cell Proteomics 1:376–386
10. Ross PL, Huang YN, Marchese JN, Williamson B, Parker K, Hattan S, Khainovski N, Pillai S, Dey S, Daniels S, Purkayastha S, Juhasz P, Martin S, Bartlet-Jones M, He F, Jacobson A, Pappin DJ (2004) Multiplexed protein quantitation in Saccharomyces cerevisiae using amine-reactive isobaric tagging reagents. Mol Cell Proteomics 3:1154–1169. doi:10.1074/mcp.M400129-MCP200, M400129-MCP200 [pii]
11. Anderson L, Hunter CL (2006) Quantitative mass spectrometric multiple reaction monitoring assays for major plasma proteins. Mol Cell Proteomics 5:573–588. doi:10.1074/mcp.M500331-MCP200
12. Nikolov M, Schmidt C, Urlaub H (2012) Quantitative mass spectrometry-based proteomics: an overview. Methods Mol Biol 893:85–100. doi:10.1007/978-1-61779-885-6_7
13. Mann M (2006) Functional and quantitative proteomics using SILAC. Nat Rev Mol Cell Biol 7:952–958. doi:10.1038/nrm2067, nrm2067 [pii]
14. Cepko C, Pear W (2001) Retrovirus infection of cells in vitro and in vivo. Curr Protoc Mol Biol Chapter 9: Unit9 14. doi:10.1002/0471142727.mb0914s36
15. Thery C, Amigorena S, Raposo G, Clayton A (2006) Isolation and characterization of exosomes from cell culture supernatants and biological fluids. Curr Protoc Cell Biol Chapter 3:Unit 3 22. doi: 10.1002/0471143030.cb0322s30
16. Cox J, Mann M (2008) MaxQuant enables high peptide identification rates, individualized p.p.b.-range mass accuracies and proteome-wide protein quantification. Nat Biotechnol 26:1367–1372. doi:10.1038/nbt.1511
17. Li M, Aliotta JM, Asara JM, Wu Q, Dooner MS, Tucker LD, Wells A, Quesenberry PJ, Ramratnam B (2010) Intercellular transfer of proteins as identified by stable isotope labeling of amino acids in cell culture. J Biol Chem 285:6285–6297. doi:10.1074/jbc.M109.057943, M109.057943 [pii]
18. Mathivanan S, Simpson RJ (2009) ExoCarta: a compendium of exosomal proteins and RNA. Proteomics 9:4997–5000. doi:10.1002/pmic.200900351
19. Mathivanan S, Fahner CJ, Reid GE, Simpson RJ (2012) ExoCarta 2012: database of exosomal proteins, RNA and lipids. Nucleic Acids Res 40:D1241–D1244. doi:10.1093/nar/gkr828, gkr828 [pii]
20. Fu W, Sanders-Beer BE, Katz KS, Maglott DR, Pruitt KD, Ptak RG (2009) Human immunodeficiency virus type 1, human protein interaction database at NCBI. Nucleic Acids Res 37:D417–D422. doi:10.1093/nar/gkn708, gkn708 [pii]
21. Bhatia VN, Perlman DH, Costello CE, McComb ME (2009) Software tool for researching annotations of proteins: open-source protein annotation software with data visualization. Anal Chem 81:9819–9823. doi:10.1021/ac901335x
22. da Huang W, Sherman BT, Lempicki RA (2009) Systematic and integrative analysis of large gene lists using DAVID bioinformatics resources. Nat Protoc 4:44–57. doi:10.1038/nprot.2008.211, nprot.2008.211 [pii]
23. Szklarczyk D, Franceschini A, Kuhn M, Simonovic M, Roth A, Minguez P, Doerks T, Stark M, Muller J, Bork P, Jensen LJ, von Mering C (2011) The STRING database in 2011: functional interaction networks of proteins, globally integrated and scored. Nucleic Acids Res 39:D561–D568. doi:10.1093/nar/gkq973, gkq973 [pii]
24. Cantin R, Diou J, Belanger D, Tremblay AM, Gilbert C (2008) Discrimination between exosomes and HIV-1: purification of both vesicles from cell-free supernatants. J Immunol Methods 338:21–30. doi:10.1016/j.jim.2008.07.007, S0022-1759(08)00216-0 [pii]
25. Zeeberg BR, Feng W, Wang G, Wang MD, Fojo AT, Sunshine M, Narasimhan S, Kane DW, Reinhold WC, Lababidi S, Bussey KJ, Riss J, Barrett JC, Weinstein JN (2003) GoMiner: a resource for biological interpretation of genomic and proteomic data. Genome Biol 4:R28

26. Mi H, Muruganujan A, Casagrande JT, Thomas PD (2013) Large-scale gene function analysis with the PANTHER classification system. Nat Protoc 8:1551–1566. doi:10.1038/nprot.2013.092, nprot.2013.092 [pii]
27. Eden E, Navon R, Steinfeld I, Lipson D, Yakhini Z (2009) GOrilla: a tool for discovery and visualization of enriched GO terms in ranked gene lists. BMC Bioinform 10:48. doi:10.1186/1471-2105-10-48, 1471-2105-10-48 [pii]
28. Kamburov A, Wierling C, Lehrach H, Herwig R (2009) ConsensusPathDB--a database for integrating human functional interaction networks. Nucleic Acids Res 37:D623–D628. doi:10.1093/nar/gkn698, gkn698 [pii]

Part VI

NeuroAIDS

Chapter 22

Detecting HIV-1 Tat in Cell Culture Supernatants by ELISA or Western Blot

Fabienne Rayne, Solène Debaisieux, Annie Tu, Christophe Chopard, Petra Tryoen-Toth, and Bruno Beaumelle

Abstract

HIV-1 Tat is efficiently secreted by HIV-1-infected or Tat-transfected cells. Accordingly, Tat concentrations in the nanomolar range have been measured in the sera of HIV-1-infected patients, and this protein acts as a viral toxin on bystander cells. Nevertheless, assaying Tat concentration in media or sera is not that straightforward because extracellular Tat is unstable and particularly sensitive to oxidation. Moreover, most anti-Tat antibodies display limited affinity. Here, we describe methods to quantify extracellular Tat using a sandwich ELISA or Western blotting when Tat is secreted by suspension or adherent cells, respectively. In both cases it is important to capture exported Tat using antibodies before any Tat oxidation occurs; otherwise it will become denatured and unreactive toward antibodies.

Key words HIV-1, Tat, Secretion, ELISA, Immunoblots

1 Introduction

HIV-1 Tat is a small (86–101 residues) and basic protein that enables efficient viral transcription and is required for HIV-1 multiplication [1]. The capacity of HIV-1-infected cells to secrete Tat in the absence of cell lysis was demonstrated in the 1990s [2]. We recently showed that this secretion process, although unconventional, is very efficient since most Tat is exported by infected cells [3]. Circulating Tat can be taken up by various cell types such as T-cells, macrophages, endothelial cells, and neurons. Tat will then cross the endosome membrane to reach the target cell cytosol and elicit a number of cell responses [4].

We first developed a sandwich ELISA assay, so that minute concentrations of Tat can be reliably assayed in the media of

The original version of this chapter was revised. The erratum to this chapter is available at: DOI 10.1007/978-1-4939-3046-3_26

Vinayaka R. Prasad and Ganjam V. Kalpana (eds.), *HIV Protocols*, Methods in Molecular Biology, vol. 1354,
DOI 10.1007/978-1-4939-3046-3_22,

suspension cells such as T-cells that are the main target cells for HIV-1 [3]. We used Jurkat cells for most experiments. During the development of this assay, we noticed that Tat in media was extremely sensitive to oxidation. We observed that reliable quantitation of Tat in the extracellular medium required prior degassing of the medium to remove oxygen as much as possible, the addition of freshly diluted β-mercaptoethanol, and the presence of immobilized anti-Tat antibodies in wells. This is why we called this assay a "cellular ELISA" because Tat-producing cells are added to wells pre-coated with the anti-Tat antibody. This enables antibodies to capture secreted Tat as soon as it is secreted by cells, before Tat is oxidated that would render it unreactive toward antibodies.

A second assay was developed for the use with adherent cells. In this case, we used Tat-FLAG-transfected PC12 cells. Anti-FLAG antibodies covalently linked to agarose beads were directly added to the medium before immunoprecipitation and Western blot. For both techniques, it is necessary to assay both intracellular Tat and secreted Tat in order to calculate the secretion efficiency.

2 Materials

2.1 Tat and Cell Culture

1. Purified HIV-1 Tat can be obtained from various commercial sources or from the NIH AIDS reagent program.
2. The Jurkat cell line (clone E6-1 from ATCC) is a $CD4^+$ T-cell line that grows in suspension.
3. PC12 cells are adherent, rat pheochromocytoma cells.
4. Fetal bovine serum (FBS) and horse serum (HS): Heat inactivate the sera in a water bath at 56 °C during 30 min and then store frozen in aliquots at −20 °C.
5. Antibiotics: Penicillin (10,000 U/ml) and streptomycin (10 mg/ml). Aliquot, store frozen at −20 °C, and dilute 100× in cell culture medium.
6. RPMI and DMEM basal medium (containing 4.5 g/L of glucose).
7. RPMI supplemented with 10 % FBS and antibiotics (RPMI/FBS): Store this medium at 4 °C, and then warm to 37 °C before adding to cells.
8. RPMI/FBS supplemented with 20 μM β-mercaptoethanol (RPMI/FBS/BME): When indicated it should be degassed for 20–40 min using a sterile vacuum Erlenmeyer flask and a pump.
9. Complete medium for PC12 cells (RPMI supplemented with 10 % heat-inactivated HS and 5 % FBS): Store complete medium at 4 °C, and then warm to 37 °C before adding to cells.
10. Immunocapture medium for PC12 cells (complete medium supplemented with 20 μM β-mercaptoethanol): Prepare fresh and degas before use.

11. Trypsin/EDTA solution (0.25 % trypsin, 1 mM EDTA in PBS with phenol red): Store at 4 °C after thawing.
12. A poly-L-lysine (PLL) solution can be used for PC12 cell plating before transfection. Use PLL of 70,000–150,000 MW to prepare a 10× PLL stock solution (100 μg PLL/ml of water) that should be stored in aliquots at −20 °C.
13. To isolate primary $CD4^+$ T-cells: Ficoll-Hypaque, a $CD4^+$ T-cell isolation kit, phytohemagglutinin (1 mg/ml), and interleukin-2.
14. For HIV-1 infection use NL4.3 virus.

2.2 Transfection

1. The use of endotoxin-free plasmids is recommended.
2. Electroporation is the method of choice to transfect T-cells. Kits are available commercially.
3. Electroporator.
4. Lipofectamine 2000 and reduced-serum Opti-MEM media are used to transfect PC 12 cells.

2.3 Immunoassays

1. ELISA 96-well plates.
2. Anti-FLAG antibodies and anti-FLAG affinity gel agarose beads.
3. Anti-Tat antibodies: Sensitivity is dependent on the antibody pair used for the assay. A number of companies provide good anti-Tat antibodies. For the monoclonal anti-Tat, we noticed that those directed toward the first N-terminal residues, such as sc-65912 and sc-65913 (Santa Cruz Biotechnologies) or 1D9 form AIDS Research and Reference Reagent Program (NIH), are often the best ones. Rabbit anti-Tat antibodies can be obtained from this reagent program.
4. Peroxidase-conjugated anti-rabbit antibodies.
5. Sodium carbonate buffer (0.1 M, pH 9.6): Filter on 0.22 μm. Prepare just before use.
6. PBS/milk (PBS containing 8 % powdered skimmed milk, *see* **Note 1**).
7. PBS/Tween (PBS containing 0.05 % Tween-20).
8. PBS/BME (PBS containing 20 μM β-mercaptoethanol): Degas before use.
9. Citrate buffer (150 mM NaCl, 30 mM citrate, 20 mM phosphate, pH 7.2).
10. Lysis buffer (150 mM NaCl, 10 % glycerol, 1 % Triton X-100, 20 mM Tris–HCl pH 7.5): Aliquots in 1.5 ml Eppendorf tubes and store them at −20 °C. Just before use, add 1 mM PMSF (from a 100 mM stock solution in isopropanol) and a protease inhibitor cocktail.

11. 3,3′,5,5′ Tetramethylbenzidine (TMB).
12. 0.5 M H_2SO_4.
13. A 96-well plate OD_{450} reader is needed.

2.4 Luciferase Assays

1. White 96-well plates.
2. Luciferase Assay Reagent (LAR).
3. A 96-well plate luminometer.

2.5 Western Blot (PC12 cells)

1. 4–20 % acrylamide gradient gels (available commercially).
2. SDS-PAGE running buffer (192 mM glycine, 0.1 % SDS, Tris–HCl, pH 8.3): Prepared as a 10× stock solution.
3. SDS/PAGE 5× reducing sample buffer (10 % SDS, 10 mM dithiothreitol, 20 % glycerol, 0.05 % bromophenol blue, 0.2 M Tris–HCl, pH 6.8).
4. Nitrocellulose membrane.
5. Wet transfer apparatus.
6. Western blot transfer buffer (192 mM glycine, 0.1 % SDS, Tris–HCl, pH 8.3, and 20 % methanol).
7. Tris-buffered saline (TBS; 0.15 M NaCl, 10 mM Tris–HCl, pH 8.0).
8. TBST (TBS containing 0.1 % Tween-20).
9. Blocking solution: 3 % BSA in TBST.
10. Chemiluminescent peroxidase substrate.
11. Chemiluminescent imaging system (or films).

3 Methods

1. Jurkat cells are grown at 37 °C in the presence of 5 % of CO_2 and 95 % humidity (i.e., in a cell culture incubator). It is cultured in RPMI/FBS. Cell density should not exceed 1.5×10^6/ml and dilutions are obtained by adding fresh medium.
2. PC12 cells are cultured in complete medium. Cells are maintained in 10 cm diameter Petri dishes containing 10 ml of culture medium. PC12 cells are adherent cells and have no contact inhibition. Confluent cells should be passed by trypsinization at least once a week and be diluted 40-fold. To this end the cell monolayer is washed with PBS before adding 2 ml of trypsin/EDTA solution (*see* **Note 2**) and incubating at 37 °C until the cells detach (*see* **Note 3**). After incubation, stop the enzymatic reaction by adding 8 ml of culture medium. Flush 3–4 times back and forth the cell suspension using a plastic pipette to obtain a homogenous cell suspension. Centrifuge at 1000 rpm

(~300 × *g*) for 5 min. The cell pellet is resuspended in complete medium by pipetting several times before counting (*see* **Note 4**). Cells are then transferred to a new tissue culture flask or plate (*see* **Note 5**). Use 1.5 million cells in 5 ml of culture medium/6 cm diameter Petri dish. Incubate cells overnight before transfection.

3. To prepare $CD4^+$ human primary T-cells, human blood from healthy volunteers can be obtained from the local blood bank following the local laws and regulations. Isolate peripheral blood mononuclear cells (PBMCs) using Ficoll-Hypaque gradients following the manufacturer's instructions. Resuspend PBMCs in RPMI/FBS at $1–4 \times 10^6$ cells/ml. Leave them for 2–4 h in tissue culture flasks to allow monocyte adherence to the flask. Non-adherent cells are peripheral blood lymphocytes (PBLs). Centrifuge PBLs (5 min × 1000 rpm) and isolate $CD4^+$ T-cells using the protocol provided by the kit manufacturer. Resuspend $CD4^+$ T-cells at $1–2 \times 10^6$ cells/ml and activate them using phytohemagglutinin (1 μg/ml) for 24 h. Centrifuge $CD4^+$ T-cells, resuspend them at $1–2 \times 10^6$ cells/ml, and then add interleukin-2 (50 U/ml) for 5–6 days.

3.1 ELISA Procedure for T-Cells: Day 0

1. Wash cells two times (1000 rpm × 5 min in a tabletop centrifuge) with RPMI (*without* serum and antibiotic).

3.1.1 Transfection of Jurkat Cells

2. Resuspend cells at 13×10^6 cells/ml in RPMI.
3. Transfer 0.7 ml (9×10^6 cells) to a standard 4 mm electroporation cuvette.
4. Dilute endotoxin-free plasmids in a maximum of 30 μl of water. We routinely used 20 μg/transfection with 18 μg and 2 μg of Tat and luciferase vector, respectively. An empty vector without Tat should be used for control cells. Mix gently without making bubbles.
5. Place the cuvette in the cuvette holder and electroporate (using an exponential decay pulse) at 270 V, 1000 μF, infinite resistance value. The pulse length should be <25 msec. Above this value, cell viability drops dramatically.
6. Transfer cells to a 25 cm^2 tissue culture flask containing 10 ml of RPMI/FBS/BME at 37 °C.
7. Cultivate cells overnight at 37 °C, 5 % CO_2.

3.1.2 Transfection of Primary T-Cells

1. Transfect cells using a kit for activated T-cells and following the manufacturer's instructions.
2. Cultivate cells overnight at 37 °C, 5 % CO_2, in RPMI/FBS/BME.

3.1.3 T-Cell Infection

Infect purified $CD4^+$ T-cells overnight with HIV-1 (NL4.3) using an MOI >0.5. Jurkat cells can also be used.

3.1.4 Day 2

1. Wash T-cells three times with RPMI/FBS/BME, count, and dilute cells to 0.5×10^6/ml (Jurkats) or 1×10^6/ml (primary $CD4^+$ T-cells).
2. Prepare the ELISA plates: Two plates are needed. The first one will be used for the secretion assay that will capture secreted Tat and the second one to assay intracellular Tat to normalize secretion data.
3. Dilute anti-Tat monoclonal antibody (1/2000 is a good starting point) in sodium carbonate buffer.
4. Add 100 µl/well of the diluted antibody.
5. Leave overnight at 4 °C.
6. Wash wells two times with 200 µl PBS.
7. Saturate wells for 1.5 h with PBS/milk.
8. Wash wells three times with 200 µl PBS, leaving wells in the last wash to prevent drying.

3.1.5 Preparing the Secretion ELISA Plate (Day 3)

1. Prepare Tat standards. Purified, endotoxin-free HIV-1 Tat should be stored at −80 °C using a concentration >100 µM (~1 µg/µl) in citrate buffer.
2. Prepare serial dilutions of Tat ranging from 1 µg/ml to 0.1 ng/ml in degassed RPMI/FBS/BME.
3. Fill the outside wells of the plate with 200 µl of degassed RPMI/FBS/BME. Important: These wells should not be used for the experiment because final readings are less reproducible in outside wells.
4. Add 100 µl of Tat dilutions to the inside wells.

3.1.6 Cell Preparation (Day 3)

1. Centrifuge cells and resuspend them at 3.75×10^6/ml (Jurkats) or 5×10^6/ml (primary $CD4^+$ T-cells) in degassed RPMI/FBS/BME, before adding 0.2 ml/well (make triplicates).
2. Wells with untransfected or uninfected cells should be used as negative controls.

3.1.7 Harvesting the Secretion ELISA Plate (Day 3)

1. After 6 h at 37 °C (*see* **Note 6**), the plate is removed from the incubator.
2. Transfer cells to 1.5 ml centrifuge tubes, and wash wells with 0.2 ml PBS to recover all cells.
3. Centrifuge cells $750 \times g \times 2$ min at RT.
4. Keep 70 µl of the supernatant, to be stored frozen for luciferase assay later.
5. Wash cells by adding 0.2 ml PBS at RT. Centrifuge at $750 \times g \times 2$ min at RT.
6. Resuspend the cell pellet in 24 µl of lysis buffer. Leave for 15 min at RT on an orbital shaker, and then place on ice.

7. In the meanwhile wash the ELISA plate four times with 0.2 ml PBS.
8. Wash the plate with PBS/Tween.
9. Add 100 µl/well of rabbit anti-Tat antibody 1/2000 in PBS/milk.
10. Leave the plate overnight at 4 °C.

3.1.8 Preparing the Intracellular ELISA Plate (Day 3)

1. Dilute 6 µl of cell lysate into 194 µl of PBS/BME.
2. Prepare serial Tat dilutions ranging from 1 µg/ml to 0.1 ng/ml in degassed PBS/BME supplemented with 6 µl lysis buffer and 194 µl PBS/BME.
3. Agitate on an orbital shaker for 2–5 min at RT.
4. Leave at 4 °C overnight.

3.1.9 Processing the Intracellular ELISA Plate (Day 4)

1. Wash wells five times with 200 µl PBS at RT.
2. Wash the plate with PBS/Tween.
3. Add 100 µl/well of rabbit anti-Tat antibody 1/2000 in PBS/milk.
4. Agitate on an orbital shaker for 1 h at RT.

3.1.10 Final ELISA Steps (Day 4)

1. Wash both secretion and intracellular ELISA plates five times with 200 µl PBS at RT.
2. Add 100 µl/well of peroxidase-conjugated anti-rabbit IgG 1/2000 in PBS/milk.
3. Agitate on an orbital shaker for 1 h at RT.
4. Wash the plates five times with PBS/Tween.
5. Add 100 µl TMB/well.
6. Place the plates back on the orbital shaker under strong agitation until a blue color appears in the key wells of the plates. It takes from 10 min (most often) to 1 h (very weak signal).
7. Stop the reaction by adding 50 µl of 0.5 M H_2SO_4/well.
8. Read the optical density at 450 nm using a plate reader (*see* **Notes 7**, **8** and **9**).

3.1.11 Luciferase Assay

1. Use a white 96-well plate.
2. To assay luciferase activity in cell lysates, add 6 µl of lysate to 30 µl of LAR/well.
3. To assay luciferase activity in media, add 20 µl of medium to 100 µl of LAR/well.
4. Typical settings for the luminometer are delay 2 s and measure 20 s.

3.1.12 Calculations of Secretion Efficiency (Jurkat Cells)

S being the amount of secreted Tat (in nanogram), and I the amount of intracellular Tat (in nanogram), the secretion efficiency (%) is $S \times 100/(S+I)$, the error on this ratio being $100 \times (I\Delta S + S\Delta I)/(S+I)^2$ with ΔS and ΔI being the SEM of S and I, respectively. Luciferase secretion efficiency is calculated using the same procedure except that relative light units (RLU) are used instead of nanogram.

The experimental flowchart (Fig. 1) summarizes the cellular ELISA procedure (*see* **Note 9**) used to assay Tat secretion by T-cells.

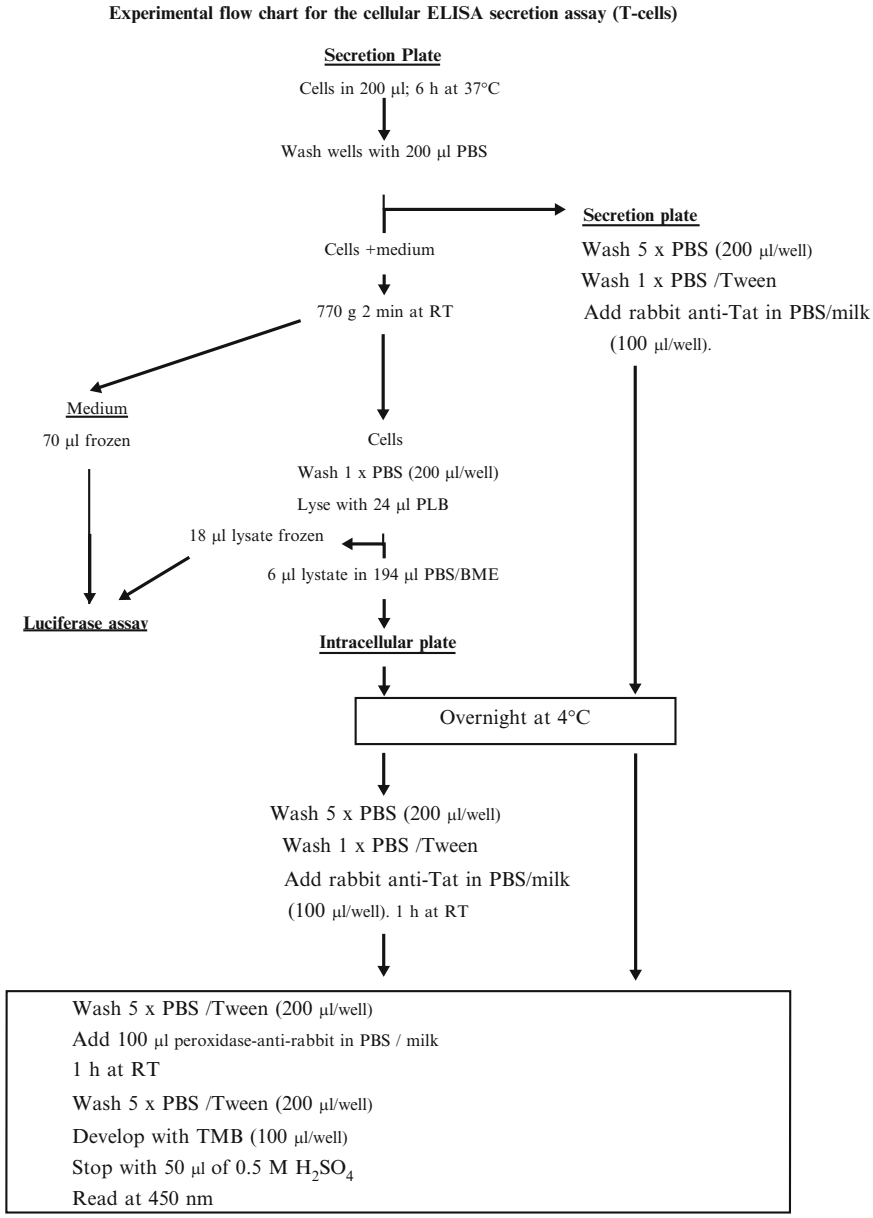

Fig. 1 Experimental flowchart.

3.2 Western Blot Procedure for Adherent Cells

3.2.1 Transfection of PC12 Cells

1. Because most anti-Tat antibodies are poorly effective for immunoprecipitation, we use Tat-FLAG and thus transfect cells with Tat-FLAG instead of Tat. Control experiments performed in Jurkat cells showed that this carboxyl-terminal tag does not affect Tat secretion efficiency. This tag also enables one to use commercially available anti-FLAG gel beads that allow one to capture Tat-FLAG in solution before it becomes oxidized and thus unreactive to antibodies. Tat is quantified using anti-FLAG Western blotting.
2. One hour before cell transfection, change the PC12 culture medium to 5 ml of Opti-MEM. Return cells to the cell culture incubator for 1 h.
3. During the incubation period prepare the mix of plasmids with Lipofectamine 2000: mix 9 μg of Tat-FLAG (or empty vector) in a volume of 500 μl of Opti-MEM. Vortex briefly. In a separate tube, dilute 18 μl of Lipofectamine 2000 in 500 μl of Opti-MEM. Vortex briefly, and then add the DNA to the diluted Lipofectamine 2000. Incubate the DNA-Lipofectamine mix for 20 min at room temperature (RT) to allow complex formation.
4. Add the mix drop by drop to the cell culture medium. Gently agitate the culture dish back and forth to homogenously distribute the complexes. Incubate for 4 h in the cell culture incubator.

   After 4 h, replace the transfection medium with 5 ml of culture medium and incubate the cells overnight.

3.2.2 Tat-FLAG Immunocapture

1. Gently rinse the cell cultures with warm DMEM and add 2 ml of immunocapture medium/dish.
2. Prepare the anti-FLAG affinity agarose beads for immunocapture: add a 20 μl aliquot of anti-FLAG affinity gel/dish to 1 ml of DMEM in an Eppendorf tube.
3. Centrifuge the tube at 200 × *g* for 1 min. Discard the supernatant. Repeat this step three times to remove all traces of glycerol from the bead suspension.
4. Resuspend the gel in 500 μl of immunocapture medium.
5. Add this suspension drop by drop to PC12 cells expressing Tat-FLAG and previously covered with 2 ml of immunocapture medium. Gently agitate the dish. Incubate for 4–6 h in the cell culture incubator.
6. After the incubation, shake the culture dish gently by making very slow rotations. It is best to use an inverted microscope to check that the movement does not lead to cell detachment. Harvest the immunocapture medium and transfer it to a 15 ml tube. Place cells on ice for lysis (*see* **steps 11** and **12**).

7. Centrifuge the tube at 200 × *g* for 1 min at 4 °C to recover the beads. Discard the supernatant and resuspend beads in 1 ml PBS.
8. Centrifuge at 200 × *g* for 1 min. Repeat this washing step three times.
9. After the last centrifugation step, add 20 µl of lysis buffer and 5 µl of 5× reducing sample buffer to the beads. Freeze the samples at −20 °C.
10. Rinse the cells carefully with 4 ml of medium. Gently rotate the dish, and then discard the medium. Repeat the washing once, keeping the cells on ice.
11. Place the dish on ice and add 1 ml of ice-cold lysis buffer/dish. Scrape the cells thoroughly and transfer the cell lysate into an Eppendorf tube. Vortex at top speed for 10 s and then place the tube on ice.
12. Take a 15 µl aliquot of anti-Flag Affinity Gel agarose beads and wash them with lysis buffer (*see* **steps 2** and **3**). Resuspend beads in 100 µl of lysis buffer and add them to the cell lysate. Mix gently without vortexing.
13. Place the tube on a rotating wheel for 90 min at 4 °C to allow Tat immunocapture.
14. Centrifuge tubes at 200 × *g* for 1 min. Wash the beads three times with 1 ml PBS.
15. Resuspend beads in 20 µl lysis buffer and 5 µl of 5× reducing sample buffer. Store the samples at −20 °C.

3.2.3 Western Blot of Immunocaptured Tat-FLAG

1. Thaw the samples prepared from the media and cell lysates. Heat them at 95 °C for 5 min. Place them on ice for 5 min and centrifuge briefly (~10 s at 10,000 × *g*).
2. In parallel, prepare the electrophoresis gel for sample loading. Take out the 4–20 % gradient acrylamide gel from its plastic wrap (*see* **Note 10**), remove the comb, and rinse the wells with purified water. Assemble the gel electrophoresis device, place the gel into the tank, fill up the tank with electrophoresis running buffer, and load the samples on the gel.
3. Run the gel at 170 V for 30 min, making sure that the dye reaches the end of the gel but does not come out of the gel (*see* **Note 11**).
4. Transfer proteins to a nitrocellulose membrane using a conventional wet transfer apparatus for 1 h at 30 V.
5. Rinse the membrane three times in TBST.
6. Incubate the membrane in blocking solution for 1 h with shaking.

7. Incubate the membrane with rabbit anti-FLAG 1:400 in blocking solution for 1 h with shaking.
8. Wash the membrane three times for 10 min in TBST.
9. Incubate the membrane with peroxidase-anti-rabbit IgG (1:25,000) for 1 h.
10. Wash the membrane four times for 10 min with TBST.
11. Incubate the membrane with the chemiluminescence substrate solution for 5 min at room temperature in the dark. Remove the excess of substrate solution, and place the membrane between two plastic sheets and immediately capture chemiluminescence signal with a cooled CCD device (or films). Use various exposure times to obtain unsaturated signal images. Tat-FLAG is detected at ~12 kDa. Dimers of Tat can also be detected at ~22 kDa.

Quantify relative band intensities using a quantification software such as ImageJ. This will enable one to evaluate the amount of Tat released into the cell culture medium (*S*) and present intracellularly (*I*). Calculations are then performed as described above for T-cells (Subheading 3.1.12). It is also possible to use cotransfected luciferase to monitor transfected cell lysis, essentially as detailed for T-cells.

4 Notes

1. Important: Use a milk powder package opened less than 2 months before.
2. It is also possible to use EDTA without trypsin to detach PC12 cells. The procedure is the same.
3. To facilitate cell detachment, gently tap the side of the Petri dish. When all cells are detached they float in the medium and this can be easily seen with the naked eyes, or using an inverted microscope if necessary. Usually 2 min is sufficient to detach PC12 cells.
4. PC12 cells tend to form small clusters in cell suspension, hence complicating counting. A confluent 10 cm diameter Petri dish contains ~10 million cells.
5. If needed, it is possible to increase the adherence of PC12 cells by pretreating the Petri dish surface with a PLL solution before cell plating. To this end, add 2 ml of sterile PLL solution to a 6 cm diameter Petri dish and incubate for 1 h at 37 °C. After incubation, remove the PLL solution and use the dish directly for cell plating.
6. Incubation can be longer if the medium does not become too much acidic, i.e., yellow.

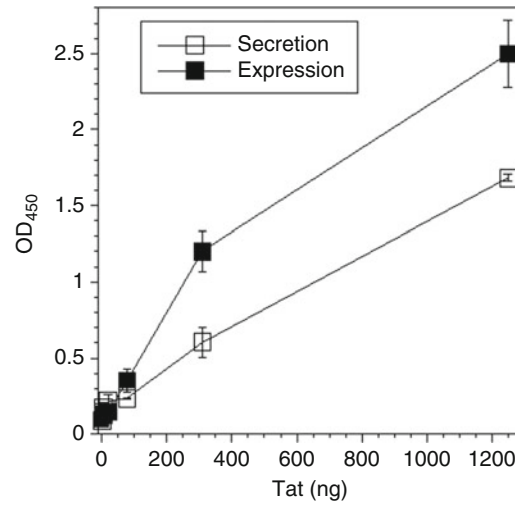

Fig. 2 Standard curves: Purified recombinant Tat was diluted in the indicated medium and assayed by ELISA. Means ± SEM ($n = 3$). Results from a typical experiment (*see* **Note 7**).

7. ELISA calculations: It should be noted that for most anti-Tat antibody pairs (monoclonal/polyclonal), standard curves will be different for the secretion and intracellular plate (Fig. 2). This is presumably due to the presence of detergent (from the lysis buffer) in the expression plate. Both standard curves are thus needed to first calculate the amount of Tat in the medium and intracellular, before calculating the secretion efficiency. Calculating directly from OD values can lead to erroneous secretion values. The extent of the error will depend on the difference between the standard curves and thus on the antibody pair.
8. Sensitivity and specificity of the ELISA assay: Figure 3 shows that the amount of secreted Tat is linear with the number of Jurkat cells present in the well, while Fig. 4 shows that luciferase release is negligible compared to Tat secretion.
9. ELISA troubleshooting: If no signal is detected, the affinity of the antibodies should be checked by Western blotting. If high background is observed, it is possible to use a biotinylated rabbit anti-Tat detected using streptavidin-peroxidase [5].
10. Alternatively, Tat can also be efficiently separated on 15 % PAGE/tricine gels [6].
11. Tat is a small protein (~11 kDa) that, depending on the gel system, can easily run out of the gel.

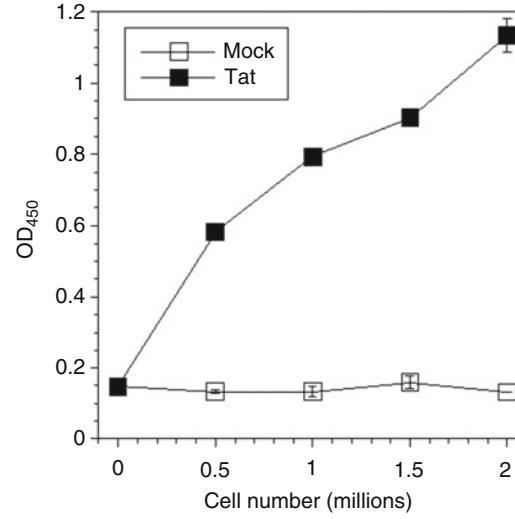

Fig. 3 Secretion efficiency: Jurkat T-cells were transfected with Tat and luciferase (Tat) or with an empty vector and luciferase (mock). The indicated number of cells was then plated in wells of a 96-well plate ($n=4$). After 6 h at 37 °C secreted and intracellular Tat were assayed by ELISA. Tat secretion is linearly dependent on cell number (*see* **Note 8**).

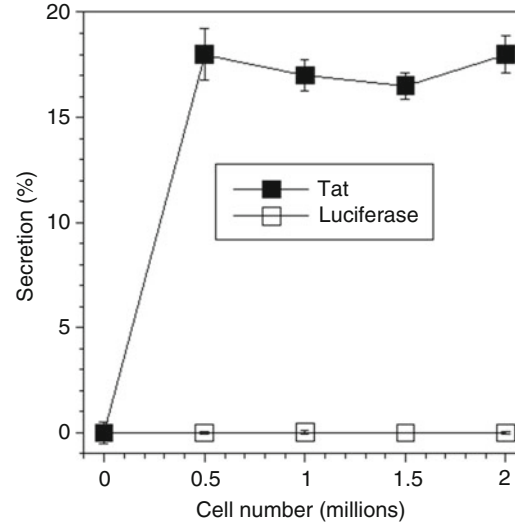

Fig. 4 Specificity of Tat secretion: Jurkat T-cells were transfected with Tat and luciferase (Tat), before essaying their extracellular and intracellular levels by ELISA ($n=4$) to calculate their secretion efficiency as described in the text. Results from a typical experiment. Luciferase release is negligible compared to Tat secretion.

Acknowledgement

This work was funded by the CNRS, the ANRS, and Sidaction.

References

1. Ott M, Geyer M, Zhou Q (2011) The control of HIV transcription: keeping RNA polymerase II on track. Cell Host Microbe 10:426–435
2. Ensoli B, Barillari G, Salahuddin SZ, Gallo RC, Wong-Staal F (1990) Tat protein of HIV-1 stimulates growth of cells derived from Kaposi's sarcoma lesions of AIDS patients. Nature 345:84–86
3. Rayne F, Debaisieux S, Yezid H, Lin YL, Mettling C, Konate K, Chazal N, Arold ST, Pugniere M, Sanchez F, Bonhoure A, Briant L, Loret E, Roy C, Beaumelle B (2010) Phosphatidylinositol-(4,5)-bisphosphate enables efficient secretion of HIV-1 Tat by infected T-cells. EMBO J 29:1348–1362
4. Debaisieux S, Rayne F, Yezid H, Beaumelle B (2012) The Ins and Outs of HIV-1 Tat. Traffic 13:355–363
5. Johnson TP, Patel K, Johnson KR, Maric D, Calabresi PA, Hasbun R, Nath A (2013) Induction of IL-17 and nonclassical T-cell activation by HIV-Tat protein. Proc Natl Acad Sci U S A 110:13588–13593
6. Schagger H (2006) Tricine-SDS-PAGE. Nat Protoc 1:16–22

Chapter 23

Protocol for Detection of HIV-Tat Protein in Cerebrospinal Fluid by a Sandwich Enzyme-Linked Immunosorbent Assay

Tory P. Johnson and Avindra Nath

Abstract

The human immunodeficiency virus (HIV) transactivator of transcription (Tat) is a virally produced protein that is required for efficient viral replication. Once formed inside an infected cell, Tat is secreted into the extracellular space where it has pathophysiological consequences on cells it interacts with. Tat has been demonstrated to be neurotoxic and is produced even under the pressures of anti-retroviral therapy; therefore Tat is suspected to contribute to the development of HIV-associated neurocognitive disorders. In this chapter, we describe a sandwich enzyme-linked immunosorbent assay protocol for the detection of Tat from cerebrospinal fluid samples.

Key words HIV, Transactivator of transcription, Tat, ELISA, Protein detection, CSF, Cell lysates

1 Introduction

Human immunodeficiency virus (HIV) is a retrovirus that encodes 15 proteins; nine proteolytically processed from three large polyprotein precursors, and six from multiply spliced transcripts [1]. One of the early viral proteins produced is the transactivator of transcription, Tat. While this protein is essential for efficient viral replication, an estimated 65 % of the produced Tat is secreted into the extracellular space [2] where it may either act directly with the neuronal cell membrane leading to excitotoxicity [3] or is taken up by other cells through endocytosis [4]. Tat secretion follows an unconventional pathway that is dependent upon interaction with phosphatidylinositol-4,5-bisphosphate at the cell membrane [2, 5, 6]. Secreted Tat has been detected from infected and transfected primary T-cells [6], T cell lines [2, 3, 5], in cerebrospinal fluid (CSF) [7], and sera [8], although the concentrations of secreted Tat vary widely. These discrepancies may reflect different viral strains, cell culture techniques, and transfection and detection efficiencies.

Vinayaka R. Prasad and Ganjam V. Kalpana (eds.), *HIV Protocols*, Methods in Molecular Biology, vol. 1354,
DOI 10.1007/978-1-4939-3046-3_23,

Once secreted, the extracellular form of the HIV protein Tat is capable of entering into almost all cell types [9]. Tat uptake has been described as clathrin mediated [4], caveolae mediated [10, 11], or dependent upon interactions with low-density lipoprotein receptor and cell surface heparan sulfate proteoglycans [12, 13]. The cellular translocation properties of Tat have been exploited by scientists for multiple purposes. For example, Tat fusion proteins and Tat-linked molecules are readily taken up by almost all cell types. This mechanism has been used to deliver molecules, such as oligonucleotides [14], peptides and full-length proteins [15], nanoparticles [16], and liposomes [15] across the cellular membranes. These molecules include chemotherapeutic agents, suicide genes, and cell-modifying proteins.

Tat has been ascribed several pathogenic and cell-modulating attributes including T-cell activation and inflammation [7, 17–19], neurotoxicity and synaptic remodeling [3, 20–22], and behavioral and potential psychological alterations [23, 24]. Tat protein and transcripts have been detected in patients with HIV encephalitis [25] and antibody levels to Tat correlate with neurocognitive impairment in individuals with HIV infection [26]. Current antiretroviral therapy (ART) has no effect on the early viral products produced by the HIV proviral DNA, including Tat [7, 27]. Therefore, the pathophysiological consequences of Tat continue to occur even during successful ART. What remains unclear is the relative contribution of Tat to these processes in vivo, as detecting and quantifying Tat in biological and clinical specimens remain difficult. Previous attempts to measure Tat in biological specimens have used Slot blots, Western blot analysis, or enzyme-linked immunosorbent assay (ELISA). However, these techniques lack the sensitivity or specificity necessary for reliably studying patient cohorts [25, 28]. The recent demonstration that Tat can be detected in CSF of patients on ART with undetectable viral loads (7) makes it critically important to develop a reliable method for monitoring Tat levels in the CSF across various cohorts of patients. The method described here is a rapid, sensitive, and reproducible ELISA, which detects Tat from CSF and cell lysates. While the method described below has been optimized for detection of Tat in CSF, it could potentially be adapted to other tissues as well. Analysis of CSF levels of Tat will give us critical insight into the contribution of Tat to HIV-associated neurological disorders (HAND).

2 Materials

1. Bicarbonate coating buffer: 3.03 g $NaCO_3$, 6.0 g $NaHCO_3$, 1000 ml distilled water. Adjust to pH 9.6.
2. 96-Well Clear Flat Bottom Polystyrene High Bind Microplate.
3. Microplate sealing tape.

4. Microplate shaker.
5. Microplate reader capable of 450 and 560 nm wavelengths.
6. Wash buffer: Phosphate-buffered saline (PBS) with 0.05 % Tween-20 (v/v).
7. Blocking buffer: PBS, 5 % nonfat dry milk (w/v), 0.05 % Tween-20 (v/v).
8. Recombinant Tat protein: Available from NIH AIDS repository or several commercial sources.
9. 3,3′,5,5′-Tetramethylbenzidine (TMB) substrate.
10. Capture antibody: Mouse monoclonal (AIDS Research and Reference Reagent Program, Division of AIDS, NIAID, NIH: HIV-1 Tat monoclonal antibody (1D9) from Dr. Dag E. Helland) [29].
11. Detector antibody: Biotinylated rabbit polyclonal (Abcam, Cambridge, MA, catalog #43015).
12. Streptavidin-poly-horseradish peroxidase (HRP).
13. Stop reagent: 1 N H_2SO_4.

3 Methods

Day 1

1. Dilute the capture antibody, Tat monoclonal antibody 1D9, to 0.002 μg/μl in bicarbonate-binding buffer.
2. Add 100 μl of antibody to each well of the plate to be used and seal the plate with tape.
3. Incubate overnight at 4 °C with gentle shaking.

Day 2

1. Wash the plate three times with 300 μl wash buffer. Tap plate well to ensure complete removal of wash buffer.
2. Block the plate with 200 μl per well of blocking buffer (*see* **Note 1**).
3. Seal the plate and incubate at room temperature for 1 h with gentle shaking.
4. Aspirate the plate and tap well.
5. Prepare the standards as follows (Fig. 1a):
   (a) Standard: Make a working solution of 1 μg Tat in 1 ml blocking buffer (*see* **Note 2**). This is 1,000,000 pg/ml.
   (b) Dilute 2.5 μl of 1,000,000 pg/ml into 500 μl blocking buffer. This is $A = 5000$ pg/ml. Prepare serial double dilutions with this solution as follows.

a

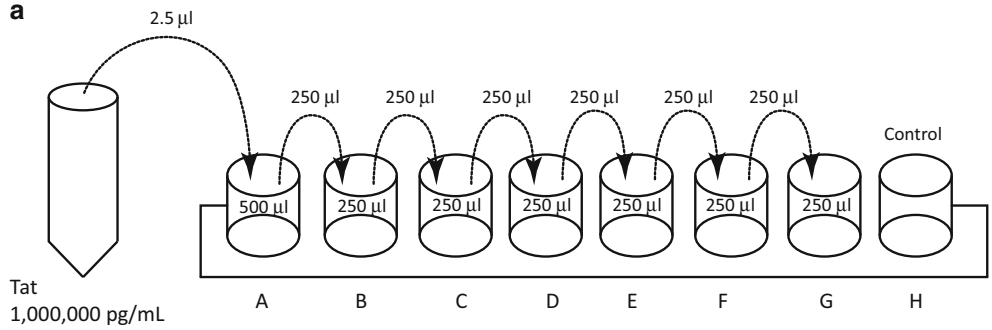

b

Date: _____ ELISA type:__ Tat___ Concentration of samples: ___ 50%____ ___

	1	2	3	4	5	6	7	8	9	10	11	12
A	5000	5000	Unknown 1	Unknown 1								
B	2500	2500	Unknown 2	Unknown 2								
C	1250	1250										
D	625	625										
E	312.5	312.25										
F	156.25	156.25										
G	78.125	78.125										
H	0	0										

Fig. 1 Preparation of the standard curve and ELISA plate setup. (**a**) Schematic illustration of the generation of serial dilutions to produce a standard curve. These samples will be used to determine the concentration of the unknown samples. (**b**) Schematic illustration of an example template for ELISA plate setup. Standards and unknown samples are plated in duplicate.

(c) Dilute 250 µl of *A* into 250 µl blocking buffer. This is *B* = 2500 pg/ml.

(d) Dilute 250 µl of *B* into 250 µl of blocking buffer. This is *C* = 1250 pg/ml.

(e) Dilute 250 µl of *C* into 250 µl of blocking buffer. This is *D* = 625 pg/ml.

(f) Dilute 250 µl of *D* into 250 µl of blocking buffer. This is *E* = 312.5 pg/ml.

(g) Dilute 250 µl of *E* into 250 µl of blocking buffer. This is *F* = 156.25 pg/ml.

(h) Dilute 250 µl of *F* into 250 µl of blocking buffer. This is *G* = 78.125 pg/ml.

(i) For *H* = use 250 µl of blocking buffer = 0 pg/ml.

6. Add 100 μl of the standards to each well in duplicate to generate the standard curve (Fig. 1b) (*see* **Note 3**).
7. Prepare the CSF samples by diluting 110 μl of CSF into 110 μl of blocking buffer (*see* **Notes 4** and **5**).
8. Add 100 μl of diluted CSF sample to wells in duplicate (*see* **Note 6**).
9. Seal the plate and incubate overnight at 4 °C with gentle shaking.

Day 3

1. Wash the plate three times with 300 μl/well of wash buffer.
2. Add 100 μl of detector antibody to each well per diagram. Dilute antibody to 0.0045 μg/μl in blocking buffer prior to use.
3. Seal the plate well and incubate for 1 h at room temperature.
4. Wash the plate six times with 300 μl of wash buffer (*see* **Note 7**).
5. Remove TMB solution from 4 °C and allow warming to room temperature (*see* **Note 8**).
6. Dilute strep-poly-HRP 1:5000 in wash buffer.
7. Add 100 μl of diluted strep-poly-HRP to each well.
8. Seal the plate well and incubate for 30 min at room temperature with gentle shaking protected from light (*see* **Note 9**).
9. Wash the plate three times with 300 μl wash buffer.
10. Add 100 μl of TMB substrate to each well.
11. Incubate for 15 min at room temperature, unsealed and protected from light (*see* **Note 9**).
12. Add 100 μl of stop reagent (H_2SO_4—1 N) to each well.
13. Read the plate at 450 nm with 560 nm background subtraction on an ELISA plate reader (*see* **Note 10**).
14. Plot the optical density (OD) versus the concentration of Tat in standard samples to generate a standard curve (Fig. 2). The equation of this line will be used to calculate the concentration of Tat in the unknown samples (*see* **Note 11**).
15. For each unknown sample, calculate the average OD and insert this into the equation generated from the standard curve to calculate the Tat concentration. Multiply this number by the dilution factor (2 in this protocol) to determine the concentration of Tat in each unknown sample (*see* **Notes 12** and **13**).

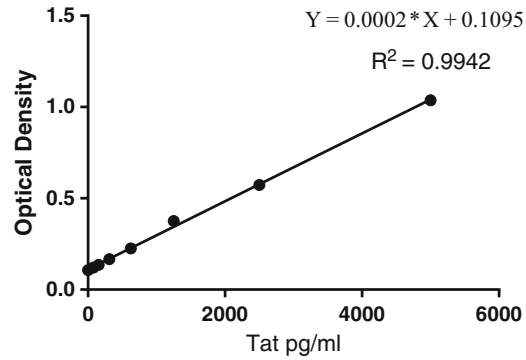

Fig. 2 Example of equation for Tat concentration calculation. Plot the average OD versus the Tat standard concentrations in the linear range. The equation of this line will be used to calculate the concentration of Tat in the unknown samples.

4 Notes

1. Make blocking buffer fresh each day. Do not reuse blocking buffer.
2. Make standard curve from stock Tat solutions maintained at no less than 1 μg/ul. Reusing diluted Tat or storing reconstituted Tat at reduced concentrations may result in lower signal.
3. Vortex all standards and samples well prior to adding them to the plate.
4. This assay has been optimized for CSF samples and cell lysate samples. It has not been tested for other biological samples such as cell supernatants or sera. For CSF and cell lysates dilutions of 50 % with blocking buffer are recommended, but if ODs are outside of the linear range further dilution of samples may be performed.
5. This assay works for detecting and measuring Tat from HIV Clades A and B. The antibodies used do not recognize Clade C Tat and therefore should not be used with samples that are likely to be predominately from a population infected with Clade C. But it would be possible to adapt this assay for measuring Tat variants such as that from Clade C by using an appropriate anti-Tat antibody that would detect it.
6. When preparing CSF samples, vortex the sample well before adding to blocking buffer and after the sample has been diluted.
7. Thorough washing of the plate is essential. Either use an automatic plate washer or be rigorous during the washing steps. Insufficient washing may result in high background OD.

8. Bring TMB to room temperature prior to use for optimum development. Using cold TMB may increase well-to-well variability.
9. Protect the plate from light during strep-poly-HRP and TMB steps.
10. Read the plate within 15 min of adding stop reagent. Delays in reading may result in higher variability and lower optical densities.
11. The range of detectable Tat for this protocol is from 100 to 5000 pg/ml. The lower level of detection was determined by setting the cutoff as the mean OD of 0 pg/ml (blank) + 3× standard deviation. The cutoff will need to be determined for each plate run.
12. This protocol has an intra-plate coefficient of variation of 4.46 % and an inter-plate coefficient of variation of 7.56 % at 1000 pg/ml of CSF with Tat. Similar intra- and inter-plate variability was confirmed for 2000 and 4000 pg/ml of Tat in CSF (Figs. 3 and 4).
13. Fractioned recovery of recombinant Tat in CSF was determined to range from 93.3 to 112.9 % (Fig. 5).

In summary, we have developed a protocol for detection of Tat protein from HIV Clades A and B in CSF and cell lysates based on a sandwich ELISA that has a sensitivity of 100 pg/ml and a broad linear range of up to 5000 pg/ml. The assay has excellent intra- and inter-plate reproducibility. The protocol requires 3 days to complete.

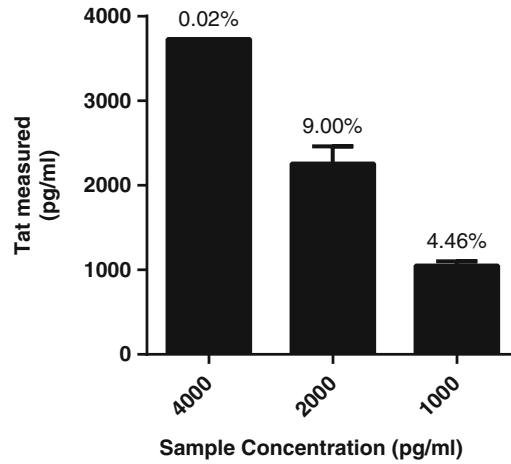

Fig. 3 Intra-plate variability from $n = 3$ samples on a single ELISA plate was performed with CSF samples spiked with 4000, 2000, and 1000 pg/ml of HIV-Clade B recombinant Tat. Data shown is the average calculated Tat measurement using the ELISA protocol. Coefficient of variation measurements are provided above each bar. All intra-plate coefficient of variation measurements are below 10 %.

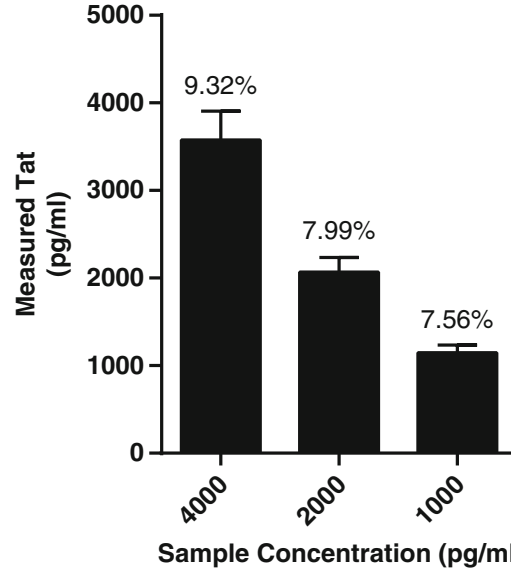

Fig. 4 Inter-plate variability from $n = 1–3$ samples on three separate ELISA plates. Protocol was performed with CSF samples spiked with 4000, 2000, and 1000 pg/ml of Clade B recombinant Tat. Data shown is the average calculated Tat measurement using the ELISA protocol. Coefficient of variation measurements are provided above each bar. All inter-plate coefficient of variation measurements are below 10 %.

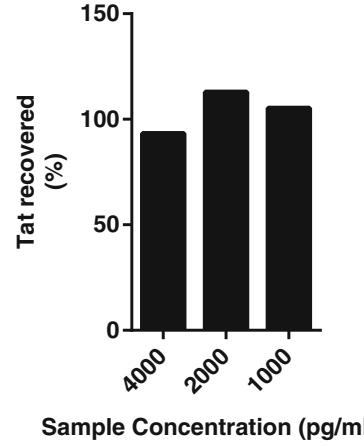

Fig. 5 Fractioned recovery of CSF samples spiked with recombinant Tat from $n = 3$ independent experiments. Data shown is the percent of Tat recovered using the ELISA protocol.

References

1. Fields BN, Knipe DM, Howley PM, Griffin DE (2001) Fields' virology, 4th edn. Lippincott Williams & Wilkins, Philadelphia, PA
2. Rayne F, Debaisieux S, Yezid H, Lin YL, Mettling C, Konate K, Chazal N, Arold ST, Pugniere M, Sanchez F, Bonhoure A, Briant L, Loret E, Roy C, Beaumelle B (2010) Phosphatidylinositol-(4,5)-bisphosphate enables efficient secretion of HIV-1 Tat by infected T-cells. EMBO J 29:1348–1362
3. Li W, Huang Y, Reid R, Steiner J, Malpica-Llanos T, Darden TA, Shankar SK, Mahadevan A, Satishchandra P, Nath A (2008) NMDA receptor activation by HIV-Tat protein is clade dependent. J Neurosci 28:12190–12198
4. Vendeville A, Rayne F, Bonhoure A, Bettache N, Montcourrier P, Beaumelle B (2004) HIV-1 Tat enters T cells using coated pits before translocating from acidified endosomes and eliciting biological responses. Mol Biol Cell 15:2347–2360
5. Ensoli B, Barillari G, Salahuddin SZ, Gallo RC, Wong-Staal F (1990) Tat protein of HIV-1 stimulates growth of cells derived from Kaposi's sarcoma lesions of AIDS patients. Nature 345:84–86
6. Rayne F, Debaisieux S, Bonhoure A, Beaumelle B (2010) HIV-1 Tat is unconventionally secreted through the plasma membrane. Cell Biol Int 34:409–413
7. Johnson TP, Patel K, Johnson KR, Maric D, Calabresi PA, Hasbun R, Nath A (2013) Induction of IL-17 and nonclassical T-cell activation by HIV-Tat protein. Proc Natl Acad Sci U S A 110:13588–13593
8. Xiao H, Neuveut C, Tiffany HL, Benkirane M, Rich EA, Murphy PM, Jeang KT (2000) Selective CXCR4 antagonism by Tat: implications for in vivo expansion of coreceptor use by HIV-1. Proc Natl Acad Sci U S A 97:11466–11471
9. Frankel AD, Pabo CO (1988) Cellular uptake of the tat protein from human immunodeficiency virus. Cell 55:1189–1193
10. Ferrari A, Pellegrini V, Arcangeli C, Fittipaldi A, Giacca M, Beltram F (2003) Caveolae-mediated internalization of extracellular HIV-1 tat fusion proteins visualized in real time. Mol Ther 8:284–294
11. Fittipaldi A, Ferrari A, Zoppe M, Arcangeli C, Pellegrini V, Beltram F, Giacca M (2003) Cell membrane lipid rafts mediate caveolar endocytosis of HIV-1 Tat fusion proteins. J Biol Chem 278:34141–34149
12. Liu Y, Jones M, Hingtgen CM, Bu G, Laribee N, Tanzi RE, Moir RD, Nath A, He JJ (2000) Uptake of HIV-1 tat protein mediated by low-density lipoprotein receptor-related protein disrupts the neuronal metabolic balance of the receptor ligands. Nat Med 6:1380–1387
13. Tyagi M, Rusnati M, Presta M, Giacca M (2001) Internalization of HIV-1 tat requires cell surface heparan sulfate proteoglycans. J Biol Chem 276:3254–3261
14. Eguchi A, Akuta T, Okuyama H, Senda T, Yokoi H, Inokuchi H, Fujita S, Hayakawa T, Takeda K, Hasegawa M, Nakanishi M (2001) Protein transduction domain of HIV-1 Tat protein promotes efficient delivery of DNA into mammalian cells. J Biol Chem 276:26204–26210
15. Wadia JS, Dowdy SF (2002) Protein transduction technology. Curr Opin Biotechnol 13: 52–56
16. Lewin M, Carlesso N, Tung CH, Tang XW, Cory D, Scadden DT, Weissleder R (2000) Tat peptide-derivatized magnetic nanoparticles allow in vivo tracking and recovery of progenitor cells. Nat Biotechnol 18:410–414
17. Abbas W, Herbein G (2013) T-Cell Signaling in HIV-1 Infection. Open Virol J 7:57–71
18. Nicoli F, Finessi V, Sicurella M, Rizzotto L, Gallerani E, Destro F, Cafaro A, Marconi P, Caputo A, Ensoli B, Gavioli R (2013) The HIV-1 Tat protein induces the activation of CD8(+) T cells and affects in vivo the magnitude and kinetics of antiviral responses. PLoS One 8:e77746
19. Secchiero P, Zella D, Curreli S, Mirandola P, Capitani S, Gallo RC, Zauli G (2000) Pivotal role of cyclic nucleoside phosphodiesterase 4 in Tat-mediated CD4+ T cell hyperactivation and HIV type 1 replication. Proc Natl Acad Sci U S A 97:14620–14625
20. Eugenin EA, King JE, Nath A, Calderon TM, Zukin RS, Bennett MV, Berman JW (2007) HIV-tat induces formation of an LRP-PSD-95-NMDAR-nNOS complex that promotes apoptosis in neurons and astrocytes. Proc Natl Acad Sci U S A 104:3438–3443. doi:10.1073/pnas.0611699104
21. Hargus NJ, Thayer SA (2013) Human immunodeficiency virus-1 Tat protein increases the number of inhibitory synapses between hippocampal neurons in culture. J Neurosci 33: 17908–17920
22. Magnuson DS, Knudsen BE, Geiger JD, Brownstone RM, Nath A (1995) Human immunodeficiency virus type 1 tat activates non-N-methyl-D-aspartate excitatory amino acid receptors and causes neurotoxicity. Ann Neurol 37:373–380
23. Hahn YK, Podhaizer EM, Farris SP, Miles MF, Hauser KF, Knapp PE (2015) Effects of chronic

HIV-1 Tat exposure in the CNS: heightened vulnerability of males versus females to changes in cell numbers, synaptic integrity, and behavior. Brain Struct Funct 220:605

24. Paris JJ, Singh HD, Ganno ML, Jackson P, McLaughlin JP (2014) Anxiety-like behavior of mice produced by conditional central expression of the HIV-1 regulatory protein, Tat. Psychopharmacology 231:2349–2360
25. Hudson L, Liu J, Nath A, Jones M, Raghavan R, Narayan O, Male D, Everall I (2000) Detection of the human immunodeficiency virus regulatory protein tat in CNS tissues. J Neurovirol 6:145–155
26. Bachani M, Sacktor N, McArthur JC, Nath A, Rumbaugh J (2013) Detection of anti-tat antibodies in CSF of individuals with HIV-associated neurocognitive disorders. J Neurovirol 19:82–88
27. Mediouni S, Darque A, Baillat G, Ravaux I, Dhiver C, Tissot-Dupont H, Mokhtari M, Moreau H, Tamalet C, Brunet C, Paul P, Dignat-George F, Stein A, Brouqui P, Spector SA, Campbell GR, Loret EP (2012) Antiretroviral therapy does not block the secretion of the human immunodeficiency virus tat protein. Infect Disord Drug Targets 12:81–86
28. Westendorp MO, Frank R, Ochsenbauer C, Stricker K, Dhein J, Walczak H, Debatin KM, Krammer PH (1995) Sensitization of T cells to CD95-mediated apoptosis by HIV-1 Tat and gp120. Nature 375:497–500
29. Valvatne H, Szilvay AM, Helland DE (1996) A monoclonal antibody defines a novel HIV type 1 Tat domain involved in trans-cellular transactivation. AIDS Res Hum Retroviruses 12: 611–619

Chapter 24

Measuring the Uptake and Transactivation Function of HIV-1 Tat Protein in a Trans-cellular Cocultivation Setup

Arthur P. Ruiz and Vinayaka R. Prasad

Abstract

HIV-1 Tat protein is secreted from infected cells and is endocytosed by uninfected bystander cells. Subsequently, Tat is translocated to the nucleus and binds to promoters of host cell genes, increasing the production of inflammatory host cytokines and chemokines. This inflammatory activation of uninfected cells by HIV-1 Tat protein contributes to the overall inflammatory burden in the central nervous system (CNS) that leads to the development of HIV-associated neurocognitive disorders (HAND). Here we describe methods to evaluate the uptake and transcriptional impact of HIV-1 Tat on uninfected cells by using a trans-cellular transactivation system. Cell lines transiently transfected with Tat expression constructs secrete Tat into the culture medium. Trans-cellular uptake and transactivation caused by secreted Tat can be measured by co-culturing LTR-responsive reporter cells with Tat-transfected cells. Such Tat-producer cells can also be co-cultured with immune cell lines, such as monocytic THP-1 cells or lymphocytic Jurkat T-cells, to evaluate transcriptional changes elicited by Tat taken up by the uninfected cells.

Key words HIV-1, Tat, Endocytosis, Transcription, Trans-cellular transactivation, Cytokine, Chemokine

1 Introduction

HIV-associated neurocognitive disorders (HAND) comprise a spectrum of neurodegenerative diseases that result from long-term exposure of the central nervous system (CNS) to HIV. HAND can range from the mildest form, asymptomatic neurocognitive impairment (ANI), to the intermediate mild neurocognitive disorder (MND) and to the most severe, HIV-associated dementia (HAD) [1]. HIV infiltrates the CNS through infected monocytes [2] and infects resident macrophages and microglia; however, neurons themselves cannot be infected by the virus. Neurons instead sustain damage by long-term exposure to neurotoxic factors released by infected cells [3], including viral proteins gp120 [4] and Tat [5, 6], as well as inflammatory host cell cytokines, including but not limited to TNF-α [7], IL-6 [8], and IL-1β [9]. The Tat protein

Vinayaka R. Prasad and Ganjam V. Kalpana (eds.), *HIV Protocols*, Methods in Molecular Biology, vol. 1354,
DOI 10.1007/978-1-4939-3046-3_24,

drives transcription of the viral genome by binding a stem-loop region in the 5′ *r* region of nascent viral transcripts termed the transactivating region (TAR), and by recruiting host transcriptional machinery to increase the processivity of HIV transcription [10]. In addition to promoting viral transcription, Tat can also drive the transcription of host cell genes [11–13]. Several mechanistic aspects are shared between viral and host genes activated by Tat [14–16]. Among the host genes promoted by Tat, the proinflammatory cytokines and chemokines play a critical role in the development of HAND.

There are several sites in the proviral LTR that bind both stimulatory (such as NF-κB and p65) and inhibitory (such as NFAT-1, AP1, and I-κB) [17] host factors. NF-κB is an important driver of proinflammatory cytokines and chemokines. Thus, both viral LTR and the proinflammatory gene promoters contain multiple NF-κB-binding sites. Tat interacts with NF-κB both by recruitment through multiple NF-κB-binding sites and via phosphorylation and degradation of the NF-κB inhibitor I-κB [18]. This activity allows Tat-mediated activation of NF-κB-driven inflammatory genes including MCP-1 [19], TNF-α and TNF-β [20, 21], IL-2 [13], IL-6 [12], and IL-8 and IL-1β [14]. In a manner very similar to its activity on the viral LTR, Tat can directly bind to a TAR-like stem-loop structure in the promoters of both the IL-6 [15] and TNF-β [16, 22] genes and recruit transcriptional host factors. An important mechanistic explanation for this pleiotropic activity of Tat derives from the presence of the NF-IL-6-binding site in the HIV LTR promoter [23], indicating a selective evolutionary pressure for the HIV LTR to adopt transcriptional regulatory features of certain host gene promoters.

In addition to altering the phenotype of HIV-infected cells, Tat has well-known paracrine functions [24], acting on uninfected cells such as T-lymphocytes [25] and neurons [26] specifically in a trans-cellular manner [27, 28]. Tat protein is efficiently secreted from infected cells in detectable quantities [29], and it is taken up by uninfected bystander cells [30] through endocytosis mediated by the Tat basic domain (amino acid residues 49–57) [31].

Because of genetic variations in Tat sequences from different subtypes around the world, it remains unknown how these variations could affect the ability of Tat to drive uptake or affect transcription. The field therefore has a need to be able to evaluate the effects of Tat variants on uninfected cells. In this chapter, we describe a method to measure cellular uptake of exogenous Tat, using a trans-cellular transactivation setup. In this setup, HeLa cells are transfected with Tat-expression constructs (these are Tat-"producer" cells that model HIV-infected cells), which are then co-cultured with the reporter cells (responsive to Tat taken up), and then assessed for the Tat-induced response signal (*see* Fig. 1). One can also use this method to measure the induction of inflammatory

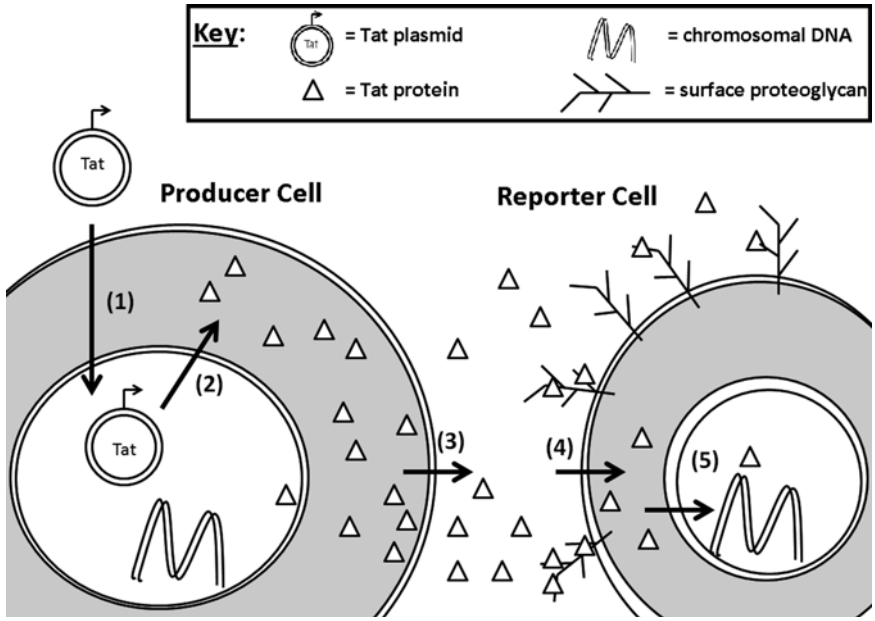

Fig. 1 A schematic of Tat trans-cellular transactivation assay: HeLa cells (shown on the *left* and labeled "Producer cells") are transfected with expression plasmids coding for Tat protein (step 1). Transfected cells are harvested and plated alongside Tat-reporter cells (shown on the *right*), either TZMbl cells (LTR-driven luciferase signal) or HLM-1 cells (containing *tat*-defective HIV provirus). Tat protein is produced from transfected plasmids in "producer cells" (step 2), secreted into the extracellular environment (step 3), and enters reporter cells by binding to extracellular proteoglycans and facilitating Tat uptake (step 4). Tat translocates to the reporter cell nucleus where it drives the expression of LTR-driven reporter signal (step 5).

host genes by Tat, by co-culturing Tat-transfected cells with PBMCs, THP-1 monocytic cells, or Jurkat T-cells. After cocultivation, the immune cells are harvested and the levels of inflammatory cytokine transcript may be assessed.

2 Materials

2.1 Cell Culture

1. DMEM and RPMI basal media (supplemented with 4.5 g/L glucose).
2. Fetal bovine serum (FBS).
3. Human serum.
4. Penicillin (10,000 U/mL) and streptomycin (10 mg/mL) (Pen-Strep antibiotic—100×).
5. TrypLE cell detachment solution, or trypsin/EDTA equivalent.
6. Lipofectamine 2000 transfection reagent.
7. HeLa cells, TZM-bl cells, and HLM-1: These adherent cell lines are cultured in DMEM media (with 10 % FBS and 1 %

Pen-Strep antibiotics). Media to culture HLM-1 cells also contains antibiotic selection G418 (10 mg/mL).

(a) TZMbl cells are derived from the parental HeLa cell line JC.53, which stably expresses large amounts of CD4 and CCR5. TZMbl cells have integrated copies of the luciferase and β-galactosidase genes under the control of the HIV-1 promoter [32].

(b) HLM-1 cells are derived from the HeLaT4$^+$ cell line, which was then transduced with the *tat*-defective mutant pM*tat*-, containing a termination codon in place of the initiator codon in the *tat* gene. The HIV provirus is derived from pHXB2gpt, a molecular clone of HIV-1_{IIIB} [33].

8. THP-1 monocytic cells are a suspension cell line derived from acute monocytic leukemia. They are grown in RPMI media (w/10% FBS, 1% HEPES buffer, and 55 μM β-mercaptoethanol) and split when cell density reaches 8×10^5 cells/mL. THP-1 cells can be differentiated by plating cells at 8×10^5 cells/mL in media supplemented with 10 nM phorbol 12-myristate 13-acetate (PMA) overnight. Differentiated cells are adherent and exhibit a well-defined pseudopod morphology.
9. Jurkat T-cells are a suspension cell line derived from T cell leukemia. They are grown in RPMI (with 10 % FBS and 1 % Pen-Strep antibiotics). Cells are split when density reaches 1×10^6 cells/mL.
10. Peripheral blood mononuclear cells (PBMCs) are prepared from donated blood (New York Blood Bank), using a sequential centrifugal isolation method. The PBMCs thus isolated are grown in a Teflon-coated flask (to minimize cell adhesion) in RPMI (with 10 % FBS, 5 % human serum, 1 % Pen-Strep) at a density of 1×10^6 cells/mL.

2.2 Expression Vectors

1. pcDNA 3.1-Tat—CMV-driven expression vectors with the gene coding for Tat subtype B (ADA strain) cloned into MCS.
   (a) A sequence coding for a human c-*myc* gene tag (N-EQKLISEEDL-C) with a 4-residue GGSG flexible linker (5′GGAGGATCCGGAgaacaaaaacttatttctgaagaagatctg-3′) has been cloned into the vector behind the Tat gene variants, to create a Tat-myc fusion protein.
2. pEGFP N1—CMV-driven superfolder GFP (sfGFP) expression vector [34] with Tat cloned into the MCS, to create a sfGFP-Tat fusion protein.
3. CMV-driven mCherry-IRES-Tat—using the pEGFP N1 vector backbone, we excised the sfGFP gene, and inserted a cassette coding for the mCherry gene, followed by an IRES sequence, and then followed by the Tat gene.

2.3 Luciferase Assay

1. 5× Luciferase Cell Culture Lysis Buffer (Promega).
2. Luciferase Assay Reagent (Promega).
3. 96-Well Luminometer plate reader.

2.4 p24 ELISA

1. p24 ELISA kit (ABL).
   (a) MicroELISA plate, coated with murine monoclonal antibodies to HIV-1 p24.
   (b) p24 standards.
   (c) Disruption buffer.
   (d) Conjugate solution.
   (e) Peroxidase solution.
   (f) Wash buffer (20×).
   (g) Stop solution.
   (h) Plate sealers.
2. 96-Well plate washer.
3. 96-Well colorimetric absorbance plate reader.

2.5 Detection of Tat in Transfected Cells by SDS-PAGE and Western Blot

1. Siliconized microcentrifuge tubes.
2. Siliconized pipet tips.
3. 1× PAGE cell lysis buffer—10 mM HEPES, 142.5 mM KCl, 2 mM $MgCl_2$, 1 % NP-40.
4. 5× sample loading buffer—10 % SDS, 10 mM dithiothreitol (DTT), 20 % v/v glycerol, 0.2 M Tris–HCl (pH 6.8), 0.05 % bromophenol blue.
5. 4 %/20 % acrylamide stacking gel.
6. Pre-stained color protein ladder, 10–250 kDa.
7. 1× Running buffer—25 mM Tris–HCl, 200 mM glycine, 0.1 % (w/v) SDS.
8. 1× Transfer buffer—25 mM Tris–HCl, 200 mM glycine, 20 % (v/v) methanol.
9. 1× TBS-T buffer—50 mM Tris–HCl, 150 mM NaCl, 0.05 % (v/v) Tween-20.
10. Nitrocellulose membrane.
11. Mouse anti-Tat monoclonal IgG antibody, clone E2.1 (provided by Dr. Udaykumar Ranga, JNCASR, Bangalore, India).
12. Mouse anti-myc monoclonal IgG antibody.
13. Mouse anti-tubulin monoclonal IgG antibody.
14. Goat anti-mouse IgG–HRP-conjugated antibody.
15. Chemiluminescent detection kit.

2.6 Measurement of Inflammatory Cytokine Transcripts by qRT-PCR

1. RNeasy RNA isolation kit (Qiagen).
2. Superscript III Reverse Transcription Kit (Invitrogen).
3. Taqman 2× qRT-PCR Master Mix (Applied Biosystems).
4. qRT-PCR instrument (Applied Biosystems, 7900-HT).
5. Nucleofector V Kit (Amaxa #VACA-1003).

3 Methods

3.1 Transfection and Cocultivation Setup

1. 24 h before transfection, seed HeLa cells in either 10 cm^2 or 6-well plates, so that they will reach 90–95 % confluency by the time of transfection (*see* **Note 1**).
2. Using Lipofectamine 2000 (LF2K), transfect cells with a Tat expression plasmid. Transfect cells with plasmids (6-well plates: 4 μg DNA + 10 μL LF2K; 10 cm^2 plate: 20 μg DNA + 40 μL LF2K) in antibiotic-free media, and 4–6 h after adding transfection reagent, replace media with fresh media containing Pen-Strep antibiotics (*see* **Note 2**). A parallel transfection using the pEGFP N1 vector (containing a CMV-driven superfolder GFP gene) should be performed, and the transfection efficiency can be assessed by the proportion of cells that are GFP positive 24 h after transfection.
3. Seed 12-well tissue culture plates with either TZM-bl or HLM-1 reporter cells the next morning, at a density that will yield ~50 % confluency (approx. 2×10^5 cells/mL per well). Allow 5–6 h for reporter cells to adhere to the plate.
4. 24 h after HeLa transfection, use siliconized pipet tips to collect supernatants from HeLa cells transfected with Tat construct into siliconized tubes (*see* **Note 3**), centrifuge ($1000 \times g$ for 10 min) to pellet dead cells and debris, and then use this cleared media to replace the supernatant of the pre-plated TZMbl or HLM-1 reporter cells. Alternatively, collect the HeLa cells transfected with Tat construct themselves by trypsinization and centrifugation, and plate along with the reporter cells (plate at 1.5×10^5 cells/mL per well into wells containing pre-plated reporter cells) (*see* **Note 4**).
5. To harvest TZMbl cultures—remove supernatant, wash cells with PBS, and then add a minimal volume of 1× luciferase cell lysis buffer to cover the cell layer (*see* **Note 5**). Incubate at room temperature for 5 min, and then firmly tap the sides of the plate to detach cells (exercising caution to avoid splashing the liquid on the sides of top of the plate).

3.2 TZM-bl Cell Harvesting and Luciferase Assay

1. Allow TZMbl cells cocultivated with *tat*-transfected HeLa cells to grow for 24 h before harvesting (*see* **Note 6**). Visually inspect the cell monolayer to ascertain a healthy level of cell density, viability, and inter-sample consistency (*see* **Note 4**).

2. Remove the media and gently wash the cells with 1 mL of PBS, and then add 1× luciferase cell culture lysis buffer to each well of TZMbl cells (*see* **Note 5**). Incubate cells in lysis buffer for 5 min at room temperature, and then tap the side of the plate several times to dislodge cells (be careful not to splash the buffer).
3. Collect the lysate by pipetting it up and down several times, being sure to rinse the bottom of the well to detach any cell clusters. Avoid bubbles. Transfer to a 1.5 mL microcentrifuge tube, vortex thoroughly, centrifuge at 12,000 × *g* for 2 min at 4 °C, and then transfer the cleared lysate to a new tube. Store lysates at −80 °C until testing.
   (a) Protein content of cell lysates can be assessed by the Bradford Colorimetric Assay (BCA, abs @ 504 nm) to determine relative protein concentrations between samples.
4. Thaw frozen TZM-bl lysates on ice. Thaw frozen aliquots of reconstituted luciferase assay reagent on ice as well. When both are thawed, bring to room temperature in an ambient water bath. Dispense 50 μL of each sample lysate into a well of a 96-well white-bottomed plate. Dispense 50 μL of LAR into each sample well, in the order that the plate reader will read each well. Immediately place into the plate reader, and run a program to read luminosity (1 s exposure time) (*see* **Note 7**) (*see* Fig. 2).
5. As an essential control, TZM-bl reporter cells should themselves be directly transfected with *tat*-expression constructs, to ascertain the maximum transactivation capacity of Tat protein when directly produced in the reporter cells themselves. This is also helpful to compare the transactivation capability of Tat

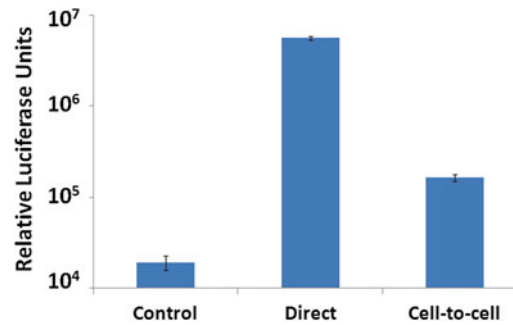

Fig. 2 Luciferase reporter signal in TZMbl cells—TZMbl cells were either transfected with empty vector, transfected with a *tat*-expression construct, or cocultivated with HeLa cells transfected with Tat-expression plasmids. Luciferase signal was measured by harvesting cells 24 h after the above treatments, preparing cell lysates, and assaying for luciferase activity.

proteins from different HIV isolates and subtypes. Directly transfect TZMbl cells in 12-well plates at a high confluency, using 1.5 μg DNA combined with 4 μL LF2K. Harvest transfected TZM-bl cells (*see* **Note 5**) and assay the lysates as described above. Transactivation signal is linearly proportional to the amount of transfected *tat* plasmid (within a range of about 0.5–3 μg per well), and can be compared with a Western blot of *tat*-transfected TZM-bl lysates to assess the relative transactivation capability of each Tat species.

3.3 HLM-1 Cells and p24 Capsid Protein ELISA

1. Allow HLM-1 cells cultivated with *tat*-transfected Hela cells or media to incubate for 48 h (although p24 is detectible in supernatant by 24 h). Visually inspect the cell monolayer to ascertain a healthy level of cell density, viability, and inter-sample consistency.
2. Collect 48 h HLM-1 supernatant in a 1.5 mL microcentrifuge tube and clear off cellular debris by centrifuging at 1000 × *g* for 10 min at 4 °C. Transfer supernatant to a new tube and store at −80 °C.
3. Thaw frozen HLM-1 supernatant on ice, and measure viral particle content by assessing p24 capsid content by ELISA. Following the instructions provided with the ABL ELISA kit, dilute supernatant to appropriate levels using cell media (*see* **Note 8**). Bring an ABL HIV p24 MicroELISA plate to room temperature. Apply the ABL kit's disruption buffer to each well (25 μL), and then add 100 μL of diluted supernatant to each well (test each sample in duplicate). Dilute the p24 standard to appropriate concentration and add to wells (containing disruption buffer) in duplicate. Seal the plate with a plate sealer, incubate at 37 °C for 1 h, then remove the seal, and wash the plate 5× using 300 μL diluted wash buffer per well. Add 100 μL of conjugate solution to each well and seal using a new plate sealer. Incubate at 37 °C for 1 h, and then wash as previously stated. Add 100 μL of peroxidase solution to each well (to be oxidized by the conjugated HRP and generate a chromogenic reaction) and incubate at room temperature for 30 min. Add 100 μL of stop solution to each well, and read absorbance at 450 nm within 20 min.
4. Use the absorbance values from the sequentially diluted p24 standard on the MicroELISA plate to create a p24 standard curve, and use the curve to calculate the p24 content of HLM-1 supernatant samples.
5. As with TZM-bl reporter cells, HLM-1 cells can themselves be directly transfected with *tat*-expression constructs. Directly transfect HLM-1 cells in 12-well plates at a high confluency, using 1.5 μg DNA combined with 10 μL LF2K. Harvest transfected HLM-1 supernatants and assay as described above (*see* **Note 9**).

As with TZM-bl cells, transactivation signal is linearly proportional to the amount of transfected *tat*-expression plasmid.

3.4 Detection of Tat in Transfected Cells by SDS-PAGE and Western Blot

1. Successful transfection of cells by Tat expression constructs can be assessed by running transfected cell lysates on an SDS-PAGE and probing by Western blotting.
2. Collect between 5×10^5 and 1×10^6 transfected cells in a siliconized microcentrifuge tube, and pellet cells by centrifuging at $1000 \times g$ for 10 min at 4 °C. Remove supernatant and store pellet at −80 °C.
3. Reconstitute pellet in 1× PAGE cell lysis buffer, at a density of 5×10^5 cells per 50 μL buffer. Vortex thoroughly, keeping the sample on ice and vortexing every 5 min for 30 min total. Centrifuge lysate at $14{,}000 \times g$ for 30 min at 4 °C.
4. Add 4 parts of cleared lysate to 1 part 5× sample loading buffer in a new siliconized microcentrifuge tube. The typical loading volume in a gel lane is 15–20 μL, so combining 20 μL lysate with 5 μL is sufficient for a single lane. Quantification of Tat may be enhanced by running one or two additional dilutions of cell lysate along the undiluted sample (dilute samples in cell lysis buffer). Heat sample at 100 °C for 5 min. Centrifuge briefly, and load in 4 %/20 % stacking gel using siliconized pipet tips.
5. Resuspend an aliquot of lyophilized recombinant Tat protein to use as a quantification standard on the gel. Dilute appropriately in loading dye, and load between 0.05 and 0.5 μg of protein per well.
6. Run gel at 120 V until dye front runs almost to the bottom of the gel (~90 min). Remove gel from the running apparatus, and using a razor blade carefully remove the 4 % stacking gel, and neatly trim off the bottom of the 20 % resolving gel below the dye front. Rinse gel briefly in 1× transfer buffer, then assemble transfer apparatus with a nitrocellulose membrane, and run in cold room at either 30 mAmp (overnight) or 350 mAmp (2 h).
7. After the transfer, remove the membrane carefully (handle with forceps instead of by hand), and use a razor blade to isolate the membrane that contacted the gel during the transfer. Cut the isolated membrane horizontally in between appropriate bands of the color-stained protein ladder—using the Bio-Rad ladder (#161-0374), cut between the bottom-most red band (25 kDa) and the blue band immediately above it (37 kDa). Make sure that you cut the top right corners of both pieces so that you can orient the gel for identification of lanes. Place the top part of the membrane (≥37 kDa) into a small

container with 5 % milk TBS-T containing diluted anti-tubulin monoclonal antibody (diluted at 1:5000). Place the bottom part of the membrane (≤25 kDa) in 5 % milk TBS-T containing either diluted anti-Tat or anti-myc antibody (either one at 1:5000). Gently rock membranes overnight in the cold.

8. Vigorously wash each membrane on a shaker three times in 1× TBS-T for 10 min each. Place each membrane in a small container with 5 % milk TBS-T containing goat anti-mouse secondary HRP-conjugated antibody (1:5000). Gently rock membranes at room temperature between 1 and 2 h.
9. Wash each membrane five times in TBS-T for 5 min each. Place membranes on plastic wrap spread out on a benchtop, and apply mixed chemiluminescent Pico ECL substrate, covering the entire membrane, for 5 min at room temperature. Remove excess ECL liquid by dabbing a corner of the membrane against a Kimwipe, and then place in a clear plastic sleeve.
10. Expose membrane to film in the dark and develop. If bands are very faint, increase exposure time, or briefly wash membrane in TBS-T and repeat chemiluminescence procedure using the stronger Femto ECL (*see* Fig. 3).

3.5 Trans-cellular Cytokine Transactivation

1. Cells transfected with *tat*-expression constructs, or their media, may be cocultivated with a variety of immunologically relevant cell types, including but not restricted to primary PBMC, undifferentiated THP-1 monocytic cells, or Jurkat T-cells—for the purposes of this method, THP-1 cells will be used as an example. After cocultivation, the immune cells can be collected

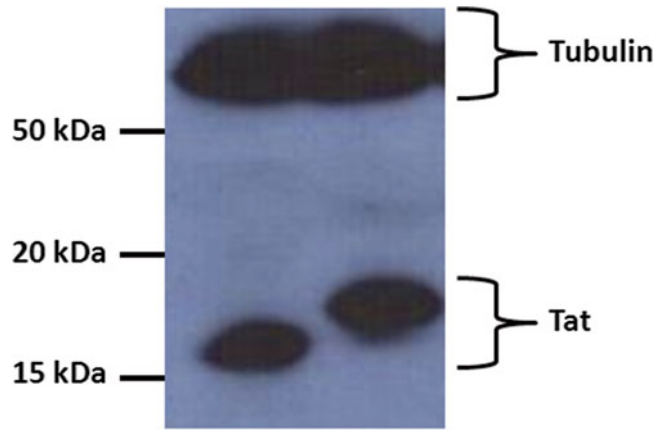

Fig. 3 Western blot of *tat*-transfected HeLa cell lysates—HeLa cells were transfected with expression plasmids coding for either (1) Tat B or (2) Tat B-*myc* fusion proteins. The cell lysates were resolved on SDS-PAGE and the western immunoblots were probed with anti-tubulin and anti-Tat antibodies.

and assayed for transcriptional differences in inflammatory cytokines between cells exposed to different variants of Tat protein.

2. THP-1 cells should be split at a low passage density the previous day, and cells collected by centrifugation ($500 \times g$ for 10 min) and resuspended in fresh media. Media from cells transfected with *tat*-expression constructs may be placed in a 12-well plate, and then 1×10^6 resuspended THP-1 cells added to the media in equal volumes. Cells transfected with Tat-expression constructs should be plated in the dish (density of $2–3 \times 10^5$ cells/mL per well) and allowed to adhere overnight. The next day, remove 500 μL HeLa media and replace with 500 μL of 1×10^6 resuspended THP-1 cells.
3. Cultivation times can vary, but significant results can be seen by 24 h. After cocultivation, carefully collect the suspension THP-1 cells, being careful not to disturb the Tat-transfected HeLa monolayer (this selection does not apply if performing a THP-1 cultivation with transfected media). Pellet the cells (store at −80 °C if they will not be processed right away) and isolate mRNA via the appropriate method (e.g., Qiagen 74104).
4. Perform a single-round reverse transcription reaction to obtain cDNA, using the Superscript III RT kid and Oligo dT primer to amplify all cellular mRNA. Measure the relative abundance of genes of interest using the relevant qRT-PCR protocol—we recommend Applied Biosystems TaqMan Master Mix and appropriate gene primer and probes. Use a housekeeping gene such as GAPDH for normalization. Supernatants from immune cells cocultivated with Tat can also be collected and assayed for secreted cytokine content using the relevant ELISA kit.
5. An important control to consider is measuring the levels of inflammatory transcripts from cells directly expressing similar levels of different Tat variants. Unlike HeLa-derived lines, primary immune cells and cell lines derived from them are difficult to transfect with expression constructs, resulting in low levels of transfection efficiency and cell viability. A variety of protocols have addressed this, but we take the following approach.
   (a) We use an expression construct containing the mCherry gene, an IRES sequence, and a *tat* gene, in succession. Transfected cells will express mCherry, and we can isolate these cells using flow cytometry sorting at a 561 nm wavelength. We thereby isolate a population of mCherry-positive cells that are also expressing Tat protein from the same transcript, which allows us to measure the relative transcription levels of inflammatory cytokines in cells directly expressing Tat. We have successfully used the Amaxa Nucleofection system. Using this system, we electroporate

cells with expression plasmid (approx. 15–20 % of cells will be transfected), allow the cells to recover for 24 h, and then sort for mCherry-positive cells (*see* **Note 10**). Cells are collected and assayed for the transcripts via qRT-PCR as described above.

4 Notes

1. High cell density is important for a successful transfection. A density of <80 % confluency tends to cause high levels of cell death the next day.
2. Replacement of transfection media with fresh media is important, as DNA:Lipofectamine complexes can persist in the media for up to 24 h after infection. If this transfection media is added to reporter cells, it can directly transfect the reporter cells with Tat constructs and confound the genuine reporter signal resulting from the uptake of Tat protein in the supernatant.
3. When handling media containing Tat, or Tat-expressing cells that will be lysed, the use of siliconized tips and tubes is very important to minimize the loss of Tat protein to surface adhesion.
4. Variable ratios of Tat-producer cells:reporter cells can be used—we have used ratios ranging from 1:3 to 3:1 and obtained appreciable signals—as long as some minimum threshold number of reporter cells are used. Upon harvest of reporter cells or media, cell density should be very high—reporter cells that are actively dividing tend to give a lower signal than cells approaching confluency.
5. For different dish sizes, minimal amounts of lysis buffer are 24-well—about 100 μL, and 12-well, about 200 μL.
6. Co-cultures can vary based on numbers of plated cells, relative proportions of Tat-producer to Tat-reporter cells, and the time of incubation. In addition, TZM-bl cells tend to yield a relatively fast cocultivation signal, giving a detectible signal as early as 6 h, while HLM-1 cells take longer to release viral particles, and generally require between 24 and 48 h of cultivation for a robust signal.
7. Luciferase reagent added to luciferase produces a sustained light-reaction signal for up to 5 min after addition. Nevertheless, it is best to minimize the amount of time between addition of LAS and plate reading. If many samples are on a plate, assay smaller subgroups of samples separately.
8. Generally, supernatant from HLM-1 cells cultivated with either transfected cell media or transfected cells requires a dilution between 50-fold and 500-fold.

9. Direct *tat* transfection of HLM-1 cells yields a higher transactivation signal than HLM-1 cells cultured with *tat*-transfected cells or media, and supernatant dilutions should be consequently increased to between 1000-fold and 10,000-fold.
10. As stated, successful transfection of primary cells and immune cell lines is not straightforward, and can require optimization to yield enough transfected cells to isolate substantial mRNA. We have successfully increased the recommended number of transfected THP-1 cells from 1×10^6–3×10^6, and also increased the amount of transfected plasmid from 0.5 to 1.5 μg. While there is a slight decrease in cell viability from these increases, the overall yield of transfected cells increases substantially. Alternatively, a specialized RNA extraction kit designed for low number of cells can also be used.

References

1. Antinori A, Arendt G, Becker JT, Brew BJ, Byrd DA, Cherner M, Clifford DB, Cinque P, Epstein LG, Goodkin K, Gisslen M, Grant I, Heaton RK, Joseph J, Marder K, Marra CM, McArthur JC, Nunn M, Price RW, Pulliam L, Robertson KR, Sacktor N, Valcour V, Wojna VE (2007) Updated research nosology for HIV-associated neurocognitive disorders. Neurology 69:1789–1799
2. Gendelman HE, Orenstein JM, Baca LM, Weiser B, Burger H, Kalter DC, Meltzer MS (1989) The macrophage in the persistence and pathogenesis of HIV infection. AIDS 3:475–495
3. Rao VR, Ruiz AP, Prasad VR (2014) Viral and cellular factors underlying neuropathogenesis in HIV associated neurocognitive disorders (HAND). AIDS Res Ther 11:13
4. Toggas SM, Masliah E, Rockenstein EM, Rall GF, Abraham CR, Mucke L (1994) Central nervous system damage produced by expression of the HIV-1 coat protein gp120 in transgenic mice. Nature 367:188–193
5. Nath A, Psooy K, Martin C, Knudsen B, Magnuson DS, Haughey N, Geiger JD (1996) Identification of a human immunodeficiency virus type 1 Tat epitope that is neuroexcitatory and neurotoxic. J Virol 70:1475–1480
6. Haughey NJ, Holden CP, Nath A, Geiger JD (1999) Involvement of inositol 1,4,5-trisphosphate-regulated stores of intracellular calcium in calcium dysregulation and neuron cell death caused by HIV-1 protein tat. J Neurochem 73:1363–1374
7. Fine SM, Angel RA, Perry SW, Epstein LG, Rothstein JD, Dewhurst S, Gelbard HA (1996) Tumor necrosis factor alpha inhibits glutamate uptake by primary human astrocytes. Implications for pathogenesis of HIV-1 dementia. J Biol Chem 271:15303–15306
8. Yeung MC, Pulliam L, Lau AS (1995) The HIV envelope protein gp120 is toxic to human brain-cell cultures through the induction of interleukin-6 and tumor necrosis factor-alpha. AIDS 9:137–143
9. Ye L, Huang Y, Zhao L, Li Y, Sun L, Zhou Y, Qian G, Zheng JC (2013) IL-1β and TNF-α induce neurotoxicity through glutamate production: a potential role for neuronal glutaminase. J Neurochem 125:897–908
10. Garcia JA, Harrich D, Soultanakis E, Wu F, Mitsuyasu R, Gaynor RB (1989) Human immunodeficiency virus type 1 LTR TATA and TAR region sequences required for transcriptional regulation. EMBO J 8:765–778
11. Nath A, Conant K, Chen P, Scott C, Major EO (1999) Transient exposure to HIV-1 Tat protein results in cytokine production in macrophages and astrocytes. A hit and run phenomenon. J Biol Chem 274:17098–17102
12. Scala G, Ruocco MR, Ambrosino C, Mallardo M, Giordano V, Baldassarre F, Dragonetti E, Quinto I, Venuta S (1994) The expression of the interleukin 6 gene is induced by the human immunodeficiency virus 1 TAT protein. J Exp Med 179:961–971
13. Westendorp MO, Li-Weber M, Frank RW, Krammer PH (1994) Human immunodeficiency virus type 1 Tat upregulates interleukin-2 secretion in activated T cells. J Virol 68:4177–4185
14. Yang Y, Wu J, Lu Y (2010) Mechanism of HIV-1-TAT induction of interleukin-1beta

from human monocytes: involvement of the phospholipase C/protein kinase C signaling cascade. J Med Virol 82:735–746

15. Ambrosino C, Ruocco MR, Chen X, Mallardo M, Baudi F, Trematerra S, Quinto I, Venuta S, Scala G (1997) HIV-1 Tat induces the expression of the interleukin-6 (IL6) gene by binding to the IL6 leader RNA and by interacting with CAAT enhancer-binding protein beta (NF-IL6) transcription factors. J Biol Chem 272: 14883–14892
16. Buonaguro L, Buonaguro FM, Giraldo G, Ensoli B (1994) The human immunodeficiency virus type 1 Tat protein transactivates tumor necrosis factor beta gene expression through a TAR-like structure. J Virol 68:2677–2682
17. Fiume G, Vecchio E, De Laurentiis A, Trimboli F, Palmieri C, Pisano A, Falcone C, Pontoriero M, Rossi A, Scialdone A, Fasanella Masci F, Scala G, Quinto I (2012) Human immunodeficiency virus-1 Tat activates NF-kappaB via physical interaction with IkappaB-alpha and p65. Nucleic Acids Res 40:3548–3562
18. Demarchi F, d'Adda di Fagagna F, Falaschi A, Giacca M (1996) Activation of transcription factor NF-kappaB by the Tat protein of human immunodeficiency virus type 1. J Virol 70: 4427–4437
19. Lim SP, Garzino-Demo A (2000) The human immunodeficiency virus type 1 Tat protein upregulates the promoter activity of the beta-chemokine monocyte chemoattractant protein 1 in the human astrocytoma cell line U-87 MG: role of SP-1, AP-1, and NF-kappaB consensus sites. J Virol 74:1632–1640
20. Buonaguro L, Barillari G, Chang HK, Bohan CA, Kao V, Morgan R, Gallo RC, Ensoli B (1992) Effects of the human immunodeficiency virus type 1 Tat protein on the expression of inflammatory cytokines. J Virol 66: 7159–7167
21. Mayne M, Bratanich AC, Chen P, Rana F, Nath A, Power C (1998) HIV-1 tat molecular diversity and induction of TNF-alpha: implications for HIV-induced neurological disease. Neuroimmunomodulation 5:184–192
22. Sharma V, Knobloch TJ, Benjamin D (1995) Differential expression of cytokine genes in HIV-1 tat transfected T and B cell lines. Biochem Biophys Res Commun 208:704–713
23. Coyle-Rink J, Sweet T, Abraham S, Sawaya B, Batuman O, Khalili K, Amini S (2002) Interaction between TGFbeta signaling proteins and C/EBP controls basal and Tat-mediated transcription of HIV-1 LTR in astrocytes. Virology 299:240–247
24. Ensoli B, Buonaguro L, Barillari G, Fiorelli V, Gendelman R, Morgan RA, Wingfield P, Gallo RC (1993) Release, uptake, and effects of extracellular human immunodeficiency virus type 1 Tat protein on cell growth and viral transactivation. J Virol 67:277–287
25. Marcuzzi A, Lowy I, Weinberger OK (1992) Transcellular activation of the human immunodeficiency virus type 1 long terminal repeat in T lymphocytes requires CD4-gp120 binding. J Virol 66:4536–4539
26. Kolson DL, Collman R, Hrin R, Balliet JW, Laughlin M, McGann KA, Debouck C, Gonzalez-Scarano F (1994) Human immunodeficiency virus type 1 Tat activity in human neuronal cells: uptake and trans-activation. J Gen Virol 75:1927–1934
27. Helland DE, Welles JL, Caputo A, Haseltine WA (1991) Transcellular transactivation by the human immunodeficiency virus type 1 tat protein. J Virol 65:4547–4549
28. Thomas CA, Dobkin J, Weinberger OK (1994) TAT-mediated transcellular activation of HIV-1 long terminal repeat directed gene expression by HIV-1-infected peripheral blood mononuclear cells. J Immunol 153:3831–3839
29. Chang HC, Samaniego F, Nair BC, Buonaguro L, Ensoli B (1997) HIV-1 Tat protein exits from cells via a leaderless secretory pathway and binds to extracellular matrix-associated heparan sulfate proteoglycans through its basic region. AIDS 11:1421–1431
30. Frankel AD, Pabo CO (1988) Cellular uptake of the tat protein from human immunodeficiency virus. Cell 55:1189–1193
31. Vives E, Brodin P, Lebleu B (1997) A truncated HIV-1 Tat protein basic domain rapidly translocates through the plasma membrane and accumulates in the cell nucleus. J Biol Chem 272:16010–16017
32. Derdeyn CA, Decker JM, Sfakianos JN, Wu X, O'Brien WA, Ratner L, Kappes JC, Shaw GM, Hunter E (2000) Sensitivity of human immunodeficiency virus type 1 to the fusion inhibitor T-20 is modulated by coreceptor specificity defined by the V3 loop of gp120. J Virol 74:8358–8367
33. Sadaie MR, Tschachler E, Valerie K, Rosenberg M, Felber BK, Pavlakis GN, Klotman ME, Wong-Staal F (1990) Activation of tat-defective human immunodeficiency virus by ultraviolet light. New Biol 2:479–486
34. Aronson DE, Costantini LM, Snapp EL (2011) Superfolder GFP is fluorescent in oxidizing environments when targeted via the Sec translocon. Traffic 12:543–548

Chapter 25

Evaluating the Role of Viral Proteins in HIV-Mediated Neurotoxicity Using Primary Human Neuronal Cultures

Vasudev R. Rao, Eliseo A. Eugenin, and Vinayaka R. Prasad

Abstract

Despite the inability of HIV-1 to infect neurons, over half of the HIV-1-infected population in the USA suffers from neurocognitive dysfunction. HIV-infected immune cells in the periphery enter the central nervous system by causing a breach in the blood–brain barrier. The damage to the neurons is mediated by viral and host toxic products released by activated and infected immune and glial cells. To evaluate the toxicity of any viral isolate, viral protein, or host inflammatory protein, we describe a protocol to assess the neuronal apoptosis and synaptic compromise in primary cultures of human neurons and astrocytes.

Key words HIV-1, Neuronal damage, Neuronal apoptosis, Neuro-inflammation, HIV-associated dementia, HAD, HIV-associated neurocognitive dysfunction, HAND, gp120, Tat, Cytokines, Chemokines

1 Introduction

HIV-infected individuals on anti-retroviral therapy are living longer; but this can result in long-standing neurological damage [1] and HIV-associated neurocognitive disorders (HAND). HAND manifests in around 50 % of the HIV-infected population despite the effective use of ARV to control peripheral viremia and immunological decline [1]. Studies have demonstrated that HIV-1 enters the brain early in the infection [2]. The disease spectrum of HAND includes the milder forms such as asymptomatic neurocognitive impairment (ANI), mild neurocognitive disorder (MND), and the severe form, HIV-associated dementia (HAD). Even though the severity of damage caused by HIV to the brain in patients on anti-retroviral therapy has decreased as evidenced by the decreasing incidence of HAD, the overall prevalence of ANI and MND is increasing worldwide [3].

CNS homeostasis and immune privilege of the brain are primarily maintained by the impermeability of the blood–brain barrier (BBB) providing separation between the central nervous

Vinayaka R. Prasad and Ganjam V. Kalpana (eds.), *HIV Protocols*, Methods in Molecular Biology, vol. 1354,
DOI 10.1007/978-1-4939-3046-3_25,

system (CNS) and the peripheral blood circulation. HIV-1 breaches the BBB early in the acute stages of infection [4]. HIV-1 infection of leukocytes increases expression of key proteins involved in transmigration and chemokine recognition, resulting in an enhanced invasion of the brain early during HIV infection by a mechanism named "Trojan horse" [5]. Once transmigrated leukocytes are inside the CNS, HIV-infected macrophages produce chemokines that recruit more immune cells from the circulation including T-cells and macrophages [6]. This influx of new transmigrated immune cells, over time, leads to an unusually high density of monocyte/macrophages in the brain including activated monocytes, macrophages, microglia resulting in enhanced inflammation, and brain tissue damage. Consequently, all these cells secrete neurotoxic viral proteins (Tat, gp120) and inflammatory chemokines/cytokines (TNF-alpha, interferon alpha, CCL2, CXCL10) [7] that have the ability to interact with the cell surface receptors present on the neurons [7] triggering neuronal apoptosis. The recent increase in efforts to identify the genetic signatures of viral proteins that are responsible for neurovirulence necessitates appropriate methods to evaluate the relative neurotoxicity of different HIV-1 isolates to help identify the neurotoxic viral and host products responsible for neurotoxicity.

Most of the neuronal apoptosis assays documented in literature are currently performed using neuroblastoma cell lines (e.g., SH-SY5Y) and rodent primary neurons. However, these immortalized cell lines or primary neurons isolated from rodents fail to accurately represent the HIV neurotoxicity observed in vivo. Use of such cells also allows investigators to simply measure cell survival using MTT or WST-1 assays. In contrast, most human cultures of neurons tend to contain variable proportions of astrocytes and an even smaller proportion of glia, complicating the interpretation of the results in cell survival assays. Here we describe a neuronal apoptosis assay employing human primary neurons to quantify the number of neurons undergoing apoptosis to get a more accurate picture of the neuropathogenesis.

2 Materials

2.1 Culture of Primary Human Neurons

1. Primary human fetal brain tissue (obtained from fetal brain tissue repository).
2. Phosphate-buffered saline (PBS).
3. Trypsin-EDTA.
4. DNase.
5. Tweezers, razor blades.
6. 250 and 150 μm Filters.

7. Minimal essential medium.
8. Fetal bovine serum.
9. Penicillin-streptomycin (10,000 U/ml).
10. Neurobasal media.
11. N2 supplement—100×.
12. TMR in situ hybridization kit.
13. Anti-neurotubulin antibodies.
14. Alexa-conjugated secondary antibody—goat anti-rabbit IgG.
15. Prolong Gold anti-fade agent with DAPI.

2.2 Virus Production

1. 293T cells.
2. Lipofectamine 2000 transfection reagent.
3. OptiMEM media.
4. DMEM tissue culture medium with L-glutamine, glucose, and sodium pyruvate.
5. Heat-inactivated pooled fetal bovine serum.
6. Penicillin-streptomycin (10,000 U/ml).
7. HIV-p24 ELISA kit.

2.3 Macrophage Differentiation and HIV Infection

1. Elutriated primary human monocytes.
2. Monocyte colony-stimulating factor (MCSF).
3. Pooled human serum.
4. 24-Well polystyrene-treated tissue culture dishes.
5. DMEM tissue culture medium with glucose and sodium pyruvate.
6. L-Glutamine—200 mM.
7. Penicillin-streptomycin (10,000 U/ml).

3 Methods

The protocol described below includes culturing primary neurons, HIV infection of human macrophages, exposure of primary cultures of neurons to HIV-infected cell supernatants, staining of neuronal cultures by nuclear staining with DAPI, staining of apoptotic cells by TUNEL (terminal deoxynucleotidyl transferase dUTP nick end labeling), and staining of neurons by neurotubulin staining. DAPI stain labels all nuclei, neurotubulin allows one to identify neurons, and TUNEL staining detects only the apoptotic nuclei; thus, one can quantitate the proportion of total cells constituted by the apoptotic neurons.

3.1 Culturing Fetal Primary Neurons

Human neuronal cultures are obtained from elective abortions. All the protocols must be approved for use by the Institutional Review Board offices. Most of the tissue employed corresponds to cortex and hippocampal tissue. In this section, we describe in detail the preparation and potential application of these cultures.

1. Place the tissue in a plate containing sterile PBS and remove the meninges using sterile forceps. Meninges contain blood and several cell types that can contaminate the purity of the CNS cell populations. Due to the fact that the tissue is of human origin, you need to use biosafety level 2+ (BL2+) handling conditions in case of contamination with human pathogens such as HIV, HCV, or CMV.
2. Mince the tissue with a razor to a fine grind, making it easy enough to pick it up with a pipet (*see* **Note 1**).
3. Tissue is cut into small sections and mixed with 1mL trypsin-EDTA and 100 μL DNase I.
4. Incubate for 45 min to an hour in a warm incubator in 50 ml Falcon tubes on a rotating shaker with trypsin-EDTA and DNase I (*see* **Note 2**).
5. After the incubation, pipet up and down to dissociate any remaining cell aggregates.
6. Then, pass the cell suspension solution through a 250 μm filter. The filtered cell suspension subsequently is filtered using a 150 μm filter to remove clumps of tissue and to obtain individual cells.
7. The cell suspension is centrifuged at $600 \times g$ for 5 min at 18 °C (*see* **Note 3**). Wash two times and remove the supernatant with care.
8. Count the cells and plate in complete medium (minimal essential medium + 10 % FBS + PenStrep). Plate the 1.2×10^8 cells in a 150 ml tissue culture flask and place in the CO_2 incubator. Do not disturb for 7–10 days.
9. After this period, observe the morphology to ensure that the cells display neuronal characteristics (*see* **Note 4**). Trypsinize with 8 ml trypsin for 1–2 min at 37 °C until you see the first evidence of adhesion loss to the plastic. Harvest the neurons and pellet the cells (quickly, $600 \times g$ for 5 min) and count.
10. Plate 10^7 cells in 15 mL Neurobasal media, 1 % FBS, N2 supplement, and PenStrep, in a T-75 flask. Half media changes are done every alternate day. These cells can be used anytime from day 5 to day 12 post-splitting. Using this protocol, you can obtain enriched neuronal cultures containing 80–90 % of neurons and 10–20 % glia.
11. In these cultures, astrocytes grow in the bottom of the plate and neurons grow on the top of the astrocytes. For these cultures,

approaches using confocal microscopy are extremely useful to evaluate cellular localization, neuronal processes, apoptosis, synaptic proteins, and glial-neuronal communication.

3.2 Virus Production

Infectious HIV-1 virus particles are produced by transient transfection of 293T cells using Lipofectamine reagent.

1. Seed 4×10^6 293T cells in 100 mm^2 culture dishes 24 h prior to transfection.
2. Replace culture medium with ~8 ml fresh, pre-warmed 2.5 % FBS DMEM antibiotic-free medium 4 h prior to transfection to stimulate cell division and prevent toxicity.
3. Prepare 24 μg DNA/Lipofectamine reagent mix in Opti-MEM media.
4. Add the DNA/Lipofectamine reagent mix in Opti-MEM to 100 mm culture dish with 293T cells by uniformly adding drops over the entire surface.
5. Incubate for 4 h at 37 °C with 5 % CO_2.
6. Add 5 ml 20 % FBS DMEM medium to the 100 mm culture dish with 293T cells.
7. After 12 h, replace culture medium with 10 ml pre-warmed 10 % FBS DMEM.
8. Collect supernatants 48 h post-transfection. Centrifuge supernatants at $3000 \times g$ for 5 min to clear the cell debris. Add 10 μl of 1 M HEPES buffer each to 1 ml aliquots of the supernatant and store at −80 °C for future use.
9. Quantitate the amount of virus obtained using HIV-p24 ELISA.

3.3 Macrophage Differentiation and Infection

Monocytes obtained by elutriating PBMCs are differentiated into macrophages using macrophage colony-stimulating factor (MCSF).

1. For differentiating monocytes into macrophages, primary human monocytes are incubated at 37 °C for 5 days in DMEM, 10 % human serum, PenStrep, L-glutamine, and MCSF (Sigma) at 6.6 ng/ml in 24-well plates with media changes every other day.
2. Following differentiation into macrophages, various viral isolates are used to infect macrophages in at least three different concentrations (*see* **Note 5**). (For full-length infectious molecular clones, virus obtained from the 293T cell transfection is used for infection and for clinical isolates, infectious PBMC supernatants are employed.)
3. Following infection, the macrophages are incubated for 5–10 days and half media changes are done every third day. Supernatants are collected every day to measuring HIV-p24

levels using ABL HIV-p24 ELISA kit. These supernatants are used to treat neuronal cultures once they exhibit equal infectivity (*see* **Note 5**).

3.4 Neurotoxicity Testing

If the sample to be tested in neurotoxicity is a protein/macromolecule such as viral proteins or chemokines/cytokines, it has to be directly added to the media, which is changed 2 days prior to treatment. If the sample to be tested for neurotoxicity is HIV-infected supernatant, then it has to be mixed with equal or greater volume of Neurobasal medium and added to the neurons. Some of these infected supernatants can be depleted of particular viral proteins, such as Tat and gp120, using immune-depleted supernatants using specific antibodies [8, 9] and the toxicity of the medium with and without immune depletion can be compared.

1. Plate approximately 100,000 primary neurons on poly-lysine-coated MatTek plates in 2 mL Neurobasal media (without FBS) for a period of 6 days in the incubator and allow them to stabilize and differentiate with half media changes every 2 days.
2. Add either diluted HIV-infected macrophage supernatant or the protein/macromolecule of interest to the Neurobasal media and incubate with the neurons for a set amount of time. In Fig. 1, primary human neurons were incubated with the HIV-1_{ADA}-infected macrophage supernatant for 24 h.
3. A dose–response curve as well as the kinetics of neuronal killing as a function of time should be performed the first time when neurotoxicity assay is performed (*see* **Note 6**).
4. Following the treatment, fix the neurons in 70 % ethanol for 15–20 min at –20 °C (if the apoptosis is massive or if the neuronal confluence is low, fix the neurons overnight).
5. Perform TUNEL assay using the TMR in situ hybridization kit (Roche; Cat No. 12156792910) (use 37 °C degree incubator with humidity control). Incubate for 1 h.
6. Following the TUNEL staining, wash the neurons two times in PBS and incubate overnight at 4 °C with anti-neurotubulin antibodies (Abcam cat. No. 21058) (primary antibody) (*see* **Note 7**).
7. Wash the neurons again and incubate with a suitable secondary antibody for 2–4 h at room temperature (low confluence/massive apoptosis again warrants overnight incubation at 4 °C).
8. Wash five times in 1× PBS with 5-min incubation between washes.
9. Add Prolong Gold anti-fade agent with DAPI (Invitrogen, cat number, P36931) to the neurons and place cover slips. Incubate overnight at 4 °C in a humid box.
10. Perform image capture and analysis using Zeiss Microscope and Zeiss Zen software. Image ten fields per treatment. For each

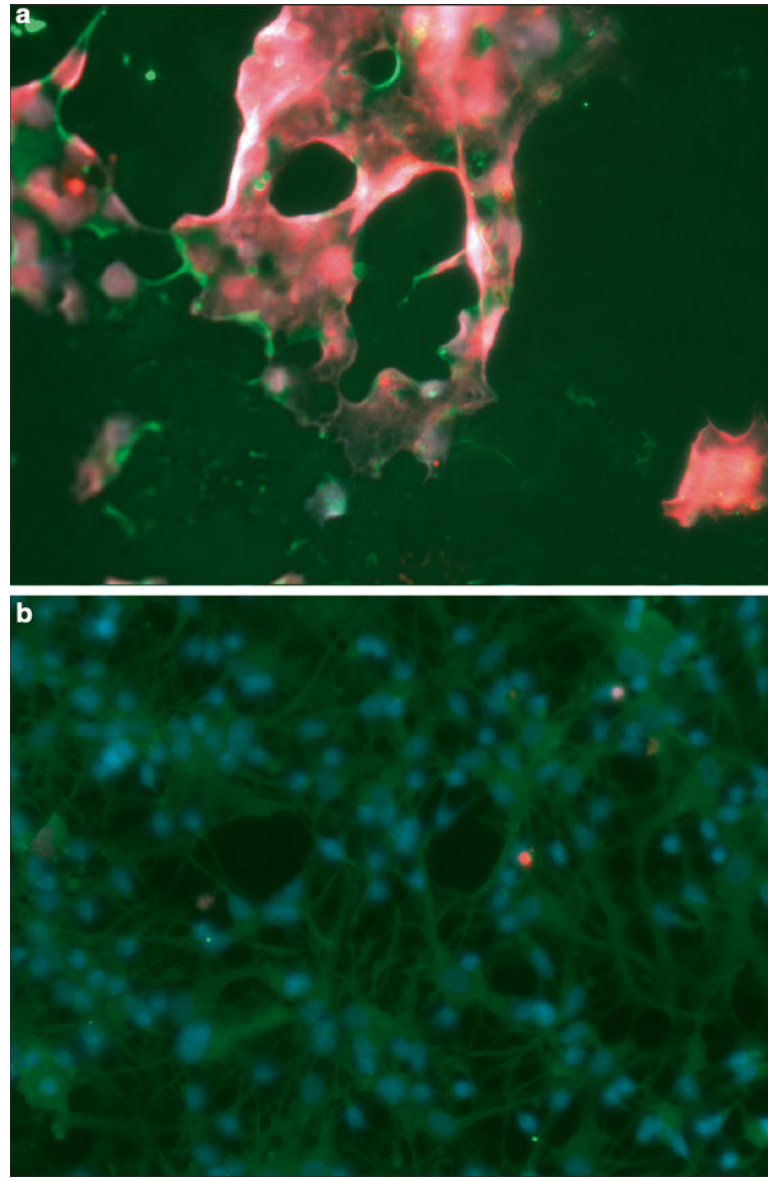

Fig. 1 Neurotubulin/TUNEL staining of primary human neurons treated with either HIV-1-infected or uninfected MDM supernatants. TUNEL-stained primary human neurons that were treated with HIV-1_{ADA}-infected or uninfected macrophage supernatant, then co-stained with anti-neurotubulin antibodies and DAPI (Prolong Gold anti-fade with DAPI, Invitrogen). Neurons treated with HIV-1-infected supernatant exhibit massive apoptosis as demonstrated by TUNEL staining.

field, you need to process all three fluorescence channels (red, green, and blue) and bright field. Each sample takes approximately an hour to process (ten fields total) (*see* Fig. 1).

11. Transfer images to Nikon NIS software for further processing. Determine the percent apoptosis/survival based on the

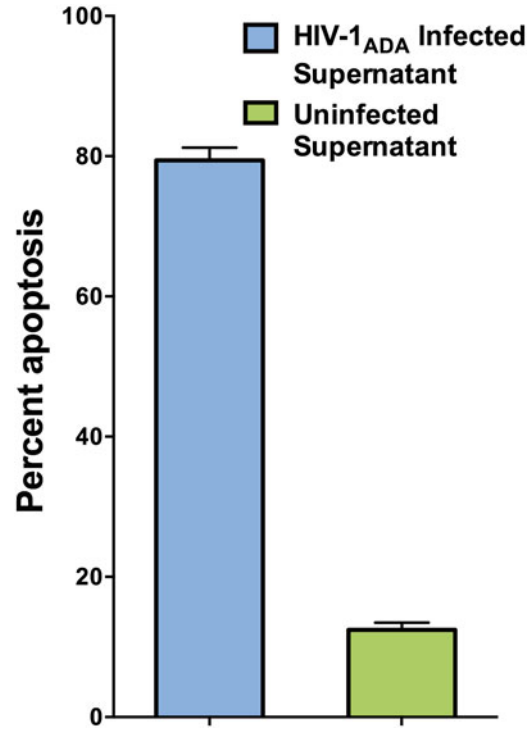

Fig. 2 HIV-1_{ADA}-infected supernatant causes neuronal apoptosis in primary human neurons. HIV-1_{ADA}-infected macrophage supernatant and uninfected macrophage supernatant were diluted with 100 μl of Neurobasal medium and incubated with primary human neurons in MatTek plates for 18 h. Percent apoptosis/survival was determined based on the proportion of cells with DAPI-neurotubulin stain that are TUNEL positive. HIV-1_{ADA} supernatant leads to a greater loss of neuronal viability when compared to uninfected supernatant.

proportion of cells with DAPI-neurotubulin stain that are TUNEL positive (Fig. 2).

12. Measure the dendrite width and length using Nikon (NIS elements) advanced research software and calculate the median dendrite width using 20–30 measurements/cell for 50–100 different cells in the field.

4 Notes

1. If the tissue is bloody, rinse it well with PBS prior to further processing. Use tweezers to separate the thick white tissue from the cortical tissue.
2. Incubations greater than an hour will lead to loss of tissue. Limit the incubations to less than 1 h.
3. The pellet at this juncture is held together loosely; therefore it should be handled with care.

4. Two distinct cell layers can be observed—a bottom layer of glial cells and a top layer of neurons. Constantly monitor trypsinized neurons for first signs of loss of adhesion.
5. Different virus isolates have varied replication rates; therefore it is critical to titer the doses of initial infection to generate infected cell cultures whose supernatants contain similar amounts of p24. Typically 10ng, 100ng and 500ng virus supernatants are used to titer the infectivity. Macrophages are plated in either 12 or 24 well plates and allowed to differentiate for a period of 72 hours in media containing MCSF (Macrophage colony stimulating factor). Once the macrophages are completely adherent and differentiated, viral isolates are tittered in various concentrations to obtain similar infectivity.
6. It is recommended to use a positive control such as LPS-treated macrophage supernatant where robust neuronal cell death can be observed.
7. Primary antibody incubation needs to be at 4 °C to preserve the TUNEL staining. Incubation at 37 °C will lead to false-positive TUNEL results.

Acknowledgements

This work was supported by NIH R01 MH083579 and R21 MH101003 (to V.R.P.). The authors would like to thank Arthur Ruiz for critically reading the manuscript.

References

1. Heaton RK, Franklin DR, Ellis RJ, McCutchan JA, Letendre SL, Leblanc S, Corkran SH, Duarte NA, Clifford DB, Woods SP, Collier AC, Marra CM, Morgello S, Mindt MR, Taylor MJ, Marcotte TD, Atkinson JH, Wolfson T, Gelman BB, McArthur JC, Simpson DM, Abramson I, Gamst A, Fennema-Notestine C, Jernigan TL, Wong J, Grant I, Group C, Group H (2011) HIV-associated neurocognitive disorders before and during the era of combination antiretroviral therapy: differences in rates, nature, and predictors. J Neurovirol 17:3–16. doi:10.1007/s13365-010-0006-1
2. Resnick L, Berger JR, Shapshak P, Tourtellotte WW (1988) Early penetration of the blood-brain-barrier by HIV. Neurology 38:9–14
3. Airoldi M, Bandera A, Trabattoni D, Tagliabue B, Arosio B, Soria A, Rainone V, Lapadula G, Annoni G, Clerici M, Gori A (2012) Neurocognitive impairment in HIV-infected naïve patients with advanced disease: the role of virus and intrathecal immune activation. Clin Dev Immunol 2012:467154. doi:10.1155/2012/467154
4. An SF, Groves M, Gray F, Scaravilli F (1999) Early entry and widespread cellular involvement of HIV-1 DNA in brains of HIV-1 positive asymptomatic individuals. J Neuropathol Exp Neurol 58:1156–1162
5. Meltzer MS, Skillman DR, Gomatos PJ, Kalter DC, Gendelman HE (1990) Role of mononuclear phagocytes in the pathogenesis of human immunodeficiency virus infection. Annu Rev Immunol 8:169–194. doi:10.1146/annurev.iy.08.040190.001125
6. Toborek M, Lee YW, Flora G, Pu H, Andras IE, Wylegala E, Hennig B, Nath A (2005)

Mechanisms of the blood-brain barrier disruption in HIV-1 infection. Cell Mol Neurobiol 25:181–199
7. Rao VR, Ruiz AP, Prasad VR (2014) Viral and cellular factors underlying neuropathogenesis in HIV associated neurocognitive disorders (HAND). AIDS Res Ther 11:13. doi:10.1186/1742-6405-11-13
8. Rao VR, Neogi U, Eugenin E, Prasad VR (2014) The gp120 protein is a second determinant of decreased neurovirulence of Indian HIV-1C isolates compared to Southern African HIV-1C isolates. PLoS One 9:e107074. doi:10.1371/journal.pone.0107074
9. Rao VR, Neogi U, Talboom JS, Padilla L, Rahman M, Fritz-French C, Gonzalez-Ramirez S, Verma A, Wood C, Ruprecht RM, Ranga U, Azim T, Joska J, Eugenin E, Shet A, Bimonte-Nelson H, Tyor WR, Prasad VR (2013) Clade C HIV-1 isolates circulating in Southern Africa exhibit a greater frequency of dicysteine motif-containing Tat variants than those in Southeast Asia and cause increased neurovirulence.Retrovirology10:61.doi:10.1186/1742-4690-10-61

ERRATUM

Detecting HIV-1 Tat in Cell Culture Supernatants by ELISA or Western Blot

Fabienne Rayne, Solène Debaisieux, Annie Tu, Christophe Chopard, Petra Tryoen-Toth, and Bruno Beaumelle

Vinayaka R. Prasad and Ganjam V. Kalpana (eds.), *HIV Protocols*, Methods in Molecular Biology, vol. 1354,
DOI 10.1007/978-1-4939-3046-3_22, © Springer Science+Business Media New York 2016

DOI 10.1007/978-1-4939-3046-3_26

One of the chapter author name, 'Petra Tryoen' was incorrect in the Table of Contents, in Contributors and also in the opening page of the chapter.

The author name has been corrected and it now reads as Petra Tryoen-Toth

The online version of the original chapter can be found at
http://dx.doi.org/10.1007/978-1-4939-3046-3_22

INDEX

A

ABCA1 281–292
ACH2 268
Affinofile cells 4, 9, 17
Affinofile system 3–18
Albumin 62, 153, 283, 306
Alkaline phosphatase 121–122, 124–125
ALLINIs 150, 151
Amino terminal copper- and nickel-binding motif (ATCUN) 94, 96, 111, 113–115
ANOVA test 78, 84
Antibodies 267, 283, 331, 335, 345, 357, 369
  α-p24 ..... 166, 167, 169, 170
  anti-Calnexin 283, 286–288, 291, 292
  anti-CD69 Biotin 246
  anti-FLAG 44, 151, 153, 161, 330, 331, 337–339
  anti-goat α-p24 ..... 169, 170, 267, 283, 286–288, 291, 357, 362, 369
  anti-Nef 283, 286–288
  anti-rabbit peroxidase-conjugated 331, 335
  anti-6xHis 151, 153
  anti-Tat
    E2.1 357
    1D9 345
    sc-65912 331
  CD4 antibody-Pacific Blue conjugate 259
  CD4 T-cell biotin-antibody cocktail 245
  CD45RA antibody-APC conjugate 259
  CD45RO antibody-PerCP conjugate 259
  CD27 antibody-APC-Alexa Fluor 750 conjugate 259
  goat anti-mouse 283, 286, 288, 291, 292, 357, 362
  goat anti-rabbit IgG 267, 283, 369
  Human gamma globulin 207, 208
  Mouse anti-human CD4-PE-Cy5 208
  Mouse anti-human CD45-FITC 208
  Mouse anti-human CD45-PE 207, 212
  Mouse anti-human CD3-PE 208
  Rat anti-mouse CD16/CD32 ..... 207, 208
Antiretroviral drug
  AZT 24, 26, 32
  elvitegravir 150
  emtricitabine 195
  preparation 208, 214–215
  raltegravir 150, 208
  tenofovir 195, 208
ApoA 281, 282, 284, 290
APOBEC3 ..... 72, 74, 81, 86
Apoptosis 368, 371–374
Astrocyte 265, 272, 277, 368, 370
ATCUN. *See* Amino terminal copper- and nickel-binding motif (ATCUN)

B

Bayesian analysis 250, 302
BEDtools 128
β-mercaptoethanol 41, 161, 177, 223, 330, 331, 356
Bicinchoninic acid (BCA) assay 317, 359
Biotin blocking kit 270
Bioinformatics 127–128, 312, 321–322
Biotin-streptavidin-fluorophore amplification 272–374
BioSafety level 370
BlaM-Vpr 24, 26, 34
Blasticidin 6
Blood 208, 215–216, 258, 263, 293, 356
Bradford assay 317, 359

C

Calnexin 282, 283, 285–287289–292
Capillary electrophoresis (CE), assembly 92, 96, 100–103, 110, 113, 115, 116
Capsid
  assembly 40, 41
  destabilization 40
  uncoating 39
cART. *See* Combination antiretroviral therapy (cART)
CCF2-AM 26, 27, 34
CCR5 ..... 3–12, 14–18, 22, 204, 221, 223, 230–232, 241, 245, 247, 356
CD8+ T cell 226, 245, 248, 249, 251

Vinayaka R. Prasad and Ganjam V. Kalpana (eds.), *HIV Protocols*, Methods in Molecular Biology, vol. 1354,
DOI 10.1007/978-1-4939-3046-3, © Springer Science+Business Media New York 2016

CD4+ T cell 190, 195–196, 208, 214, 228, 241, 245–246, 258–260
central memory
adoptive transfer 195–196
expansion 190, 195–196
infection 195–196
culturing 239–251
isolation 241, 242, 245–246, 258
monitoring levels
by FACS 208, 214
naïve
isolation 142, 228, 258–260
plating 245–246
resting
isolation 241, 245–246
purification 245–246
Cell free infection 21–23, 142–143
Cell labeling 22, 28–29, 35
Cell lines
ACH2 268
CEM 82, 257, 261–262
GHOST-R5 12
HEK 293T 190
HeLa 356
HLM-1 cells 356
Jurkat 330
MOLT-4/CCR5 ..... 240, 241, 243–245
MT-4 cells 24, 26
OM-10 ..... 267, 268
PC12 ..... 330, 332, 337
293T 190
THP-1 ..... 282, 283, 356
U373-MAGI-CXCR4 ..... 73, 74, 76–78
Cell lysate 142, 228, 285, 309, 335, 338, 344, 349, 359, 361, 362
preparation 134, 136, 137, 140–141
Cell-to-cell HIV-1 infection 21–36
Cell-to-cell membrane fusion 24, 26–27, 29, 32–34
Cell-to-cell transfer 23, 24, 29–32, 34, 36
CEM cell 257, 261, 262
CCRF-CEM 313
Central nervous system (CNS) 353, 367, 368, 370
Cerebrospinal fluid (CSF) 224, 225, 293, 343–350
CFSE 241
Chemokine 3, 251, 354, 368, 372
Cholesterol, [^{3}H] labeled 282, 284, 285, 291
Cholesterol efflux 281–292
CHO-pgsA-745 ..... 51, 53, 55
Chromatography
HPLC 61, 153, 154, 314, 315, 318
LC 296, 297, 300, 306, 307, 319
LC-MS 296, 318
CLIP library 127, 130
CLIP-seq 119–130
CNS. *See* Central nervous system (CNS)
Cochran-Mantel-Haenszel test 82, 86
Cocultivation 353–365
Combination antiretroviral therapy (cART) 239, 241, 255
activation 256
Confocal microscopy 166, 266, 274–277, 283, 285–290, 371
CpG island 94, 111
CPSF6 protein 41–44
CS-source irradiator 242, 245
CSF. *See* Cerebrospinal fluid (CSF)
CXCR4 ..... 3, 7, 22, 73, 74, 76–78, 82, 204, 241, 244
Cyclophilin A 49
Cytokine transcripts 355
qRT-PCR 358

D

Databases
DAVID 315, 322, 324
exosome 315, 321
gene ontology 321, 322, 324
Human Protein Interaction 321
STRING 315, 322
SwissProt 299, 307
UniProt 299, 307, 308, 321, 322
DEAE-Dextran 224, 225
Dendritic cells (DCs) 22, 68, 204, 226, 276
Deoxynucleoside triphosphates (dNTPs) 61–66, 68, 70, 75, 80, 101, 127, 138, 140
DNAse I treatment of virus 76, 83
dNTP assay 62, 64–66
Dolutegravir 150
Doxycycline 5–811–13, 17
DynaBeads 136, 139, 190, 195, 242, 248, 249
Human T-Activator CD3/CD28 ..... 258, 260, 262
Dynal MPC-1 magnetic particle concentrator 242

E

Electroporation 331, 333
ELISA
cellular 330, 336
sandwich 329, 349
End-labeling 102, 121–122, 124–125
Endocytosis 57, 343, 354
Endosome 329
Endoplasmic reticulum (ER) 165, 282, 292
Endothelial cells 329
Env 3–18, 22, 25, 34, 35, 52, 72, 74, 82, 83, 162, 165, 221, 222, 224, 225, 256, 291
Exosomes
HIEP 321–322, 324
isolation 316–317, 323

preparation....317
protein extraction....312, 317
proteomics of....311–324
Extraction of genomic DNA....80–82

F

FACS. *See* Fluorescence-activated cell sorting (FACS)
Fetal bovine serum....330, 355, 369
Ficoll-Plague Plus....26, 205, 209, 242, 267
Fisher's exact test....82, 86
Fluorescence-activated cell sorting (FACS)....6, 8, 9, 17, 74, 75, 78–80, 85, 208, 214, 261, 262, 271
Footpad injection....192–195
Footprinting....93, 103, 112, 113
Formic acid....295, 296, 315, 318

G

G418....74, 243, 245, 283, 356
Gag Pr^{55}
highly basic region....175
myristoylated....180
Gag-iGFP....24, 25, 31, 34
Gag-membrane interactions....177, 178, 180–182
Gag-Pol....165, 167, 168
GALT. *See* Gut-associated lymphatic tissue (GALT)
GraphPad Prism....75, 77, 78
Gut-associated lymphatic tissue (GALT)....21

H

H9 cell....313
HAND. *See* HIV-associated neurological disorders (HAND)
HEK 293T cells....190, 193, 257, 261
HeLa
HeLa T4+ cells....313
HeLa-ABCA1-GFP cell line....283, 286, 287
JC.53....356
Hematopoietic stem cells (HSC)....204, 222
CD34+....204–206, 209–211
High performance liquid chromatography-mass spectrometry....61, 96, 123, 153, 154, 296, 314, 315, 318, 319
nanoflow....315, 319
High-performance liquid chromatography-mass spectrometry (HPLC-MS)....61, 62
HIV-associated neurological disorders (HAND)....344, 353, 354, 367
HIV-Gag-iCherryΔEnv....52
HIV-Gag-iGFPΔEnv....51, 52
HIV NL-GI....24, 25, 33, 34
HIV-1....119, 120, 193–195, 224–225, 371
ADA....356
assembly....119, 175
Biotinylation....136
CCR5-tropic....241
Clade....348, 349
CXCR4-tropic....82, 204, 241
infectious
generation....225
titration....225
NL4-3....138, 167, 168, 291, 316
p6....175
p24....154, 159, 241, 243, 267, 268, 272, 275–277, 323, 357, 360–361, 369, 372
measuring....224–225, 371
reporter....7, 25, 79, 190–192
preparation of high-titer....193–195
subtype....256, 257
HIV-1 Gag
imaging....171–173
localization....165–174
quantitation....173
HIV-1 IN
cross-linking....152, 154, 159, 161
multimerization assay....153
HIV-1 infection
by parenteral route....207, 213
by rectal mucosal route....207, 212–213
by vaginal route....207, 212–213
HIV-1 latency....240, 241, 256, 257
HIV-1 molecular clones
ADA....356
HIV-1Bal....224
HIV-1JR-CSF....224
IIIB....356
pHXB2gpt....356
HIV-1 Nef....285–287
HIV-1 provirus....240, 241
HIV-1 reporter viruses
HIV-LucR....225, 230
HIV-nLucR....231, 232, 234
NL-LucR.T2A-Bal.ecto....224, 231
NL-LucR.T2A-JR-CSF.ecto....225
HIV-1 RNA....92, 133–145, 207
In vitro transcription....139–140
HIV-1 RNP....134–136, 139–140
isolation....134–136, 139–140
HIV-1 RTC....51
HIV-1 Tat....221, 259, 329, 330, 334, 345
trans-cellular transactivation....353
HIV-1 viremia....204, 207–208, 213–214
monitoring....207–208, 213–214
HIV associated neurocognitive disorders (HAND)....353, 367
HLM-1 cells....355, 356, 360–361, 364, 365

Homogeneous time-resolved fluorescence resonance (HTRF) 151–153, 155–156, 161
instrument 153
microplates 153
HPLC. *See* High-performance liquid chromatography (HPLC)
HPLC-MS. *See* High-performance liquid chromatography-mass spectrometry (HPLC-MS)
HSC. *See* Hematopoietic stem cells (HSC)
HTLV-1 22
Hu-HSC mice 205, 206, 211
Preparation 206, 211
Humanized mice (hu-mice) 203, 204, 207, 209, 211, 212, 216
hu-mice. *See* Humanized mice (hu-mice)
Hu-PBL-SCID mice 203
HVI-1
Assembly 158
Hygromycin B 283

I

IL-2 ..... 26, 203, 223, 225, 242, 244, 262, 354
Image analysis 166, 169, 191, 193, 197, 283, 285–290
software 166, 169, 192, 197
ImageJ 52, 55, 166, 168, 169, 173
Image processing 192, 197–198
Immunoblotting 154–155, 159–160
Immunodepletion 29, 305
Immunofluorescence 169–171
Immunoprecipitation 121, 125, 129, 137, 330, 337
Infectious units/mL 83, 195, 225, 226, 228
Inflammation 344, 368
50 % inhibitory concentration (IC50) 151, 156
In situ imaging 50
Infectious 17, 22, 72, 73, 77, 83, 119, 137, 165, 195, 225, 263, 305, 371
Institutional Review Board 305, 370
Intasome 149, 150, 158
Integration 22, 23, 25, 49, 84, 149, 241, 250, 256, 263, 289
Integrins 22
Internal ribosome entry site (IRES) 25, 78, 224, 256, 356, 363
In vitro liposome-binding assay 175
In vitro transcription/translation (TNT) 180
In vivo fluorescent assay 50
IRES. *See* Internal ribosome entry site (IRES)
iTRAQ 293, 311, 312
IVIS Spectrum imager 225–227

J

Jurkat cells 24, 27, 29, 34, 36, 257, 261, 329, 332, 333, 336, 337, 340
transfection of 333

K

Klenow fragment 62
Kruskal–Wallis analysis 271

L

LEDGF/p75 149–151
Lentivirus packaging 258–259, 261
Leukocyte analysis 269–270
Leukopaks 242, 243
LGIT in vitro latency model 255–263
Lipid rafts 281
Liposomes
multilamellar 178–180
preparing 177–180
unilamellar 178–180
Liposome flotation 176, 177, 180–183
Longitudinal studies 240
Long terminal repeat (LTR) 207, 213, 214, 256, 354, 355
LTR. *See* Long terminal repeat (LTR)
Luciferase
assay 224, 225, 231, 332, 334, 335, 357–360
firefly 162, 224, 225, 233
Measuring 224–225, 359
NanoLuc 224
Renilla 224, 228
Luminometer 224 228, 233, 332, 335, 357
Lymphoblasts 239–242, 244, 245, 248–250, 313
CD8 depleted+B270 ..... 241, 242, 245, 248, 249

M

Matrix protein (MA) 25, 50, 51, 122, 167, 175, 176, 225, 267, 345
Macrophage colony stimulating factor 371, 375
Macrophages 3, 61, 204, 221, 223, 226, 265, 276, 277, 291, 329, 368, 369, 371, 375
MACS Separator Magnets 242
Malvern Zetasizer Nano S90 154
Mass spectroscopy 293
Media
Dulbecco's modified Eagle's medium 51, 74, 154, 257, 283
Iscove's Modified Dulbecco's Media 206
RPMI 26, 142, 190, 195, 223, 257, 313, 355
Meth treatment 229, 231, 233
Methidiumpropyl-EDTA (MPE) 93, 94, 96, 110–113, 115
Mice
BALB/c-Rag1nullγcnull 206
BALB/c-Rag2nullγcnull 206
BLT mice 193, 205, 206, 211–212, 217
hCD4/R5/cT1 ..... 223, 224, 230–233

HIV-1 infection 203, 204, 207
Hu-mice 203, 204, 207, 209, 211, 212, 216
construction
Hu-HSC mice 205, 206, 211
preparation
hu-spl-PBMC-NSG 222
NOD-scid IL2Rγnull 206
NSG 206, 222, 223, 228–230
Microbeads
anti-biotin 246, 258
Anti-HLA-DR 242, 246
Human CD25 242
human CD69 kit 242
Microglia 289
Microscopyconfocal
Axio Observer Z1 289
MINIS 151
Microscopy
Confocal 166, 266, 275–277, 283, 285, 289, 371
Axio Observer Z1
fluorescent 24
intravital 191–193, 195, 196
multiphoton 189, 192, 196, 197, 200
software 289
Zen Blue
MOI 7, 11, 12, 17, 145, 261, 262, 333
MOLT-4/CCR5 ..... 240, 241, 243–245, 247, 249, 250
Monocytes 371
MPE. *See* Methidiumpropyl-EDTA (MPE)
MPE-Fe(II) 94, 110–113, 115
MTS cell proliferation assay 242, 244
MTT assay 315
Multiple reaction monitoring 311
Mutant frequencies 71–86
Mutation spectra 71–, 86

N

N-hydroxysulfosuccinimide 152
Nef 25, 224, 256, 272, 277, 282, 283, 285–288, 290
Neutralization assay 29, 32
Neuroblastoma 369
Neurons, primary human 368
Culturing 209, 225, 244, 355, 369, 370
Neurotoxicity 372–374
NL4-3 ..... 34, 83, 291, 316
Nucleocapsid (NC) 119, 175
Nucleofection 26–28, 363

O

OM-10 ..... 267, 268
Oxyrase/Oxyfluor 57

P

^{32}P-ATP 125
p24
ELISA 369, 371
PAR-CLIP 120
Paraformaldehyde (PFA) 267
Paracrine 354
PBMCs. *See* Peripheral blood mononuclear cells (PBMCs)
PC12 Cells
transfection 337
pCherryVpr 51
pCMV-dR8.2 dVpr 51
pCMV-VSV-G 51, 258
PCR amplification 80
pEGFP N1 ..... 356, 358
penicillin-streptomycin 169
Peripheral blood lymphocytes 333
Peripheral blood mononuclear cells 356
Peripheral blood mononuclear cells (PBMCs) 215, 222, 225, 226, 228, 241, 243–246, 248, 249, 251, 258–260, 269, 277, 333, 355, 356, 371
Isolation 225, 243–245, 356
pGFPVpr 51
PHA. *See* Phytohemagglutinin (PHA)
Phorbol 12-myristate-13-acetate (PMA) 242, 244, 267, 268, 282–284, 356
photobleaching 53, 56–58
phototoxicity 53, 56–58
Phusion Hot Start II 75, 80, 81, 85
Phytohemagglutinin (PHA) 223, 225, 241, 242, 244–247, 249, 251
PI(4,5)P2 ..... 175–178, 182, 183
Plasma
membrane 22, 165–167, 173–175, 311
PMA. *See* Phorbol 12-myristate-13-acetate (PMA)
Pharmacokinetic analysis 208, 215
Phosphatidylinositol (4,5) bisphosphate 175
Phosphorimaging 67, 103
Photobleaching 53, 54, 56–58, 189
Phototoxicity 53, 56–58
pmCherry-IRES-Tat 356
pMM310 ..... 26, 34
pNL4-3 HIG 83
pNL4-3 MIG 73, 74, 76, 80, 83
Polybrene 51
Ponasterone A 5–7
Popliteal lymphocytes 191–193, 195, 196
POPC 176–178
POPS 176–178
PrEP
oral 204, 208, 214–215
topical 204, 208, 215

Primary T-Cells
Transfection....333
Primer labeling....64–65
Probenecid....26
Protease (PR)
inhibitor....294
Protein....121, 122, 125–126, 293–296, 301, 307
Extraction....312, 316, 317
Quantification....166, 173, 296, 306, 319
Proteome....293, 299, 311, 312, 323
Proteomics
Exosomes....311–324
limitations of....305
plasma/serum....305
techniques
iTRAQ....293
ICAT....293
MRM....311, 312
TMT....293
shotgun....293, 294
SILAC....293, 311–313, 315, 319, 320, 322–324
super-SILAC....293
SWATH-MS....294–296, 301, 307
pSPAX2....51, 52
p-value....79, 250, 303, 304, 322

Q

Quantitative viral outgrowth assay (Q-VOA)....241

R

Rabbit reticulocyte lysate....177
Radioactivity....67, 284
Radio immuno precipitation assay (RIPA)....137, 314, 317
Raltegravir....150, 208
Real-time quantitative PCR....207–208, 213
RediJect Coelenterazine h....225–227
Reverse transcriptase....61–70, 72, 74, 96, 101, 103, 138, 213
Reverse transcription....62–63, 96, 100–101, 137–138, 144, 358
Ribonucleoprotein complexes....133–146
RIPA. *See* Radio immuno precipitation assay (RIPA)
RNA....119, 120, 122, 123, 125–127, 129, 130
affinity chromatography....134, 141, 142
composer....94, 107, 113
folding....95–100, 105, 107, 111, 113, 114
fractionation....93, 98–99
fractionation by ND page....98–99
Hydroxy radical cleavage....110, 112
IP....143
isolation....108, 243, 248, 358
modeling....94
modeling 2-D....105–107, 110, 113, 115
modeling 3-D....107, 110, 113
modification, with NMIA....95
Purification....122, 125–126
quantitation....93, 95, 99, 100
refolding....182
Structure (software)....92, 106, 107, 120
UV Shadowing....108–109
RNA Immunoprecipitation....143–144
RNASe T1....129
RNAComposer....94, 107, 113
RNP
RNA.affinity isolation....133–136, 143
Virion-Associated....142–144
RRE....92–94, 97, 98, 107–109, 111, 113
RT-qPCR....145, 240, 241, 243, 248, 251
RXR receptor....4, 5

S

Sampling
Blood....263
Tissue....208, 215–216
SAMtools....128
Scintillation....282
SDS-PAGE....125, 129, 138, 142, 145, 160, 177, 183, 314, 317, 332, 357, 361–362
Preparative....142, 177
Sequencing
FASTA....300
ladders....96, 101, 102
STRING....315, 322
Serum....52, 74, 76, 154, 157, 207, 209, 229, 242, 290, 291, 293–309, 331, 333
SHAPE
data normalization....103, 104
ensemble....92–94, 97–100, 104, 105, 110, 113, 115
in-gel....92–94, 99, 107, 109
mathematical deconvolution....104
ShapeFinder....96, 102, 103, 110, 113, 115
SILAC....293, 311–313, 315, 319, 320, 322–324
Spectral library....295, 299, 300, 307
Sphingolipids....281
Software
Andromeda....315
ConsensusPathDB....324
GoMiner....324
GORILLA....324
ImageJ....169, 173
ImageStudio....315, 319
Ingenuity....324
Leica Microsystems LAS....169, 171
Mascot....315, 319
MAXQuant....315, 319
Nikon NIS....373
PANTHER....324

Silacratioanalyser 315
STRAP.....315, 322
Stable synaptic complex (SSC).....7, 9, 149, 150, 217
Stable Isotope Labeling by Amino acids.....311–313, 315, 319, 320, 322–324 (*see also* SILAC)
Statistics
ANOVA 303, 304
p-value 303, 304
Student's t-test.....304
STCM. *See* Super T cell medium (STCM)
Strepavidin 135
Super T cell medium (STCM) 242, 244–249, 251
Surgical anesthesia..... 191, 196, 200
SYBR Green 95, 98–100, 108
SWATH-MS 294–297, 299, 301, 307, 308
sample processing 295–296
SwissProt.....307

T

TAR. *See* Transactivating region (TAR)
Tat 356
Detection.....344, 349, 357, 361–362
Expression vectors
pmCherry-IRES-Tat 356
pcDNA 3.1-Tat 356
neurotoxicity.....344
secretion efficiency.....330, 337
uptake 344
Tat-FLAG.....330, 337–338
TCGF. *See* T cell growth factor (TCGF)
293T cells 73, 76, 83, 168, 170, 223–225, 232, 369, 371
T cell activation markers.....241
T cell growth factor (TCGF) 242–244251
Preparation 242–244
Tet-On 5
Tetracycline 4, 5, 17
THP-1 ..... 282, 283, 355, 356, 362, 363, 365
Thymidine kinase 72
Titering viral stocks.....76–77, 83
TO-901317 ..... 282, 284, 290
Transactivating region (TAR)..... 134, 222, 354
Transcription 127, 139–140, 180–183
in vitro 134, 135, 139, 180–183
T-Tropism.....3, 4
Transfection
fugene 6 224
Metafecten.....287
Transferrin.....306
TRIMcypA 58
Triton X-100 .....154, 282, 283, 288, 331
Trojan horse.....368
Trichostatin A (TSA).....259, 261–263
TRIM5α.....58
Trypan blue 26, 29, 217, 231, 258, 260, 313, 315
TUNEL 369, 372–375
TMR in situ hybridization 369, 372
Tukey's Post Test 78, 84
TZM-bl reporter cell line.....223

U

Uncoating.....22, 23, 39, 50–52, 55, 57
UniProt-SwissProt 299
Urea-PAGE.....66–67
UTR..... 92, 93, 134, 135
UV-cross linking.....121, 124

V

Vesicle.....311
VERSA metrics.....4, 14–18
VgEcr 4, 5
Vif 72, 277
Viral particles 21, 22, 25, 51, 54, 56, 57, 120, 151, 152, 154, 157, 160, 364
Isolation.....157–158
Viral-associated RNPs.....142
Viral protein expression constructs
pCMV-VSV-G.....258
pMDLs/pRRE 258
pRSV-Rev 258, 261
Virological synapse 22, 23
VPR.....24, 26, 49–52, 55, 72

W

WST-1 assay 368

Z

z-score 303
z-stack 54, 56–58, 166, 172, 174, 290